Tue. Jun 4, 2019

Room K

International Session | International Session | [ES] E-1 Knowledge engineering

[1K4-E-1] Knowledge engineering

Chair: Kazushi Okamoto (The University of Electro-Communications), Reviewer: Yasufumi Takama (Tokyo Metropolitan University)
5:20 PM - 7:00 PM Room K (201A Medium meeting room)

[1K4-E-1-01] How is Social Capital Associated with Perception of AI?
○Yoji Inaba[1] （1. Nihon University）
5:20 PM - 5:40 PM

[1K4-E-1-02] Multimodal Neural Network– based Health Platform for Knowledge Decision-Making
○Kyungyong Chung[1] （1. Kyonggi University）
5:40 PM - 6:00 PM

[1K4-E-1-03] Variables Extraction in Natural (English) Language Through Possessive Relationships
○Danilo Eidy Miura[1], Teruaki Hayashi[1], Yukio Ohsawa[1] （1. The University of Tokyo）
6:00 PM - 6:20 PM

[1K4-E-1-04] Using Sequence Constraints for Modelling Network Interactions
Johannes De Smedt[2], ○Junichiro Mori[1], Masanao Ochi[1] （1. The University of Tokyo, 2. The University of Edinburgh）
6:20 PM - 6:40 PM

[1K4-E-1-05] CTransE : Confidence-Based Translation Model for Uncertain Knowledge Graph Embedding
○Natthawut Kertkeidkachorn[1,2], Xin Liu[1], Ryutaro Ichise[2,1] （1. National Institute of Advanced Industrial Science and Technology, 2. National Institute of Informatics）
6:40 PM - 7:00 PM

Wed. Jun 5, 2019

Room A

International Session | International Session | [ES] E-2 Machine learning

[2A4-E-2] Machine learning: method extensions

Chair: Junichiro Mori (The University of Tokyo)
3:20 PM - 5:00 PM Room A (2F Main hall A)

[2A4-E-2-01] Multi-carrier energy hub management through deep deterministic policy gradient over continuous action space

Hioki Tomoyuki[1], ○Tomah Sogabe[1,2,3], Dinesh Malla[3], Kei Takahashi[1], Masaru Sogabe[3], Katsuyoshi Sakamoto[1], Kouichi Yamaguchi[1] (1. Department of Engineering Science ,The University ofElectro-Communications, 2. Info-Powered Energy System Research Center, 3. Grid Inc.)

3:20 PM - 3:40 PM

[2A4-E-2-02] Attention-masking extended deep Q network (AME-DQN) reinforcement learning algorithm for combinatory optimization of smart-grid energy

○Dinesh Bahadur Malla[3], Hioki Tomoyuki [2], Kei Takahashi[2], Masaru Sogabe[3], Katsuyoshi Sakamoto[1,2], Koichi Yamaguchi[1,2], Tomah Sogabe[1,2,3] (1. i-PERC, The University ofElectro-Communications, 2. The University ofElectro-Communications, 3. Grid Inc.)

3:40 PM - 4:00 PM

[2A4-E-2-03] Exploring Machine Learning Techniques for Irony Detection

○Zheng Lin Chia[1], Michal Ptaszynski[1], Fumito Masui[1] (1. Kitami Institute of Technology)

4:00 PM - 4:20 PM

[2A4-E-2-04] A Matrix-Operation Fast Approximated Solution for Logistic Regression with Strong L2 Regularization

○Zeke Xie[1], Jinze Yu[1], Yanping Deng[2] (1. University of Tokyo, 2. Waseda University)

4:20 PM - 4:40 PM

[2A4-E-2-05] Final Sample Batch Normalization For Quantized Neural Networks

○Joel Owen Nicholls[1], Atsunori Kanemura[1] (1. LeapMind Inc.)

4:40 PM - 5:00 PM

International Session | International Session | [ES] E-5 Human interface, education aid

[2A3-E-5] Human interface, education aid: chance discoveries

Chair: Akinori Abe (Chiba University), Reviewer: Naohiro Matsumura (Osaka University)
1:20 PM - 2:20 PM Room A (2F Main hall A)

[2A3-E-5-01] How to enable the utility data under the lower sampling rate and less attribute for making smart cities

○Eiji Murakami[1] (1. Azbil kimmon Co.,Ltd.)

1:20 PM - 1:40 PM

[2A3-E-5-02] Proposal of Context-aware Music Recommender System Using Negative Sampling

○Jin-cheng ZHANG[1], Yasufumi TAKAMA[1] (1. Tokyo Metropolitan University)

1:40 PM - 2:00 PM

[2A3-E-5-03] Entropy-based Knowledge Space Visualization for Data-driven Decision Support

○Qi Wang[1], Teruaki Hayashi[1], Yukio Ohsawa[1] (1. The University of Tokyo)

2:00 PM - 2:20 PM

Room C

International Session | International Session | [ES] E-5 Human interface, education aid

[2C5-E-5] Human interface, education aid: places of design

Chair: Katsutoshi Yada (Kansai University)
5:20 PM - 7:00 PM Room C (4F International conference hall)

[2C5-E-5-01] The Influence of Story Creating Activities while Appreciating Abstract Artworks

○Kotone Tadaki[1], Akinori Abe[1] (1. Chiba University)

5:20 PM - 5:40 PM

[2C5-E-5-02] AI, Making Software for Humans

○Mika Yasuoka[1], Rune Moeller Jensen[2] (1. GLOCOM, 2. IT University of Copenhagen)

5:40 PM - 6:00 PM

[2C5-E-5-03] The effect of eye-catching object on sampling at supermarket

○Rihoko Mae[1], Naohiro Matsumura[1] (1. Osaka University)

6:00 PM - 6:20 PM

[2C5-E-5-04] Vision Based Analysis on Trajectories of

Notes Representing Ideas Toward Workshop Summarization

○Yuji Oyamada[1], Mikihiko Mori[2], Haruhiko Maenami[1] (1. Tottori University, 2. Hosei University)

6:20 PM - 6:40 PM

[2C5-E-5-05] Intuitive Automatic Music Arrangement System for Wave Files Following Sensitivity Words

○Koichi Yamagata[1], Shota Miyoshi[1], Maki Sakamoto[1] (1. The University of Electro-Communications)

6:40 PM - 7:00 PM

Room D

International Session | International Session | [ES] E-4 Robots and real worlds

[2D3-E-4] Robots and real worlds: planning and control

Chair: Eri Sato-Shimokawara (Tokyo Metropolitan University), Reviewer: Hiroki Shibata (Tokyo Metropolitan University)
1:20 PM - 2:20 PM Room D (301B Medium meeting room)

[2D3-E-4-01] Mahalanobis Taguchi Fukuda Approach to Motion Control

○Shuichi Fukuda[1] (1. Keio University)

1:20 PM - 1:40 PM

[2D3-E-4-02] Flexibility of Emulation Learning from Pioneers in Nonstationary Environments

Moto Shinriki[1], ○Hiroaki Wakabayashi[1], Yu Kono[1], Tatsuji Takahashi[1] (1. Tokyo Denki University)

1:40 PM - 2:00 PM

[2D3-E-4-03] A Multimodal Target-Source Classifier Model for Object Fetching from Natural Language Instructions

○Aly Magassouba[1], Komei Sugiura[1], Hisashi Kawai[1] (1. NICT)

2:00 PM - 2:20 PM

Room F

International Session | International Session | [ES] E-3 Agents

[2F1-E-3] Agents: interaction and decision

Chair: Shigeo Matsubara (Kyoto University), Reviewer: Takayuki Ito (Nagoya Institute of Technology)
9:00 AM - 10:40 AM Room F (302B Medium meeting room)

[2F1-E-3-01] ANAC 2018: Repeated Multilateral Negotiation League

Reyhan Aydogan[1,4], ○Katsuhide Fujita[2], Tim Baarslag[3], Catholijn M. Jonker[4], Takayuki Ito[5] (1. Ozyegin University, 2. Tokyo University of Agriculture and Technology Tokyo, 3. Centrum Wiskunde &Informatica, 4. Delft University of Technology, 5. Nagoya Institute of Technology)

9:00 AM - 9:20 AM

[2F1-E-3-02] Extraction of Online Discussion Structures for Automated Facilitation Agent

○Shota Suzuki[1], Naoko Yamaguchi[1], Tomohiro Nishida[1], Ahmed Moustafa[1], Daichi Shibata[1], Kai Yoshino[1], Kentaro Hiraishi[1], Takayuki Ito[1] (1. Nagoya Institute of Technology)

9:20 AM - 9:40 AM

[2F1-E-3-03] An Automated Negotiating Agent that Searches the Bids around Nash Bargaining Solution to Obtain High Joint Utilities

Shan Liu[1], ○Ahmed Moustafa[1], Takayuki Ito[1] (1. Nagoya Institute of Technology)

9:40 AM - 10:00 AM

[2F1-E-3-04] Analysis of Incentive Ratio in Top-Trading-Cycles Algorithms

○Taiki Todo[1] (1. Kyushu University)

10:00 AM - 10:20 AM

[2F1-E-3-05] Multi-Agent Traffic Signal Control System Using Deep Q-Network

○YOHEI KANZAKI[1], Keisuke Ohno[1], Eichi Takaya[1], Satoshi Kurihara[1] (1. Keio University)

10:20 AM - 10:40 AM

Room H

International Session | International Session | [ES] E-2 Machine learning

[2H4-E-2] Machine learning: fusion of models

Chair: Naohiro Matsumura (Osaka University)
3:20 PM - 5:00 PM Room H (303+304 Small meeting rooms)

[2H4-E-2-01] Curiosity Driven by Self Capability Prediction

○Nicolas Bougie[1,2], Ryutaro Ichise[2,1] (1. Sokendai, The Graduate University for Advanced Studies, 2. National Institute of Informatics)

3:20 PM - 3:40 PM

[2H4-E-2-02] Improvement of Product Shipment Forecast based on LSTM Incorporating On-Site Knowledge as Residual Connection

○Takeshi Morinibu[1], Tomohiro Noda[1], Shota Tanaka[1] (1. Daikin Industries, Ltd. Technology and Innovation Center)

3:40 PM - 4:00 PM

[2H4-E-2-03] Unsupervised Joint Learning for Headline Generation and Discourse Structure of Reviews

○Masaru Isonuma[1], Junichiro Mori[1], Ichiro Sakata[1] (1. The University of Tokyo)

4:00 PM - 4:20 PM

[2H4-E-2-04] Gradient Descent Optimization by Reinforcement Learning

○Yingda Zhu[1], Teruaki Hayashi[1], Yukio Ohsawa[1] (1. The University of Tokyo)

4:20 PM - 4:40 PM

[2H4-E-2-05] Reducing the Number of Multiplications in Convolutional Recurrent Neural Networks (ConvRNNs)

○Daria Vazhenina[1], Atsunori Kanemura[1] (1. Leapmind Inc.)

4:40 PM - 5:00 PM

International Session | International Session | [ES] E-2 Machine learning

[2H5-E-2] Machine learning: new modeling

Chair: Junichiro Mori (The University of Tokyo)
5:20 PM - 6:40 PM Room H (303+304 Small meeting rooms)

[2H5-E-2-01] Local Feature Fitting Learning Network for Point Cloud Classification

○Lu SUN[1] (1. Chiba University)

5:20 PM - 5:40 PM

[2H5-E-2-02] Feasible Affect Recognition in Advertising based on Physiological Responses from Wearable Sensors

○Taweesak Emsawas[1] (1. Osaka University)

5:40 PM - 6:00 PM

[2H5-E-2-03] Deep Markov Models for Data Assimilation in Chaotic Dynamical Systems

○Calvin Janitra Halim[1], Kazuhiko Kawamoto[1] (1. Chiba University)

6:00 PM - 6:20 PM

[2H5-E-2-04] Modelling Naturalistic Work Stress Using Spectral HRV Representations and Deep Learning

○Juan Lorenzo Mutia Hagad[1], Ken-ichi Fukui[1], Masayuki Numao[1] (1. Osaka University)

6:20 PM - 6:40 PM

Room J

International Session | International Session | [ES] E-5 Human interface, education aid

[2J1-E-5] Human interface, education aid: education

Chair: Katsutoshi Yada (Kansai University)
9:00 AM - 10:40 AM Room J (201B Medium meeting room)

[2J1-E-5-01] Teaching Reinforcement Learning and Computer Games with 2048-Like Games

○Hung Guei[1], Ting-Han Wei[1], I-Chen Wu[1] (1. National Chiao Tung University)

9:00 AM - 9:20 AM

[2J1-E-5-02] Feature Extraction of Onomatopoeia Considering Phonotactics for Automatic Semantic Usage Classification of Onomatopoeia

○Hiromu Takayama[1], Nastumi Takeuchi[1], Daiki Urata[1], Tsuyoshi Nakamura[1], Ahmed Moustafa[1], Takayuki Ito[1] (1. Nagoya Institute of Technology)

9:20 AM - 9:40 AM

[2J1-E-5-03] Vibrational Artificial Subtle Expressions to Convey System’ s Confidence Level to Users

○Takanori Komatsu[1], Kazuki Kobayashi[2], Seiji Yamada[3], Kotaro Funakoshi[4], Mikio Nakano[4] (1. Meiji University, 2. Shinshu University, 3. National Institute of Informatics/Tokyo Institute of Technology/SOKENDAI, 4. Honda Research Institute Japan)

9:40 AM - 10:00 AM

[2J1-E-5-04] A think-programming method based on free texts “ almost” in English

○Keisuke Nakamura[1] (1. KnowrelSystem,Inc.)

10:00 AM - 10:20 AM

[2J1-E-5-05] Affective Tutoring for Programming Education

○Thomas James Zarraga Tiam-Lee[1], Kaoru Sumi[1] (1. Future University Hakodate)

10:20 AM - 10:40 AM

Room K

International Session | International Session | [ES] E-1 Knowledge engineering

[2K3-E-1] Knowledge engineering

Chair: Tadahiko Murata (Kansai University), Reviewer: Yasufumi

Takama (Tokyo Metropolitan University)
1:20 PM - 2:40 PM Room K (201A Medium meeting room)

[2K3-E-1-01] Mobile Website Creation based on Web Data eXtraction and Reuse
○Chia-Hui Chang[1], Yan-Kai Lai[1], Yu-An Chou[1], Oviliani Yenty Yuliana[1] (1. National Central University)
1:20 PM - 1:40 PM

[2K3-E-1-02] Reduction of Erasable Itemset Mining to Frequent Itemset Mining
○Tzung-Pei Hong[1,2], Chun-Ho Wang[2], Chia-Che Li[2], Wen-Yang Lin[1] (1. National University of Kaohsiung, 2. National Sun Yat-sen University)
1:40 PM - 2:00 PM

[2K3-E-1-03] Consideration of the relationship between explicit knowledge and tacit knowledge in an intellectual task
○Itsuki Takiguchi[1] (1. Graduate School of Humanities and Studies on Public Affairs Chiba University)
2:00 PM - 2:20 PM

[2K3-E-1-04] k-th Order Intelligences: Learning To Learn To Do
○Francisco J Arjonilla[1], Yuichi Kobayashi[1] (1. Graduate School of Science and Technology, Shizuoka University)
2:20 PM - 2:40 PM

Room O

International Session | International Session | [ES] E-3 Agents

[2O5-E-3] Agents: reasoning and integration

Chair: Naoki Fukuda (Sizuoka University), Reviewer: Takayuki Ito (Nagoya Institute of Technology)
5:20 PM - 7:00 PM Room O (Front-left room of 1F Exhibition hall)

[2O5-E-3-01] Improving the Accuracy of the Collective Prediction by Maintaining the Diversity of Opinions: Preliminary Report
○Rui Chen[1], Shigeo Matsubara[1] (1. Kyoto University)
5:20 PM - 5:40 PM

[2O5-E-3-02] An Approach to Knowledge Graph Completion based on Discussion Agents using IBIS Structure
○Xiangyu Zhang[1], Shun Shiramatsu[2] (1. Department of Computer Science, Faculty of Engineering, Nagoya Institute of Technology, 2. Department of Computer Science, Graduate School of Engineering, Nagoya Institute of Technology)
5:40 PM - 6:00 PM

[2O5-E-3-03] Using Q-learning and Estimation of Role in Werewolf Game
○Makoto Hagiwara[1], Ahmed Moustafa[1], Takayuki Ito[1] (1. Nagoya Institute of Technology)
6:00 PM - 6:20 PM

[2O5-E-3-04] Inferring Agent's Goals from Observing Successful Traces
○Guillaume LORTHIOIR[1,2], Katsumi INOUE[1,2], Gauvain Bourgne[3] (1. SOKENDAI (The Graduate University for Advanced Studies), 2. National Institute of Informatics, 3. Sorbonne Université, UPMC CNRS, UMR 7606,LIP6, F-75005, Paris, France)
6:20 PM - 6:40 PM

[2O5-E-3-05] A New Character Decision-Making System by combining Behavior Tree and State Machine
○Youichiro Miyake[1] (1. SQUARE ENIX)
6:40 PM - 7:00 PM

Thu. Jun 6, 2019

Room B

International Session | International Session | [ES] E-2 Machine learning

[3B3-E-2] Machine learning: image recognition and generation

Chair: Masakazu Ishihata (NTT)
1:50 PM - 3:30 PM Room B (2F Main hall B)

[3B3-E-2-01] Design a Loss Function which Generates a Spatial configuration of Image In-betweening
○Paulino Cristovao[1], Hidemoto Nakada[1,2], Yusuke Tanimura[1,2], Hideki Asoh[2] (1. University of Tsukuba, 2. National Advanced Institute of Science and Technology of Japan (AIST))
1:50 PM - 2:10 PM

[3B3-E-2-02] One-shot Learning using Triplet Network with kNN classifier
○Mu Zhou[1,2], Yusuke Tanimura[2,1], Hidemoto Nakada[2,1] (1. University of Tsukuba, 2. Artifical Intelligence Research Center, National Institute of Advanced Institute of Technology)
2:10 PM - 2:30 PM

[3B3-E-2-03] Cycle Sketch GAN: Unpaired Sketch to Sketch Translation Based on Cycle GAN Algorithm
○Takeshi Kojima[1] (1. Peach Aviation Limited)
2:30 PM - 2:50 PM

[3B3-E-2-04] Conditional DCGAN's Challenge: Generating Handwritten Character Digit, Alphabet and Katakana
○Rina Komatsu[1], Tad Gonsalves[1] (1. Sophia University)
2:50 PM - 3:10 PM

[3B3-E-2-05] Sparse Damage Per-pixel Prognosis Indices via Semantic Segmentation
○Takato Yasuno[1] (1. Research Institute for Infrastructure Paradigm Shift (RIIPS))
3:10 PM - 3:30 PM

International Session | International Session | [ES] E-2 Machine learning

[3B4-E-2] Machine learning: social links

Chair: Lieu-Hen Chen (National Chi Nan University), Reviewer: Yasufumi Takama (Tokyo Metropolitan University)
3:50 PM - 5:30 PM Room B (2F Main hall B)

[3B4-E-2-01] Social Influence Prediction by a Community-based Convolutional Neural Network
Shao-Hsuan Tai[1], Hao-Shang Ma[1], ○Jen-Wei Huang[1] (1. National Cheng Kung University)
3:50 PM - 4:10 PM

[3B4-E-2-02] A Community Sensing Approach for User Identity Linkage
○Zexuan Wang[1], Teruaki Hayashi[1], Yukio Ohsawa[1] (1. Department of Systems Innovation, School of Engineering, The University of Tokyo)
4:10 PM - 4:30 PM

[3B4-E-2-03] Learning Sequential Behavior for Next-Item Prediction
○Na Lu[1], Yukio Ohsawa[1], Teruaki Hayashi[1] (1. The University of Tokyo)
4:30 PM - 4:50 PM

[3B4-E-2-04] Application of Unsupervised NMT Technique to Japanese--Chinese Machine Translation
○Yuting Zhao[1], Longtu Zhang[1], Mamoru Komachi[1] (1. Tokyo Metropolitan University)
4:50 PM - 5:10 PM

[3B4-E-2-05] Synthetic and Distribution Method of Japanese Synthesized Population for Real-Scale Social Simulations
○Tadahiko Murata[1], Takuya Harada[1] (1. Kansai University)
5:10 PM - 5:30 PM

Room H

International Session | International Session | [ES] E-3 Agents

[3H3-E-3] Agents: safe and cooperative society

Chair: Ahmed Moustafa (Nagoya Institute of Technology), Reviewer: Takayuki Ito (Nagoya Institute of Technology)
1:50 PM - 3:30 PM Room H (303+304 Small meeting rooms)

[3H3-E-3-01] An Autonomous Cooperative Randomization Approach to Prevent Attacks Based on Traffic Trends in the Communication Destination Anonymization Problem
○Keita Sugiyama[1], Naoki Fukuta[1] (1. Shizuoka University)
1:50 PM - 2:10 PM

[3H3-E-3-02] Cooperation Model for Improving Scalability of the Multi-Blockchains System
○Keyang Liu[1], Yukio Ohsawa[1], Teruaki Hayashi [1] (1. University of Tokyo, Graduate school of engineer)
2:10 PM - 2:30 PM

[3H3-E-3-03] Effect of Visible Meta-Rewards on Consumer Generated Media

○Fujio Toriumi[1], Hitoshi Yamamoto[2], Isamu Okada[3] (1. The University of Tokyo, 2. Rissho University, 3. Soka University)

2:30 PM - 2:50 PM

[3H3-E-3-04] Toward machine learning-based facilitation for online discussion in crowd-scale deliberation

○Chunsheng Yang[1], Takayuki Ito[2], Wen GU[2] (1. National Research Council Canada, 2. Nagoya Institute of Technology)

2:50 PM - 3:10 PM

[3H3-E-3-05] An automated privacy information detection approach for protecting individual online social network users

○Weihua Li[1], Jiaqi Wu[1], Quan Bai[2] (1. Auckland University of Technology, 2. University of Tasmania)

3:10 PM - 3:30 PM

Room J

International Session | International Session | [ES] E-4 Robots and real worlds

[3J3-E-4] Robots and real worlds: Human Interactions

Chair: Yihsin Ho (Takushoku University), Eri Sato-Shimokawara (Tokyo Metropolitan University)

1:50 PM - 3:10 PM Room J (201B Medium meeting room)

[3J3-E-4-01] Automatic Advertisement Copy Generation System from Images

○Koichi Yamagata[1], Masato Konno[1], Maki Sakamoto[1] (1. The University of Electro-Communications)

1:50 PM - 2:10 PM

[3J3-E-4-02] Eye-gaze in Social Robot Interactions

Koki Ijuin[2], ○Kristiina Jokinen Jokinen[1], Tsuneo Kato[2], Seiichi Yamamoto[2] (1. AIRC, AIST Tokyo Waterfront, 2. Doshisha University)

2:10 PM - 2:30 PM

[3J3-E-4-03] A Team Negotiation Strategy that Considers Team Interdependencies

○Daiki Setoguchi[1], Ahmed Moustafa[1], Takayuki Ito[1] (1. Nagoya Institute of Technology)

2:30 PM - 2:50 PM

[3J3-E-4-04] Identity Verification Using Face Recognition Improved by Managing Check-in Behavior of Event Attendees

○Akitoshi Okumura[1], Susumu Handa[1], Takamichi Hoshino[1], Naoki Tokunaga[1], Masami Kanda[1] (1. NEC Solution Innovators, Ltd.)

2:50 PM - 3:10 PM

Fri. Jun 7, 2019

Room D

International Session | International Session | [ES] E-2 Machine learning

[4D3-E-2] Machine learning: living environment

Chair: Junichiro Mori (The University of Tokyo)
2:00 PM - 3:40 PM Room D (301B Medium meeting room)

[4D3-E-2-01] Privacy-Preserving Resident Monitoring System with Ultra Low-Resolution Imaging and the Examination of Its Ease of Installation

○Takumi Kimura[1], Shogo Murakami[1], Ikuko Egushi Yairi[1] （1. Sophia University）

2:00 PM - 2:20 PM

[4D3-E-2-02] Trees Detection on Google Street View Images Using Deep Learning and City Open Data

○Lieu-Hen Chen[1], Hao-Ming Hung[1], Cheng-Yu Sun[1], Eric Hsiao-Kuang Wu[2], Toru Yamaguchi[3], Eri Sato-Shimokawara[3], Hao Chen[1] （1. Nantional Chi Nan University, 2. National Central University, 3. Tokyo Metropolitan University）

2:20 PM - 2:40 PM

[4D3-E-2-03] Scoring and Classifying Regions via Multimodal Transportation Networks

○Aaron Bramson[1,2,3,4], Megumi Hori[1], Zha Bingran[1], Hirohisa Inamoto[1] （1. GA Technologies, 2. RIKEN Center for Biosystems Dynamics Research, 3. Ghent Univeristy, 4. UNC - Charlotte）

2:40 PM - 3:00 PM

[4D3-E-2-04] Evaluating Road Surface Condition by using Wheelchair Driving Data and Positional Information based Weakly Supervision

○Takumi Watanabe[1], Hiroki Takahashi[1], Yusuke Iwasawa[2], Yutaka Matsuo[2], Ikuko Eguchi Yairi[1] （1. Sophia Univ., 2. Univ. of Tokyo）

3:00 PM - 3:20 PM

[4D3-E-2-05] Prediction of the Onset of Lifestyle-related Diseases Using Regular Health Checkup Data

○Mitsuru Tsunekawa[1], Natsuki Oka[1], Masahiro Araki[1], Motoshi Shintani[2], Masataka Yoshikawa[3], Takashi Tanigawa[4] （1. Kyoto Institute of Technology, 2. SG Holdings Group Health Insurance Association, 3. Japan System Techniques Co.,Ltd., 4. Juntendo University）

3:20 PM - 3:40 PM

Room H

International Session | International Session | [ES] E-5 Human interface, education aid

[4H2-E-5] Human interface, education aid: human evaluation

Chair: Naohiro Matsumura (Osaka University)
12:00 PM - 1:40 PM Room H (303+304 Small meeting rooms)

[4H2-E-5-01] Recognition of Kuzushi-ji with Deep Learning Method

○Xiaoran Hu[1], Mariko Inamoto[2], Akihiko Konagaya[1] （1. Tokyo Institute of Technology, 2. Keisen University）

12:00 PM - 12:20 PM

[4H2-E-5-02] Computerized Adaptive Testing Method using Integer Programming to Minimize Item Exposure

○Yoshimitsu MIYAZAWA[1], Maomi UENO[2] （1. The National Center for University Entrance Examinations, 2. The University of Electro-Communications）

12:20 PM - 12:40 PM

[4H2-E-5-03] Maximizing accuracy of group peer assessment using item response theory and integer programming

○Masaki Uto[1], Duc-Thien Nguyen[1], Maomi Ueno[1] （1. University of Electro-Communications）

12:40 PM - 1:00 PM

[4H2-E-5-04] Waveform Processing of Electrocardiogram with Neural Network and Non-contact Measurement using Kinect for Driver Evaluation

○HAO ZHANG[1], Takashi IMAMURA[1] （1. Niigata University）

1:00 PM - 1:20 PM

[4H2-E-5-05] Probability based scaffolding system using Deep Learning

○Ryo Kinoshita[1], Maomi Ueno[1] （1. The University of Electro-Communications.）

1:20 PM - 1:40 PM

International Session | International Session | [ES] E-1 Knowledge engineering

[1K4-E-1] Knowledge engineering

Chair: Kazushi Okamoto (The University of Electro-Communications), Reviewer: Yasufumi Takama (Tokyo Metropolitan University)

Tue. Jun 4, 2019 5:20 PM - 7:00 PM Room K (201A Medium meeting room)

[1K4-E-1-01] How is Social Capital Associated with Perception of AI?

○Yoji Inaba[1] （1. Nihon University）

5:20 PM - 5:40 PM

[1K4-E-1-02] Multimodal Neural Network– based Health Platform for Knowledge Decision-Making

○Kyungyong Chung[1] （1. Kyonggi University）

5:40 PM - 6:00 PM

[1K4-E-1-03] Variables Extraction in Natural (English) Language Through Possessive Relationships

○Danilo Eidy Miura[1], Teruaki Hayashi[1], Yukio Ohsawa[1] （1. The University of Tokyo）

6:00 PM - 6:20 PM

[1K4-E-1-04] Using Sequence Constraints for Modelling Network Interactions

Johannes De Smedt[2], ○Junichiro Mori[1], Masanao Ochi[1] （1. The University of Tokyo, 2. The University of Edinburgh）

6:20 PM - 6:40 PM

[1K4-E-1-05] CTransE : Confidence-Based Translation Model for Uncertain Knowledge Graph Embedding

○Natthawut Kertkeidkachorn[1,2], Xin Liu[1], Ryutaro Ichise[2,1] （1. National Institute of Advanced Industrial Science and Technology, 2. National Institute of Informatics）

6:40 PM - 7:00 PM

The 33rd Annual Conference of the Japanese Society for Artificial Intelligence, 2019

How is Social Capital Associated with Perception of AI? – An Observation from a Survey of Residents in Metropolitan Tokyo Area

Yoji Inaba*

*1 Nihon university

Abstract

Numerous studies over the past 30 years have examined the relationship between social capital (SC) and information and communication technology (ICT). However, few studies have examined the association between artificial intelligence (AI) and SC. This study addresses this gap using a Web survey (N=5000) carried out in the Tokyo metropolitan area in Japan in 2018. The survey included questions on ICT literacy and SC (networks, trust, norms of reciprocity), as well as questions on perceptions of AI including its impact on society. The author found a statistically significant positive association between cognitive SC (trust and norms of reciprocity) and positive perceptions of AI. However, the impact of structural SC (networks) on AI perceptions was either nonexistent or negative. Structural SC created by group participation, as well as contact with others, including those in the workplace, does not create positive perceptions of AI, and could even be a source of negative perceptions of AI. Cognitive SC may function as a promoter of AI, while structural SC may function as a precaution to AI. Both types of SC might assume important roles for the smooth transition to the AI era.

Keyword: Social Capital, ICT, AI, Networks

1. Introduction

1. Introduction

Numerous papers and articles have been written on the relation between social capital (SC) and information communication technologies (ICT) in the past thirty years. Artificial intelligence (AI) which obviously overlaps with ICT is another popular subject in recent years. Yet few papers deal with the association between AI and SC. This paper is an attempt to fulfill the gap based on a web survey (N=5000) the author carried out in the metropolitan Tokyo area in Japan in 2018. The survey asked questions on ICT literacy, SC (networks, trust, norms of reciprocity) as well as perceptions on the AI and its impact on society.

2. Preceding studies and research questions

2.1 Preceding studies

Introduction of ICT until the middle of 2000s functioned both complementary and/or substitutionary to the existing offline SC (1st Wave). Then online structural SC created by ICT mainly enhanced offline cognitive SC (2nd Wave). Currently the offline SC backed up by online structural SC mostly seems to have positive impact on ICT applications to the society. Although ICT literacy and SC were originally mutually correlated, main concern on causality have shifted from ICT to SC rather than vice versa.

2.2 Research questions

The present study deals with the following research questions which have not been fully fulfilled by preceding studies.

RQ1 How will SC affect ICT literacy? Although many papers have dealt with ICT, most of them examined impact of just a particular type of ICT. The lack of comprehensiveness could be said about the preceding studies dealing with SC. As for SC, it covers various concepts including networks, trust, and norms. To the best of our knowledge, there is no paper which is based upon comprehensive pictures of both ICT literacy and SC. This is especially the case on the impact of SC to the ICT literacy. Therefore the present paper shed the light on this aspect.

RQ2 How will SC affect the perception of AI? Are there any implications which could be inferred by the way SC is associated with ICT applications?

RQ3 How will AI affect SC? Are there any implications which could be inferred from an analysis on the way ICT literacy is associated with SC?

Contact: Yoji Inaba, Nihon Univesity, Phone +81-03-5275-8636, Fax +81-03-5936-1780, inaba.yoji@nihon-u.ac.jp

RQ4 What are the policy implications to cope with negative impact of AI introduction if there is any?

3. Materials and Methods

3.1 Data

The dataset used in this study comes from a questionnaire survey that we conducted between September 4th and 10th, 2018 over the internet. The survey covers residents in Metropolitan Tokyo area including Tokyo, Kanagawa, Chiba, and Saitama prefectures between the ages of 20 and 69 years. The survey questionnaires were sent and recovered through the internet. We got reply from 5000 people.

The Questionnaire survey was conducted on the following topics:

① ICT literacy

・8 questions on the availability of ICT devices (yes or no),

・14 questions on the frequency of use of ICT devices and web services with a three-point Likert scale,

・8 questions on capability of soft wares and web services usage with a four-point Likert scale,

・6 questions on the experience of using AI related equipment with a three-point Likert scale.

② SC

12 questions are asked with regard to SC.

・8 questions related to structural SC including group participation, relationships with neighbors, family members and relatives, friends and acquaintances, and colleagues (from four to seven-point Likert scales),

・4 questions related to cognitive SC including trust and norm of reciprocity with a four-point Likert scale.

② Perception on AI

The questionnaire dealt with 30 items on respondents' perception with regard to AI.

・7 questions about evaluations on the influence of AI (one five-choice question and 6 Likert scale questions with a four-point)

・8 questions related to pros & cons on AI use in our society at 8 situations with a five-point Likert scale,

・8 questions on personal preference of AI use at 8 situations with a five-point Likert scale,

・7 questions on the choice between AI or human beings at 7 situations with a four-point Likert scale.

In addition, the survey asked personal attributes of respondents including sex, age, educational attainment, marital status, occupation, forms of employment (permanent or temporary), family income, number of cohabiting people, duration of residence, the name of municipality they reside, and perception on risk.

Concerning the ethical appropriateness of the contents of the questionnaire, the survey was checked and approved by the ethical committee (social science) of the Tohoku University.

3.2 Methodology

I conducted three factor analyses using the above mentioned data on ICT literacy, SC, and perception of AI in order to get basic factors out of these questions in each of the three groups. Then, using factor scores as explanatory variables, two logistic regressions are carried out. First, logistic regressions between ICT literacy and SC. As an extension of the third wave of preceding studies which try to explain the behavior of ICT by SC, we used SC factors as independent variables to explain the changes in ICT literacy factors. Secondly, another series of logistic regression on perceptions of AI, using SC as independent variable controlling ICT literacy and characteristics of respondents.

4. Results

Statistically significant positive associations between cognitive SC and affirmative perception of AI use were observed. However, impact of structural SC on AI perception is either none existent or negative. Structural SC created by group participation as well as contacts with others including those at work place does not create affirmative perception on AI. On the contrary, they could be a source of negative AI perception.

References

Ahmed, Zafor (2018) "Explaining the unpredictability : a social capital perspective on ICT intervention", International Journal of Information Management,38, 175-186.

Bauernschuster.S, F.Oliver, W. Ludger,(2014) "Surfing alone? The internet and social capital: Evidence from an unforeseeable technological mistake", Journal of Public Economics, vol. 117, issue C,73-89

Terashima. K, and A. Miura(2013) "Does use of SNS develop offline/online social caital", Kwansei Gakuin University Bulletin of Psycological Science, Vol.39,59-67. (in Japanese)

Kobayashi, T., & Ikeda, K.(2006). The development of social capital in communities in an online game: A perspective o-n a"spill over"effect into the offline world. Japanese Journal of Social Psychology, vol.22-1, 58−71.(in Japanese)

Hsieh, J.J.P., Rai, A., & Keil, M. (2010). Addressing digital inequality for the socio- economically disadvantaged through government initiatives; Forms of capital that affect ICT utilization. Information Systems Research, 233-253.

Ishizuka, M, et al. (2017) "Introduction" In The Japan Society for Artificial Intelligence (ed.) Encyclopedia of Artificial Intelligence, Kyouritsu Publishing, p.2 (in Japanese) .

Li, Xiaoqian and Wenhong Chen (2014) "Facebook or Renren? A comparative study of social networking site use and social capital among Chinese international students in the United States" Computers in Human Behavior 35,116–123

Lu, J., Yang, J., & Yu, C. (2013). Is social capital effective for online learning? Information & Management, 50, 507-522.

Miyakawa, Tadao, and Omori Takashi (2004) Social Capital, Toyo Keizai (in Japanese).

Miyta, Kakuko (2005a) Social Phycology of the Internet – the function of the internet from a viewpoint of social capital, Kazama Syobo (in Japanese).

Miyata, Kakuko(2005b) Media as a bridge among human ties – Social Capital in the Era of the Internet, NTT Publishing (in Japanese).

Miyata, Kakuko, Barry Wellman, and Jeffrey Boase. (2005c) "The Wired — and Wireless — Japanese: Webphones, PCs and Social Networks." Mobile Communications. Computer Supported Cooperative Work, Springer, vol 31. pp.427-449.

Naranjo-Zolotov, Mijail et al. (2019) “Examining social capital and individual motivators to explain the adoption of online citizen participation”, Future Generation Computer Systems, 92 302–311

Nie, Norman, and Lutz Erbring (2002) “Internet and society: Preliminary Report”, IT and SOCIETY, Vol 1, 275-283.

Nolan.S, Hendricks.J, Amanda.T,(2015) “ Social networking sites (SNS); exploring their uses and associated value for adolescent mothers in Western Australia in terms of social support provision and building social capital” Midwifery 31,912–919

Norris,Pippa (2003),“Social Capital and ICTs: Widening or Reinforcing Social Networks?”presented at the“International Forum on Social Capital for Economic Revival”held by the Economic and Social Research Institute, Cabinet Office, Japan in Tokyo,24-25th March 2003、

Penard,Thierry and Nicolas Poussing (2010) Internet use and social capital; the strength of virtual ties, Journal of Economic Issues, 44(3), 569-595.

Ryan, S. (2010). Information system and healthcare XXXVI: Building and maintaining social Capital-Evidence from the field. Communications of the Association of Information Systems, 27(18), 307-322.

Salahuddin, Mohammad et al. (2016) “Does internet stimulate the accumulation of social capital? A macro-persective from Australia” Economic Analysis and Policy, 49, 43-55.

Zhong, Zhi-Jin (2014) “Civic engagement among educated Chinese youth: The role of SNS (Social Networking Services), bonding and bridging social capital” Computers & Education 75,263–273urname of the first author Year] Names of authors, Title, Journal, Publisher, Year.

The 33rd Annual Conference of the Japanese Society for Artificial Intelligence, 2019

Multimodal Neural Network-based Health Platform for Knowledge Decision-Making

Joo-Chung Kim[1], Ji-Won Baek[2], Hyun Yoo[3], Kyungyong Chung[*4]

[1,2]Data Mining Lab., Dept. of Computer Science, Kyonggi University, South Korea

[3]Dept. of Computer Information Engineering, Sangji University, South Korea

[*4]Division of Computer Science and Engineering, Kyonggi University, South Korea

There is a need for artificial intelligence-oriented information technologies (aimed at continuous monitoring and life-care of chronic diseases through health platforms) that can discover potential health-risk-factor changes and predict emerging risks. In this paper, we propose a multimodal neural network-based health platform for knowledge decision-making. The proposed method learns the relationships present between heterogeneous data and the multimodal neural network, and extracts the common information shared between the modals to estimate health-risk factors. The correlation of variables appearing in the health platform is used to construct a multimodal neural network, and shared common information is combined to estimate the health-risk factors. The correlations of the variables are shown as positive correlations and negative correlations. A positive correlation indicates a relationship in which two variables change in the same direction, and a negative correlation indicates a relationship in which they change in a different direction. The proposed multimodal neural network is used to solve the health-risk–factor problem in the health platform, improving the reliability of the data.

1. Introduction

Due to the development of information-gathering technology, a variety of data is gathered from various fields, such as society, science, and industry, and is being accumulated as big data (Rho et al., 2015). This is characterized by a continuous increase in volume, rapid change, and various properties (Chung and Roy, 2016). Especially in the health platform, the scope is expanding with the development of information processing and collection technologies such as the electronic medical record (EMR), personal health record (PHR), and life-log (Kim and Chung, 2017). In a health platform, data are mainly continuous, changing over time. Data related to human health are affected by internal and external environments. Health status changes over a short period of time or over a long period of time from variables such as weather, physical information, nutrition, and activity, etc. (Larose et al., 2014; Kim and Chung, 2018; Yoo and Chung, 2018). In these health data, the collection range changes depending on the user's surrounding environment or the device held. Missing values are likely to be generated in collected data due to differences in environments or devices among users (Sarwar et al., 2001; Chung et al., 2016). In particular, devices using low power have difficulty collecting real-time data, leading to missing values. In addition, even if the same type of device is used, the obtained data may show different properties.

Previous research (Kim and Chung, 2018) presented data mining of health-risk factors using the PHR, the EMR, and health status similarities from medical big data in a hybrid peer-to-peer (P2P) network environment. This data mining is used to provide a health service and a user-oriented healthcare promotion service for chronic diseases requiring constant care, life care, and elderly health care in health platforms. In addition, the present study predicts the potential health status of chronic diseases using a similarity-based sequence-mining algorithm.

This study is organized as follows: Section 2 describes the related researches of the health-risk factors of the health matrix, Section 3 describes the proposed multimodal neural network-based health platform for knowledge decision-making, Section 4 describes the multimodal based ontology mining for an adaptive knowledge processing, and Section 5 provides a conclusion

2. Related Works

Medical big data have a health-risk–factor problem in which the values of certain properties are missing due to human, natural, and mechanical errors in the collection process (Kim et al., 2017). Health-risk factors create a null state where there is no value for a variable or property at a particular point in time (Kim et al., 2014; Chung and Lee, 2004). Health factors are an important issue in data analysis and utilization, and various studies are under way to solve this problem. In addition, a higher percentage of missing values causes problems in the reliability of the results from a data analysis (Jung and Chung, 2016; Yoo and Chung, 2018; Phanich et al., 2010).

Health-risk–factor processing mainly uses value estimation or a substitution method, and if the influence of a property causing a large amount of health-risk factors is small, the property itself is removed. There are various methods to deal with health-risk factors: mean/median value substitution, the artificial neural network, the regression model, k-nearest neighbors, and collaborative filtering. Of the various methods, artificial neural networks have received much attention in recent years. This is an issue in various fields, such as object recognition, classification, and artificial intelligence, as well as in health-risk–factor estimation (EI-Dosuky et al., 2010; Jung and Chung, 2016; Kim

Contact: Kyungyong Chung, Kyonggi University, South Korea, 82-10-6362-4555, dragonhci@gmail.com

et al., 2014). In an artificial neural network, nodes and weights can be flexibly configured according to data characteristics.

3. Multimodal Neural Network–based Health Platform for Knowledge Decision-Making

3.1 Data Features in Health Platforms

Health data can be collected based on the same time, and they show a time-series characteristic that varies with time. An analysis of this makes it possible to distinguish whether the variables are positively or negatively correlated (Specht, 1993; Deshpande and Karypis, 2004; Chung et al., 2018). The closer the variables are to -1, the higher the negative correlation, and the closer to +1, the higher the positive correlation (Orciuoli and Parente, 2017; Adomavicius and Tuzhilin, 2015). Figure 1 shows the process of health-risk factors in health platforms.

In addition, being closer to 0 indicates that the two variables have no effect on each other. In this paper, health-risk factors are estimated through the neural network configuration using the correlations between variables.

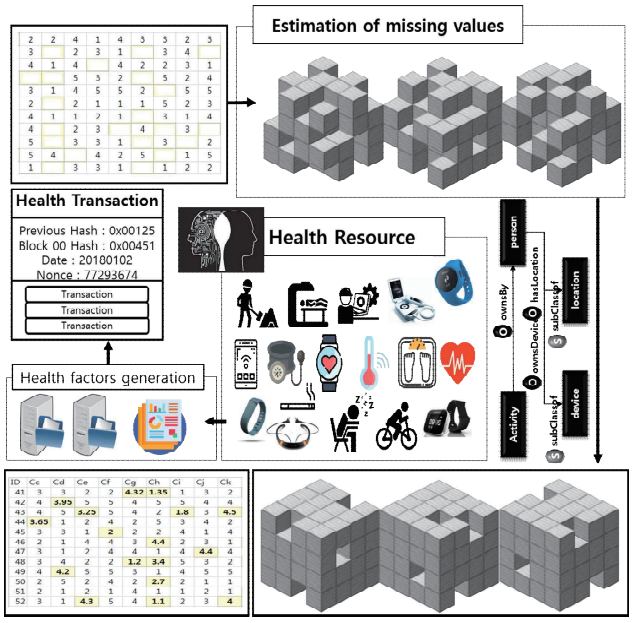

Figure 1 Process of health-risk factors in health platform

3.2 Mining Health-risk Factors using a Multimodal Neural Network

This is a correlation-based neural network for estimating health-risk factors in the platform. Figure 2 shows the estimation of health-risk factors using a multimodal neural network in a health platform.

Positive correlations and negative correlations between the variables are analyzed, and the variables representing positive correlations are grouped into neural networks. According to the results of the analysis, a fully connected network is constructed with input values by grouping the variables with a high positive correlation. This makes it possible to estimate the health-risk factors appearing in the health data. The relationship between multimodals is learned from large-capacity heterogeneous data, and common information shared between modals is extracted from multimodal input based on it.

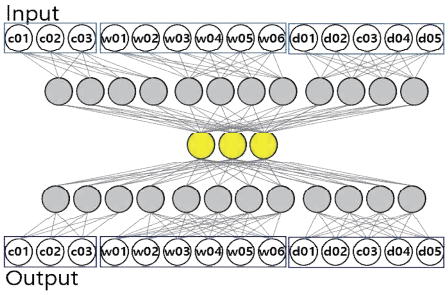

Figure 2 Process of health-risk factors in health platform

4. Multimodal based Ontology Mining for Adaptive Knowledge Processing

4.1 Adaptive Ontological Knowledge Representation

Health platforms use ontology-reasoning engines to express knowledge based on natural language. Mining is used to discover rules and to create knowledge using the discovered reasoning rules. In addition, knowledge is expanded by using inference engines according to the changing situations. Ontological knowledge representation specifies the relationship between data and attributes, and creates adaptive knowledge using language-based sequence tagging models. It consists of a top-level ontology for real-time service, and expansion in the previously developed health ontology (Chen and Tsai, 2018; Orciuoli and Parente, 2017). Figure 3 shows an adaptive ontological knowledge representation using ontology-reasoning engines.

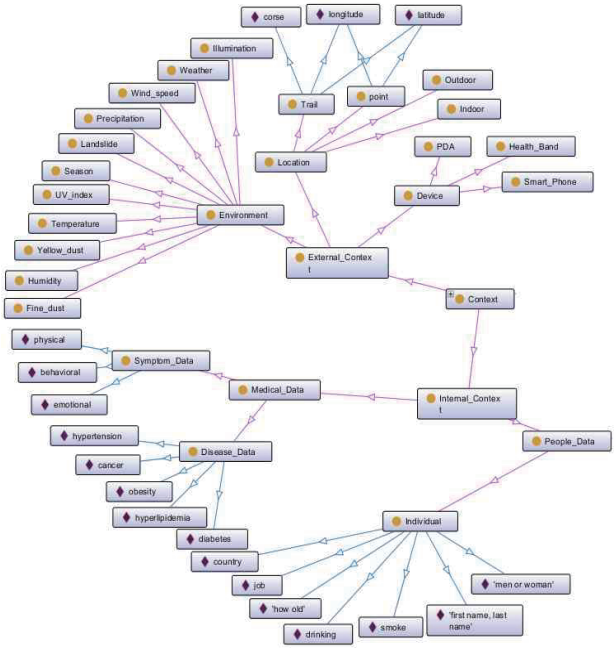

Figure 3 Adaptive ontological knowledge representation

The mining model is derived by using optimal tag prediction methods, using tag accuracy that is generated repeatedly by acquiring and refining natural language–based knowledge. An ontological knowledge model is also used to develop knowledge representation, knowledge-type conversion, and generation

technologies to deal with learning data in three dimensions (Adomavicius and Tuzhilin, 2015). This can resolve the problem of a shortage in learning data by increasing the utility of learning and the use of knowledge. Knowledge is efficiently integrated and managed by configuring mining models according to predefined learning models. The model is configured to improve time, cost, and the integrity of knowledge management.

4.2 Multimodal-based Ontology Mining in Health Platforms

In the health platform, a mining model discovers association rules by constructing transactions from ontological knowledge. The life-log is collected in real-time through ambient sensors and is processed using multimodal knowledge acquisition technologies. In order to acquire knowledge based on natural language, a model is developed to extract and refine data that are considered knowledge from unstructured, semi-structured, and structured data. In the case of incomplete knowledge about the acquired information, characteristics that have not been acquired from the knowledge are inferred through mining using deep learning (Kim et al., 2014; Kim and Chung, 2017). Behavioral tips or potential risks are provided based on the inference rules related to healthcare. Users can avoid or prevent health risks by reflecting information they receive from making decisions based on behavioral predictions in their daily lives. In addition, changes in time series data are predicted through mining to provide warnings and countermeasures to users. Figure 4 shows the multimodal-based ontology mining process of health data sources, knowledge collection, knowledge processing, and knowledge analysis in health platforms.

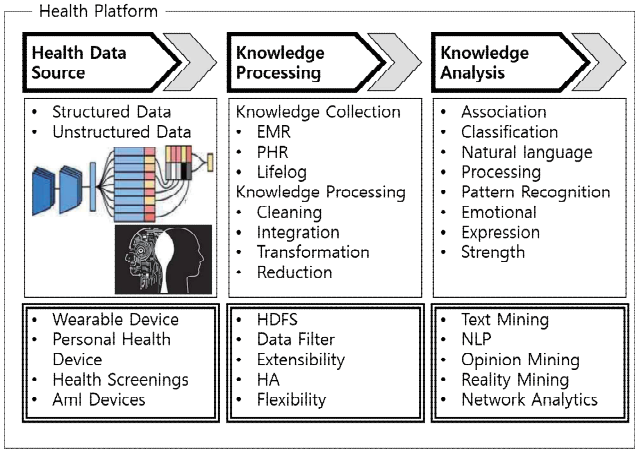

Figure 4 Multimodal-based ontology mining process

5. Conclusion

In this paper, we proposed a multimodal neural network-based health platform for knowledge decision-making. This is solved by a multimodal neural network that extracts common information about health-risk factors from multiple heterogeneous devices. In order to reflect the dynamic characteristics of the time series data, the variables showing a high correlation are grouped into multimodal neural networks for each cluster, and the health-risk factors are estimated by integrating them. The correlations between the variables were positively correlated with negative correlations. By using the proposed multimodal neural network, it is possible to construct the data with higher reliability in the health platform when estimating health-risk factors.

Acknowledgments

This research was supported by Basic Science Research Program through the National Research Foundation of Korea (NRF) funded by the Ministry of Education (No. NRF-2016R1D1A1A09917313)

References

[1] M. J. Rho, K. S. Jang, K. Y. Chung, I. Y. Choi, "Comparison of Knowledge, Attitudes, and Trust for the Use of Personal Health Information in Clinical Research", Multimedia Tools and Applications, Vol. 74, No. 7, pp. 2391-2404, 2015.

[2] K. Chung, Roy C. Park, "PHR Open Platform based Smart Health Service using Distributed Object Group Framework", Cluster Computing, Vol. 19, No. 1, pp. 505-517, 2016.

[3] J. C. Kim, K. Chung, "Depression Index Service using Knowledge based Crowdsourcing in Smart Health", Wireless Personal Communication, Vol. 93, No. 1, pp. 255-268, 2017.

[4] D. T. Larose, C. D. Larose, "Discovering Knowledge in Data: An Introduction to Data Mining", John Wiley & Sons, 2014.

[5] J. C. Kim, K. Chung, "Mining Health-Risk Factors using PHR Similarity in a Hybrid P2P Network", Peer-to-Peer Networking and Applications, Vol. 11, No. 6, pp. 1278-1287, 2018.

[6] B. Sarwar, G. Karypis, J. Konstan, J. Riedl, "Item-based collaborative filtering recommendation algorithms", In Proc. of the 10th international conference on World Wide Web, pp. 285-295, 2001.

[7] K. Chung, J. C. Kim, R. C. Park, "Knowledge-based Health Service considering User Convenience using Hybrid Wi-Fi P2P", Information Technology and Management, Vol. 17, No. 1, pp. 67-80, 2016.

[8] J. C. Kim, K. Chung, "Depression Index Service using Knowledge based Crowdsourcing in Smart Health", Wireless Personal Communication, Vol. 93, No. 1, pp. 255-268, 2017.

[9] J. H. Kim, D. Lee, K. Y. Chung, "Item Recommendation based on Context-aware Model for Personalized u-Healthcare Service", Multimedia Tools and Applications, Vol. 71, No. 2, pp. 855-872, 2014.

[10] K. Y. Chung, J. H. Lee, "User Preference Mining through Hybrid Collaborative Filtering and Content-based Filtering in Recommendation System", IEICE Transaction on Information and Systems, Vol. E87-D, No. 12, pp. 2781-2790, 2004.

[11] H. Jung, K. Chung, "Knowledge-based dietary nutrition recommendation for obese management", Information Technology and Management, Vol. 17, No. 1, pp. 29-42, 2016.

[12] H. Yoo, K. Chung, "Mining-based Lifecare Recommendation using Peer-to-Peer Dataset and Adaptive Decision Feedback", Peer-to-Peer Networking and Applications, Vol. 11, No. 6, pp. 1309-1320, 2018.

[13] M. Phanich, P. Pholkul, S. Phimoltares, "Food Recommendation System Using Clustering Analysis for

Diabetic Patients", In Proc. of the International Conference on Information Science and Applications, pp. 1-8. 2010.

[14] M. A. El-Dosuky, M. Z. Rashad, T. T. Hamza, A. H. El-Bassiouny, "Food Recommendation Using Ontology and Heuristics", In Proc. of the International Conference on Advanced Machine Learning Technologies and Applications, pp. 423-429, 2012.

[15] H. Jung, K. Chung, "Life Style Improvement Mobile Service for High Risk Chronic Disease based on PHR Platform", Cluster Computing, Vol. 19, No. 2, pp. 967-977, 2016.

[16] J. H. Kim, J. Kim, D. Lee, K. Y. Chung, "Ontology Driven Interactive Healthcare with Wearable Sensors", Multimedia Tools and Applications, Vol. 71, No. 2, pp. 827-841, 2014.

[17] D. F. Specht, "The General Regression Neural Network-rediscovered. Neural Networks", Vol. 6, No. 7, pp. 1033-1034. 1993.

[18] M. Deshpande, G. Karypis, "Item-based top-n recommendation algorithms", ACM Transactions on Information Systems (TOIS), Vol. 22, No. 1, pp. 143-177, 2004.

[19] K. Chung, H. Yoo, D. E. Choe, "Ambient Context-based Modeling for Health Risk Assessment Using Deep Neural Network", Journal of Ambient Intelligence and Humanized Computing, 2018. DOI: 10.1007/s12652-018-1033-7

[20] T. Chen, H. R. Tsai, "Application of industrial engineering concepts and techniques to ambient intelligence: a case study", Journal of Ambient Intelligence and Humanized Computing, Vol 9, No. 2, pp. 215-223, 2018.

[21] F. Orciuoli, M. Parente, "An ontology-driven context-aware recommender system for indoor shopping based on cellular automata", Journal of Ambient Intelligence and Humanized Computing, Vol 8, No. 6, pp. 937-955, 2017.

[22] G. Adomavicius, A. Tuzhilin, "Context-Aware Recommender Systems", Recommender Systems Handbook pp 191-226, 2015.

The 33rd Annual Conference of the Japanese Society for Artificial Intelligence, 2019

Variables Extraction in Natural (English) Language Through Possessive Relationships

Danilo Eidy Miura
The University of Tokyo

Teruaki Hayashi
The University of Tokyo

Yukio Ohsawa
The University of Tokyo

The already highlighted importance of the 'flow' of data in the Market of Data brings needs of development of ways to better explore the utilization of data. Aware of the existence of rich knowledge stored and shared in text format, this paper aims to propose a form of representation of variable names that can be identified in natural language written knowledge. With the use of possessive relationships between words in Noun Phrases, we supported the representation of variable name relating a variable to a thing or event. A simple experiment was performed to demonstrate the efficacy of the proposed representation supported by Data Jacket Store, where we can find well-form variable names under the name of Variable Labels.

1. Introduction

The Chance Discovery in the Market of Data is a field of research that aims to design the flow of data in the society through creative methods and find hidden patterns. From the generation, through supply, processing, distribution to utilization of data, discoveries can enhance the demands and pull the consumption of data in the society. Therefore, the perception of the value of data through its utilization is the essential force to innovate in market. Although data is offered and advertised in online repositories, such as Data Jacket Store (Hayashi & Ohsawa, 2015), potential users of data may not be aware of the potential utilization of the offered data. Knowledge of data analysis and processing is required to explore the applications of data.

In order to support data users or suppliers to assess the value of their data, the exploration of potential utilization is the basis for valuing what is not in use yet. To support users in the exploration of potential use of data, we aim to recognize potential use of data from repositories of knowledge recorded in texts, such as research papers and data analytics reports. In this paper we explain the formal representation of data as a well formed variable name (WFVN) that can be used to discover potential new variable labels to name data.

In the field of Knowledge Engineering, the recognition of variables is an essential step to design the knowledge-based system. Implemented systems will contain well-formed variables and knowledge representation. But in natural language, the variables may be expressed in free style, enabling a direct codification to computer-readable language. In order to get the advantage of accumulated knowledge written in natural language, the variable identification and its formal representation may allow knowledge-based systems users to explore possibilities of data utilization.

Contact: Danilo Eidy Miura, The University of Tokyo, daneidyucb@gmail.com

2. Related Work

2.1.Knowledge Representation

In previous works in knowledge representation (Studer et al., 1998, Davis et al., 1993), we learned that the representation of the knowledge depends on the intended task to perform, giving the limited capacity to codify the complete reality of the represented knowledge. Therefore, the representation of the knowledge should be limited and defined according to convenience to the given task. In the definition of the representation, the level of formalism of the representation may enable the use of the represented knowledge in different ways (Guarino, 1995). In this study, the functional approach to representation was adopted to enable further analysis of the represented knowledge (Hayashi & Ohsawa, 2015), as defined in later section.

2.2.Named Entity Recognition

In Natural Language Processing (NLP), Named Entity recognition and Classification (NERC) is a kind of task that identifies entities according to predefined classes. The use of textual features support the identification of entities.

Possessive Noun Phrases (PNP) are the expressions for possessive relationships possessor-possessed. With the use of textual features, such as markers and syntax , relationships between elements of the sentence can be identified and named. According to WALS (Nichols & Bickel, 2013), there are 4 main locus of marking in PNPs:

1)Possessor is head-marked,
2)Possessor is dependent-marked,
3)Possessor is double-marked, and
4)Possessor has no marking.

Markings in PNP explain the existence of various forms of expression of possessive relationships, given the emphasis on of different elements in the phrase.

Given the nature of variables in data analysis in the Market of Data, possessive expressions including pronouns, which are relevant in narratives, are not relevant to our task. The focus of this study is the identification of variables of entities and events, and not possessions of people.

3. Variable Identification

Our aim is to identify and extract well-formed variable names (WFVN) from the natural language text and discover potential variable labels. Recognizing essential elements of a PNP, and defining their relationship and roles, we formally represent the knowledge of the variable.

In order to understand the WFVN, let's consider the variable as an abstract sense of varieties (attributes, properties, features, qualities, etc.) that needs a paired representative (thing of event) that provides a more concrete sense of what variables may vary to. Between the pair, should exist a possessive relation that places a variable as a qualifier of the concrete sense.

Let PNP be represented by the expression *has* (*x* , *y*) where *x* is the possessor noun and *y* is the possessed noun. For the identification of PNP as a WFVN, the Formal Representation of a Variable should satisfy the following conditions of possessor should be a thing (or event) and possessed should be a variable:

$$\text{has}(x, y) \wedge E(x) \wedge V(y) \rightarrow \text{WFVN}(\text{has}(x, y)) \quad (1)$$

1) has (x , y) : Possessor has possessed.
2) *E (x) : Possessor is a thing or an event.*
3) V (y) : Possessed is a variable.

In possessive nouns phrases, we can identify the noun that represents possessor and the noun that represents possessed. To satisfy the condition 1, the possessive relationship will be identified with three patterns of PNPs, as follows:

a)Pd + of + Pr, (ex. temperature of water)
b)Pr + 's + Pd, (ex. water's temperature)
c)Pd + Pr (ex. water temperature)
Pd: Possessed noun
Pr: Possessor noun

In order to satisfy the conditions 2 and 3, it is needed to take in account the relation between the noun and their relative abstractness and concreteness. The relation between Pr and Pd should make a clear distinction between their senses and provide both abstract and concrete sense. This consideration regards the fact of PNPs without clear distinction may not a full sense of the variable:

A) Level of temperature (double abstract)
B) Pool water (double concrete)

In the example A, the level of abstraction of both nouns are high, and we don't have a full sense of the variable, missing the concrete sense of and event (ice, melting, boiling, condensing, …)

In the example B, the problem is on the lack of abstraction. Since both nouns provide concrete sense, we don't have a clear idea possession. This example allows us to have interpretation without possession:

Instead of *Water of pool*,
Interpret W*ater in pool*

4. Experiment on Data Jacket Store

An experiment was designed to verify the performance of the identification of WFVN. Possessive relationships can be identified with use of the three patterns of PNPs, defined before. And regarding the conditions 2 and 3 discussed before, we considered the use of Wordnet hypernyms (Scott & Matin, 1998) as features to establish the concrete-abstract relationship between the nouns in the phrase.

Using a database containing natural language contents and variable names, we could attribute a score to the candidates of variables. Data Jacket Store is a catalog of more than 1000 Data Jackets (Hayashi & Ohsawa, 2015), digest information about the datasets that contain natural language description of the data, as well as variable labels.

In the experiment, we tested the use of hypernyms as features to distinguish PNPs that represent WFVN from the others. Assuming features of WFVN supports the identification of new variable names with similar features, we defined the probability of a new PNP be a WFVN is defined by the probability of the new PNP to have similar hypernyms of WFVN.

Given *n* as a noun in a new PNP, H as a *i* number of hypernyms of *n*, extracted from Wordnet, *v* is the condition of being a variable, and *e* is the condition of being a thing (or event). We define the probability of role (*v* or *e*) of the noun in a new PNP as the average of the probabilities of each PNP's hypernym to be a variable's hypernym:

$$P(v|n) = \sum_{1}^{i} P(v|Hi) * P(Hi|n) \quad (2)$$

$$P(e|n) = \sum_{1}^{i} P(e|Hi) * P(Hi|n) \quad (3)$$

The probability of a given hypernym to be a variable's hypernym can be defined by the probability of the given hypernym be the VLs' hypernym.

4.1. Procedures

The experiment was design to demonstrate the performance of the Classifier with the use of trained data.

1) Define the probability of hypernyms to be variable's hypernyms by the distribution of hypernyms of VLs of DJ Store.

2) Identify and extract PNPs in the DJ's outlines.

3) Calculate the probability of the PNPs to be variables, according to the equation in previous session.

4) Classify PNPs according to the existence in VLs list and satisfaction of the following criteria:
   $P (v | n) > P (\neg v | n)$

5. Results of DJ Store Experiment

In total of 1032 DJ Outlines, 8660 PNPs were identified according to the three patterns of PNP. In total, DJ Store provided 5836 Variable Labels from which 3788 different representations were extracted.

The formal representation of the variable names solved the problem of variances in the expression of possessive relationships due to the markings of the language (Nichols & Bickel, 2013). The formal representation eliminates markings and different patterns of PNP are represented in the same way. Possessive Noun Phrases such as *temperature of water*, *water's temperature* and *water temperature* will be uniquely represented as has (water , temperature).

Regarding the performance of the experimental test to discover potential Variable Labels, discovery is shown as the identification of variables that does not exist in DJ Store VL list. Using the formal representation of variable, we could discover 2017 new PNPs that satisfied the defined criteria. It suggests the information from DJ Outlines shows latent Variable Labels that can be considered in the utilization of that data.

Examples of new identified variables:

Temperature of air,
Efficiency of fuel,
Number of climbers,
Number of surgeries, …

6. Discussion and Future Work

In this paper, the proposal of use of Possessive Relationships as feature of variable names was demonstrated through a simple experiment using DJ Store. And results point to a potential use of the possessive relations as feature to identify variables in text. But it suggests the need of improvements in the selection of candidate relations.

In future work, we aim to refine variable selection with better understanding of types of variables and more accurate algorithms. We also should consider variables that are not considered measurable, such as classes or unstructured data.

Acknowledgements

This work was made possible thanks to to the initiatives of Data Jacket Promotion Work Group which provided the access to the DJ Store data for experiments and it was funded by JST CREST No. JPMJCR1304, JSPS KAKENHI JP16H01836, and JP16K12428, and industrial collaborators.

References

Guarino, N. (1995). Formal ontology, conceptual analysis and knowledge representation. International journal of human-computer studies, 43(5-6), 625-640.

Johanna Nichols, Balthasar Bickel. 2013. Locus of Marking in Possessive Noun Phrases. In: Dryer, Matthew S. & Haspelmath, Martin (eds.) The World Atlas of Language Structures Online. Leipzig: Max Planck Institute for Evolutionary Anthropology. (Available online at http://wals.info/chapter/24, Accessed on 2019-01-28.)

Nadeau, D., & Sekine, S. (2007). A survey of named entity recognition and classification. Lingvisticae Investigationes, 30(1), 3-26.

Studer, R., Benjamins, V. R., & Fensel, D. (1998). Knowledge engineering: principles and methods. Data and knowledge engineering, 25(1), 161-198.

Davis, R., Shrobe, H., & Szolovits, P. (1993). What is a knowledge representation?. AI magazine, 14(1), 17.

Hayashi, T., & Ohsawa, Y. (2015). Knowledge Structuring and Reuse System Using RDF for Supporting Scenario Generation. Procedia Computer Science, 60, 1281-1288.

Scott, S., & Matwin, S. (1998). Text classification using WordNet hypernyms. Usage of WordNet in Natural Language Processing Systems.

The 33rd Annual Conference of the Japanese Society for Artificial Intelligence, 2019

Using Sequence Constraints for Modelling Network Interactions

Johannes De Smedt*1 Junichiro Mori*2 Masanao Ochi*2

*1 The University of Edinburgh *2 The University of Tokyo

The ubiquitous nature of networks has led a vast number of works dedicated to the study of capturing their information. Various graph-based techniques exist that report on the characteristics of nodes and edges, e.g., author-citation networks, social interactions, and so on. A significant amount of information can be extracted by summarizing the surrounding network structure of nodes, e.g., by capturing motives, or walk patterns. In this work, we present a new way of capturing the interaction between nodes in a network by making use of the sequence in which they occur. (1) The objective of this paper is to make use of behavioural constraint patterns; a concise but detailed report of node's interactions can be constructed that can be used for various purposes. (2) It is shown how the constraint patterns can be mined form interaction data, and how they can be used for various applications.

1. Introduction

Networks are often formed by the interaction of various actors. For example, social networks grow based on friendship or interested-based relations, forum posts and emails link users according to their communication patterns, and citation networks are formed through authors referencing peers in their field. Typically, the construction of these networks is based on either undirected, or directed edges with weights. Furthermore, many network techniques focus on static relationships, I.e., the evolution over time is not investigated. However, a range of new techniques emerged recently that focus on the time-aspect of a network. Most notably, the use of motifs [Paranjape 17], and streams [Latapy 18] allow to capture the evolution of a network over time. In this paper, we describe a new approach based on behavioral constraints, I.e., constraints based on sequence patterns that allow to describe the order of the interactions of nodes.

We investigate how they can be constructed from a network dataset, and use the various patterns to describe the evolution of the network over time. In particular, we apply the sequence mining method to the question-and-answer interaction-based network. Our preliminary results show that profiling network interactions patterns with sequence mining enables track the behaviour of nodes in a transactional network without relying on the typical partial-order based results.

This paper is structured as follows. In Section 2, the methodology is presented to mine constraints from network data. Next, Section 3 reports on the application on real-life datasets. Section 4 concludes the paper and reports on the future directions.

2. Behavioural constraint patterns in networks

In this section, a detailed overview of the constraints is given, and how they can be leveraged for various network analysis applications.

Contact: Johannes De Smedt, The University of Edinburgh, johannes.desmedt@ed.ac.uk

2.1 Constraint set

Behavioural constraint templates have been long used in various areas of computer science. Most notably, a comprehensive set of Linear Temporal Logic (LTL) templates was proposed for the formal verification of program execution [Dwyer 99]. LTL provides an adequate formalism to search for various temporal properties, such as whether something happens eventually, next, and so on, and can be used in conjunction with typical logical operators to construct expressive relations. The initial set was extended to include various other relations, most notably unary ones. While initially proposed as LTL formulae which are convertible to Büchi automata, finite trace equivalent regular expressions were introduced in [Di Ciccio 13]. Models allowing for multiple constraints at the same time can be obtained by conjoining the automata to obtain a global language or automaton, over which all constraints hold.

In Table 1, an overview of the most-commonly used constraints in literature. They are organized according to 7 different categories, including unary and binary constraints. Most notably, the binary constraints are exhibit a hierarchy which is reported in [Di Ciccio 13] and which covers unordered up to chain ordered (using the next operator). Besides, the inclusion of negative constraints is unique, as typically only existing patterns are reported. Including negative behaviour can be used to find relations that are not apparent at first sight, e.g., in Figure 1 , the fact that nodes A and E are both present in the sequence of C, but do not have interactions themselves, still allows the inference of not succession(A,E).

Despite not being useful for capturing interaction effects, the unary constraints can be used for adding information to a node's feature vector in case any exist. I.e., if a particular node is always occurring first in a sequence, this might signify a particular pattern, e.g., a person reporting recently-occurred disasters.

Not every constraint is suitable for binary interaction within a network context, i.e., not chain succession is, in general, not suitable for profiling behavior, as it holds in many situations. Besides, absence is hard to identify unless a particular node is scrutinized for this behaviour in the sequence of another node. Exclusive choice and not co-

Table 1: An overview of Declare constraint templates with their corresponding regular expression.

Template	Regular Expression
Existence(A,n)	.*(A.*){n}
Absence(A,n)	[^A]*(A?[^A]*){n-1}
Exactly(A,n)	[^A]*(A[^A]*){n}
Init(A)	(A.*)?
Last(A)	.*A
Responded existence(A,B)	[^A]*((A.*B.*) |(B.*A.*))?
Co-existence(A,B)	[^AB]*((A.*B.*) |(B.*A.*))?
Response(A,B)	[^A]*(A.*B)*[^A]*
Precedence(A,B)	[^B]*(A.*B)*[^B]*
Succession(A,B)	[^AB]*(A.*B)*[^AB]*
Alternate response(A,B)	[^A]*(A[^A]*B[^A]*)*
Alternate precedence(A,B)	[^B]*(A[^B]*B[^B]*)*
Alternate succession(A,B)	[^AB]*(A[^AB]*B[^AB]*)*
Chain response(A,B)	[^A]*(AB[^A]*)*
Chain precedence(A,B)	[^B]*(AB[^B]*)*
Chain succession(A,B)	[^AB]*(AB[^AB]*)*
Not co-existence(A,B)	[^AB]*((A[^B]*) |(B[^A]*))?
Not succession(A,B)	[^A]*(A[^B]*)*
Not chain succession(A,B)	[^A]*(A+[^AB][^A]*)*A*
Choice(A,B)	.*[AB].*
Exclusive choice(A,B)	([^B]*A[^B]*) |.*[AB].*([^A]*B[^A]*)

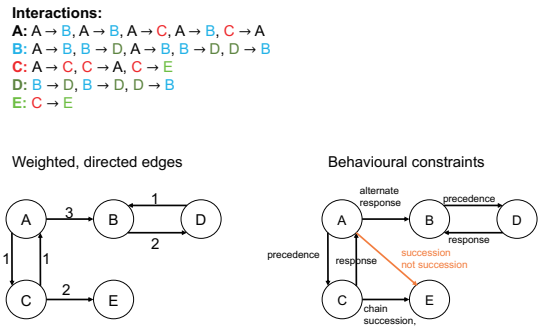

Figure 1: Running example

existence are similar in this respect, where the latter does not require the presence of either. Similar to not chain succession, this might lead to the discovery of many frequently non-occurring pairs.

2.2 Mining the patterns

We define transactional network data as an ordered set of interactions T between nodes from the set N, where each transaction is a tuple $(n_1, n_2, ts) \in T$ with $n_1 \in N$ the initiating node, $n_2 \in N$ the receiving node, and $ts \in \mathbb{N}^+$ a timestamp. T can be read sequentially, where each node $n \in N$ has a sequence $s_n \subset 2^{|N|}$ that is extended whenever a transaction $t \in T$ is for that node is witnessed. I.e., s_n gets extended with $\langle n, n_o \rangle$ whenever n is the initiating node, and with $\langle n_o, n \rangle$ when n is on the receiving end given another node $n_o \in N$.

By using the interesting Behavioural Constraint Miner [De Smedt 17], we can mine all patterns in a a sequence s_n to obtain a set of constraints C_{s_n}. Note, however, that if a given binary constraint $c(n, n_2) \in C_{s_n}$ holds for n in its own sequence, this still has to be verified with the sequence of the other node. If $c(n, n_2)$ is not present in that sequence, the constraints does not hold. Consider for example the interaction in Figure 1. Despite the evidence in the sequence of A that there exists an alternate succession relationship between A and B due to the alternating ABABAAB pattern, the sequence of B rather indicates that other occurrences of B happen in between (e.g. B→D), breaking the pattern. Hence, a final step is required to recursively ensure that $C_n = \{c \mid c \in C_n \wedge c \in C_{n_i} \forall n_i \in \mathcal{N}(n) \vee c \notin C_n \wedge c \notin C_{n_i} \forall n_i \in \mathcal{N}(n)\}$ where $\mathcal{N}(n) \subseteq N$ denotes the neighbourhood of node n to check that all constraint pertaining to n are either both in its constraint set and the constraint set of its neighbours to avoid conflict, or that it is present in an unrelated node (e.g. the connection succession(A,E) in Figure 1). To conclude the discovery of sequence templates from the network interactions, the sets C_n are pruned according to the constraint hierarchy.

2.3 Applications

The mining of interactions in a network as sequences has several applications. Most notably, the sequence information can be used for analyzing the interactions' evolution over time. By tracking what patterns exist, and whether they return over time gives an overview of how certain relations change and what the underlying sequential behaviour is.

Next, the sequence patterns can be used as features of a node. In this case, also unary constraints help define the node in terms of where in a sequence, how often, and with what other nodes the node is interacting. The features can be used towards node classification [Bhagat 11]. Finally, by using the transitivity properties of the constraints, link inference/prediction [Liben 07] can also be made.

3. Results

We apply the sequence method to the Math Overflow dataset, as used in [Paranjape 17]. On the Overflow web sites, users post questions and receive answers from other users, and users may comment on both questions and answers. We derive a transactional network by creating an edge (u, v, t) if, at time t, user u: (1) posts an answer to user vs question, (2) comments on user vs question, or (3) comments on user vs answer. The data contains 24,818 nodes with 506,550 interactions over 2,350 days and deals with question-and-answer data from users regarding mathematical problems.

We retrieve the constraints over the dataset by splitting the interactions into contingent blocks of a varying time length. In this case, we used blocks of 4 hours, 2 days, 100 days, and 1,000 days in order to track the evolution of the constraints. For this analysis, we limit the constraint set to the 7 most common sequence patterns. In order to illustrate the usefulness of the results, we focus on two active users with a different background. The first user (denoted B) is considered an authority as that node in the network has the highest authority score [Ding 04]. The high authority is pointed to by many high hubs and high hub points to many high authorities. Authority and hub scores are obtained by this iterative scoring.

Table 2: An overview of the proportion of constraints that shift from one sequence pattern into another, both for incoming and outgoing constraints of nodes A and B. The colours denote the place in the distribution, where red is higher and green lower. Scores with different colours and equal scores indicate a difference in value behind the significant digits.

	In								Out							
4 hours - A	**0**	**1**	**2**	**3**	**4**	**5**	**6**	**7**	**0**	**1**	**2**	**3**	**4**	**5**	**6**	**7**
NotSuc (1)	0.15	0.04	0.01	0.00	0.02	0.02	0.00	0.01	0.14	0.05	0.05	0.00	0.02	0.02	0.00	0.04
Prec (2)	0.14	0.03	0.02	0.00	0.01	0.01	0.00	0.01	0.13	0.01	0.03	0.00	0.01	0.02	0.00	0.02
AltPrec (3)	0.00	0.00	0.00	0.00	0.00	0.00	0.00	0.00	0.00	0.00	0.00	0.00	0.00	0.00	0.00	0.01
ChainPrec (4)	0.03	0.03	0.02	0.00	0.03	0.02	0.00	0.00	0.09	0.02	0.05	0.00	0.02	0.03	0.00	0.04
Resp (5)	0.15	0.02	0.01	0.00	0.01	0.03	0.00	0.01	0.11	0.01	0.00	0.00	0.00	0.03	0.00	0.00
AltRes (6)	0.00	0.00	0.00	0.00	0.00	0.00	0.00	0.00	0.00	0.00	0.00	0.00	0.00	0.00	0.00	0.00
ChainRes (7)	0.04	0.05	0.01	0.00	0.01	0.02	0.00	0.04	0.13	0.00	0.02	0.00	0.01	0.02	0.00	0.15
4 hours - B																
NotSuc	0.17	0.02	0.02	0.00	0.01	0.01	0.00	0.01	0.21	0.02	0.03	0.00	0.01	0.02	0.00	0.01
Prec	0.22	0.02	0.02	0.00	0.01	0.01	0.00	0.01	0.19	0.01	0.02	0.00	0.00	0.01	0.00	0.01
AltPrec	0.00	0.00	0.00	0.00	0.00	0.00	0.00	0.00	0.00	0.00	0.00	0.00	0.00	0.00	0.00	0.00
ChainPrec	0.05	0.01	0.01	0.00	0.00	0.01	0.00	0.01	0.06	0.01	0.01	0.00	0.00	0.01	0.00	0.01
Resp	0.21	0.02	0.01	0.00	0.00	0.02	0.00	0.01	0.20	0.02	0.01	0.00	0.00	0.02	0.00	0.00
AltRes	0.00	0.00	0.00	0.00	0.00	0.00	0.00	0.00	0.00	0.00	0.00	0.00	0.00	0.00	0.00	0.00
ChainRes	0.07	0.01	0.01	0.00	0.00	0.01	0.00	0.03	0.06	0.01	0.01	0.00	0.00	0.02	0.00	0.02
2 days - A																
NotSuc	0.19	0.01	0.01	0.00	0.00	0.01	0.00	0.00	0.26	0.01	0.01	0.00	0.00	0.01	0.00	0.00
Prec	0.32	0.01	0.02	0.00	0.00	0.00	0.00	0.00	0.24	0.01	0.01	0.00	0.00	0.01	0.00	0.00
AltPrec	0.01	0.00	0.00	0.00	0.00	0.00	0.00	0.00	0.00	0.00	0.00	0.00	0.00	0.00	0.00	0.00
ChainPrec	0.01	0.00	0.00	0.00	0.00	0.00	0.00	0.00	0.02	0.00	0.00	0.00	0.00	0.00	0.00	0.00
Resp	0.33	0.01	0.00	0.00	0.00	0.02	0.00	0.00	0.25	0.01	0.00	0.00	0.00	0.02	0.00	0.00
AltRes	0.01	0.00	0.00	0.00	0.00	0.00	0.00	0.00	0.00	0.00	0.00	0.00	0.00	0.00	0.00	0.00
ChainRes	0.01	0.00	0.00	0.00	0.00	0.00	0.00	0.00	0.02	0.00	0.00	0.00	0.00	0.00	0.00	0.00
2 days - B																
NotSuc	0.21	0.02	0.02	0.00	0.00	0.02	0.00	0.00	0.23	0.01	0.02	0.00	0.00	0.02	0.00	0.00
Prec	0.29	0.02	0.02	0.00	0.00	0.01	0.00	0.00	0.27	0.02	0.02	0.00	0.00	0.01	0.00	0.00
AltPrec	0.01	0.00	0.00	0.00	0.00	0.00	0.00	0.00	0.01	0.00	0.00	0.00	0.00	0.00	0.00	0.00
ChainPrec	0.01	0.00	0.00	0.00	0.00	0.00	0.00	0.00	0.01	0.00	0.00	0.00	0.00	0.00	0.00	0.00
Resp	0.29	0.02	0.01	0.00	0.00	0.02	0.00	0.00	0.28	0.02	0.00	0.00	0.00	0.03	0.00	0.00
AltRes	0.01	0.00	0.00	0.00	0.00	0.00	0.00	0.00	0.01	0.00	0.00	0.00	0.00	0.00	0.00	0.00
ChainRes	0.02	0.00	0.00	0.00	0.00	0.00	0.00	0.00	0.01	0.00	0.00	0.00	0.00	0.00	0.00	0.00

Table 3: Similar overview as Table 3 containing the 100 and 1,000 days time frames.

	In								Out							
100 days - A	**0**	**1**	**2**	**3**	**4**	**5**	**6**	**7**	**0**	**1**	**2**	**3**	**4**	**5**	**6**	**7**
NotSuc	0.13	0.02	0.03	0.00	0.00	0.04	0.00	0.00	0.18	0.04	0.04	0.00	0.00	0.04	0.00	0.00
Prec	0.24	0.04	0.07	0.00	0.00	0.02	0.00	0.00	0.19	0.04	0.05	0.00	0.00	0.01	0.00	0.00
AltPrec	0.00	0.00	0.00	0.00	0.00	0.00	0.00	0.00	0.01	0.00	0.00	0.00	0.00	0.00	0.00	0.00
ChainPrec	0.00	0.00	0.00	0.00	0.00	0.00	0.00	0.00	0.00	0.00	0.00	0.00	0.00	0.00	0.00	0.00
Resp	0.25	0.04	0.02	0.00	0.00	0.07	0.00	0.00	0.18	0.04	0.01	0.00	0.00	0.04	0.00	0.00
AltRes	0.01	0.00	0.00	0.00	0.00	0.00	0.00	0.00	0.00	0.00	0.00	0.00	0.00	0.00	0.00	0.00
ChainRes	0.00	0.00	0.00	0.00	0.00	0.00	0.00	0.00	0.00	0.00	0.00	0.00	0.00	0.00	0.00	0.00
100 days - B																
NotSuc	0.10	0.02	0.04	0.00	0.00	0.05	0.00	0.00	0.15	0.05	0.06	0.00	0.00	0.05	0.00	0.00
Prec	0.19	0.04	0.08	0.00	0.00	0.03	0.00	0.00	0.16	0.05	0.07	0.00	0.00	0.02	0.00	0.00
AltPrec	0.00	0.00	0.00	0.00	0.00	0.00	0.00	0.00	0.00	0.00	0.00	0.00	0.00	0.00	0.00	0.00
ChainPrec	0.00	0.00	0.00	0.00	0.00	0.00	0.00	0.00	0.00	0.00	0.00	0.00	0.00	0.00	0.00	0.00
Resp	0.22	0.05	0.02	0.00	0.00	0.11	0.00	0.00	0.13	0.04	0.02	0.00	0.00	0.05	0.00	0.00
AltRes	0.01	0.00	0.00	0.00	0.00	0.00	0.00	0.00	0.00	0.00	0.00	0.00	0.00	0.00	0.00	0.00
ChainRes	0.00	0.00	0.00	0.00	0.00	0.00	0.00	0.00	0.00	0.00	0.00	0.00	0.00	0.00	0.00	0.00
1000 days - A																
NotSuc	0.07	0.03	0.06	0.00	0.00	0.07	0.00	0.00	0.11	0.04	0.07	0.00	0.00	0.06	0.00	0.00
Prec	0.14	0.04	0.09	0.00	0.00	0.06	0.00	0.00	0.12	0.06	0.09	0.00	0.00	0.03	0.00	0.00
AltPrec	0.01	0.00	0.00	0.00	0.00	0.00	0.00	0.00	0.00	0.00	0.00	0.00	0.00	0.00	0.00	0.00
ChainPrec	0.00	0.00	0.00	0.00	0.00	0.00	0.00	0.00	0.00	0.00	0.00	0.00	0.00	0.00	0.00	0.00
Resp	0.17	0.06	0.04	0.00	0.00	0.14	0.00	0.00	0.10	0.05	0.04	0.00	0.00	0.07	0.00	0.00
AltRes	0.01	0.00	0.00	0.00	0.00	0.00	0.00	0.00	0.00	0.00	0.00	0.00	0.00	0.00	0.00	0.00
ChainRes	0.00	0.00	0.00	0.00	0.00	0.00	0.00	0.00	0.00	0.00	0.00	0.00	0.00	0.00	0.00	0.00
1000 days - B																
NotSuc	0.01	0.03	0.01	0.00	0.00	0.05	0.00	0.00	0.06	0.02	0.19	0.01	0.00	0.09	0.00	0.00
Prec	0.08	0.06	0.05	0.00	0.00	0.12	0.00	0.00	0.05	0.02	0.23	0.01	0.00	0.03	0.00	0.00
AltPrec	0.00	0.00	0.00	0.00	0.00	0.00	0.00	0.00	0.00	0.00	0.00	0.00	0.00	0.00	0.00	0.00
ChainPrec	0.00	0.00	0.00	0.00	0.00	0.00	0.00	0.00	0.00	0.00	0.00	0.00	0.00	0.00	0.00	0.00
Resp	0.14	0.10	0.04	0.00	0.00	0.29	0.01	0.00	0.02	0.01	0.05	0.00	0.00	0.05	0.00	0.00
AltRes	0.00	0.00	0.00	0.00	0.00	0.01	0.00	0.00	0.00	0.00	0.00	0.00	0.00	0.00	0.00	0.00
ChainRes	0.00	0.00	0.00	0.00	0.00	0.00	0.00	0.00	0.00	0.00	0.00	0.00	0.00	0.00	0.00	0.00

The other user (denoted A) has a similarly high degree (high number of connections in the network), but a lower authority score. Our hypothesis is that the interactions of the authority user result in several constraint patterns as he gains the authority through answering and commenting to questions within his expertise.

The results of the shifts in constraint patterns as expressed in their proportions, are included in Tables 2 and 3 for both incoming and outgoing constraints of both nodes. The cells indicate the proportion of connections between the same nodes that are both present again in two subsequent time frames that shifted from the template in the rows, to the template in the columns. '0' signifies that the constraint is no longer present between both rows.

Firstly, it can be seen that there is a high number of constraints that are not reoccurring over time, meaning they are not repeated in the subsequent time frame. This behaviour is expected, given that many question-answering threads stop after a few posts, and many users only tend to intervene in a limited number of threads. Considering different lengths of time frames, however, we note that especially for node B (the authority) the number of vanishing interactions is drastically lower for 1,000 days. In case of incoming constraints, we see many re-occurring response constraints, and with outgoing ones we see many precedence and not succession constraints appearing. This is in line with how we would expect question-answering is handled by an authority, who responds to all questions within his area of expertise.

Overall, the two nodes behave relatively similarly in terms of proportions of constraints up until the 1,000 days threshold. The change incurred by increasing the time frames does not yield drastically different results, but it can be noted that more connections are reoccurring (mostly response and precedence relationships) rather than vanishing (as captured by column '0'). Hence, nodes that are surviving longer, and hence are reoccurring themselves, seem to maintain their relations over time. Also, any 'stronger' constraints that model alternating or chain relations are very often not present. One final observation is interesting. The high number of chain response connections that are going out from node A indicates that many immediate answer-response messages were exchanged over a period of 4 hours, indicating that single conversations where picked up of which many reoccurred as well.

4. Conclusion and future work

In this paper, we have shown how mining network interaction patterns can be profiled using sequence mining techniques. We apply the sequence mining method to the question-and-answer interaction-based network. Our preliminary results show that employing sequence patterns enables us track the behaviour of nodes in a transactional network and summarize their interactions without relying on the typical partial-order based results that are offered in sequence mining, while still going beyond the typical general nature of motifs that focus on directed arcs between 2 or 3 actors [Paranjape 17] . In a small experimental evaluation, we demonstrate the usefulness of the approach in the context of message board analysis.

For future work, we envision to focus on testing the patterns in the context of feature engineering, and link inference.

References

[Paranjape 17] Paranjape, A., Benson, A. R., & Leskovec, J.: Motifs in temporal networks, Proceedings of the Tenth ACM International Conference on Web Search and Data Mining (2017)

[Namaki 17] Namaki, M. H., Wu, Y., Song, Q., Lin, P., & e, T.: Discovering graph temporal association rules, Proceedings of the 2017 ACM Conference on Information and Knowledge Management (2017)

[Dwyer 99] Dwyer, M. B., Avrunin, G. S., & Corbett, J. C.: Patterns in property specifications for finite-state verification, Proceedings of the 21st international conference on Software engineering (1999)

[Latapy 18] Latapy, M., Viard, T., & Magnien, C.: Stream graphs and link streams for the modeling of interactions over time. Social Network Analysis and Mining, 8(1) (2018)

[Di Ciccio 13] Di Ciccio, C., & Mecella, M.: A two-step fast algorithm for the automated discovery of declarative workflows, 2013 IEEE Symposium on Computational Intelligence and Data Mining (2013)

[De Smedt 17] De Smedt, J., Deeva, G., & De Weerdt, J.: Behavioral Constraint Template-Based Sequence Classification, European Conference on Machine Learning (2017)

[Ding 04] Ding, C. H., Zha, H., He, X., Husbands, P., & Simon, H. D.: Link analysis: hubs and authorities on the World Wide Web, SIAM review, 46(2) (2004)

[Bhagat 11] Bhagat, S., Cormode, G., & Muthukrishnan, S.: Node classification in social networks, Social network data analytics, Springer (2011)

[Liben 07] LibenNowell, D., & Kleinberg, J.: The linkprediction problem for social networks, Journal of the American society for information science and technology, 58(7) (2007)

The 33rd Annual Conference of the Japanese Society for Artificial Intelligence, 2019

CTransE : Confidence-Based Translation Model for Uncertain Knowledge Graph Embedding

Natthawut Kertkeidkachorn[*1*2] Xin Liu[*1] Ryutaro Ichise[*2*1]

[*1] National Institute of Advanced Industrial Science and Technology, Tokyo, Japan
[*2] National Institute of Informatics, Tokyo, Japan

Knowledge graphs play an important role in many AI applications such as fact checking. Many studies focused on learning representations of a knowledge graph in a low-dimensional continuous vector space. However, most of the recent studies do not learn embedding representations on uncertain knowledge graphs. Uncertain knowledge graphs, e.g., NELL and Knowledge Vault, are valuable because they can automatically populate themselves with new facts. Nevertheless, the automatic process basically induces uncertainty to knowledge. In this study, we introduced knowledge graph embedding on uncertain knowledge graphs by using adapting confidence-margin-based loss function for translation-based models, namely CTransE, to deal with uncertainty on knowledge graphs. The results show that CTransE can robustly learn representations of uncertain knowledge graphs and outperforms the conventional method on knowledge graph completion task.

1. Introduction

A knowledge graph is a structured knowledge base, which provides real-world facts as knowledge. A knowledge in a knowledge graph is represented as a triple (h, r, t), where h and t are entities and r is a relation directed from h to t. Such knowledge has been widely used in many recent AI applications such as fact checking. Since Knowledge graphs become popular, the research community has made a great effort in constructing them. Currently, there are many publicly available knowledge graphs, such as DBpedia and Freebase. However, these knowledge graphs require manual effort to curate and keep up-to-date.

Unlike the above efforts, other approaches try to automatically build knowledge graphs [3]. However, automated construction of Knowledge Graphs often results in noisy and inaccurate facts, whose degree of reliability can be expressed by a score. The well-known uncertain knowledge graphs are Reverb and NELL.

Recently, knowledge graph embedding has gained the attention of many researchers. Knowledge graph embedding learns to capture latent representations of triples in a knowledge graph by projecting the entities and the relations of triples in the knowledge graph to a continuous low-dimensional vector space without considering the uncertainty of a knowledge graph. Generally, the uncertainty of a triple provides the reliability of the triple. Ignoring such reliability, noisy triples could induce the problem on the representation learning process.

In this paper, we introduce a confidence margin-based loss function on the translation model, namely CTransE, to deal with the uncertainty of triples in Knowledge Graphs. In CTransE, an uncertainty score is treated as the weight for a triple. The higher weight is, the lower the uncertainty is. A higher weight means that it is more likely a triple is true. CTransE handles the weight by adjusting the margin of the translation model in order to encode uncertainty into the representation.

Contact: Natthawut Kertkeidkachorn, natthawut@nii.ac.jp

2. Problem Definition

Given an uncertain knowledge graph denoted by $G = (E, R, Q)$, where E, R, and Q are the entity set, relationship set, and fact set, respectively. A fact is represented by a quadruple $q = (h, r, t, s)$, where $h, t \in E$, $r \in R$, and $s \in \mathbb{R}_{[0,1]}$. It indicates that entities h and t are connected by a relation r with score s, uncertain knowledge graph embedding is to learn embedding representations of an entity $\vec{e} \in \mathbb{R}^K$ for each $e \in E$ and a relation $\vec{r} \in \mathbb{R}^K$ for each $r \in R$ such that for each $(h, r, t, s) \in Q$; $f(h, r, t) \propto 1 - s$, where $f(h, r, t)$ is any arbitrary score function for q, such as $|\vec{h} + \vec{r} - \vec{t}|$, i.e. the facts can be preserved in $\mathbb{R}^K$ while considering their confidence.

3. Related Work

One of the popular models for knowledge graph embedding is the translation model. The translation models embed representations by using the relation r from the head entity h to the tail entity t as a dissimilarity score. The first model for the translation model is TransE [1]. TransE computes the triple's dissimilarity score by (h, r, t) as $\vec{h} + \vec{r} = \vec{t}$. With this translation, it can capture the first-order rules. Later, there are many models improving TransE by proposed the different dissimilarity functions.

However, such models are not supported uncertain knowledge graphs. In an uncertain knowledge graph, the level of reliability of a fact is represented in terms of a confidence s. So far, the translation methods do not take the confidence s of each fact into account. In practice, we can ignore the confidence of the facts and learn the embedding. Nevertheless, without confidence as an indicator, noisy facts can degrade the quality of the embedding representations. In this study, we therefore aim to introduce a new margin-

based loss function for supporting the uncertain knowledge graph embedding on the translation models.

4. Uncertain Knowledge Graph Embedding

The confidence margin-based translation model (CTransE) is to improve the margin-based loss function in translation models in order to support confidence on the quadruple q. The margin-based loss function is as follows.

$$L = \sum_{(h,r,t)\in T} \sum_{(h',r,t')\in T'} [f(h,r,t) - f(h',r,t') + M]_+ \quad (1)$$

, where $[x]_+$ is the positive part of x, $f(\cdot)$ is a score function, M is a margin, and (h', r, t') is a negative sample in T'. To preserve the embedding in the vector space, TransE uses normalization as the regularization in each iteration.

As shown in Eq. 1, the margin-based loss function does not consider the score s in the quadruple q. As a result, the reliability of triples is ignored. To overcome this problem, we propose a confidence margin-based loss function for translation models by varying the margin M of each triple based upon the score s. The idea behind is that the higher the uncertainty of the quadruple, the less margin should be used to keep the relation because (e, e') is likely to be noise. The relation r then should not be held with the margin M due to such uncertainty. We therefore derive the confidence margin-based loss function as follows.

$$L = \sum_{(h,r,t,s)\in Q} \sum_{(h',r,t',s)\in Q'} [f(h,r,t) - f(h',r,t') + sM]_+ \quad (2)$$

where $[x]_+$ is the positive part of x, $f(\cdot)$ is the score function for (h, r, t) of the quadruple q, M is the margin, $(h', r, t', 1.0)$ is a negative sample in Q' generated in the same way as T' and s is the confidence of the quadruple.

5. Experiments and Results

To evaluate CTransE for learning embedding representations for an uncertain knowledge graph, we conducted the experiment knowledge graph completion. Knowledge graph completion is a task to fill the knowledge graph by predicting missing relationships between entities. Given an incomplete uncertain knowledge graph G, the task is to fill in G by predicting the set of missing quadruples $Q' = \{(h, r, t, \cdot) \mid h, t \in E, r \in R, (h, r, t, \cdot) \notin Q\}$.

Currently, there are many datasets for the knowledge graph completion. However, these datasets do not contain uncertainty of triples. We, therefore, constructed the dataset from a real knowledge graph, NELL [2]. NELL provides a confidence score for each triple. To build our dataset, we first collected quadruples form NELL at the 995^{th} iteration. Then, we followed the cleaning process [4]. However, we did not add the inverse relation to the dataset as was done in that study. As a result, we obtained 75,491 entities, 200 relations, 134,213 training, 10,000 validation, and 10,000 testing quadruples.

Table 1: Results of knowledge graph completion

Method	% Hit@		MR
	1	10	
TransE	10.44	30.15	0.175
CTransE	**11.11**	**30.47**	**0.180**

The experimental setup and the evaluation protocol of the experiment are similar to the study in TransE [1]. Although our confidence-margin-based loss function can be applied to any arbitrary translation models, we select TransE to study due to its simplicity. As a result, the dissimilarity function in the experiment is set as L1-norm and TransE becomes the baseline for the experiment. The implementations of TransE and CTransE both used the grid search algorithm to find appropriate parameters. The dimension was selected from {20,50,100,200}. The search range for the margin M was set at {1,5,10,50,100}. The learning rate was selected from {0.1,0.001,0.0001}. In the evaluation process, we employed three evaluation metrics: Hit@1, Hit@10 and mean reciprocal rank (MR) as the study [1].

The experimental result is presented in Table 1. The result shows that CTransE outperforms TransE. This result indicates that the confidence of the triples affects the learning representation on uncertain knowledge graph and CTransE can capture such uncertainty to improve embedding representations.

6. Conclusion

We introduced a new confidence-margin-based loss function, namely CTransE, for the translation model. The preliminary results show that CTransE could encode the uncertainty of knowledge graphs and that better learn the embedding representation than the traditional margin-based loss function on uncertain knowledge graph.

References

[1] A. Bordes, N. Usunier, A. Garcia-Duran, J. Weston, and O. Yakhnenko. Translating embeddings for modeling multi-relational data. In *NIPS*, pages 2787–2795, 2013.

[2] A. Carlson, J. Betteridge, B. Kisiel, B. Settles, E. R. Hruschka Jr, and T. M. Mitchell. Toward an Architecture for Never-Ending Language Learning. In *AAAI*, pages 1306–1313, 2010.

[3] N. Kertkeidkachorn and R. Ichise. An automatic knowledge graph creation framework from natural language text. *IEICE Transaction on Information and Systems*, 101(1):90–98, 2018.

[4] W. Xiong, T. Hoang, and W. Y. Wang. Deeppath: A reinforcement learning method for knowledge graph reasoning. In *EMNLP*, pages 564–573, 2017.

International Session | International Session | [ES] E-2 Machine learning

[2A4-E-2] Machine learning: method extensions

Chair: Junichiro Mori (The University of Tokyo)

Wed. Jun 5, 2019 3:20 PM - 5:00 PM Room A (2F Main hall A)

The room is connected with B.

[2A4-E-2-01] Multi-carrier energy hub management through deep deterministic policy gradient over continuous action space

Hioki Tomoyuki[1], ○Tomah Sogabe[1,2,3], Dinesh Malla[3], Kei Takahashi[1], Masaru Sogabe[3], Katsuyoshi Sakamoto[1], Kouichi Yamaguchi[1] （1. Department of Engineering Science ,The University ofElectro-Communications, 2. Info-Powered Energy System Research Center, 3. Grid Inc.）

3:20 PM - 3:40 PM

[2A4-E-2-02] Attention-masking extended deep Q network (AME-DQN) reinforcement learning algorithm for combinatory optimization of smart-grid energy

○Dinesh Bahadur Malla[3], Hioki Tomoyuki [2], Kei Takahashi[2], Masaru Sogabe[3], Katsuyoshi Sakamoto[1,2], Koichi Yamaguchi[1,2], Tomah Sogabe[1,2,3] （1. i-PERC, The University ofElectro-Communications, 2. The University ofElectro-Communications, 3. Grid Inc.）

3:40 PM - 4:00 PM

[2A4-E-2-03] Exploring Machine Learning Techniques for Irony Detection

○Zheng Lin Chia[1], Michal Ptaszynski[1], Fumito Masui[1] （1. Kitami Institute of Technology）

4:00 PM - 4:20 PM

[2A4-E-2-04] A Matrix-Operation Fast Approximated Solution for Logistic Regression with Strong L2 Regularization

○Zeke Xie[1], Jinze Yu[1], Yanping Deng[2] （1. University of Tokyo, 2. Waseda University）

4:20 PM - 4:40 PM

[2A4-E-2-05] Final Sample Batch Normalization For Quantized Neural Networks

○Joel Owen Nicholls[1], Atsunori Kanemura[1] （1. LeapMind Inc.）

4:40 PM - 5:00 PM

The 33rd Annual Conference of the Japanese Society for Artificial Intelligence, 2019

Multi-carrier energy hub management through deep deterministic policy gradient over continuous action space

Tomah Sogabe[*1,2,3] Dinesh Bahadur Malla[*1,3] Tomoyuki Hioki[*2], Kei Takahashi[*2], Masaru Sogabe[*3], Katsuyoshi Sakamoto[*1,2], Koichi Yamaguchi[*1,2]

[*1] Info-Powered Energy System Research Center,
[*2]Department of Engineering Science
The University of Electro-Communications, Chofu, Tokyo, 182-8585, Japan
[*3] Technology Solution Group, Grid Inc., Kita Aoyama, Minato-ku, Tokyo, 107-0061, Japan

Abstract: Multi-carrier energy hub has provided more flexibility for energy management systems. On the other hand, due to the mutual impact of different energy carriers in an energy hub's energy management becomes more challengeable. For energy management purpose Mathematic optimization tools are used, but real-time optimization challenges the optimal management. On the other hand, energy demand and supply are very changeable so optimization objectives may vary or more than one. For real-time management, changing environment and multi-objective options AI is purposed. In this work operation of multi-carrier energy hub optimization has been solved by executing a multiagent AI algorithm, which contain deep deterministic policy gradient(DDPG) algorithm. Research multi-agent simulation results show that AI agent can manage a balance between demand and supply, proper charging and discharging of storage agent to optimize energy hub cost. It also describes the price determination method by using AI, which is good for demand and supply management purpose for a market.

1. Introduction

An energy hub is a conceptual model of multi-carrier energy systems used to represent the interactions of multiple energy conversion and storage technologies [1]. The energy hub concept was emerged because or world's energy crisis and its related problems caused a considerable movement into efficient utilization of energy systems. This comprehensive attitude to energy, which presented in the energy hub idea, persuaded the researchers to design future energy systems based on this idea [2]. In the energy hub concept, the whole of energy systems is investigated instead of individual management of energy carriers such as electricity, natural gas and so on. It also combined renewable energy source with a nonrenewable source to minimize carbon emissions for an environmental objective. The main question in the optimization of energy hub operation problem is that what is an optimum arrangement of energy components in each time for providing demands with minimum cost [1]. The energy system is a very changing environment to manage this feature the energy hub contain energy utility, which is capable of energy conversion, energy storage and direct connection of multi-energy carriers [3]. The objective of energy hub optimization is normally cost minimization, which generally includes both technology investment and operation costs [4].

Multi-carrier energy hub management is a process of energy flow optimization in a hub system, which investigates the flow of energy carriers in an integrated system by considering technical constraints of each system [5]. The mathematic optimization is a popular method in system optimization, for example, MILP, game optimization software, genetic algorithm, dynamic relaxation etc. The mathematics optimization tools are expensive and more difficult with the increase in parameter and objectives. So, we purposed for AI which refers to a Reinforcement learning process where agents to learn optimal behavior under different conditions. Key concepts in reinforcement learning are state, action, reward, and policy. The state refers to the state of the environment calculation at a given time. The action refers to the specific action taken by an agent, e.g. the direction and distance of an agent's movement within a given interval of time. The reward refers to the feedback signal (often a simple scalar value) given to an agent as a result of a specific action taken within a specific state. The policy links the states and actions of an agent and refers to the action(s) with the estimated highest reward value in any given state. The aim of reinforcement learning is normally to facilitate agents in identifying an optimal policy. For the problem-solving purpose, we can use two kinds of actions that can be continuous or discrete. Nature of Environment and problem optimization it's taking action will have determined. In this work, we used continuous actions algorithm DDPG [6]. Because we want to learn how much quantity purchase or sell and what will be the price? So according to the nature of optimization continuous action are preferred. If we use discrete nature actions, it will suggest doing buy or sell or pre-defined quantity of purchase and sell.

Contact: Tomah Sogabe, i-PERC, The University of Electro-communications, sogabe@uec.ac.jp

2. Model and learning algorithm

2.1 Model

Energy hub concept is very board concept, it contains a lot of devices and technologies. Our assumed energy hub input energy carriers are electricity, natural gas and the output side consist of electrical demand, heat demand [7]. The internal devices are the electrical transformer, CHP, boiler, electrical and thermal storage systems, PV and wind form. For hub energy supply and demand management, there are markets, hub's input and output situations are responsible for determining optimal operation based on received database on an agent action. The Energy hub model is figure in Fig.1. For selling and buying price determination purpose we divide the model learning in to two case which is described in section 3.

2.2 Learning algorithm

We used DDPG [6] as our learning algorithm, which is a limiting case of stochastic policy gradient in the actor-critic approach used for solving continuous tasks. To solve complex continuous action tasks, it requires a policy with stable learning and faster convergence, since policy may converge to sub-optimal solutions at the early stage of policy learning. There are mainly two networks in the DDPG they are actor and critic network which are in Fig.1. In the learning process critic network is updated with TD (temporal difference) of state and next state. The actor parameters are updated in the gradient of critic output with respect to policy parameters.

3. Simulation information

For demonstrating how energy demand market and its price affect the hub's operation, the simulation results are dividing into two case studies. These case studies are as follows:

Case1: With constant agent's buy and sell price and variable demand and supply.

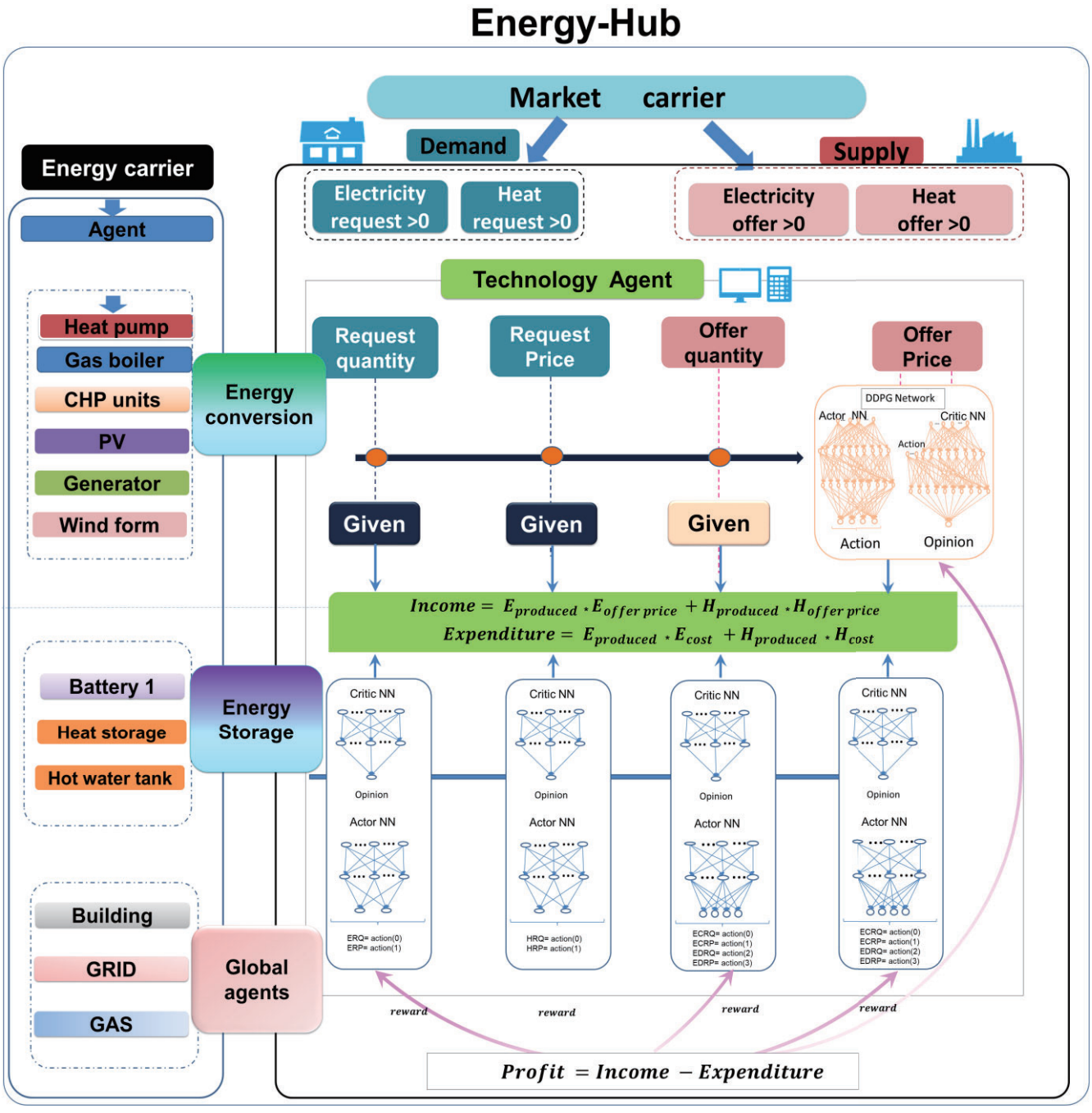

Fig. 1. Multi carrier Learning agent's architecture

Case2: With the variable price, demand, and supply.

In the case1 There is selling and buying price is constant for GRID and house agent. But another agent like storage, Boiler, Power generator's demand is variable. In this case, we assume that selling and buying price is determined by the standard or global agent like GRID in the real world. So, based on the GRID fixed price other agent calculate the quantity to sell and buy, which optimize their profit. In case2 selling and buying price with quantity are variable. So every agent learns what quantity and price make the total profit maximum for this point in time. We assumed that there is a free market where all agent has selling and buying price determination right, and they also fix their buying and selling quantity. After fixing individual price and quantity, we go to the global market where a higher buying price agent with lower selling price agent mechanism fixed the quantity sell and buy.

Based on the agent network state and actions are as follows:

Agent Name	Contribution to states	Actions			
		Buy quantity	Sell quantity	Buy price	Sell price
Boiler	Heat production	-	O	-	O
CHP	Heat production Electricity production	-	O	-	O
Heat storage	Current SOC	O	O	O	O
Photo voltaic	PV generation	-	-	-	O
Power generator	Maximum generation	-	O	-	O
Power storage	Current SOC	O	O	O	O

Fig.2. Agent and action data chart

4. Simulation result and discussion

Here we present simulation results which are based on section 2 model and AI algorithm. And results are divided in two case study which was discussed in section 3. Multi-carrier energy system contains many carriers and According to the content, it's level of difficulty will be ranked difficult or sample. Here in this work, we take a few carrier hub systems to minimize the power use cost per day. Case study 1 and case study 2 contain differ carrier. There are Electrical storage, heat storage, CHP, boiler, windfarm, and GRID in case study 1. A building, solar PV, power generator, power storage, GRID are in case study 2. According to the case study results are discussed below:

Case study 1:

In this case, we have a GRID, wind farm, boiler, CHP, electrical storage, heat storage and demand. Demand contain electricity demand, heat demand and gas demand for houses hold in total for 24 hours 24 discrete form. Here we have a 24-hour total cost for an electricity minimization problem. The Fig.3 shows the

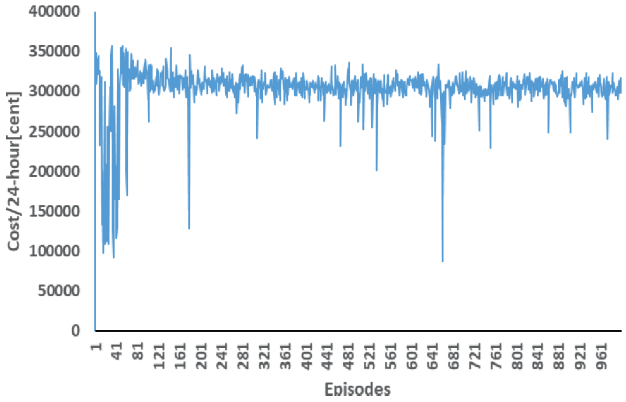

Fig. 3. 24-hour agent contribution total cost

learning time optimization cost for 24 hours. At the beginning of the learning time, the 24-hour cost was 430000[cent]. And after the 1000 episode, its 24-hour total cost is 395316.45[cent]. For optimization purpose storage agent like electricity storage for

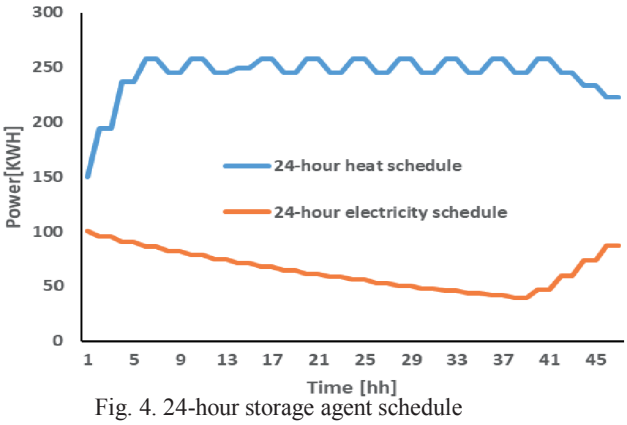

Fig. 4. 24-hour storage agent schedule

electricity and heat storage for heat, storage plays a very significant role. The test time electricity storage and heat storage schedule for 24-hour is in Fig.4. We set electricity storage's maxing storage capacity is 200[KWH] and initial time is half of the maximization. Heat storage max capacity is 300[KWH] and initial is half of the max. We also set minimum level, which is for storage safety, after long time learning agent is able not to discharge below the minimum level. This case study is based on [7] MILP optimization for energy conversion and management. We use a multiagent algorithm (section 2.2) for minimizing the

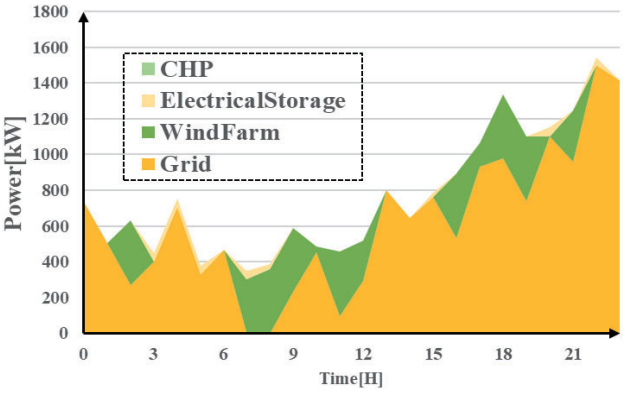

Fig. 5. 24-hour electricity contributor agent

cost. We have storage, CHP and boiler agents, they learn the quantity to supply for demand fulfillment. Here GRID is a global agent and can supply the unbalance quantity of electricity and heat. Fig.5 shows the total contributor for 24-hour electricity almost GRID and wind farm agent supply to the demand but another agent has small capacity and their contribution also small.

Case study 2:

In this case, we have the battery, power generator and PV are student agents, building and GRID are fixed-learning agents Student agent learns to sell/buy price and quantity from their action interact with the environment. In Fig.6 blue line is the

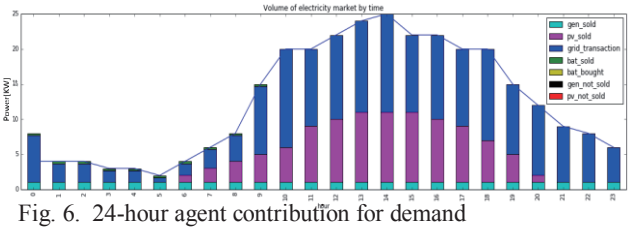

Fig. 6. 24-hour agent contribution for demand

demand of the day and other colored bar are agent contribution for demand. The model is based on the GRID global agent it can buy and can sell too. Start to hour power generator production and GRID are used for the demand of building and after PV starting to produce power it also included. But in increasing in demand PV and generator production does not fulfill the demand so, more power from GRID is use. We use agent wise profit and total profit as a reward in the learning process. In the start of the learning time, all agent does not know how much they can sell

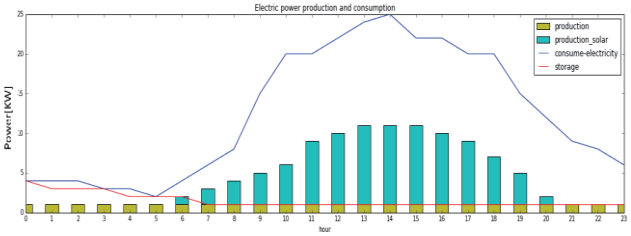

Fig. 7. 24-hour agent contribution for demand other than

and what price will good for sell/ buy. So in the beginning quantity not sold remain but increase in learning they balance the demand and supply. We also use fixed cost and variable cost concept for making profit real. Power generator agent almost fixed for all 24 hours after learning, and battery agent most of the time discharge before to its minimum level but charging actions are very low in Fig.7. The learning time reward graph in Fig.8.

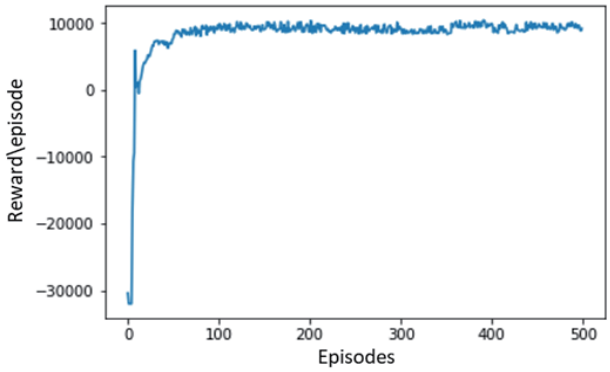

Fig. 8. Reward of multi-agent reinforcement learning

5. Conclusion

Increasing energy scarcity leads to the energy hub concept. It presented a comprehensive attitude towards the energy management problem. Optimal operation of an energy hub with consideration new conditions can help to find out about multi-carrier concept more and move to make it practical. This paper studied presents AI to optimal operation of the energy hub with consideration energy markets and system uncertainties with real-time action. The presented new ways of energy free market operation significantly power up energy market based on forecasting and its sustainability. Artificial intelligence for optimization not only diminish the cost but it also helps to optimize forecast near to very real time. The current work can extend by integrating more power and heat systems in the future. Also, the addition of forecasting agent can make more efficient energy market. Which is not consider in this work and the future works focus on forecasting and real-time optimization.

References

[1] Geidl and G. Andersson. Optimal power flow of multiple energy carriers. IEEE Transactions on Power Systems, 22:145.155, 2007.

[2] Favre-Perrod P. A vision of future energy networks. In: 2005 IEEE power engineering society inaugural conference and exposition in Africa. IEEE; 2005.p. 13–7.

[3] Zhang X, Shahidehpour M, Alabdulwahab A, Abusorrah A. Optimal expansionplanning of energy hub with multiple energy infrastructures. IEEE Trans SmartGrid 2015;6(5):2302–11.

[4] Skarvelis-Kazakos S, Papadopoulos P, Unda IG, Gorman T, Belaidi A, Zigan S.Multiple energy carrier optimisation with intelligent agents. Appl Energy 2016;167:323–35

[5] Shabanpour-Haghighi A, Seifi AR. Simultaneous integrated optimal energy flow of electricity, gas, and heat. Energy Convers Manage 2015;101:579–91

[6] D. Silver, G. Lever, N. Heess, T. Degris, D. Wierstra, and M. Riedmiller. Deterministic policy gradient algorithms. In Int. Conf on Machine Learning, 2014.

[7] M.J. Vahid-Pakdel, Sayyad Nojavan, B. Mohammadi-ivatloo, Kazem Zare. Stochastic optimization of energy hub operation with consideration of thermal energy market and demand response. Energy Conversion and Management 145 (2017) 117–1

The 33rd Annual Conference of the Japanese Society for Artificial Intelligence, 2019

Attention-masking extended deep Q network（AME-DQN）reinforcement learning algorithm for combinatory optimization of smart-grid energy

Dinesh Bahadur Malla[*1,3] Tomoyuki Hioki[*2], Kei Takahashi[*2], Masaru Sogabe[*3], Katsuyoshi Sakamoto[*1,2], Koichi Yamaguchi[*1,2], Tomah Sogabe[*1,2,3]

[*1] Info-Powered Energy System Research Center,
[*2]Department of Engineering Science
The University of Electro-Communications, Chofu, Tokyo, 182-8585, Japan
[*3] Technology Solution Group, Grid Inc., Kita Aoyama, Minato-ku, Tokyo, 107-0061, Japan

Recently deep neural network-based reinforcement learning (DRL) methods, which demonstrated unprecedented success in game and robotic control, are gradually gaining attention to solve the combinatory optimization problem. However, effective operation in smart grid system has to be submitted to various constraints such as power demand-supply relation, lower and upper bound of battery electricity, market price etc. Because of these constraints, DRL algorithm is not efficient to get an optimized result. In this paper we address this issue by developing an attention-masking extended deep Q network（AME-DQN）reinforcement learning algorithm. Special focus was lied on the prediction ability of the trained AME-DQN model given various weather conditions and demand profile. These results were further compared with MILP results and finally we demonstrate that the AME-DQN are able to predict optimized actions which satisfy all the constraints while the MILP failed to meet the conditions in most of the cases.

1. Introduction

Defining the Energy system apart from the smart grid system is very difficult, improvement in research and artificial intelligence (AI) also makes system intelligent day by day. It's can be reasoning some authors even argue that it is "too hard" to define the smart concept [1]. The smart grid is an innovation that has the potential to revolutionize the transmission, distribution, and conservation of energy. Actually, the current electric power delivery system is almost entirely a mechanical system, with only limited use of sensors, minimal electronic communication and almost no electronic control [2]. Construction of efficient smart grid system is in principle a control optimization mathematical problem. Because of complexity wide range of methods have been proposed to tackle this challenge including linear and dynamic programming as well as heuristic methods such as PSO, GA, game or fuzzy theory and so on [3]. The mathematical process synthesis typically deals with the optimization with one objective and increase in parameter exponential increase in cost.

So, what is reinforcement learning? Reinforcement learning is a process where agents to learn optimal behavior under different conditions. Key concepts in reinforcement learning are state, action, reward, and policy [4]. The state refers to the state of the environment calculation at a given time. The action refers to the specific action taken by an agent, e.g. the direction and distance of an agent's movement within a given interval of time. The reward refers to the feedback signal (often a simple scalar value) given to an agent as a result of a specific action taken within a specific state. The policy links the states and actions of an agent and refers to the action(s) with the estimated highest reward value in any given state.

In this paper, we have an optimization objective for the energy grid system. Because of the complex system, we plan to solve small subsystem power cost optimization. Grid system has one household having Photovoltaic power production, having power storage battery and grid power supply. Where Production and consumption are not controllable but storing the power and use the storage can control, because of controllability optimization concept emerge. Small optimization for the household makes a huge quantity of the whole grid system, and subsystem optimization can connect with whole system optimization.

Contact: Tomah Sogabe, i-PERC, The University of Electro-communications, sogabe@uec.ac.jp

2. Model and Algorithm

Smart grid system based communication technology helps to know the current power demand, power production, battery SOC and other needed information. Basically digitalized electricity meter PV control system and sensing sensor plays a very important role collect the data and information. Base on the information we can optimize our system by taking what action makes out cost minimum. Our basic model is a small grid having one household for power consumption, one PV and one battery

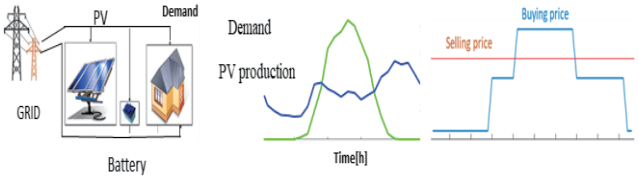

Fig.1 The basic model for power balance

for power storage and power supply for the consumption. The Q-attention-masking Algorithm is as below.

2.1 Reinforcement learning

We propose a framework that uses deep Q-learning to learn a high-level tactical decision-making policy, and also introduce, action-masking for the time of not constraints fulfill by the next-

state, a novel technique that forces the agent to explore and learn only a subspace of Q-values [7]. This subspace is directly governed by a constraints module that consists of prior knowledge about the system. Constraints of the problem and information from the same input state make the input data for the action-masking network. Not only does action-masking provide the tight integration between the two paradigms: learning high-level policy and using state action control, but also heavily simplifies the reward function and makes learning faster and data efficient. Not only Q-learning and action-masking are efficient to optimize our objective we use the learning from scratch, where agent updates their parameter by using search from scratch. We use epsilon-greedy for learning process which helps agent learn from scratch, the first agent selects action randomly and after the decrease in epsilon, agent use action by its learned result and agent able to optimize the goal.

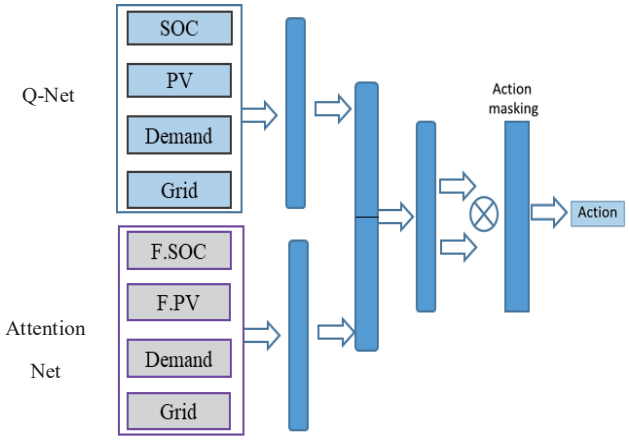

Fig.2 Attention-masking extended Deep Q algorithm

We use an attention network to parallel with normal Q-network, where attention network contains the information about the next state but not the state like next state. Attention network is a network, which informs the network about the current state and its impact to next state are fulfilling constrains or not. The cross-validation of state with attention state helps to make the good decision, and it helps the network to take the right decision based on the state to make next state. We start from scratch, with the help of the epsilon-greedy method we reduce the dependency of Q-network from random action. The decrease in epsilon helps our agent to calculate the action from the learned weight. Our attention states are so simple if constraint will satisfy in the next state they remain same, if not satisfy we just symbolized the state to -1.

After the layer of a network, we concatenate the state and future state result and calculate the action. For the purpose of hard constraints, we use an action masking process. Hard constraints are those constraints which are necessary to get the reward. After fulfilling the hard constraints, we have to fulfill the soft constraints which maximize or minimize the reward in the network and daily consumption cost of the electricity in the energy system. The network learns from energy optimization actions outcomes with the help of rewards by estimating the optimal Q-value function. Until the terminal time agent don't get a reward (like Monte Carlo samples), it gets a reward if satisfied all constraints if not it gets terminate punishment.

2.2 Mixed Integer Linear Programming (MILP)

MILP is a mathematical optimization program in which some or all of the variables are restricted to be integers. The mathematic optimization methods can divide into three parts where the first is a single numerical quantity objective function which is to maximized or minimized. The second is a collection of variables which are quantities whose values can manipulate in order to optimize the objective. The third is a set of constraints which are restrictions on the values that the variable can take. Here in work our objective function is as below: $minimize\ \sum_{h=1}^{48} C_{buy}P_{buy}(h) - C_{sell}P_{sell}(h)$ and constraints are :

$$P_{demand} = P_{buy} - P_{sell} + P_{battD} - P_{battC} + P_{PV} \ldots (1)$$

$$P_{battE}(1) = P_{battE}(48) = P_{battEmax} \qquad \ldots (2)$$

$$P_{battE} + dt\ P_{battC} \leq P_{battCAP} \qquad \ldots (3)$$

The Constraints 1 means power demand needs to be equal with power buy minus power sell and adding PV with a battery charge. The Constraint 2 for battery state of charge (SOC) at end of the day is equal to the start of the day. The Constraints 3 is for battery capacity is always greater than battery current adding with powered charged in the battery.

3. Results and discussion

We already discuss RL algorithm in section 2.1, Base on that algorithm we obtain the different result that we discuss in this section. First, shortly describe coming for this algorithm. The field of optimization is totally obtained by the mathematical optimization methods, which is very good for one objective optimization. But it is not cost effective and not good enough after the increase in a parameter and objectives. So, the optional method is reinforcement learning, but RL is very weak in constraint fulfillment but very cost effective. We purpose this reinforcement algorithm for constraints based optimization problem. The obtained results are here below:

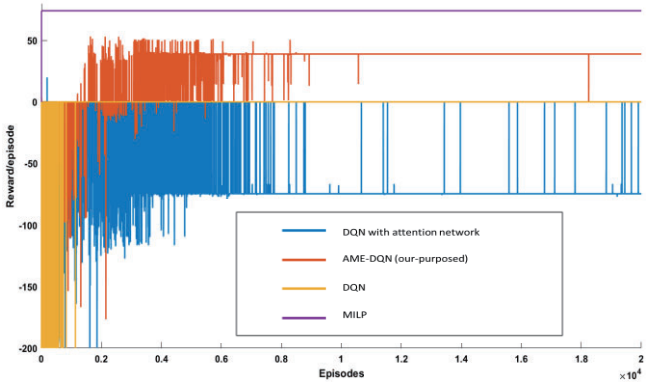

Fig.3 Reward per episodes of different R L algorithm

The Fig.3. is the reward results per episodes of our suggested algorithms. Here we used a reinforcement learning algorithm to optimize the power cost per day. In reward plot 0 mean some or one constraint is not fulfilling. The negative reward means a daily cost to pay for electricity consumption and positive means income from the electricity transaction. The DQN is the similar algorithm presented by the deep mind team[5]. The DQN Attention Mask network is the algorithm combination of DQN, attention, and masking, where attention network used in language processing techniques and masking is also one of the actions clarifying technique used in RL recent year. The DQN Attention network is the combination of DQN and attention network. The above graph clearly presents that, only DQN algorithm is unable to satisfy the constraints. In the beginning time a random process of taking action helps to satisfy the constraints but decrease randomness, it does not satisfy the total constraints. The other DQN with Attention is able to satisfy the constraints but it is also unable to minimize the cost and DQN with Attention and mask network is quite satisfactory to compare with DQN and DQN with Attention network.

3.1 AME-DQN test

Reuse is the main benefit of RL, so it is cost effective, and it is efficient to optimize the similar nature problems with the previous learned network or agent. For the test purpose, we defined the similar nature power problems and use the above discussed AME-DQN agent to solve the problem, the results are discussed in this section. In Fig.4. PV production curve represents the low production of PV or cloudy weather PV

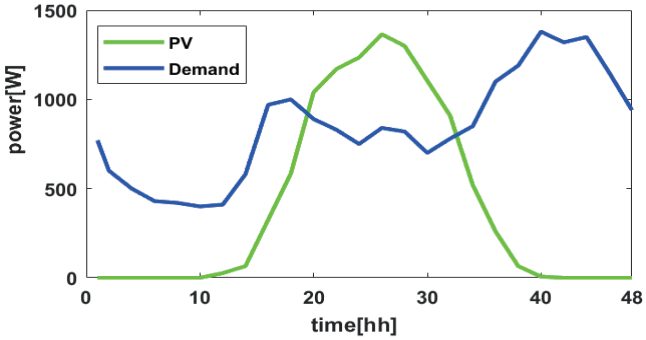

Fig.4 Demand and PV production curve

production. The total production of the day is 19959[W], and demand is 40400[W]. The optimization result of MILP and test result of RL plotted in the below Fig.4, Fig.5. The MILP mathematic optimization algorithm [6], and the RL side only use the learned weight to solve the problem. Here in this test, only PV production is different from the above-solved problem, but MILP needs to recalculate the problem to solve or optimize the result but not to the RL. MLP optimized result is lower than the RL test optimized cost for the day, but this is the result of weight used where MILP optimized result is 74 JPY/day, and RL has only 38JPY/day. At the test time, all the constraint is fulfilled and it also near to optimized result also.

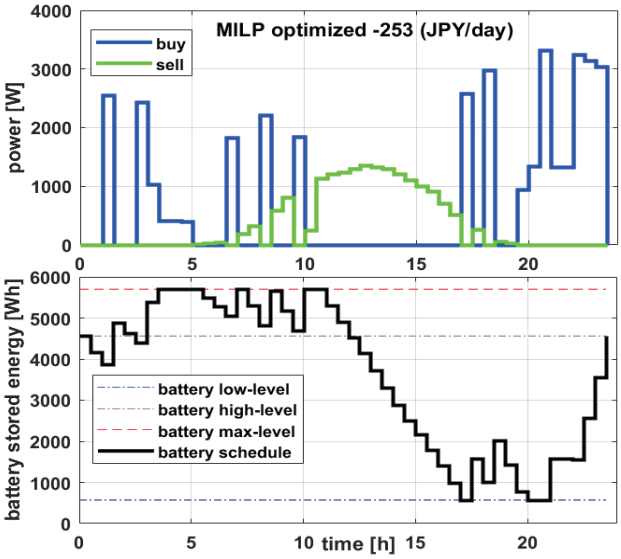

Fig.5 Buy and sell schedule from MILP optimization

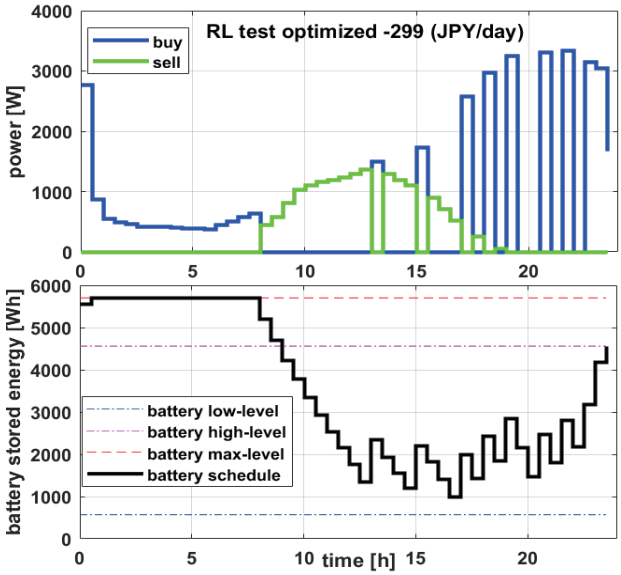

Fig.6 Buy and sell schedule from RL test

3.2 AME-DQN and MILP test

In this section, we present the same power system learned AME-DQN and MILP. MILP test is a quite unfamiliar term, we used MILP optimization time actions for the same time step of the problem to test, and AME-DQN is using the learned weight to forecast the test. Here in this work, we used the last optimization time actions of MILP because all PV production and demand are not the same. Both of the algorithms have learned the same problem whose total reward is plotted in Fig.3. This time test problem demand and PV production curve is in as Fig.7. MILP and AME-DQN results are plotted in Fig.8 and Fig 9 respectively. The problem contains different PV production curve and higher demand of the 24 hours.

Form the test results we can see a different scenario, which is not an unbelievable pattern from the MILP optimization. But in the test time we haven't calculated the optimized result, we only

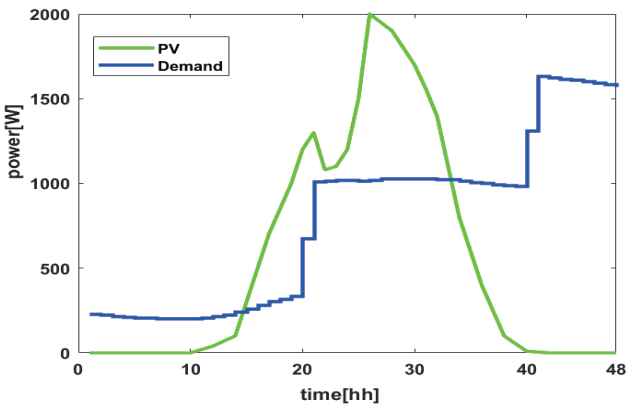

Fig.7 Demand and PV production curve

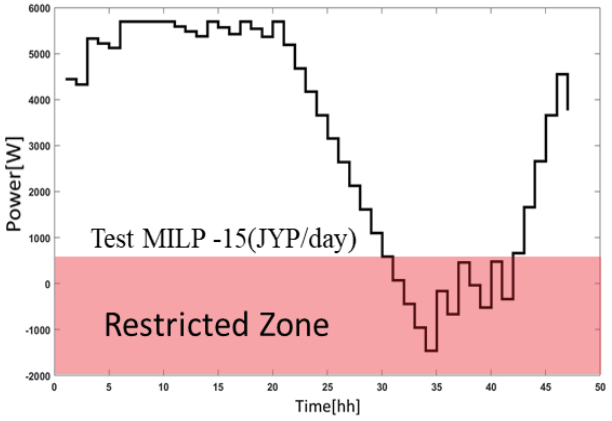

Fig.8. test time battery schedule by MILP

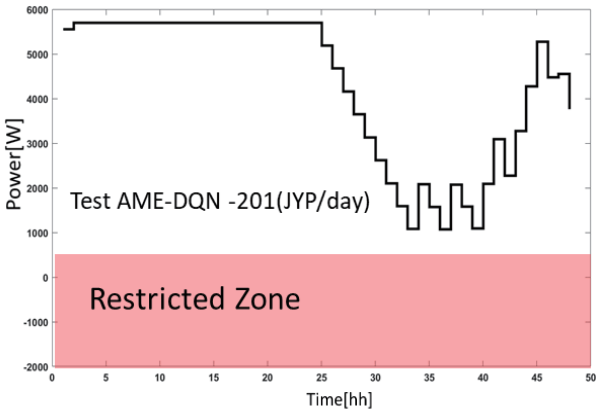

Fig.9. test time battery schedule by AME-DQN

predict on the base of optimization time scenario. So, MILP is not for prediction purpose, but average from predicted different scenario can make it better. The test result shows that MILP is not obeying the lower bound constraints at a test, but AME-DQN fulfills all the constraints.

4. Conclusions

In this paper, we present a reinforcement learning method for smart grid optimization. From the different result discussed above in results and analysis section, the agent was able to catch the feature involved in the balance of load demand, PV power surplus and battery discharge/charge, as well as grid, integrate. The agent successfully learned how to tune its action profile to maximize the reward function during training. The RL agent satisfies all the constraints, which is one step toward the optimization. Our learning agent is not able to get the global goal but can be useful for similar kind of problems. So, there are many beneficial parts for using the RL agent than the using MILP or another mathematical optimization result. Mathematical optimizations are good for one objective optimization but increasing in data, parameter and objectives make it incompatible. If we want a multi-objective result that is only fulfilled by a reinforcement learning agent, it is also cost-effective and we can model without knowing the problem from the root. The RL for an optimized result is difficult but not impossible. RL agent can optimize the problem from scratch now our RL agent fulfill the constraints which are difficult to fulfill so far. The current work can continue by uniting more power sources in the future. Also, works focus on global optimization and optional roots search for optimization. This research helps us to know about the constraint application in RL learning process, how to define soft and hard constraint as well.

References

[1] Miller, J., “The Smart Grid – How Do We Get There?”, Smart Grid News, June 26, 2008

[2] http://smartgrid.epri.com

[3] M. R. Alam, M. St-Hilaire, and T. Kunz, "Computational methods for residential energy cost optimization in smart grids: A survey," *ACM Comput. Surv.*, vol. 49, pp. 22-34, Apr. 2016.

[4] L.A. Bollinger and R. Evins. “Multi-agent reinforcement learning for optimizing technology deployment
in distributed multi-energy systems”. EMPA20160705

[5] Mnih, V., Kavukcuoglu, K., Silver, D., Rusu, A. A., Veness, J., Bellemare, M. G., Graves, A., Riedmiller, M., Fidjeland, A. K., Ostrovski, G., Petersen, S., Beattie, C., Sadik, A., Antonoglou, I., King, H., Kumaran, D., Wierstra, D., Legg, S., and Hassabis, D. 2015. “Human-level control through deep reinforcement learning.” Nature 518(7540):529–533.

[6] M.J. Vahid-Pakdel, Sayyad Nojavan, B. Mohammadi-ivatloo, Kazem Zare. Stochastic optimization of energy hub operation with consideration of thermal energy market and demand response. Energy Conversion and Management 145 (2017) 117–1

[7] Mustafa Mukadam, Akansel Cosgun, Alireza Nakhaei, Kikuo Fujimura. “Tactical Decision Making for Lane Changing with Deep Reinforcement Learning”. 31st Conference on Neural Information Processing Systems (NIPS 2017), Long Beach, CA, USA.

The 33rd Annual Conference of the Japanese Society for Artificial Intelligence, 2019

Exploring Machine Learning Techniques for Irony Detection

Chia Zheng Lin*1 Michal Ptaszynski*2 Fumito Masui*3

Kitami Institute of Technology, Kitami, Japan

Irony detection is considered a complex task in Natural Language Processing. This paper first introduce and cover the recently state of irony detection. Then we review and summarize previous related research on text-based irony detection. Finally we compare various classifiers including the proposed CNN model on three dataset of tweets, and analysis and discuss the results. We conclude that CNN is effective for irony detection under various situation with our model outperforming all the other classifiers.

1. Introduction

Irony is considered an important component of human communication recognized as one of the most prominent and pervasive device of figurative and creative language widely used dating back to ancient religious texts to modern time [Ghosh et al 2017]. Merriam Webster, a popular online dictionary, defines irony "as the use of words to express something other than and especially opposite off the literal meaning" [https://merriam-webster.com/].

Due to its nature, irony has important implications for Nature Language Processing (NLP) tasks, which aim to understand and produce human language. In fact, automatic irony detection has a large potential for various applications in the domain of text mining [Van Hee et al. 2018]. Rosenthal et al [2014] demonstrated the impact of irony on automatic sentiment classification by attempting to analyze a test set of irony tweets with standard sentiment analysis tools, and showing the inability of those tools to maintain high performance on irony texts.

In the recent years, studies in irony detection and classification have gained popularity and have been widely applied as sentiment analysis tasks. Various types of approaches were developed and improved to tackle the problem of irony detection. Some of the most popular approaches with better performance are rule-based, statistical, or Deep Learning-based approaches.

Among many Social Networking Services, the one that became one of the most popular for people to express their opinions, share their thoughts and report real-time events, etc., has been Twitter [https://twitter.com/] [Bouazizi and Otsuki 2016]. Many companies and organizations have been interested in these data for the purpose of studying the opinion of people. Therefore it has been suggested that data sets of tweets may be able to bring out the best performance of irony detection approaches.

Whilst many studies has been carried out on irony detection, there have been few empirical investigations into the best and optimal approach for the task. The aim of this paper is to evaluate whether it is possible to develop a classification model for irony detection with various Natural Language Processing (NLP) methods, with particular focus on recent developments in NLP and Artificial Intelligence (AI), such as Deep Neural Networks. In this paper we study, review and analyze previous related researches on text-based irony detection, investigate the potential of other methods,to compare them, and identify the applications of irony detection in various platforms.

The rest of this paper is organized in the following way. Firstly, we describe the problem of irony detection and present some of the previous research. Next, we describe the data set used in this research and approaches applied in experiment for comparison. Further, we explain the evaluation settings, followed by the analysis of experiment results and discussion.

Contact: Name, Affiliation, Address, Phone number, Facsimile number, and E-mail address

2. Research Background

2.1 Definition of Irony

The word irony originates from an Ancient Greek word ε ρ ω ν ε α, meaning dissimulation or feigned ignorance. Irony is often described as a rhetorical device, literary technique, or event in which what appears, on the surface, differs radically from what is actually the conveyed.

The relationship between irony and sarcasm have been confused in many studies. Van Hee [2017] concludes a number of differences between verbal irony and sarcasm, such as the level of aggressiveness, the presence of a target, the intention to hurt, and even some vocal clues. In this research, we will be performing experiments in irony detection, therefore, we will not distinguish between sarcasm and verbal irony, and instead we will be implementing the general term 'irony'.

2.2 Previous Research on Irony Detection

Some of the earliest research dealing with irony detection was a spoken dialogue system using feature extraction approach which included irony detection as a subtask [Tepperman et al. 2006]. As for the later research, Davidov et al. [2010] mainly focused on irony detection from tweets and Amazon product reviews, and Gonzalez-Ibanez et al. [2011] proposed a machine learning model composed of various features.

Numerous studies have attempted to describe the recent trend on approaches to irony detection, which can roughly be classified into three parts: rule-based, machine learning (statistical approach) and deep-learning approaches [Ku-

mar et al. 2017; Barbieri 2017]. Rule- based approaches attempt to identify irony through specific evidences which can be captured with specific rules. Barbieri [2017] reported that rule-based approaches which require no training mostly rely on lexical information and do not perform as well as statistical systems. Reyes et al. [2013] designed another system with different feature types exploiting lexical, syntactic and semantic information.

However, most of the work on irony detection apply statistical approaches. Statistical approaches vary in terms of features and learning algorithms, which mostly composed of two phases. Firstly the data is converted into a feature vector which will be calculated with various methods. Then a machine learning algorithm is used to classify them. Some of the most often used algorithms are Support Vector Machines and Naives Bayes. Liebrecht et al. [2013] implemented bi-gram and tri-gram based features and designed an irony detector that marks unseen tweets as being irony or not.

With the work of Amir et al. [2016] which used a standard binary classification with Convolutional Neural Network (CNN) and Poria et al. [2016] who used a combination of CNNs trained on different tasks, Deep Learning approaches have been brought into the scene of irony detection. Popular deep learning algorithms such as CNN [LeCun et al., 1998] and Long Short Term Memory (LSTM)[Hochreiter and Schmidhuber, 1997] have been widely used in recent works. Amir et al. [2016] and Poria et al. [2016] used CNN in irony detection. LSTM is also considered another popular deep learning algorithm in text classification. Ghosh and Veale [2016] proposed a network model composed of CNN and followed by a LSTM network. The model outperformed state-of-the-art text-based methods for irony detection at the publishing time.

Following the Semantic Evaluation 2018 Task 3: Irony Detection in English Tweets [Van Hee et al., 2018] which received submissions from 43 teams for the binary classification Task A, deep learning algorithms were further optimized for irony detection task. The best ranked system by team THU_NGN [Wu et al., 2018] consisted of densely connected LSTM network with multi-task learning strategy. One of the top teams, NTUA-SLP [Baziotis et al., 2018] ensembled two independent models, based on bi-directional LSTM networks. The systems that were submitted represent a variety of neural-network-based approaches and other popular classification algorithms include SVM, Maximum Entropy, Random Forest, and Naive Bayes [Van Hee et al., 2018]. Overall, there seems to be some evidence to indicate that approaches with ensemble learners are the current trend to further challenge the detection of irony however there is still no definitively best method for detecting irony automatically.

3. Proposed Methods

3.1 Data Preprocessing

Light normalization were applied to the data set. All of the tweets were transformed into lowercases and emojis were represented with their labels (e.g. :smileyface:). Furthermore, all URLs and tagged users are replaced with specific tokens "_url_" and "_tagged_" because they are not likely to be contributing to the classification.

3.2 Feature Extraction

Referring to Ptaszynski et al. [2017] work on data preparation, the following feature preprocessing was done after the normalization. Traditional weight calculation scheme, namely term frequency with inverse document frequency (TF-IDF) were applied to both dataset with and without hashtags. Term frequency t f (t,d) refers here to the traditional raw frequency, meaning the number of times a term t (word, token) occurs in a document d. Inverse document frequency idf (t,D) is the logarithm of the total number of documents containing the term nt. Finally tf*idf refers to the term frequency multiplied by inverse document frequency.

3.3 Classifiers

Several types of classifiers are applied for comparison in this research.

Naive Bayes classifier is a supervised learning algorithms applying Bayes' theorem which assign class labels to problem instance represented as vectors of feature values, often applied as a baseline in text classification task.

Next the k-Nearest Neighbors (kNN) classifier takes an input k-closest training samples and classifies them based on the majority vote . It is often used as a baseline after Naive Bayes. For the input sample to be assigned to the class of the first nearest neighbor, k=1 setting is used here.

JRip also known as Repeated Incremental Pruning to Produce Error Reduction (RIPPER) which is efficient in classifying noisy text [Sasaki and Kita, 1998], learns rules incrementally in order to optimize them. Also J48 which is implemented with C4.5 decision tree algorithm, builds decision trees from dataset and the optimal splitting criterion are further chosen from tree nodes to make the decision.

Support Vector Machines (SVM) is a supervised machine learning algorithm designed for classification or regression problems which uses a technique called kernel trick to transform data and finds an optimal boundary between the possible output. Two types of SVM functions are used here, linear and radial.

Lastly, Convolutional Neural Networks (CNN) which are a type of feed-forward neural network, were applied with Rectified Linear Units (ReLU) as neuron activation function. The proposed CNN method consisted of two hidden convolutional layers, containing 20 and 100 feature maps with both layers having 5x5 size of patch and 2x2 max-pooling, and Stochastic Gradient Descent [LeCun et al., 2012].

4. Experiment

4.1 Dataset

The dataset used in this research is the dataset provided by Semantic Evaluation 2018 Task 3: Irony Detection in English Tweets [Van Hee et al., 2018] which was constructed by searching Twitter for the hashtags #irony, #sarcasm

and #not, which could occur anywhere in the tweet that was finally included in the corpus. All tweets were collected between 2014/12/01 and 2015/01/04 and represent 2,676 unique users, and were manually labelled using a fine-grained annotation scheme for irony [Van Hee et al., 2016a]. The entire corpus was cleaned by removing retweets, duplicates and non-English tweets and replacing XML-escaped characters (e.g. &).

The dataset consists of 4,618 tweets (2,222 ironic + 2,396 non-ironic) that were manually labelled by three students using the brat rapid annotation tool with an inter annotator agreement study set up to assess the reliability of the annotations. Additionally, there are two duplicate sets of the data with all the ironic hashtags removed and with only hashtags.

4.2 Evaluation setup

Three separate datasets provided from the original preprocessed dataset are being performed in the experiment, with and without hashtags. Each of the classifiers mentioned in 3.4 was tested on both version of the dataset in a 10-fold cross validation procedure. The results were calculated using standard Accuracy (A), Precision (P), Recall (R) and balanced F-score (F1). The results were determined based on the highest achieved balance F-score.

4.3 Results discussion

Table 1 shows the summarization of all results. We can see that the results the from dataset with hashtags included are significantly higher than the other dataset without hashtags. As stated by Maynard and Greenwood [2014], even without considering ironic hashtags, the presence of hashtags greatly increase the results of irony detection.

The kNN scored the lowest result among the classifiers for both dataset and Naive Bayes barely came after it. Even though these classifiers may be able to do well in typical sentiment analysis, stemming and parsing are not applied to the dataset, hence the noisy language might be a challenge for them.

For the decision tree-based classifiers, J48 did better than Random Forest with hashtag included but scored as low as kNN when hashtags are removed. Random Forest scored third highest for both dataset but it is unfortunately impractical because it is time-inefficient when comparing to SVM. The rule learner algorithm, JRip scored highest when hashtags are included but just performed better than kNN and J48 when hashtags are removed.

The most used algorithms in irony detection are SVMs. As we can observe, the radial-SVM is comparable to the proposed CNN. They achieved the same F score on dataset with hashtags and SVM ranked second just after CNN for the dataset without hashtags. The linear-SVM, however, did not perform well enough in both condition.

When it comes to the proposed CNN with two hidden layers, 5x5 patch size, max-pooling, and Stochastic Gradient, it outperformed all of the classifiers in the harsh situation where all hashtags were removed (F-score= 0.66). While CNN is time-efficient comparing to other classifiers in small datasets, larger dataset might produce different result. One of the best irony detection system so far is also a network model composed of CNN, but applied to a data set of 39K tweets [Ghosh and Veale, 2016].

Table 1: Experiment result F-score

Classifiers	with hashtag	no hashtag	only hashtag
kNN	0.753	0.571	0.881
Naive Bayes	0.808	0.621	0.758
Random Forest	0.883	0.641	0.898
J48	0.883	0.641	0.884
JRip	0.899	0.616	0.897
SVM-linear	0.826	0.615	0.893
SVM-radial	0.844	0.644	0.833
CNN	0.844	0.660	N/A

The last column of Table 1 shows the results of the dataset which consists of only the hashtags. Besides CNN which the results could not be calculated due to the lack of suitable environment, all the remaining classifiers attain high F-score comparable to the dataset with hashtag. Together these results provide important insights into the presence of hashtags in a tweets especially ironic hashtag for irony detection.

These findings enhance our understanding of the impact of hashtag, which makes great difference in irony detection. In general, irony detection is still an unsolved problem, but it will be an easy task on Twitter thanks to the presence of deliberated hashtag. Taken together, these results also suggest that hashtag is the product of authors who realize that their ironic phrases alone may not be enough for their audience to understand. This redefines irony in textual communication especially on social network services from figurative speech to direct speech.

5. Conclusion

In this paper we reviewed and summarized previous related works on text-based irony detection. We covered various types of systems designed in the past works such as rule-based, statistical based, and deep learning based approaches. Then we compared a few different classifiers including the proposed optimized CNN model on two datasets with and without hashtags.

With minimal preprocessing done, the proposed CNN model outperformed all the other classifiers under the same condition even though the results are still far away from the known state-of-the-art system (F-score=0.92). We found that CNN is effective for irony detection under various situation.

In the future, we plan to evaluate the proposed method with other classifiers on larger corpus with more preprocessing. Future work will also focus on optimizing the feature extraction of the dataset.

References

[Ghosh 17] Aniruddha Ghosh and Tony Veale, Fracking Sarcasm using Neural Network, Proceedings of

NAACL-HLT 2016, Association for Computational Linguistics (2017)

[Van Hee 18] Cynthia Van Hee, Els Lefever and Veronique Hoste, SemEval-2018 Task 3: Irony Detection in English Tweets, Proceedings of the 12th International Workshop on Semantic Evaluation(SemEval-2018), Association for Computational Linguistics (2018)

[Poria 16] Soujanya Poria, Erik Cambria, Devamanyu Hazarika, Prateek Vij, A Deeper Look into Sarcastic Tweets Using Deep Convolutional Neural Networks, COLING 2016 (2016)

[Kumar 17] Lakshya Kumar, Arpan Somani and Pushpak Bhattacharyya, Approaches for Computational Sarcasm Detection: A Survey, ACM CSUR (2017)

[Ptaszynski 17] Michal Ptaszynski, Juuso Kalevi Kristian Eronen, and Fumito Masui, Learning Deep on Cyberbullying is Always Better Than Brute Force, LaCATODA2017, (2017)

[Van Hee 17] Cynthia Van Hee, Can machines sense irony? Exploring automatic irony detection on social media, University Gent (2017)

[Barbieri 17] Francesco Barbieri, Machine Learning Methods for Understanding Social Media Communication: Modeling Irony and Emojis, Departament DTIC (2017)

[Wu 18] Chuhan Wu, Fangzhao Wu, Sixing Wu, Junxin Liu, Zhigang Yuan and Yongfeng Huang, THU_NGN at SemEval-2018 Task 3: Tweet Irony Detection with Densely Connected LSTM and Multi-task Learning, Proceedings of the 12th International Workshop on Semantic Evaluation(SemEval-2018), Association for Computational Linguistics (2018)

[Vu 18] Thanh Vy, Dat Quoc Nguyen, Xuan-son Vu, Dai Quoc Nguyen, Michael Catt and Michael Trenell, NIHRIO at SemEval-2018 Task 3: A Simple and Accurate Neural Network Model for Irony Detection in Twitter, Proceedings of the 12th International Workshop on Semantic Evaluation(SemEval-2018), Association for Computational Linguistics (2018)

[Tepperman 06] Joseph Tepperman, David Traum, and Shrikanth Narayanan, "YEAH RIGHT": Sarcasm Recognition for Spoken Dialogue Systems, Interspeech 2006, ICSLP (2006)

[Bouazizi 16] Mondher Bouazizi and Tomoaki Otsuki, A Pattern-Based Approach for Sarcasm Detection on Twitter, Digital Object Identifier, IEEE Access (2016)

[Davidov 10] Dmitry Davidov, Oren Tsur and Ari Rappoport, Semi-Supervised Recognition of Sarcastic Sentences in Twitter and Amazon, Proceedings of the Fourteenth Conference on Computational Natural Language Learning, Association of Computational Linguistics (2010)

[Gonzalez-Ibanez 11] Roberto Gonzalez-Ibanez, Smaranda Muresan, and Nina Wacholder, Identifying Sarcasm in Twitter: A Closer Look, Proceedings of the 49th Annual Meeting of the Association For Computational Linguistics, Association for Computational Linguistic (2011)

[Reyes 13] Antonio Reyes, Paolo Rosso, and Tony Veale, A multidimensional approach for detecting irony in Twitter,Lang Resources & Evaluation (2013)

[Liebrecht 13] Christine Liebrecht, Florian Kunneman, and Antal Van den Bosch, The perfect solution for detecting sarcasm in tweets #not, Proceedings of the 4th Wiorkshop on Computational Approaches to Subjectivity, Sentiment and Social Media Analysis (2013)

[Amir 16] ilvio Amir, Byron C. Wallace, Hao Lyu, Paula Carvalho, and Mario J. Silva, Modelling Context with User Embeddings for Sarcasm Detection in Social Media, Proceedings of the 20th SIGNLL Conference on Computational Natural Language Learning (CoNLL), Association for Computational Linguistic (2016)

[LeCun 98] Yann LeCun, Leon Bottou, Yoshua Bengio, and Patrick Haffner, Gradient-Based Learning Applied To Document Recognition, Proc of the IEEE (1998)

[Hochreiter 97] Sepp Hochreiter and Jurgen Schmidhuber, Long Short-Term Memory, Neural Computation 9(8) (1997)

[Baziotis 18] Christos Baziotis, Nikos Athanasiou, Pinelopu Papalampidi, Athanasia Kolovou, Georgios Paraskevopoulos, Mikolaos Ellinas, Alexandros Potamianos, NTUA-SLP at SemEval-2018 Task 3: Tracking Ironic Tweets using Ensembles of Word and Character Level Attentive RNNs, Proceedings of the 12th International Workshop on Semantic Evaluation(SemEval-2018), Association for Computational Linguistics (2018)

[Sasaki 98] Minoru Sasaki and Kenji Kita, Rule-Based Text Categorization Using Hierarchical Categories, Systems, Man, and Cybernetics, 1998 (1998)

[Maynard 14] Diana Maynard and Mark A. Greenwood, Who cares about sarcastic tweets? Investigating the impact of sarcasm on sentiment analysis, LREC 2014 Proceedings (2014)

The 33rd Annual Conference of the Japanese Society for Artificial Intelligence, 2019

A Matrix-Operation Fast Approximated Solution for Logistic Regression with Strong L2 Regularization

Zeke Xie[1], Jinze Yu*[1], and Yanping Deng[2]

[1]The University of Tokyo, Japan
[2]Waseda University

We propose a second-order approximated solution for Logistic Regression with strong L2 regularization based on matrix operations. As training a Logistic Regression model is a convex optimization, researchers have efficient techniques solving it, such as Gradient Descent. But, to our best knowledge, a solution in the form of matrix operations has not been revealed. Generally speaking, matrix operation is faster and more convenient than solving optimization problems. In principle, the matrix-operation approximated solution is only applicable to Logistic Regression with very strong L2 regularization, however, it also works as a pretty good approximated solution in our empirical analysis even when the L2 regularization strength is set in a practical range. This method can also generate good parameter initialization efficiently. The mathematical proof is presented in this paper.

1. Introduction

Logistic regression is the appropriate regression analysis to conduct when dealing with dichotomous (binary) problem. Like all regression analyses, the logistic regression is a predictive analysis. Logistic regression is used to describe data and to explain the relationship between one dependent binary variable and one or more nominal, ordinal, interval or ratio-level independent variables. For machine learning task, Logics Regression model is largely used for unlinear classifiers [Mitchell 05]. As training a Logistic Regression model is a convex optimization, researchers have efficient techniques, such as Gradient Descent, solving it. But, to our best knowledge, a solution in the form of matrix operations has not been revealed. Generally speaking, matrix operation is faster and more convenient than solving optimization problems. In principle, the matrix-operation approximated solution is only applicable to Logistic Regression with very strong L2 regularization, however, it also works as a pretty good approximated solution in our empirical analysis even when the L2 regularization strength is set in a practical range. This method can also generate good parameter initialization efficiently. We propose a second-order approximated solution for Logistic Regression with strong L2 regularization based on matrix operations. The mathematical proof is presented in this paper.

2. Logistic Regression with strong $L2$ regularization

Suppose we are given a data set $X \in R^{n\times m}, y \in \{0, +1\}$ for a binary classification problem. X, a $n \times m$ data matrix, contains n data samples, and each feature vector x^i has m attributes. The target variable vector y is a binary-value column vector with a length of n. Assume we decide to learn a Logistic Regression model mapping from X to y. θ is a column vector parameterizing

Contact: Name, Affiliation, Address, Phone number, Facsimile number, and E-mail address

$$p(y = 1|x) = h_\theta(x) = \frac{e^{-x^T\theta}}{1 + e^{-x^T\theta}} \tag{1}$$

In our discussion, we ignore the intercept term for the simplicity of our notation. The maximum log-likelihood method gives

$$\begin{aligned} l(\theta) &= \sum_{i=1}^{n} lnp(y^{(i)}|x^{(i)}; \theta) \\ &= \sum_{i=1}^{n} (-y_i x^{(i)T}\theta + ln(1 + e^{x^{(i)T}\theta})) \end{aligned} \tag{2}$$

To prevent over-fitting, people often add a regularization term into the log-likelihood. We choose L2-norm regularization and use λ control the strength of regularization, and we obtain the expression of θ as

$$\theta(\lambda) = {}_{\theta\in R^m}(l(\theta) + \lambda\|\theta\|_2^2) \tag{3}$$

where the weight vector θ only depends on λ given a certain data set X, y.

We present the matrix-operation approximated solution first, and then discuss the mathematical proof in next section. With the strong $l2$ regularization limit, the parameter vector θ is a vector with a length of nearly zero, which means $\|\theta\|_2 \to 0$ when $\lambda \to +\infty$. In this situation, only the direction of vector θ still matters. Logistic regression employs the hyperplane $z = \theta x$ to discriminate samples. In logistic regression, $z > 0$ makes positive prediction, and $z < 0$ makes negative prediction. The normalized θ may be written as

$$\begin{aligned} e_\theta(\lambda) &= \frac{\theta(\lambda)}{\|\theta(\lambda)\|_2} \\ e_\theta(\lambda) &= \frac{{}_{\theta\in R^p}(l(\theta) + \lambda\|\theta\|_2^2)}{\|{}_{\theta\in R^p}(l(\theta) + \lambda\|\theta\|_2^2)\|_2} \end{aligned} \tag{4}$$

where the normalization may change the predicted probability but makes no difference on the classification result.

And we present the second-order approximated solution for Logistic Regression as follows:

$$\hat{\theta} \approx (2\lambda I + \frac{1}{4}X^T X)^{-1} X^T (y - \frac{1}{2}) \tag{5}$$

applicable when λ is large, e.g. $\lambda > 1000$. We find out that $\|\theta\|_2 \sim O(\frac{1}{\lambda})$. It indicates the fact that $\|\theta\|_2$ is a first-order small quantity if λ is a first-order large quantity. And its direction vector is given by

$$\hat{e}_\theta \approx \frac{(2\lambda I + \frac{1}{4}X^T X)^{-1} X^T (y - \frac{1}{2})}{\|(2\lambda I + \frac{1}{4}X^T X)^{-1} X^T (y - \frac{1}{2})\|_2} \tag{6}$$

With the limit of strong L2 regularization, we can use the simpler approximated solution

$$\hat{e}_\theta = \lim_{\lambda \to +\infty} \frac{\theta(\lambda)}{\|\theta(\lambda)\|_2} = \frac{X^T (y - \frac{1}{2})}{\|X^T (y - \frac{1}{2})\|_2} \tag{7}$$

where we denote the column vector $(1, \ldots, 1)^T$ as 1.

3. Mathematical Proof

In this section, we organize the proof of the matrix-operation solution. We decide to Taylor expand the regularized log-likelihood function. And we first Taylor expand the second term, a multivariable function, $ln(1+e^{x^T\theta})$, and thus have

$$ln(1 + e^{x^T\theta}) = ln2 + \frac{x^T\theta}{2} + \sum_{i,j=1}^{m} \frac{x_j(x_i - 1)}{8} + O(\theta^3) \tag{8}$$

$$ln(1 + e^{x^T\theta}) = ln2 + \frac{x^T\theta}{2} + \frac{x^T\theta(x^T\theta - 1^T\theta)}{8} + O(\theta^3) \tag{9}$$

using multivariate Taylor Expansion. As we know that θ is a first-order small quantity, we may ignore the three-order small quantities with no impact on the second-order approximated solution. So we write the log-likelihood in the form of

$$l(\theta) = \sum_{i=1}^{n} [ln2 + (\frac{1}{2} - y^{(i)})x^{(i)T}\theta + \frac{x^{(i)T}\theta(x^{(i)T}\theta - 1^T\theta)}{8} + \frac{\lambda}{n}\theta^T\theta + O(\theta^3)] \tag{10}$$

And we have its partial derivative as

$$\frac{\partial l(\theta)}{\partial \theta_j} = \sum_{i=1}^{n} [(\frac{1}{2} - y^{(i)})x_j^{(i)} + \frac{2\lambda}{n}\theta_j + \frac{(2x_j^{(i)} - 1)}{8}x^{(i)T}\theta - \frac{x_j^{(i)}}{8}1^T\theta + O(\theta^2)] \tag{11}$$

Here we assume the data matrix satisfies the mean normalization $\sum_{i=1}^{n} x_j^{(i)} = 0$.

$$\frac{\partial l(\theta)}{\partial \theta_j} = \sum_{i=1}^{n} [(\frac{1}{2} - y^{(i)})x_j^{(i)} + \frac{2\lambda}{n}\theta_j + \frac{1}{4}x_j^{(i)}x^{(i)T}\theta + O(\theta^2)] \tag{12}$$

$$\frac{\partial l(\theta)}{\partial \theta_j} = \sum_{i=1}^{n} [(\frac{1}{2} - y^{(i)})x_j^{(i)} + \frac{2\lambda}{n}\theta_j + \sum_{k=1}^{m} \frac{1}{4}x_j^{(i)}x_k^{(i)T}\theta_k + O(\theta^2)] \tag{13}$$

We ignore high-order small quantities $O(\theta_2)$ in the above system of equations.

$$\frac{\partial l(\theta)}{\partial \theta_j} = \sum_{i=1}^{n} [(\frac{1}{2} - y^{(i)})x_j^{(i)} + \frac{2\lambda}{n}\theta_j + \sum_{k=1}^{m} \frac{1}{4}x_j^{(i)}x_k^{(i)T}\theta_k] \tag{14}$$

We denote the system of linear equations as $M\theta = N$, where $M = 2\lambda I + \frac{1}{4}X^T X$ and $N = X^T(y - \frac{1}{2})$. It simply implies that the second-order approximated matrix-operation solution for Logistic Regression with strong L2-regularization is

$$\hat{\theta} \approx (2\lambda I + \frac{1}{4}X^T X)^{-1} X^T (y - \frac{1}{2}) \tag{15}$$

And its direction vector is given by

$$\hat{e}_\theta \approx \frac{(2\lambda I + \frac{1}{4}X^T X)^{-1} X^T (y - \frac{1}{2})}{\|(2\lambda I + \frac{1}{4}X^T X)^{-1} X^T (y - \frac{1}{2})\|_2} \tag{16}$$

With the limit of strong L2 regularization, we can use the simpler approximated solution

$$\hat{e}_\theta \approx \frac{X^T (y - \frac{1}{2})}{\|X^T (y - \frac{1}{2})\|_2} \tag{17}$$

4. Summary and Conclusion

Logics Regression model is largely used for unlinear classifiers. To solve a Logics Regression model, the efficient way is to use numeric solver such as gradient descent. In this paper, we proposed a Matrix-Operation Fast Approximated Solution for Logistic Regression with Strong L2 Regularization. We conclude that the proposed solution is much faster than the conventional solution. And, in practice, the proposed solution works very closely to the conventional solution.

References

[Mitchell 05] T. Mitchell, Generative and Discriminative Classifiers: Naive Bayes and Logistic Regression. Draft Version, 2005

The 33rd Annual Conference of the Japanese Society for Artificial Intelligence, 2019

Final Sample Batch Normalization For Quantized Neural Networks

Joel Nicholls Atsunori Kanemura

LeapMind Inc.

We outline and conduct an empirical study into the effectiveness of a modified version of batch normalization, for combination with quantized neural networks. The proposed method uses only the statistics of the final batch for determining the batch normalization operation at the inference stage. This contrasts with the usual implementation, where population statistics are accumulated over many batches of training. The proposed and existing methods are compared over several models and datasets, which span both classification and object detection tasks. Overall, the proposed method exceeds the value and consistency of test performance compared to the usual batch normalization, in the case of quantized networks. For floating point precision networks, the usual method is best.

1. Introduction

Both batch normalization and quantization are widely used in the deep learning community for improving the training and inference speed of neural networks, respectively. However, it has been recently observed that the training of quantized neural networks can suffer from fluctuating performance, which is related to the way that batch normalization is implemented [8].

Batch normalization has for some time been an important technique in the deep learning toolkit. Primarily, batch normalization is used to accelerate the training of deep neural networks. Some argue that it eases training by reducing internal covariate shift [7], while others say that it smooths the loss landscape [13]. Either way, this technique has been empirically useful for deep learning practitioners to improve training.

Quantization is used for streamlining neural network models. Deep learning typically results in large models that are computationally expensive in the inference stage (e.g. to make predictions on new data). Quantized neural networks deal with this deficiency by greatly reducing the precision of the majority of parameters and computations involved, without significantly hurting the accuracy of the model.

To be explicit, here we are talking about very low precision, where the neural network must be trained in a quantization-aware way in order to give good performance. Weights and activations can be only a few bits [16], or even binary [3], to rapidly accelerate inference.

Prompted by the issue of fluctuating test performance of quantized neural networks and its relation to batch normalization, we have undertaken investigations on how to better combine these two techniques. In particular, we find that the quantized neural network has both higher test accuracy and is more consistent (has less jitter), when the statistics of only the most recent batch are used for determining the batch normalization used at inference.

This is in contrast to the standard method for batch normalization in floating point precision neural networks, which uses population statistics accumulated over many batches. We refer to our proposed method as *final sample batch normalization*.

Contact: Joel Nicholls, LeapMind Inc. Tokyo 150-0044, `joel@leapmind.io`

2. Method

For the neural network model and quantization functionality, we use the Blueoil framework [6]. Blueoil is based on TensorFlow [1] and provides convolutional neural networks in both floating point and quantized precision.

Within the Blueoil framework (and within Tensorflow also), there is an argument to the batch normalization operation called `decay`, which is a hyperparameter that controls how batch normalization statistics are accumulated.

The default batch normalization `decay` hyperparameter of Blueoil is 0.99. This value is close to 1, which means that population statistics are being used. Furthermore, both PyTorch [10] and Tensorflow [14] use population statistics by default. We will abbreviate this (standard) implementation of batch normalization as *BN-pop*. Throughout the experiments, BN-pop will refer to neural network models with `decay` of 0.99.

Our proposed modification to batch normalization can be easily implemented in Blueoil using a `decay` hyperparameter of 0.0. This uses the final batch statistics, so we will abbreviate the method as *BN-final*. Through empirical comparisons, we show that for quantized neural networks, our proposed BN-final performs equally well or better than BN-pop.

The quantized models of Blueoil use a combination of techniques from the literature on quantized networks [2, 11, 16]. For all experiments in this paper, the quantized neural networks have 2 bit activations and 1 bit weights, except for the first and last layers.

To evaluate the effectiveness of our proposed final sample batch normalization, we use classification and object detection models. There are more specific hyperparameter details in Appendix A. We compared BN-final and BN-pop over floating point precision and quantized models for 3 classification datasets (CIFAR-10, CIFAR-100 [9], and Caltech 101 [5]), and 1 object detection dataset (PASCAL VOC [4]). Making a range of comparisons is important to empirically establish the usefulness of our proposed change to the batch normalization method.

3. Results

The main thrust of the results is the empirical comparsion between the existing method BN-pop, and our proposed modification BN-final. Therefore, multiple training runs over various datasets were made and the test performance was measured. For classification, top-1 accuracy was used. For object detection, mean average

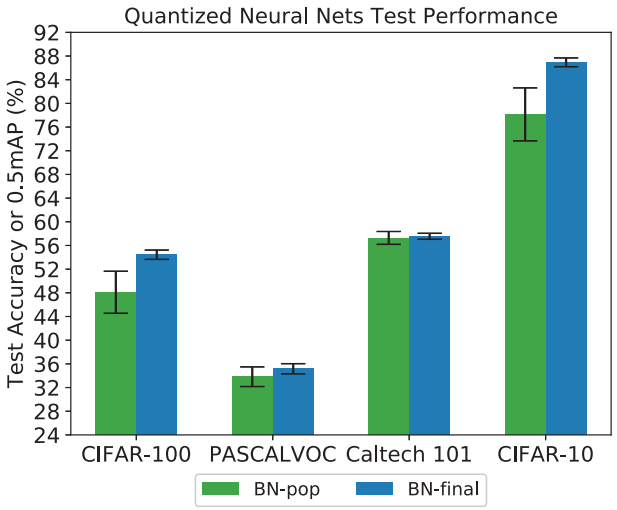

Figure 1: Test accuracy and 0.5mAP for existing batch normalization (BN-pop) and proposed batch normalization (BN-final) on quantized neural network models.

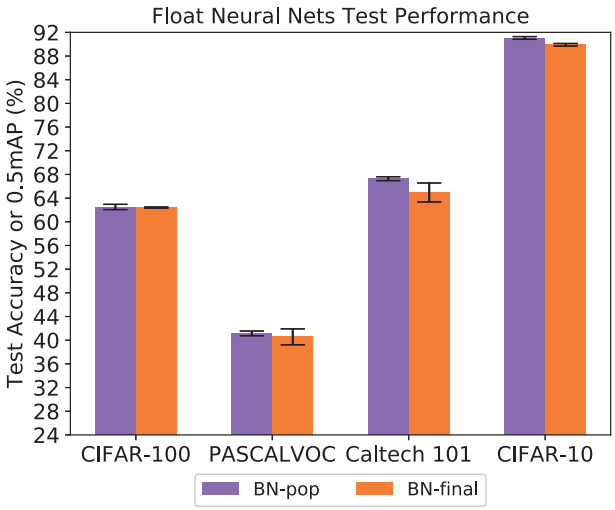

Figure 2: Test performance compared between existing BN-pop and proposed BN-final, for floating point precision neural networks.

precision (mAP) with 0.5 overlap threshold was used.

3.1 Main comparisons

The comparisons for quantized neural networks are given in Figure 1. In all cases, BN-final gave higher test performance than BN-pop. The CIFAR dataset shows the greatest difference.

The same comparisons are shown for floating point precision neural networks in Figure 2. For this set, BN-pop gives higher test performance. The order of preference of batch normalization method is reversed.

This suggests that the proposed BN-final should be used for quantized networks, but the usual BN-pop is better for floating point precision networks. Many of the investigations on batch normalization in the literature have focused on floating point precision networks. BN-final is not effective on floating point precision networks, which is a possible reason that it had not been previously explored.

3.2 Calculation of error bars

Here, we give more details about the values and error bars shown in Figure 1, Figure 2, and Figure 4. Two independent training runs were conducted for each experiment. However, two data points are not enough to get meaningful error bars.

Therefore, for each experiment, we took the last 3 test accuracies from the two training runs. These 6 data points were used to calculate the mean and standard deviation for the experiment.

The test steps are separated by only 1 000 train steps. Therefore, the last 3 test accuracies are not totally independent. But, they do give a rough idea of the fluctuations that can be expected. The error bars shown in the Figures are therefore generally an underestimate of the true standard deviation that would be obtained if all data points were completely uncorrelated.

Another point to note is that by taking the last 3 test steps, the model is still being trained during that time. There is a possibility that the performance is still increasing due to the training. However, by eyeballing the plots of TensorFlow training, the test accuracy has already levelled off at that late stage of training.

3.3 Test accuracy curve

Looking at the test accuracy of an example model over the training run, as in Figure 3, it can be seen that BN-final allows for much smoother generalization accuracy, consistently over the whole training process.

The accuracy on the train dataset was not shown because the two methods (BN-pop and BN-final), both act in the same way on the training dataset. It is worthwhile to note that the point of the final sample batch normalization method is to allow the trained model to transfer to an inference model in a better way than the existing batch normalization, for quantized networks.

In addition to the mean value of the test accuracy, the smoothness of test accuracy over the training of quantized neural networks is a positive point. It results in more consistent generalization accuracy, even if the deep learning practitioner decides to finish training early. The error bars shown in Figure 1 for various datasets also indicates more consistent test accuracy for BN-final, in comparison to BN-pop.

3.4 Additional quantizations

For classification on the CIFAR-100 dataset using quantized neural networks, two additional model versions were used. These other versions implement quantization in slightly different ways, giving a broader view on the compatibility between quantization and final sample batch normalization. They are shown in Figure 4.

Firstly, `usual_quant` makes use of channelwise quantization (this is the same as was shown for the CIFAR-100 category in Figure 1). Secondly, the network labelled `layerwise_quant` uses layerwise scaling factors. This can be useful to reduce the number of floating point precision computations in the neural network even further than channelwise quantization.

Thirdly, the network `divide255_quant` uses 8 bit inputs for the first convolutional layer. This differs with the usual kind of quantized neural network, which uses image standardization to provide floating point precision inputs to the first convolutional layer. The benefit of using `divide255_quant` is that the required precision of the first layer convolution is lowered, resulting in more efficient inference.

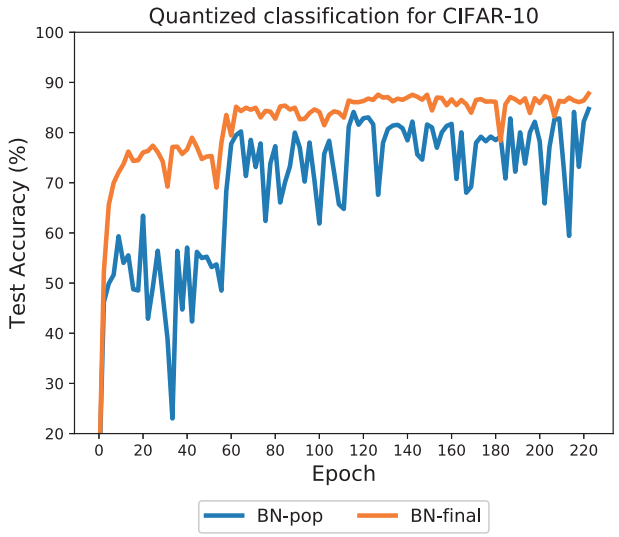

Figure 3: Time series plot for the test accuracy of the quantized neural network against epochs of training completed. Both BN-pop and BN-final are compared, for classification on the CIFAR-10 dataset. In this experiment, the batch size was 100, with 45 000 training images. The test accuracy was calculated once every 1 000 training steps, corresponding to once every $2.\overline{2}$ epochs, where the overline indicates a repeating decimal.

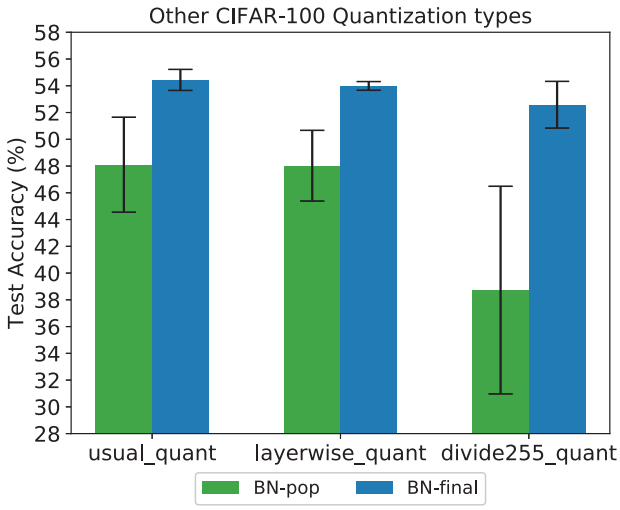

Figure 4: Test accuracy compared between BN-pop and BN-final, for different methods of quantization. In each case, the network performs classification on the CIFAR-100 dataset.

The main point to note from Figure 4 is that the `divide255_quant` network does a lot worse than the other two networks, when using BN-pop. Instead, if using BN-final, all three networks have similar performance.

This suggests that `divide255_quant` is especially sensitive to the change between training model and inference model. One possible reason for why BN-final improves this network so significantly in the inference is that it allows for more stability with respect to the inputs. The results here are not enough to fully support this kind of hypothesis, which is an area for further work.

4. Related works

Several other works have tampered with the standard batch normalization. For example, instance normalization [15] uses the batch normalization behaviour of training for the inference stage, averaging over only the spatial dimensions of the batch in order to improve on other works. Their batch normalization at inference is not an affine transformation, so they have increased the computational cost of inference to improve style transfer. Our motivation and implementation are quite different, since we are interested in increasing the efficiency of deep learning.

Some works also consider batch normalization in the context of quantized neural networks. Courbariaux et al. [3] implement an approximate shift-based batch normalization to decrease the computational effort by using bit shifting. This technique saves computation in the training, and seems to be compatible with final sample batch normalization. We have not tested this combination because our main interest is in improving speed and accuracy of inference. In the inference stage, the affine transformation of batch normalization can be folded into scaling factors and layer bias, resulting in only a small computation cost relative to the convolutional layers.

Finally, Krishnamoorthi [8] implements a modification called batch normalization freezing. After a certain number of training steps, the updates of batch normalization statistics are frozen and the batch normalization behaviour during training switches to that of the inference stage. In this sense, the batch normalization becomes an affine transformation after the freeze step (which is a hyperparameter). This method reduces jitter by a large amount. However, the batch normalization is effectively switched off (frozen), at the later steps of training. It is hard to make a direct comparison with their work without more experiments because their whitepaper shows the effect of batch normalization on 8 bit weights and activations, whereas our experiments involve 1 bit weights and 2 bit activations.

5. Conclusion

For float point precision networks, there is no benefit in changing to BN-final. If anything, BN-pop is better. However, for quantized networks, BN-final gives higher and more consistent test accuracy. Moreover, using BN-final does not add any computational overhead compared to the usual method of batch normalization. This makes BN-final an excellent candidate for reducing the gap in performance between quantized and floating point precision neural networks.

It seems that both the CIFAR dataset and the `divide255_quant` network benefit especially well from BN-final. We hypothesise that this dataset and network have something in common that causes them to benefit most from BN-final: in both these cases the forward function of the neural network model is a sensitive (easily perturbed) function of its inputs. The CIFAR dataset provides very low resolution inputs. The `divide255_quant` network enables higher efficiency, but has a more sensitive first layer.

There is a difference between the forward functions in training and inference due to the change in batch normalization behaviour to an affine transformation. This increases the efficiency for inference, but it generally causes a decrease in test accuracy. Therefore, one possible reason for the success of BN-final is that it reduces the

difference between the forward function in training and inference. This gives the most benefit in cases (such as those mentioned in the previous paragraph), where the forward function is a sensitive function on its inputs. Here is an exciting direction for possible future research.

A major test case that we have missed out is comparison for the ImageNet [12] dataset. It is an important case because it is often used as pretraining for other datasets, and is used in the deep learning literature as a difficult and realistic problem. However, there was not sufficient time to gather results on this dataset for the current paper.

Another point to note about our proposed method is the case where some batches contain outlier data, are imbalanced, or especially small. In the case of a dataset where some batches contain poor quality outlier data, it is possible that the final batch is not representative of the overall dataset. This could result in low test accuracy.

One possible partial remedy is to save the model at multiple steps near the end of training, and choose the best model based on validation accuracy. When the batch size is imbalanced or small, the single batch statistics will naturally be less consistent between batches. This may exacerbate the issue of imbalanced datasets.

A Extra detail on experimental setup

Here we give further explanation on hyperparameters, as well as the method for constructing the train and test datasets used in the experiments.

CIFAR-10: 45 000 images were used for the train dataset and 10 000 images for the test dataset. The image size was 32×32 pixels. We used 100 000 train steps, `divide255_quant`, and channelwise scaling factors. The network in Blueoil is `LmnetV1Quantize`. For the floating point precision version, network `LmnetV1` and scaling `PerImageStandardization` were used.

CIFAR-100: 45 000 images were used for the train dataset and 10 000 images for the test dataset. The image size was 32 × 32 pixels. We used 100 000 train steps. We used `PerImageStandardization` and channelwise scaling except where stated. For the quantized version, we used the network `LmnetV1Quantize`, and for floating point precision version `LmnetV1`.

Caltech 101: 7 809 images were used for the train dataset and 868 images for the test dataset. For Caltech 101 experiments, we trained without augmentation. We used 10 000 steps, `PerImageStandardization`, `Image_Size` = 128, and `batch_size` of 64.

PASCALVOC: The test dataset consists of 4 952 images from PASCAL VOC 2007. The train dataset consists of 16 551 images from a mix of the remaining images of PASCAL VOC 2007 and 2012. We resize the images to 320 × 320 pixels. We used `divide255_quant`, channelwise scaling, and 100 000 train steps. In Blueoil, the network is called `LMFYoloQuantize`. The config file is `lm_fyolo_quantize_pascalvoc_2007_2012.py`.

Acknowledgements

We thank Hiroyuki Tokunaga and Takuya Wakisaka from LeapMind Inc. for their useful advice on this paper.

References

[1] Martín Abadi et al. TensorFlow: Large-scale machine learning on heterogeneous systems, 2015. Software available from `https://www.tensorflow.org/`.

[2] Zhaowei Cai, Xiaodong He, Jian Sun, and Nuno Vasconcelos. Deep learning with low precision by half-wave Gaussian quantization. In *IEEE Conference on Computer Vision and Pattern Recognition (CVPR)*, pages 5406–5414, July 2017.

[3] Matthieu Courbariaux, Itay Hubara, Daniel Soudry, Ran El-Yaniv, and Yoshua Bengio. Binarized neural networks: Training deep neural networks with weights and activations constrained to +1 or −1. *arXiv:1602.02830 [cs.LG]*, 2016.

[4] Mark Everingham, Luc Van Gool, Christopher K. I. Williams, John Winn, and Andrew Zisserman. The Pascal Visual Object Classes (VOC) challenge. *International Journal of Computer Vision*, 88(2):303–338, September 2009.

[5] Li Fei-Fei, Rob Fergus, and Pietro Perona. Learning generative visual models from few training examples: An incremental Bayesian approach tested on 101 object categories. In *CVPR Workshop on Generative Model Based Vision*, 2004.

[6] LeapMind Inc.˙ Blueoil. `https://github.com/blue-oil/blueoil`, 2018. [Online; accessed 5-Feb-2019].

[7] Sergey Ioffe and Christian Szegedy. Batch normalization accelerating deep network training by reducing internal covariate shift. In *International Conference on International Conference on Machine Learning (ICML)*, 2015.

[8] Raghuraman Krishnamoorthi. Quantizing deep convolutional networks for efficient inference: A whitepaper. *arXiv:1806.08342 [cs.LG]*, June 2018.

[9] Alex Krizhevsky. Learning multiple layers of features from tiny images. Technical report, University of Toronto, 2009.

[10] PyTorch. Normalization layers, torch.nn, pytorch documentation. `https://pytorch.org/docs/stable/nn.html#normalization-layers`. [Online; accessed 5-Feb-2019].

[11] Mohammad Rastegari, Vicente Ordonez, Joseph Redmon, and Ali Farhadi. XNOR-Net: ImageNet classification using binary convolutional neural networks. In *European Conference on Computer Vision (ECCV)*, pages 525–542, 2016.

[12] Olga Russakovsky et al. ImageNet Large Scale Visual Recognition Challenge. *International Journal of Computer Vision*, 115(3):211–252, 2015.

[13] Shibani Santurkar, Dimitris Tsipras, Andrew Ilyas, and Aleksander Madry. How does batch normalization help optimization? *arXiv:1805.11604 [stat.ML]*, May 2018.

[14] TensorFlow. tf.contrib.layers.batch_norm. `https://www.tensorflow.org/api_docs/python/tf/contrib/layers/batch_norm`. [Online; accessed 5-Feb-2019].

[15] Dmitry Ulyanov, Andrea Vedaldi, and Victor Lempitsky. Instance Normalization: The Missing Ingredient for Fast Stylization. *arXiv:1607.08022 [cs.CV]*, July 2016.

[16] Shuchang Zhou, Yuxin Wu, Zekun Ni, Xinyu Zhou, He Wen, and Yuheng Zou. DoReFa-Net: Training low bitwidth convolutional neural networks with low bitwidth gradients. *arXiv:1606.06160 [cs.NE]*, June 2016.

International Session | International Session | [ES] E-5 Human interface, education aid

[2A3-E-5] Human interface, education aid: chance discoveries

Chair: Akinori Abe (Chiba University), Reviewer: Naohiro Matsumura (Osaka University)

Wed. Jun 5, 2019 1:20 PM - 2:20 PM Room A (2F Main hall A)

The room is connected with B.

[2A3-E-5-01] How to enable the utility data under the lower sampling rate and less attribute for making smart cities

○Eiji Murakami[1] （1. Azbil kimmon Co.,Ltd.）

1:20 PM - 1:40 PM

[2A3-E-5-02] Proposal of Context-aware Music Recommender System Using Negative Sampling

○Jin-cheng ZHANG[1], Yasufumi TAKAMA[1] （1. Tokyo Metropolitan University）

1:40 PM - 2:00 PM

[2A3-E-5-03] Entropy-based Knowledge Space Visualization for Data-driven Decision Support

○Qi Wang[1], Teruaki Hayashi[1], Yukio Ohsawa[1] （1. The University of Tokyo）

2:00 PM - 2:20 PM

The 33rd Annual Conference of the Japanese Society for Artificial Intelligence, 2019

How to enable the utility data under the lower sampling rate and less attribute for making smart cities

Eiji Murakami[*1]

[*1] Azbil Kimmon Co., Ltd.

This paper discusses the utility data analysis under the different sampling rate makes variety of result. Otherwise, we use the high sampling data and much attributes, we start to think combination of the data which haven't measured at same time of utility data has measured. To come up the idea of data combination, the method of idea creation should employ for making the innovation. This paper will show the difficulties and some of the existing method to overcome them.

1. Introduction

The research for the utility data analysis has been conducted on electricity consumption of electric power meters, where is mainly in Europe. In 2019, Internet of things (IoT) of gas and water meter will be started using 4G LTE of mobile communication technology in Japan.

As a result of employing the IoT technology, the measuring consumption of utility data which has been conventionally done every once a month or every two months, now it could carry out at least every day and even more frequent to measure utility data every hour if necessary. In this paper, we show an example of utility data and discuss how difficult to analyze if the sampling rate is lower and the sampling data is reduced. We also discuss how difficult will be made in analyzing utility data with less attribute data. Finally, I will describe what is expected in the future when utility data is collected under the lower sampling rate and less attribute data.

2. Utility data analysis

2.1 Data sampling rate

The data sampling rate is important in utility data analysis. Table 1 shows the relationship between sampling rate and acquired data. When the sampling rate is 1 hr - 15 min then acquisition data is visualized, it becomes a only bar chart showing the result that is consumption of utility in each time span.

Data Sampling Frequency	1 hr – 15 min	1 min – 1 sec	10Hz – 2KHz	10KHz – 15KHz	> 1MHz
Data Appearance	1 hr PG&E	<1 min Sampling	Similar to adjacent graphs	KHz Sampling	MHz Sampling

Table1 Sampling rate and graph pattern, cited from [Armel11]

When the sampling rate is 1 min - 1 sec then acquired data is visualized, it becomes a line graph with sampling data. It can be estimate the consumption of utility, and could be inferred the purpose from gas or water service had been consumed in the consumption pattern.

2.2 Utility data of 1 min sampling rate

Fig 1 is a graph of the power consumption in the electric power meter with one minute period

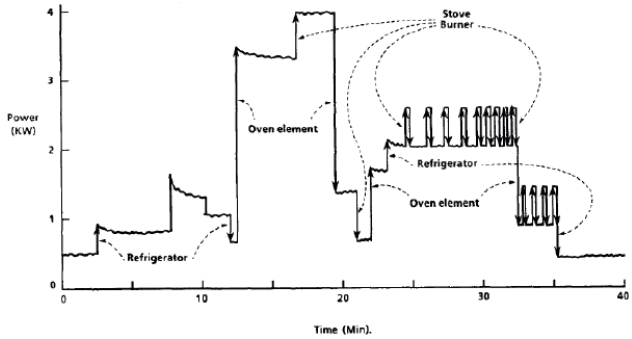

Fig 1 One min sampling rate and graph pattern, cited from [Armel11]

According to the Fig1, it can be categorized by the pattern of energy consumption for all appliances. This is an example where it is feasible if the data sampling rate is 1 minute or less with having appropriate technology.

3. Study for data analysis of REAL restaurant

Fig 2 shows an example of measuring utility data, temperature and humidity at a restaurant.

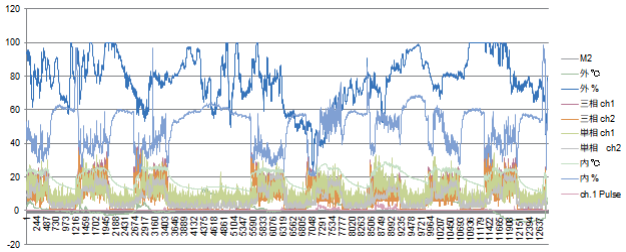

Fig 2 REAL restaurant various data

The meaning of Legend (symbol) of the graph is as follows. M2 is gas consumption, 外 is outdoor, ch1 and ch2 are electrical

Contact: Eiji Murakami, Azbil kimmon Co.,Ltd., 1-14-3 Kita-Otsuka, Toshima-ku Tokyo, 170-0004

power consumption reading of power meter, 内 is inside (room). The horizontal axis shows elapsed time from the start of measurement in seconds. In the vertical axis, the measured value was normalized between 0% and 100%. Ch1.pulse is the human sensor value installed at the entrance of the restaurant. All the data has sampled by 1 minute. So we can measure the gas consumption, outdoor temperature and humidity, room temperature and humidity, power consumption and human sensor value by each one minute.

The one analysis method is observing the graph pattern. The other analysis is we employ statistical method as follows, correlation analysis, factor analysis, and principal component analysis. From principal component analysis, the following facts are discovered.

The combination of gas consumption, indoor temperature and single-phase electrical power consumption ch 1 have same behavior (in principal component analysis, if the values of principal component are near same, these variable belong to same category). The combination of the single-phase electrical power consumption ch 2 and the three-phase electrical power consumption ch 1 and ch 2 have the same behavior according to result of principal component. Outdoor temperature and human sensor value are correlated.

On the other hand, outdoor humidity and room humidity have no correlation.

One hypothesis has been obtained, paying attention to the correlation between the outdoor temperature and the value of the human sensor, there is a tendency for customer wants to come restaurant more often when outdoor temperature gets low in winter season. As a hypothesis verification, this phenomenon can be explained from the fact that this restaurant is a ramen shop located in Sapporo.

4. Data with low sampling rate and less attribute

Section 3 shows the example where there are sufficient attribute data at high sampling rate. In section 3, let us consider a case where the sampling rate has changed from one minute to one hour. When the sampling rate is 1 minute, the graph pattern is a line graph in plotting measured values of each sample and connecting each sample with a line. When the sampling rate is 1 hour, the measured value of each sample is represented by a bar graph. The fluctuation of the sample value generated within one hour is invisible on the graph. Any changes in sample values generated within one hour are unknown. This is a specific harmful effect when the sampling rate changes to a lower rate.

Next, let us consider the case where available attribute data decreases in section 3. In section 3, we applied statistical methods to all data and discovered that there is a correlation between outdoor temperature and human sensor of restaurant door by counting how many people comes in with principal component analysis. The obtained findings are natural for ramen shop in Sapporo, but it is not easy to choose the limited sampling data for measuring with limited sensor from the beginning, rather than try and error exploratory way. Also it is not easy for hypothesis verification by one shot analysis with limited data.

5. Discussion and future work

[Toki 18] solved the vehicle routing problem of LP gas cylinder which is a special case of travelling salesman problem (TSP). The necessary data for the vehicle routing problem is the delivery address and delivery date. By the gas meter IoT, gas consumption data can be obtained every day, so we can determine the delivery date to minimize the delivery cost. Once the delivery date is determined, sort out the all address of the LP gas consumer then full charged LP gas cylinder should be delivered at the same day which is today. Then search the optimal the delivery route for all customer location.

The necessary data for vehicle routing to deliver the LP gas cylinder is only gas consumption and customer's address. Now we think about other applications that could enrich our living life with restricted information.

Fig. 3 shows an example of adding the certain color on map after the gas consumption has been calculated for each customer. There could be various meanings of the color, for example it can changes to red when the gas consumption is high. We know the whole volume of the LP gas cylinder, the remaining gas volume of the LP gas cylinder can be calculated from the gas consumption volume. If the remaining gas is very low volume, we can change the color like red on map which might have special meaning such as energy supply for customer has been critical condition at the potential risk of LP gas company. The meaning of area which is colored on map may be varied depending on the application. However, the data to use is the same as [Toki 18], and only difference is adding the geographic information. The applications that use geographic information in this way called Geographic Information System (GIS).

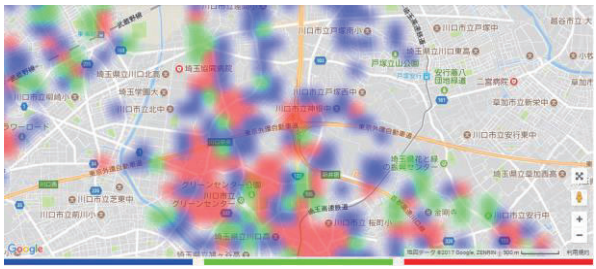

Fig 3 Example of several colors on map (The map copyright belongs to Google and ZENRIN)

The future work would be using utility data obtained by low sampling rate like [Toki 18] uses daily gas consumption and use few number of attribute data, otherwise using the geographical information have society enrich by application or service [Kumar14] under the restricted information should be studied more. Also the methodology for create the innovation like IMDJ [Ohsawa 17] which can share the same goal as I explain just before would like to apply.

References

[Armel11] Carrie Armel, Energy Disaggregation, Precourt Energy Efficiency Center, Stanford, 2011

[Kumar14] TM Vinod Kumar, Geographic Information System for Smart Cities, Copal Publishing Group, 2014

[Ohsawa17] Yukio Ohsawa,Teruaki Hayashi,Masahiro Akimoto,Noriyuki Kushiro,Jun Nakamura,Masahiko Teramoto, MoDAT Market of Data, Kindaikagaku publisher, 2017

[Toki18] Soma Toki,Naoshi Shiono,Eiji Murakami,A practical approach to the vehicle routing problem in cylinder gas distribution, INFORMS Annual meeting, 2018

The 33rd Annual Conference of the Japanese Society for Artificial Intelligence, 2019

Proposal of Context-aware Music Recommender System Using Negative Sampling

Jin-cheng ZHANG*1 Yasufumi TAKAMA*1

*1 Graduate School of System Design, Tokyo Metropolitan University

This paper proposes a method for recommending music items considering listeners' context information. Recently, users can enjoy music easily regardless of time and a place due to evolution of online music services such as Spotify. However, it is difficult for us to find appropriate music items from enormous resources. On the other hand, because of listening style and characteristic of music items, music items do not usually have explicit rating. Therefore, implicit feedback such as playing count has been popular to construct recommender systems. As additional information, this paper considers listeners' context. The proposed method employs FMs (Factorization Machines), in which the context information is treated as factors. Negative sampling is applied to reduce the number of negative samples (music items a user has yet to be listened). The effectiveness of the proposed method and the effect of negative sampling are shown with an offline experiment.

1. Introduction

This paper proposes a method for recommending music items considering listeners' context information. Recently, with the development of communication technology and portable electronic devices, online music services such as Spotify, AWA, Amazon Music has grown rapidly and become popular in a short period of time. The number of users who utilize online music services has exceeded 17 millions on 2017 in Japan.

To help users find their favorite music items, music recommendation systems have been studied. One of the challenges of music recommendation is that explicit feedback such as rating is not usually available due to the way of listening to music and characteristic of music items. Therefore, existing music recommender systems often use implicit feedback such as playing count[Koren 08]. Another challenge is that the influence of users' context while listening to music on their preference is higher than other domains. By extending the conventional matrix factorization approach, a tensor factorization method can consider context axis in addition to user and item axes [Adomavicius 11]. However, it is difficult to optimize the use of contexts due to high time complexity. Therefore, this paper employs Factorization Machines (FMs), in which listeners' contexts are used as factors. It is shown that FMs can flexibly consider the interaction of users, items, and context with relatively low time complexity [Rendle 12].

As FMs needs both positive and negative samples, LEs (Listening events) are used as positive samples, and music items a user has yet to be listened are used as negative samples. To reduce the number of negative samples, this paper employs negative sampling. Effectiveness of the proposed method is shown by comparing it with wALS (weighted Alternating Least Squares). The effect of negative sampling is also investigated.

Contact: Yasufumi TAKAMA, Graduate School of System Design, Tokyo Metropolitan University, ytakama@tmu.ac.jp

2. Related work

2.1 Implicit collaborative filtering

Koren et al. proposed a collaborative filtering method called wALS for implicit feedback datasets[Koren 08]. As an implicit feedback such as play count is not as reliable as explicit rating, it is difficult to make recommendation by solving the same loss function as methods based on Matrix Factorization. Eq. (1) shows the loss function of wALS,

$$Ł(x_u, y_i) = \sum_{u,i} c_{u,i}(p_{u,i} - x_u^T y_i)^2 + \lambda(\sum_u ||x_u||^2 + \sum_i ||y_i||^2), \quad (1)$$

where x_u, y_i is the latent factors of users and items, $p_{u,i}$ is the element of user-item binary matrix representing whether or not a user u played a music item i. $c_{u,i}$ is the element of confidence matrix: $c_{u,i} = 1 + \alpha r_{u,i}$, where α is a hyperparameter and $r_{u,i}$ is the play count of i by u.

2.2 Factorization Machines

FMs[Rendle 12] can not only learn the latent factors of user and items like Matrix Factorization methods, but also flexibly consider the interaction of users, items, and any other features with relatively low time complexity. The model equation for a FMs of degree $d = 2$ is defined as:

$$\hat{r}(\boldsymbol{x}) := \omega_0 + \sum_{i=1}^{n} \omega_i x_i + \sum_{i=1}^{n} \sum_{j=i+1}^{n} (\sum_{f=1}^{k} v_{i,f} \cdot v_{j,f}) x_i x_j, \quad (2)$$

where $x_i \in \boldsymbol{x}$ is rating, which corresponds to a LE in this paper, ω_0 is the global bias, ω_i is the strength of x_i. $\sum_{f=1}^{k} v_{i,f} \cdot v_{j,f}$ shows the interaction of x_i and x_j with k factors. The $\hat{r}(\boldsymbol{x})$ are the prediction values for all LEs.

3. Proposed Method

This paper considers season, time zone, time stamp and mother language when a user listened music item as context information. Those are used as additional factors $v_{i,f}$.

We set $r(x_i) = 1$ for positive samples, and $r(x_i) = 0$ for negative samples.

Regarding all music items a user has yet to be listened as negative is a naive method. Although it could be effective in Matrix Factorization method such as wALS, the number of negative samples becomes huge, and cause a problem of time complexity when training a model by FMs.

To solve the problem, this paper employs negative sampling, which selects a part of music items that a user has yet to be listened as negative samples. In particular, this paper proposes to select negative samples according to the hypothesis that **if a music item is not played by a user in some context, s/he would not be interested in it in that context.** Because a negative sample is not real LE, it is not used in evaluation process for ensuring the fairness.

4. Experiment

Dataset We use nowplaying-RS dataset[*1] that is generated from all tweets tagged by hashtag #nowplaying of 2014. This dataset also includes above-mentioned users' listening context. For avoiding the influence of tweet bot and extremely not active users, we removed the users who listened less than 10 and larger than 5000 music items from the dataset. After preprocessing, the number of users, music items, and LEs are 18,946, 22,023, and 1,835,993, respectively.

Evaluation metric This paper employs MPR (Mean Percentage Ranking) (Eq. (3)) to evaluate the performance of each method. $rank_{u,i}$ represents the percentile-ranking of a music item in the recommend list, and $r_{u,i}$ corresponds to $r(x_i)$ in Eq. (2): $r_{u,1} = 1$ if a user u actually listened a music item i, otherwise 0. Smaller MPR indicates better performance.

$$MPR = \frac{\sum_{u,i} r_{u,i} \times rank_{u,i}}{\sum_{u,i} r_{u,i}} \tag{3}$$

Experiments are done with 5-fold cross-validation based on time series. Experiments are repeated 5 times, and use t-test to confirm whether or not significant difference to wALS is observed. Used parameters are: $\alpha = 250$, $\#latent\ factor = 15$, $\lambda = 0.05$ for wALS by hyperparameter tunning, and $k = 3$ for the proposed method.

Table 1 shows MPR with the p-value among wALS, UO (user-oriented negative sample)+FMs and UO+FMs+Contexts. Table 1 shows that UO+FMs is more effective than wALS, and its performance is improved by introducing context information.

Fig. 1 shows the MPR against the ratio of negative samples to positive samples (denoted by k). It is observed that setting k larger than 2 can obtain more effective result than wALS. Although MPR decreases as k increases, the effect is gradually reduced. The computation time when $k = 2$ and 6 are 688(s) and 2142(s) per fold in cross-validation, respectively. This mean that k should be set by considering the balance between time complexity and accuracy of recommendation.

Table 1: Experimental result

p-value	wALS	UO+FMs	UO+FMs +Contexts
wALS	-	2.363e-05	5.368e-07
UO+FMs	2.363e-05	-	0.0003
UO+FMs +Contexts	5.368e-07	0.0003	-
MPR	0.1092	**0.1041**	**0.1017**

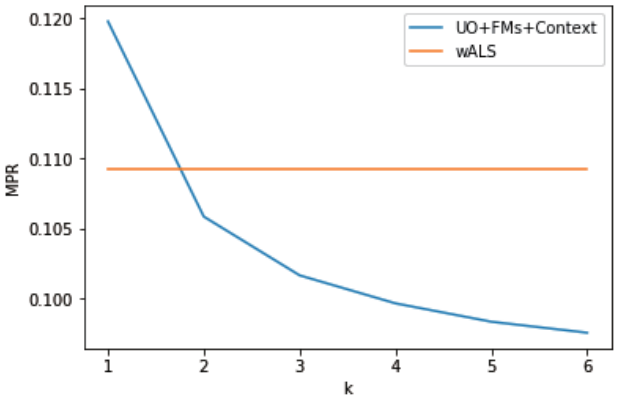

Figure 1: Effect k on MPR

5. Conclusion and Future work

This paper proposes a method for recommending music items considering listeners' context information. An experimental result shows the proposed method is more effective than wALS. In future work, we will investigate other negative sampling methods to improve performance, and evaluate the proposed method with other metrics such as diversity and novelty.

References

[Koren 08] Hu Yifan, Yehuda Koren, and Chris Volinsky, "Collaborative filtering for implicit feedback datasets," ICDM'08, pp.263-272, 2008.

[Rendle 12] Rendle Steffen, "Factorization machines with libfm," ACM Transactions on Intelligent Systems and Technology, Vol.3, No.3, Article No.57, 2012.

[Adomavicius 11] Adomavicius Gediminas and Alexander Tuzhilin, "Context-aware recommender systems," Recommender systems handbook, pp.217-253, 2011.

*1 http://dbis-nowplaying.uibk.ac.at/#nowplayingrs

The 33rd Annual Conference of the Japanese Society for Artificial Intelligence, 2019

Entropy-based Knowledge Space Visualization for Data-driven Decision Support

Qi Wang Teruaki Hayashi Yukio Ohsawa

Department of Systems Innovation, School of Engineering, The University of Tokyo

This paper describes an entropy-based visualization for extracting utilization value of data in data-driven decision support. There is an increasing demand for data utilization from different domains to create new businesses or solve existing problems. Many researches focus on extracting similar data to create business value. However, data utilization is a more human-interactive field thus reusing data utilization knowledge is a more important task to define data relations in the field of solving multidisciplinary problems. That is to say, knowing the application fields of data is vital in promoting data utilization for problem-solving. Thus, this paper reuses the knowledge of data utilization to re-design data relations in visualization of knowledge space to assist data utilization recognition and decision-making processes. The Innovators' Marketplace on Data Jackets is employed to collect data utilization knowledge, and we use data co-occurrence entropy to reflect people's recognition process on data utilization because co-occurrence between data in utilization knowledge is an informative prior supporting for decision-making. The experimental results show the proposed entropy-based visualization method suppresses baseline methods in the data-utilization proposal numbers and qualities, which verifies proposed method assists people's recognition and decision-making processes in data utilization.

1. Introduction

1.1 Background

In recent years, data utilization is becoming an increasing demand to dig out the potential value of various data. However, the lack of data market to communicate and collaborate with data transaction stakeholders is the main obstacle of data utilization. In other words, the market of data needs a platform to facilitate data-driven decision-making to explore the utility value of data. The platform is supposed to help open and provide data information in the market to potential users while considering privacy and confidential policies; data users and data holders, as well as data analysts, can negotiate to discuss the potential use value of data; data transactions and collaborations can be conducted at reasonable conditions by negotiation. Under such data market platform, the value of data can be negotiated in a reasonable condition facilitating data utilization, thus to build a data-driven society. However, there is still a difficulty of data sharing policy in the first stage of the platform.

1.2 Literature Review

1.2.1 Data Jackets

On the one hand, data users hardly discover suitable data for their problem-solving without disclosure of datasets and utilization method; on the other hand, data providers such as individuals and companies are not willing to open and share their datasets because of privacy and security issues of sharing data. To overcome these problems, a novel conception of Data Jacket (hereafter DJ) is proposed to promote data exchanges and transactions [Ohsawa 13]. DJ, an analogue of CD jackets in CD shops, is the metadata of the dataset which illustrates the necessary information without disclosing data detailed contents. By this technique, stakeholders can share the information of data and discuss the potential use approaches of data without sharing data itself. Besides, DJ transfer unstructured datasets into structured data information. Thus, it is an ideal method for stakeholders to discuss the value of data while reducing the risk of security management cost and business loss, encouraging stakeholders to share information and combine latent related datasets from different domains to solve problems.

1.2.2 Innovators' Marketplace on Data Jackets

However, although the data sharing problem has been solved by adopting DJ, stakeholders still need a platform to negotiate and collaborate on data utilization. Inspired by the collaborative game of Innovators' Market Game [Ohsawa 13] and its extension [Wang 13], Innovators' Marketplace on Data Jackets (hereafter IMDJ) combining data mining and visualization is supposed to detect potential data utilization in one stage [Liu 13, Ohsawa 15]. The participants in the innovative game can communicate or think by themselves to explore potential connections of data through visualization graphs. They can recognize the utility of different domains of data and negotiate to exchange or collaborate with the data.

In the process of IMDJ, data users will elaborate their problems as requirements; analysts are expected to provide insights into data utilization for problem-solving by looking at a given DJ visualization graph which showing DJ relations and connections; data-utilization scenario proposals as solutions will be evaluated by others, and transactions can be negotiated in the final phase.

1.2.3 Entropy Distance

Information entropy was introduced by Claude Shannon to measure the average amount of information value produced by a stochastic source of events [Shannon 48]. The measurement of information entropy [Arndt 04] described as S, the sum of negative logarithm of the probability mass function multiples corresponding possible data value, which formulates as follows:

Contact: Qi Wang, The University of Tokyo, Hongo7-3-1, Bunkyo, Tokyo, Japan, 07044242665, wangqi940519@gmail.com

$$S = -\sum_i P_i ln P_i \quad (1)$$

Where P_i represents the probability of ith event occurs [Pathria 11]. The base of the logarithm is usually taken 2 in Shannon entropy as a measurement in bits.

The basic idea of entropy is described as a measurement of the unpredictability of the event, or in other words, the average information content the event conveys. When the event occurs with low-probability, it conveys more information than when the data has a higher-probability value [Martin 11]. The information entropy is the expected value of the random variable which is the amount of information carried by each event [Stone 14].

Recent years, the concept of information entropy has been extended to many research fields and used in many applications. For instance, in the field of graph theory [Tsai 08, Dehmer 08] and probability theory such as application in the Markov process [McCallum 00]. A similar application like this work, Liu discussed the relations of entropy, distance measure, and similarity measure with the fuzzy sets [Xuecheng 92]. [Shi 16] measures distance applied information entropy, and [Parker 16] uses entropy information to measure distance compared with Jaccard distance.

2. Method Proposal

2.1 Problem Statement

In the previous researches, few works focus on visualization techniques supporting data-driven decision-making processes, though many related works concentrate on data mining algorithms or retrieval systems. This paper will contribute to the visualization algorithm based on the literature review of IMDJ platform to support data utilization activities. As mentioned above, from the previous experiments, participants pay attention to the distance of DJs to define their relations. As a result, there is a demand to re-define the distance of DJs to further assist the data-driven decision-making process. The restriction of distance computation is supposed to enable subjects to understand the relations of DJs better and discover the hidden value of so-called data solutions by combining useful data quickly and feasibly. Information hidden in the distances between DJs reveals the latent relations of data.

2.2 Hypothesis

From the perspective of attention mechanism, human beings focus on only parts of the whole work at once. Thus, the short distance between DJs will enable participants to think their relations at first. This paper utilizes information theory integrating visual analytics to construct a knowledge space to support users recognition processes and data-driven decision-making processes. First of all, the information entropy proposed by Shannon is defined as the average amount of information produced by a stochastic source of data, and it can measure the uncertainty of an event or the diversity. The higher value of entropy is, the more unpredictable the event is. On the contrary, low entropy means a certain probability of the occurrence of an event. In this case, the event is the usage of DJ in solutions. The prior probability of co-occurrence of two DJs in solutions can compute their entropy which defines their relations. The high entropy reveals the independence of two DJs which means the uncertainty of data usage. On the other hand, low entropy represents certain relations of two DJs whether high dependence or low-frequent co-occurrence. In either case, the certainty of co-occurrence will assist users to think data relations easier and quickly exclude useless data from solutions.

DJs with high entropy mean they have complicated relations and their co-occurrences in solutions are unpredictable and need more information make decisions. That is to say, the information entropy value of DJs represents relations of data revealed in the visualization graph. The low entropy implicit little amount of information which is needed to decide whether the DJ is useful in the solution or not. Contrarily, high entropy means it is so complicated that needs more information to make decisions. Thus, the DJs with small entropy should be grouped to be a cognition cluster. By this mechanism, participants firstly consider simple things which are easy to think out solutions for data utilization. And then they can extend to the DJs which are far away from it to deeply consider the utilization method of DJs. In our hypothesis, the knowledge space constructed is supposed to support the decision-making process and enable to build a data-driven society exploring the true value of data.

2.3 Data Knowledge Structure

Based on our hypothesis above, the whole procedures can be described as follows. First of all, we define the data-utilization knowledge structure. Data can be combined to create new value to solve social or personal problems which are the proposed requirements by data users. The process of problem-solving in IMDJ is called data-utilization scenario proposals or so-called solutions. The data analysts can discuss the value of data by negotiating with the solution providers to find satisfactory solutions and conclude deals in a reasonable condition. The knowledge of data-utilization can be defined as the follows [Hayashi 15]:

$$\mathrm{U}_{1,\cdots k}\,\text{Data Jackets} \xrightarrow{combined} \text{solutions} \xrightarrow{satisfy} \text{requirements}$$

From the previous workshop experiments, the data-utilization knowledge has been collected and stored in Data Jacket Store, and we can use this knowledge to construct a knowledge space for data-utilization. There are several steps: first of all, extracting the knowledge structure needed to construct a knowledge matrix. The matrix is a binary matrix with rows of solutions and columns of DJs. The entry is 1 when the target DJ is used in the corresponding solution. Otherwise, the entry is 0.

2.4 Relation Matrix Generation

After obtaining the relation matrix of DJs with solutions, a distance matrix between DJs can be computed by conditional information entropy of pairwise DJs. To be specific, for shortening thinking process of subjects thus accelerating the making decisions process in IMDJ, it plays crucial roles in the circumstances of both the interdependence relations between DJs as well as the low-frequency co-existence of DJs representing hints for data utilization chances. On the other hand, DJs with uncertain applications or usages in different fields of problem-solving can be regarded as noninformative prior thus the distance between them should be far from certain ones. Under the hypothesis, we design the distance calculation method as:

$$R(X,Y) = \left(-P(X|Y)\log_2 P(X|Y) - \left(1-P(X|Y)\right)\log_2\left(1-P(X|Y)\right)\right) + \left(-P(Y|X)\log_2 P(Y|X) - \left(1-P(Y|X)\right)\log_2\left(1-P(Y|X)\right)\right) \quad (2)$$

$$P(X|Y) = \frac{|X \cap Y|}{|Y|} \quad (3)$$

$$P(Y|X) = \frac{|X \cap Y|}{|X|} \quad (4)$$

Where X, Y are the binary sets whether DJ_x and DJ_y are included in the solution respectively. And P is the conditional probability of pairwise DJs co-existence in the same solutions under the condition of the frequency of single DJ existence, or the complement of the possibility vice versa.

2.5 Visualization Configuration

Given that the computed distance matrix between DJs, a dimensionality reduction method of multidimensional scaling (MDS) is adopted. Since MDS is an algorithm to reduce dimensions preserving the relations of data points in the original data space, it applies to many other works such as psychology to explicate the disparities of cognitions in the map [Leeuw 88]. In this paper, we use MDS to distribute the DJs in the 2-dimensional Euclidean space to easily captured by subjects and enhance the insights cognition of them. As for our distance matrix does not meet the Euclidean space, a majorization algorithm of Scaling by MAjorizing a COmplicated Function (SMACOF) is employed to reach a minimum of the stress loss function [Leeuw 11]. Thus the configuration of coordinates of DJs can be used to plot the visualization map.

3. Experiments and Results

3.1 Experiment Procedures

Based on the hypothesis, we conduct experiments to evaluate the distance visualization method implementing on DJs proposed above, to inspect and verify whether the distance computation method based on information entropy in data-utilization knowledge space is feasible for guiding the recognition process and play a role of decision-making assistance in IMDJ.

We expect to gather experimenters to conduct revised edition of single person IMDJ comparing with other visualization maps to see whether there is the difference between them. For the baseline distances calculation methods to draw the visualization maps, we choose two other methods. One is Jaccard distance which also a binary distance calculation method. The relation matrix of DJs can be the same one with our approach, but the computation steps are different corresponding to each method. Another distance calculation method is based on word vector space, say, the word2vec method in this case because there is a related word showing the advantages of word2vec distances between DJs during IMDJ.

The purpose of this experiment is to compare the performance of these three distance calculation methods of DJs revealing in the visualization graph on the results of solutions in personal IMDJ. Experiment subjects are separated into 3 groups, each of subjects conduct single experiment with different themes and methods for 3 times, each theme including 10 DJs. They are encouraged to raise proposals as much as possible in a limited 10 minutes.

Table 1. Illustration of Experiment Groups

	Dataset1: Olympics Preparation	Dataset2: Town Development	Dataset3: Regional Revitalization
Method1: Entropy Distance	Group1	Group3	Group2
Method2: Word Vector Distance	Group2	Group1	Group3
Method3: Jaccard Distance	Group3	Group2	Group1

Visualization graphs given to subjects only show the DJ numbers as figure1 in order to eliminate bias. DJ details can be checked in the appendix by participants.

Figure 1. Example of Visualization Graph

3.2 Quantitative Evaluation

As a result, 375 pieces of data have been collected from the experiments. The data is described as the knowledge flow as defined above: data-utilization scenario proposals drive from combinations of DJs.

Table 2. Results of Proposal Numbers

# of proposals	Method1	Method2	Method3	Total
Theme1	51	40	37	128
Theme2	50	38	36	124
Theme3	47	37	39	123
Total	148	115	112	375

*Method1: Entropy-based distance; Method2: Word vector distance; Method3: Jaccard distance

From the results we can see there is no statistic significant difference between method2 and method3 using Kruskal-Wallis test, whereas method1 differs from the method2 and other two methods. The total proposal number of method1 is greater than the other two methods. It verifies the effectiveness of the decision support function of the proposed method. To draw the conclusion, the proposed method of distance between DJs outperforms the other two methods on the number of proposals. That is to say, the hints of distance between DJs revealed in the visualization map assist subjects' cognition process, which is a decision making of whether pairwise DJs have a possibility to be combined for solving problems.

3.3 Qualitative Evaluation

To evaluate the quality of proposals, a third-party has been involved to rate on a five-point scale: 5 to 1 represents for excellent, good, average, below average and poor respectively. The three criteria are as follows:

(1 Novelty: do you think the proposal is a new idea or an existing one? (2 Feasibility: do you think the proposal can be realized by real actions or not? (3 Utility: do you think the proposal is useful or valuable if it been conducted/analyzed?

The results are shown in table3. From the statistic results, we can see there is a significant difference between method 1 and method2 in novelty, feasibility and utility, and method 1 differs from method3 in novelty and feasibility at the significance level of 0.05.

Table 3. Results of Significance Analyses

	Novelty	Feasibility	Utility
Method1	3.714	3.664	3.608
Method2	3.475	3.330	3.217
Method3	3.631	3.577	3.536
Method1-Method2	**	**	**
Method1-Method3	*	*	n.s.
Method2-Method3	**	**	**

n.s.: non significance *: P<0.05, **: P<0.01

The entropy-based distance algorithm can help trigger more novel and feasible insights for ideas. We can conclude that proposed data knowledge space influences the outcomes of data-utilization proposals. From the questionnaire analyses, we conclude that low co-occurrence DJs clusters will trigger more novel ideas because participants can notice rare but significant relations from the visualization distance. The emphasis on infrequent pair-wise DJs is the reason for high quality and novelty proposals.

4. Conclusion and Future Work

In this work, we construct the data knowledge space and re-define the data relations revealed by distances of DJs in the visualization graph. To design distance algorithm assisting thinking and decision-making processes, information entropy is adopted. The distance between two DJs is defined as their addition of conditional entropy of their co-occurrence in solutions. The experimental results show outperformance of proposed method in quantitative and qualitative evaluation. Thus we conclude that proposed entropy-based visualization of knowledge space can support for the data-driven decision-making in the market of data.

For the market of data, our method is supposed to facilitate data stakeholders' recognition process that can correctly grasp the value of data consisting of utilization approaches to using it. Furthermore, the data-driven society can be built as we reduce the uncertainty of business loss and waste opportunity by digging out the value of data.

This study is not finished by this thesis; there are still improvements remained for further research. As mentioned above, we will continue to elucidate the visual influences on data utilization efficiency, excavate the use value of data, and extend the method to other fields as support for visual analytics decision making.

Acknowledgement

This work was funded by JSPS KAKENHI JP16H01836, JP16K12428, and industrial collaborators.

References

[Ohsawa 13] Ohsawa Y, Kido H, Hayashi T, et al. Data jackets for synthesizing values in the market of data. Procedia Computer Science, 2013, 22: 709-716.

[Hayashi 13] Hayashi T, Ohsawa Y. Processing combinatorial thinking: Innovators marketplace as role-based game plus action planning. International Journal of Knowledge and Systems Science (IJKSS), 2013, 4(3): 14-38.

[Wang 13] Wang H, Ohsawa Y. Idea discovery: A scenario-based systematic approach for decision making in market innovation. Expert Systems with Applications, 2013, 40(2): 429-438.

[Liu 13] Liu C, Ohsawa Y, Suda Y. Valuation of data through use-scenarios in innovators' marketplace on data jackets. Data Mining Workshops (ICDMW), 2013 IEEE 13th International Conference on. IEEE, 2013: 694-701.

[Ohsawa 15] Ohsawa Y, Kido H, Hayashi T, et al. Innovators marketplace on data jackets, for valuating, sharing, and synthesizing data. Knowledge-Based Information Systems in Practice. Springer, Cham, 2015: 83-97.

[Shannon 48] Shannon C E. A mathematical theory of communication. Bell system technical journal, 1948, 27(3): 379-423.

[Arndt 04] Arndt, C. (2004), Information Measures: Information and its Description in Science and Engineering, Springer, ISBN 978-3-540-40855-0

[Pathria 11] Pathria, R. K.; Beale, Paul (2011). Statistical Mechanics (Third Edition). Academic Press. p. 51. ISBN 978-0123821881.

[Martin 11] Martin, Nathaniel F.G. & England, James W. (2011). Mathematical Theory of Entropy. Cambridge University Press. ISBN 978-0-521-17738-2.

[Stone 14] Stone, J. V. (2014), Chapter 1 of Information Theory: A Tutorial Introduction, University of Sheffield, England. ISBN 978-0956372857.

[Tsai 08] Tsai D Y, Lee Y, Matsuyama E. Information entropy measure for evaluation of image quality. Journal of digital imaging, 2008, 21(3): 338-347

[Dehmer 08] Dehmer M. Information processing in complex networks: Graph entropy and information functionals. Applied Mathematics and Computation, 2008, 201(1-2): 82-94.

[McCallum 00] McCallum A, Freitag D, Pereira F C N. Maximum Entropy Markov Models for Information Extraction and Segmentation. Icml. 2000, 17(2000): 591-598.

[Xuecheng 92] Xuecheng L. Entropy, distance measure and similarity measure of fuzzy sets and their relations. Fuzzy sets and systems, 1992, 52(3): 305-318.

[Parker 16] Parker A J, Yancey K B, Yancey M P. Regular Language Distance and Entropy. arXiv preprint arXiv:1602.07715, 2016.

[Hayashi 15] Hayashi, T., Ohsawa, Y.: Knowledge Structuring and Reuse System Design Using RDF for Creating a Market of Data, 2nd International Conference on Signal Processing and Integrated Networks, pp.566-571, 2015.

[Leeuw 88] De Leeuw J. Convergence of the majorization method for multidimensional scaling. Journal of classification, 1988, 5(2): 163-180.

[Leeuw 11] De Leeuw J, Mair P. Multidimensional scaling using majorization: SMACOF in R. 2011

[Shi 16] Shi Q, Chen Z, Fang C, et al. Measuring the diversity of a test set with distance entropy. IEEE Transactions on Reliability, 2016, 65(1): 19-27.

International Session | International Session | [ES] E-5 Human interface, education aid

[2C5-E-5] Human interface, education aid: places of design

Chair: Katsutoshi Yada (Kansai University)

Wed. Jun 5, 2019 5:20 PM - 7:00 PM Room C (4F International conference hall)

[2C5-E-5-01] The Influence of Story Creating Activities while Appreciating Abstract Artworks

○Kotone Tadaki[1], Akinori Abe[1] （1. Chiba University）

5:20 PM - 5:40 PM

[2C5-E-5-02] AI, Making Software for Humans

○Mika Yasuoka[1], Rune Moeller Jensen[2] （1. GLOCOM, 2. IT University of Copenhagen）

5:40 PM - 6:00 PM

[2C5-E-5-03] The effect of eye-catching object on sampling at supermarket

○Rihoko Mae[1], Naohiro Matsumura[1] （1. Osaka University）

6:00 PM - 6:20 PM

[2C5-E-5-04] Vision Based Analysis on Trajectories of Notes Representing Ideas Toward Workshop Summarization

○Yuji Oyamada[1], Mikihiko Mori[2], Haruhiko Maenami[1] （1. Tottori University, 2. Hosei University）

6:20 PM - 6:40 PM

[2C5-E-5-05] Intuitive Automatic Music Arrangement System for Wave Files Following Sensitivity Words

○Koichi Yamagata[1], Shota Miyoshi[1], Maki Sakamoto[1] （1. The University of Electro-Communications）

6:40 PM - 7:00 PM

The 33rd Annual Conference of the Japanese Society for Artificial Intelligence, 2019

The Influence of Story Creating Activities while Appreciating Abstract Artworks

Kotone Tadaki[*1] Akinori Abe[*2]

*1*2 Graduate School of Humanities and Public Affairs, Chiba University

In this paper, the authors will introduce our experiment to determine the influence of story creation on the appreciation of abstract artworks. From previous researches, it was known that novice viewers tend to dislike abstract artworks than representative artworks because abstract artworks lack the forms. The authors tried to relax this trend by creating a story about the artwork while appreciating. To answer our research question which is "will individual viewers create similar stories for artworks?", the authors conducted the experiment. The participants answer the worksheet while appreciating abstract artworks and representational artworks. As results, we found out that individual viewers create the similar story to the same artwork from the corresponding analysis and bold lines on the artworks was the important factor to imagine a story. Our result can suggest the possible advantages and disadvantages of using similar activities and how to create effective captions for the artworks.

1. Introduction

1.1 Abstract and Representational Paintings

The mechanism of art appreciation has been a major issue for years. Schmidt et al. (1989) focused on a novice who never thought art appreciation (visual analysis) nor creation as a professional artist and monitored their verbal protocols during the art appreciation. Using these data, Schmidt et al. (1989) tried to clarify the novice strategies for understanding paintings to build a computer-based education program. Based on these researches, they showed that novices tend to use the semantic features or contents (e.g. theme, symbolism) than formal elements (e.g. lines, shape, colour) when appreciating representational paintings. However, when they are appreciating abstract paintings, the result was completely opposite which means novices more frequently use the formal elements than semantic features. Since instructors in schools and museums tend to use formal elements when they teach visual analysis to novices, this result suggested that art education might be unsuitable for a novice. In addition, O'hare (1976) pointed out that novices tend to dislike abstract artworks.

Okada and Inoue (1991) described that these differences in art appreciation occur because abstract paintings lack the specific form. They conducted an experiment to determine how novice will evaluate abstract and representational artworks. They concluded that the artistic evaluation of abstract artworks is highly affected by the tenderness and the taste whereas the artistic evaluation of representational artworks is highly affected by the strangeness and the impact of the artwork.

Ishibashi and Okada (2010) call this phenomenon the reality constraint and pointed out that nowadays art education (usually in elementary and secondary school) tend to focus on representational artworks, not abstract paintings. Ishibashi and Okada (2010) showed that the reality constraint can be relaxed by copying the artwork by experiment. From this result, they suggested by copying the artwork, novice played the artist's role and acquired the artist's point of view.

Tanaka and Matsumoto (2013) tried to relax the reality constraint by using a commentary which is a short text explaining the artwork. The result suggested that reading a commentary with technical information (style, colour, technique and various technical aspects of the artwork) relaxed the reality constraint. The participant's descriptions about the artwork showed that when reading these commentaries, novice tried to understand beyond what was drawn on the painting.

1.2 Creating story about abstract paintings

There are two possible solutions to relax the reality constraint. Two research groups (Ishibashi Okada, 2010) (Tanaka Matsumoto, 2013) tried to relax the reality constraint by obtaining the artist's point of view. Viewers in their experiment playing a role (copying the work) and knowing how they created the artwork technically. However, they never tried to overcome the lack of forms.

In this paper, we discuss whether novice can overcome the lack of forms by creating a story about abstract artworks. When creating a story, we need a character, stage, situation and many other elements. When we trying to create a story form an abstract artwork which lacks a specific form, we need to imagine the form. In other words, a viewer may create their own imaginal forms in abstract artworks.

In art museums, we can find several kinds of tools and activities which aim to make visitors create a story about artworks. In this section, we will introduce tools and activities in museums.

The most typical tools are worksheets. When we visit art museums, we obtain information from captions displayed next to the artwork. However, since the amount of information which can installed on captions are very limited, art museums usually provide a tool to help visitor's understanding. The most popular

連絡先：kotonetadaki@yahoo.co.jp

type of tools is worksheets with a short question (e.g. “What is this girl on the artwork doing?”) and empty space to write in the answer to the question.

The Metropolitan Museum of Art (2005)’s family guide “Shall We Dance?”, they focused on three artworks related to dancing and provided detailed facts and activities to help visitors understanding. The work-sheet instructed to create own story and suggested to eight sample sentences such as “Once upon a time there was a young girl and boy. Their names were…and…”, “They went to a costume party to celebrate the…” or “The party was held at…”. This worksheet can be downloaded from The Metropolitan Museum’s website.

The National Museum of Modern Art, Tokyo (MOMAT)’s MOMAT Collection Children’s Self Guide also have questions to encourage visitors to create a story. On one Ryusei Kishida’s artwork, there is a brown-coloured road crossing the canvas bottom to up. On background, we can see blue sky with white clouds. The question on the sheet is “if you walk up the road, what will you see?” and the smaller text on the same page says “You are climbing up the hill road step by step. You can see blue sky in front of you.”. There is a blank box below the text to answer the question.

In addition, art museums in Japan usually provide activities such as a guided tour and a workshop. Many of the tour and worksheets are based on the idea of Visual Thinking Strategies (VTS) (Visual Thinking Strategies Site by Joel Smith Media, 2018). In Japan, this methodology is widely accepted in art museums. VTS is a methodology of art appreciation which focus on explaining and sharing viewers’ impression between viewers. The first question in VTS workshop is “what is going on in this picture?”. Viewers answer, explain and share what they saw in the artwork.

1.3 Explaining abstract paintings

Our research question is that will individual viewers create similar stories for artworks? In this article, the authors will introduce the result correspond to the research question and discuss the outcomes of the experiment overall.

We should note that the experiment in this paper was conducted in Japanese. All stimuli used in the experiment was written in Japanese. Therefore, this research procedures and results of this paper may improve art museums in Japan. However, it might not fit non-Japanese museums or visitors.

2. Materials and Methods

2.1 Participants

Participants were 29 adults including university students and teachers. All the participants are asked to answer about their art education background. Based on that answer sheet, we chose participants who never educated or had experienced to create their own artworks as a professional artist so that we could regard them as novices.

2.2 Stimuli

The experiment was conducted in a room in Chiba University on 23rd December 2017.

We used 18 artworks created in from 1947 to 2017 as stimuli. Six of them were representational paintings and others were abstract paintings. Each artwork had numbers to distinguish them.

All artworks were displayed with simple captions and labels. Information included in captions were chosen based on Tanaka and Matsumoto (2013)’s experiment.

All participants answer the worksheet and questionnaire during appreciating the artwork. The questionnaire included questions asked about participants’ experience of art education and creation. We made two types of worksheets to apply to them according conditions. The first type of worksheet is a worksheet with two questions which are Q1) Write about your impression about the artwork and Q2) Mark the point which fits best to your impression on the following list. Q2 was based on a semantic differential technique (SD) used in Okada and Inoue (1991)’s experiment. The second type of worksheet includes additional question between Q1 and Q2. Questions in the worksheets were Q1) Write about your impression about the artwork, Q2) Create a story from the artwork and Q3) Mark the point which fits best to your impression on the following list.

2.3 Conditions

We used three conditions for each participant (within-subject factor). As they enter the room, they saw six abstract paintings without creating a story (abstract condition), six representational paintings without creating a story (representational condition) and six abstract paintings using a worksheet to create a story (story condition). All participants followed this order.

If the story creating worksheet helped to image a form on the painting, in other words, if the hypothesis was true, the result from story condition will have a similar trend comparing to the representational condition and different trend comparing to the abstract condition.

2.4 Hypothesis

The hypothesis is that stories created for an artwork are different from stories created for other artworks. In other words, all viewers create similar stories for the same artwork.

3. Results and Discussion

3.1 Similar stories for an artwork

Our hypothesis was “Stories created for an artwork is different from stories created for other artworks”. We used the data from story condition in this analysis. The result in Fig.2 showed that there are three groups in stories and each group are isolated from other groups by correspondence analysis. We used KH coder (Higuchi, 2016) (Higuchi, 2017) which is a free software for text mining and analysis. Since answers from participants were all written in Japanese, the result on Fig.3 is plotted with English labels translated by the authors.

First, we focused on the words which participants frequently used. Numbers in square shape such as “C13” are an artwork number which means C13 corresponding to No.13. there are three groups on the top left (No.15), bottom left (No.16, No.17, No.18) and bottom right (No.13, No.14).

In the dimension 2 (y-axis in Fig.3), words such as “gingko tree (イチョウ)”, “modern (現代)”, “art (芸術)”, “window (窓)”

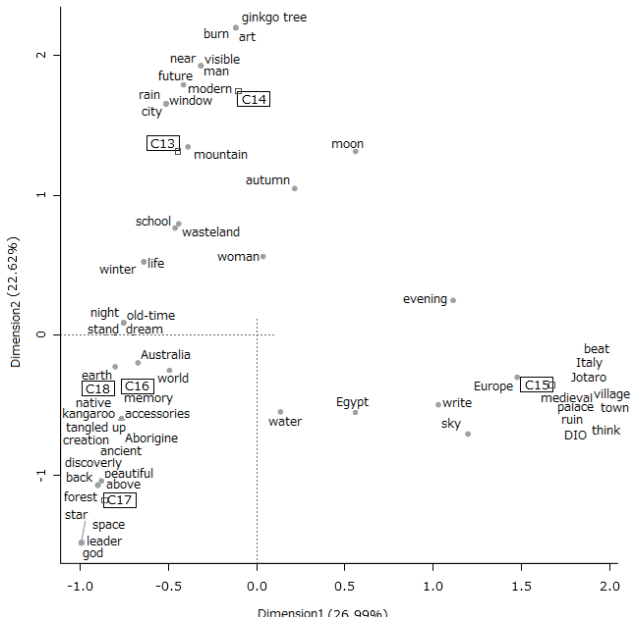

Fig. 1 correspondence analysis result

whereas words such as “space (宇宙)”, “ancient (大昔)”, “god (神)”, “native peoples (先住民)”, “palace (王宮)” and “ruin (荒廃)” concentrate on negative side. We can estimate dimension 2 (y-axis) as a time axis.

In the dimension 1 (x-axis in Fig.3), words such as “think (思う)”, “village (村)”, “Italy (イタリア)” concentrated on the positive side of x-axis whereas words such as “star (星)”, “accessory (アクセサリー)”, “school (学校)”, “mountain (山)” and “future (未来)” concentrate on negative side. In the middle, there are words such as “moon (月)”, “Egypt (エジプト)” and “water (水)”. From this result, we could not estimate what this axis indicates.

However, when looking at artworks, No.16, No.17 and No.18’ have strong and bold lines in common. Of course, since these artworks are abstract paintings, we could not identify what is drawn. No.15 on the positive side of x-axis was an artwork painted with strong colours and its compositions. This result suggests the importance of strong lines to show the object’s form. Okada and Inoue (1991) suggested that abstract paintings are difficult to appreciate for a novice because they lack forms. Our result can add to Okada and Inoue (1991)’s suggestion that strong lines are the important factor to decide the presence of forms.

This result showed that there are three patterns of stories created for abstract artworks in this experiment. And when comparing the groups of stories, we suggested strong and bold line is the reason for these groups. This result means the bold lines are the important factor in appreciation, however, this result will not mean that the appreciation is easier in some artworks.

3.2 Settings: place

In this section, we focused on settings of the viewers’ story. We assumed that stories have more detailed and familiar when the appreciation is easier.

The stories include information about the place where the story took place. For example, viewers wrote “under the water (水中)”, “near the sun (太陽の近く)” and “a village in Europe (ヨーロッパのある村)” in their stories about artworks.

We picked up the word about the place and added labels to each story based on their stories setting place. For each answer, a label chosen from three types which are “common noun”, “mixed” and “proper noun”. Label “mixed” is for the word with common noun qualified by the phrase include proper nouns such as “huge wasteland like we see in the USA or Australia (アメリカやオーストラリアのような広大な荒野)”. We chose these three labels because we tend to use proper nouns when talking about the familiar or specific places.

Fig.3 is the result of each artwork. There are significant differences between No.15 - No.13 (p= 0.003) and No.15 - No.17 (p= 0.034) by Tukey’s HSD test when converting labels into scores. There is a more proper noun used to explain No.15 than No.13 and No.17. This result has a similar pattern with the result from correspondence analysis shown on Fig.2.

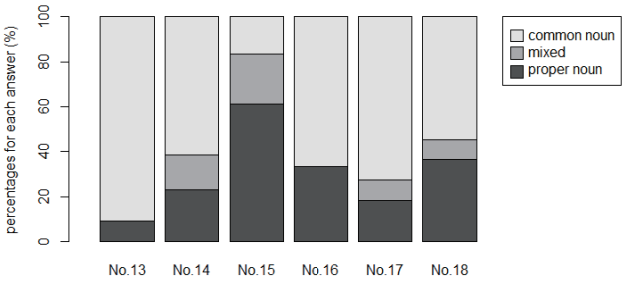

Fig. 2 Artworks and noun types in story

There is a place impossible to reach such as “another planet (異星)” and easy to reach such as “school (学校)”. We added three labels which are “went”, “possible” and “impossible”. The place which considered viewer have visited such as school and their laboratory is labelled as “went”. The result was shown in Fig.4. However, there is no significant difference found by Tukey’s HSD test when converting labels into scores.

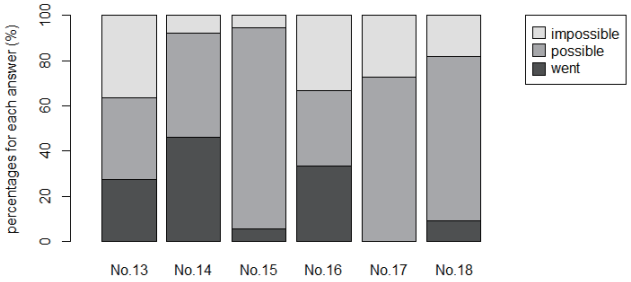

Fig. 3 Artworks and possibility to reach there

3.3 Settings: time

There is also information about the time when the story happens such as “yesterday (昨日)” and “raining night (雨の降る夜)”.

We picked up the word about the time and added labels. For each answer, a label chosen from six types which are not-limited (eg. “future (未来)”) , period (eg. “medieval (中世)”), year (eg. “1970”), season (eg. “before harvesting wheat (麦の収穫前)”), day (eg. “December 20th 2015”), hour (eg. “evening (夕方)”).

Fig.5 is showing the result plotted for each artwork. There are significant differences between No.15 - No.13 (p=0.038) and No.13 - No.17 (p=0.038) by Tukey's HSD test when converting labels into scores. This result also had a similar pattern with the analysis shown in Fig.2 and Fig.3 which means the three groups found in Fig.2 were isolated from each other.

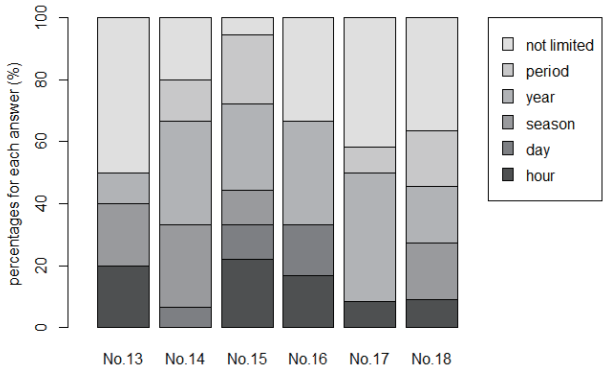

Fig. 4 Artworks and setting of the story

4. Results and Discussion

We conducted the experiment to test the hypothesis whether stories created for an artwork is different from stories created for other artworks.

We found out that individual viewers create a similar story to the same artwork from corresponding analysis. In addition, our result suggested some patterns exists when creating stories about artworks. The important suggestion from these results is that story creating activity is effective for some kinds of artworks but not for other kinds of artworks. We could not decide features of these artworks at this point. Correspondence analysis's result suggests artworks with clear bold lines (No.16, 17, 18) are effective where analysis about settings suggest artwork with colour composition (No.15) is effective.

Since museums are the facility with the educational and conservational aim, museums must appeal the importance of conservation of cultural and natural heritage through their exhibitions and educational programs. This research aimed to help art museums to create the effective activities (educational programs) for visitors who are mainly novices. Therefore, we tried to relax the feelings of "dislike" to abstract artworks by converting abstract artworks to representational artworks in viewers' mind by creating a story.

However, we could not assume that the feeling of "like" is the main aim of art appreciation. Some artworks even tried to raise an issue by inducing the negative feeling. We need further research and discussion about what is exactly the art appreciation is and what is exactly the "fun" art appreciation is. This point will not affect the outcomes of our experiment discussed above, however, we must continue discussing these topics when we are trying to somehow evaluate or verbalise the other people's art appreciation experience.

References

[J. A. Schmidt 1989] J. A. Schmidt, J. P. McLaughlin, P. Leighten, "Novice Strategies for Understanding Paintings," Applied Cognitive Psychology, 3, pp. 65-72, 1989.

[D. O'hare 1976] D. O'hare, "Individual differences in perceived similarity and preference for visual art: A multidimensional scaling analysis," Perception & Psychophysics, 20(6), pp. 445-452, 1976.

[M. Okada 1991] M. Okada, J. Inoue, "A psychological analysis about the elements of artistic evaluation on viewing paintings," The educational sciences. Journal of the Yokohama National University, 31, pp. 45-66, 1991.

[K. Ishibashi 2010] K. Ishibashi, T. Okada, "Facilitating Creative Drawing by Copying Art Works by Others," Cognitive studies: bulletin of the Japanese Cognitive Science Society, 17(1), pp. 196-223, 2010.

[Y. Tanaka 2013] Y. Tanaka, S. Matsumoto, "Cognitive Constraints and its Relaxation in Appreciation of Painting," Cognitive studies: bulletin of the Japanese Cognitive Science Society, 20(1), pp. 130-151, 2013.

[The Metropolitan Museum of Art 2005] The Metropolitan Museum of Art, "Family Guides," 2005. [online]. Available: https://www.metmuseum.org/learn/kids-and-families/family-guides.

[Visual Thinking Strategies Site by Joel Smith Media 2018] Visual Thinking Strategies Site by Joel Smith Media, "Visual Thinking Strategies," 2018. [online]. Available: https://vtshome.org.

[K. Tadaki 2018] K. Tadaki, A. Abe, "The Influence of Story Writing Worksheets on Art Appreciation,": The 2018 International Conference on Artificial ALife and Robotics (ICAROB2018), Beppu (Japan), 2018.

[K. Tadaki 2018] K. Tadaki, A. Abe, "Effects of Context Creation Work in Impression of Abstract Paintings (in Japanese),": The 32th Annual Conference of The Japanese Society for Artificial Intelligence (JSAI2018), Kagoshima (Japan), 2018.

[K. Higuchi 2016] K. Higuchi, ""A Two-Step Approach to Quantitative Content Analysis: KH Coder Tutorial Using Anne of Green Gables (Part I)," Ritsumeikan Social Science Review, 52(3), pp. 77-91, 2016.

[K. Higuchi 2017] K. Higuchi, "A Two-Step Approach to Quantitative Content Analysis: KH Coder Tutorial Using Anne of Green Gables (Part II)," Ritsumeikan Social Science Review, 53(1), pp. 137-147, 2017.

The 33rd Annual Conference of the Japanese Society for Artificial Intelligence, 2019

AI, Making Software for Humans

Mika Yasuoka [*1]

[*1] GLOCOM

Rune Møller Jensen [*2]

[*2] IT University of Copenhagen

Artificial Intelligence (AI) algorithms are expected to have substantial impact on high-end white-collar jobs like lawyers, physicians, and financial advisors in a near future. A non-technical challenge of this development is that advanced Decision Support Tools (DSTs) often are rejected by practitioners or have low uptake. This paper proposes Living Lab as a design approach for developing human centered AI-tools. First, the paper exemplifies the use of AI in the current society with cases the authors are engaged in, and then show two design approaches for social implementation of AI. Based on the presented cases, the paper argues for the benefits of utilizing the Living Lab approach for societal AI.

1. Introduction

Artificial Intelligence (AI) has attracted attention as well as raised uneasiness globally in the last decades. The advent of singularity, exceeding human intelligence, goes far beyond the comprehension of ordinary minds. The legendary forecast of human work in the future is that AI will steal work from humans. This has brought many ordinary people to the conclusion that they have no choice but to think about how AI will impact their lives. It is certain that AI changes the future of work, however, with which consequence is less agreed. As Hori argues [Hori, 2018], in our society, AI has been gradually embedded and melted into the society than ever and has become invisible to ordinary eyes. Liquid modernity [Bauman 2000] is happening to reality. At the same time, AI-based systems in high-end jobs comes in the form of Decision Support Tools (DSTs) that already since the expert system era in the 1980s have been known to be hard to integrate in work processes.

Based on four cases that the authors have been involved in, this paper portrays the present situation as well as near future scenarios, where AI enters every corner of society and blends into our daily lives. By presenting the application of two typical design methods of utilization of AI in society, this paper argues for the importance of social implementation through Living Lab approach by exemplifying presented cases.

2. Living Lab

Living Lab is a demonstration space in daily life context [fx. Ehn 2014; Yasuoka 2018]. In Scandinavia, it is generally regarded as a part of participatory design, and co-creation (Co-Design) approach for solving social problems with complex and high uncertainty. It can be used as innovative test bed in organizational context of IT development [Leminen 2013], and as a social innovation space [Bergvall-Kåreborn et al. 2009]. Ultimate goal of Living Lab is to design socially embedded IT systems in real life context with wider stakeholders. Bergvall-Kåreborn and colleagues define living lab as "a user-centric innovation milieu built on every- day practice and research, with and approach that facilities user influence in open and distributed innovation processes engaging all relevant partners in real-life contexts, aiming to create sustainable values.". In a conceptual model authors proposed (Fig 1), ten critical aspects for Living Lab is depicted; 1. Familiar Context 2. Activity with multi-layer 3. Co-Creation 4. Dialogue and Reflection 5.Evaluation 6.Discovery 7.Long-term Engagement, 8.Purpose & Vision 9 Empowerment 10.Openness.

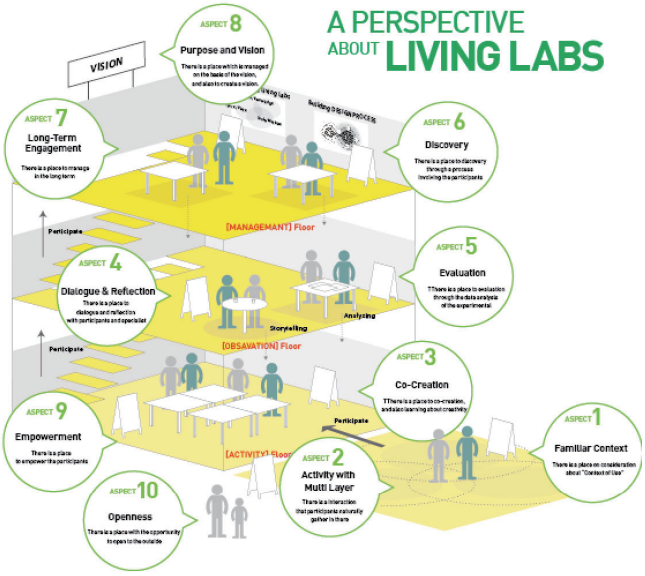

<Fig.1; Conceptual Model of Living Lab>

The infographic utilizes a building metaphor with three floors, indicating community structure and its user involvements. Three floors consist of activity floor, observation floor and management floor. In this building metaphor, one user enters the building (community) and views each floor (aspects) step by step. This presentation indicates importance of; 1) widening view to understand current activities and plan future activities, and then acquire holistic view; 2) recognizing a progressive involvement process to the community; 3) categorizing and organizing activities with certain perspectives.

3. Applied AI Cases

In this section, exemplified with four projects that the authors are involved in, this section portrays how an AI embedded society and its future scenarios can be.

Contact: Mika Yasuoka, GLOCOM Address, Phone number, mika@yasuoka.dk.

3.1 Knowledge Transfer

Due to the advancement of describing human tacit and explicit knowledge in varied modes of data, knowledge management empowered with AI becomes a reality.

In our knowledge management project with a metal casting industry [Hirata 2018], we designed a knowledge transfer system *T2S2*, which captures and passes on distributed knowledge of metal casting experts. Traditionally, it was believed that the knowledge of expert craft practitioners was transmitted only through demonstrating practice in master- apprentice relations, and intuition accumulated based on their long experiences is indispensable. Thus, many companies including the company we worked with, had believed designing an intelligent knowledge management system was not possible.

Our achievement became possible only because we worked together with traditional skilled crafts practitioners at Living Lab. The longitudinal interactions with craftsman clarified that some explicit and tacit knowledge were describable intelligence while other knowledge remained at human hands, but supported by digital means. This field project implies human knowledge benefits from being described with different external representations.

The decision about which knowledge should be digitized relies largely on a deep understanding of the professional activity. For designing the knowledge management system, understanding of associated human cognitive activity in the field for a long duration was very important.

3.2 Big data and deep learning

The expectations of what we can do with large amounts of data have increased surprisingly. By collecting and analyzing human behavior data from sensors, AI deep learning might identify outliers in human behavior and improve quality of life.

The REACH project[1] is a five-year EU Horizon 2020 project [Schäpers 17], conducted by a consortium consisting of academic institutions, medical and healthcare organizations, healthcare IT companies, insurance companies, municipalities, and citizens from Denmark, Switzerland, Netherlands and Germany. The objective of the project is to develop REACH health eco system for senior citizens, which detect outliers and intervene in daily activities through monitoring and big data analysis of health conditions based on real data from installed and wearable sensors.

To achieve this goal, REACH applies the Living Lab approach for collecting the feedback and input from users. By developing the system together with stakeholders, the REACH experienced various changes in data collection methods, data utilization, implementation of field inputs to eco system design in earlier stage. For example, personal health data through wearable sensors was originally regarded too sensitive to collect. However, our study showed that accumulation of trust in the systems could easily overcome this sensitivity challenge. A good balance on adequacy of behavior advice, ethics towards implicit motivation push (nudge) is another challenge to be negotiated along the way.

This project implies that interaction with users at stake can clarify which data is usable and what data granularity is needed for analytics.

3.3 Network

The possibility of discovering relationships among humans, between humans and things is expanding as the relations can be visualized in more detail.

This project with KDDI aims at designing better communication support systems among family members. Starting with a field study and a qualitative data collection in 2017, the project conducted a long-term Living Lab experiments with test system, by inviting ordinary households and its family members. Together with target families, the project also conducted a few concept development workshops, using a typical concept design methods. While the majority of proposed ideas at the workshop were novice and creative, many ideas focused only on either convenience or efficiency in communication. Interestingly, quantitative fields data from long-term Living Lab experiments, and interviews showed the importance of “role play” among family members and interaction on family role communication. All families with own roles (37% of all target families) tend to successfully utilize the system for longer periods with higher satisfaction rate.

This project implies that it is critical to understand values acquired in real-life contexts to get design implications. Given the support of social networks in the future, closed laboratory settings or innovation workshops can only offer limited understanding of real of social relations and networks.

3.4 Planning

Planning algorithms are changing the actual business. In the stowage planning of container ships, skilled workers usually spend 2-3 hours to allocate all containers for each port. For a long time, stowage planning is regarded as a field of experiences skilled workers as in traditional crafts, and untouchable for AI researchers. Typical academic stowage planning system has often been made based on the fictitious data and unrealistic contexts.

SAM, the stowage planning system designed based on the detailed field observations on stowage planners work process, in collaboration with stakeholders, achieved a record stow in 2018. At the present stage, it is indispensable to understand and reflect the detailed process of stowage experts for the algorithm. The result indicates that the stowage system is a system not for replacing humans, but for supporting decision making. At least now, the world record stowage system does not reach to the conclusion that all stowage process is to be automated.

This project implies that current DSTs require in-depth understanding of the work process of professionals to be used in a real-world context. With high probability, future DSTs require that human experts take final decisions due to their responsibility of the solution. Interleaving automated decisions carried out with AI tools with decision points of responsible humans in a seamless work-process is a major challenge for many white-collar applications of AI. Research on DST uptake in other fields [e.g, Rose, 2016] summarize bottom-line performance, ease of use, trust, cost, and work process compliance as some of the key success factors for DST uptake.

[1] http://www.reach2020.eu/ REACH (*Responsive Engagement of the elderly promoting Activity and Customized Health care*)

4. Two Design Approaches for AI

If AI is to be used in society and to be positioned to support humans, it is essential to understand situated human behavior in depth. There has been, largely speaking, two approaches to design AI in society from human centered perspective. The first is a conventional technology driven approach, which adjust architecture to fit to the societal needs. For example, current work attempts to make machine translation available for daily life [Ishida 2011]. The machine translation receives particular context based knowledge by defining contexts of use such as hospital situation and sightseeing situation.

The second is a usage-need driven approach. It first investigates situated human behavior and then realizes human needs for advanced intelligent systems. The co-design approach as well as stakeholder involvement approaches such as Participatory Design [e.g. Ehn 2014 & Yasuoka 2018] and Living Lab are typical examples.

5. Why Living Lab for AI

Living lab is particularly relevant for the AI community. AI is an exploration of human intelligence, but still discussion for application of AI in society and socialization of AI has been quite limited for a long time. Today the situation is changing drastically. AI in society is more obvious, thus cognitive support becomes indispensable when considering AI. AI will soon produce intimidating software, if it not already is. As shown in Case 1 (Knowledge transfer) and Case 4 (Planning), craftsmen and planners are hesitant towards intelligent system because of their fear of AI invasion to their territory. For them, it is difficult to judge what to compromise and to understand the limitations of AI. It was hard for them to appropriate AI as supportive for their expert activities.

In Case 2, the senior user may not define their behavior change is based on self-decision or their motivation is manipulated or nudged. Thus, people probably conclude that they will not want to use AI. However, when trust is granted, and when tacit knowledge and its visualization in system actually helps further refinements of their casting skills (Case 1), and when visualized foot step records became a trigger of taking a walk (Case 2), the advantage of incorporating human activities with AI can be positively recognized.

This paper is an initial attempt to bridge current AI and society from Living Lab perspectives. It first introduced four cases that the authors were involved in to exemplify the challenges of adopting AI in society. Living Lab can be one of the indispensable instruments to consider future socially embedded AI design.

References

[Bauman 2000] Bauman Z, Liquid Modernity, 2000.

[Bergvall-Kåreborn 2009] Bergvall-Kåreborn, B. and Ståhlbrust, A. Living Lab; An Open and Citizen-Centric approach for Innovation, International Journal of Innovation and Regional Development, 1(4), 35-370. 2009.

[Hirata 18] Hirata S, Yasuoka M. Consideration of Tacit Knowledge Sharing by Automation for Reinforcement of Human Abilities: Empirical Comparison of Conservation Techniques Between Japan and Denmark. International Journal of Automation Technology. Vol.12 No.4. p553-563. 2018.

[Hori 2018] 堀浩一, 人工知能として認識されない人工知能の埋め込まれる社会に向けて, Journal of Information and Communications Policy Vol.2. No.1.

[Ishida 2011] Ishida T, The Language Grid, Springer-Verlag, 2011.

[Leminen 2013] Leminen, S., Coordination and Participation in Living Lab Networks. Technology Innovation Management Review, 3(11): 5–14, 2013.

[Rose 2016] Rose D.C., Sutherland W.J., Parker C., Lobley M., Winther M., Morris C., Twinning S., Ffoulkes C., Amano T., and Dicks L.V., Decision support tools for agriculture: Towards effective design and delivery. Agricultural Systems 149, 165-174, 2016.

[Ehn 2014] Ehn P, Elisabet M. Nilsson, Richard (eds.) Making Futures: Marginal Notes on Innovation, Design, and Democracy, 2014.

[Schäpers 17] Schäpers, B. Yasuoka, M. et al. Determining Design Requirement s for Active Ageing: Use Cases, Personas, and Stakeholders. Journal of Gerontechnology – Special Issue – REACH: Responsive Engagement of the Elderly promoting Activity and Customized Healthcare, 16(3), 139-150. 2017.

[Yasuoka 2018] Yasuoka M, Akasaka F., Kimura A., Ihara M., Living Lab as a methodology for Service Design: Analysis based on cases and discussion form the viewpoint of systems approach. Design Conference. 2018.

The 33rd Annual Conference of the Japanese Society for Artificial Intelligence, 2019

The effect of eye-catching object on sampling at supermarket

Rihoko Mae[*1] Naohiro Matsumura[*1]

[*1] Graduate School of Economics, Osaka University

This paper considers how consumers pay attention to and participate in sales promotions. To achieve this purpose, we conducted experiments on sampling jam at a supermarket. We did comparison experiments with four conditions using an eye-catching object to encourage shoppers to notice the samples and a voting-style gimmick to encourage them to try the samples. Experimental results show that the object and the gimmick were useful for encouraging shoppers to participate in the sampling. This tendency was noted among people of certain age groups, in pairs, and coming from the entrance.

1. Introduction

This research considers the method and possibility of promoting consumers' attention in sales promotion. Specifically, we measured consumers ' reactions to jam sampling. We conducted the sampling using low-relevance goods that can be substituted and that consumers do not purchase on a daily basis. Even if they would not normally purchase the product, it is added to the consideration set of consumers, and the possibility that they would purchase the jam in the near future would rise. We also used an eye-catching object to catch consumers ' attention. Ordinary sampling is not enough to attract the attention of consumers; however, an eye-catching object gives consumers a positive sense of incompatibility in their sight and can raise interest in products. Therefore, the possibility that the product will remain in the long-term memory of consumers will rise.

2. Literature Review

According to Chandon et al. [Chandon 00], the benefits of sales promotions are explained as a perceived value attached to the promotion experience. This means that customers respond to a promotional offer because of the positive experience and value. They suggest that promotions can help consumers to find the product they want or remind them of the product and quantity they need to buy. This can reduce search and decision costs and improve shopping efficiency and convenience.

There are various empirical studies on sales promotions and purchasing environments in grocery stores. Iyengar and Lepper [Iyengar 00] conducted a jam sampling experiment at a supermarket in the US. Two pattern displays, a table with samples of six kinds of jam, and a table with samples of 24 types of jam were presented to shoppers. The percentage of shoppers who stopped was 20% higher at the extensive-selection display of jams, but the percentage of shoppers who actually purchased items at the limited-selection display of jams was ten times higher. Zhang [Zhang 17] conducted a bread sampling experiment at a bakery in Japan and introduced a voting-style sampling of two kinds of bread. It was demonstrated that this reduced consumer-perceived risk and improved the efficiency of tasting sales.

Contact: Naohiro Matsumura, Graduate School of Economics, Osaka University, 1-7 Machikaneyama, Toyonaka, Osaka, 560-0043 JAPAN, matumura@econ.osaka-u.ac.jp

3. Our Approach

In this experiment, we added two elements to encourage the participation of shoppers in the conventional sales promotion of food sampling. The first was an eye-catching object. Such an object attracts shoppers, and they notice the table of samples. The biggest problem in conducting sales promotion is that consumers are unaware of the existence of the promotion in the first place. Expanding an attractive promotion is meaningless if consumers are unaware of it. The object solves that problem.

We prepared a conspicuous fake food (Figures 1) that looks like jam falling onto a piece of toast in the air. Shoppers walking near the fake food would be highly likely to see it because it was fixed at about eye level. We designed it so as to increase visibility. Specifically, we made it larger than actual toast and jam bottles, and the colors were closer to a complementary color relationship to make it more conspicuous. There are two reasons for adding a fake food (toast) to encourage jam sampling. First, we thought that one scene where people eat jam is breakfast time. We aimed to let shoppers who were not interested in jam before coming to the supermarket develop interest. The second reason is because the bread was necessary for the voting style (described later), so we thought this was an appropriate combination.

The second element encouraging the participation of shoppers in the food sampling was a voting-style gimmick (Figure 2). The gimmick gives them the motivation to actively participate in order to enhance the effectiveness of the promotion. According to Zhang, food sampling as a sales promotion has perceived risk for consumers. Once they sample a food, they feel obligated to buy the goods, so they may decline the samples. In order to alleviate this risk, the voting-style gimmick was invented. In our experiment, we treated jam as the main product, but we decided to accompany the jam with bread to carry out the voting-style gimmick using toothpicks.

Figure 1: The eye-catching object.

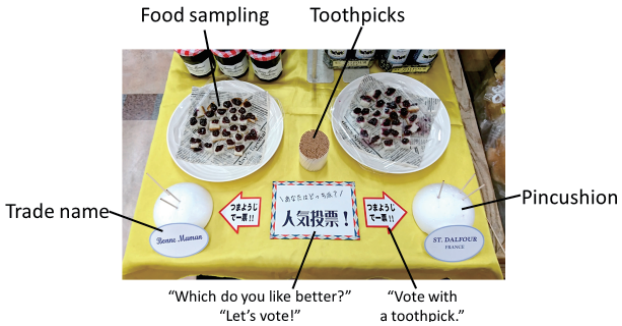

Figure 2: The voting-style gimmick.

4. Hypothesis

We formed two hypotheses on shoppers' reactions to samples at a supermarket.

Hypothesis I: As the eye-catching object attracts shoppers, the possibility that they will notice the sales promotion increases.

Hypothesis II: As the voting-style gimmick lowers the perceived risk of shoppers, they will actively participate in the promotion.

5. Method

Over four days (Wednesday, September 26th to Saturday the 29th, 2018), we conducted a jam sampling experiment at a super market in Fukuoka, Japan. We set up only experimental materials without any salespeople, and we left all actions to the freedom of the shoppers. The staff made observations so as to be inconspicuous from afar. Observation items were "they looked at the sampling," "they stopped," "they ate the sampling food," and so on. We observed for 5 hours each at various times of day and under 4 conditions. Condition 1 was in the basic form of all experiments. Pincushions for voting were not essential, but one was installed in order to align the experimental conditions. In Condition 2 we added the voting style to Condition 1. People who tasted were urged to vote by placing their used toothpicks into one of the pincushions beside the jam that they preferred. In Condition 3 we added the eye-catching object to Condition 1. We placed only one pincushion for the same reason as in Condition 1. Condition 4 synthesized Conditions 1 through 3.

We observed 2,147 people, and 2,073 people were useful samples, measured as passersby who were nearby and reacted to the sampling. There were 1,653 women and 420 men. Participants were not informed that they were being observed, so their characteristics were based on the observer's estimation.

6. Results

In order to verify the hypothesis, a logistic regression analysis revealed the effect of eye-catching objects and environmental factors on shoppers' behavior. *Attention*, *stopping*, *sampling*, and *voting* were the dependent variables. *Attention* included three other dependent variables and also included weak reactions, such as glances. We made all of these as dummy variables.

When the dependent variables were *attention*, *stopping*, and *sampling*, the output indicated that *object*, the independent variable, was significantly related with positive coefficients. There was no significant result for voting as a dependent variable. When the dependent variables were *stopping* and *sampling*, the output indicated that *vote*, the independent variable, was significantly related with positive coefficients. There were no significant results for *attention* or *voting*. These results partially supported Hypothesis I and II. Thus, it turns out that the eye-catching object had a positive effect on consumers' behavior.

7. Conclusion

We conducted this experiment with emphasis on promotion within stores because the importance of sales promotion is increasing due to the commoditization of consumer goods. We hypothesized that it is possible to increase the effects of promotions by adding an eye-catching object and a voting-style gimmick to food sampling as a conventional sales promotion. As a result, it was revealed that the object and gimmick were able to enhance the possibility of shoppers reacting to the sampling. A relatively wide age group of shoppers reacted to the sampling.

References

[Chandon 00] Chandon, P., Wansink, B., and Laurent, G.: A Benefit Congruency Framework of Sales Promotion Effectiveness, Journal of Marketing, Vol. 64, Oct 2016, pp. 65–81 (2000).

[Iyengar 00] Iyengar, S. S, Lepper, M.: When Choice is Demotivating: Can One Desire Too Much of a Good Thing?, Journal of Personality and Social Psychology, Vol. 79, No. 6, pp. 995–1006 (2000).

[Zhang 17] Zhang, L.: The Effect of Introducing a Voting-Style on Tasting Promotion, Graduate School of Economics, Osaka University, Master thesis (unpublished) (2017).

The 33rd Annual Conference of the Japanese Society for Artificial Intelligence, 2019

Vision Based Analysis on Trajectories of Notes Representing Ideas Toward Workshop Summarization

Yuji Oyamada*1 Mikihiko Mori*2 Haruhiko Maenami*1

*1Tottori University *2Hosei University

In some workshops, the participants use sticky notes to represent their ideas and the notes are regarded as one of the outputs. When workshop analysts summarize a workshop afterwards, they compare those notes and recorded video and/or audio by hand. We hypothesize that spatial and sequential information of the notes represents how ideas are came up with and how discussions flow. Therefore, we propose a vision based system analyzes trajectories of such notes during workshops. This paper introduces our prototype system that analyzes trajectories of notes representing ideas. During the workshop, the system recognizes and tracks each note separately from camera observation. The recognition and tracking results are saved and used for further offline analysis. From preliminary experiments, we confirmed that the proposed system can potentially reduce the manual tasks.

1. Introduction

Today, the workshop [Geurts 01] departs from the original meaning such as "workplace" or "studio", it means a method to learn or create ideas through experience, work, discussion, emergence among participants, devise solutions for problems. A typical example is people learn to make things by hand or to play music/theater through work participation and physical expression. Also, workshops are using for corporate training in recent years, and it is also frequently used as a means of formulating public policy, citizen participational consensus building or disaster prevention measures.

Considering the discussions in workshops, argument mining [Moens 18] occupies a position to find contextual meanings from the discussions to analyze. Thus, the area of argument mining typically aims to analyze the structure and important words and sentences from text data of utterance.

Discussion mining considers the progress and turning points of discussion [Nagao 04]. Focusing on meetings using slides, their works record the video of the meeting as well as statements and their types of the statements. From those recorded information, we can overlook the structure of discussion [Nagao 04] and presenter's tasks [Nagao 15].

Workshop reflector records a wide variety of activities during workshops to reflect them [Tomobe 08]. A workshop is semi-automatically recorded as pictures, videos, and audios. After the recording, texts or handwritten images are annotated to those recorded data. Once the annotation is done, participants in the workshop can reflect the discussion from those annotated contents with time-line or card style representations.

Contrast to the state-of-the arts, we extract a different type of information from workshop outputs to support workshop analysts. Figure 2 (a) shows our target situation. Workshop participants sit/stand surrounding a table. During the workshop, the participants write their idea and keywords on idea notes, a kind of small sheet of paper, and put them on the table. Following their discussion, the participants move the idea notes to represent their connectivity by their physical distance. When a group of idea notes form a group, the participants put a special idea note to assign a label to the group. Finally, we obtain a set of idea notes and their corresponding groups.

Workshop analysts need to summarize a workshop from its output such as notes representing ideas and their spatial relationship. This task requires them to compare the workshop outputs and recorded video/audio several times by hand, which is time consuming. We hypothesize that spatial and sequential information of the notes represents how ideas are came up with and how discussions flow. Therefore, we propose a vision based system analyzes trajectories of such notes during workshops.

Contact: Yuji Oyamada, Tottori University, Japan, oyamada@tottori-u.ac.jp

2. Our prototype system

We aim to support workshop analysts summarizing discussions in a workshop to confirm their progression retrospectively. As a first step of this ultimate goal, this paper proposes our prototype system of vision based progress recorder to analyze workshops.

As mentioned above, our aim is to support workshop analysts summarizing the progress of a workshop. In this paper, we introduce our prototype system based on simple computer vision technique. Specifically, we record idea notes put on the table and analyze the recorded sequence in real-time. Using computer vision technique, we can detect idea notes from the recorded picture and recognize their ID in real-time. Hence, we can record (1) when and where each idea note appears on the table, (2) how each idea note moves, and (3) which idea notes form a group. We regard those recorded information as a representation of the discussion progress. So, workshop analysts can retrospect the workshop from the information: idea notes' creation time represents when the idea comes out, idea notes' trajectory represents how the idea interact each other, and groups represent the relationship between the ideas.

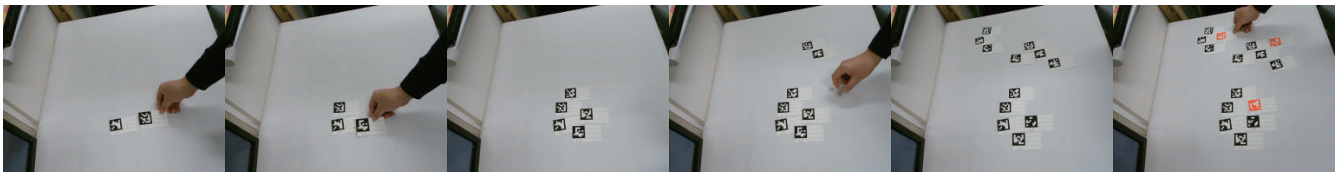

(a) Input sequence

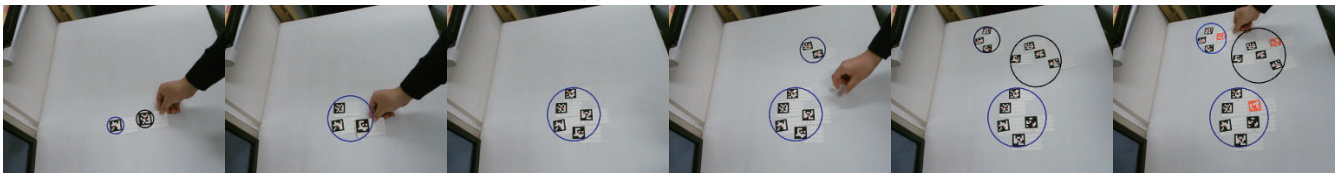

(b) Real-time analysis result

Figure 1: The video sequences. (Top) The input video sequence. (Bottom) A sequence visualizing the grouping result.

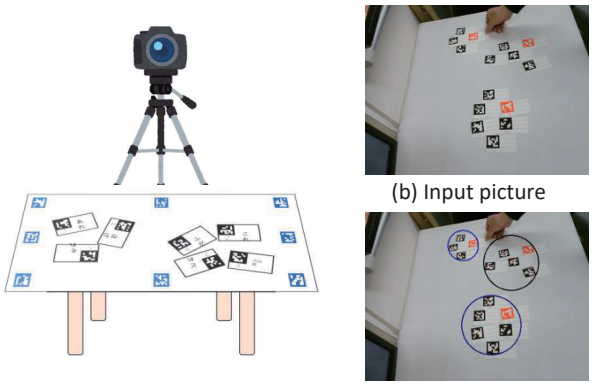

Figure 2: The proposed system.

2.1 System Configuration

Figure 2 (a) shows our system setup. We put a camera over a table to observe an entire table. The camera sends a video sequence to a PC. The PC detects and recognizes idea notes put on the table and group them into some groups in real-time. The position of each detected idea note as well as the pgrouping information are stored with recorded time information. Fig. 2 (b) shows a sketch of input picture and analysis result.

To enable idea notes detection and recognition easier, we design a special idea notes as shown in Fig. 3. Each idea note consists of three parts:

1. 2D barcode part on the left top is for the PC to detect and recognize the idea note.
2. ID part on the left bottom is for the participants to recognize the idea note.
3. text part on the right is for the participants to write their idea and keywords.

We design two types of idea notes, one for normal use and the other for labeling. The participants use normal idea notes (Fig. 3 (a)) for writing their ideas. Only when they

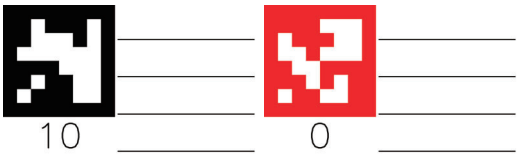

(a) Normal (b) Label

Figure 3: Example of the designed idea notes.

label groups, labeling idea notes are used. For ease of understanding, we differentiate these different type idea notes by color.

2.2 Vision based progress analysis

This section briefly explains how our prototype system analyzes the workshop progress.

2.2.1 On-line idea note grouping

On-line idea note grouping is done by two steps. The first step is idea note detection and recognition. We use ArUco [Garrido-Jurado 16, J.Romero-Ramirez 18] for this process. ArUco is an open source library for camera pose estimation using squared markers such as 2D barcodes shown in Fig. 3. As a pre-processing, ArUco builds a database storing the relation between 2D barcode and idea note's ID. During system operation, ArUco takes a picture from the camera and detects and recognizes 2D barcodes appearing on the picture. As results, ArUco outputs a set of idea notes information, each of which consists of its ID and detected spatial position in the 2D picture coordinate.

The second step is to group the idea notes. Assuming that all idea notes assigned to a group must be closer, we solve this grouping problem by the following ad-hoc aggregation.

1. computes a threshold distance for each idea note,
2. computes a pairwise distance between all pair of the idea notes,
3. aggregates multiple idea notes into a single group if their pairwise distance is less than one of their threshold distances.

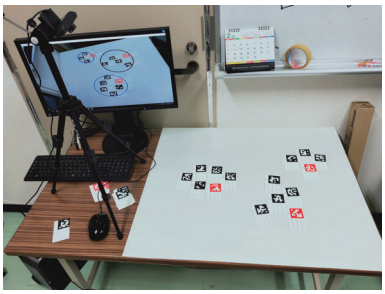

Figure 4: Experimental setup.

2.2.2 Off-line trajectory analysis

Off-line trajectory analysis visualizes trajectories of idea notes so that workshop analysts can reflect the discussions from idea notes' activity. We propose two type of visualization. Both visualization encode time stamp by color. The first visualization draws the trajectories of interests as shown in Fig. 6 (a). A symbol is assigned to each idea note and their position at each frame is plot with associated color. The second visualization draws the trajectories of all idea notes as shown in Fig. 6 (b). Contrast to the above one, this visualization uses same symbol for all idea notes. Thus, this visualization is to see when participants moves the idea notes more.

3. Experiments

We conducted a preliminary experiment to show how our prototype system works and to show its potential. Figure 4 shows the experimental setup. We prepared a half-A0 size white paper on a table. The paper area was used for idea note based discussion. We put a camera at the left hand side of the table to observe the scene. An operator checked the real-time analysis result on a computer monitor behind the tripod.

In this experiment, an operator performed fake discussion as shown in Fig. 1 (a). The idea notes history is as follows

1. made a group of five idea notes in the middle,
2. made another group of two idea notes in the top right
3. moved an idea note from the first group to the second one,
4. added one idea note to each group,
5. made the third group of 3 idea notes in the top left,
6. assigned a label idea note to each group.

After the fake discussion, the operator captured pictures of idea notes assigned to each group. The computer automatically cropped each of the assigned idea notes and saved them as separate files.

3.1 Real-time grouping results

Figure 1 (b) visualizes the on-line grouping results corresponding to their counterparts in Fig. 1 (a). All markers assigned to a single group is bounded by a unique colored ellipse. As the figure shows, idea notes grouping worked well. For a 24bit picture of 640×480 resolution, the on-line analysis worked in real-time on an ordinary computer.

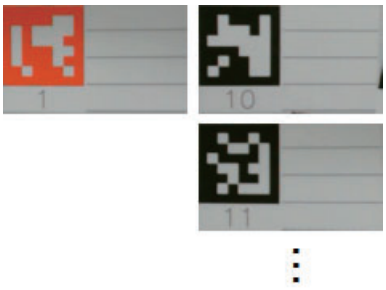

(a) Idea notes assigned to Group 0

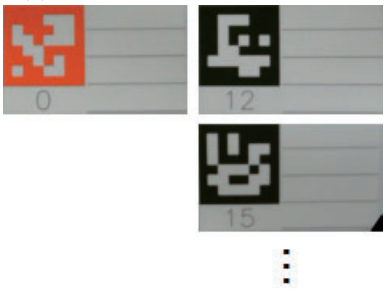

(b) Idea notes assigned to Group 1

Figure 5: Grouping results.

Figure 5 shows the label idea note and some normal idea notes of first two groups. Even though we just saved the cropped notes, we believe that we can extract text written on the notes by OCR and use such information for further reflection.

3.2 Off-line trajectory analysis

Figure 6 shows off-line trajectory analysis result. We can see that the active region moves from the middle to the top and that a single idea note moves from the middle to the top region. These results are consistent with Fig. 1.

4. Conclusion

Considering recent trend style of discussions and workshops, we aim to offer workshop analysts useful tools. As a first step of this ultimate goal, we introduced our prototype system of vision based workshop progress analysis. The preliminary experiments show some potential of our prototype system.

Acknowledgment

This work was partially supported by JSPS KAKENHI Grant Number 18K02834 and Tottori Unversity CBR Grant Program.

References

[Garrido-Jurado 16] Garrido-Jurado, S., Salinas, noz R. M., Madrid-Cuevas, F., and Medina-Carnicer, R.: Generation of fiducial marker dictionaries using Mixed

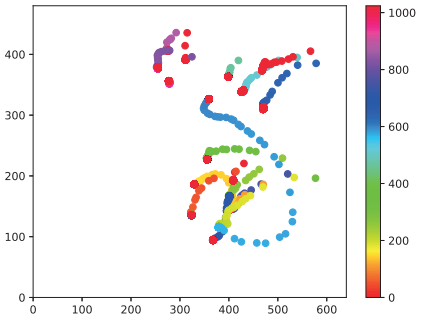

(a) Trajectory of all idea notes.

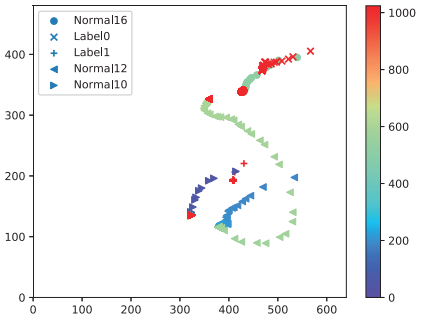

(b) Trajectory of some idea notes.

Figure 6: Off-line trajectory analysis.

Integer Linear Programming, *Pattern Recognition*, Vol. 51, pp. 481–491 (2016)

[Geurts 01] Geurts, J. and Joldersma, C.: Methodology for participatory policy analysis, *European Journal of Operational Research*, Vol. 128, No. 2, pp. 300–310 (2001), Complex Societal Problems

[J.Romero-Ramirez 18] J.Romero-Ramirez, F., Salinas, noz R. M., and Medina-Carnicer, R.: Speeded up detection of squared fiducial markers, *Image and Vision Computing*, Vol. 76, pp. 38–47 (2018)

[Moens 18] Moens, M.-F.: Argumentation Mining: How Can a Machine Acquire Common Sense and World Knowledge?, *Argument & Computation*, Vol. 9, No. 1, pp. 1–14 (2018)

[Nagao 04] Nagao, K., Kaji, K., Yamamoto, D., and Tomobe, H.: Discussion Mining: Annotation-Based Knowledge Discovery from Real World Activities, in *Pacific-Rim Conference on Multimedia*, pp. 522–531 (2004)

[Nagao 15] Nagao, K., Inoue, K., Morita, N., and Matsubara, S.: Automatic Extraction of Task Statements from Structured Meeting Content, in *International Joint Conference on Knowledge Discovery, Knowledge Engineering and Knowledge Management*, pp. 307–315 (2015)

[Tomobe 08] Tomobe, H.: Workshop Reector: An Interface for Reecting Processes of Human Activities on Workshops, in *International Workshop on Content Creation Activity Support by Networked Sensing (CCASNS)* (2008)

The 33rd Annual Conference of the Japanese Society for Artificial Intelligence, 2019

Intuitive Automatic Music Arrangement System for Wave Files Following Sensitivity Words

Koichi Yamagata[*1], Shota Miyoshi[*1], Maki Sakamoto[*1]

[*1] Graduate School of Informatics and Engineering, The University of Electro-Communications

Music is frequently used to guide the atmosphere. However, when we play our favorite music, that music is not always suitable for atmosphere of the place. We propose a method to arrange music automatically so that music follows given sensitivity adjective words. We use music files in wave format for practicality and arrange only tempo and pitch for the purpose. This system is based on an experiment that subjects arranged music wave files from ten genres to follow 16 adjectives. Hypothesis tests on a psychological evaluation experiment confirmed that adjustment of tempo and pitch of our system is sufficiently effective to derive sensitivity.

1. Introduction

Music plays an important role in people's lives because music is effective for proper induction of people's emotions. The relation between emotion and music has been studied for a long time. Hevner [Hevner 1935, 1936, 1937] and Bruner [Bruner 1990] revealed the relationship between music factors (tempo, pitch, rhythm, etc.) and sensitivity words. From these research, it is recognized that slow tempo music induces sensitivities such as "serene", and fast tempo music induces sensitivities such as "exciting". Meanwhile, low pitch music induces "sad", and high pitch music induces "graceful".

Based on these knowledge, various systems about music and sensitivity such as music retrieval systems have been proposed [Ikezoe 2001, Tsuyoshi 2005]. Further, various methods of automatic music editing or music composition with sensitivities have been proposed [Cruz 2007, Tokairin 2008, Akiguchi 2009]. However, existing systems are based on the assumption that users have music files in midi format containing musical score information.

The purpose of this study is to develop a system to arrange music wave files automatically so that music follows given sensitivity adjectives. The wave format is more practical than midi because most selling music can be easily converted to wave format.

2. Materials and Methods

2.1 Task Design

We conducted a psychological experiment to acquire the data set necessary for the development of automatic music arrangement system. In this experiment, the subjects are asked to change the tempo and pitch so as to match the given sensitivity to the music of 10 different genres. From this data, we confirm the effect of target sensitivity words on the arrangement music. Based on this data, we construct a system to arrange music by sensitivity words automatically.

Contact: Koichi Yamagata, UEC, 1-5-1, Chofugaoka, Chofu, Tokyo182-8585, Japan, koichi.yamagata@uec.ac.jp, 042-443-5535

2.2 Participants

The number of participants were 10 (2 women and 8 men, mean age = 22.3). They have no known impediment in speech or in hearing. They were not informed of the purpose of the experiment.

2.3 Apparatus and Stimuli

In this study, we used ten music files as the experimental stimuli obtained from the GTZAN Genre Collection, which is one of the first publicly available dataset for research purposes. This database was used for the well-known paper in genre classification [Tzanetakis 2002]. These files were collected in 2000-2001 from a variety of sources including personal CDs, radio, microphone recordings, in order to represent a variety of recording conditions. It contains 10 genres (blues, classical, country, disco, hiphop, jazz, metal, pop, reggae, rock) and consists of 1000 audio tracks in .wav format. We selected one music file from each of 10 genres.

To change tempo and pitch of music freely, we adopted Hayaemon (http://hayaemon.jp/) which is an Android tablet application operated by touch control (Fig. 1).

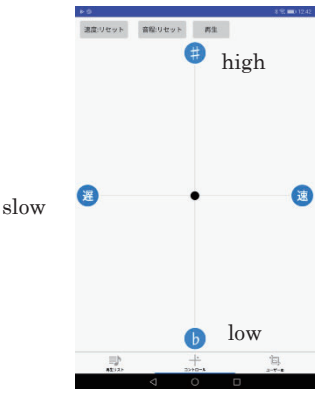

Fig. 1: The operation screen of Hayaemon which is an android tablet application to change tempo and pitch of music.

2.4 Procedure

We asked each participant to arrange tempo and pitch of music so that the atmosphere of music followed a given adjective. For example, if the given adjective was "bright", the participant arranged tempo and pitch to be bright. We extracted eight

adjective pairs implying features of music from 43 sensitivity adjective pairs used in [Doizaki 2013] with referring to [Ikezoe 2001] as shown in Table 1. Other sensitivity adjectives can be associated with any one of the eight adjective pairs by comparing correlation coefficients.

Table 1. Eight adjective pairs

	Positive adjective		Negative adjective
1	bright	9	dark
2	heavy	10	light
3	hard	11	soft
4	stable	12	unstable
5	clean	13	dirty
6	smooth	14	rough
7	intense	15	calm
8	thick	16	thin

Fig. 2 shows the result of this experiment for ten genres of music when adjectives were bright (red) and dark (blue). The horizontal and vertical axis represent arranged tempo and logarithm of pitch, respectively. We can see that red and blue points are clustered. Fig. 3 shows result for other pairs of adjectives. Red and blue points correspond to positive and negative adjectives, respectively. In this figure, points for all genres are combined because of space limitations. We can see that red and blue points for most adjective pairs tend to form different clusters.

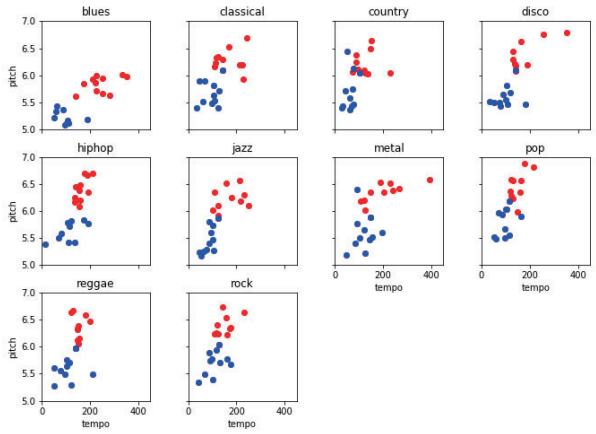

Fig. 2: Result of the experiment for ten genres of music when adjectives were bright (red) and dark (blue). The horizontal and vertical axis represent arranged tempo and logarithm of pitch, respectively.

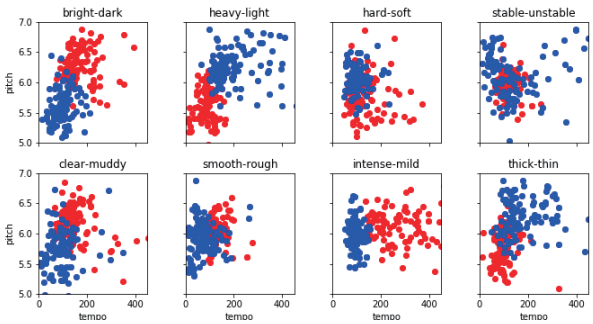

Fig. 3: Result of the experiment for eight adjective pairs. Red and blue points indicate results of positive and negative adjectives, respectively. Points for all genres are combined.

2.5 Data analysis

At first, to assess the effect of adjectives on tempo and pitch, we conducted two-way factorial analysis of variance (two-way ANOVA), where adjectives and music are independent variables, and tempo and pitch are dependent variables. Table 2 shows result of two-way ANOVA for tempo as an independent variable. Table 3 shows result for pitch in like manner. Numerical values in these tables are p-values from f-ratios under the null hypothesis that there is no effect of adjectives and/or music genres as independent variables. From p-values for adjectives of the f-tests, we can see that all of the eight adjective pairs have significant effect for both tempo and pitch. The p-values for music also imply that the effect of music genre is not negligible.

Table 2: P-values from two-way ANOVA for tempo as an independent variable.

		P-values from f-ratio		
Positive adjective	Negative adjective	Adjective	Music	Adjective: Music
bright	dark	1.51×10^{-23}	2.17×10^{-5}	0.006
heavy	light	1.08×10^{-25}	0.018	0.162
hard	soft	5.50×10^{-5}	0.153	0.886
stable	unstable	1.66×10^{-2}	0.273	0.776
clear	muddy	9.26×10^{-10}	0.437	0.909
smooth	rough	5.32×10^{-11}	0.204	0.141
intense	mild	1.27×10^{-42}	1.68×10^{-4}	0.008
thick	thin	2.35×10^{-17}	2.80×10^{-3}	0.506

Table 3. P-values from two-way ANOVA for pitch as an independent variable.

		P-values from f-ratios		
Positive adjective	Negative adjective	Adjective	Music	Adjective: Music
bright	dark	1.13×10^{-51}	8.94×10^{-13}	0.744
heavy	light	4.3×10^{-42}	1.66×10^{-11}	0.934
hard	soft	8.50×10^{-14}	8.17×10^{-14}	0.756
stable	unstable	5.16×10^{-4}	1.17×10^{-10}	0.771
clear	muddy	2.67×10^{-26}	2.58×10^{-13}	0.516
smooth	rough	2.07×10^{-6}	5.27×10^{-12}	0.903
intense	mild	5.75×10^{-5}	1.35×10^{-12}	0.414
thick	thin	3.58×10^{-34}	3.07×10^{-11}	0.799

Above experimental data enable us to devolve a system to arrange tempo and pitch automatically so that music follows given adjective. When target degrees of adjectives are given by 16-dimensional vector $x = (x_1, \dots, x_{16}) \in [0,1]^{16}$, arranged tempo t and pitch p for a music genre g are calculated as follows:

$$(t, p) = (t_{g0}, p_{g0}) + \frac{\sum_{i=1}^{16} x_i^3 (dt_{gi}, dp_{gi})}{\sum_{i=1}^{16} x_i^2}, \qquad (1)$$

where t_{g0} and p_{g0} are the total averages of tempo and pitch in the experiential data for genre g, $(t_{g0} + dt_{gi}, p_{g0} + dp_{gi})$ is the representative point of experimental data for the genre g and the i-th adjective. Note that (t, p) is identical to $(t_{g0} + dt_{g1}, p_{g0} + dp_{g1})$ when $x = (1,0, \dots, 0)$, and (t, p) is identical to (t_{g0}, p_{g0}) when $x = (0, \dots, 0)$.

3. System Evaluation

To evaluate the accuracy of our system, we conducted a psychological experiment to 16 participants (2 women and 14 men, mean age = 22.9). They were asked to evaluate the music arranged by our system for 16 target adjectives and 10 genres of music. Every target adjective obtained 40 samples (10 genres × 4 trials), that are enough for the central limit theorem and z-tests. Participants were not informed the target adjective, and answered scores of all 8 adjective pairs on a scale from -3 to 3. Table 4 shows p-values from one-sided z-tests under the null hypothesis that the mean score of the target adjective is zero for each adjective. These result of z-test show that means of scores for most target adjectives are significantly different from zero at the 5 percent level except for “hard”, “smooth”, and “soft”.

Table 4: Results of one-side z-tests under the null hypothesis that the mean score of evaluation of arranged music for each adjective is zero.

Adjective	Mean	Standard deviation	Z-value	P-value
bright	-1.90	0.98	-12.24	9.70×10^{-35}
heavy	-1.73	1.34	-8.14	1.90×10^{-16}
hard	-0.43	1.96	-1.37	0.09
stable	-1.13	1.52	-4.67	1.48×10^{-6}
clear	-0.90	1.57	-3.64	1.39×10^{-4}
smooth	-0.45	1.78	-1.60	0.055
intense	-1.75	1.43	-7.75	4.52×10^{-15}
thick	-1.65	1.25	-8.34	3.80×10^{-17}
dark	1.53	1.38	7.00	1.25×10^{-12}
light	2.00	1.55	8.15	1.86×10^{-16}
soft	0.08	1.69	0.28	0.39
unstable	0.68	2.14	1.99	0.02
muddy	1.20	1.52	4.98	3.10×10^{-7}
rough	2.63	0.87	19.13	7.18×10^{-82}
mild	1.00	1.26	5.02	2.64×10^{-7}
thin	1.10	1.34	5.21	9.56×10^{-8}

4. Conclusion

This study proposed a method to arrange music automatically so that music follows given sensitivity adjective words. We used music files in wave format for practicality. The arranged tempos and pitches are calculated from experimental data that subjects arranged music wave files from ten genres to follow 16 adjectives because f-tests of our experimental data indicated that not only adjective but also music genre is significant factor to determine tempo and pitch. The results of z-tests on psychological evaluation experiment confirmed that adjustment of tempo and pitch of our system is sufficiently effective to derive sensitivity.

Acknowledgements

This work was supported by JST-Mirai Program Grant Number JPMJMI17DB, Japan.

References

[Hevner 35] Hevner, K.: The Affective Character of the Major and Minor Modes in Music, The American Journal of Psychology, Vol.47, No.1, pp.103-118 (1935)

[Hevner 36] Hevner, K.: Experimental Studies of the Elements of Expression in Music, The American Journal if Psychology, Vol.48, No.2, pp.246-268 (1936)

[Hevner 37] Hevner, K.: The Affective Value of Pitch and Tempo in Music, The American Journal of Psychology, Vol.49, No.4, pp.621-630 (1937)

[Bruner 90] Bruner, G. C.: Music, Mood, and Marketing, Journal of Marketing, No.4, pp.94-104 (1990)

[Ikezoe 01] Ikezoe, T., Kajikawa, Y., and Nomura, Y.: Music Database Retrieval System with Sensitivity Words Using Music Sensitivity Space. The Journal of Information Processing Society 42(12), 3201–3212 (2001)

[Tsuyoshi 05] Takayama, T., Ikeda, T., Kuroda, S., and Takeda, Y.: Retrieval Interface ‘2D-RIB’ for Music Database by the Combination of Values of Fixed Numbers of Opposite Impression Pairs, DBSJ Letters, Vol. 3, No. 4, pp. 29-32 (2005)

[Cruz 07] Cruz, R., Brisson, A., Paiva, A., and Lopes, E.: I-Sounds - Emotion-Based Music Generation for Virtual Environments, ACII 2007 Springer, LNCS 4738, pp. 769-770 (2007)

[Tokairin 08] Tokairin, M., Sizuka, H.: Automatic Music Composition System through KANSEI Adjectives, Transactions of Japan Society of Kansei Engineering, Vol. 8, Issue 1, pp. 119-127 (2008)

[Akiguchi 09] Akiguchi, S.; Development of Melody Automatic Generation System from Music Impression Using Soft-Computing Method, Journal of Japan Society for Fuzzy Theory and Intelligent Informatics, Vol. 21, Issue 5, pp. 782-791 (2009)

[Tzanetakis 02] Tzanetakis, G. and Cook, P.: Musical genre classification of audio signals, IEEE Trans. Speech Audio Process., vol. 10, no. 5, pp. 293–302 (2002)

[Doizaki 13] Doizaki, R., Oikawa, A., Shimizu, Y., and Sakamoto, M.: Intuitive Color Design Support System Using Onomatopoeia, Proceedings of the 5th International Congress of International Association of Societies of Design Research (IASDR 2013), 757-766 (2013)

International Session | International Session | [ES] E-4 Robots and real worlds

[2D3-E-4] Robots and real worlds: planning and control

Chair: Eri Sato-Shimokawara (Tokyo Metropolitan University), Reviewer: Hiroki Shibata (Tokyo Metropolitan University)

Wed. Jun 5, 2019 1:20 PM - 2:20 PM Room D (301B Medium meeting room)

[2D3-E-4-01] Mahalanobis Taguchi Fukuda Approach to Motion Control

○Shuichi Fukuda[1] （1. Keio University）

1:20 PM - 1:40 PM

[2D3-E-4-02] Flexibility of Emulation Learning from Pioneers in Nonstationary Environments

Moto Shinriki[1], ○Hiroaki Wakabayashi[1], Yu Kono[1], Tatsuji Takahashi[1] （1. Tokyo Denki University）

1:40 PM - 2:00 PM

[2D3-E-4-03] A Multimodal Target-Source Classifier Model for Object Fetching from Natural Language Instructions

○Aly Magassouba[1], Komei Sugiura[1], Hisashi Kawai[1] （1. NICT）

2:00 PM - 2:20 PM

The 33rd Annual Conference of the Japanese Society for Artificial Intelligence, 2019

Mahalanobis Taguchi Fukuda Approach to Motion Control

Shuichi Fukuda [*1]

[*1] Keio University, System Design and Management Research Laboratory

As the environments and situations change frequently and extensively and these changes are unpredictable, interaction with the outer world increases its importance. Yesterday, changes were smooth, so they are mathematically differentiable, and we could predict the future. Thus, reproducibility was important, and we could develop model-based approaches. But situations being such, adaptability becomes increasingly important. In the case of motion control, coordination or balancing becomes important, but there is very few, if any, researches on how to learn to control motions. Most researches present the successful cases. But to learn to control, we need an approach to learn by trial and error, or, to learn from failures. Shuichi Fukuda proposed a new approach by extending Mahalanobis-Taguchi approach.

1. Introduction

It is pointed out in this paper that changes yesterday and today are different and changes today are unpredictable. Further, motion control is related to the problem of coordination or balancing. When our world was closed with boundaries, it was easy to develop a model and to solve the problem analytically.

But today changes are unpredictable, so adaptability is increasing importance. To cope with such changes, interaction with the outer world should be taken into consideration. But since the environments and situations change frequently and extensively, and unpredictably. What is needed now is not knowledge, but wisdom.

To be wise, we need to learn from failures. We solve the problem by trial and error. But there are very few approaches to support us to learn from failures.

Shuichi Fukuda extended Mahalanobis-Taguchi approach to learning from failures and proposes here the new approach Mahalanobis-Taguchi-Fukuda approach. This approach will be effective even in such an environment and situation of swmming, which is almost impossible to apply traditional model based approach.

2. Motion Control: What are the Issues?

Although there are many measurement tools for motion control, they only show us the successful motions. We do not understand how we can learn to control our motion to this final success.

Nikolai Burnstein pointed out human motion control is very difficult due to its large number of degrees of freedom. Fig.1 shows his famous cyclogram of hammering.

Fig. 1 Human motion of hammering

As this cyclogram shows, human motion trajectory varies widely every time, but near the target, the trajectory is fixed, i.e,. the number of degrees of freedom of trajectories is very large far away from the target, but it is reduced to the minimum near the target. The large number of degrees of freedom is to balance a body.

In other words, balancing plays a very important role in human motion control. Bernstein used the word “co-ordination” [Bernstein 1967] and he emphasized how important co-ordination, or balancing is.

Apart from such jobs, humans need balancing to move in daily life. Therefore, we need to know how we can secure balancing in the case of humans, But the mechanism of proprioception or deep sensation is still not clear.

Although Bernstein did not point out, but we may safety say that current engineering is based on the model when human motions are fixed near the target. As the number of degrees of freedom is reduced to the minimum, we can easily apply mathematical analyses. But with the rapid expansion of our world and disappearing of boundaries, engineering is shifting from an individual machine/product to a team machine/product. Therefore, the number of degrees of freedom increases exponentially. Thus, our world is shifting from explicit to tacit or from verbal to nonverbal. Thus, balancing or coordination is a critical problem in engineering, especially in robotics.

Shuichi Fukuda, Keio University, System Design and Management Research Institute,
4-1-1, Hiyoshi, Kohoku-ku, Yokohama, 223-8526, Japan
shufukuda@gmail.com

Thus, what is missing today in motion control is how we can learn from failures. We learn to control motion by trial and error. So, we need a support tool to gudie us how we can balance better the next time. The current one only shows the final successful motion and does not provide any clue how we can do that.

Italians, Cecilia Laschi for example [Laschi 2012], [Laschi 2016] proposed Robosoft. Current robotics are based on a model approach or knowledge-based approach. But they insist that as environments and situations change frequently and extensively and in an unpredictable manner, such interaction-focused approach is increasing importance as we see in the octopuses. Octopuses make decisions how to adapt by trial and error. When their baby is born, parents die. So, there is no knowledge transfer from generation to generation. Further, octopuses have eight arms. If we study how they can coordinate these arms to perceive and understand the situation and to act to adapt to that current situation, it will help us to develop new tools for engineering which is quickly becoming multi-dimensional.

This problem is associated with the fact why we do not have swimming robots. Water changes every minute and our traditional engineering approach of system identification cannot be applied. But we learn to swim by trial and error.

Thus, how we learn to coordinate, or balance motion is a pressing issue today. This paper proposes one approach which works good for human motion control and is expected to be useful for wide applications in learning how to control motions.

3. Changes Yesterday and Today

There were changes yesterday. But changes yesterday were smooth so that they were mathematically differentiable. Therefore, we could predict the future. So, we could develop a mathematical analysis model, and solved the problem algebraically.

But changes today are sharp. So, we cannot differentiate them. Thus, we cannot predict the future. And adaptability becomes more important than reproducibility. We need to develop adaptive network in an age of teamworking to cope with this situation.

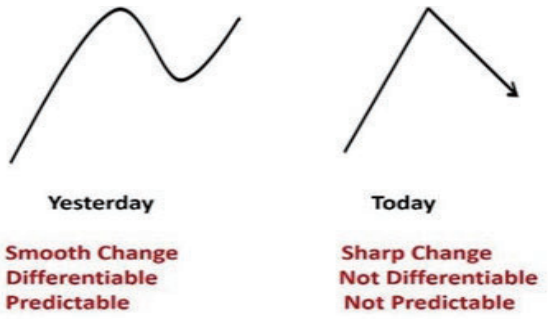

Fig. 2 Changes yesterday and today

4. Mahalanobis Taguchi Fukuda Approach

4.1 Mahalanobis-Distance

As space is limited, detailed explanation of Mahalanobis Distance (MD) is omitted here. The YouTube video [Clapham 2016] illustrates very well what MD is and how useful it is. In short, MD enables us to measure multivariate dimension variables.

4.2 Taguchi - Pattern Identification

Genichi Taguchi realized that Mahalanobis Distance is very useful for pattern identification. Patterns are multi-dimensional, and these dimensions are well defined [Taguchi 2002]

4.3 Fukuda – Learning from Failures

Taguchi set up a threshold MD and if MD of a pattern is within the threshold level, then it is identified as the same pattern. If MD exceeds the threshold, that pattern is different.

Fukuda regards musculoskeletal system as a pattern, although most robotics researchers use it as a basis for their model. Learners observe the change of MD. Successful motion varies from person to person, but we can utilize the generally accepted successful motion as a reference pattern for defining threshold. If learners control their motion to reduce their difference of MD and get closer to the threshold level, then he is improving. When he finally succeeds to control the motion, then we can set up his own threshold level.

5. Summary

Engineering and Robotics tomorrow should shift focus from nodes to links, if we use graph theory terms. Traditional engineering has paid efforts to make each node (model) richer or to advance its model further ahead. But in such environments and situations, where unpredictable changes occur frequently and extensively, i.e., our world is becoming nonverbal and increasing the number of degrees of freedom, we must develop sensors and actuators which directly interact with the outer world in multiple ways, just as the octopus does. We should study how we can increase the number of links or how we can enrich them. Thus, engineering is shifting from node-based to link-focused.

Such a shift calls for pragmatic approaches. We need to advance by trial and error. Thus, learning from failures becomes very important. We must develop approaches which help us to understand how we can control better next time by trial and error.

Shuichi Fukuda proposed here to extend Mahalanobis-Taguchi Approach to motion learning. We should extend it from pattern identification to pattern creation.

References

[Matthew E. Clapham, YouTube, Feb. 8, 2016] https://www.youtube.com/watch?v=spNpfmWZBmg, 2016.

[Taguchi 2002] Genichi Taguchi, Rajesh Yugulum, The Mahalanobis-Taguchi Strategy: A Pattern Techology System, John Wiley and Sons, 2002.

[Laschi 2012] C. Laschi, M. Cianchetti, B. Mazzolai, L. Margheri, M. Follador, Soft Robot Arm Inspired by the Octopus, Taylor and Francis, 2012.

[Laschi 2016] C. Laschi, B. Mazzolai, M. Cianchetti , Soft Robotics: Technologies and Systems Pushing the Boundaries of Robot Abilities, Science Robotics, eaah3690, 2016.

The 33rd Annual Conference of the Japanese Society for Artificial Intelligence, 2019

Flexibility of Emulation Learning from Pioneers in Nonstationary Environments

Moto Shinriki*1 Hiroaki Wakabayashi*1 Yu Kono*1 Tatsuji Takahashi*1

*1School of Science and Engineering, Tokyo Denki University

In imitation learning, the agent observes specific action-state pair sequences of another agent (expert) and somehow reflect them into its own action. One of its implementations in reinforcement learning is the inverse reinforcement learning. We propose a new framework for social learning, emulation learning, which requires much less information from another agent (pioneer). In emulation learning, the agent is given only a certain level of achievement (accumulated rewards per episode). In this study, we implement emulation learning in the reinforcement learning setting by applying a model of satisficing action policy. We show that the emulation learning algorithm works well in a non-stationary reinforcement learning tasks, breaking the often observed trade-off like relationship between optimality and flexibility.

1. Introduction

Humans usually begin learning with some kind of prior knowledge. If the knowledge is about the structure of the environment, the past experience, or other's action history, the learning will be somehow model-based, by transfer, or supervised (or inverse), respectively. Imitation learning requires an *expert* who provides an exemplar behavior. However, the expert's action data may be very expensive or unavailable in general. On the other hand, there are cases where (only) the information of someone's achievement level is obtained. Our search is often accelerated by a peer's high achievement or record breaking, as in sports or in invention. As it is closely related to *end state emulation* in social learning[1], we call this form of learning *emulation learning*. In emulation, the outcome of an action sequence ("what") is socially learned, while in imitation the process or the procedure ("how") is observed and assimilated.

In this study, from two aspect, we test the performance of the three algorithms: the vanilla Q-learning, imitation learning with inverse reinforcement learning, and our emulation learning with satisficing reinforcement learning. The first aspect is the speed of the learning algorithms. The second aspect is the flexibility of the algorithms. The learning task is a nonstationary reinforcement learning task, and we evaluate how flexibly the algorithm can respond to the environmental changes.

2. The Reinforcement Learning Algorithms

Reinforcement Learning is a type of machine learning in which an agent learns an appropriate action sequence through interaction, trial and error, in the environment. Recently, as researches on game AI and autonomous robot have been actively conducted, reinforcement learning is gaining more attention as a method for autonomous learning in unknown environments.

Contact: Tatsuji Takahashi, School of Science and Engineering, Tokyo Denki University, Ishizaka, Hatoyama, Hikigun, Saitama, Japan 350-0394, Tel: 049-296-5416, tatsujit@mail.dendai.ac.jp

2.1 Q-Learning

There is a representative method of reinforcement learning called Q-learning. The action value $Q(s_t, a_t)$ of Q learning is updated based on the estimation policy. When the estimation policy is set as the greedy policy, the action value $Q(s_t, a_t)$ is updated as:

$$Q(s_t, a_t) \leftarrow Q(s_t, a_t) + \alpha\Big(r_t + \gamma \max_a Q(s_{t+1}, a) - Q(s_t, a_t)\Big), \quad (1)$$

where α is the learning rate and γ is the discount rate.

2.2 Inverse Reinfocement Learning as Imitation

Inverse reinforcement learning (IRL) is a form of learning of which the goal is to infer a reward function $R(s)$ from the expert's behavior trajectory T. A reward function $R(s)$ is usually a function which returns a reward calculated by multiplying the parameter θ and the one-hot-vector of the state. The behavior trajectory is a pair of expert's states and actions, $(s_0, a_0, s_1, a_1, ...)$. In this study, we used the maximum entropy IRL (MaxEntIRL) as the implementation[3].

2.3 Emulation by Risk-sensitive Satisficing (RS)

Humans tend not to exhaustively search for optimazation. Rather, we satisfice. That is, we confront a task with certain reference level (aspiration) and finish searching when we find an satisfactory actoin better than the reference [6]. When the aspiration is given socially, satisficing means emulation. Satisicing policy will converge the actions to take, when the aspiration is satisfied, after the limited search. We implement emulation with the RS model, a cognitive satisficing value function with reflective risk attitudes as in the prospect theory in behavioral economics [2]. The RS value funtion is defined as follows:

$$RS(s_t, a_t) = \tau(s_t, a_t)\Big(Q(s_t, a_t) - \aleph(s_t)\Big) \quad (2)$$

$$a_t^{\mathrm{sel}} = \arg\max_a RS(s_t, a) \quad (3)$$

RS's valuation qualitatively changes according to the sign of the difference between the aspiration and the Q value. It considers the reliablity of the Q value with τ that approximates how many times the action has been chosen. τ is defined as follows, where γ_τ is the discount rate and α_τ is the learning rate.

$$\tau(s_t, a_t) = \tau_{\text{curr}}(s_t, a_t) + \tau_{\text{post}}(s_t, a_t) \quad (4)$$

$$\tau_{\text{curr}}(s_t, a_t) \leftarrow \tau_{\text{curr}}(s_t, a_t) + 1 \quad (5)$$

$$\tau_{\text{post}}(s_t, a_t) \leftarrow (1 - \alpha_\tau)\tau_{\text{post}}(s_t, a_t) + \alpha_\tau \gamma_\tau \tau(s_{t+1}, a^{\text{sel}}_{t+1}) \quad (6)$$

2.3.1 Global reference conversion (GRC)

While RS works as intended in the multi-armed bandit problems that may be considered as a single state reinforcement learning task, it is generally difficult to assign the optimal aspiration to each state, when the global aspiration (for the entire episode) is avaiable from a pioneer. The global reference conversion (GRC) allocates optimal reference values to each state by defining the global observed expectation E_G and the global satisficing reference value $\aleph_G$ defined below. It is this $\aleph_G$ that works as a social goal-setting trigger, such as someone's high performance or record breaking. E_G is defined using the temporary expectation (E_{tmp}) which is periodically reset.

$$E_G \leftarrow \frac{E_{\text{tmp}} + \gamma_G N_G E_G}{1 + \gamma_G N_G} \quad (7)$$

$$N_G \leftarrow 1 + \gamma_G N_G \quad (8)$$

$$\delta_G = \min(E_G - \aleph_G, 0) \quad (9)$$

$$\aleph(s_i) = \max_a Q(s_i, a) - \zeta(s_i)\delta_G \quad (10)$$

The parameter $\zeta(s_i)$ is introduced to adjust the scale of the global reference value and the Q value.

3. Task: UnsteadySwitchWorld

To test the speed and flexibility of the learning algorithms, we conducted an experiment, based a task called SwitchWorld introduced in the previous study by some of the authors [4]. In this experiment, we used a *UnsteadySwitchWorld* task in which the switches change their places periodically. The state space of the task is shown in Fig. 1. The red cells are where a switch is placed, and the green cell is where the agent is placed at the initial step of an episode. The agent can move to one of the upper, lower, left, or right adjacent cell in an action. When the agent passes through one of the switch cells, the agent is notified of it (an augmented state space [5]). When the agent has acted for 99 times, each episode ends. In order for the agent to gain a reward, the switches must be pressed in a correct order: switch 1, 2, and then 3. When the agent presses the last switch, a reward 1 is given, and the state of the switches resets. In this experiment, the agent ran 10000 episodes and calculated the average of 1000 simulations. The switch changes its place randomly every 1000 episodes, under the constraint that the new switch configuration is not the same at the previous one. The maximum reward in an episode is always six, because a lap (from switch 1 to 2 to 3) takes 16 moves.

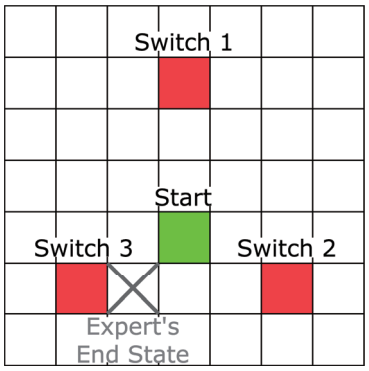

Fig. 1: Unsteady Switch World Task

4. Simulation and Result

QL and MaxEntIRL are operated under the ϵ-greedy policy, in which the agent selects an action at random at probability ϵ and selects the greedy action a with the highest action value $Q(s_t, a_t)$ at probability $1 - \epsilon$. ϵ starts from 1.0 and then decreases by 0.005 per episode, until it reaches 0.025 at episode 200. The aspiration level for *RS*+GRC, $\aleph(s_t)$, is assigned to each state by the Global Reference conversion (GRC). The global aspiration for entire episodes was $\aleph_G = 0.06$. γ_G was set to 0.9. The scaling parameter $\zeta(s_i) = 1.0$ for all s_i[7]. Learning rate α is 0.1 in all methods, and the discount rate γ is set to 0.5 for MaxEntIRL and 0.9 for all the other algorithms. The sample size of expert's trajectory for MaxEntIRL is 100, the learning rate β is 0.01 for reward function estimation and the epoch is 20. For generating the expert's trajectories, we used the Q values of the QL agent, which has already been learned. However, the starting position of the expert was uniformly randomly selected from the state space with an exception, setting the coordinates of the left upper cell $(0, 0)$, the $(2, 5)$ was avoided. The reason why cordinates $(2, 5)$ was avoided is because the experts trajectory starts from the coordinates that is set randomly and ends at $(2, 5)$. In addition, the parameter θ used in the estimated reward function is normalized while keeping the scale with the maximum value being 0.5.

Figure 2 shows the time development of the obtained reward for each episode. *RS*+GRC was overall capable to obtain the rewards, while MaxEntIRL failed to obtain the reward stably. QL can gradually adapt to the environmental change, slower than *RS*+GRC.

5. Discussion

From the results of this experiment, we see that *RS*+GRC can learn faster than QL and MaxEntIRL. MaxEntIRL could not cope well with unsteady environment. Considering the learning speed of *RS*+GRC, *RS*+GRC is conducting a search with an optimistic directionality based

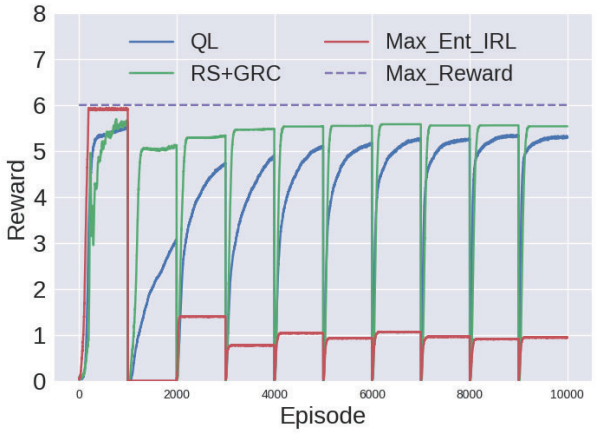

Fig. 2: Time development of reward per episode

on the satisficing policy and searching without much inefficient samplings, rather than ϵ-greedy applied to QL, which is a random search with no directionality.

We would discuss the difference in the behavior of *RS*+GRC and MaxEntIRL in the unsteady environment. The difference between the two is that *RS*+GRC is given only the reference value ($\aleph_G = 0.06$) and MaxEntIRL is given the expert's trajectory as the prior information. For that reason, *RS*+GRC judges the superiority or inferiority of the action sequence only with its result, compared to $\aleph_G$. MaxEntIRL compares the whole action sequence with the action sequence of the expert to judge the superiority or inferiority of the action series. Therefore, *RS*+GRC was able to cope with an unsteady environment because it can truncate the existing action sequence and search for a new action sequence if the result is lower than the reference level.

6. Conclusion

In this study, we showed that emulation implemented in RS can learn faster than QL, and has more flexible search capability than imitation implemented as MaxEntIRL. One of the future tasks is to test our emulation algorithm compared with imitation in continuous environments and to clarify the functional roles of imitation and emulation learning in a broader perspective such as general machine intelligence.

References

[1] Whiten, A. et al.: Emulation, imitation, over-imitation and the scope of culture for child and chimpanzee, *Phil. Trans. of the Royal Soc. B*, 364(1528), 2417–2428. 364 (2009)

[2] Takahashi, T., Kono, Y., Uragami, D., Cognitive Satisficing: Bounded Rationality in Reinforcement Learning, *Trans. Jap. Soc. AI*, 31, 6, AI30-M_1–11. (2016)

[3] Ziebart, B.D. et al.: Maximum Entropy Inverse Reinforcement Learning,*AAAI 2008*. (2008)

[4] Shinriki, M., Kono, Y., Takahashi, T., Emulation Learning from Pioneers, In: *Proc. of JNNS 2018*, PaperID-43, P1-30 ,(2018)

[5] Levy, K.Y., Shimkin, N.: Unified Inter and Intra Options Learning Using Policy Gradient Methods, In *EWRL*, 153164, (2011)

[6] Simon, H.A.: Rational choice and the structure of the environment, *Psychological Review*, Vol. 63, No. 2, pp. 129–138 (1956)

[7] Ushida, U., Kono, U., Takahashi, T., Proc. of JSAI 2017, 4C2-2in2. (2017)

The 33rd Annual Conference of the Japanese Society for Artificial Intelligence, 2019

A Multimodal Target-Source Classifier Model for Object Fetching from Natural Language Instructions

Aly Magassouba*1 Komei Sugiura*1 Hisahi Kawai*1

*1 National Institute of Information and Communications Technology

In this paper, we address the fetching task from ambiguous instructions. A typical fetching task consists of picking up a target object specified by ambiguous instructions. We specifically propose a multimodal target-source classifier model (MTCM) that grounds the instructions in the scene. More explicitly, MCTM can predict the likelihood of a target object in addition to the source of this target using linguistic and visual features. Our approach improves the accuracy of the previous state-of-the-art method for target object prediction in fetching task.

1. Introduction

Natural interactions with robots that strive to understand spoken language and assist humans requires versatile functions. Endowing robots with such functionality is particularly valuable for domestic service robots (DSRs) [1] that are expected to interact with non-expert users.

Given this background, we address the fetching task, which is one of the most crucial manipulation tasks, from ambiguous instructions. This task consists of picking up a target object instructed by a user. However, understanding and grounding the fetching instruction is particularly complex because it does not follow any predefined rule: the information may be truncated, hidden, or expressed in a multitude of ways. The unpredictability and richness of language make this task difficult to solve for DSRs that are required to infer the user's intention. .

Data-driven methods [2, 3] aim to solve similar tasks by combining visual and linguistic knowledge. Inspired by these approaches, we develop a solution that can understand free-form language and predict the likelihood of a target object in addition to its source given the initial instruction. Our method, the multimodal target-source classifier model (MTCM), addresses language understanding from visual and linguistic modalities.

2. Problem Statement

We aim to solve fetching task based on instructions such as "Give me the yellow doll on the desk". Our approach consists in understanding the target object (*e.g.*"yellow doll") and the source of this target (*e.g.*"on the desk"). Considering environments in daily life, several grounding challenges arise regarding understanding instructions. In particular, users tend to use referring expressions to describe an object. For instance, the target object in the previous example "yellow doll" is characterized by its color. Similarly the source of the target object may be mentioned or not depending on the context. For instance, "Give me the yellow doll" is a likely instruction when there is no ambiguity about the source. One or several of these grounding challenges may appear in a single instruction. To solve this problem and the related grounding challenges, we consider the following inputs and outputs for our system:

- **Inputs**: Linguistic instructions and pre-collected candidate target and source data.
- **Output**: Likelihood of the potential target object and source of the target object.

The likelihood refers to the possibility that the candidate object corresponds to the object in the user's instructions. This likelihood is expressed as a binary classification problem.

Contact: Aly Magassouba, NICT, 3 Chome-5 Hikaridai, Seika, Soraku District, Kyoto Prefecture 619-0237, aly.amagassouba@nict.go.jp

3. Proposed method

Inspired by the latest advancements in image comprehension [2], in addition to natural language understanding, we propose the MTCM method illustrated in Fig. 1. MTCM combines a convolutional neural network (CNN) in addition to a long short-term memory (LSTM) network that process the visual and linguistic inputs, respectively. The set of inputs of the MTCM is $\{\mathbf{x}_{instr}, \mathbf{x}_v, \mathbf{x}_{rel}\}$, where $\mathbf{x}_v$ denotes the visual inputs, $\mathbf{x}_{instr}$ denotes the linguistic inputs, and $\mathbf{x}_{rel}$ denotes the relational feature inputs. Input $\mathbf{x}_{rel}$ denotes the relational feature between the target object and the environment, that is, the position in the scene, position within the source, and position with respect to neighboring objects.

Visual inputs $\mathbf{x}_v$ correspond more explicitly to the cropped image of target object $\mathbf{y}$. A CNN is used to process image $\mathbf{x}_v$. In our approach, we consider the 16-layer network VGG16 [5] to encode each image. The output of the fully connected layer (FC7) is used to extract visual features.

By contrast, the linguistic features are embedded and then encoded by a multi-layer bidirectional LSTM (Bi-LSTM) network. Instead of directly training an embedding model from scratch, we use a pre-trained sub-word embedding model, BERT [6], to initialize the embedding vectors. The word embedding model is then fine-tuned on

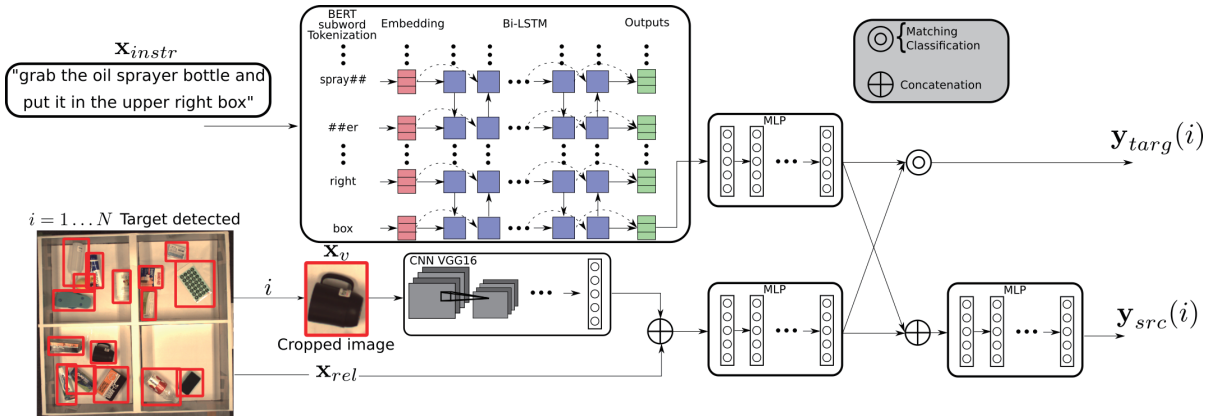

Figure 1: Proposed method framework: the MTCM is based on a CNN-LSTM architecture to process linguistic and visual inputs. The model predicts the likelihood of a target object using binary classification, in addition to the source of the target object. For comparison, we also implement a matching function to directly predict the object, as performed in [4]

Table 1: Difference between (a) typical word-tokens with pre-processing for rare and or erroneous word and (b) sub-word tokenization: in word representation rare words may be replaced by <UNK> tag

Expression	(a)	(b)
topright object	topright, object	top, right, object
sprayer	<UNK>	spray, er
greyis bottle	<UNK> , bottle	grey, is, bottle

the dataset as the MTCM is trained. BERT is a language encoding model based on bi-directional transformers. This approach provides more flexibility and generalization ability to the LSTM network. Indeed, the undesirable effect of rare words in the dataset is avoided because most BERT is pre-trained on 3.5 billion words. Additionally, instead of a word-based representation, BERT is based on the sub-word [7]. A sub-word representation is more robust to word misspelling in the model, as given in Table 1

The concatenation of the last hidden layers of the forward layer and backward layer of the Bi-LSTM is extracted to encode the linguistic inputs.

After encoding the visual, relational, and linguistic inputs, a common latent representation is required to compare the extracted features from the CNN and LSTM. Two multi-layer perceptrons (MLPs) are used for this purpose. In parallel, an MLP is used to predict the source of the target object based on the output of the linguistic and visual MLPs

Finally, the output of the MCTM is given by $\mathbf{y}_R = \{\mathbf{y}_{targ}, \mathbf{y}_{src}\}$, where y_{targ} is the likelihood of the target object and y_{src} is the predicted class of the target source

In the case of the binary classification, the prediction task is solved by minimizing a cross-entropy function so that J is

$$J(\mathbf{y}) = -\sum_n \sum_j y^*_{n_j} \log p(y_{n_j}), \tag{1}$$

where $y^*_{n_j}$ denotes the label of the j-th dimension of the n-th sample. The loss function J_M of the network is then given by:

$$J_M = \lambda_1 J_{targ} + \lambda_2 J_{src} \tag{2}$$

where $J_{src} = J(\mathbf{y}_{src})$ and target $J_{targ} = J(\mathbf{y}_{targ})$ from (1), while λ_1 and λ_2 are some weighting parameters. On the other hand, a Hinge loss function is used for J_{targ} when the tasks consists in matching the most likely object with the initial instruction. This loss consists in increasing the similarity between correct pairs of linguistic and visual/relational features and the dissimilarity between incorrect pairs. With s_i as an instruction and y_i a target object, the cost function J_{targ} becomes:

$$J_{targ} = \sum_n \max(0, M + f(s_n, y_m) - f(s_n, y_n)) + \max((0, M + f(s_k, y_n) - f(s_n, y_n)), \tag{3}$$

where M is the margin, and $f(.)$ is the similarity function (*e.g.* cosine similarity). The incorrect target object (y_m) and sentences (s_k) are randomly sampled from the same image as the real target object.

4. Experiments

To assess the performance of our method in a real-word scenario, we applied the MCTM module to the PFN-PIC dataset [4]. We used the same dataset as that in their original paper, with 89,861 sentences and 25,517 bounding boxes in the training set, and 898 sentences and 352 bounding boxes in the validation set. In each image, target objects were placed randomly in four boxes (see Fig.2). These boxes were the target sources.

For the linguistic processing of the MCTM, each sub-word was first encoded as a 1,024-sized vector using BERT. We used the largest version of pre-trained BERT (24 layers) considering uncased words. The embedded vectors were input into a three-layer Bi-LSTM, with 1,024-sized cells. The last hidden state of the Bi-LSTM was eventually extracted. In parallel, the images were processed in a CNN. We used a VGG16 pre-trained model and extracted the output of the seventh fully connected (FC7) layer. Both linguistic and

Table 2: Mean validation top-1 accuracy and binary on the PFNPIC data set considering a baseline method given [4], and MCTM. The binary accuracy for several positive/negative samples ratio γ are also reported. These results are based on five trials.

Method	**Target accuracy**					**Source accuracy**
	Top-1	**Binary accuracy**				
		$\gamma = 1.0$	$\gamma = 0.5$	$\gamma = 0.25$	$\gamma = 0.2$	
Baseline (Hatori et al. [4])	88.0	–	–	–	–	–
Ours (MCTM)	88.8	94.5	95.4	96.1	96.3	99.8

visual/relational features were transformed by three-layer MLPs with dimension $d = 1024$. We applied batch normalization and the ReLU activation function for each layer of the MLP. The third MLP that predicted the source also had three layers and dimension $d = 2048$. Similar to the previous MLPs, the ReLU activation function was used, except for the last layer, which used a softmax function for the prediction. Finally, the network was trained using the Adam optimizer with an initial learning rate of $2e^{-4}$. The weighting parameters of the loss function were set to $\lambda_1 = 1$ and $\lambda_2 = 0.7$

The results of our experiments are reported in Table 2. In the first column, for a fair comparison with the state-of-the-art method, we also provide the top-one accuracy of the MCTM. The results over five trials of the MCTM demonstrate that our method improved to 88.8% of the accuracy previously obtained in [4] with a CNN-LSTM framework.

Besides, we also provide the binary accuracy of our approach. The accuracy in Table 2 is then given for different ratio γ of correct/incorrect visual and linguistic pairs. As expected, the accuracy of MTCM improved from 94.5% to 96.3% by adding more negative samples. Finally, our method is able to correctly predict the source of the target object with an accuracy of 99.8%.

Additionally, the qualitative results of MCTM are shown in Fig. 2, which illustrates typical true and false predictions. In the two samples, the likelihood of each object in the image was reported given the initial instruction: overall accurate results were obtained. The right figure reports the case of multiple likely objects that fit the instruction "move the white bottle to the upper right box." Even for a human subject, this case is difficult to solve because three white bottle-like objects are in the scene. Semantically, the binary likelihood of these target objects is not erroneous, given the instruction. Interestingly, unlike K-class methods that would only predict the most probable object, our approach provides the most likely objects to the user, that would be able to select the desired target object in a second hand.

5. CONCLUSION

Following the increasing demand for DSRs, we proposed the MTCM, which can predict the likelihood of target objects and their respective source given ambiguous instructions for the picking task. Our binary target object classifier had an accuracy of 96% and source box prediction reached 99.8%. In parallel, our results improved the state-of-the-art baseline by 0.8% on a standard dataset.

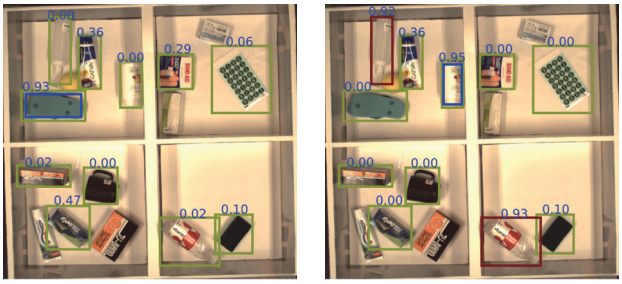

(a) take the blue sandal an move it to the lower left box

(b) move the white bottle to the upper right box

Figure 2: Predictions of the MCTM network. The likelihood is given for each object given the initial sentence. Targets with a prediction above 0.5 are considered as likely. In green the correctly labelled targets and in red the incorrectly labelled targets, while the target object of the instruction is in blue.

Acknowledgements

This work was partially supported by JST CREST and SCOPE.

References

[1] L. Iocchi, D. Holz, J. Ruiz-del Solar, K. Sugiura, and T. Van Der Zant, "Robocup@ home: Analysis and results of evolving competitions for domestic and service robots," *Artificial Intelligence*, pp. 258–281, 2015.

[2] L. Yu, H. Tan, M. Bansal, and T L. Berg, "A joint speaker listener-reinforcer model for referring expressions," *CVPR*, 2017.

[3] A. Magassouba, K. Sugiura, and H. Kawai, "A multimodal classifier generative adversarial network for carry and place tasks from ambiguous language instructions," *IEEE RAL*, vol. 3, no. 4, pp. 3113–3120, 2018.

[4] J. Hatori et al., "Interactively picking real-world objects with unconstrained spoken language instructions," *IEEE ICRA*, pp. 3774–3781, 2018.

[5] K. Simonyan and A. Zisserman, "Very deep convolutional networks for large-scale image recognition," *arXiv preprint arXiv:1409.1556*, 2014.

[6] J. Devlin, M-W. Chang, K. Lee, and K. Toutanova, "Bert: Pre-training of deep bidirectional transformers for language understanding," *arXiv preprint arXiv:1810.04805*, 2018.

International Session | International Session | [ES] E-3 Agents

[2F1-E-3] Agents: interaction and decision

Chair: Shigeo Matsubara (Kyoto University), Reviewer: Takayuki Ito (Nagoya Institute of Technology)
Wed. Jun 5, 2019 9:00 AM - 10:40 AM Room F (302B Medium meeting room)

[2F1-E-3-01] ANAC 2018: Repeated Multilateral Negotiation League

Reyhan Aydogan[1,4], ○Katsuhide Fujita[2], Tim Baarslag[3], Catholijn M. Jonker[4], Takayuki Ito[5]
（1. Ozyegin University, 2. Tokyo University of Agriculture and Technology Tokyo, 3. Centrum Wiskunde &Informatica, 4. Delft University of Technology, 5. Nagoya Institute of Technology）

9:00 AM - 9:20 AM

[2F1-E-3-02] Extraction of Online Discussion Structures for Automated Facilitation Agent

○Shota Suzuki[1], Naoko Yamaguchi[1], Tomohiro Nishida[1], Ahmed Moustafa[1], Daichi Shibata[1], Kai Yoshino[1], Kentaro Hiraishi[1], Takayuki Ito[1] （1. Nagoya Institute of Technology）

9:20 AM - 9:40 AM

[2F1-E-3-03] An Automated Negotiating Agent that Searches the Bids around Nash Bargaining Solution to Obtain High Joint Utilities

Shan Liu[1], ○Ahmed Moustafa[1], Takayuki Ito[1] （1. Nagoya Institute of Technology）

9:40 AM - 10:00 AM

[2F1-E-3-04] Analysis of Incentive Ratio in Top-Trading-Cycles Algorithms

○Taiki Todo[1] （1. Kyushu University）

10:00 AM - 10:20 AM

[2F1-E-3-05] Multi-Agent Traffic Signal Control System Using Deep Q-Network

○YOHEI KANZAKI[1], Keisuke Ohno[1], Eichi Takaya[1], Satoshi Kurihara[1] （1. Keio University）

10:20 AM - 10:40 AM

The 33rd Annual Conference of the Japanese Society for Artificial Intelligence, 2019

ANAC 2018: Repeated Multilateral Negotiation League

Reyhan Aydoğan[*1] Katsuhide Fujita[*2] Tim Baarslag[*3] Catholijn M. Jonker[*4]
Takayuki Ito[*5]

[*1] Department of Computer Science, Özyeğin University, Istanbul, Turkey
[*2] Institute of Engineering, Tokyo University of Agriculture and Technology Tokyo, Japan
[*3] Centrum Wiskunde & Informatica (CWI), Amsterdam, The Netherlands
[*4] Interactive Intelligence Group, Delft University of Technology, Delft, The Netherlands
[*5] Nagoya Institute of Technology, Nagoya, Japan

There are a number of research challenges in the field of Automated Negotiation. The Ninth International Automated Negotiating Agent Competition aimed to encourage participants to develop effective negotiating agents, which can negotiate with multiple opponents more than once. This paper discusses essential research challenges for such negotiations as well as presenting the competition set-up and results. Results showed that winner agents mostly adopt hybrid bidding strategies and take their opponents' preferences as well as their strategy into account.

1. Introduction

In multi-agent systems, agents mostly interact and collaborate with each other to achieve their goals; however, their interests and preferences may sometimes conflict. In such situations, agents can resolve their conflict and come up a consensus through negotiation. Therefore, it is important to design and develop efficient negotiation strategies for autonomous agents [Jennings 98, Baarslag 15, Fatima 14]. In order to facilitate the research on negotiation in multi-agent systems and to provide unique benchmarks for evaluation of the developed negotiation strategies, an international competition on automated negotiation namely ANAC [Jonker 17] has been organized for several years. As the main organizers of this competition, we aim to address a variety of research challenges (e.g. uncertainty about opponent, reasoning on complex preferences, negotiating with multiple opponents). In ANAC 2018, we introduced three leagues: Human-agent negotiation [Mell 18], Negotiation Strategies for Diplomacy Game [Jonge 19] and Repeated Multilateral Negotiation. This paper presents the competition setup and evaluation results of the repeated multilateral negotiation as well as pointing out the main challenges.

In multilateral negotiation, there are more than two agents searching for a consensus. Since it involves more conflicts and interactions, it is more complicated than bilateral negotiation [Aydoğan 14, Fujita 12, Fujita 14]. When those agents have a long term relation, they may need to negotiate with each other more than once. In such a situation, it is important for agents to understand their opponents' needs and strategy well and adjust their strategy accordingly so to find a better deal. It is also essential to recall that they are going to negotiate with the same opponents again. If their strategy is based on completely exploiting the other sides, their negotiation may end up with a failure. In ANAC 2018, we encourage the participants to pursue designing effective negotiation strategies for such repeated multilateral negotiations.

Competition results showed that successful agents mostly employ a hybrid bidding strategy in order to avoid being exploited and consider their opponents' best offer in their previous negotiation. Furthermore, they usually adopt a frequency based opponent modeling. Some agents model the likelihood of an offer to be accepted by other agents by analyzing the bids in their past negotiations while others use opponents' best offers in their bidding strategy. In the rest of this paper, the essential research challenges are discussed, and competition setup and results are explained.

2. ANAC 2018 Competition Challenges

Although agents negotiate with the same opponents several times, they do not know their exact preferences and strategies. The essential research goal is to model their opponents' behaviour or preferences based on their past negotiations and to incorporate those models into their bidding strategy so as to improve their negotiation outcome. However, this is not trivial since their opponents may change their behaviour over time in spite of having the same preferences. Therefore, learnt model may mislead the agents. Furthermore, if an agent tries to exploit its opponents based on what it learnt about them, they may reciprocate in a similar way next time. It would result in decreasing utility for all agents. Moreover, when agents negotiate with the same opponents, they should establish a good relationship while still aiming at maximizing their own utility. There is a trade-off between to what extent act nicely and to what extent consider its own benefit.

3. Competition Setup

In the competition, three agents negotiate on multiple issues to reach a consensus by following the Stacked Alter-

Contact: Reyhan Aydoğan, Özyeğin University, Özyeğin University, Istanbul, Turkey, Reyhan Aydoğan

native Offers Protocol (SAOP) [Aydoğan 17]. According to this protocol, one of the agents starts the negotiation with an offer. Agents can take their action in a turn-taking fashion. When an offer is made by any agent and the next agent in line can take the following actions:

- Make a counter offer (overriding the previous offer)
- Accept the current offer
- Walk away (e.g. ending the negotiation without any agreement)

This process continues in a turn taking fashion until agents reach an agreement or the given deadline, or one of the agents walks away. It is worth noting that an agreement is reached if and only if all agents accept the agreed offer. If negotiation fails, agents receive their reservation utility (i.e., BATNA). The utility of agreement for each agent is calculated with respect to their own preferences. Note that in the competition preferences of each agent are represented by means of additive utility function as shown in Equation 1 where $V_n(v_j)$ denotes agent n's valuation of the value for the issue j in the given bid and $w_{n,j}$ denotes the weights of that issue. In other words, agents sum up their weighted valuation of each issue value to calculate the overall utility. It is worth noting that each agent can only access their own preferences during the negotiation; that is, they do not know each others' truth preferences.

$$u_n(b^t) = \sum_{j \in I} V_n(b_j^t) \cdot w_{n,j} \quad (1)$$

In the competition, the deadline is set to three minutes and each negotiation session is repeated five times. Agents are allowed to access provided historical data from their past negotiations. The historical data involves the utility distribution of the exchanged offers in previous negotiation sessions according to agent's own utility space and previous agreements. In addition, agents are allowed to model their opponents' preferences by examining the bids exchanged during their negotiation and to store the learnt model where they can access in their further negotiations.

Genius 8.0.4 [Lin 14] was used to run negotiation tournaments in the competition. Agents were evaluated in four different negotiation scenarios described in Table 1. Note that all participants submitted a negotiation scenario consisting of three conflicting preference profiles and four of them were chosen for the tournaments based on varying size of their outcome space.

Table 1: Negotiation Scenarios

Name	# of Issue	# of Values	# of Outcomes
Meng wan	6	4,4,4,4,3,4	3072
BetaOne	3	4,4,4	64
IQSon	7	7,6,5,3,4,4,4	40320
Hamada	4	5,5,5,5	625

In order to complete such an extensive set of tournaments within a limited time frame, we used some high-spec computers, made available by Tokyo University of Agriculture and Technology, Japan. Specifically, each of these machines contained an *Intel Core i7* CPU, at least 64GB of DDR3 memory, and a hard drive with at least 2TB of capacity.

Agent Name	Individual Utility	Social Welfare
meng wan	0.586923478	1.632116151
AgentHerb	0.49193542	1.854380384
IQSun2018	0.583185484	1.759158992
PonPokoRampage	0.567184966	1.547263306
FullAgent	0.549039084	1.766976108
Seto	0.551805443	1.449438396
Lancelot	0.517828051	1.53437244

Figure 1: Results of Qualification Round for Pool-A

4. Result of the Competition

We have received 21 submissions from 10 institutions in eight different countries. The performance of the agents were evaluated according to their average *individual utility* and average sum of utilities (*social welfare*). The competition consists of two stages. In the *qualification round*, finalist agents are determined while the winners for each category (*individual* and *social welfare*) are determined in the *final round*. In the following sections, results for each round are presented.

4.1 Qualification Results

Running the whole tournament involving 21 agents in four domains with 5 repetitions were not feasible within the given time. Therefore, three agent pools were generated randomly as follows:

- **Pool-A:** Meng wan, AgentHerb, IQSun2018, PonPokoRampage, FullAgent, Seto, Lancelot
- **Pool-B:** Beta One, Yeela, SMAC_Agent, AgreeableAgent2018, ConDAgent, Shiboy, Libra
- **Pool-C:** AgentNP1, GroupY, ATeamAgent, Sontag, Agent33, Agent_Hama, Exp-Rubick

The top 3 performing agents in each pool proceeded to the final. Therefore, there were nine finalists for each category after the qualification round.

According to the results of the pool-A, the *Mengwan*, *IQSun2018*, and *PonPokoRampage* qualified for the final round in the individual utility category. As far as the average sum of the utilities are concerned, *AgentHerb*, *IQSun2018*, and *FullAgent* are qualified for the final round.

According to the results of the pool-B, the *BetaOne*, *AgreeableAgent2018*, and *Shiboy* qualified for the final round in the individual utility category. As far as the average sum of the utilities are concerned, *Yeela*, *AgreeableAgent2018*, and *ConDAgent* are qualified for the final round.

According to the results of the pool-C, the *AgentNP1*, *GroupY*, and *Sontag* qualified for the final round in the individual utility category. As far as the average sum of the utilities are concerned, *AgentNP1*, *Sontag*, and *Agent33* are qualified for the final round.

Agent Name	Individual Utility	Social Welfare
Beta One	0.482887311	1.404794645
Yeela	0.399430418	1.422654384
SMAC_Agent	0.464635439	1.325276881
AgreeableAgent2018	0.505584897	1.505251211
ConDAgent	0.471002153	1.518896956
Shiboy	0.502585371	1.411124211
Libra	0.445786573	1.227738202

Figure 2: Results of Qualification Round for Pool-B

Agent Name	Individual Utility	Social Welfare
AgentNP1	0.512177707	1.52976242
GroupY	0.485323479	1.33874982
ATeamAgent	0.345297603	0.980979189
Sontag	0.484535782	1.515047114
Agent33	0.428666974	1.419233621
Agent_Hama	0.469592183	1.393009022

Figure 3: Results of Qualification Round for Pool-C

4.2 Final Results: Individual Utility Category

Figure 4 shows the average individual utility gained by each finalist over 2520 negotiations. Recall that each negotiating agent negotiates with all other agents five times for each negotiation scenario in Table 1. *AgreeableAgent2018* gained 0.59 on average and won the competition. *Meng wan* and *Beta One* agents were awarded second and third place respectively. The detailed description of the winner strategies according to the individual utility, are given.

- ***AgreeableAgent2018 by Sahar Mirzayi (University of Tehran, Iran):*** This agent tries to learn its opponents' preferences during the ongoing negotiations by using a frequency based modeling. It uses a time-based bidding strategy, which takes its opponents' preferences into account. Basically, it generates all candidate bids above estimated target utility and sorts those candidates according to opponent models. It makes the bid selected by using Roulette Wheel Selection. It employs ACNext acceptance strategy. It also accepts it opponents' bid, which is higher than reservation utility if it is almost deadline.
- ***Meng wan by Meng Wan, Hui Cui (University of Southampton, UK):*** It employs a hybrid bidding strategy composed of three bidding strategy. The first strategy generates a random bid above an estimated target utility (time-based) while the second strategy chooses a random bid among opponents' best offers so far. The third bidding strategy makes a bid whose utility is higher than target utility, which also maximizes its opponents' utility based on estimated frequency-based opponent models. It employs a time-based acceptance strategy, which is not inclined to accept any offer at the beginning. By the end of negotiation, this agent tends to ask opponents' best offers so far.
- ***Beta One by Alper Sekerci, Abdulkadir Nurkalem (Özyeğin University):*** This agent has a tendency to be more stubborn against stubborn opponents while more generous against generous opponents. For the opponent modelling, the agent uses statistical analysis to decide whether it should concede or not. The personality of the agent is parameterized. By analyzing the history, the agent is able to tune its parameters (e.g. selfish ratio) to try to perform better in the upcoming negotiations.

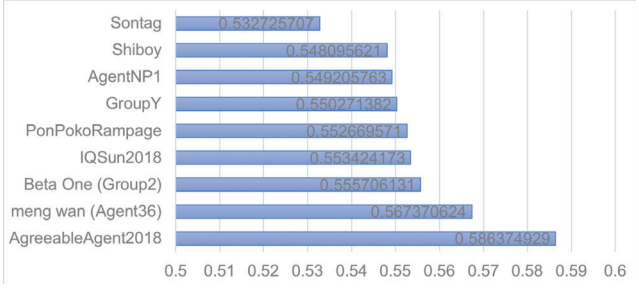

Figure 4: Overall Ranking w.r.t. Individual Utility

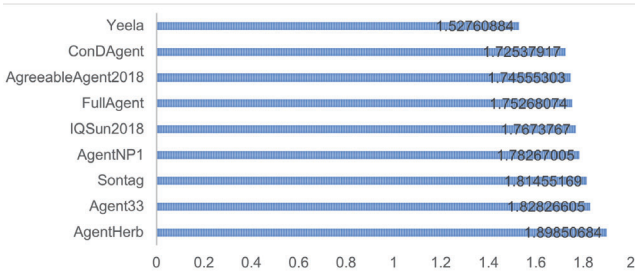

Figure 5: Overall Ranking wrt. Social Welfare

4.3 Social Welfare Category

Figure 5 shows the average sum of utilities of the agreements reached by each agent. *AgentHerb* gained 1.89 on average and won the competition where *Agent33* and *Sontag* agents took the second and third place respectively. The description of the winner strategies are given below.

- ***AgentHerb by Alon Stern, Amit Moryossef, Yehudit Reyzer, Karin Dahan (Bar Ilan University, Israel):*** This agent records the history of bids for each opponent and whether they were accepted or rejected by the opponents. Accordingly, Agent Herb uses a logistic regression model to predict the likelihood of acceptance of a bid by the opponents. It makes its bids based on its chances of acceptance by all the opponents while taking its own utility into account. The agent employs ACNext acceptance strategy with a discount factor.
- ***Agent33 by Liu Shan (Nagoya Institute of Technology, Japan):*** The bidding Strategy aims to propose bids around Nash bargaining solution (NBS). Agent33 uses a novel heuristic method in order to find

Table 2: Detailed Results of Winners Tournaments

	Agreeable	**MengWan**	**BetaOne**	**Social Welfare**	**Dist. to Pareto**	**Dist. to Nash**
Individual Category	0.769856823	**0.805217872**	0.787584175	2.362659083	0.019035083	0.223667667
	Agent Herb	**Agent33**	**Sontag**	**Social Welfare**	**Dist. to Pareto**	**Dist. to Nash**
Social Category	0.634797437	0.688591936	**0.899989331**	2.223378333	0.027012083	0.32230525

the promising bids around the NBS. The proposed heuristic method aims to construct a list of the opponents prior issues, which is incrementally updated throughout the negotiation process by calculating the standard deviation of each issue value's frequency and the standard deviation of each issue's value.

- ***Sontag by Ryohei Kawata (Tokyo University of Agriculture and Technology, Japan):*** Sontag makes concessions in early to increase social welfare. Sontag does not model opponents and no learning from negotiation history. In other words, it expects that the opponents will make a concession finally. The proposal and acceptance of the bids are based on the following equation: $f(t) = t/2.5 - \log(t/2 + 0.1)$.

4.4 Further Analysis of ANAC2018 Winners

After competition, we ran another tournament among the winners per each category. The settings of tournaments are same as ANAC2018; however, the agents in the tournament consists of only the winners of each category (Individual Utility Category: AgreeableAgent2018, MengWan, BetaOne; Social Welfare Category: AgentHerb, Agent33, Sontag). According to the results listed in Table 2, MengWan received the highest average utility although this agent took the second place in the competition. Similarly, when only winners of the social welfare category negotiate with each other, Songtag outperforms other winners. The result should not surprise us because negotiation outcome highly depends on whom we are negotiating with. Similarly, the winners in individual category received higher average social welfare than the winners of social category. In addition, it can be seen that winners made agreements that are closer to the Pareto Frontier, received higher social welfare.

5. Conclusion

This paper discusses main research challenges in repeated multilateral negotiations as well as explaining the ANAC 2018 competition setup and results briefly. As a future work, it would be interesting to analyze the performance of agents elaborately in a more extensive setup. Furthermore, we are planning to run additional tournaments including ANAC 2017 winner agents and compare their performances.

References

[Aydoğan 17] Aydoğan, R., Festen, D., Hindriks, K. V., and Jonker, C. M.: Alternating offers protocols for multilateral negotiation, in Fujita, K., Bai, Q., Ito, T., Zhang, M., Ren, F., Aydoğan, R., and Hadfi, R. eds., *Modern Approaches to Agent-based Complex Automated Negotiation*, pp. 153–167, Springer Publishing (2017)

[Aydoğan 14] Aydoğan, R., Hindriks, K. V., and Jonker, C. M.: Multilateral mediated negotiation protocols with feedback, in *Novel Insights in Agent-based Complex Automated Negotiation*, pp. 43–59, Springer (2014)

[Baarslag 15] Baarslag, T., Gerding, E. H., Aydoğan, R., and Schraefel, M.: Optimal negotiation decision functions in time-sensitive domains, in *IEEE International Conference on Web Intelligence and Intelligent Agent Technology*, Vol. 2, pp. 190–197IEEE (2015)

[Fatima 14] Fatima, S., Kraus, S., and Wooldridge, M.: *Principles of Automated Negotiation*, Cambridge University Press, New York, NY, USA (2014)

[Fujita 12] Fujita, K., Ito, T., and Klein, M.: A Secure and Fair Protocol that Addresses Weaknesses of the Nash Bargaining Solution in Nonlinear Negotiation, *Group Decision and Negotiation*, Vol. 21, No. 1, pp. 29–47 (2012)

[Fujita 14] Fujita, K., Ito, T., and Klein, M.: Efficient issue-grouping approach for multiple interdependent issues negotiation between exaggerator agents, *Decision Support Systems*, Vol. 60, pp. 10–17 (2014)

[Jennings 98] Jennings, N. R., Faratin, P., Lomuscio, A., Parsons, S., Sierra, C., and Wooldridge, M.: Automated Negotiation : Prospects , Methods and Challenges (1998)

[Jonge 19] Jonge, de D., Baarslag, T., Aydoğan, R., Jonker, C. M., Fujita, K., and Ito, T.: The Challenge of Negotiation in the Game of Diplomacy, in *Proceedings of the 6th Conference on Agreement Technologies* (2019)

[Jonker 17] Jonker, C. M., Aydoğan, R., Baarslag, T., Fujita, K., Ito, T., and Hindriks, K. V.: Automated Negotiating Agents Competition (ANAC)., in *AAAI*, pp. 5070–5072 (2017)

[Lin 14] Lin, R., Kraus, S., Baarslag, T., Tykhonov, D., Hindriks, K., and Jonker, C. M.: Genius: An integrated environment for supporting the design of generic automated negotiators, *Computational Intelligence*, Vol. 30, No. 1, pp. 48–70 (2014)

[Mell 18] Mell, J., Gratch, J., Baarslag, T., Aydoğan, R., and Jonker, C. M.: Results of the First Annual Human-Agent League of the Automated Negotiating Agents Competition, in *Proceedings of the 18th International Conference on Intelligent Virtual Agents*, IVA '18, pp. 23–28, New York, NY, USA (2018), ACM

The 33rd Annual Conference of the Japanese Society for Artificial Intelligence, 2019

Extraction of Online Discussion Structures for Automated Facilitation Agent

Shota Suzuki Naoko Yamaguchi Tomohiro Nishida Ahmed Moustafa Daichi Shibata
Kai Yoshino Kentaro Hiraishi Takayuki Ito

Nagoya Institute of Technology

This paper proposes an approach that aims to extract the discussion structure from large-scale text-based online discussions. The ultimate goal is to develop an automated facilitation agent that is able to extract discussion structures from large-scale online discussions. To support this facilitation agent, an extraction approach is needed. Towards this end, we adopt the issue-based information system (IBIS), as a suitable format for structuring online discussions. In this context, we model the task of extracting an IBIS structure as it consists of node extraction and link extraction. Towards this end, a deep neural network based approach is employed in order to perform these two extraction subtasks. In order to evaluate the proposed approach, a set of experiments has been conducted on the data collected from the discussions in the online discussion support system called D-Agree. The experimental results show that the proposed approach is efficient for extracting online discussion structures.

1. Introduction

Several research attempts have been proposed in order to build intelligent online discussion forums because they are the cornerstone of the next-generation open and public deliberative democracy. Towards this end, an intelligent crowd decision support system that has facilitator functions was developed and deployed for several real-world online discussion forums [Ito 14, Ito 15, Sengoku 16, Takahashi 16]. This facilitator-mediated online discussion model leads online discussions to better directions. In this regard, human facilitators play an important role to coordinate, lead, integrate, classify, and summarize discussions in order to reach an acceptable consensus. Therefore, our ultimate goal becomes to create intelligent software agents that can function as automated facilitators.

In this regard, when an automated agent facilitates online discussions, extracting discussion structures is required because this facilitation agent needs to analyze the structure during these online discussions. As a result, this automated facilitation agent will be able to understand whether a discussion topic is positive or negative, what words are being focused on, and which words are important. Towards this end, we adopt the issue-based information system (IBIS) [Kunz 70] as an approach for structuring online discussions. The elements of IBIS are "issues" that need to be answered, "ideas" that are possible answers, "arguments" that support or object to a given idea. In this study, we use the term "pros" to refer to the arguments that support an idea and "cons" to refer to the arguments that oppose an idea. We also use the term "nodes" in order to refer to the issues, ideas, pros, and cons, and "links" in order to refer to the relationships amongst these nodes. As a result, our goal becomes to extract this "IBIS structure" from large-scale online discussions.

In order to achieve this goal, we propose an approach that includes two steps which are node extraction and link extraction. In this context, extracting nodes means classifying sentences which composes the submissions in online discussions into the elements of IBIS. On the other hand, extracting links means extracting the relationships amongst these nodes. Eventually, we construct a tree-like discussion structure that consists of the nodes and their relationships in IBIS. Towards this end, we employ bidirectional long short-term memory (Bi-LSTM) for both of node extraction and link extraction.

The results of the experiments that are conducted on the data collected from the discussion support system called D-Agree demonstrate that the proposed approach is efficient for extracting discussion structures. Therefore, we conclude that extracting discussion structures is efficient with the proposed deep learning approach.

Contact: Shota Suzuki, Nagoya Institute of Technology, Gokiso-cho, Showa-ku, Nagoya-shi, Aichi-ken, 466-8555, Japan, +81-52-735-5000, suzuki.shota@itolab.nitech.ac.jp

2. Extracting IBIS Structure with Deep Learning

The problem of extracting nodes from online discussions can be formulated as follows. Given a data thread in the form of natural language $X = \{x_1, x_2, \ldots, x_n\}$, where x_i is the i^{th} submission. Each submission consists of sentences $x_i = \{x_{i1}, x_{i2}, \ldots, x_{im}\}$, where x_{ij} is the j^{th} sentence. The proposed model classify sentences into four types of issues, ideas, pros, and cons which are the elements of IBIS. Figure 1 shows the sentence about "Let's discuss town development with IoT and AI." is classified into issues, the sentence about "I propose signs that provide information." is classified into ideas, and the sentence about "It is nice idea because the signs are easy to understand." is classified into pros. In order to support node extraction, we employ Bi-LSTM which is a type of RNN model that aims at classifying time series data. The input is the embedding of each

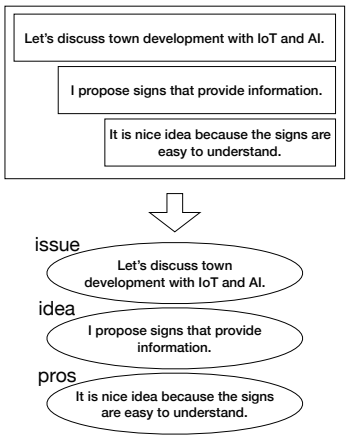

Figure 1: Node-extraction

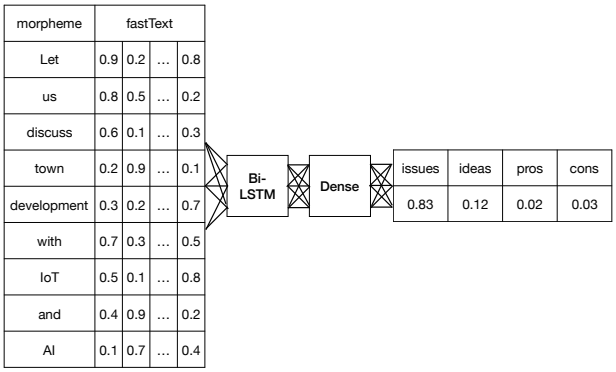

Figure 2: Node-extraction architecture

word by fastText [Bojanowski 16, Joulin 16] and the output is a normalized probability. Then, we consider a sentence as the type of the node that acquires the highest probability. This node-extraction architecture is shown in Figure 2.

On the other hand, the problem of link extraction can be formulated as follows. Given the extracted nodes in the form of natural language $S_1, S_2, \ldots, S_n$ and $T_1, T_2, \ldots, T_m$. Note that $S_k (1 \leq k \leq n)$ has a relation with $T_l (l \in \{1, 2, \ldots, m\})$. For example, the idea node about "I propose signs that provide information." has a relation with the issue node about "Let's discuss town development with IoT and AI.". Therefore, in order to address the link extraction challenge, we model it as a prediction of the head of the arrow. It should be noted that this prediction model adopts a regression technique. Towards this end, we calculate the cosine similarities between the prediction model output and the embedded candidate nodes in order to find an adequate link from these candidate nodes. In this context, we consider that the input node points to the nearest node, among these candidate nodes, to the output. In addition, we limit the space of candidate nodes using the structure of the discussion support system. Please note that

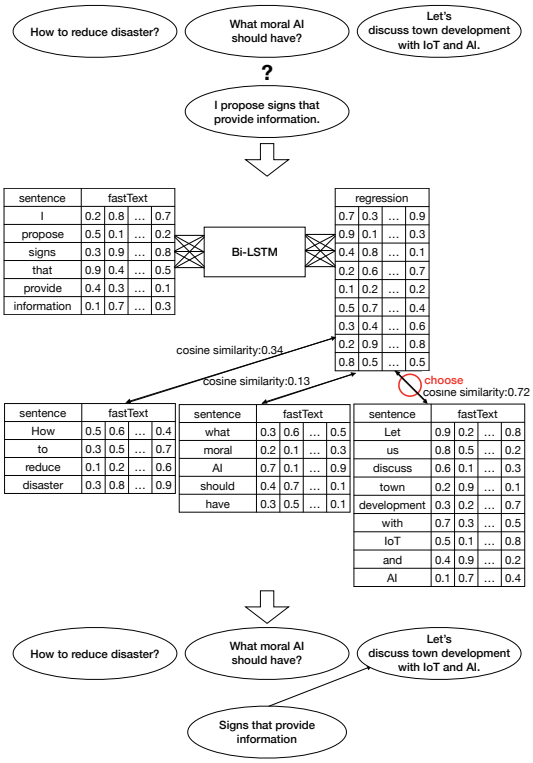

Figure 3: Link-extraction architecture

we also use Bi-LSTM as in the node extraction step. This link-extraction architecture is shown in Figure 3.

3. Experiments and Discussions

3.1 Experiment settings

D-Agree is an intelligent crowd decision support system that is developed by AI research center at Nagoya Institute of Technology (NIT). We gathered the experimental data from a number of online discussions (19 discussions) that were created in D-Agree. The themes of these discussions were chosen from the topics which are relevant to Nagoya, AI, IoT, and city development. In addition, we chose topics about which participates can easily think. Furthermore, we set a threshold of at least five participates per discussion. During these online discussions in D-Agree, one person acted as facilitator in accordance with IBIS structure. Those who have facilitated the online discussions in D-Agree did also annotate the experimental data.

3.2 Results

We conducted a set of experiments in order to evaluate the node-extraction performance of the proposed approach using Bi-LSTM. The results of these experiments are demonstrated in Figure 4. The results in Figure 4 represent the values of precision, recall, and F1 score for sentence classification. Please note that each value is the average of leave-one-out cross-validation. The results in Figure 1 show that the proposed approach achieved an F1 score value of 0.887 in issues/node extraction, 0.761 in ideas/node extrac-

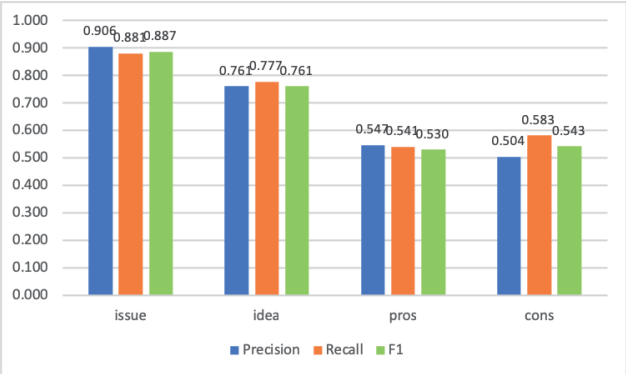

Figure 4: Experimental results of node extraction

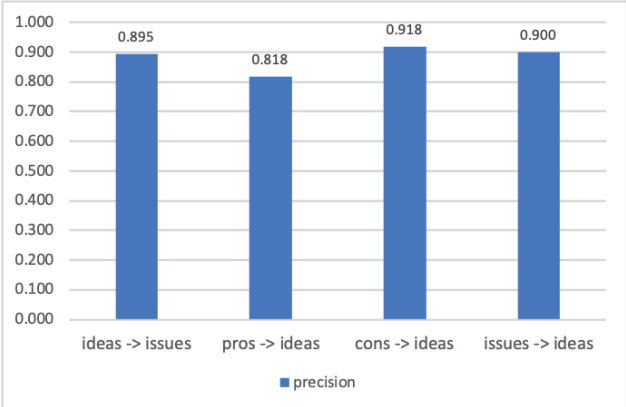

Figure 5: Experimental results of link extraction

tion, 0.530 in pros/node extraction and 0.543 in cons/node extraction.

In addition, we conducted a second set of experiments in order to evaluate the link-extraction performance of the proposed approach. The results of these experiments are demonstrated in Figure 5, which represent the precision values for link extraction using Bi-LSTM. Please note that we did not calculate the recall and F1 score values because the proposed approach aims to predict the point of the link (head of the arrow), not to classify it. As demonstrated in Figure 5, the proposed approach obtained a precision value of 0.895 when extracting the links from ideas nodes to issues nodes, 0.818 when extracting the links from pros nodes to ideas nodes, 0.918 when extracting the links from cons nodes to ideas nodes, and 0.900 when extracting the links from issues nodes to ideas nodes. These high precision values are competitive amongst the state of art technologies in the field of argumentation mining [Stab 14]. Therefor, it becomes promising that the availability of more data will increase the precision values when extracting other links.

3.3 Discussions

To summarize, the experimental results demonstrate the efficiency of the proposed approach in extracting IBIS structures from online discussions. In specific, the results of link-extraction express high precision values in predicting all types of links. In this regard, it is worth mentioning that the precision value of extracting the link from pros to ideas is slightly less than other precision values. This result is attributed to the fact that similar ideas are extracted from a single discussion domain/topic where the range of ideas is narrow. On the other hand, the results of node-extraction show lower F1 scores when extracting pros and cons. These results are attributed to the existence of certain sentences which are classified with dependencies on their context. A number of sentences is sometimes classified into pros, sometimes into cons by its context. It is, therefore, concluded that the proposed approach that is not use context as features is not able to classify into pros and cons. An approach which regards context as a feature to classify is expected to improve the results.

4. Conclusions and Future Work

This paper proposes a novel approach that aims to promote automated facilitation in large-scale online discussion platforms. The proposed approach employs deep learning in order to extract the IBIS structure from online discussions. Towards this end, the proposed approach employs a novel two-step method, that involves node extraction and link extraction, that aims to construct IBIS structures. In order to evaluate the performance of the proposed approach, a set of experiments are conducted using the discussion that are created in D-Agree system. The experimental results demonstrate the ability of the proposed approach to extract the IBIS structures efficiently. Future work is planned to involve improving the accuracy of the extraction of IBIS structures. Another direction will be developing an automated facilitation agent that promotes large-scale online discussions. This agent needs the abilities of questioning and making remarks to facilitate online discussions.

Acknowledgement

This work was supported by JST CREST Grant Number JPMJCR15E1, Japan.

References

[Bojanowski 16] Bojanowski, P., Grave, E., Joulin, A., and Mikolov, T.: Enriching word vectors with subword information, arXiv preprint arXiv:1607.04606 (2016)

[Ito 14] Ito, T., Imi, Y., Ito, T., and Hideshima, E.: COLLAGREE: A facilitator-mediated large-scale consensus support system, Collective Intelligence 2014 (2014)

[Ito 15] Ito, T., Imi, Y., Sato, M., Ito, T., and Hideshima, E.: Incentive mechanism for managing large-scale internet-based discussions on collagree, Collective Intelligence 2015 (2015)

[Joulin 16] Joulin, A., Grave, E., Bojanowski, P., and Mikolov, T.: Bag of tricks for efficient text classification, arXiv preprint arXiv:1607.01759 (2016)

[Kunz 70] Kunz, W., and Rittel, H. W.: Issues as elements of information systems (Vol. 131). Berkeley, California:

Institute of Urban and Regional Development, University of California (1970)

[Sengoku 16] Sengoku, A., Ito, T., Takahashi, K., Shiramatsu, S., Ito, T., Hideshima, E., and Fujita, K.: Discussion tree for managing large-scale internet-based discussions, Collective Intelligence 2016 (2016)

[Stab 14] Stab, C., and Gurevych, I.: Identifying argumentative discourse structures in persuasive essays. In Proceedings of the 2014 Conference on Empirical Methods in Natural Language Processing (EMNLP), pp. 46-56 (2014)

[Takahashi 16] Takahashi, K., Ito, T., Ito, T., Hideshima, E., Shiramatsu, S., Sengoku, A., and Fujita, K.: Incentive mechanism based on qualit of opinion for Large-Scale discussion support, Collective Intelligence 2016, p. 16 (2016)

The 33rd Annual Conference of the Japanese Society for Artificial Intelligence, 2019

An Automated Negotiating Agent that Searches the Bids around Nash Bargaining Solution to Obtain High Joint Utilities

Shan Liu*1 Ahmed Moustafa*2 Takayuki Ito*3

*1 *2 *3 Nagoya Institute of Technology

The International Automated Negotiating Agents Competition (ANAC) and the Pacific Rim International Automated Negotiation Agents Competition (PRIANAC) are being held annually in order to bring together the researchers from the multi-agent automated negotiation community. In this paper, we present a negotiating agent that is capable of searching the suitable bids that obtain high joint utility values near Nash bargaining solution by using a novel bid searching strategy. The proposed agent has participated in both competitions and finished in second place in the social welfare category in ANAC 2018 and in first place in the social welfare category in PRIANAC 2018.

1. Introduction

In this paper, we present a novel bid searching strategy that is proposed for an automated negotiating agent in order to participate in ANAC Repeated Multilateral Negotiation League (RMNL) 2018 and PRIANAC 2018[1]. As a competitive challenge in ANAC 2018 [2], RMNL requires the participants to design and implement an automated negotiating agent, that is able to negotiate with two opponent agents and is capable of learning from its previous negotiation experiences. The same challenge in PRIANAC 2018 requires the design of the same type of automated agent that is able to negotiate only with one opponent agent. In addition, this challenge permits the usage of a local file in order to save the bids that were offered by the opponent agent, and a machine learning library. In order to address this challenge, we propose a novel negotiation strategy that is capable of finding the preference issues and values of each agent, then combining those issues and values in order to generate the bids that provide high joint utility values near Nash bargaining solution.

2. Negotiation Environment

2.1 Negotiation Competition

RMNL in ANAC 2018 is a repeated multi-party closed negotiation competition among three agents. RMNL assumes no previous knowledge of the preferences and strategies of the opponent agents, wherein the negotiating agents use the Stacked Alternating Offers Protocol (SAOP)[3]. In this context, each agent is given three minutes to deliberate. Each negotiation round is repeated five times. Also, the utility functions are linear and the participant agents are able to negotiate about a large set of previously unknown preferences. Similarly, PRIANAC 2018 is a bilateral negotiation competition. In this context, PRIANAC 2018 competition assumes no previous knowledge of the preferences of the opponent agents, wherein the negotiating agents use the Alternative Offer Protocol (AOP)[3]. Each negotiation round has ten seconds and the number of negotiation rounds on the same configuration is set to 100. Both competitions use GENIUS[4] platform.

Contact: Shan Liu, Nagoya Institute of Technology, Gokiso-cho, Showa-ku, Nagoya, Aichi, 466-8555 Japan, +818028807597, liu.shan@itolab.nitech.ac.jp

2.2 Preferences of the Negotiating Agents

The preferences for each agent in all negotiation domains are represented by a weighted sum utility function. In this regard, each agent has its own utility function. This utility function is expressed as follows:

$$u_a(b^t) = \sum_{j \in I} V_a(b_j^t) \cdot w_{a,j} \quad (1)$$

According to Equation (1), each negotiation issue $j \in I$ can take a value v_j from a predefined set of valid values for that issue which is denoted by D_j (i.e., $v_j \in D_j$), where each agent can access this domain information. In addition, a bid $b = (b_1,...,b_{|I|})$ is an assignment of values to all issues where $b_1 \in D_1$. $V_a(v_j)$ denotes Agent a valuation of the value of issue j.

3. Proposed Approach

3.1 Bid Searching Strategy

The proposed bid searching strategy aims to find the bids around Nash bargaining solution because these bids are expected to possess higher values of the joint utility function. In order to achieve this goal, the proposed method aims to find the priority issues for each opponent agent after analyzing the series of bids offered by this agent.

The main idea is dividing these bids into negotiation issue units, selecting the priority issue and value for each opponent agent and then generating new bids which not only have high utilities, but also include those prior issues and values. Therefore, the bid searching space becomes unrestricted to the already offered bids, instead, the new bids which include all the preference issues from different agents are expected. In addition, in PRIANAC 2018, we save and analyze all the bids that are offered by the opponent agents, in all negotiation rounds of the same negotiation domain, to

a local file. With the increasing number of bids, the accuracy of determining the preference for the opponent agent also increases. This bid searching strategy that is used in both ANAC 2018 and PRIANAC 2018 includes five steps.

The bid searching strategy is represented by Algorithm 1 as follows:

Algorithm 1 Bid Searching Strategy

Issues: given by a scenario, such as: ***a, b, c, d, e.***
Values: given for each issue by a scenario, such as: ***a1, a2, a3, a4, a5*** *for issue* ***a.***
for all *opponent participant agents* **do**
  for all *issues:* ***a, b, c, d, e*** **do**
    calculate the average of all the values in all offered bids
    calculate the standard deviation of all the values (VSD)
  end for
  calculate the standard deviation of all the issues' VSD (ISD)
  if $ISD > 0.0$ **then**
    The agent has preference
    Compare the preference of issues
    Choose the prior issue and the prior value
  else
    Choose the prior issue and the prior value randomly
  end if
end for
while true **do**
  generate the bid with the prior issues and values of opponent participant agents
  if *the utility of the generated bid ¿ threshold* **then**
    offer the bid
  end if
end while
if *the offered bid is accepted by all opponent agents* **then**
  negotiation succeeds
  save the list of offered bids to a local file
else
  update offered bids list and go to step 3
end if

In addition, a sample demonstration is shown in Figure 1 according to the following steps. First, calculate the standard deviation of each value in each issue, which is denoted as value standard deviation. Second, calculate the standard deviation of value standard deviation of each issue, which is denoted as issue standard deviation. Third, set issues with high value standard deviation as prior issues, and values with high frequency as prior values. Fourth, search the utility of the bids with prior issues and prior values, randomly. If the utilities of these bids are higher than a predefined threshold value, make an offer. Fifth, if the negotiation succeeds, save the list of offered bids to a local file. Otherwise, update the list of offered bids and return to the first step.

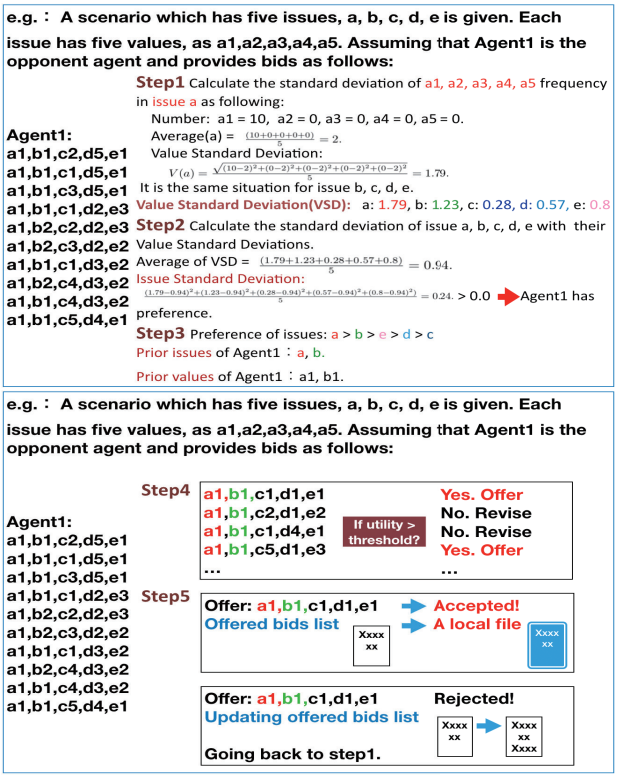

Figure 1: An example of bid reconstruction method

3.2 Bid Acceptance Strategy

A compromise function is used in order to judge whether or not to accept an offered bid. If the utility of a certain bid is greater than a preset threshold value, then the proposed agent accepts this bid. This threshold value decreases as time passes. In this context, this threshold value is calculated using the following equation.

$$Threshold = \max\{(1-(1-df)\cdot\log(e-1.9+(e-1)^{\alpha})\cdot t), emax\} \quad (2)$$

In this equation, df represents a discount factor. α is a parameter which we set as 4.5. t represents the current time. $emax$ represents the estimated maximum utility which is calculated using the following equation.

$$emax(t) = \mu(t) + (1 - \mu(t)) \cdot d(t) \quad (3)$$

Where, $\mu(t)$ is the mean utility of the opponent offers in the utility space of a certain agent. $d(t)$ [5] is a function for estimating the utility width of the opponent offers in the utility space of this agent. This utility width is given by Farma Agent in the ANAC 2016 competition as follow:

$$d(t) = \frac{\sqrt{3}\sigma(t)}{\sqrt{\mu(t)(1-\mu(t))}} \quad (4)$$

Where, σ is the standard deviation.

4. Results and Evaluation

Both competitions, i.e., ANAC 2018 and PRIANAC 2018 have two categories: the individual category, in which the

participant agents are ranked according to the individual utility they have obtained; and the social welfare category in which the participant agents are ranked by their social utility. This social utility is the sum of the individual utilities of all agents. The proposed agent won the second place in the final round of the social welfare category in ANAC 2018 and also won the first place of the social welfare category in PRIANAC 2018. These results demonstrate the efficiency of the proposed agent and its ability to find high joint utility solutions.

ANAC 2018 The final round has been run among nine finalists in each category with four selected scenarios submitted by the participants. For each scenario, 2520 negotiations were run. The results of the qualifying round and the final round of the social welfare category are presented in Figure 2.

Qualify Round Result (Pool C)

Agent Name	Individual Utility	Social Welfare
AgentNP1	0.512177707	1.52976242
GroupY	0.485323479	1.33874982
ATeamAgent	0.345297603	0.980979189
Sontag	0.484535782	1.515047114
Agent33	0.428666974	1.419233621
Agent_Hama	0.469592183	1.393009022
Exp-Rubick	-	-

Figure 2: Qualify Round Result in ANAC 2018

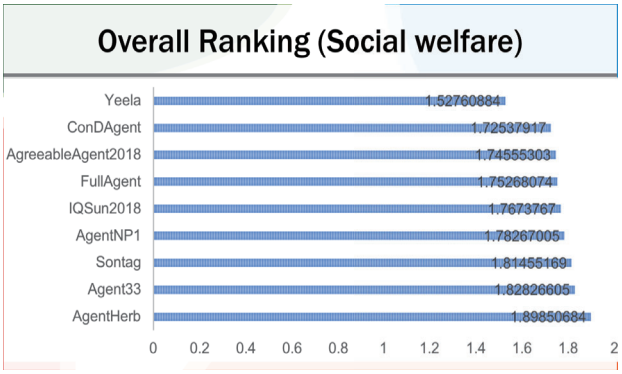

Figure 3: Results in ANAC 2018

PRIANAC 2018 The competition has been held among 6 agents with 120 negotiation scenarios which are generated by the organizers. In each tournament, 12,000 sessions were run. The results of the social welfare category are presented in Figure 3.

5. Conclusion and Future Work

This paper proposes a negotiating agent that implements a novel bid reconstruction method in order to search the suitable bids that obtain high joint utility values. Towards this end, the bid reconstruction method utilizes the previously offered bids by the opponent agents in order to construct the successful bids around Nash bargaining solution. The final round results of ANAC RMNL 2018 competition and the results of PRIANAC 2018 competition demonstrate that the proposed agent is able to search the scope of suitable bids around Nash bargaining solution and succeeds to lead other participant agents where the negotiating agent achieves higher values of joint utilities. Future work is set to study the necessary improvements that are needed to achieve a high individual utility value and to investigate the usage of machine learning to help reduce the scope of bid searching.

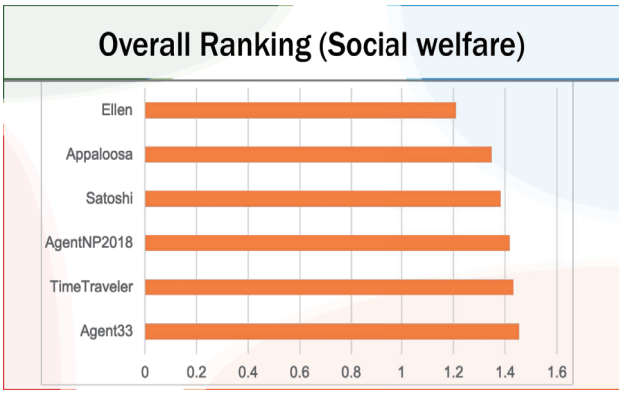

Figure 4: Overall Ranking (Social Welfare) in PRIANAC 2018

References

[1] PRIANAC 2018 (Pacific Rim International Automated Negotiation Agents Competition), http://web.tuat.ac.jp/ katfuji/PRIANAC2018/.

[2] ANAC 2018 (Ninth International Automated Negotiating Agents Competition), http://web.tuat.ac.jp/katfuji/ANAC2018/.

[3] Aydoğan, R., Festen, D., Hindriks, K. V., & Jonker, C. M. (2017). Alternating offers protocols for multilateral negotiation. In Modern Approaches to Agent-based Complex Automated Negotiation (pp. 153-167). Springer, Cham.

[4] Lin, R., Kraus, S., Baarslag, T., Tykhonov, D., Hindriks, K., & Jonker, C. M. (2014). Genius: An integrated environment for supporting the design of generic automated negotiators. Computational Intelligence, 30(1), 48-70.

[5] Toyama T., Takayuki, I. (2016). Concession based on Maximum Utilities Estimated by a Divided Uniform Distribution.

The 33rd Annual Conference of the Japanese Society for Artificial Intelligence, 2019

Analysis of Incentive Ratio in Top-Trading-Cycles Algorithms

Taiki Todo[*1*2]

[*1]Department of Informatics, Graduate School of ISEE, Kyushu University
[*2]Multi-Agent Optimization Team, RIKEN AIP

The main objective of this paper is to analyze some variants of the classical top-trading-cycles (TTC) algorithm for slightly modified models of the housing market. Extensions of TTC for such modified models are not necessarily strategy-proof, as pointed out by Fujita et al. (2015), and thus some alternative analysis of agents' selfish behavior is needed. In this paper, the incentive ratio, originally proposed by Chen et al. (2011), of the variants of TTC algorithm is analyzed in both (i) the multi-item exchange and (ii) an exchange model with a specific form of externalities.

1. Introduction

Exchange of indivisible items is a fundamental problem in the literature of economic theory, where each agent is endowed with a set of indivisible item and a preference over the items in the market, and monetary transfer is not allowed. The objective is the find an exchange rule that returns a socially-desirable redistribution (outcome) of items among agents. Most researches on exchange, especially those on the mechanism design perspective, have investigated agents' incentives, such as *strategy-proofness* that requires no agent can benefit by misreporting its preference to the mechanism.

The *housing market* [Shapley 74], is one of the well-studied model of exchange, where each agent's endowments are restricted to a single item. The *top-trading-cycles* (TTC) algorithm is a well-known exchange rule for the housing market, which satisfies strategy-proofness, and returns an efficient outcome in polynomial time. Furthermore, Ma showed that TTC is the only exchange rule that satisfies, under a natural condition, those two properties [Ma 94]. Recent years, there have been several extensions of TTC for various modified exchange problems, in the fields of economics and artificial intelligence [Pápai 00, Alcalde-Unzu 11, Aziz 12, Saban 13, Sonoda 14, Sun 15, Sikdar 17].

Strategy-proofness is, in general, a too demanding property, and is not compatible with optimal outcomes, e.g., Pareto efficient ones, in many realistic extensions, including exchange of multiple items [Sönmez 99]. Therefore, many researches in the literature of mechanism design have focused on developing sub-optimal mechanisms, in order to guarantee strategy-proofness [Todo 14].

However, it is still important to analyze, under mechanisms that are not strategy-proof, to what extent an agent can benefit by his selfish behavior. In particular, mechanism that are popular or easy-to-understand are, even if they are not strategy-proof, more likely to be used in practice, as the first-price auction is for selling items. One of such analysis is based on *incentive ratio* [Chen 11, Chen 17a, Chen 17b], which quantitatively evaluates the (ratio of) possible gain by a manipulation.

In this paper, we first algorithmically analyze the incentive ratio of some TTC variants, which indicates how much in the worst case an agent can gain by misreporting its preference under TTC. For the case of multi-item exchange, we show that (a) the incentive ratio is unbounded in general, and (b) it becomes 2 when the valuation is assumed to be lexicographic. For the case of service exchange, which is a special case of exchange with externalities, we show that (c) the incentive ratio is unbounded, even if the valuations have an upper bound.

2. General Model

In this section we introduce a general model of exchange. Let N be the set of n agents, and K be the set of indivisible items. Each agent $i \in N$ has an *endowment* $e_i \subseteq K$, satisfying $\bigcup_{i \in N} e_i = K$, $e_i \neq \emptyset$ for any $i \in N$, and $e_i \cap e_j = \emptyset$ for any pair $i, j \in N$. The profile $e := (e_i)_{i \in N}$ is called an *endowment profile*. An n-partition $(a_i)_{i \in N}$ of the set K, satisfying $\bigcup_{i \in N} a_i = K$, $a_i \neq \emptyset$ for any $i \in N$, and and $a_i \cap a_j = \emptyset$ for any pair $i, j \in N$, is called an *outcome*. Let A be the set of all outcomes. By definition, the endowment profile e is also an outcome, i.e., $e \in A$.

Each agent $i \in N$ also has a *valuation function* $v_i : A \to \mathbb{R}_{>0}$, which assigns a non-negative value for each outcome. The value $v_i(a)$ indicates the level of happiness for agent i when outcome a realizes. Let V be the set of all possible valuation functions. An *exchange rule* $f : A \times V \to A$ is a function that takes an endowment profile and a profile of valuation functions as an input and returns an outcome[*1].

In the literature of mechanism design, an incentive property called *strategy-proofness* has been extensively studied. An exchange rule is said to be strategy-proof if no agent can benefit by misreporting his valuation function, i.e., truth-telling is a dominant strategy of the game. Formally, it requires that $\forall N$, $\forall K$, $\forall e \in A$, $\forall i \in N$, $\forall v_{-i} \in V^{n-1}$,

Contact: Taiki Todo, Department of Informatics, Kyushu University, Motooka 744, Nishi-Ward, Fukuoka, Japan 819-0395, +81-92-802-3576, todo@inf.kyushu-u.ac.jp

*1 While we restrict our attention in this paper to deterministic exchange rules, most of the concepts defined in this paper can easily apply for *randomized exchange rules*, which returns a probability distribution over outcomes.

$\forall v_i \in V$, and $\forall v_i' \in V$,

$$v_i(f(e,(v_i,v_{-i}))) \geq v_i(f(e,(v_i',v_{-i}))).$$

As readers may wonder, however, the condition of strategy-proofness is quite demanding and actually very hard to satisfy; the inequality must hold for any profile of other agents' valuations and any misreport of the manipulator. Indeed, under very natural assumptions, strategy-proofness, and its variants such as false-name-proofness, are not achievable in various mechanism design problems [Gibbard 73, Satterthwaite 75, Yokoo 04, Todo 14].

Accordingly, Chen et al. [Chen 11] proposed an alternative measure, called *incentive ratio*, to evaluate the robustness of mechanisms/rules against agents' selfish behaviors.

Definition 1 (Incentive Ratio)**.** *For a given exchange rule f, the* incentive ratio in f *is $\alpha \in \mathbb{R}_{\geq 1}$ if α is the minimum real number such that $\forall N$, $\forall K$, $\forall e \in A$, $\forall i \in N$, $\forall v_{-i}$, $\forall v_i$, $\forall v_i'$,*

$$\alpha \cdot v_i(f(e,(v_i,v_{-i}))) \geq v_i(f(e,(v_i',v_{-i}))).$$

Obviously, when an exchange rule f is strategy-proof, the incentive ratio of f is one. The smaller, i.e., closer to one, the incentive ratio is, the more robust it is against manipulations (in our framework, against valuation misreports).

3. Housing Market and TTC

The classical *housing market*, originally proposed by Shapley and Scarf, is represented as a special case of our exchange problem*2, by setting $|K| = n$ (and thus, automatically $|e_i| = |a_i| = 1$ for any $i \in N$ and $a \in A$) and $v_i(a) = v_i(b)$ if and only if $a_i = b_i$ for any $i \in N$ and any pair $a, b \in A$. Each outcome therefore corresponds to a permutation of endowments among agents. The following algorithm is called *Top-Trading-Cycles* (TTC in short), which is proposed to solve the housing market problem [Shapley 74].

Definition 2 (Top-Trading-Cycles)**.**

Step 1 *Construct a DAG with two types of vertices, agents and items, so that draw a directed edge from each agent vertex to his favorite item vertex, and a directed edge from each item vertex to its owner (agent) vertex. Assign to each agent, in each cycle, the item to which he is pointing and remove all such item vertices and agent vertices from the graph. Go to* **Step** 2.

Step $t(\geq 2)$ *The algorithm halts if no agent vertex remains; otherwise, each agent in the graph points to his favorite item among the remaining ones and each item points to its owner. Assign to each agent, in each cycle, the item to which he points and remove all such items and agents from the graph. Go to* **Step** $t+1$.

It was proven that the TTC algorithm is strategy-proof, and therefore, the incentive ratio of TTC in the housing market is 1.

*2 The original housing market is defined only with ordinal preferences, rather than with valuation functions. However, all the discussion on incentives in their paper can easily apply for the case with valuation functions.

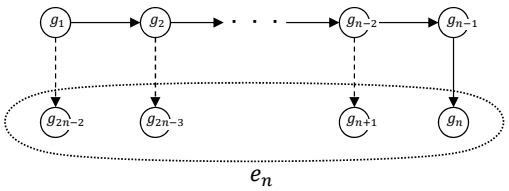

Figure 1: Example in Proof of Lemma 1

4. Multi-Item Exchange

Fujita et al. [Fujita 15] extended the classical housing market to *multi-item exchange* problem, in which agents' endowments are not restricted to a single item, i.e., remove the constraints of $|K| = n$ from the housing market.

They proposed a modification of TTC, so-called augmented TTC (ATTC), that still runs in polynomial times and always selects a core outcome. ATTC first splits each agent i into atomic players, so that each atomic player has the same valuation function with agent i only over single items, and owns exactly one item from e_i. ATTC then run the TTC algorithm for the market consisting of the atomic players. By definition, each agent finally obtains the same number of items as his original endowment, i.e., $|a_i| = |e_i|$ for any $a \in A$ and any $i \in N$. To simplify the notation, let us focus on the following *additive* valuation functions: there exists $u_i : K \to \mathbb{R}_{>0}$ such that $v_i(a_i) = \sum_{g \in a_i} u_i(g)$.

As they pointed out, ATTC is not strategy-proof. On the other hand, they also pointed out by Proposition 2 in [Fujita 18], even though ATTC is not strategy-proof, the best item that an agent receives under truth-telling cannot be improved by any misreport of valuation function.

Here, we provide a further observation on the manipulability of ATTC: there exists a problem instance under which an agent can improve all the other items, except for the best one, as much as possible.

Lemma 1. *For any N, there is a problem instance (K, e, v) such that an agent $i \in N$ with endowment $e_i \subset K$, who originally receives the best item and the worst $|e_i|-1$ items, receives the top $|e_i|$ item by misreporting valuation function.*

Proof. Consider $N = \{1, \ldots, n\}$, $K = \{g_1, g_2, \ldots, g_n, g_{n+1}, g_{n+2}, \ldots, g_{2n-2}\}$, $e = (e_i)_{i \in N} = (\{g_1\}, \{g_2\}, \ldots, \{g_n, g_{n+1}, g_{n+2}, \ldots, g_{2n-2}\})$, and the valuation functions $(v_i)_{i \in N}$ is given as follows:

$$\begin{aligned}
&u_1(g_2) > u_1(g_{2n-2}) > \cdots \\
&u_2(g_3) > u_2(g_{2n-3}) > \cdots \\
&\vdots \\
&u_{n-2}(g_{n-1}) > u_{n-2}(g_{n+1}) > \cdots \\
&u_{n-1}(g_n) > \cdots \\
&u_n(g_1) > u_n(g_2) > \cdots > u_n(g_n) > \cdots > u_n(g_{2n-2})
\end{aligned}$$

Figure 1 indicates the first and second best items for each agent except the manipulator $n \in N$.

When every agent truthfully reports their valuations, a cycle $g_1 \to g_2 \to \cdots \to g_n \to g_1$ is constructed at round

1 of ATTC. In the subsequent rounds only atomic players made for agent n remain. Agent n finally obtains $\{g_1, g_{n+1}, g_{n+2}, \ldots, g_{2n-2}\}$, one of which is the best item and the others are the worst $n-2$ items.

Now consider the misreport v'_n by agent n, associated with u'_i given as follows:

$$u'_n(g_{n-1}) > u'_n(g_{n-2}) > \cdots > u'_n(g_1) > u'_n(g_n) > \cdots$$

Under this misreport, at each round r ($1 \leq r \leq n-1$) of ATTC, an atomic player, made for agent n, receives g_{n-r} for item g_{n+r-1}. Agent n thus finally obtains $\{g_1, g_2, \ldots, g_{n-1}\}$, which are the best $n-1$ items. □

Obviously this is the best possible gain by an agent's valuation misreport, and thus the incentive ratio of ATTC is given as:

$$\frac{\sum_{k=1}^{n-1} u_n(g_k)}{u_n(g_1) + \sum_{l=n+1}^{2n-2} u_n(g_l)} \tag{1}$$

Based on this observation, we can now analyze the incentive ratio of ATTC in detail.

Theorem 1. *When the agents' valuation functions are additive, the ATTC for multi-item exchange has an unbounded incentive ratio.*

Proof. For given n, the maximum value of the incentive ratio, given in Eq. 1, approaches $n-1$, which realizes, for instance, when the first $n-1$ values, $u_n(g_1), \ldots, u_n(g_{n-1})$, are close enough to one and all the lower values, $u_n(g_n), \ldots, u_n(g_{2n-2})$, are almost zero. The ratio is therefore unbounded when $n \to \infty$. □

An additive valuation function is said to be *lexicographic* if its associated u_i satisfies the following:

$$\forall g \in K, u_i(g) \geq \sum_{h \in K \text{ s.t. } u_i(g) > u_i(h)} u_i(h).$$

Considering such a valuation function is natural when agents have extreme preferences so that their utility is determined almost solely by the best item they receives, and each of the other items he receives is considered as an extra. Under this assumption, the incentive ratio of ATTC is slightly improved.

Theorem 2. *When the agents' valuation functions are lexicographic, the ATTC for multi-item exchange has the incentive ratio of 2.*

Proof. When the valuation function u_n is given as

$$\forall g_k \in K, u_n(g_k) = 2^{|K|-k},$$

the incentive ratio becomes

$$\frac{2^{2n-3} + 2^{2n-4} + \cdots + 2^n}{2^{2n-3} + 2^{n-2} + \cdots + 2^0},$$

which converges to 2 for $n \to \infty$. □

5. Exchange with Externalities

Considering externalities in agents' utilities is a promising approach [Mumcu 07], as in most of the real-life market, a person's utility usually depends on other people's information/actions. However, in many mechanism design problems, including the exchange problem for housing market, such externality in agents' utilities causes a negative results, such as the non-existence of strategy-proof mechanisms.

A natural approach to avoid falling into such negative results is to focus on some specific structure of externalities. The *service exchange problem*, proposed by Lesca and Todo [Lesca 18] as a simple extension of the housing market, is one of such an approach. In their model, each agent considers both the item he receives *and* the agent who receives his endowment.

The service exchange problem is also a special case of exchange problem, which can be represented by setting $|K| = n$ and for any $i \in N$ and any pair $a, b(\neq a) \in A$, $v_i(a) = v_i(b)$ if and only if both $a_i = b_i$ and $\exists j \in N$ such that $a_j = b_j = e_i$. In words, an agent i is indifferent between two outcomes a and b if and only if (i) he receives the same item, and (ii) his endowment is taken by the same agent. To simplify the model, let us focus on the following valuation functions; there exists $p_i : V \to \mathbb{R}_{>0}$ and $q_i : N \to \mathbb{R}_{>0}$ such that $v_i(a) = p_i(a_i) + q_i(j)$, where $j \in N$ is the agent who takes e_i and $q_i(i) = 0$.

One naive way to implement the idea of TTC for the service exchange problem is to ignore the externality term q_i in agents' valuations and focus only on the item that each agent receives. By focusing on the receiving item, we can guarantee that the classical TTC runs without any modification.

The following theorem shows that the TTC for the problem has an unbounded incentive ratio.

Theorem 3. *The TTC for exchange with externalities has an unbounded incentive ratio, even if agents' externalities, $(q_i)_{i \in N}$, have an upper bound.*

Proof. Consider $N = \{1, 2, 3\}$, $K = \{g_1, g_2, g_3\}$, $e = (e_i)_{i \in N} = (\{g_1\}, \{g_2\}, \{g_3\})$, and the functions of manipulating agent 3, p_3 and q_3, are given as follows:

$$p_3(g_1) = p_3(g_2) + \epsilon$$
$$q_3(1) \ll q_3(2)$$

When both agents 1 and 2 most prefers item g_3, the TTC assigns g_1 to agent 3 and g_3 is assigned to agent 1, in which agent 3's valuation is $p_3(g_1) + q_3(1)$. By misreporting his valuation, agent 3 can receive g_2 and give his endowment g_3 to agent 2, in which his valuation is $p_3(g_2) + q_3(2)$. The ratio is therefore unbounded, since we can choose small enough $p_i(1)$. The ratio is still unbounded when both p_i and q_i have the same upper bound because, by adding more agents and items, we may find the above case in the very last step of TTC, where only a few items having small enough values p for agent 3 is left in the market, which still have large values q. □

6. Conclusions

Note that the analysis of incentive ratio still focuses on the worst case behavior of the market/algorithm, as the analysis of strategy-proofness does. It should be interesting to theoretically analyze the average case incentives [Kojima 09]. It is obvious that the TTC algorithms cannot always achieve the optimal outcome for extensions of , i.e., the one which maximizes *social welfare* which is defined as the sum of agents' valuations. Accordingly, analyzing their approximation factors is an open question, as several papers on both algorithms and mechanism design have considered for various problems. Developing different exchange rules that are still easy to understand, as well as having a better, i.e., smaller, incentive ratio, is another interesting direction.

Acknowledgement

This work is supported by JSPS KAKENHI Grant Numbers JP17H00761 and JP17H04695. The author thanks Etsushi Fujita, Julien Lesca, Akihisa Sonoda, and Makoto Yokoo for their helpful comments and discussion. All errors are my own.

References

[Alcalde-Unzu 11] Alcalde-Unzu, J. and Molis, E.: Exchange of indivisible goods and indifferences: The Top Trading Absorbing Sets mechanisms, *Games and Economic Behavior*, Vol. 73, No. 1, pp. 1 – 16 (2011)

[Aziz 12] Aziz, H. and Keijzer, de B.: Housing Markets with Indifferences: A Tale of Two Mechanisms, in *Proc. AAAI'12*, pp. 1249–1255 (2012)

[Chen 11] Chen, N., Deng, X., and Zhang, J.: How Profitable Are Strategic Behaviors in a Market?, in *Proc. the 19th Europ. Symp. Algorithms (ESA'11)*, pp. 106–118 (2011)

[Chen 17a] Chen, Z., Cheng, Y., Deng, X., Qi, Q., and Yan, X.: Agent Incentives of Strategic Behavior in Resource Exchange, in Proc. SAGT'17, pp. 227–239 (2017)

[Chen 17b] Chen, Z., Cheng, Y., Deng, X., Qi, Q., and Yan, X.: Limiting User's Sybil Attack in Resource Sharing, in *Proc. WINE'17*, pp. 103–119 (2017)

[Fujita 15] Fujita, E., Lesca, J., Sonoda, A., Todo, T., and Yokoo, M.: A Complexity Approach for Core-Selecting Exchange with Multiple Indivisible Goods under Lexicographic Preferences, in *Proc. AAAI'15*, pp. 907–913 (2015)

[Fujita 18] Fujita, E., Lesca, J., Sonoda, A., Todo, T., and Yokoo, M.: A Complexity Approach for Core-Selecting Exchange under Conditionally Lexicographic Preferences, *J. Artif. Intell. Res.*, Vol. 63, pp. 515–555 (2018)

[Gibbard 73] Gibbard, A.: Manipulation of voting schmes, *Econometrica*, Vol. 41, pp. 587–602 (1973)

[Kojima 09] Kojima, F. and Pathak, P. A.: Incentives and Stability in Large Two-Sided Matching Markets, *Amer. Econ. Rev.*, Vol. 99, No. 3, pp. 608–627 (2009)

[Lesca 18] Lesca, J. and Todo, T.: Service Exchange Problems, in *Proc. IJCAI-ECAI'18*, pp. 354–360 (2018)

[Ma 94] Ma, J.: Strategy-proofness and the strict core in a market with indivisibilities, *Intl. J. Game Theory*, Vol. 23, No. 1, pp. 75–83 (1994)

[Mumcu 07] Mumcu, A. and Saglam, I.: The core of a housing market with externalities, *Economics Bulletin*, Vol. 3, No. 57, pp. 1–5 (2007)

[Pápai 00] Pápai, S.: Strategyproof Assignment by Hierarchical Exchange, *Econometrica*, Vol. 68, No. 6, pp. 1403–1433 (2000)

[Saban 13] Saban, D. and Sethuraman, J.: House Allocation with Indifferences: A Generalization and a Unified View, in *Proc. ACM-EC'13*, pp. 803–820 (2013)

[Satterthwaite 75] Satterthwaite, M. A.: Strategy-proofness and Arrow's conditions: existence and correspondence theorems for voting procedures and social welfare functions, *J. Econ. Theory*, Vol. 10, pp. 187–217 (1975)

[Shapley 74] Shapley, L. and Scarf, H.: On cores and indivisibility, *J. Mathe. Econ.*, Vol. 1, No. 1, pp. 23–37 (1974)

[Sikdar 17] Sikdar, S., Adali, S., and Xia, L.: Mechanism Design for Multi-Type Housing Markets, in *Proc. AAAI'17*, pp. 684–690 (2017)

[Sönmez 99] Sönmez, T.: Strategy-proofness and Essentially Single-valued Cores, *Econometrica*, Vol. 67, No. 3, pp. 677–689 (1999)

[Sonoda 14] Sonoda, A., Fujita, E., Todo, T., and Yokoo, M.: Two Case Studies for Trading Multiple Indivisible Goods with Indifferences, in *Proc. AAAI'14*, pp. 791–797 (2014)

[Sun 15] Sun, Z., Hata, H., Todo, T., and Yokoo, M.: Exchange of Indivisible Objects with Asymmetry, in *Proc. IJCAI'15*, pp. 97–103 (2015)

[Todo 14] Todo, T., Sun, H., and Yokoo, M.: Strategyproof Exchange with Multiple Private Endowments, in *Proc. AAAI'14*, pp. 805–811 (2014)

[Yokoo 04] Yokoo, M., Sakurai, Y., and Matsubara, S.: The Effect of False-name Bids in Combinatorial Auctions: New Fraud in Internet Auctions, *Games and Economic Behavior*, Vol. 46, No. 1, pp. 174–188 (2004)

The 33rd Annual Conference of the Japanese Society for Artificial Intelligence, 2019

Multi-Agent Traffic Signal Control System Using Deep Q-Network

*1Yohei Kanzaki Keisuke Ohno Eichi Takaya Satoshi Kurihara

*1Keio University

In urban areas, temporal and economic losses due to traffic congestion are getting worse. It has a great influence on our lives. As a cause of traffic congestion, on ordinary road, inappropriate signal switching may be cited. Parameter manipulation in the general signal control is set based on experiences by human hands, and it is never optimal. Therefore, controlling traffic lights to improve traffic behavior is possible way to solve traffic congestion. In this study, we combine multi agent system with Deep Q-Network method. We used an intersection as an agent and conducted experiment in road environment with multiple intersections. As a result, it was shown that agents can perform appropriate parameter manipulation by mutual exchange of information among agents.

1. Introduction

In recent years, temporal and economic losses due to traffic jams in urban areas are getting worse and exert a great influence on our lives. Parameter manipulation in the general signal control is set based on experiences by human hands and it is never optimal. Therefore, controlling traffic lights and improving traffic behavior is one way to solve traffic congestion. In this study, we combine a multi-agent system with a method using Deep Q-Network (DQN) [Mnih et al.2013]. This is a combination of deep learning with high feature extraction capability and Q learning which is one of reinforcement learning methods to learn optimal behavior based on rewards. In consequence, we propose a signal control system aiming at appropriate parameter manipulation in road environment with multiple intersections.

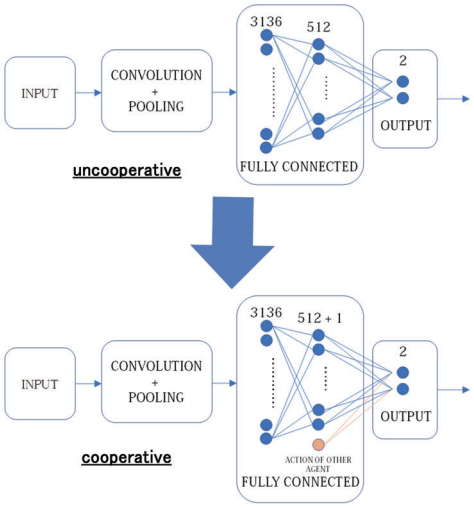

Figure 1: CNN in uncooperative / collaborative learning

2. Traffic Signal Control with Deep Q-Network

Previous study[Sato et al.2017] uses DQN to control traffic signal. However, it is necessary to cover the operation pattern of traffic lights as many as the number of intersections. If the number of traffic lights increases, the amount of calculation becomes enormous and it becomes difficult to perform appropriate parameter control. Therefore, we propose a multi-agent signal control system using DQN aiming at reducing the computational complexity compared with method of Sato et al. by preparing agents as many as the number of intersections where signal operations are performed and coordinating agents together.

3. Proposed Method

In this study, we use the traffic flow simulator image as input value by using DQN. Design of DQN in a single agent, we follow Sato et al. In order to cooperate among agents, we have the agent exchange information on other agent's behavior. In order to be able to share behaviors among agents, we use 513 values by adding the value of action of other agent to 512 input values in fully connected layer. As a result, the values of the actions is updated considering the behavior of other agents. (See Figure 1).

Contact: Yohei Kanzaki 0wrkan@keio.jp

4. Experiment and Evaluation

We used the number of waiting cars as evaluation criteria and compared them with several methods and examined the effect of the proposed method and its usefulness. In this study, we performed experiments using the micro traffic flow simulator SUMO. This is an open source simulator developed around the German Aerospace Center. It is possible to set various parameter freely, such as the speed of the car, the acceleration, the traveling route and the installation of traffic lights and roads. We prepared the following three comparative methods.

4.1 Comparative method 1: static signal control

First, we prepared a static situation in which traffic lights are switched at regular intervals according to the traffic

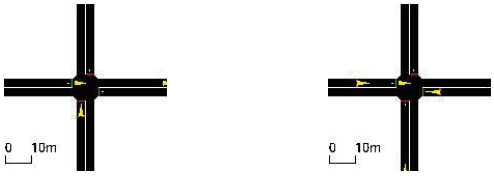

Figure 2: Input image of SUMO for multi-agent

Figure 3: Input image of SUMO for single-agent

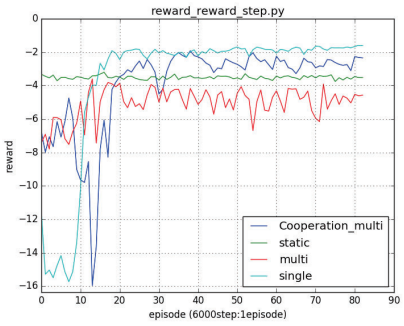

Figure 4: Experimental Results of Proposed Method and Comparative Method

flow. We set the offset [*1] to 15 seconds.

4.2 Comparative method 2: Signal control by non-cooperative multi-agent using Deep Q-Network

Second method is an situation with multiple agents with DQN as agent and agents do not share information(Figure 2).

4.3 Comparative method 3: Signal control by single-agent using Deep Q-Network

Third method is a single agent situation using method of Sato et al. DQN is used as an agent which learns while reading the entire road situationnt image(Figure 3).

5. Experimental Result

For both the proposed method and the comparative methods, we performed 500,000 step experiments and showed the result of simulation by taking the average of the number of waiting cars every 6,000 steps(Figure 4). The horizontal axis is every 6,000 steps and the vertical axis is the number of waiting cars as negative reward. For each line, the proposed method, comparative method 1, method 2 and method 3 are corresponding to "Cooperation_multi", "static ", "multi", "single" respectively. As the number of episodes increases, Comparative Method 3 was better than any other methods and it is understood that it was the ideal method to solve the most congestion, but it took about 1.8 times as long as the proposed method. In addition, the proposed method surpassed Method 1 and Method 2, and was approaching Method 3. Therefore, the proposed method can reduce the computational complexity while obtain the similar result as Sato et al 's method.

6. Conclusion

In this study, we proposed the method of traffic signal control with multi-agent Deep Q-Network. Experimental result showed it was able to control traffic signals appropriately with reducing the computational complexity than the comparative method. Cooperation among agents in signal control using DQN worked effectively in our experiment. However, it is impractical to use images taken from the sky at each intersection. Therefore, we replace the information obtained from the radar with a simulator(Figure 5). By using radio wave radar we get information on the speed, length, position etc. of the car. Information obtained from the simulator is entered into the agent as a matrix. In this way, we are beginning to examine even the reality-appropriate method.

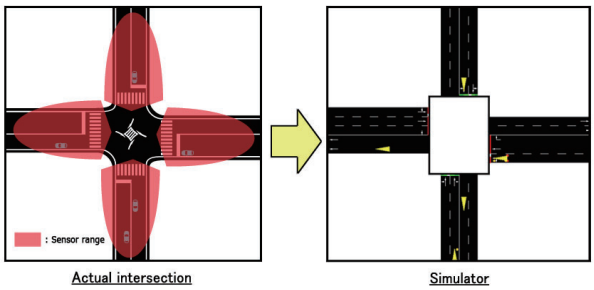

Figure 5: Convert real road to simulator

References

Mnih, V.; Kavukcuoglu, K.; Silver, D.; Graves, A.; Antonoglou, I.; Wierstra, D.; and Riedmiller, M. 2013. Playing atari with deep reinforcement learning. *arXiv preprint arXiv:1312.5602*.

Sato, K.; Takaya, E.; Ogawa, R.; Ashihara, Y.; and Kurihara., S. 2017. Development of traffic control system by use of deep q-network. In *The 31st Annual Conference of the Japanese Society for Artificial Intelligence, 2017*, 3I2OS13b4–3I2OS13b4. Japanese Society for Artificial Intelligence.

∗1 Number of seconds to shift the timing at which traffic lights switch to green light for each intersection.

International Session | International Session | [ES] E-2 Machine learning

[2H4-E-2] Machine learning: fusion of models

Chair: Naohiro Matsumura (Osaka University)

Wed. Jun 5, 2019 3:20 PM - 5:00 PM Room H (303+304 Small meeting rooms)

[2H4-E-2-01] Curiosity Driven by Self Capability Prediction

○Nicolas Bougie[1,2], Ryutaro Ichise[2,1] （1. Sokendai, The Graduate University for Advanced Studies, 2. National Institute of Informatics）

3:20 PM - 3:40 PM

[2H4-E-2-02] Improvement of Product Shipment Forecast based on LSTM Incorporating On-Site Knowledge as Residual Connection

○Takeshi Morinibu[1], Tomohiro Noda[1], Shota Tanaka[1] （1. Daikin Industries, Ltd. Technology and Innovation Center）

3:40 PM - 4:00 PM

[2H4-E-2-03] Unsupervised Joint Learning for Headline Generation and Discourse Structure of Reviews

○Masaru Isonuma[1], Junichiro Mori[1], Ichiro Sakata[1] （1. The University of Tokyo）

4:00 PM - 4:20 PM

[2H4-E-2-04] Gradient Descent Optimization by Reinforcement Learning

○Yingda Zhu[1], Teruaki Hayashi[1], Yukio Ohsawa[1] （1. The University of Tokyo）

4:20 PM - 4:40 PM

[2H4-E-2-05] Reducing the Number of Multiplications in Convolutional Recurrent Neural Networks (ConvRNNs)

○Daria Vazhenina[1], Atsunori Kanemura[1] （1. Leapmind Inc.）

4:40 PM - 5:00 PM

The 33rd Annual Conference of the Japanese Society for Artificial Intelligence, 2019

Curiosity Driven by Self Capability Prediction

Nicolas Bougie[*1*2] Ryutaro Ichise[*2*1]

[*1] Sokendai, The Graduate University for Advanced Studies
[*2] National Institute of Informatics

Reinforcement learning is a powerful method to solve tasks using a reward signal; however, it struggles in sparse reward scenarios. One solution to this problem is the use of reward shaping but, it requires complicated human engineering in complex environments. Instead, our solution relies on exploration driven by curiosity. In this paper, we formulate the curiosity as the ability of the agent to predict its knowledge about the task. The prediction is based on the combination of intermediate goals and deep learning. Our end-to-end method scales to high-dimensional state spaces such as images. As proof-of-concept, we present a preliminary implementation of our algorithm using only raw pixels as input.

1. Introduction

Reinforcement learning (RL) methods have led to remarkable successes in a wide variety of tasks. RL can be used to train an algorithm to learn policies by optimizing a reward function. For instance, they have been used in autonomous vehicle control [Abbeel et al., 2007] or robotic control [Levine et al., 2016]. Another significant technique is the combination of deep neural networks and Q-learning, resulting in "Deep Q-Learning" (DQN) [Mnih et al., 2013], able to achieve human performance on many tasks including Atari video games [Bellemare et al., 2015]. However, in many real-world tasks, rewards are sparse or poorly defined, which entails that they learn slowly.

In order to guide the agent, an additional intrinsic signal can be provided to the agent. Multiple techniques have been tested. For example, Racaniere et al., base the exploration of the agent on the surprise - the ability of the agent to predict future [Racanière et al., 2017]. Pathak et al., estimate the surprise of the agent by predicting the consequences of the actions of the agent on the environment [Pathak et al., 2017]. Namely, they use an inverse model and the prediction error as the intrinsic reward. Another attempt aims to predict the features of a fixed random neural network on the observation of the agent [Burda et al., 2018]. Nevertheless, the low sample efficiency doesn't show clearly how to adapt this method to large scale tasks.

We propose an alternative solution to the curiosity mechanism by defining the exploration bonus as the capability of the agent to predict the sub-tasks that it masters - the agent learns to predict its own capabilities. We introduce the idea of goals to automatically decompose a task into several easier sub-tasks. Namely, given the current observation, the agent learns to predict which intermediate goals it masters. By acquiring knowledge about its abilities, we can improve exploration by forcing the agent to explore unknown parts of the environment. Our method relies on two deep neural networks: one to embedded the states and goals and the other one to predict the capabilities of the agent. In order to measure the distance between a goal and an observation, we base the goals and states representation on a latent variable model, a variational autoencoder [Kingma and Welling, 2014]. In the preliminary implementation, our architecture can learn policies in large continuous states spaces with sparse rewards. Note that our agent can learn policies from raw pixels without any supervision.

Contact: Nicolas Bougie, Sokendai, The Graduate University for Advanced Studies, Tokyo, Japan, +81-3-4212-2000, nicolas-bougie@nii.ac.jp

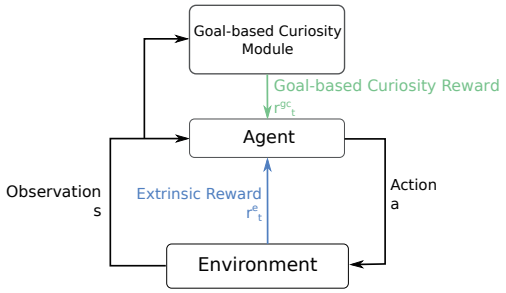

Figure 1: The agent in a state s interacts with the environment by performing an action a and, receives an extrinsic reward r^e. A policy $\pi(s_t;\theta_P)$ is trained to optimize the sum of r^e and r^{gc}. The intrinsic reward r^{gc} is generated by the goal-based curiosity module to favor the exploration of novel states.

2. Method

2.1 Curiosity as Reward Signal

Training an agent in a sparse reward environment is challenging since the agent generally receives no reward or a negative reward. We can introduce a new bonus to encourage the agent to explore sparse reward scenarios. In addition to the extrinsic rewards r^e of the environment, we introduce a goal-based curiosity reward signal r^{gc} (Figure 1). At time t the agent receives the sum of these two rewards $r_t = r^e_t + r^{gc}_t$. To encourage the agent to explore the environment, we design r^{gc} to be higher in novel states than in frequently visited states.

The policy $\pi(s_t;\theta_P)$ is represented by a deep neural net-

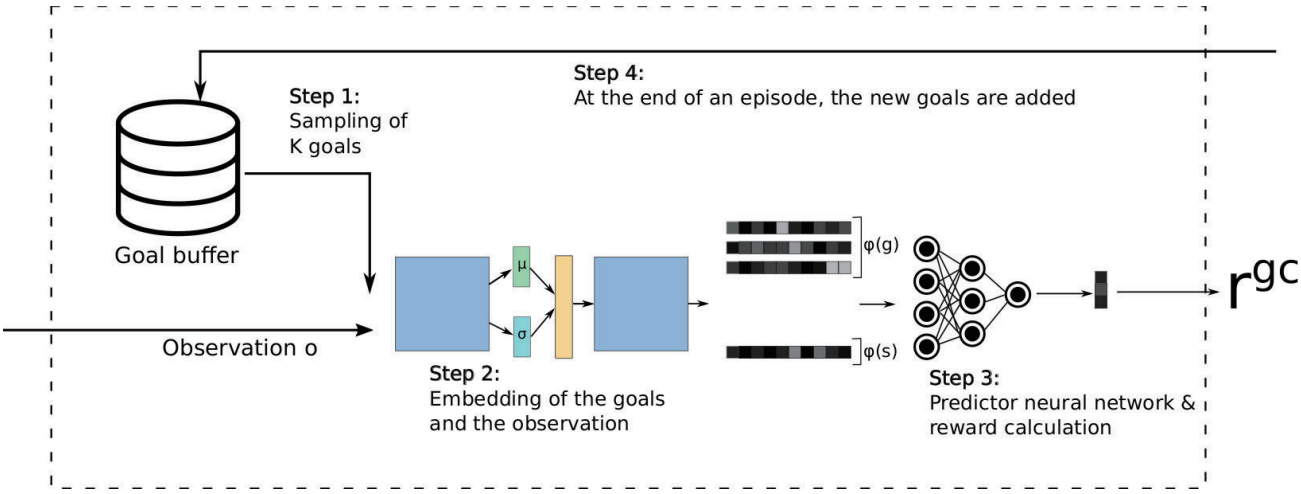

Figure 2: Goal-based curiosity module. The module takes as input an observation o and, at the beginning of every episode randomly samples multiple goals. The goals and the observation are embedded during step 2, $\phi(g)$ and $\phi(s)$ respectively. Step 3 predicts the probability that each goal is mastered and given this vector of probabilities, calculates the new reward signal r^{gc}. A the end of each episode, the new goals are added to the goal buffer based on the experienced states.

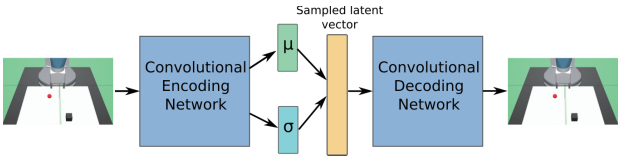

Figure 3: Variational Auto Encoder structure. The input image is passed through an encoder network which outputs the parameters μ and σ of a multivariate Gaussian distribution. A latent vector is sampled and the decoder network decodes it into an image.

works. Its parameters θ_P are optimized to maximize the following equation:

$$\max_{\theta_P} \mathbb{E}_{\pi(s_t;\theta_P)}[\sum_t r_t] \tag{1}$$

In this work, we use twin delayed deep deterministic policy gradients (TD2) [Silver et al., 2014] as policy learning method. Our main contribution is to design a new exploration mechanism, the goal-based curiosity module that we describe in the following section. Given the current observation, the module generates a goal-based curiosity reward signal r^{gc}.

2.2 Goal-based Curiosity Module

We based the goal-based curiosity module (GCM) on the following intuition. If the agent can predict whether or not it can achieve a goal given an observation then, we can reward more the agent when the uncertainty to solve it is high - to force the agent to explore novel states.

In sparse reward environments, reaching the final goal may be infrequent, entailing that for most of the episodes the agent only experiences failures. Therefore, training a probabilistic model for predicting if the final goal is mastered is highly inaccurate. Instead, we propose to estimate if the agent can solve multiple intermediate goals. Since these goals are easier to master (to reach), the estimation becomes more accurate while providing information about the agent's knowledge. Our model can be trained using multiple goals which produces a vector of probabilities. The method to select the goal is explained in Section 2.2.1.

In details, the GCM is an end-to-end module. It takes as input the current observation and produces r^{gc}. The algorithm can be broken down in fours parts (Figure 2). First, at the beginning of an episode, K goals are randomly sampled with $1 \leq K \in \mathbb{N}$. Second, at every step, the goals and the current observation are embedded by a variational autoencoder $f : O \rightarrow \mathbb{R}^n$ (Figure 3). Third, the agent predicts the probability that each goal can be achieved. Our implementation relies on a deep predictor neural network which predicts the probability that a goal can be reached $\hat{f} : \mathbb{R}^n \times \mathbb{R}^n \rightarrow [0-1]$. Finally, at the end of the episode, the GCM is updated according to the experienced observations and the predictor neural network is retrained to fit with the new knowledge of the agent.

To produce the reward signal and improve exploration, we design the reward to be higher in novel states. Namely, we take advantage of uncertainty given the probabilities that the goals are mastered by the agent. We give details about the reward calculation is Section 2.2.2.

2.2.1 Goals

We define the goals $g \in G$ as $f_g : S \rightarrow \{0, 1\}$ that defines if the goal is achieved by the agent. In the case that a goal g is solved in a state s, $f_g(s) = 1$. In order to keep a consistent representation, we suppose the goals as $G = \mathbb{R}^n$. Note that we assume the goal space G to be the same as the state space S.

At each iteration, a sub-sets g' of goals latent $\phi(g)$ are sampled given a distribution function f_p:

$$g' = \{\phi(g) \sim f_p(g)\} \text{ sample K goals} \in G \tag{2}$$

In the current implementation, the probability of sampling a goal $f_p(g)$ is uniform for all the goals. In future work, we anticipate more complex distributions to take into about the difficulties of the goals.

During training, the goals aim to provide additional feedback to the agent to improve exploration. At the end of an episode, we add a mechanism to further enable sample-efficient learning. In addition to the state reached at the end of the episode, we artificially generate new goals by randomly selecting states visited during the episode. The new goals are stored in the replay buffer that is used to train an RL algorithm.

2.2.2 Reward Calculation

At every time step, the deep predictor neural network outputs the probability that the active goals are mastered by the agent $g_{active} = \langle p(g_1, ..., g_K) \rangle$. Given these predictions we define the goal-based curiosity reward:

$$r^{gc} = \delta \times g(\langle \alpha \rangle - \langle p(g_1, ..., g_K \rangle) \tag{3}$$

with g the function mapping the probabilities to the reward, the parameters δ the scale of the new reward, and $\langle \alpha \rangle$ the sign of the new reward. In the current implementation, we use $\alpha = \langle 1.0 \rangle$ a uniform vector of 1 and $g = \max()$.

In other words, predicting that the agent doesn't master a goal will result in a higher curiosity-based reward. One issue with the combination of extrinsic reward and curiosity-based reward is the scaling of the reward which may vary between the tasks. In order to mitigate this scaling problem, we normalize the curiosity-based reward:

$$r_t^{gc} = \frac{r_t^{gc}}{\sigma(R_{gc})} \tag{4}$$

with $\sigma(R_e)$ the standard deviations of the curiosity-based reward returns.

3. Conclusion

This paper introduces a new mechanism for generating curiosity based rewards on the idea of predicting the capabilities of the agent. This allows our agent to learn policies in sparse reward environments without human engineering. Our model works in the latent space to generate a compact representation of the states and goals which are used by a deep neural network to predict the capabilities of the agents. By acquiring knowledge about itself, the agent can use its curiosity to explore unseen states of the environment. As a result, we can expect to solve a large set of tasks requiring more supervision than the extrinsic reward of the environment.

We are interested in testing our method on a set of tasks such as *MuJoCo*, or *Super Mario Bros*, two sparse reward environments. In the future, we are willing to introduce human feedback during the choice of the goals and improve the goal sampling method.

References

[Abbeel et al., 2007] Abbeel, P., Coates, A., Quigley, M., and Ng, A. Y. (2007). An application of reinforcement learning to aerobatic helicopter flight. In *Proceedings of Advances in Neural Information Processing Systems*, pages 1–8.

[Bellemare et al., 2015] Bellemare, M. G., Naddaf, Y., Veness, J., and Bowling, M. (2015). The arcade learning environment: an evaluation platform for general agents. In *Proceedings of the International Conference on Artificial Intelligence*, pages 4148–4152.

[Burda et al., 2018] Burda, Y., Edwards, H., Storkey, A. J., and Klimov, O. (2018). Exploration by random network distillation. *CoRR*, abs/1810.12894.

[Kingma and Welling, 2014] Kingma, D. P. and Welling, M. (2014). Auto-encoding variational Bayes. In *International Conference on Learning Representations*.

[Levine et al., 2016] Levine, S., Finn, C., Darrell, T., and Abbeel, P. (2016). End-to-end training of deep visuomotor policies. *The Journal of Machine Learning Research*, 17(1):1334–1373.

[Mnih et al., 2013] Mnih, V., Kavukcuoglu, K., Silver, D., Graves, A., Antonoglou, I., Wierstra, D., and Riedmiller, M. (2013). Playing atari with deep reinforcement learning. *arXiv preprint arXiv:1312.5602*.

[Pathak et al., 2017] Pathak, D., Agrawal, P., Efros, A. A., and Darrell, T. (2017). Curiosity-driven exploration by self-supervised prediction. In *Proceedings of the International Conference on International Conference on Machine Learning*.

[Racanière et al., 2017] Racanière, S., Weber, T., Reichert, D., Buesing, L., Guez, A., Jimenez Rezende, D., Puigdomènech Badia, A., Vinyals, O., Heess, N., Li, Y., Pascanu, R., Battaglia, P., Hassabis, D., Silver, D., and Wierstra, D. (2017). Imagination-augmented agents for deep reinforcement learning. In Guyon, I., Luxburg, U. V., Bengio, S., Wallach, H., Fergus, R., Vishwanathan, S., and Garnett, R., editors, *Proceedings of Advances in Neural Information Processing Systems*, pages 5690–5701. Curran Associates, Inc.

[Silver et al., 2014] Silver, D., Lever, G., Heess, N., Degris, T., Wierstra, D., and Riedmiller, M. (2014). Deterministic policy gradient algorithms. In *Proceedings of the International Conference on International Conference on Machine Learning*, pages I–387–I–395.

The 33rd Annual Conference of the Japanese Society for Artificial Intelligence, 2019

Improvement of Product Shipment Forecast based on LSTM Incorporating On-Site Knowledge as Residual Connection

Takeshi Morinibu Tomohiro Noda Shota Tanaka

Daikin Industries, Ltd. Technology and Innovation Center

It is important to predict shipments for the purpose of making a production plan of air conditioners. Although ARIMA was used for that prediction for a long time, it turned out that some products we manage had less accurate prediction score. In order to get more precise prediction, we applied LSTM to forecast shipments. Despite the complexity of LSTM, we could not get what we expected. Therefore, we further improved the accuracy by adding on-site knowledge to network structure of LSTM as residual mechanism.

1. Introduction

In order to make profit efficiently in the manufacturing industry, it is necessary to minimize the warehouse cost due to excessive inventory and the missed selling caused by sales suspension due to out of stock. Since predicted values of shipment quantity are used to make a production plan for managing that stock, better prediction accuracy is required.

ARIMA is widely used as a traditional method for time series prediction including shipment quantity. For example, there is an application for wholesale of vegetables [Shukla 13]. Even in the case of air conditioners, an ARIMA was able to make good predictions in many cases. The word "series" we describe is a group of products summarized with certain features. When we conducted a survey, however, we found that there are some series with extremely low precision among major series. We attempted to improve it.

In recent years, application of RNN to various time series data has been widespread and its superiority has been confirmed [Li 18], so we tried first to improve accuracy by using a plain LSTM. Even so, the prediction accuracy of the LSTM was not much better than the ARIMA. Hence we challenge to alter the structure of the plain LSTM to solve the problem. The idea to realize it comes from ResNet.

ResNet recorded amazing precision in the field of image recognition by using Residual block [He 16]. It ensures an information flow, leading to optimizing loss function for very deep structure efficiently. It is also used as a feature extraction before connecting to an LSTM layer [Wei 18] or applied to LSTM directly to enhance information flow [Wang 16]. There is a more challenging study creating skip connections dynamically [Gui 18].

The LSTM that is different from these LSTMs with the residual connections in that it doesn't have such a deep structure with respect to the time direction. We have incorporated that mechanism described above into the LSTM to reflect the idea of the site manager, not to prevent vanishing gradient. The improved LSTM, we equate it as "Res-LSTM" below, achieve higher accuracy than the LSTM and the ARIMA.

Contact: Takeshi Morinibu, Daikin Industries, Ltd. Technology and Innovation Center, 06-6195-7184, takeshi.morinibu@daikin.co.jp

2. Method

2.1 Dataset and previous results

The data we used is the shipping number of series per month for 2013 to 2018. As the evaluation measures, we use the average value of RMSE (Root Mean Squared Error) and MAPE (Mean Absolute Percentage Error) within the prediction period. RMSE is used to compare the accuracy of the model and MAPE is used to compare series. We have been updating the ARIMA and forecasting the number of series shipments every month since last year and summarized the average accuracy of the major series over the period. From the results: Table 1, it was found that the prediction accuracy of series B was not better than the others in the major series.

Table 1: Accuracy of previous model for major series

Series	A	B	C	D	E
MAPE	11.4	17.4	8.10	13.3	12.1
RMSE	573	239	1038	301	324

According to Figure 1 and Figure 2, the strong seasonality of the year is common to both, but series B has larger variance over its cycle than A. This seems to be one of the factors that lower the prediction accuracy of the ARIMA.

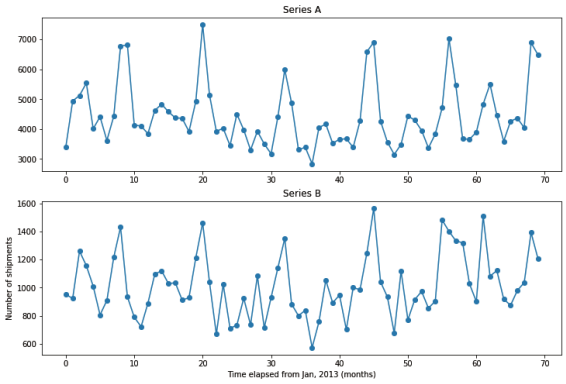

Figure 1: Comparison of observed shipments of series A and B

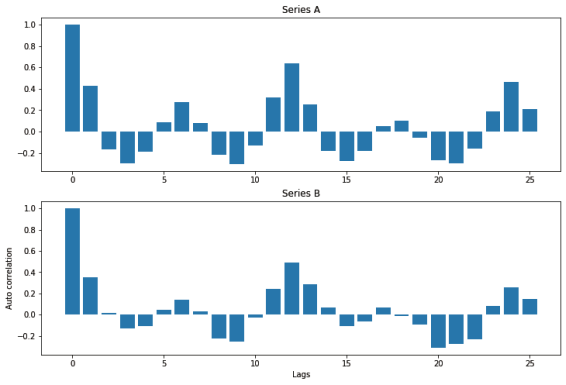

Figure 2: Comparison of autocorrelation coefficient of series A and B

According to the actual prediction result shown in Figure 3, the ARIMA can capture features well for series A but not for series B. Establishing a production plan using this forecast value can cause excessive inventory. To solve this problem, it is necessary to use a model that can deal with more complicated problems than the ARIMA conventionally. In this case, LSTM is appropriate for that model.

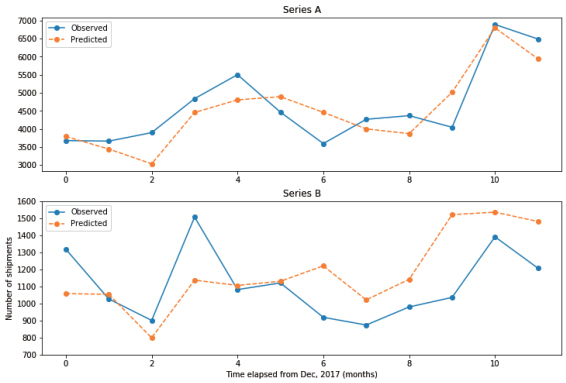

Figure 3: The difference of predicted values by ARIMA between series A and B

2.2 LSTM

LSTM is a type of RNN solves the problem of a vanishing or exploding gradient and makes it possible for network to correctly remember information far back in the sequence [Hochreiter 97]. Due to its characteristics, LSTM has resulted in a wide range of fields such as natural language processing and time series data.

Figure 4 shows the LSTM we implemented in this paper. This model predicts one-month-ahead shipments using series data of length 12 as input. The structure of this network is based on the site experience that the value of the past year is helpful. In spite of our efforts, this model did not give much better accuracy than the ARIMA as described later. Therefore we extended the network structure to make use of the additional on-site knowledge for the LSTM.

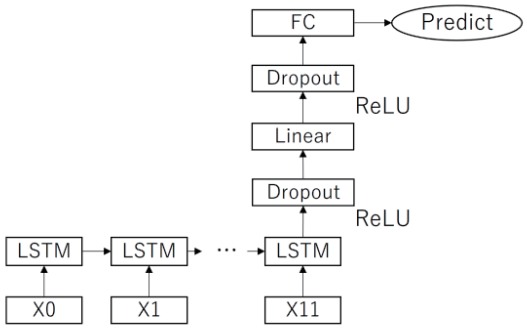

Figure 4: The structure of the plain LSTM

2.3 Res-LSTM

Product managers say that in order to predict one-month-ahead shipments, the monthly data of that just one year ago is particularly beneficial. Depending on the structure of the sequence data, the first output of the LSTM strongly reflects the data of the same month last year, accordingly we sum the first and the last output of the LSTM and connect to the next layer. Figure 5 shows its structure.

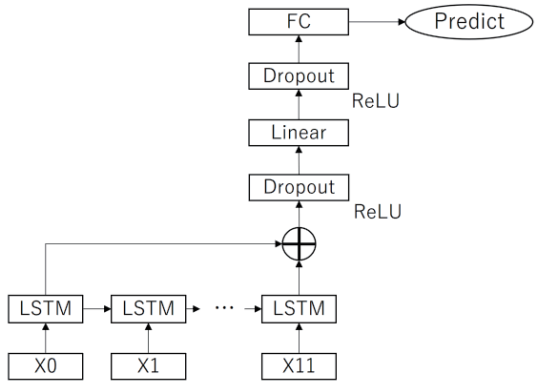

Figure 5: The structure of the Res-LSTM

2.4 Hyperparameters

We adapted Bayesian optimization instead of Grid Search owing to the fairly large space of hyperparameters to search appropriate ones. A variety of Bayesian optimization algorithms have been studied, and [Shahriari 16] introduces its features and the libraries that are implemented in some programing languages. We chose TPE (Tree-structured Parzen Estimator) as an algorithm [Bergstra 11]. It is possible for the TPE to search efficiently and apply it stably to the space containing categorical variables. The search ran 500 times within the range of the table 2.

Table 2: Space of hyperparameters

	range
Hidden1	(5, 20)
Hiddne2	(5, 20)
Optimize	(Adam, RMSprop)
Learning rate	(0.001, 0.1)
Dropout1	(0.1, 0.5)
Dropout2	(0.1, 0.5)
Epoch	(10, 100)

2.5 Experiment

We implemented both models using "PyTorch" and used "Hyperopt" library of Python for searching hyperparameters [Bergstra 15]. Predicted values over the year was made using the data up to 2016/11 for the verification and up to 2017/11 for the test. Figure 6 represents it graphically. Hyperparameters of each LSTM were optimized by Hyperopt with the verification score, and the result of testing with that value is taken as prediction accuracy. Then, we used MSE(Mean Squared Error) as the loss function and batch size as 18.

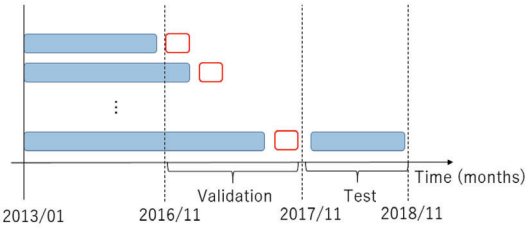

Figure 6: Division method for verification and testing

3. Results

3.1 Optimized hyperparameters

Figure 7 shows the search result of hyperparameters. Compared with the plain LSTM, the Res-LSTM shows higher verification score during training. Table 3 shows what was selected from them. Optimized hyperparameters has differences depending on the structure of the model. We will discuss it later in section 4.

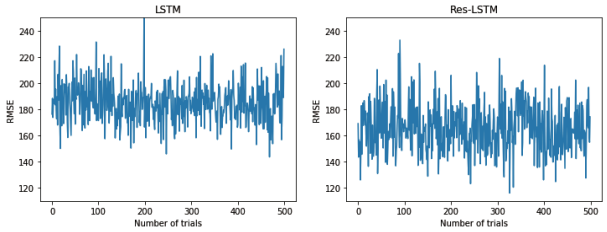

Figure 7: Result of trials while verification. The parameter of the point where the best score is recorded is used.

Table 3: Values for the respective hyperparameters in the LSTM and Res-LSTM

	LSTM	Res-LSTM
Hidden1	7	8
Hiddne2	7	9
Optimize	Adam	RMSprop
Learning rate	0.02	0.04
Dropout1	0.25	0.09
Dropout2	0.36	0.24
Epoch	39	69

3.2 Accuracy

Table 4 describes the test accuracy of each model for series B. The Res-LSTM achieved the best accuracy in terms of both RMSE and MAPE and it was better than other major series. Consequently, we managed to achieve our original objectives.

Table 4: Accuracy of each model for series B

	MAPE	RMSE
ARIMA	17.4	239
LSTM	17.3	176
Res-LSTM	11.1	146

3.3 Prediction

A comparison of predicted values of the LSTM and the Res-LSTM is shown in Figure 8, and a comparison between those of the Res-LSTM and the ARIMA is shown in Figure 9. The plain LSTM did not grasp the trend well and the ARIMA was able to grasp it, but the individual value greatly exceeded. On the other hand, the Res-LSTM catched the trend and is adaptable to each values. The value exceeding 1,500 observed at point 3 is probably Large-volume shipping. Large-volume shipping occurs rarely and it is difficult to predict from data, but in business it is often understood beforehand. Except for that, the model has made a fairly good prediction.

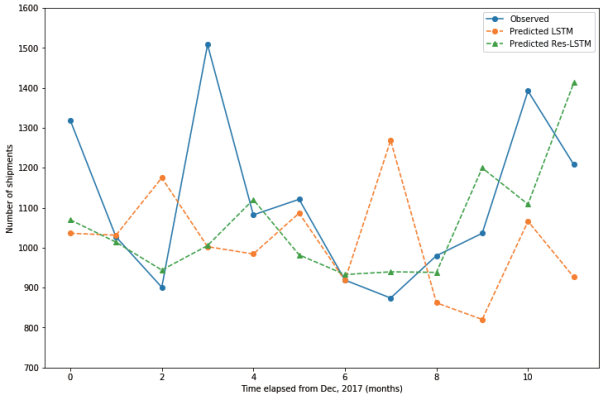

Figure 8: LSTM vs Res-LSTM

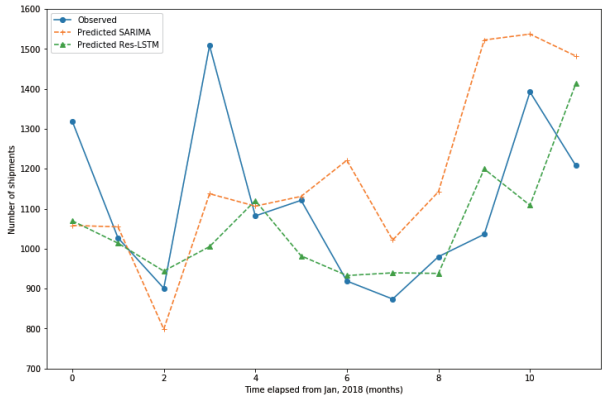

Figure 9: ARIMA vs Res-LSTM

4. Discussion

The Res-LSTM was able to significantly improve the accuracy compared with previous models. We will estimate factors that caused such results. The hyperparameters obtained by the verification: Table 3, shows that the learning rate and the epoch number of the LSTM are lower than those of the Res-LSTM. This is because the LSTM has reached the limit parameter to avoid over-fitting during the search. The over-fitting line of the Res-LSTM was higher than that of the LSTM, so it seems that it was able to acquire generalization performance even if further learning is advanced. In addition, Table 3 shows that the ResLSTM has lower Dropout rate than the LSTM. This is probably because the information that the LSTM handled stochastically was handled by the network structure of the ResLSTM.

5. Conclusion

In this paper, we showed that the Res-LSTM we proposed outperforms prediction accuracy of the plain LSTM and the ARIMA for predicting shipment quantity. Moreover, it seems that the residual mechanism is working to reflect the information of the structure of the series data rather than preventing the gradient disappearance. Although this may not be effective in all cases, it was able to solve a specific problem like this time. In the future, it is necessary to investigate whether there is effective for the others.

In this way, it is sometimes more effective to incorporate knowledge of the domain into the network structure, so we will continue to conduct research on those policies in the future.

Acknowledgment

We would like to thank Yamauchi, S. and Shiimado, T. in the SCM department of our company for providing data and knowledge about it.

References

[Bergstra 11] Bergstra, J., Bardenet,R., Bengio, Y. and Kgl, B.: Algorithms for Hyper-Parameter Optimization. In *NIPS 24*, pp. 2546-2554, (2011).

[Bergstra 15] Bergstra, J., Komer, B., Eliasmith, C., Yamins, D., Cox, D.D.: Hyperopt: A Python Library for Optimizing the Hyperparameters of Machine Learning Algorithms. *Computational Science and Discovery*, 8(1), (2015).

[Gui 18] Gui, T., Zhang, Q., Zhao, L., Lin, Y., Peng, M., Gong, J. and Huang, X..: Long Short-Term Memory with Dynamic Skip Connections. *arXiv*, (2018).

[He 16] He, K., Zhang, X., Ren, S. and Sun, J.: Deep Residual Learning for Image Recognition. In *Proceedings of the IEEE Computer Society Conference on Computer Vision and Pattern Recognition*, pp. 770-778, (2016).

[Hochreiter 97] Hochreiter, S. and Schmidhuber, J.: Long short-term memory. *Neural Computation*, 9(8), pp. 1735-1780, (1997).

[Li 18] Li, Y. and Cao, H.: Prediction for Tourism Flow based on LSTM Neural Network. *Procedia Computer Science*, 129, pp. 277-283, (2018).

[Shahriari 16] Shahriari, B., Swersky, K., Wang, Z., Adams, R.P. and De Freitas, N.: Taking the Human Out of the Loop: A Review of Bayesian Optimization. In *Proceedings of the IEEE*, pp. 148-175, (2016).

[Shukla 13] Shukla, M., Jharkharia, S.: Applicability of ARIMA Models in Wholesale Vegetable Market: An Investigation. *International Journal of Information Systems and Supply Chain Management*, 6(3), pp. 105-119, (2013).

[Wang 16] Wang, Y. and Tian, F.: Recurrent residual learning for sequence classification. In *Proceedings of the EMNLP*, pp. 938–943, (2016).

[Wei 18] Wei, H., Zhou, H., Sankaranarayanan, J. and Sengupta, S.: Residual Convolutional LSTM for Tweet Count Prediction. In *Proceedings of the The Web Conference*, pp. 1309-1316, (2018).

The 33rd Annual Conference of the Japanese Society for Artificial Intelligence, 2019

Unsupervised Joint Learning for Headline Generation and Discourse Structure of Reviews

Masaru Isonuma*1 Junichiro Mori*1 Ichiro Sakata*1

*1 The University of Tokyo

Recently, using a large amount of reference summary, supervised neural summarization models have achieved success. However, such datasets are rare, and trained models cannot be shared across domains. Although an unsupervised approach is a possible solution, models applicable for single-document summary or headline generation have not been established. Our work focuses on generating headlines for reviews, without supervision. We assume that reviews contain a discourse tree in which the headline is the root and the child sentences elaborate on the parent. By estimating the parent from their child recursively, our model learns such a structure and generates a headline that describes the entire review. Through the evaluation of the generated headline on actual reviews, our model achieved competitive performance with supervised models, especially on relatively long reviews. In induced structures, we confirmed that the child-sentences explain the parent in detail and generated headline abstracts for the entire review.

1. Introduction

The need for automatic document summarization is widely increasing, with the recently growing vast amounts of online textual data such as reviews on E-commerce websites. Under these circumstances, supervised neural network models have widely achieved success, using a large amount of reference summary. However, the model trained from them cannot be adopted in other domains as salient phrases are not common across domains. Few or no examples of summaries exist for most documents, and preparing such large volumes of reference summaries is very expensive.

An unsupervised approach is a possible solution for such a problem. Traditionally, the unsupervised approach has been widely applied to sentence extraction [Erkan 04]. The extractive approach can be effective for some types of documents, e.g. news articles, since the salient sentences should be the summary even though they describe only a part of the document. On the other hand, as for reviews, an appropriate summary is generally concise sentences that summarize the entire review. Therefore, the abstractive method is more effective for reviews because it condenses an entire review via paraphrasing and generalization [Gerani 14]. Our work focuses on headline generation of reviews; a kind of abstractive summarization tasks, without supervision.

Abstractive summarization techniques sometimes use discourse parsers [Hirao 13, Gerani 14]; however, [Ji 17] indicates the limitations of using external discourse parsers. In this context, [Liu 18] proposed a model that encodes a document while automatically inducing the discourse tree. Following [Liu 18], we aim to generate a headline based on the discourse tree, which is automatically constructed.

Figure 1 shows an example of a review about a jigsaw puzzle and its dependency-based discourse tree [Hirao 13] constructed manually. The headline describes its quality, and the child sentences explain it in terms of size and thickness. Each child sentence elaborate on the parent in detail.

Contact: Masaru Isonuma, isonuma@ipr-ctr.t.u-tokyo.ac.jp

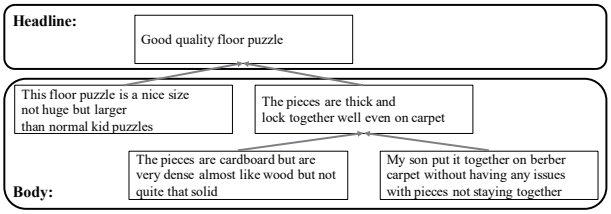

Figure 1: An example of discourse tree in a review

Thus, we assume that reviews can generally be described as a multi-root non-projective discourse tree in which the headline is the root, and the sentences construct each node. In such trees, child sentences elaborate on or provide background to the parent sentence. By estimating the parent from their children recursively, our model learns such a discourse tree and generates a headline.

In this work, we propose a model that generates the headline of a single review without reference through learning the discourse tree. Although there has been previous work without supervision using the Abstract Meaning Representation (AMR) parser [Dohare 18], our work is, to our knowledge, the first headline-generation model that requires no external parser. Through the evaluation of the headlines generated for actual online reviews and the induced discourse tree, we validate our assumption; child sentences elaborate on the parent sentences, and as a result, the generated headline summarizes the entire review.

2. Related research

2.1 Un-/Semi-supervised Summarization

Most of unsupervised summarization techniques have been focused on sentence extraction. [Erkan 04] constructed a graph that consists of sentences as the nodes, with their similarities as the edge. They extracted sentences with a higher eigenvector centrality so that the selected sentences are heavily connected to each sentence in the input document. On the other hand, with the re-

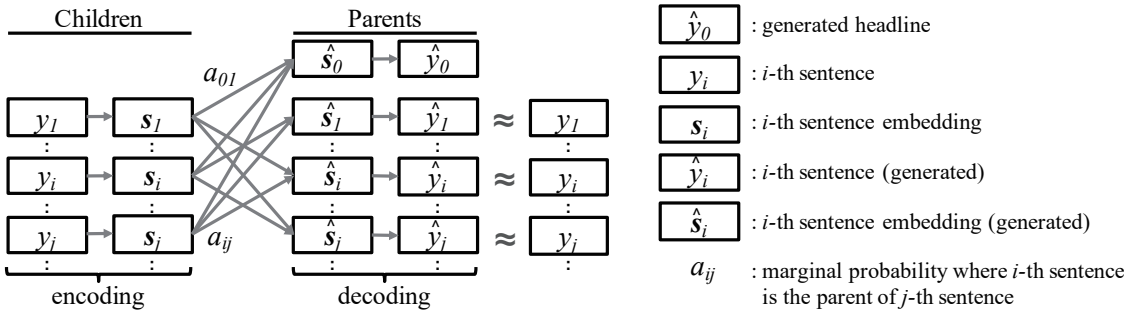

Figure 2: The outline of the proposed model

cently growing neural summarization models, unsupervised or semi-supervised summary generation is being attempted. [Miao 16] introduced the idea that compressed sentences that do not lose meaningful phrases can decode the input sentences. They applied a variational auto-encoder for the sentence compression task. [Chu 18] proposed a model that consists of an auto-encoder trained so that the mean of the representations of the input reviews is decoded to the summary. However, their model does not aim to generate the summary or headline of a single document. Against such a background, our model generates the headline of a single review without reference.

2.2 Discourse Parsing and its Application

Discourse parsing is broadly researched and used for various applications that utilize knowledge on conjunctions or corpora in which rhetorical structure is annotated. [Hirao 13] transformed a rhetorical structure theory-based discourse tree (RST-DT) into a dependency-based discourse tree to take a tree-trimming approach to summarization. [Ji 17] also constructed a dependency-based discourse tree, and applied a recursive neural network model for document classification. They indicated the limitations of using external parsers, showing that the performance depends on the amount of the RST-DT and the domain of documents. Against such a background, [Liu 18] proposed a model that can encode a document while automatically inducing a latent document structure. They reported that the child presents additional information regarding the parent in the induced document structure. Inspired by [Liu 18], we obtain a discourse tree without external parsers by estimating parent sentences from the children.

3. Proposed Model

In this section, we present our headline generation model by inducing a discourse tree without external parsers. Figure 2 shows the outline of our proposed model. In the following, we explain the training method and computation of the marginal probability of the dependency edges.

3.1 Model Training

In Figure 2, y_i and $\boldsymbol{s}_i \in \mathcal{R}^d$ indicate i-th sentence and its embedding in a document $D = \{y_1, y_2, \ldots, y_n\}$ respectively. w_i^t is t-th word in a sentence $y_i = \{w_i^1, w_i^2, \ldots, w_i^l\}$. $\boldsymbol{s}_i$ is computed via max-pooling operation across hidden states $\boldsymbol{h}_i^t \in \mathcal{R}^d$ of Bi-directional Gated Recurrent Units (Bi-GRU):

$$\overrightarrow{\boldsymbol{h}}_i^t = \overrightarrow{\mathrm{GRU}}(\overrightarrow{\boldsymbol{h}}_i^{t-1}, w_i^t) \quad (1)$$

$$\overleftarrow{\boldsymbol{h}}_i^t = \overleftarrow{\mathrm{GRU}}(\overleftarrow{\boldsymbol{h}}_i^{t+1}, w_i^t) \quad (2)$$

$$\boldsymbol{h}_i^t = [\overrightarrow{\boldsymbol{h}}_i^t, \overleftarrow{\boldsymbol{h}}_i^t] \quad (3)$$

$$\forall m \in \{1, \ldots, d\},\ \boldsymbol{s}_{i,m} = \max_t \boldsymbol{h}_{i,m}^t \quad (4)$$

Here, we assume that the document D involves a discourse tree in which the root is the headline, and all the sentences are the nodes. We denote a_{ij} and a_{0j} as the marginal probability, where sentence i and the root are the parent node of sentence j under the constraint $\sum_{i=0}^{n} a_{ij} = 1$ (see Figure 2). From the sentence embeddings and a_{ij}, we compute the embedding of the parent sentence $\hat{s}_i$ and that of the headline $\hat{s}_0$. $\hat{s}_i$ $(i \in \{0, \ldots, n\})$ are defined with parameters $\boldsymbol{W}_s \in \mathcal{R}^{d*d}$ and $\boldsymbol{b}_s \in \mathcal{R}^d$ as shown below:

$$\hat{\boldsymbol{s}}_i = \tanh\Big\{\boldsymbol{W}_s(\sum_{j=1}^{n} a_{ij}\boldsymbol{s}_j) + \boldsymbol{b}_s\Big\} \quad (5)$$

The higher the marginal probability a_{ij} is, the more the information of $\boldsymbol{s}_j$ are input into $\hat{\boldsymbol{s}}_i$. From $\hat{\boldsymbol{s}}_i$, the GRU-decoder learns to reconstruct the sentence i, i.e., search the parameters $\boldsymbol{\theta}$ that maximize the following log likelihood:

$$\sum_{i=1}^{n}\sum_{t=1}^{l} \log P(w_i^t | w_i^{<t}, \hat{\boldsymbol{s}}_i, \boldsymbol{\theta}) \quad (6)$$

Here, we explain how training the model contributes to headline generation. By reconstructing the sentences in documents, the decoder learns a language model to generate grammatical sentences. Therefore, the model can decode the headline embedding $\hat{\boldsymbol{s}}_0$ as a fluent sentence.

Besides, the more the j-th sentence contributes to generating the i-th sentence, the higher a_{ij} can be. This mechanism models our assumption; child sentences can generate their parent, but not vice versa, because the children have more information than the parents. Based on this assumption, the most abstractive k-th sentences in the body make less contribution to reconstruction of any other sentences. From the constraint $\sum_{i=0}^{n} a_{ik} = 1$, a_{0k} is expected to be larger and contribute toward generating the headline.

3.2 Marginal Probability of Dependency

We explain how to calculate the marginal probability a_{ij}. We first define the unnormalized weight f_{ij} of the edge between a parent node i and the child node j via a bilinear function and a linear function. For convenience, we assume the weighted adjacency matrix $\boldsymbol{F} = (f_{ij}) \in \mathcal{R}^{(n+1)*(n+1)}$. The index of the first column and row are 0, which denotes the root node. We assume that the discourse structure can be described as a multi-root non-projective tree. Therefore, based on [Liu 18], f_{ij} is defined as :

$$f_{ij} = \begin{cases} \exp(\boldsymbol{w}_r^\top \boldsymbol{s}_j) & (i = 0 \wedge j \geq 1) \\ \exp(\boldsymbol{p}_i^\top \boldsymbol{W}_f \boldsymbol{c}_j) & (i \geq 1 \wedge j \geq 1 \wedge i \neq j) \\ 0 & (j = 0 \vee i = j) \end{cases} \quad (7)$$

$$\boldsymbol{p}_i = \tanh(\boldsymbol{W}_p \boldsymbol{s}_i + \boldsymbol{b}_p) \quad (8)$$

$$\boldsymbol{c}_j = \tanh(\boldsymbol{W}_c \boldsymbol{s}_j + \boldsymbol{b}_c) \quad (9)$$

where $\boldsymbol{W}_f \in \mathcal{R}^{d*d}$ and $\boldsymbol{w}_r \in \mathcal{R}^d$ are parameters for the transformation. $\boldsymbol{W}_p \in \mathcal{R}^{d*d}$ and $\boldsymbol{b}_p \in \mathcal{R}^d$ are the weights and the bias for constructing the representation of the parent nodes. $\boldsymbol{W}_c \in \mathcal{R}^{d*d}$ and $\boldsymbol{b}_c \in \mathcal{R}^d$ are those of the child nodes.

We normalize f_{ij} into a_{ij}, following [Koo 07]. a_{ij} corresponds the proportion of the total weight of all the spanning trees containing the edge (i, j):

$$\begin{aligned} a_{ij}(\boldsymbol{F}) &= \frac{\sum_{g \in G:(i,j) \in g} v(g|\boldsymbol{F})}{\sum_{g \in G} v(g|\boldsymbol{F})} \\ &= \frac{\partial \log Z(\boldsymbol{F})}{\partial f_{ij}} \end{aligned} \quad (10)$$

$$v(g|\boldsymbol{F}) = \prod_{(i,j) \in g} f_{ij} \quad (11)$$

$$Z(\boldsymbol{F}) = \sum_{g \in G} v(g|\boldsymbol{F}) \quad (12)$$

Here, G denotes the set of all the spanning trees in a document D. $v(g|\boldsymbol{F})$ is the weight of a tree $g \in G$, and $Z(\boldsymbol{F})$ denotes the sum of the weights of all the trees in G. From the Matrix-Tree Theorem, $Z(\boldsymbol{F})$ can be rephrased as:

$$Z(\boldsymbol{F}) = L^{(0,0)}(\boldsymbol{F}) \quad (13)$$

where $L(\boldsymbol{F})$ and $L^{(0,0)}(\boldsymbol{F})$ be the Laplacian matrix of $\boldsymbol{F}$ and its minor, with respect to the row 0 and the column 0.

4. Experiments

In this section we present our experiments for evaluating the performance of headline generation. We compared the generated headlines on actual online reviews. The following explains the details of our experiments and the results.

Table 1: ROUGE-F1 score on the evaluation set (%)

Models	ROUGE-1	ROUGE-2	ROUGE-L
Seq-Seq	12.8	1.8	10.2
Seq-Seq-att	13.8	2.5	10.9
Our Model	11.4	1.6	9.1

4.1 Dataset

Our experiment uses Amazon product review data (Toys and Games) [He 16], which [Ma 18] used as evaluation for their supervised headline generation model. This dataset contains actual online reviews and their headlines.

Because our model generates a headline via learning the discourse tree, we assume that training will fail if the number of sentences in the review is too small. Therefore, we use reviews in which the number of sentence is in $[10, 20)$ for training and $[5, 20)$ for validation and evaluation. The number of reviews for training, validation, and evaluation are 21791, 416, and 464, respectively.

4.2 Experimental Details

For all the experiments, our model has 300-dimensional word embeddings and Bi-GRU with 256-dimensional hidden states. We initialize the word embeddings with pre-trained GloVe (840B tokens) [Pennington 14]. We train the model using Ada-grad with a learning rate of 10^{-1}, an initial accumulator value of 0.1, and a batch size of 16. At evaluation time, we use a beam search with a beam size of 10.

Similar to [Ma 18], our evaluation metric is the ROUGE-F1 score. We use ROUGE-1, ROUGE-2, and ROUGE-L.

4.3 Baseline

Following previous work [Ma 18], our baseline models are the supervised sequence-to-sequence models for headline generation. We denote the sequence-to-sequence model as Seq-Seq and that with the attention mechanism as Seq-Seq-att. Implementation details are the same as above.

4.4 Results

Table 1 shows the ROUGE score of our model and the baseline models on the evaluation sets. Our model achieves a slightly low performance, compared to Seq-Seq.

In Figure 3, we report the performance on the evaluation sets in which the number of the sentences are in $[5, 10)$, $[10, 15)$ and $[15, 20)$, respectively. We compared to the supervised baseline model (Seq-Seq-Att). In the case of the dataset with under 10 sentences, the performance of our model is inferior to that of the baseline. On the other hand, on the one with 10 or more sentences, our model achieves a competitive performance as for ROUGE-1 and ROUGE-L. Because our model generates headlines via learning discourse tree, our model sometimes appears to fail at constructing a tree as for short documents. It results in a decline in the performance.

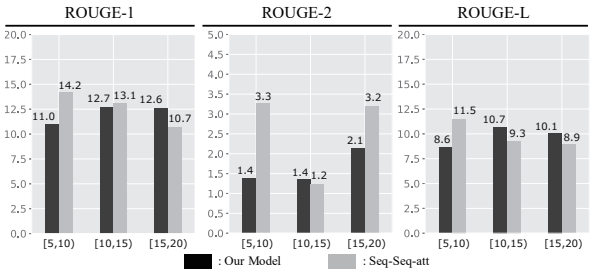

Figure 3: ROUGE-F1 score on evaluation set with various number of sentences

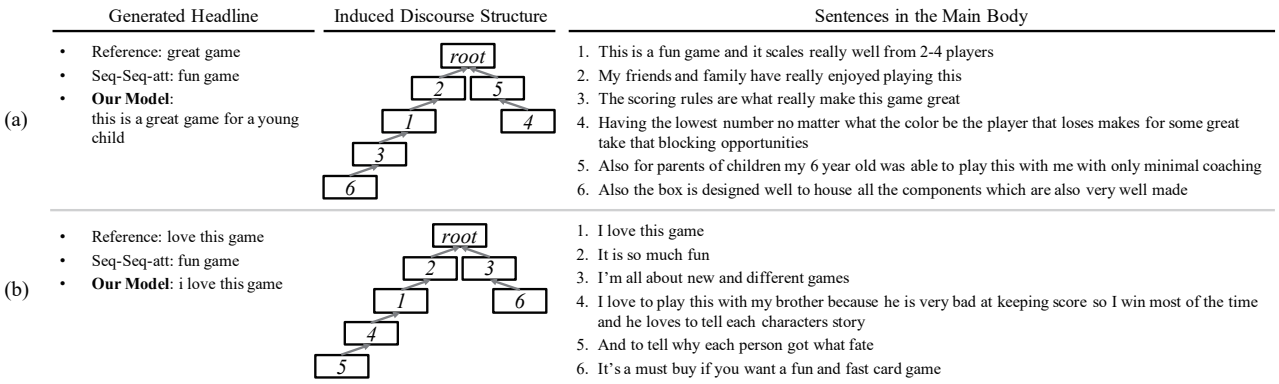

Figure 4: Examples of generated headline and induced discourse tree

5. Discussion

Figure 4 shows the generated headline and the discourse tree induced by our model. We obtain the maximum spanning tree from the probability distribution of dependency, using Chu–Liu–Edmonds algorithm. In Figure 4 (a), our model generates the headline, "this is a great game for a young child" while the actual headline is "great game." On the discourse tree, the child nodes of the root are the 2nd and 5th sentence. Both of them elaborate on the generated headline. The 3rd sentence explains the parent, the 1st sentence, by explaining the cause of fun.

Figure 4 (b) shows that the generated headline is "i love this game," while the reference is "love this game". In the induced tree, the 2nd sentence elaborates on the generated headline, while the 3rd sentence describes its background. The 4th and 5th sentences describe why the author loves the game, i.e., they explain the 1st sentence in detail.

As shown above, we confirmed that the child sentences elaborate on the parent in the induced discourse tree, while the headline abstracts for the child sentences.

6. Conclusion

In this work, we proposed a model to generate the headline of reviews by learning the latent discourse tree with neither a reference summary nor an external parser.

We evaluate our proposed model in comparison with supervised models on actual reviews. Our model achieves a competitive performance when the number of sentences is relatively large. On the reviews that contain few sentences, our model fails to construct the discourse tree and generate a reasonable headline.

Furthermore, our model induced a discourse tree in which the child sentences elaborate on the parent. We also confirmed that the headline abstracts for the entire review.

Acknowledgements

This work was supported by CREST, JST, the New Energy and Industrial Technology Development Organization (NEDO) and Deloitte Tohmatsu Financial Advisory LLC.

References

[Chu 18] Chu, E. and Liu, P. J.: Unsupervised Neural Multi-document Abstractive Summarization, *arXiv preprint arXiv:1810.05739* (2018)

[Dohare 18] Dohare, S., et al.: Unsupervised Semantic Abstractive Summarization, in *ACL Student Research Workshop*, pp. 74–83 (2018)

[Erkan 04] Erkan, G. and Radev, D. R.: LexPageRank: Prestige in Multi-Document Text Summarization, in *EMNLP*, Vol. 4, pp. 365–371 (2004)

[Gerani 14] Gerani, S., et al.: Abstractive summarization of product reviews using discourse structure, in *EMNLP*, pp. 1602–1613 (2014)

[He 16] He, R. and McAuley, J.: Ups and downs: Modeling the visual evolution of fashion trends with one-class collaborative filtering, in *WWW*, pp. 507–517 (2016)

[Hirao 13] Hirao, T., et al.: Single-document summarization as a tree knapsack problem, in *EMNLP*, pp. 1515–1520 (2013)

[Ji 17] Ji, Y. and Smith, N. A.: Neural Discourse Structure for Text Categorization, in *ACL*, Vol. 1, pp. 996–1005 (2017)

[Koo 07] Koo, T., et al.: Structured prediction models via the matrix-tree theorem, in *EMNLP-CoNLL* (2007)

[Liu 18] Liu, Y. and Lapata, M.: Learning structured text representations, *TACL*, Vol. 6, pp. 63–75 (2018)

[Ma 18] Ma, S., et al.: A Hierarchical End-to-End Model for Jointly Improving Text Summarization and Sentiment Classification, in *IJCAI*, pp. 4251–4257 (2018)

[Miao 16] Miao, Y. and Blunsom, P.: Language as a Latent Variable: Discrete Generative Models for Sentence Compression, in *EMNLP*, pp. 319–328 (2016)

[Pennington 14] Pennington, J., et al.: Glove: Global vectors for word representation, in *EMNLP*, pp. 1532–1543 (2014)

The 33rd Annual Conference of the Japanese Society for Artificial Intelligence, 2019

Gradient Descent Optimization by Reinforcement Learning

Yingda Zhu, Teruaki Hayashi, Yukio Ohsawa

Department of Systems Innovation, Graduate School of Engineering, The University of Tokyo

Gradient descent, which helps to search the global minimum of a complex (high dimension) function, is widely used in the deep neural network to minimize the total loss. The representative methods: stochastic gradient descent (SGD) and ADAM (Kingma & Ba, 2014) are the dominant ones to train neural network today. While some sensitive hyper-parameters like learning rate will affect the descent speed or even the convergence. In previous work, these hyper-parameters are often fixed or set by feedback and experience. I propose using reinforcement learning (RL) to optimize the gradient descent process with neural network feedback as input and hyper-parameter action as output to control these hyper-parameters. The experiment results of using RL based optimizer in both fixed and random start point shows better performance than normal optimizers which are set by default hyper-parameters.

1. Introduction

With the rapid development of deep learning these years, a lot of methods and models are proposed. While their cores, which are based on deep neural networks (DNN), are to minimize the DNN functions. Different from usual function minimization, dealing with DNN function which contains millions or even billions of parameters, it is nearly impossible to search the optimum solution. Gradient descent (GD) is an effective method to find the greedy solution which is good enough to be utilized in most cases. According to the related work these years, among the several GD methods, SGD and ADAM (Kingma & Ba, 2014) are the most popular and powerful ones which are used in diverse deep learning researches and applications. Some sensitive hyper-parameters in such methods (like learning rate (lr) in SGD) should be artificially set and may affect the descent speed and convergence. And related works use more complex optimizer structure to realize weight decay, but the optimization of GD might be affected by more diverse information which needs neural networks to express.

Reinforcement learning (RL), using states and rewards from the environment as input and the actions from the agent as output, whose training process is to find the actions in continuous states to maximize the total rewards. The feature of RL model, especially deep RL model, let it have strong ability in making strategy and actions which could deal with complex environment and adjust the optimizers' hyper-parameters through the observed states and given rewards in GD process.

2. Related Works

In this section, the related work of GD method and RL method will be reviewed.

The development of gradient descent was a long time before the popularity of deep learning these years. SGD is the simplest but most essential one which is currently widely used even if many latest complex methods are proposed. Momentum SGD (Jacobs, 1988) solved the problem that GD process may slow down or stop in a saddle point or a local minimum. After 2008, several methods which benefit to deep neural networks were proposed since the backpropagation was widely used. Adagrad (Duchi *et al*. 2011) and RMSprop (Tieleman & Hinton, 2012) use the gradient square accumulation in the denominator to decay the learning rate(lr). lr control in SGD by Actor-Critic is also proved possible (Xu el at 2017). And Adam (Kingma & Ba, 2014) which combines the feature of Momentum and RMSprop shows the relatively good performance in various tasks. While AMSGrad (Reddi *et al*. 2018) revises some parts of ADAM which could lead nonconvergence in some special cases due to the fixed hyper-parameters. It seems hard to explore the best optimizer which could lead fast and stable descent process in many cases for the reason that the hyper-parameters in these methods are set by human experience or theoretical calculation which made the performance good in average.

Reinforcement learning (Sutton & Barto, 1988), different from supervised or unsupervised learning, was also put forward early and can solve the problem with no concrete labels. Q-learning (Watkins & Dayan, 1992) and SARSA (Rummery & Niranjan, 1994) are two typical value-based RL algorithm and deep RL combine RL and DNN which let multidimensional input become possible. Policy-based RL like DDPG (TP Lillicrap, 2015) and PPO (Schulman *et al*. 2017) can output continuous actions which perform well in special tasks that need precise control. Recent work like Deep Q-Network (Mnih *et al*. 2015) and AlphaGo (Silver *et al*.,2016) stabilized the learning and achieved outstanding results. The advantage of RL is not only to search the proper action in each step but make a strategy to maximize the long-term rewards.

3. Method and Algorithm

In this section, RL based optimizer structure and the detailed algorithm will be shown. The optimizer is mainly based on related work in gradient descent research, and the algorithm combines Deep Q-Network and GD process in target neural network.

3.1 Optimizer Structure

According to related work of optimizers in Table 1, the structure of optimizer can be summarized to two parts, learning rate decay with the root of quadratic polynomial (second-moment estimate) and momentum with linear polynomial (first-moment estimate) which are widely used in recent gradient descent research.

Contact: Zhu Yingda, University of Tokyo,
7 Chome-3-1 Hongo, Bunkyō, Tokyo, Japan, 113-8654,
(81)70-3342-1110, zhuyingda18@gmail.com

Table 1: Optimizer functions in related works

Define learning rate η, descent step g_t', gradient g_t, parameter θ_t, constant ϵ , step t, hyper-parameter β_1 and β_2
GD: $\theta_t = \theta_{t-1} - g_t'$, **SGD:** $g_t' = \eta g_t$,
First moment estimate and bias-corrected
$v_t = \beta_1 v_{t-1} + (1-\beta_1) g_t$, $\widehat{v_t} = \frac{v_t}{1-{\beta_1}^t}$ *where* $v_0 = 0$
Second moment estimate and bias-corrected by
$s_t = \beta_2 s_{t-1} + (1-\beta_2) g_t \odot g_t$, $\widehat{s_t} = \frac{s_t}{1-{\beta_2}^t}$ *where* $s_0 = 0$

Adagrad: $g_t' = \frac{\eta}{\sqrt{s_t{}' + \epsilon}} g_t$, $s_t{}' = s_{t-1} + g_t \odot g_t$ (2011)

Rmsprop: $g_t' = \frac{\eta}{\sqrt{s_t + \epsilon}} g_t$ (2012)

Adadelta: $g_t' = \frac{\sqrt{\Delta x_{t-1} + \epsilon}}{\sqrt{s_t + \epsilon}} g_t$, *where* $\Delta x_0 = 0$ (2012)
and $\Delta x_t = \beta_2 \Delta x_{t-1} + (1-\beta_2) g_t{}' \odot g_t{}'$

ADAM : $g_t' = \frac{\eta}{\sqrt{\widehat{s_t} + \epsilon}} \widehat{v_t}$ (2014)

Adamax: $g_t' = \frac{\eta}{u_t} \widehat{v_t}$, $u_t = \max(\beta_1 v_{t-1}, |g_t|)$ (2014)

SGDR: $g_t' = \eta_t g_t$, with i is the index of the run (2016)
$\eta_t = {\eta_{min}}^i + \frac{1}{2}({\eta_{max}}^i - {\eta_{min}}^i)(1 + \cos\left(\frac{T_{cur}}{T_i}\pi\right))$
T_{cur} and T_i *are epochs* from latest restart and initial restart. η_{max}, η_{min} are defined from restart.

AMSGrad: $g_t' = \frac{\eta}{\sqrt{\hat{s}_t + \epsilon}} v_t$, $\hat{s}_t = \max(\hat{s}_{t-1}, s_t)$ (2018)

ADAM (Kingma and Ba, 2014) is the method which combines these two parts and hyper-parameters β_1 , β_2 can control them respectively. Thus, (η, β_1, β_2) become three essential hyper-parameters which are fixed by (0.1,0.9,0.999) in ADAM. But default value are not perfect in all cases. There are works which fixed weight decay of η in SGD and ADAM (Loshchilov & Hutter, 2016 & 2017) and AMSGrad (Reddi *et al*. 2018) which used adaptive $\beta_2 = 0.999 \; or \; 1$ in specified conditions. So, the optimizer function could be written in the following structures:

$$g_t' = \frac{\eta}{\sqrt{P(g_t)}} Q(g_t) = h(\mu)$$
$$P(g_t) = a_1 P(g_{t-1}) + a_2 g_t \odot g_t + a_3$$
$$Q(g_t) = b_1 Q(g_{t-1}) + b_2 g_t + b_3$$

The hyper-parameters μ in this optimizer will be at most 7 which are $\eta, a_1, a_2, a_3, b_1, b_2, b_3$. Where $\eta, (a_1, a_2), (b_1, b_2), (a_3, b_3)$ are equals learning rate, weight decay, momentum and epsilon respectively. In this work, only learning rate η became the main action of DQN to test the possibility of using RL in GD process.

3.2 Gradient Descent with Deep Q-Learning

Since the performance of hyper-parameter is in the real number field, the change of them in two adjacent states would not be very violent, and the sensitivity of hyper-parameters to GD process does not need precision in such high level. Thus, Deep Q-Network (DQN) (Mnih *et al*., 2015), the typical method of deep RL, is utilized in hyper-parameter update process.

Algorithm 1 shows the detailed process on how to use DQN to update the target network (CNN) parameters. At the first step, initial hyper-parameters are used to update CNN once and get the states (i.e. gradient, loss) and rewards to update DQN next. Experience replay performs well in this case because the next GD step does not only depend on the current states information but the previous states, which is mainly caused by the general neural network structure.

Algorithm 1: CNN gradient descent process with Deep Q-learning optimizer $h(\mu_0)$

Initialize main and target network Q and $\widehat{\mathrm{Q}}$ with parameter θ and θ^- ,with action list a and a' respectively, hyper-parameters of optimizer μ_0, threshold $score_0$, constant C
for *episode* = 1 to M **do**
  Initialize CNN model P , sequence $s_1 = \{x_1\}$ and pre-processed $\phi_1 = \phi(s_1)$, $score = 0$, action a_1, reward r_1
  update parameter of P once with $h(\mu_0)$
  for t = 1 to T **do**
    $a_{t+1} = \begin{cases} a\,random\,action & if\,in\,possibility\,\varepsilon \\ argmax_a\, Q(\phi(s_1), a; \theta) & otherwise \end{cases}$
    update parameter of P once with $h(\mu_t)$ by a_{t+1}
    calculate state x_{t+1}, reward r_{t+1} with CNN feedback
    update $s_{t+1} = s_t$, $\phi_{t+1} = \phi(s_{t+1})$
    store $(\phi_t, a_t, r_t \phi_{t+1})$, sample random $(\phi_j, a_j, r_j, \phi_{j+1})$
    $y_{t+1} = \begin{cases} r_{t+1} & if\,episode\,terminates\,at\,step\,j+1 \\ r_{t+1} + \gamma \max_{a'} \widehat{Q}(\phi_{j+1}, a'; \theta^-) & otherwise \end{cases}$
    Perform a gradient descent step on $(y_j - \widehat{Q}(\phi_j, a_j; \theta))^2$
    Update Q with y_{t+1}, reset $\widehat{Q} = Q$ every C steps,
    $score = score + r_{t+1}$
    if $score < score_0$:**break**
  end
end

4. Experiment and Results

The experiments are based on shallow CNN (3 layers with 28938 parameters) and use 8000 MNIST data in training and validation. The training process of CNN contains 10 episodes, each of which has 250 steps with batch size equals 32. The DQN optimizer is based on SGD which control changeable learning rate η and the action and reward definitions are highly related to loss behavior with different learning rates (lr).

4.1 Action and Reward Definition

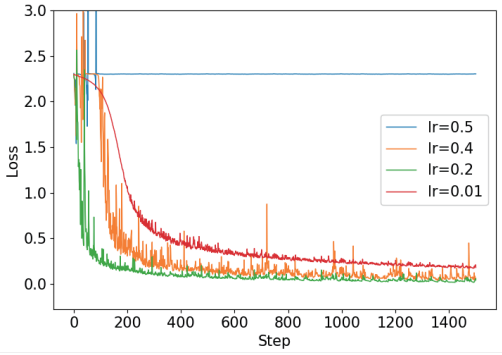

Figure 1: Performance comparison of different learning rate which with the same start point and same batch order, the learning rates are 0.5, 0.4, 0.2, 0.01 respectively.

Action, which equals the change of lr in this case, is initially set at $lr = 1, act = (0.9, 1, 1/0.9)$ are three choices of action and let $lr = lr * act$ in each step.

Figure 1 shows that there are 4 types of performance of the loss curve with different learning rates. The blue curve shows loss performance will stay at a high level when lr are too big. In this case, the loss is hard to decrease later in any learning rate, which should be avoided as much as possible. The orange curve shows frequent fluctuation and slow decrease, which indicates that lr could be much smaller. Big lr can help decrease fast in steep

condition but hard to converge at last. The green one shows the curve performance when lr is proper. But notice that, the appropriate lr could also has some fluctuation which can help it escape some saddle points or local minimums. The red curve shows the situation when lr is too small. The curve is almost monotonically decreasing, but speed is low.

With the performance in Figure 1, rewards are separated into 3 priorities. The latter priority will be ignored if one reward is given. The first priority is to set the upper/lower bound of lr. If over bound, give large negative reward and break (In this experiment, upper = 0.5 and lower = 0.001 are set). The second priority uses the range of fluctuation in the latest 20 losses to judge whether the lr is too small. If so, continuous negative rewards would be given. In the third priority, if the current loss is larger than the minimum of first half of the loss data, lr will be judged too big and give a normal negative reward. If the loss reaches a new minimum or the threshold loss (0.02 in this experiment), a positive reward will be given according to the total steps.

4.2 States Definition

The simplest way to define states is using all the parameters directly. But simultaneously it means that there are too many states which should be considered and the model will be hard to train. Proper states are significant to ensure the convergence and training speed to a RL model. In this experiment, following types of information of CNN are considered:

(1) Total step (2) Loss based: max(Loss), min(Loss), previous Loss, delta(Loss), (3) Parameter based: increase/decrease parameter number, parameter average change ratio (4) Gradient based: gradient in previous 3 epochs, absolute value of gradient, sum of positive/negative gradient (5) others: monotonically decrease number of loss, hyper-parameters.

4.3 Results in fixed start point

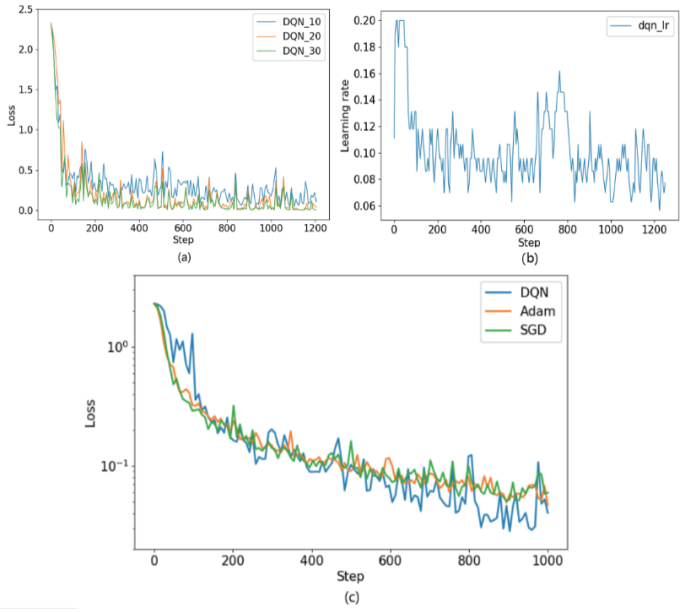

Figure 2 : (a) is the results of DQN optimizer after 10, 20 and 30 epochs' training, (c) is the comparison to SGD (lr = 0.1) and ADAM (lr = 0.001). Notice that the start point and batch order in (a) and (c) are the same. (b) shows the learning rate change of DQN model shown in (c).

Using to the action, reward, states definition in **4.1** and **4.2**, the training model will have 3 actions and 18 states. With the experience replay size of 2000 and target network update frequency of 100, the DQN model was trained for 50 epochs with the fixed start point. Figure 2.(a) shows the loss performance of the training process that becomes better in first 30 epochs. Compared to SGD, ADAM (figure 2.(c)), the performance of DQN optimizer shows strong ability to reach the lower loss and has larger fluctuation. Learning rate of DQN in figure 2.(b) goes to 0.2 at an early period and decrease to 0.1 whose fluctuation range is between 0.06 to 0.14.

4.4 Results in random start point

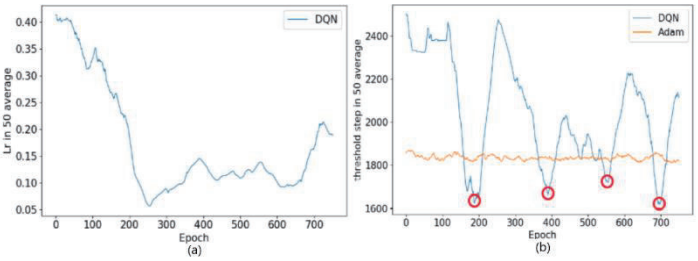

Figure 3: DQN training results of 800 epochs with a random start point. (a) shows the average learning rate and (b) shows the minimum step for each GD to reach the threshold loss (0.02) with DQN and Adam. Red circles point out the best result in each cycle. And both (a) and (b) are averaged in 50 adjacent data.

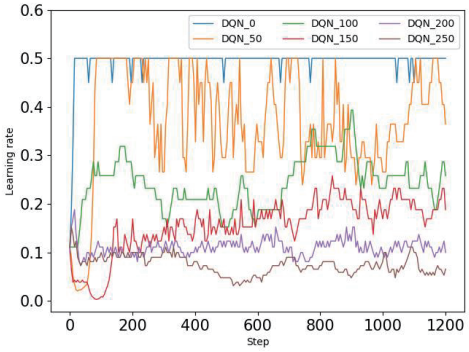

Figure 4: Learning rate (lr) curve of DQN optimizer after 0, 50, 100, 150, 200 and 250 epochs' training with random start point. After 250 epochs' training, the lr curve will fluctuate between DQN_50 to DQN_200.

Without the limitation of a fixed start point, it needs more training episodes to ensure the convergence of DQN. Each start point is saved and trained with ADAM again to do the comparison.

From the lr performance shown in Figure 3.(a), the average lr decrease in the first 250 epochs, then turn to increase and fluctuate. Combined with Figure 4, we found that the adjustment of strategy is first to decrease the average lr and limit the fluctuation which could avoid to get a large negative reward and relatively conservative. After the lr is near 0.05 which could let it get continuous negative reward written in **4.1**, it began to rise and fluctuate in a range. In Figure 3(b), the minimum step curve to reach the threshold (0.02) is shown which indicates that if the DQN model reaches the best solution under the current strategy, it will 'try' to change strategy as to find a better solution. The convergence of cycle is not obvious, but get a result which is better than Adam in each cycle.

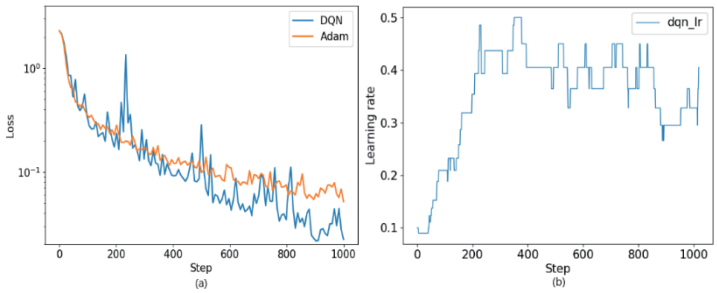

Figure 5: (a) is the validation data results of DQN optimizer after 729 epochs' training with a random start point, which compares to ADAM (lr = 0.001). (b) shows the learning rate change of DQN model shown in (a).

Figure 5.(a) shows the relatively good result in 800 episodes, whose performance is better than Adam in the same condition. From the lr curve in Figure 5.(b), the strategy of DQN gradually raise the learning rate in order not to leave GD area, then stay in a quite high level (0.4). It takes more time than starting from a fixed start point in **4.3** but has better performance.
Notice that the lr performances in Figure 2.(b) and Figure 5.(b) are different which might be the result of specific and random distributed samples. Compared with the result in **4.3**, tens times of training time is taken. But if the demand is not extremely high, we can also use the trained DQN model near 200 epochs which is already good enough.(Figure 3.(b))

5. Conclusion

The hyper-parameters in optimizers can greatly affect the decrease speed and convergence stability in gradient descent process. Such like SGD, learning rate should be adjusted lower if the loss curve seems to converge but higher when met a saddle point.
In this work, reinforcement learning is used to consider more information which was feedbacked by the target network and adjust the hyper-parameter quickly and precisely. The general performance of DQN-based optimizer shows good potential within limited training episodes both in fixed and random condition. Simultaneously using DQN optimizer would not take much more time than other optimizers during the training process. If a DNN model is planning to train several times, for the structure of the network will not change, the DQN optimizer might be a good method to choose.

6. Future Direction

DQN model is the basic model in value-based deep reinforcement learning. In the future work, other latest models like Rainbow (Hessel *et al*. 2018) or policy-based models like DDPG (Lillicrap *et al*. 2015) can also be considered to improve the result. Also, the layer depth of CNN in this work is shallow (3 layers). Deeper neural networks or other types like RNN could be tested.
More hyper-parameters and a new type of optimizer structure could contain more factors. Decreasing speed and escape ability are contradictions in GD process and the required minimum loss level will affect related reward design. A changeable parameter in the reward system can also operate training tendencies and lead to different results.

7. Acknowledgement

This work was funded by JSPS KAKENHI JP16H01836, JP16K12428, and industrial collaborators.

References

[Jacobs, 1988] Jacobs R A. Increased rates of convergence through learning rate adaptation[J]. Neural networks, 1988, 1(4): 295-307.

[Duchi *et al*. 2011] Duchi J, Hazan E, Singer Y. Adaptive subgradient methods for online learning and stochastic optimization[J]. Journal of Machine Learning Research, 2011, 12(Jul): 2121-2159.

[Tieleman & Hinton, 2012] Tieleman T, Hinton G. Lecture 6.5-rmsprop: Divide the gradient by a running average of its recent magnitude[J]. COURSERA: Neural networks for machine learning, 2012, 4(2): 26-31.

[Zeiler, 2012]Zeiler M D. ADADELTA: an adaptive learning rate method[J]. arXiv preprint arXiv:1212.5701, 2012.

[Kingma & Ba. 2014] Kingma D P, Ba J. Adam: A method for stochastic optimization[J]. arXiv preprint arXiv:1412.6980, 2014.

[Loshchilov & Hutter, 2016] Loshchilov I, Hutter F. Sgdr: Stochastic gradient descent with warm restarts[J]. arXiv preprint arXiv:1608.03983, 2016.

[Loshchilov & Hutter, 2017] Loshchilov I, Hutter F. Fixing weight decay regularization in adam[J]. arXiv preprint arXiv:1711.05101, 2017.

[Reddi *et al*. 2018] Reddi S J, Kale S, Kumar S. On the convergence of adam and beyond[J]. 2018.

[Sutton & Barto. 1988] Sutton R S, Barto A G. Reinforcement learning: An introduction[M]. MIT press, 1988.

[Watkins & Dayan, 1992] Watkins C J C H, Dayan P. Q-learning[J]. Machine learning, 1992, 8(3-4): 279-292.

[Rummery & Niranjan, 1994] Rummery G A, Niranjan M. On-line Q-learning using connectionist systems[M]. Cambridge, England: University of Cambridge, Department of Engineering, 1994

[Mnih *et al*. 2015] Mnih V, Kavukcuoglu K, Silver D, *et al*. Human-level control through deep reinforcement learning[J]. Nature, 2015, 518(7540): 529.

[Hessel *et al*. 2018] Hessel M, Modayil J, Van Hasselt H, *et al*. Rainbow: Combining improvements in deep reinforcement learning[C]//Thirty-Second AAAI Conference on Artificial Intelligence. 2018.

[Lillicrap *et al*. 2015] Lillicrap T P, Hunt J J, Pritzel A, *et al*. Continuous control with deep reinforcement learning[J]. arXiv preprint arXiv:1509.02971, 2015.

[Schulman *et al*. 2017] Schulman J, Wolski F, Dhariwal P, *et al*. Proximal policy optimization algorithms[J]. arXiv preprint arXiv:1707.06347, 2017.

[Silver & Hassabis, 2016] Silver D, Hassabis D. AlphaGo: Mastering the ancient game of Go with Machine Learning[J]. Research Blog, 2016.

[Xu *et al*. 2017] Xu C, Qin T, Wang G, *et al*. Reinforcement Learning for Learning Rate Control[J]. arXiv preprint arXiv:1705.11159, 2017.

The 33rd Annual Conference of the Japanese Society for Artificial Intelligence, 2019

Reducing the Number of Multiplications in Convolutional Recurrent Neural Networks (ConvRNNs)

Daria Vazhenina Atsunori Kanemura

LeapMind Inc.

Convolutional variants of recurrent neural networks, ConvRNNs, are widely used for spatio-temporal modeling. Although ConvRNNs are suited to model two-dimensional sequences, the introduction of convolution operation brings additional parameters and increases the computational complexity. The computation load can be obstacles in putting ConvRNNs in operation in real-world applications. We propose to reduce the number of parameters and multiplications by substituting some convolutional operations with the Hadamard product. We evaluate our proposal using the task of next video frame prediction and the Moving MNIST dataset. The proposed method requires 38% less multiplications and 21% less parameters compared to the fully convolutional counterpart. In price of the reduced computational complexity, the performance measured by for structural similarity index measure (SSIM) decreased about 1.5%. ConvRNNs with reduced computations can be used in more various situations like in web apps or embedded systems.

1. Introduction

Convolutional recurrent neural networks (ConvRNNs) are widely used because of their ability to model temporal information using 2D input. Donahue et al. [2] proposed to stack CNN and LSTM layers for sequential video processing. Xingjian et al. [6] combined those techniques in ConvLSTM layer and showed its effectiveness on two different tasks with 2D input and temporal dependencies. It allowed to obtain informative representation that improve overall model performance. Representations (or features) of a video are useful in video contents description, activity recognition, and other tasks. ConvRNNs parse video frames sequentially and encode frame-level information.

While lots of work were done on speeding up and improving performance of conventional (i.e. non-convolutional) RNNs, less attention was paid to ConvRNNs. Similar to conventional RNNs, gated variants were proposed for their convolutional conterparts, such as ConvLSTM [6] with three gates, ConvGRU [1] with two gates, and reduced-gate ConvLSTM [3] with one gate, which is variant of non-convolutional JaNet [9]. Gates are sensitive to short-term and long-term patterns in the input and help to overcome vanishing gradient problem. Other improvements for ConvRNNs focused on fitting better to their target task and increased overall model performance, but they resulted in increasing memory footprint, the number of parameters, and the number of floating point multiplications [7, 10].

Recently, for conventional RNNs, Li et al. [4] proposed to reduce the numbers of multiplications and parameters by substituting matrix multiplication between a weight matrix and an input vector to the Hadamard product. It allowed to build a deeper network of up to 21 layers and slightly outperformed state-of-the-art models for three different tasks.

We investigate the influence of substituting convolution with the Hadamard product in ConvLSTM, ConvGRU, and reduced-gate LSTM. It is expected that such substitution would result in a large performance drop. Then, instead of replacing all the convolution operations in a network, we used the Hadamard product only in some parts of a network, in order to keep a good balance between reducing the numbers of parameters and multiplications and performance drops.

As an example of using ConvRNN, we selected the task of next video frame prediction, which learns video sequence representations of individual video frames in an unsupervised manner [8]. The next frame prediction problem is useful because 1) we don't need to obtain lots of labeled data, which is often a difficult task before adopting deep learning, and 2) whereas a system trained for one specific task will learn representations for that specific task, internal representations learned by the model for predicting next frames will be re-usable for other tasks [8]. Also, targets in supervised learning contain much less information than input data, especially in terms of video action recognition, where there is only one label per many frames. That is why learning how to forecast the future of an image sequence requires the prediction model to understand and efficiently encode the content and dynamics for a certain period of time.

Contact: Daria Vazhenina, LeapMind Inc., Tokyo 150-0044, Japan, daria@leapmind.io

2. ConvRNNs

2.1 Basic ConvRNN architecture

The most widely used variant of ConvRNN is ConvLSTM, proposed in [6], where conventional LSTM is modified by replacing matrix multiplication with convolution and changing the shape of input X_t to 2D from 1D. A ConvLSTM cell is described by the following equations:

$$i_t = \sigma(X_t * W_{xi} + h_{t-1} * W_{hi} + b_i), \quad (1)$$

$$f_t = \sigma(X_t * W_{xf} + h_{t-1} * W_{hf} + b_f), \quad (2)$$

$$o_t = \sigma(X_t * W_{xo} + h_{t-1} * W_{h0} + b_o), \quad (3)$$

$$c_t = f_t \odot c_{t-1} + i_t \odot \tanh(X_t * W_{xc} + h_{t-1} * W_{hc} + b_c), \quad (4)$$

$$h_t = \tanh(c_t \odot o_t), \quad (5)$$

where $*$ means convolutional operation; $W_{..}$ is a set of convolutional kernels; h_t and h_{t-1} are current and previous hidden states, respectively; i_t, f_t, and o_t are input, forget, and output gates, respectively; and c_t is cell output.

2.2 Next video frame prediction model using ConvRNN

In unsupervised video representation model, ConvRNN cells are combined in composite model described in [8], which has an encoder-decoder pipeline with two different decoders termed a predictor and a reconstructor. In the composite model, several video frames are fed into recurrent encoder and then its final hidden state, so called a learned representation, is used as the initial hidden state in the predictor decoder and the reconstructor decoder, while the two decoders do not share all other parameters (e.g. weight matrices). Learning the two tasks of prediction and reconstruction using the same encoder allows us to improve overall model performance, rather than using different encoders. The loss function is defined to be the sum of one for the reconstructor and the other for the predictor, and we can do backpropagation on it.

Our experiments in this paper are based on the network architecture proposed in [5], where the next frame prediction pipeline has been improved by stacking recurrent layers on the top of the CNN layers in the encoder part and reversing those recurrent and CNN layers in the decoder part, changing the CNN layers into so-called deconvolution layers. This stacking technique reduces the resolution of input image frames with convolutional layers before feeding it to the recurrent ones, thus reducing the number of parameters in the recurrent layers. This significantly reduce mean square error (MSE) of the model for both prediction and reconstruction tasks.

3. Proposed improvements

We investigated and analyzed replacing convolutional operation with Hadamard product in ConvRNN cells. This idea was inspired by IndRNN [4], which reduces the number of multiplications in the vanilla recurrent cell. Since IndRNN was proposed for RNNs without gates, we cannot adopt it for our purpose of improving ConvLSTM, which includes many gates. This reduction of the number of multiplications has not been investigated so far for gated convolutional recurrent units.

Here is the comparison of the expected computational complexity (CC; lower is better) and performance mean square error (MSE; lower is better):

$$CC_{\text{Hadamard}} < CC_{\text{Combi}} \ll CC_{\text{Baseline}},$$
$$MSE_{\text{Hadamard}} \gg MSE_{\text{Combi}} \geq MSE_{\text{Baseline}}$$

where the notation is as follows:

- Baseline (Conv*): The baseline model with standard ConvRNN structure,
- Combi (ConvIndConv*): Proposed combination of convolution and Hadamard product,
- Hadamard (ConvInd*): The model where convolution is replaced with Hadamard product.

Here the asterisk sign "*" means LSTM, GRU, or Janet. That is, "ConvInd*" means ConvIndLSTM, ConvIndGRU, or ConvIndJanet.

As baselines for applying Hadamard product, we used ConvLSTM, ConvGRU, and ConvJanet. Hadamard product was used to calculate gates and cell unit in ConvInd* models:

$$i_t = \sigma(X_t * W_{xi} + h_{t-1} \odot W_{hi} + b_i), \quad (6)$$
$$f_t = \sigma(X_t * W_{xf} + h_{t-1} \odot W_{hf} + b_f), \quad (7)$$
$$o_t = \sigma(X_t * W_{xo} + h_{t-1} \odot W_{h0} + b_o), \quad (8)$$
$$c_t = f_t \odot c_{t-1} + i_t \odot \tanh(X_t * W_{xc} + h_{t-1} \odot W_{hc} + b_c), \quad (9)$$
$$h_t = \tanh(c_t \odot o_t) \quad (10)$$

and Hadamard product was used for gates calculations only in ConvIndConv* models, so c_t is calculated as follows:

$$c_t = f_t \odot c_{t-1} + i_t \odot \tanh(X_t * W_{xc} + h_{t-1} * W_{hc} + b_c) \quad (11)$$

4. Experimental results

4.1 Database description

We use the moving MNIST dataset, which has been widely used to evaluate video frame prediction models. We used same train and test settings as in [8]. Each sequence in this dataset consists of 20 image frames of size 64×64 with two random moving digits from the MNIST dataset. The performance in next frame prediction was measured by MSE (the low this value the better) and SSIM (the higher this value the better) between prediction and the ground truth [11].

4.2 Performance evaluation

We evaluated three types of ConvRNNs and their ConvInd* and ConvIndConv* variants described in Section 3.. We considered the number of multiplications and the number of parameters for complexity evaluation.

As shown in Fig. 1, the model with ConvLSTM cell showed the best performance in terms of SSIM, while the model with ConvGRU cell was slightly better in terms of MSE. All models with ConvInd* cell showed significant drop in performance about 30% relative to their fully convolutional counterparts. Returning one convolution operation in the ConvIndConv* cell allowed to reduce performance drop to about 5% relative to their fully convolutional counterparts.

Fig. 2 shows that the best performing model with ConvLSTM cell requires the largest numbers of multiplications and parameters. The model with ConvIndConvLSTM cell showed the second best SSIM value and required about 37.5% less multiplications and about 21% less parameters. Its relative drop of SSIM value is 1.54% and MSE is 4.2%. This shows that it is possible to use less parameters and multiplications for gates calculations without big loss in performance.

5. Conclusions

In this work, we compared three gated ConvRNN variants using next video frame prediction task. We showed that it is possible to reduce the number of parameters and multiplications in the ConvRNN architecture with a small drop in the performance of the overall model. ConvInd* models provide significant reduction in the number of parameters and multiplications, but drop in performance of those models is pretty large. Proposed ConvIndConv* models, where convolution operation is kept in the cell computation, allowed to achieve minor drop in performance compared to ConvInd* models, and also kept number of parameters and multiplications smaller compared to Conv* models.

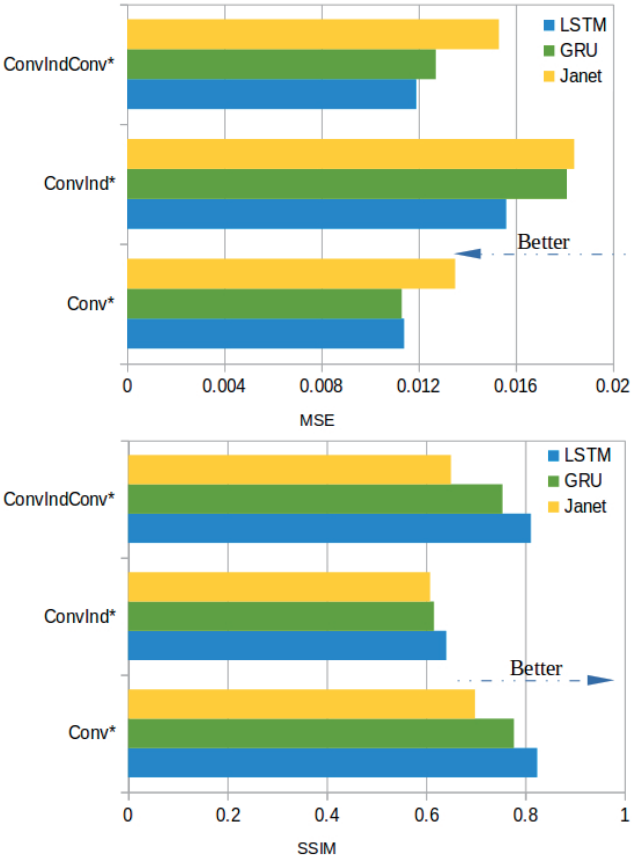

Figure 1: ConvInd* and ConvIndConv* models performance evaluation in terms of MSE and SSIM.

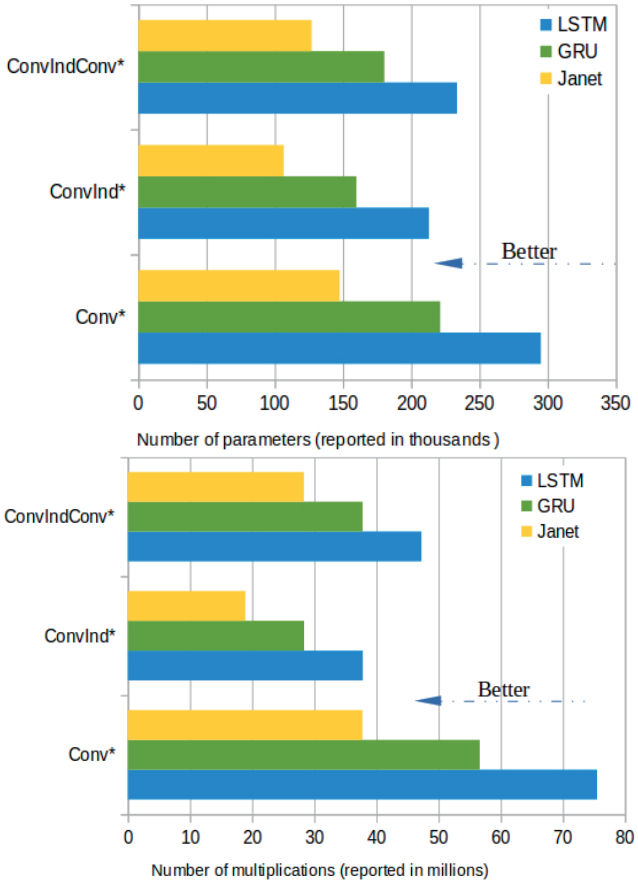

Figure 2: ConvInd* and ConvIndConv* models performance evaluation in terms of number of parameters and multiplications.

References

[1] N. Ballas, L. Yao, C. Pal, and A. Courville. Delving deeper into convolutional networks for learning video representations. In *Int. Conf. Learning Representations (ICLR)*, 2016.

[2] J. Donahue, L. A. Hendricks, S. Guadarrama, M. Rohrbach, S. Venugopalan, K. Saenko, and T. Darrell. Long-term recurrent convolutional networks for visual recognition and description. In *IEEE Conf. Computer Vision and Pattern Recognition (CVPR)*, pages 2625–2634, 2015.

[3] N. Elsayed, A. S. Maida, and M. Bayoumi. Reduced-gate convolutional LSTM using predictive coding for spatiotemporal prediction. *arXiv:1810.07251*, 2018.

[4] S. Li, W. Li, C. Cook, C. Zhu, and Y. Gao. Independently recurrent neural network (IndRNN): Building a longer and deeper RNN. In *IEEE Conf. Computer Vision and Pattern Recognition (CVPR)*, pages 5457–5466, 2018.

[5] B. Sautermeister. Deep learning approaches to predict future frames in videos. Master's thesis, Technishe Universität München, 2016.

[6] X. Shi, Z. Chen, H. Wang, D.-Y. Yeung, W. Wong, and W. Woo. Convolutional LSTM network: A machine learning approach for precipitation nowcasting. In *Advances in Neural Information Processing Systems (NIPS)*, pages 802–810, 2015.

[7] X. Shi, Z. Gao, L. Lausen, H. Wang, D.-Y. Yeung, W. Wong, and W. Woo. Deep learning for precipitation nowcasting: A benchmark and a new model. In *Advances in Neural Information Processing Systems (NIPS)*, pages 5617–5627, 2017.

[8] N. Srivastava, E. Mansimov, and R. Salakhudinov. Unsupervised learning of video representations using LSTMs. In *Int. Conf. Machine Learning (ICML)*, pages 843–852, 2015.

[9] J. van der Westhuizen and J. Lasenby. The unreasonable effectiveness of the forget gate. *arXiv:1804.04849*, 2018.

[10] Y. Wang, Z. Gao, M. Long, J. Wang, and P. S. Yu. PredRNN++: Towards a resolution of the deep-in-time dilemma in spatiotemporal predictive learning. In *Int. Conf. Machine Learning (ICML)*, 2018.

[11] Z. Wang, A. C. Bovik, H. R. Sheikh, and E. P. Simoncelli. Image quality assessment: from error visibility to structural similarity. *IEEE Trans. Image Process.*, 13(4):600–612, 2004.

International Session | International Session | [ES] E-2 Machine learning

[2H5-E-2] Machine learning: new modeling

Chair: Junichiro Mori (The University of Tokyo)

Wed. Jun 5, 2019 5:20 PM - 6:40 PM Room H (303+304 Small meeting rooms)

[2H5-E-2-01] Local Feature Fitting Learning Network for Point Cloud Classification

○Lu SUN[1] （1. Chiba University ）

5:20 PM - 5:40 PM

[2H5-E-2-02] Feasible Affect Recognition in Advertising based on Physiological Responses from Wearable Sensors

○Taweesak Emsawas[1] （1. Osaka University）

5:40 PM - 6:00 PM

[2H5-E-2-03] Deep Markov Models for Data Assimilation in Chaotic Dynamical Systems

○Calvin Janitra Halim[1], Kazuhiko Kawamoto[1] （1. Chiba University）

6:00 PM - 6:20 PM

[2H5-E-2-04] Modelling Naturalistic Work Stress Using Spectral HRV Representations and Deep Learning

○Juan Lorenzo Mutia Hagad[1], Ken-ichi Fukui[1], Masayuki Numao[1] （1. Osaka University）

6:20 PM - 6:40 PM

The 33rd Annual Conference of the Japanese Society for Artificial Intelligence, 2019

Local Feature Fitting Learning Network for Point Cloud Classification

Lu SUN [*1] Yoshitsugu MANABE [*1]

[*1] CHIBA University

We propose a deep learning network framework to solve the classification task of three-dimensional point clouds. According to different functions, the network can be divided into the resampling block, transform block, local feature fitting block, and classification block. Unlike other classification methods based on point cloud, we try to fit local point cloud and use the fitting function as a local feature to enter the classification layer. Though simple, Local feature fitting learning network (LFFLN) is highly efficient and effective. It achieves excellent performance in the ModelNet40 without any tricks.

1. Introduction

In recent years, deep learning tools have made great achievements in image-based works. However, it is difficult to apply the image-based network framework to three-dimensional models directly. Therefore, the accuracy of image classification is more than 99%, while the accuracy of the three-dimensional model classification is mostly hovering at 85%. The main problem is that point clouds cannot be convoluted directly. The main contribution of this study is to simulate the convolution operation with the local fitting of point clouds and to find the local characteristics of point clouds.

2. Related Work

2.1 Non-point Cloud Method

To use convolution in three-dimensional models, some researchers use voxels to represent three-dimensional models [Wang 2017] [Maturana 2015]. This kind of method can directly use 3D convolution to convolute voxels. However, voxels are not a good way to express three-dimensional models. The resolution of three-dimensional models expressed by voxels is not high. If we want to improve the resolution, we need to take up a lot of storage space.

Another method is based on picture groups [Su 2015]. Based on the method of picture group, the images from different angles are convoluted for 2D and merged into the classification layer. This method is not strictly based on three-dimensional models and requires a lot of pre-operation.

2.2 Point Cloud Method

Because point cloud can be used to express the three-dimensional model effectively, many researchers are studying the classification method based on point cloud now. The main difficulty of point cloud-based method is the disorder of point cloud. PointNet [Qi 2016] using symmetry function to solve disorder problems. PointCNN [Li 2018] explored the idea of equivariance instead of invariance. They train the possible sequence of point cloud directly.

We have come up with completely different ideas. Considering that point clouds belong to space coordinates, there always exists a function to abstractly express point clouds when they are placed on coordinate axes. As long as we can find this function, point clouds can be classified according to the output of the function. Of course, this function may be very complex, but it doesn't matter. Deep learning tools are very suitable for solving this problem.

Contact: Lu SUN, CHIBA University, 1-33, Yayoicho, Inage Ward, Chiba-shi, Chiba, 263-8522 Japan, 080-3974-0897, yeelou@chiba-u.jp

3. Local Feature Fitting Learning Network

Before introducing the network structure, I would like to review how convolution works in images. Example, computing any pixel on an image with convolution kernel 3×3. The first step is to find eight points adjacent to the pixel, then multiply the nine pixels with the corresponding position of the convolution core, and finally add up all the results. From the point cloud-based convolution operation, finding neighborhoods and building convolution kernels are the key steps for point clouds. So, we divide the network into four blocks according to the functional requirements. First resampling block is to find the neighborhood. Transform block and local feature fitting block are to determine the convolution kernels. The last block is to classify the extracted features. The network structure is shown in Figure 1.

3.1 Resampling

The purpose of this section is to resample the point cloud and make it look like many small point groups. It is required here that for a large point cloud, the number of small point groups is fixed, and the number of points of small groups is fixed.

Firstly, we sampled uniformly in point clouds. To get the core of the point group and then search the neighborhood based on these cores to get the point group.

As shown in Figure 1.A, the point cloud format changes from $n \times 3$ to $pg \times pn \times 3$. Where n is the point's number, pg is point group's number, pn is point number of point group.

3.2 Transform

The purpose of building this block is that the function expression does not have rotation and translation invariance for point clouds.

Although the center of the whole point cloud is at the origin of the coordinates, however, due to resampling, all point groups need to be standardized first.

$$x_{std}^{(i)} = \frac{x_i - \mu_x}{\delta_x}$$

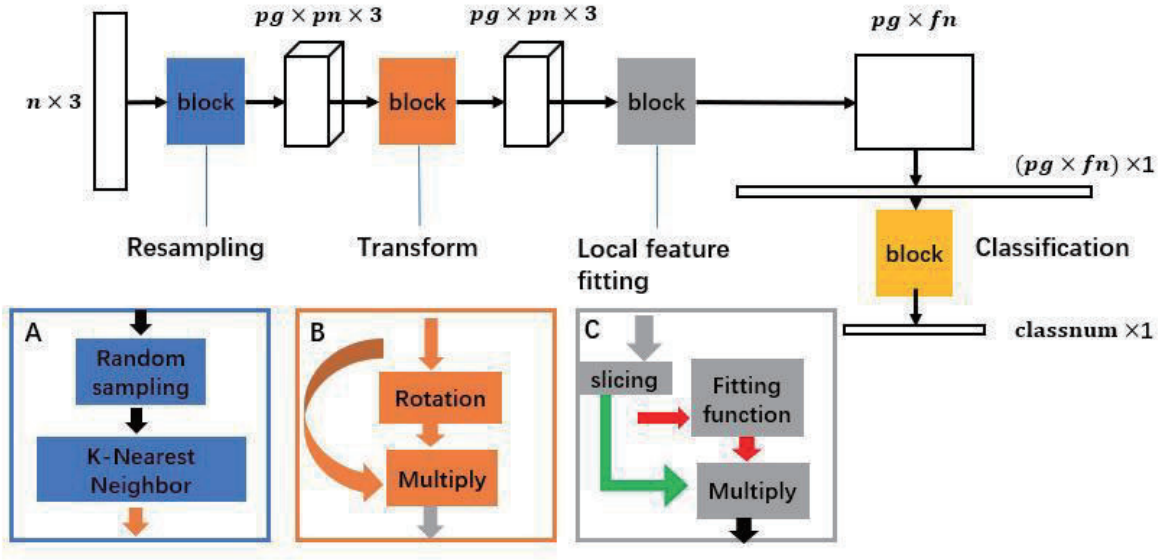

Fig 1. Local feature fitting learning network (LFFLN) architecture

Where $x_{std}^{(i)}$ is a normalized feature, x_i is an input feature, μ_x is the mean of the features, δ_x is the standard deviation of features.

Then we calculate the rotation matrix by regression of the point group itself. As shown in Figure 1.B, we only use simple non-linear regression, superimpose two dense layers, and then multiply this 3×3 matrix with itself to get the rotated point group. The input and output format of this block is unchanged.

3.3 Local Feature Fitting

The main purpose of this block is to make a convolution kernel. Because point clouds of the same shape have a different distribution of points. To get the same feature, a function needs to be calculated. From this function, we can get convolution kernels of any fixed shape.

First, cut the input of this block.

$$(\mathrm{pg} \times \mathrm{pn} \times 3) \rightarrow M\colon (\mathrm{pg} \times \mathrm{pn} \times 2), N(\mathrm{pg} \times \mathrm{pn} \times 1)$$

M retains the first two values of the point group (x, y), N retains the last values of the point group (z).

Then we put M into the fitting network to calculate a value N' (z'), This value is a small part of the convolution kernel. By adding all Z members N, we get the convolution result of a point group. By multiplying N' and N separately and adding the results, we can get one convolution result of a group of points.

$$feature_{conv} = \sum_{pn} \mathrm{F}(M) \times N$$

Where F( ) is a fitting function. We can construct multiple functions to obtain multiple features. Like the transform block, the function consists of two simple dense layers.

As shown in Figure 1.C, the input format changes from $\mathrm{pg} \times \mathrm{pn} \times 3$ to $\mathrm{pg} \times \mathrm{fn}$ where fn is the function's number.

3.4 Classification

There's nothing special about this piece. Pull the input into a one-dimensional vector and put into three layers of dense to get the final classification result.

3.5 Loss

The loss function of this method is based on cross-entropy loss. However, there is a rotating block before, and the network cannot converge very well. To guide the network learning, we will transform the point group by SVD before input the rotating block. We will calculate mean squared error loss by rotating the characteristic matrix and the result of the rotating block.

$$\mathrm{Loss} = loss_{ce} + \alpha loss_{rmse}$$

Where α is the weight of $loss_{rmse}$. As the training progresses, it gradually decreases.

4. Experiment

Our network learns a global point cloud feature that can be used for object classification. We evaluate our model on the ModelNet40 [Wu 2015] shape classification benchmark. The data set split into 9,843 for training and 2,468 for testing.

In Table 1, we compare our model with previous works; Our model achieved excellent performance among methods based on 3D input (volumetric, image and point cloud).

Table 1: Object classification results on ModelNet40

Method	Input	accuracy avg. class	accuracy overall
3DShapeNets	volume	77.3	84.7
VoxNet	volume	83.0	85.9
MVCNN	image	90.1	-
PointNet	point	86.2	89.2
PointCNN	point	88.1	91.2
Ours	point	86.9	88.1

We input the result of feature fitting directly into the classification part. This results in that the classification results are based on the local features of point clouds. However, the types of point clouds in this data set vary greatly. So although it is based

on the classification of local point clouds, good results are obtained.

5. Discuss

We want to discuss some hyperparameters. In Section 3.1, pg and pn are the number of point groups and the number of points in point group. In an image, the stride of the general convolution operation is 1. For 3×3 convolution kernel, each operation overlaps by 66%. So we sampled four adjacent points evenly in the point cloud and then set 27 adjacent points as a group of points, $\mathrm{pg} = 512$, and $\mathrm{pn} = 27$.

We calculate the rotation matrix by regression of the point group itself in Section 3.2. Considering that there are only 27 points in a point group, so we don't need too complicated network model to return to a 3×3 matrix. We superimpose two layers of dense at first. But the rotation matrix is a very complicated process. Although we add an item to the rotation matrix independently in the loss function, when we check the training results, we find that this part of the network can not converge very well. Therefore, in the follow-up study, we consider increasing the complexity of this part of the network and improving the overall accuracy.

After resampling, feature rotation and feature fitting, we can think that this is a convolution operation for point clouds. In this study, these features are directly put into the classification network for classification. We know that one-layer convolution is not enough for image classification, so if the feature is sampled, rotated and fitted continuously, the classification accuracy can be improved. Attention should be paid to the convergence of the rotation matrix for features. It is not possible to add a function on this part of the loss function. How to train this part of the network is the focus of future research.

Although we are not the most precise model, we still have a lot to improve. For example, we have performed a convolution operation now. If we add more convolution operations later, I believe the result will be better.

6. Conclusion

We have designed a point cloud feature extraction method by simulated convolution, which achieves good results when only one layer of simulated convolution is used, and no tricks are used. The plan is to add more simulated convolution layer and use various tricks to improve accuracy.

References

[Surname of the first author Year] Names of authors, Title, Journal, Publisher, Year.

[Wang 2017] P.-S. Wang, Y. Liu, Y.-X. Guo, C.-Y. Sun, and X. Tong. O-CNN: Octree-based convolutional neural networks for 3d shape analysis. ACM Transactions on Graphics, 2017

[Maturana 2015] D. Maturana and S. Scherer. Voxnet: A 3d convolutional neural network for real-time object recognition. In IEEE/RSJ International Conference on Intelligent Robots and Systems, 2015

[Su 2015] H. Su, S. Maji, E. Kalogerakis, and E. G. Learned-Miller. Multi-view convolutional neural networks for 3d shape recognition. In IEEE International Conference on Computer Vision, 2015

[Qi 2016] C. R. Qi, H. Su, K. Mo, and L. J. Guibas. Pointnet: Deep learning on point sets for 3d classification and segmentation. Computing Research Repository - arXiv, 2016

[Li 2018] Y. Li, R. Bu, M. Sun, and B. Chen. Pointcnn. arXiv:1801.07791, 2018

[Wu 2015] Z. Wu, S. Song, A. Khosla, F. Yu, L. Zhang, X. Tang, and J. Xiao. 3d shapenets: A deep representation for volumetric shapes. In Proceedings of the IEEE Conference on Computer Vision and Pattern Recognition, 2015

The 33rd Annual Conference of the Japanese Society for Artificial Intelligence, 2019

Feasible Affect Recognition in Advertising based on Physiological Responses from Wearable Sensors

Taweesak Emsawas[*1] Ken-ichi Fukui[*2] Masayuki Numao[*2]

[*1] Graduate School of Information Science and Technology, Osaka University
[*2] The Institute of Scientific and Industrial Research (ISIR), Osaka University

Recent studies in affective computing have facilitated and stimulated the development of systems and sensors that can recognize and interpret human affects. Affective computing has been applied in various domains, and one of the applied domains is in the marketing area to increase the consumers' appeal and attraction. In particular, advertisements (ads) can convey amounts of information in a short time. Therefore, using physiological responses can help to acquire a user's feedback and obtain an advantage. This study proposes non-invasive affect recognition in each scene of an advertising video using electroencephalogram (EEG), electrocardiogram (ECG) and eye-tracking. The preliminary analysis of EEG shows the relationship between scene feeling score and emotional affects regarding physiological responses. Hence, we also trained two types of recognition models: window recognition and sequence learning. The models learned from the physiological responses and questionnaires on a user's preference in each ad scene.

1. Introduction

In the marketing area, Marketer always tries to reach maximum customer for getting their attraction and sales. Consequently, the ads have been created in various ways such as articles, billboards, videos, and so on. Nowadays, TV commercial plays a role in human life, and consumer commonly watches many ad videos through various channels. The goal of creating ads video is to convey amounts of information in a short time. For this reason, all scene in the ads is essential information and should make an impression. To comprehend feedback and obtain an advantage, consumers' response is needed, and there can gather in many ways such as questionnaires, external appearances, and internal appearances.

Recently, the studies are interested in understanding the user's preferences regarding human affect or emotion. Hence, emotion recognition based on physiological signals has been a hot topic and applied in various domains such as health care, game and commercial [Shu 2018]. The emotion can be represented in various ways. In psychology, human affect is a concept to describe the experience of feeling or emotion, and affect transmits physiological responses with stimuli (e.g., pictures, audio and videos). To acquire the data from a subject, Sensors have been developed for different purposes such as for laboratory or wearable depend on the feasibility and accurate circumstances [Ragot 2017].

In recognition method based on physiological data, after extracting and selecting the features, various researches utilize these features to train a model and classify different emotional states. However, each model applies a different method to represent input data or physiological signals. General techniques train with the whole signal data and classify labels such as multilayer perceptron (MLP), support vector machine (SVM) and so on. While another technique, which studies continuous time interval of sequential behavior, or sequence learning in affective computing recognizes the continuous human affects appropriately. Long-short term memory (LSTM) networks are efficient sequence learner that suits to recognition tasks.

This study focuses on continuous ads-affect recognition that considers how the strength of changing states during watching ads. We propose subject-independent recognition [Chen 2017] using non-invasive wearable sensors, and a 15-second ad video was selected as stimuli. In this study, we study the subject affects as negative or positive (low or high) emotional affects each scene interval. First, in preliminary experiment, the result shows a relation between the scene-feeling score of questionnaires and the physiological responses. Thus, machine learning techniques including MLP, SVM and LSTM networks were performed to recognize these emotional human affects. The results of continuous affect recognition can support the interpretation of the scene interesting and how subjects interact with ad scenes.

2. Data Acquisition and Preprocessing

In this study, 130 subjects between 20 and 50 years of age including half of males and females participated in the experiments, and all subjects had never watched the ad video before, to assure a genuine reactions. The 15-second ad video of toothpaste was chosen as stimuli to elicit emotional affect from the subjects. This ad video contains 11 scenes which respectively present tooth problems, bacteria illustration, brushing teeth, cleaning up and toothpaste products. The subjects were asked to watch the video while wearing Neurosky's sensors. Then, after watching the video, all subjects were asked to fill out the questionnaires concerning scene feeling based on 7 scales of preference (-4 to 4). We represent the score of 0 to 4 and -1 to -4 as positive and

Contact: Taweesak Emsawas, Department of Information and Physical Sciences, Information Science and Technology, Osaka University, E-mail: taweesak@ai.sanken.osaka-u.ac.jp

negative labels respectively.

2.1 Electroencephalogram (EEG)

The frontal-brain activity plays a crucial role in emotion recognition and distinguishes emotional affects which were known to vary in affective valence such as positive and negative [Schmidt 2001]. EEG data were acquired from one electrode and consequently power spectral density (PSD) was employed to extract features from EEG signal into five frequency bands: delta (0-4 Hz) , theta (4-8 Hz), alpha (8-13 Hz), beta(13-30 Hz), and gamma (>30 Hz) from low to high frequencies [Jenke 2014]. Neurosky's sensor calculated and recorded five frequency bands in each second.

2.2 Electrocardiogram (ECG)

CardioChip/BMD10X-based devices of Neurosky's sensors recorded and converted to ECG signals. ECG signal consists of P-QRS-T waves in each one cardiac cycle. The features were extracted throughout the whole P-QRS-T segment as the standard deviation of the RR intervals (SNDD), the number of pairs of successive RR intervals that differ by more than 50 ms (NN50) and the proportion of NN50 that divides by the total number of NN intervals (PNN50)[Karpagachelvi 2010].

2.3 Eye-tracking

Video-based method of eye tracking is widely used in commercial eye trackers which measures horizontal and vertical components of the movements of both eyes [Chennamma 2013]. The distance of each X and Y pairs was calculated and used as an eye-tracking feature.

To synchronized all physiological features, the lower-frequency feature was duplicated multiple times unit it matches the timestamp with the higher-frequency feature. For example, in the case of all features, EEG and ECG features were duplicate until they match with eye-tracking features.

For the sake of simplicity, the targeted labels of affect recognition were extracted from questionnaires using mapping and rearrangement depend on the scene period. Thus, each second which involves more than 2 scenes would calculate the average of time-weighting by

$$f_t = \sum_{i}^{N_t} (sf_i * t_i) \tag{1}$$

where f_t is feeling score at time t, sf_i is feeling score at scene i, t_i is time weight at scene i, N_t is the number of scene which relates to time t and t is observed timestamp $(1, 2, 3, ..., 15)$

3. Research Methodology

In this study, we used trend value to comprehend the relation of physiological data over time. For affect recognition, the emotional affect was classified as positive and negative. The techniques can be divided into two types: window recognition and sequence learning. The input and output data were constructed from extracted features and questionnaires, which are shown in Figure 1.

3.1 Data Trends

To observe the relationship of physiological data and feeling score, representation of the same axis is required to indicates whether each particular band is increasing or decreasing over time, and how strong each data values. We present the data trend by using trend value or r which represents the trend of data over time. Each trend value calculated by using the 4-second sliding window technique. The positive value is a direct variation of data values over time, and the negative value is an inverse variation. The trend value can be calculated by

$$r = \frac{\sum_i^n (x_i - \bar{x})(t_i - \bar{t})}{\sqrt{\sum_i^n (x_i - \bar{x})^2} \sqrt{\sum_i^n (t_i - \bar{t})^2}} \tag{2}$$

where n is sliding window size, x is data value, t is time in second and i is running number of sliding window.

3.2 Window recognition

Window recognition recognizes emotional affects each second which this study applied the 4-second sliding window for segmentation technique to analyze temporal data and recognize emotional affects over time. The model input was constructed from the trend values in section 3.1. Then, the values were mapped to the time axis for data and label consistency. Meanwhile, the label or output was the feeling score value at each second. Therefore, MLP and SVM which are ubiquitous techniques were chosen in this experiment. However, these techniques are not able to transmit useful information between each window entirely but can learn along the values according to the sliding window size.

3.3 Sequence learning

We also applied sequence learning as LSTM networks which improve from a recurrent neural network (RNN). The main idea of the RNN is to memorize previous information in the network's internal states by using self-connections. The benefit of an RNN is the ability to use contextual information from the whole data sequence, and the dependencies of inputs can remain in the network. The LSTM architecture preserves information by using memory cells and gate units which allows the exhibiting of temporal dynamic behavior for a time series data. In the experiment of sequence learning, the LSTM networks were used to learn the dependencies of physiological responses. After constructing from the trend values in section 3.1, we perform a 1-second sliding window that contains the data values, and each feeling score in a second was used as the label. The sliding window is shifted along the data waves to construct an input vector for each window. After having been trained, the network can be used to predict the label sequence of feeling score.

4. Experiments and Results

4.1 Preliminary Experiment

In our preliminary experiment, we calculated and investigated the trends considering the five frequency bands of only EEG data over time. The subject's averages between EEG data over time are shown in Figure 2, and the average time-weighting of the feeling score is shown in Figure 3, respectively.

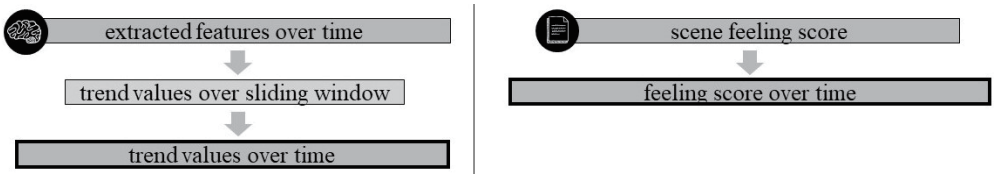

Figure 1: the input representation from extracted feature values (left) and output representation from questionnaires (right)

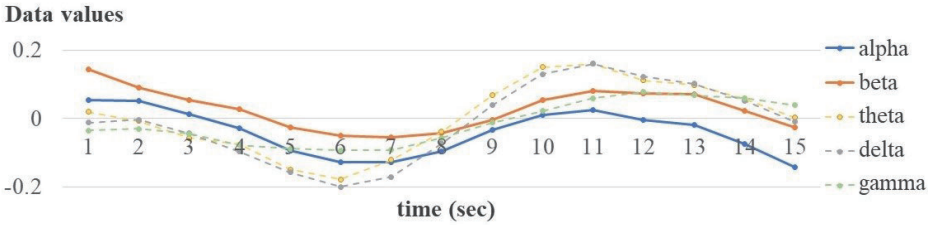

Figure 2: Average data trends of EEG data over time for all subjects

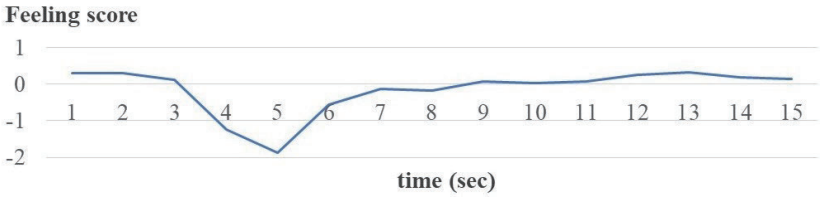

Figure 3: Average feeling score overtime for all subjects

Considering these two figures, we found the evidence that shows the relation between EEG responses and scene feeling score. Fortunately, we can indicate the unusual point around 3 to 7 seconds which is the disgusting scene of bacteria. Hence, we continued to examine the recognition experiment based on physiological responses using machine learning techniques.

4.2 Recognition Experiment

In this section, we divide the experiments, according to the features used, into two experiments: only EEG features and all features. These two experiments applied MLP, SVM and LSTM network to recognize the output label or feeling score each second. 5-fold cross-validation was performed for all subjects. The trend values and feeling score over time were used as the dataset and labels. This dataset was proportionally divided into 5 fold and used for train and test the models. In addition, MLP and LSTM need the validation set in the training process, so the training sets of each fold were divided into the training set and validation set with 80% and 20% respectively. The results are shown in Table 1. In the experiment of only EEG features, LSTM achieved the highest accuracy at 76.4%, and SVM and MLP achieved 70.3% and 68.8% respectively. Unfortunately, all features experiment achieved an accuracy of 72.8%, 69.2%, 61.9% respectively.

	MLP	SVM	LSTM
Only EEG features	68.8	70.3	76.4
All features	61.9	69.2	72.8

Table 1: Accuracy of affect recognition

5. Discussion and Conclusion

In this study, we present a study of emotional affect recognition based on physiological responses from wearable sensors. the models constructed through this study approach can be used for detecting the emotional affects change over time. Based on the recognition results, the best results are achieved in recognition when only EEG features are used. Considering ECG features and according to previous researches, we found that ECG features could not perform good results in a short duration. While eye tracking features in this experiment could not denote the emotional affects, the subjects just watched the interesting points in each scene. In recognition techniques, we present general recognition and sequence learning techniques. These two techniques could gain a continuous affect along the duration and apply to comprehend the feedback and obtain an advantage from the interesting points in ads. In addition, the sequence learning outperformed the accuracy through learning of data sequence.

References

[Shu 2018] L. Shu, J. Xie, M. Yang, Z. Li, Z. Li, D. Liao, X. Xu, X. Yang; A Review of Emotion Recognition Using Physiological Signals, Sensors, 18(7), 2018.

[Ragot 2017] M. Ragot, N. Martin, S. Em, N. Pallamin, J. Diverrez; Emotion Recognition Using Physiological Signals: Laboratory vs. Wearable Sensors, Advances in Human Factors in Wearable Technologies and Game Design, pp.15-22, 2017.

[Chen 2017] J. Chen, B. Hu, Y. Wang, P. Moore, Y. Dai, L. Feng, Z. Ding; Subject-independent emotion recognition based on physiological signals a three-stage decision method, BMC Medical Informatics and Decision Making, 17(3), 2017.

[Schmidt 2001] L.A. Schmidt and L.J. Trainor; Frontal brain electrical activity EEG distinguishes valence and intensity of musical emotions, Cognition and Emotion, 15(4), pp.487–500, 2001.

[Jenke 2014] R. Jenke, A. Peer, M. Buss; Feature Extraction and Selection for Emotion Recognition from EEG, IEEE Transactions on Affective Computing, 5(3), pp.327-339, 2014.

[Karpagachelvi 2010] S. Karpagachelvi, M. Arthanari, M. Sivakumar; ECG Feature Extraction Techniques - A Survey Approach, 2010.

[Chennamma 2013] H.R. Chennamma, X. Yuan; A Survey on Eye-Gaze Tracking Techniques, Indian Journal of Computer Science and Engineering, 4(5), pp. 388-393, 2013.

The 33rd Annual Conference of the Japanese Society for Artificial Intelligence, 2019

Deep Markov Models for Data Assimilation in Chaotic Dynamical Systems

Calvin Janitra Halim Kazuhiko Kawamoto

Chiba University

Recently, the use of deep learning in data assimilation has been gaining traction. One particular time series model known as deep Markov model has been proposed, along with an inference network that is trained together using variational inference. However, the original paper did not address the full capability of the model in data assimilation problem. Therefore, we aim to evaluate the suitability of a deep Markov model and its inference network against a chaotic dynamical system, which often shows up as a problem in data assimilation. We evaluate the model in various generative conditions. We show that when information about part of the target model is known, the model is able to match the capability of a smoothed unscented Kalman filter, even when there are process and observation noise involved.

1. Introduction

The advancement of computer processors has allowed the simulation of real-world processes, modelled by dynamical systems and numerical models. However, hurdles such as chaos and numerical errors prevented the use of these models for long term forecasting. This gave rise to data assimilation (DA) methods, utilizing both observations and numerical models as inputs to statistical methods to reduce estimation error.

Successes of deep learning have led researchers to focus on combining traditional DA methods with deep learning [Cintra 18]. One specific method trains a neural network-based Gaussian state-space model (GSSM) and an inference network together using variational inference [Krishnan 17].

Nevertheless, [Krishnan 17] didn't evaluate the model on chaotic dynamical systems, the primary target of DA, and the paper didn't address the capability of the model when only part of the generative model is available (namely, transition function and emission function), which indirectly shows the adaptive characteristics of the model. Thus, we aim to assess whether this method can be applied to such systems on various conditions (the availability of transition function or emission function during training).

2. Deep Markov Model

Krishnan et al. proposed a method consisting of a generative model and an inference network trained with variational inference [Krishnan 17]. The method uses evidence lower bound (ELBO) as an objective function, comparing the posterior latents generated by inference network with prior latents, along with maximizing the expected log-likelihood of observations generated by the generative network.

2.1 Generative Model

The generative model takes a sequence of latents and produces the corresponding observations. The model is a GSSM, whose transition and emission function can be substituted with neural networks, hence the name *deep Markov model* (DMM). The transition function uses a gated transition function (GTU), which is essentially a gated recurrent unit (GRU) [Cho 14] without being conditioned by the observations, similar to the Markovian properties of the latents.

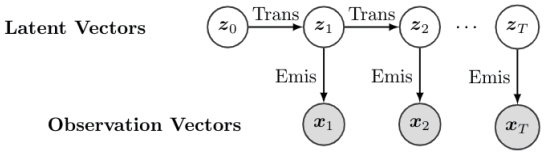

Figure 1: Generative Model (GSSM)

2.2 Inference Network

The inference network takes an observation sequence and infer its corresponding latents. This inference network is structured upon the factorization of the posterior latent distribution, which can be referred to [Krishnan 17]. [Krishnan 17] followed the factorization using a backward recurrent neural network (RNN), which outputs hidden unit for each time step, and then uses a *combiner* function, with the hidden unit and previous latent as input, to output/sample the approximate latent for current time step. As the RNN is propagated from future to the past, [Krishnan 17] uses the notation ST-R, which stands for *STructured-Right*, which we will also adopt. The structure for both generative model and inference network is shown by Figure 1 and Figure 2.

3. Experiments and Results

3.1 Dataset and Evaluation Methods

We train and evaluate the model on Lorenz-96 model [Lorenz 95], which exhibits chaos and is often used on many DA method evaluations. This model also has an atmospheric-like movement, which is similar to real-world atmospherical model. The model is defined by the differen-

Contact: Kazuhiko Kawamoto, Chiba University, 1-33, Yayoicho, Inage Ward, Chiba-shi, Chiba, 263-8522 Japan, +81-43-290-3508, kawa@faculty.chiba-u.jp

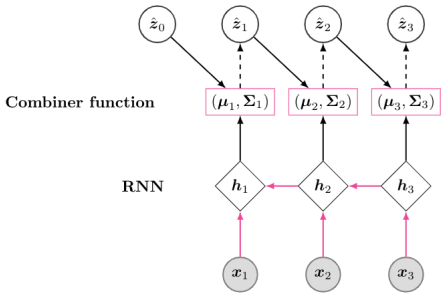

Figure 2: Inference Network (sequence length of 3)

tial equation:

$$\frac{dy^{(i)}}{dt} = (y^{(i+1)} - y^{(i-2)})y^{(i-1)} - y^{(i)} + F \tag{1}$$

where $y^{(i)}$ is the i-th state of the model, $y^{(-1)} = y^{(N-1)}, y^{(0)} = y^{(N)}, y^{(N+1)} = y^{(1)}$ and $\frac{dy^{(i)}}{dt}$ is the derivative of $y^{(i)}$ w.r.t time t. The F here is the forcing constant, which is set into 8.0 to give the model a chaotic movement [Lorenz 95]. We then set the transition and emission function of the generative model into stochastic processes:

$$\textbf{Transtion} : \boldsymbol{z}_t \sim \mathcal{N}(\text{Lorenz96RK4}(\boldsymbol{z}_{t-1}), 5I) \tag{2}$$

$$\textbf{Emission} : \boldsymbol{x}_t \sim \mathcal{N}(\boldsymbol{z}_t, 5I) \tag{3}$$

where I is identity matrix, the function Lorenz96RK4(.) is a 4th order Runge-kutta integration function of Lorenz-96 model, with time step difference of 0.01, and $\mathcal{N}(\boldsymbol{\mu}, \Sigma)$ denoting a multivariate Gaussian distribution with mean vector $\boldsymbol{\mu}$ and covariance matrix Σ. Both the latent and observation sizes are 20. The training and validation data has 5000 and 500 data each, with sequence length of 25.

We use a smoothed unscented Kalman filter (UKF) as baseline, and take the root-mean-square error (RMSE) between true latents, observations and their reconstructed counterparts as the measurement of the model capability. We also evaluated the model on 4 conditions imposed on the generative model:

1. Condition 1: *fixed transition and emission*
2. Condition 2: *unknown transition and fixed emission*
3. Condition 3: *fixed transition and unknown emission*
4. Condition 4: *unknown transition and emission.*

Here, *fixed* means setting the corresponding function of the generative model into the Equation 2 or 3, and *unknown* means setting the function to be not *known*, which is substituted with neural network that is to be inferred during training process. Also note that the smoothed UKF here is only evaluated on condition 1, as UKF is not an adaptive filter.

3.2 Results

The evaluation result is shown on Figure 3. *ST-R*, *UKF*, *Observations* denote the RMSE (vertical axis) of the DMM (with ST-R), UKF, and observations respectively, and the horizontal axis shows the training epochs. The result shows

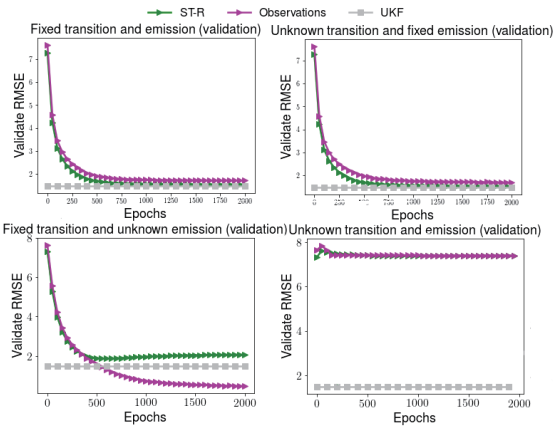

Figure 3: Validation RMSE on 4 conditions

that the RMSE of DMM converges to that of UKF as the training continues on condition 1, 2, and 3. This implies that DMM is capable of state estimation that rivals that of UKF, and is also able to infer part of the generative model when it is not given, showing the capability of DMM as an adaptive filter. However, the model couldn't estimate a system when only the observations are given. We believe that the reason for this lies in the insufficient information of the sampled observations in inferring a generative network that is unknown.

4. Conclusion

We showed that DMM is suitable enough to be used as a DA method, even with a chaotic dynamical system (with the addition of stochasticity) as the target. We plan to experiment further with harder grid problems and improve the model inference capability to surpass current DA methods.

Acknowledgements

This work was supported by JSPS KAKENHI Grant Number JP16K00231.

References

[Cintra 18] Cintra, R. S. and Velho, H. F. C.: Data assimilation by artificial neural networks for an atmospheric general circulation model. In *Advanced Applications for Artificial Neural Networks*, ch. 14 (2018)

[Krishnan 17] Krishnan, R. G., Shalit, U. and Sontag, D.: Structured inference networks for nonlinear state space model. In *AAAI* (2017)

[Cho 14] Cho, K., Merrinboer, B., Glehre, ., Bahdanau, D., Bougares, F., Schwenk, H. and Bengio, Y.: Learning phrase representations using rnn encoder-decoder for statistical machine translation. In *Proceedings of the 2014 Conference on EMNLP*, pp. 1724-1734 (2014)

[Lorenz 95] Lorenz, E.: Predictability: a problem partly solved. In *Seminar on Predictability*, Vol. 1, pp. 1-18 (1995)

The 33rd Annual Conference of the Japanese Society for Artificial Intelligence, 2019

Modelling Naturalistic Work Stress Using Spectral HRV Representations and Deep Learning

Juan Lorenzo Hagad[*1] Ken-ichi Fukui[*2] Masayuki Numao[*2]

[*1]Graduate School of Information Science and Technology
[*2] Institute of Scientific and Industrial Research
Osaka University, Japan

With the proliferation of wearable devices and the inflow of new health data, artificial intelligence is expected to revolutionize the field of wellness and health management by providing potential tools for analyzing harmful conditions like prolonged stress. Currently, one of the standard measurements used by medical practitioners to measure stress is heart rate variability (HRV), a set of numerical indices that reflect autonomic balance. However, recent advances in machine learning have shown that learned features tend to outperform hand-crafted features. In this work we propose a more expressive intermediate data representation based on Lomb-Scargle periodograms combined with the feature learning capabilities of deep learning. Using stress data from naturalistic work activities, we tested different shallow and deep learning architectures and show that significant improvements can be achieved compared to traditional HRV indices. Results show that models trained on our spectral-temporal representation significantly outperform models trained on traditional HRV indices for predicting naturalistic work stress.

1. Introduction

Findings from a large number of clinical studies [5, 8] have linked cardio-vascular disorders to psychological stressors. In particular, long-term exposure to stressful environments, such as those commonly found in offices, has been shown to be a major risk factor for major depressive disorder (MDD), a disorder that affects an estimated 350 million people across the world [9]. In response to this, we have witnessed a surge in the development of ambient intelligences for the purpose of mental health and stress monitoring [1].

1.1 HRV Stress Analysis

Historically, heart rate variability (HRV) spectrograms were used by medical practitioners as the primary tool to measure cardiac neural regulation externally. This was brought out by findings that mental and physical states have certain effects on cardiac rhythm that could easily and unintrusively be measured with electrocardiographs (ECG) [6]. In the past few decades, studies have established the connection between HRV and the sympatho-vagal stress response as being visible in both the time and frequency domains. Through experiments and empirical anlaysis, these works have identified indices which show high correlations with physical and mental stress, particulary with the high and low frequency ranges [10]. However, even now there is no widely accepted standard for stress evaluation based on HRV features. In recent surveys [14, 7] it has been found that neurobiological evidence links some components of HRV to activity in cortical regions related to stress appraisal as well as other brain mechanisms. As it stands, it seems that one of the main challenges is identifying which components of HRV may be relevant to evaluating stress.

Contact: Juan Lorenzo Hagad, Department of Architecture for Intelligence, 8-1 Mihogaoka, Ibaraki, Osaka, 567-0047, Japan, +81-6-6879-8426, hagad@ai.sanken.osaka-u.ac.jp

1.2 Deep Learning and Heart Rate Analysis

Traditionally, affective analysis such as those done for stress have mostly focused towards using visual or auditory measures [15], where deep learning has been found to be effective. In recent years, others works in the field of ECG analysis for medical applications have also pushed for end-to-end applications of deep learning. In one of the most prominent works [12] they used a 34-layer residual convolutional neural network (CNN) to analyze raw ECG sequences in order to identify 14 different types of arrhythmia. Using a very large dataset of over 60,000 recordings they were able to train a model that performed better on average than actual cardiologists recruited for the experiment. Their work demonstrates how deep learning is able to identify structural patterns in heart rate data. In our work, we attempt to exclude morphological patterns and instead focus on frequency-related features of heart beats. Towards this end we introduce the use of short-time Lomb-Scargle (LS) spectrograms to train CNNs.

2. Methodology

This work aims to use spectral HRV data representations together with deep learning models to predict mental stress. Specifically, we use a sliding window Lomb-Scargle approach to build a spectrogram of heart rate in lieu of the traditional short-term Fourier transform (STFT). Next, we use pre-built deep models designed for image recognition and compared them with more simplified architectures and train them to recognize stress. In the following sections we describe the experiments and tools used in this research.

2.1 Dataset

For the following experiments we use the same work stress dataset introduced in a previous work [4]. It consists of ECG recordings of subjects performing naturalistic desk work activities in front of a PC. The dataset was gathered

from four subjects each contributing five separate hour-long sessions. This provided us with a total of 20 hours of ECG data that was used for training and testing.

2.2 Signal Processing

Previous works on spectral anlaysis of HRV applied the fast fourier transform (FFT) [17] to produce periodograms from which the power of different frequency bands can be measured and compared. However, one limitation of the FFT algorithm is that it assumes that all samples used for analysis are evenly spaced in time. This poses a fundamental issue for heart rate since the RR intervals used to represent detected heart beats are not evenly sampled. A study [2] has shown that data resampling methods used to align RR interval data for FFT analysis can lead to artifacting and higher errors in the final PSD estimation. A better alternative has been put forward in the form of the Lomb-Scargle periodogram, a method based on FFT that does not require evenly sampled data.

2.2.1 Lomb-Scargle Periodogram

Periodograms are some of the most basic tools used for spectral analysis, the most common of which is the discrete Fourier transform (DFT). The DFT can be defined for any sampled dataset, $X(t_i), i = 1, 2, ..., N_0$ as,

$$FT_X(\omega) = \sum_{j=1}^{N_0} X(t_j) \exp(-i\omega t_j). \tag{1}$$

The periodogram can then be defined as,

$$\begin{aligned} P_X(\omega) &= \frac{1}{N_0}|FT_x(\omega)|^2 \\ &= \frac{1}{N_0}\left|\sum_{j=1}^{N_0} X(t_j)\exp(-i\omega t_j)\right|^2 \\ &= \frac{1}{N_0}\left[\left(\sum_j X_j \cos\omega t_j\right)^2 + \left(\sum_j X_j \sin\omega t_j\right)^2\right] \end{aligned}, \tag{2}$$

[3] which while sufficient for calculating an accurate estimation of the FFT of most signals was found to be sensitive to noisy signals and other artifacts [16]. In practice, it is necessary to apply additional spectral smoothing equations, such as *spectral window functions*, to reduce the variances of the spectrum. Most of these methods are designed to be applied on evenly sampled data. Though some may also be applied to the unevenly sampled case, such as in RR intervals, it has been found that it can lead to higher error and increased sensitivity to signal noise [11]. This can also be mitigated by the addition of more data for calculating the spectra as a way to taper off the signal-to-noise ratio, but this may not be an option for data-scarce or time-intensive domains. A reasonable alternative is the Lomb-Scargle periodogram [13], a notable method designed for use in calculating frequency spectrograms from unevenly sampled data streams such as heart beats. The equation is based on the FFT and is wholly similar but addresses some of the noise sensitivity and *spectral leakage* issues of the standard FFT equation. Here, the periodogram is defined as,

$$P_X(\omega) = \frac{1}{2}\left\{\frac{\left[\sum_j X_j \cos\omega(t_j-\tau)\right]^2}{\sum_j \cos^2\omega(t_j-\tau)}\right\} + \frac{\left[\sum_j X_j \sin\omega(t_j-\tau)\right]^2}{\sum_j \sin^2\omega(t_j-\tau)} \tag{3}$$

with τ defined as,

$$\tan(2\omega\tau) = \left(\sum_j \sin 2\omega t_j\right) \Big/ \left(\sum_j \cos 2\omega t_j\right). \tag{4}$$

This modified equation, outputs similar values to the original FFT in most cases, however it has a simpler statistical behavior and is equivalent to the reduction of the sum of squares in least-squares fitting of sin waves to data [13]. It is also time-translation invariant and reduces to a similar representation as DFT in cases where data is evenly spaced. This makes it ideal for HRV analysis and is the method used in this research. The next issue is how to tackle the non-stationary nature of heart rate. For this, we construct spectrograms from the periodograms.

2.2.2 Spectrogram Analysis

Spectrograms are visual representations of frequency spectra over time. They are tools that are used extensively in applications that deal with audio and radio signals. Recently, they have also seen frequent application in the analysis of physiological signals such as brainwaves and heart rate. The most common method used for building spectrograms is the short-time Fourier transform (STFT). Put simply it is built by applying the DFT over a pre-defined window of data and sliding the windowed function over the data series using a fixed amount of overlap. Formally, for any series $x(n)$ we can defined the STFT as,

$$X_w(mS, \omega) = \sum_{n=-\infty}^{\infty} x(n)w(n - mS)\exp(-j\omega n) \tag{5}$$

for analysis window w, frame index m and step size S [18]. The internal equation $\sum_{n=-\infty}^{\infty} x(n)w(n - mS)\exp(-j\omega n)$ represents the Fourier transform of $x_w(mS, \omega)$ and is stored in the matrix $\hat{X}$ whose columns are Fourier periodograms $P_X(\omega)$. To adapt the spectrogram to the unevenly sampled heart rate data, we replace this equation with the Lomb-Scargle equation,

$$\begin{aligned} X_w(mS, \omega) = \frac{1}{2}&\left\{\frac{\left[\sum_j x(n)\cos\omega(t_j-\tau)\right]^2}{\sum_j \cos^2\omega(t_j-\tau)}\right\} \\ &+ \frac{\left[\sum_j x(n)\sin\omega(t_j-\tau)\right]^2}{\sum_j \sin^2\omega(t_j-\tau)} \end{aligned} \tag{6}$$

In this way we mitigate the sensitivity of the standard STFT while maintaining its ability to capture the nonstationary patterns in the temporal data. In effect, we end up with a very high dimensional representation that could potentially have more expressive and appropriate features for detecting stress. The next step is to use machine learning to discover these features and compare the performance

difference with models based on traditional HRV features. Due to the 2D spatial nature of data representation, convolutional neural networks should provide an efficient learning architecture.

3. Experiments and Validation

3.1 Dataset and Models

For the following experiments, we applied a sliding window method to the stress dataset in order to segment the data. This method also lends itself to real-time processing in the future. Through empirical testing, we found that 505-beat windows (6 mins) showed the best balance between stability and expressiveness while staying above the 5-minute minimum length recommended for short-term HRV analysis. We also applied a modal labelling scheme for segments which overlapped between multiple labels. However, we tweaked the unimodal threshold to 70% so segments with modal valued samples greater than the threshold could be labelled with the modal value, otherwise it would be marked as a "transitional" segment. The final experiment dataset was comprised of 1,500 windowed samples which were either labelled based on the 4-level stress annotation or as transitions.

For modeling, we trained perceptron and autoencoder models using the stress HRV data to serve as baselines and compared these to convolutional neural network (CNN) models trained on our spectral HRV data representation. The convolutional layers were topped with a 128-unit dense layer to match the ones used for the non-deep HRV stress models. For the CNN models, we tested both standard deep learning models typically used for image classification tasks as well as shallower CNN architectures to verify the hierarchical feature requirements of the dataset. Performance was validated using stratified 10-fold cross-validation.

3.2 Results and Discussion

First, we analyze the performance results for models trained on the standard HRV features, which were 14 time and frequency domain features, and compared them to the deep ResNet model trained on the LS spectrum data. As seen in Figure 1, the baseline HRV-MLP model achieved 52% test accuracy which was improved by up to 60% by applying denoising autoencoders for more efficient latent feature selection. These results are well-above the 20% random classification on this 5-class dataset.

3.2.1 Deep Spectral Model

Moving over to the spectral models, ResNet50 was able to achieve over 80% testing accuracy, which is well above both of the traditional HRV baselines. These significant gains could be explained by the effective combination of the more expressive spectral data with the feature learning ability of deep learning algorithms. The traditional indices used in traditional HRV analysis help humans understand physical conditions, but they may also obfuscate some intricate features that may be necessary for deeper affective analysis. By allowing the model to learn from a spatial-spectral representation, we are able to train a more effective model. However, this comes at the cost of increased complexity since the standard 50-residual unit model requires over 25 million parameters. This not only leads to higher data requirements, but may also lead to more challenges in interpretation and optimization.

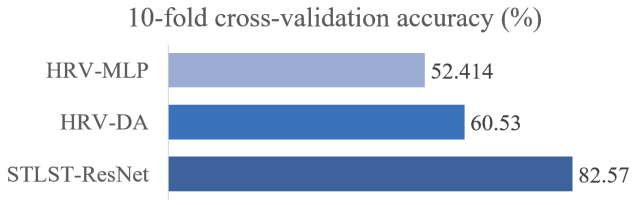

Figure 1: Comparison of test performance results between models trained on standard HRV features (MLP and DA) and the ResNet model trained on STLST heart rate spectrum data.

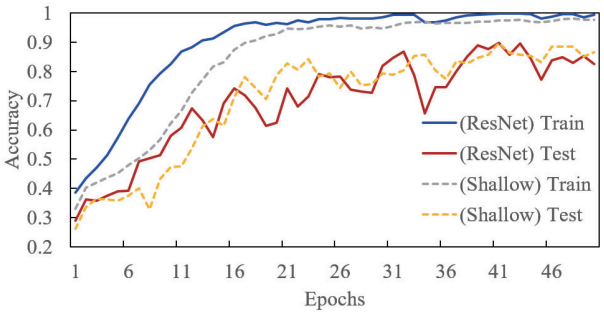

Figure 2: Learning and test performance of ResNet50 and the shallower 5-layer CNN model.

3.2.2 Shallow Spectral Model

To help alleviate the problem of increased complexity, we attempted to train a more compact model. For these tests, the goal was to reduce the depth and overall complexity of our model without compromising performance. This ultimately culminated in a model featuring 5 intermediate 128-filter CNN layers with BatchNorm for regularization. The relatively shallow model also meant residual units were unnecessary and training was much faster than the deeper model. It should also be noted that tests were also performed on shallower models below 5 layers, but this typically lead to larger performance variations and more noticeable overfitting. Figure 2 shows a comparison of the learning process of both the deep and shallow models. Despite using less than 1 million parameters, as opposed to the over 25 million of ResNet50, the shallow model is able to match the performance of the much larger ResNet model while also avoiding overfitting. Actual training time could also reduced by up to 5x which may be useful in situations where occasional retraining is necessary.

4. Summary and Future Work

In this work we trained a deep model of work stress using a spectral representation of heart rate extracted using short-time Lomb-Scargle transform. The experiments showed that the deep models trained on the spectral rep-

resentation could easily outperform those trained on the traditional HRV features for detecting naturalistic stress levels. Additionally, we show that even relatively shallow models featuring at least 5 convolutional layers can match the performance of ResNet50, this could indicate that at least some shallow hierarchical features may be important for effectively modelling naturalistic stress from heart rate. In future work we plan to investigate further the specific features learned by our model through feature activation analysis. We also plan to train and compare the performance of the model on other affective computing datasets for emotion. Finally, it would benefit the affective computing community greatly if we can develop optimal representations that can enable the aggregation of data using different devices and dataset to build a single model that contains all the richest features for HRV analysis.

References

[1] G. Acampora, D.J. Cook, P. Rashidi, and A.V. Vasilakos. A survey on ambient intelligence in healthcare. *Proceedings of the IEEE*, 101(12):2470–2494, Dec 2013.

[2] Gari D Clifford and Lionel Tarassenko. Quantifying errors in spectral estimates of hrv due to beat replacement and resampling. *IEEE transactions on biomedical engineering*, 52(4):630–638, 2005.

[3] T Jr Deeming. Fourier analysis with unequally-spaced data. *Astrophysics and Space Science*, 36(1):137–158, 1975.

[4] Juan Lorenzo Hagad, Ken-ichi Fukui, and Masayuki Numao. A hierarchical model of authentic work stress using physiological signals and stress coping profiles. In 人工知能学会全国大会論文集 *2016* 年度人工知能学会全国大会 *(*第 *30* 回*)* 論文集, pages 3E34–3E34. 一般社団法人人工知能学会, 2016.

[5] H. Iso, C. Date, A. Yamamoto, H. Toyoshima, N. Tanabe, S. Kikuchi, T. Kondo, Y. Watanabe, Y. Wada, T. Ishibashi, H. Suzuki, A. Koizumi, Y. Inaba, A. Tamakoshi, and Y. Ohno. Perceived mental stress and mortality from cardiovascular disease among Japanese men and women: the Japan Collaborative Cohort Study for Evaluation of Cancer Risk Sponsored by Monbusho (JACC Study). *Circulation*, 106(10):1229–1236, Sep 2002.

[6] Markad V Kamath, Dhanjoo N Ghista, Ernest L Fallen, David Fitchett, Donald Miller, and Robert McKelvie. Heart rate variability power spectrogram as a potential noninvasive signature of cardiac regulatory system response, mechanisms, and disorders. *Heart and vessels*, 3(1):33–41, 1987.

[7] Hye-Geum Kim, Eun-Jin Cheon, Dai-Seg Bai, Young Hwan Lee, and Bon-Hoon Koo. Stress and heart rate variability: A meta-analysis and review of the literature. *Psychiatry investigation*, 15(3):235, 2018.

[8] E. Kowata, A. Hozawa, M. Kakizaki, Y. Tomata, M. Nagai, Y. Sugawara, S. Kuriyama, and I. Tsuji. [Perceived stress and cardiovascular disease mortality. The Ohsaki Cohort Study]. *Nihon Koshu Eisei Zasshi*, 59(2):82–91, Feb 2012.

[9] M. Marcus, M.T. Yasamy, M. van Ommeren, and D. Chisholm. Depression: A global public health concern. Technical report, World Health Organization, 2012.

[10] Paolo Melillo, Marcello Bracale, and Leandro Pecchia. Nonlinear heart rate variability features for real-life stress detection. case study: students under stress due to university examination. *BioMedical Engineering OnLine*, 10:96+, November 2011.

[11] G.B. Moody. Spectral analysis of heart rate without resampling. In *Computers in Cardiology 1993, Proceedings.*, pages 715–718, Sep 1993.

[12] Pranav Rajpurkar, Awni Y Hannun, Masoumeh Haghpanahi, Codie Bourn, and Andrew Y Ng. Cardiologist-level arrhythmia detection with convolutional neural networks. *arXiv preprint arXiv:1707.01836*, 2017.

[13] Jeffrey D Scargle. Studies in astronomical time series analysis. ii-statistical aspects of spectral analysis of unevenly spaced data. *The Astrophysical Journal*, 263:835–853, 1982.

[14] Julian F Thayer, Fredrik Åhs, Mats Fredrikson, John J Sollers III, and Tor D Wager. A meta-analysis of heart rate variability and neuroimaging studies: implications for heart rate variability as a marker of stress and health. *Neuroscience & Biobehavioral Reviews*, 36(2):747–756, 2012.

[15] Panagiotis Tzirakis, George Trigeorgis, Mihalis A Nicolaou, Björn W Schuller, and Stefanos Zafeiriou. End-to-end multimodal emotion recognition using deep neural networks. *IEEE Journal of Selected Topics in Signal Processing*, 11(8):1301–1309, 2017.

[16] Jacob T VanderPlas. Understanding the lomb–scargle periodogram. *The Astrophysical Journal Supplement Series*, 236(1):16, 2018.

[17] Peter Welch. The use of fast fourier transform for the estimation of power spectra: a method based on time averaging over short, modified periodograms. *IEEE Transactions on audio and electroacoustics*, 15(2):70–73, 1967.

[18] Xinglei Zhu, Gerald T Beauregard, and Lonce L Wyse. Real-time signal estimation from modified short-time fourier transform magnitude spectra. *IEEE Transactions on Audio, Speech, and Language Processing*, 15(5):1645–1653, 2007.

International Session | International Session | [ES] E-5 Human interface, education aid

[2J1-E-5] Human interface, education aid: education

Chair: Katsutoshi Yada (Kansai University)

Wed. Jun 5, 2019 9:00 AM - 10:40 AM Room J (201B Medium meeting room)

[2J1-E-5-01] Teaching Reinforcement Learning and Computer Games with 2048-Like Games

○Hung Guei[1], Ting-Han Wei[1], I-Chen Wu[1] (1. National Chiao Tung University)

9:00 AM - 9:20 AM

[2J1-E-5-02] Feature Extraction of Onomatopoeia Considering Phonotactics for Automatic Semantic Usage Classification of Onomatopoeia

○Hiromu Takayama[1], Nastumi Takeuchi[1], Daiki Urata[1], Tsuyoshi Nakamura[1], Ahmed Moustafa[1], Takayuki Ito[1] (1. Nagoya Institute of Technology)

9:20 AM - 9:40 AM

[2J1-E-5-03] Vibrational Artificial Subtle Expressions to Convey System's Confidence Level to Users

○Takanori Komatsu[1], Kazuki Kobayashi[2], Seiji Yamada[3], Kotaro Funakoshi[4], Mikio Nakano[4] (1. Meiji University, 2. Shinshu University, 3. National Institute of Informatics/Tokyo Institute of Technology/SOKENDAI, 4. Honda Research Institute Japan)

9:40 AM - 10:00 AM

[2J1-E-5-04] A think-programming method based on free texts "almost" in English

○Keisuke Nakamura[1] (1. KnowrelSystem,Inc.)

10:00 AM - 10:20 AM

[2J1-E-5-05] Affective Tutoring for Programming Education

○Thomas James Zarraga Tiam-Lee[1], Kaoru Sumi[1] (1. Future University Hakodate)

10:20 AM - 10:40 AM

The 33rd Annual Conference of the Japanese Society for Artificial Intelligence, 2019

Teaching Reinforcement Learning and Computer Games with 2048-Like Games

Hung Guei* Ting-Han Wei* I-Chen Wu*

* Department of Computer Science, National Chiao Tung University, Hsinchu, Taiwan

2048-like games are a family of single-player stochastic puzzle games, which consist of sliding numbered-tiles that combine to form tiles with larger numbers. Notable examples of games in this family include Threes!, 2048, and 2584. 2048-like games are highly suitable for educational purposes due to their simplicity and popularity. Numerous machine learning methods have been proposed for 2048, which provide a good opportunity for students to gain first-hand experience in applying these techniques. This paper summarizes the experience of using different 2048-like games, namely Threes! and 2584, as pedagogical tools for teaching reinforcement learning and computer game algorithms. With two classes of graduate level students, the average win rates for 2584 and Threes! reached 96.1% and 93.5%, respectively. The course designs were also well received by students, with 4.21/5 and 4.35/5 points from student feedbacks.

1. Introduction

2048 is a single-player stochastic puzzle game introduced as a variant of 1024 and Threes! [Cirulli 2014]. 2048 is easy to learn and to play reasonably well, yet mastering the game is far from trivial. Many machine learning methods have been applied to 2048 such as the well-known Temporal Difference Learning [Szubert 2014]. As a teaching tool, 2048's popularity can increase student engagement, while the existing machine learning methods for it provide a well-established basis to educate from.

We have summarized the experience of using 2584, a variant of 2048, as the pedagogical tool for teaching reinforcement learning and computer game algorithms [Guei 2018]. In this paper, we extend our previous work, propose a new course design for Threes! and summarize the experiences and list the differences between using Threes! and 2584 in the curriculum. With two consecutive classes of graduate level students, the average win rate for 2584 and Threes! student projects reached 96.1% and 93.5%. The course projects were also well received by students, with 4.21/5 and 4.35/5 points from feedbacks.

This paper is organized as follows. Section 2 introduces 2048-like games and reviews existing related techniques. Section 3 shows how teaching material is designed with Threes! in our courses, summarizes student results, and compares differences with previous 2584 lectures. Section 4 provides student feedback and makes concluding remarks.

2. Background and Related Techniques

In this section, we will first introduce some 2048-like games, then briefly review important relevant algorithms and techniques.

2.1 Single-player 2048-like Games

We first describe the game, 2048[1], and then 2584[2] and Threes![3], the first two of which are derived from Threes!. 2048 is a 4×4 puzzle (16 grids), starting with two tiles. Each grid on the puzzle is either empty or contains a numbered tile with a value that is a power of two. The objective is to slide the puzzle such that the tiles merge into larger tiles.

Upon the player sliding the puzzle, all tiles will slide to the specified direction as far as possible. Adjacent tiles with the same value, say v-tile, will be merged into a larger tile, $2v$-tile, and the player will receive a reward $2v$. A sliding direction is illegal if the puzzle remains unchanged after sliding.

The environment immediately generates a new tile after the player slides the puzzle. The new tile can be either a 2-tile or a 4-tile, with the probabilities of 0.9 and 0.1, respectively. The new tile will be randomly placed at any empty grid.

After the new tile has been added, the player continues to slide the puzzle. This process repeats until no legal direction is possible. The final score is the sum of rewards gained from merging. Players win if a 2048-tile is generated.

For 2584, tiles are labeled by the numbers in the Fibonacci series, instead of powers of two. The environment generates 1-tiles and 2-tiles with the probabilities of 0.9 and 0.1. However, instead of merging tiles with the same value, two adjacent tiles whose values are adjacent numbers in the series are merged. Players win if a 2584-tile is generated.

Threes! is a game originally developed by Vollmer and Wohlwend. In Threes!, the game starts with nine initial tiles. The sliding distance is at most one. A 1-tile and a 2-tile can be merged into a 3-tile; for tiles with values v between $3 \leq v < 6144$, two v-tiles can be merged into a $2v$-tile. The 6144-tile is designed so that it can no longer be merged.

In Threes!, a *hint* is observable for the next generated tile before sliding the puzzle. The generated tile will be randomly placed at a newly cleared empty space (generated by sliding a 1-tile) on the opposite side of the last sliding direction. The type of generated tiles is controlled by the so-called *bag rule* and *bonus rule*. Consider a bag of 12 tiles composed of equal amounts of 1-, 2-, and 3-tiles. A tile is randomly selected and removed from the bag during tile generation, until the bag is empty and then refilled. The bonus rule states that when the largest tile on the current puzzle,

Contact: I-Chen Wu, Department of Computer Science, National Chiao Tung University, Taiwan, +886-3-5731855, +886-3-5733777, icwu@cs.nctu.edu.tw

[1] Available at https://gabrielecirulli.github.io/2048/

[2] Available at https://davidagross.github.io/2048/

[3] Available at http://asherv.com/threes/ and http://threesjs.com/

the $v_{\max}$-tile, is at least a 48-tile, there is a probability of $1/21$ to generate a bonus v_+-tile where $6 \leq v_+ \leq 1/8 \times v_{\max}$ and each possible value for v_+ has equal probability. For the remaining $20/21$ cases, bag tiles are generated.

The game ends when the player has no legal direction to slide. The final score is the sum of $3^{\log_2(v/3)+1}$ of all v-tiles with $v \geq 3$. In this paper, players are said to win if a 384-tile is generated.

2.2 Two-player 2048-like Games

In this paper, 2048-like games are modified into a two-player games as follows. While one player is still called *player*, his opponent is called *adversary* to play the role of an antagonistic environment that makes the player more difficult to play, i.e., the player maximizes the score, while the adversary minimizes it.

Thus, the modified two-player game begins with the adversarial side. First, the adversary places some tiles on an empty puzzle. Then, the player and the adversary take turns sliding the puzzle or placing a tile. The game ends when the player is unable to slide.

2.3 Generic Framework of 2048-like Games

All the puzzles in 2048-like games can be categorized into two kinds of states: *before-states* and *after-states*. An instance of a 2048-like game begins with a special before-state called the *initial state*. The player performs an *action*, i.e., sliding the puzzle, to the before-state, upon which the before-state will transform into an after-state. The environment then makes changes to the after-state, which renders it into another before-state for the next *time step*. The game continues until reaching a *terminal state*, which is a before-state for which the player is unable to perform any actions.

2.4 Techniques Related to 2048-like Games

(1) Tree Search

The original single-player 2048 is an expectimax game. In the case of a two-player game where the adversary can determine both the type and the position of new tiles, the game follows the minimax paradigm. Conversely, if the type of new tile is decided randomly and the adversary can only determine the position, the game conforms to the expectiminimax paradigm. In practice, heuristic or value functions are combined with tree search since there tends to be insufficient time to expand to leaf nodes.

(2) Temporal Difference Learning

Temporal Difference Learning (TD) is a reinforcement learning method [Sutton 1998] which was first applied to 2048 in 2014. [Szubert 2014]. The simplest TD(0) updates the value function $\mathrm{V}(s_t)$ with the prediction error $\delta = r_t + \gamma \mathrm{V}(s_{t+1}) - \mathrm{V}(s_t)$ from subsequent values through $\mathrm{V}(s_t) \leftarrow \mathrm{V}(s_t) + \alpha\delta$, where t is the time step, α is the learning rate, and γ is the discount factor. The value function $\mathrm{V}(s_t)$ can be viewed as the expected return of a given state s_t. Therefore, a policy $\pi(s_t)$ can be derived as $\pi(s_t) = \underset{a_t}{\operatorname{argmax}}\big(r_t + \mathrm{P}(s'_t, s_{t+1})\mathrm{V}(s_{t+1})\big)$, where $\mathrm{P}(s'_t, s_{t+1})$ is the probability of transition from an after-state s'_t to a state s_{t+1}.

The general form, TD(λ), updates the value function with all subsequent errors with a trace decay parameter λ. Higher λ values increase the proportion of prediction error from more distant states and actions [Sutton 1998]. TD(0.5) has been successfully applied to 2048 [Yeh 2017] [Jaśkowski 2017].

Forward update and backward update are both possible for TD implementation. Forward update here refers to the scheme where all states are updated in order of an episode from initial state to terminal state; backward update reverses the order. Backward update is slightly better than forward update when the training episodes are the same [Matsuzaki 2017a]. Also, backward update is easier for students to understand and implement [Guei 2018].

Multi-stage Temporal Difference Learning (MS-TD) divides the entire episode into several stages, each with a unique function approximator. It has been applied to 2048 and has successfully reached the first-ever game with 65536-tile by computer program [Wu 2014] [Yeh 2017]. Several other implementations have also been investigated, such as finding more optimal ways to divide stages [Jaśkowski 2017] [Matsuzaki 2017b].

Temporal Coherence Learning (TC) is a variant of TD with adaptive learning rates, which has been applied to 2048 [Jaśkowski 2017]. The update amount is controlled by the parameter α and the coherence $\sum|\delta|/|\sum\delta|$, where δ is the TD error of each update. Therefore, the update amount decreases if the TD error δ starts to oscillate between positive and negative values.

(3) Function Approximator

The state spaces of 2048-like games are quite large, which makes it unaffordable for current computers to store the entire state space with a direct mapping table. Therefore, a function approximator can be an efficient way to obtain state values.

N-tuple networks are a well-known function approximator for 2048-like games since 2014 [Szubert 2014]. An n-tuple network estimates the value of a state by extracting features from the state and accumulating feature values, where features are usually sub-puzzles in 2048-like games. The performance of n-tuple networks is highly correlated with feature design. Good configurations are not trivial, and have been investigated as a topic of research [Yeh 2017] [Matsuzaki 2016]. Each feature maps to an entry of a lookup table. The value function is therefore $\mathrm{V}(s) = \sum_i^m \mathrm{LUT}[\phi_i(s)]$, where LUT is the weight table, m is the total number of features, and ϕ_i refers to the i^{th} feature. Features are updated as follows, $\mathrm{LUT}[\phi_i(s)] \leftarrow \mathrm{LUT}[\phi_i(s)] + (1/m)\alpha\delta$.

Deep neural networks (DNN) and convolutional neural networks (CNN) can also be used as function approximators for 2048 [Guei 2016] [Wei 2019]. Compared with n-tuple networks, DNNs usually consist of fewer weights overall, but more weights are involved for each output. At the time of writing, strong 2048-like game programs currently use n-tuple networks as the function approximator [Yeh 2017] [Jaśkowski 2017]. Using DNNs efficiently for 2048-like games is still an open research topic.

3. Course Design and Student Results

Theory of Computer Games is a course taught by Professor I-Chen Wu at National Chiao Tung University, Hsinchu, Taiwan. The course is designed for graduate level students, and the prerequisites are Algorithms and Data Structures. Also, students are expected to be moderately proficient at programming.

Students are required to develop a game-playing program as the term project during the semester, which spans about five months. The overall program is broken down into six projects, which are built on top of each other. In the series of projects, students are required to develop their program step by step.

In the subsequent subsections, we will first give a short summary of each project, and then compare the difference of using 2584 and Threes! in the curricula for 2017 and 2018, respectively.

- Project 1: Learning to use the framework
- Project 2: Train the player using TD and n-tuple networks
- Project 3: Solve a reduced game by expectimax
- Project 4: Further improve the performance of the player
- Project 5: Design the adversarial environment
- Project 6: Participate in the final tournament

3.1 Learning to Use the Framework

First of all, students need to set up the framework and prepare the training environment for the coming projects in two weeks. We provide a demo of 2048 as the framework[4], where the students are expected to modify the rules to the target game. Since the original rules for Threes! is complex, we simplify them as in Table 1.

Table 1. Rule simplifications in Project 1

2584	The same as original 2584.
Threes!	Bag size is set to 3; no bonus tiles. New tiles can be placed at any empty position on the opposite side of the last sliding direction.

3.2 Train the Player Using TD and N-tuple Networks

Students are required to train a strong player using TD with n-tuple networks in one month. The main purpose is to ensure that students understand the mechanism of TD and n-tuple networks.

The environments follow that described in Table 1. We recommend students to start with the simplest feature design, which contains 4 rows and 4 columns, for a total of 8 standalone 4-tuple patterns. The initial learning rate α is 0.1.

Table 2. Average win rate and n-tuple in Project 2

	Avg. win rate	Avg. n for n-tuples
2584 34 students	$96.1\% \pm 4.2\%$ 10 reached 100%	4.6 ± 0.8 # of {4,5,6}-tuple: {20,7,7}
Threes! 43 students	$93.5\% \pm 11.2\%$ 5 reached 100%	5.6 ± 0.8 # of {4,5,6}-tuple: {9,1,33}

We use the win rate to analyze the performance of student programs. As shown in Table 2, reaching the 2584-tile in 2584 seems to be easier than reaching the 384-tile in the simplified version of Threes!.

The average n of n-tuples is also different. Most of the students applied a 6-tuple configuration in Threes! since it has better performance. However, not so many students tried 6-tuples in 2584 since the tile indices can easily grow to more than 20, resulting in a much higher memory cost.

3.3 Solve a Reduced Game by Expectimax

The aim of this project is to familiarize the students with the expectimax paradigm. Students need to use the expectimax search to solve a reduced game with a puzzle size of 2×3. The time allocated for this project is at most one month.

The environments are still the same. However, there is only one initial tile for Threes!. In project 3, student solvers are required to answer the expected value of given input questions. The average numbers of solved questions are listed in Table 3.

Solving 2×3 Threes! seems to be harder than 2×3 2584, as shown in Table 3. There are two potential reasons for this. First, we observed that the students ran into difficulties implementing expectimax search with hints, which was unique to Threes!. Since the framework we provided was designed for 2048, students needed to program hint processing on their own. Second, we introduced some changes to Threes! in 2018 to increase the project difficulty, so that we can better discriminate student performance.

Table 3. Average questions solved in Project 3

	Avg. solved
2584 34 students	$99.9\% \pm 0.5\%$ 31 reached 100%
Threes! 35 students	$92.5\% \pm 15.5\%$ 24 reached 100%

In 2018, students need to answer not only the expected value, but also the best and the worst value. The best value occurs when the player is extremely lucky, i.e., the environment coincidentally generates tiles which leads the player to the highest score under oracle play. The worst value is exactly the opposite. Although this definition is not difficult to understand, more specifications tend to lead to more avenues of error for students.

3.4 Further Improve the Performance of the Player

The objective is encouraging students to improve their player with optional methods. Project 4 is similar to Project 2, but with more stringent environments, which we show in Table 4.

Table 4. Rule modifications in Project 4

2584	*1-tiles and 3-tiles* are generated with probabilities of *0.75 and 0.25*, respectively.
Threes!	*Bag size and bonus tiles follow original*. New tiles can be placed at any empty position on the opposite side of the last sliding direction.

Note: Differences between Project 4 and Project 2 are in italic.

Students are required to retrain their players under the new environments. Several possible improvements are needed to achieve a comparable level of performance. Regardless of the method chosen, Project 4 is expected to be finished in one month.

Our first suggestion to students is adding the expectimax search that has already been implemented in Project 3. The second is using complex network structures, isomorphism of features may also be needed to avoid high memory usage and to speed up training. The third is decreasing the learning rate if they have not yet done so. The last suggestion is trying some advanced TD methods, such as using TD(λ), TC, or MS-TD.

Table 5. Average win rate, n-tuple, and depth in Project 4

	Avg. win rate	Avg. n for n-tuples	Avg. depth*
2584 31 students	$82.0\% \pm 11.3\%$ 12 reached 90%	5.5 ± 0.7 # of {4,5,6}-tuple: {4,8,19}	2.6 ± 0.8 25 applied
Threes! 40 students	$88.8\% \pm 15.1\%$ 26 reached 90%	6.3 ± 0.7 # of {4,5,6,7†}-tuple: {2,0,21,17}	1.5 ± 0.9 10 applied

* The depth for no extra search is 1; for an additional 1-ply search is 3.
† Extra encoding such as hints is counted as 1.

The final results of Project 4 are shown in Table 5. Contrary to previous results, students got better performances in Threes!. One reason is that the rule changes for 2584 is much more difficult, as 3-tiles are unmergeable with neither 1-tiles nor other 3-tiles, and are generated with a high probability of 0.25. Another possible reason for this result is the usage of large networks. Many students encoded the hint for the next generated tile into their network,

[4] https://github.com/moporgic/2048-Framework/branches/

which greatly improved the performance. Since the tile is limited to 6144-tile (14^{th}), students can also enlarge the network easily.

Since the expectimax project for Threes! in 2018 was quite difficult, relatively fewer students added expectimax into their player. The average win rate might have been higher if expectimax was applied more often.

3.5 Design the Adversarial Environment

The objective of Project 5 is to build an adversary, which is a clear departure from previous projects where students work solely from the perspective of the player. The adversary in two-player Threes! can control both the type and position of a new tile, which conforms to the minimax paradigm. In contrast, the adversary in 2584 can only control the position, while the type is randomly generated, which conforms to an expectiminimax paradigm.

One month is given for Project 5. The best practice is retraining networks for player and adversary under the new paradigms. Note that it is possible to make an adversary by reusing the network and choosing the minimum value. However, the performance may drop slightly due to paradigm mismatch.

Table 6. Average win rate, n-tuple, and depth in Project 5

	Avg. win rate	Avg. n for n-tuples	Avg. depth*
2584 31 students	87.5% ± 14.7% 18 reached 90%	5.5 ± 0.7 # of {4,5,6}-tuple: {4,7,20}	2.9 ± 0.5 29 applied
Threes! 37 students	52.7% ± 35.6% 9 reached 90%	6.4 ± 0.7 # of {4,5,6,7†}-tuple: {2,0,17,18}	2.4 ± 0.9 25 applied

* The additional 1-layer search of reusing the network is not included.
† Extra encoding of the network such as hints is counted as 1.

We also grade the adversary by its win rate, defined as the rate at which the player loses. The results are listed in Table 6. The variance of adversary performance in Threes! is quite large; this was unexpected since the minimax setting should have been easier to handle than the expectiminimax setting for 2584. It is possible that hint processing in search is much more complex, mistakes were made during network reuse, or minimax search was implemented incorrectly.

3.6 Participate in the Final Tournament

All students are required to participate in the final tournament. To determine the result between two students, two games are necessary: each student acts as the player and the adversary exactly once. The student whose player gets the higher score wins and receives one point. The ranking is then determined by the total number of points.

30 students participated in the 2584 tournament in 2017, and 40 students in the Threes! tournament in 2018. The top ranked student got 28 points in 29 matches in 2017; the winner for 2018 got 109 points in 117 matches for Threes!. It is worth mentioning that the top ranked programs adopted different strategies. The 1^{st} place 2584 program applied a simple 4-tuple network, while the 1^{st} place Threes! program applied a complex 7-tuple network.

Another difference between the above two tournaments was the wide use of advanced TD methods in 2018. Only a few students applied TC in 2017. However, many advanced TD methods such as TC, TC(λ), MS-TD appeared in 2018. This increased the strength of the highest-performing programs and intensified the competition between students.

4. Summary

For the popularity and simplicity of 2048, 2048-like games have become a staple application for reinforcement learning in the term project starting from 2014. From positive student feedbacks (4.21/5 and 4.35/5 points), experience sharing of students[5], and gradual improvement in program strength over years of using 2048-like games as term projects, we think 2048-like games are highly suitable for teaching computer game programming techniques and machine learning, especially for reinforcement learning. It can be a good pedagogical tool to motivate young minds in joining our field and community.

References

[Cirulli 2014] G. Cirulli, “2048, success and me”, Retrieved from http://gabrielecirulli.com/articles/2048-success-and-me, 2014.

[Guei 2016] H. Guei, T.-H. Wei, J.-B. Huang, and I-C. Wu, “An Empirical Study on Applying Deep Reinforcement Learning to the Game 2048”, Workshop Neural Networks in Games in the International Conference on Computers and Games, Springer, 2016.

[Guei 2018] H. Guei, T.-H. Wei, and I-C. Wu, “Using 2048-like Games as a Pedagogical Tool for Reinforcement Learning”, International Conference on Computers and Games, Springer, 2018.

[Jaśkowski 2017] W. Jaśkowski, “Mastering 2048 with delayed temporal coherence learning, multi-stage weight promotion, redundant encoding and carousel shaping”, Transactions on Computational Intelligence and AI in Games, IEEE, 2017.

[Matsuzaki 2016] K. Matsuzaki, “Systematic selection of N-tuple networks with consideration of interinfluence for game 2048”, Technologies and Applications of Artificial Intelligence, IEEE, 2016.

[Matsuzaki 2017a] K. Matsuzaki, “Developing a 2048 Player with Backward Temporal Coherence Learning and Restart”, Advances in Computer Games, Springer, 2017.

[Matsuzaki 2017b] K. Matsuzaki, “Evaluation of Multi-staging and Weight Promotion for Game 2048”, 高知工科大學紀要テクニカルレポート, 2017.

[Sutton 1998] R. S. Sutton, and A. G. Barto, “Reinforcement learning: An introduction”, MIT press, 1998.

[Szubert 2014] M. G. Szubert, and W. Jaśkowski, “Temporal difference learning of N-tuple networks for the game 2048”, Computational Intelligence and Games, IEEE, 2014.

[Wei 2019] T.-J. Wei, “A Deep Learning AI for 2048”, Retrieved from https://github.com/tjwei/2048-NN, 2019.

[Wu 2014] I-C. Wu, K.-H. Yeh, C.-C. Liang, C.-C. Chang, and H. Chiang, “Multi-stage Temporal Difference Learning for 2048”, Conference on Technologies and Applications of Artificial Intelligence, Springer, 2014.

[Yeh 2017] K.-H. Yeh, I-C. Wu, C.-H. Hsueh, C.-C. Chang, C.-C. Liang, and H. Chiang, “Multistage Temporal Difference Learning for 2048-Like Games”, Transactions on Computational Intelligence and AI in Games, IEEE, 2017.

[5] Some experiences of students are shared (in Chinese) at http://blog.sharknevercries.tw/2018/01/23/2584-AI and https://junmo1215.github.io/tags.html#2584-fibonacci-ref.

The 33rd Annual Conference of the Japanese Society for Artificial Intelligence, 2019

Feature Extraction of Onomatopoeia Considering Phonotactics for Automatic Semantic Usage Classification of Onomatopoeia

Hiromu Takayama[*1] Natsumi Takeuchi[*1] Daiki Urata[*1]

Tsuyoshi Nakamura[*1] Ahmed Moustafa [*1] Takayuki Ito[*1]

[*1] Nagoya Institute of Technology

Onomatopoeia is a language that imitates sounds and state of things. In particular, Japanese onomatopoeia has the merit of being able to communicate intuitively and concisely. On the other hand, onomatopoeia is a language that is hard to understand for people who do not speak Japanese natively. Therefore, this paper aims at estimating the meaning of onomatopoeia to support Japanese learners. Towards this end, I design a learner that automatically classifies Japanese onomatopoeia into their semantic usage. The input feature of this learner is extracted by focusing on the sound symbolism which is assumed to be the most important property of onomatopoeia. Therefore, this paper proposes a method to extract features of onomatopoeia considering their phonotactics. In the evaluation experiment, the efficiency of the proposed method is demonstrated by the fact that the precision of the proposed feature classifier exceeded those of the existing research.

1. Introduction

1.1 Background

In recent years, the number of foreigners (Japanese learners) who learn Japanese has been increasing. In this regard, Agency for Cultural Affairs [Agency for Cultural Affairs 1999] promotes policies for Japanese language education. However, there are some Japanese expressions which are difficult to learn and understand for Japanese learners. Onomatopoeia is a typical example.

onomatopoeia is generic term for onomatopoeic and mimetic words. Mimetic words represent and imitate state of things and living such as "zarazara"(rough), "sowasowa"(fidgeting) and the like, and mimetic terms, and onomatopoeias are represented by mimicking the sounds of nature and organisms such as "gatangoton"(trains run) , "gagya"(Humans cry). In addition, onomatopoeia has the advantage that it can realize more intuitive and realistic depictions than general vocabulary. For example, Fujino et al. [Fujino 2006] indicated that sports learning can be done efficiently by speaking onomatopoeia at the time of sports instruction. These results based on the hypothesis that the sound symbolism of onomatopoeia is strongly influenced by the people's five senses. Sound symbolism means that there exists a certain relationship between sound and meaning. This sound symbolism is unique to the mother tongue language, and it is recognized that any language contains sound symbolism. [Hinton 1995] Among them, there are these languages with strong sound symbolism such as Japanese and Korean, [Akimoto 2007] that is, these languages have many onomatopoeias. In particular, Japanese onomatopoeia are not only in large numbers but also with wide variety of meaning. As a result, onomatopoeia has been regarded as an important linguistic element in Japanese because of its very broad range of expressions compared to other languages. However, as mentioned above, there is the problem that the estimation of onomatopoeic meaning is difficult for those who do not have Japanese as their mother tongue, because the variety of onomatopoeia meaning and sound symbolism are unique to Japanese.

Therefore, this paper aims to support semantic estimation of onomatopoeia. Towards the end, we propose designing an automatic semantic usage classifier of onomatopoeia as the aim of this research.

1.2 Related works

Ample studies aimed at auto-classifying onomatopoeias into their semantic usage category. Towards this end, Ichioka et al. [Ichioka 2009] proposed frequency of vowels / consonants that are contained in onomatopoeia as an input feature (hereinafter referred to as phoneme feature) and attempts to auto-classify onomatopoeia that have similarity. In addition, Urata et al. [Urata 2017] proposed an acoustic model called mel-frequency cepstrum coefficients (MFCC) as input feature (hereinafter referred to as acoustic feature) and classified onomatopoeias into six semantic usage category. Moreover, Goriki et al. [Goriki 2018] attempted auto-classifying mimetic words into six semantic usage categories, using the estimated value that is obtained by integrating the results of the classifier of each of the phoneme feature and the acoustic feature described above.

Both of these studies extract features of onomatopoeia by focusing on the sound symbolism, and the proposed approach in this paper is based on this idea as well. However, in the previous studies, there exist two limitations. Firstly, in the work of Goriki et al. [Goriki 2018]., attention is focused only on the "frequency" of onomatopoeic vowel / consonant phoneme feature, and information on the "position" of the phoneme is not taken into consideration at all. For example, there are onomatopoeias have

Contact: Hiromu Takayama, Nagoya Institute of Technology, Gokiso-cho, Showa-ku, Nagoya-city, Aichi-prefecture, 466-8555, Japan, +81-52-735-5000
takayama.hiromu@itolab.nitech.ac.jp

two different meanings, such as "tobotobo" related to walking motion, and "botoboto" related to water and liquid, but their method, these two onomatopoeias have the same frequencies of vowels / consonants, As a result, their classifier will derive the same estimated value. Thus, since the onomatopoeic sound symbolism is constituted by the vowel / consonant belonging to onomatopoeia and also its "position", the feature extraction of the conventional method can't fully capture the features of onomatopoeia. Therefore, in the phoneme feature of onomatopoeia, "phoneme arrangement"(hereinafter referred to as phonotactics) should also be taken into consideration. Secondly, in the approach proposed by Goriki et al. [Goriki 2018], There is insufficient discussion on the accuracy evaluation of the proposed semantic auto-classifier of onomatopoeia. Conventional research showed the effectiveness of semantic estimation by deriving classifier accuracy using cross validation methods [Goriki 2018], but this only shows the estimation accuracy in machine (classifier). Therefore, it becomes important to investigate whether the estimation accuracy by the proposed classifier is the same as that of a human.

In order to overcome the above limitations, this paper proposes design of phoneme features that takes phoneme arrangement into account for auto-classifying the semantic usage of onomatopoeia, the effectiveness of the proposed method is shown by comparison experiment of classification accuracy of human and machine.

2. Preliminary

This paper proposes design of phoneme features that takes phoneme arrangement into account for auto-classifying onomatopoeia into their semantic usage. In particular, it is Hamano [Hamano 2014] that studied the phoneme sequence theory in detail, and in this paper we also extract features of onomatopoeia according to the onomatopoeic semantic structure model of Hamano [Hamano 2014]. In specific, Hamano assumed that onomatopoeia had two semantic structural patterns of CV type and CVCV type. Figure 1 demonstrate the CVCV type of the onomatopoeic semantic structure model of Hamano.

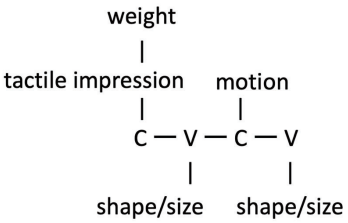

Figure 1. CVCV type

In this regard, it is apparent that the meanings change depending on the position of the phoneme that belong to onomatopoeia. For example, "kira" meaning of sparkling is "lightly stiff (tactile impression)" by /k/, "radiating line (shape)" by /i/, "fluent movement (movement)" by /r/ "Spread (shape)" by /a/.

Therefore, the sound symbolism of onomatopoeias varies depending on the phoneme type as well as the phoneme position. Table 1 shows basic sound symbols of consonants. According to these models, we propose to convert onomatopoeia into a mathematical model.

3. Proposed Approach

3.1 Problem Formulation

In order to convert Hamano's model into a mathematical model,

Table 1. Sound symbols of consonants

	C of CV		C_1 of CVCV		C_2 of CVCV
p	Impact to the surface on tension or rupture	Light, small	Tensiony surface, obese	Light, small	Burst, breaking, covered swelling
b		Heavy, large, coarse		Heavy, large, coarse	
t	Weak tension tapping the surface	Light, small	Weak tension surface, relaxation not conspicuous	Light, small	Tap, touch close, match
d		Heavy, large, coarse		Heavy, large, coarse	
k	Hard surface, Severity of motion, tightness, certainty	Light, small	Hard surface tightness, certainty	Light, small	Open, from inside comes out,
g		Heavy, large, coarse		Heavy, large, coarse	
s	Slip surface without resistance liquid, fluid	Light, small	Surface, liquid, fluid without resistance	Light, small	Moving while touching, friction
z		Heavy, large, coarse		Heavy, large, coarse	
n	Hard to capture		Slip, difficult to catch, stickiness, curviness		Nothing of power bending
y			Shaking, unreliable movement		The outline is not dangerous
h	breath		Beauty, weakness		
w	Excitement				Softness weakness
m	suppression				
r					Movement like flowing
Palatization	Childiness, miscellaneous things, insufficient control				

the phoneme itself must be expressed as a mathematical expression. In this research, we digitize phonemes by using a method in which the sound symbol of elements of Japanese consonants, vowels, etc. proposed by Akiyama et al. [Akiyama 2011]. In specific, Akiyama et al conducted a questionnaire survey, considering the impression of consonants / vowels as being evaluated by 43 adjective pairs. Then, the questionnaire results of these adjective pairs were compressed into four dimensions by factor analysis, and it was made to be the four attribute vector of the sound symbol. Table 2 shows the results of factor analysis.

Table 2. Factor analysis result for extraction of attribute type

	factor1	factor2	factor3	factor4
clear-cloudy	**0.73**	0.07	-0.02	0.04
neat-dull	**0.68**	-0.04	-0.01	0.06
beautiful-ugly	**0.67**	0.26	-0.10	0.00
brilliant-blurred	**0.57**	-0.09	0.18	0.06
detail of texture-rough	**0.53**	0.05	-0.15	-0.24
quick-curse	**0.51**	-0.28	0.25	-0.12
high tone-Low tone	**0.51**	0.07	0.37	-0.29
articulate-vague	**0.45**	-0.27	0.19	0.16
fast-slow	**0.45**	-0.31	0.29	-0.11
dull-sharp	**−0.49**	0.38	-0.09	0.03
bad crisp-sharp	**−0.57**	0.26	-0.04	-0.08
repetitious-crisp	**−0.64**	0.05	0.12	0.05
dirty-clean	**−0.71**	-0.21	0.17	-0.02
soft-hard	0.00	**0.79**	0.04	-0.18
round-square	-0.11	**0.74**	0.01	-0.05
loose-nervous	-0.12	**0.64**	-0.01	-0.05
moisture-dried	0.10	**0.56**	0.00	0.00
smooth-not smooth	0.22	**0.55**	-0.06	-0.01
warm-cold	-0.17	**0.48**	0.22	0.24
extensive-not extensive	0.10	**0.44**	0.11	0.29
crowded-free	-0.22	**−0.49**	-0.16	-0.11
sharp-roundish	0.19	**−0.65**	0.08	-0.04
excited-calm	-0.14	-0.07	**0.79**	-0.12
dynamic-static	-0.10	0.00	**0.71**	0.05
flashy-sober	0.18	0.10	**0.61**	0.02
bustling-lonely	0.03	0.21	**0.61**	0.02
stupid-gentle	-0.03	-0.33	**0.56**	-0.04
active-Inactive	0.25	0.03	**0.52**	0.12
hilarious-gloomy	0.28	0.29	**0.44**	0.13
bright-dark	0.39	0.30	**0.44**	0.07
quiet-noisy	0.21	0.04	**−0.78**	0.01
large-small	-0.29	0.04	0.05	**0.64**
strong-weak	-0.06	-0.34	0.15	**0.60**
rich-paltry	0.04	0.29	0.09	**0.51**
stable-unstable	0.34	0.16	-0.23	**0.45**

3.2 Algorithm

The proposed algorithm of design of phoneme features taking phoneme arrangement into account which is the proposed method. In this regards, let us take the onomatopoeia "katakata" as an example below.

I. The feature vector as shown in Figure 2 was designed based on the four attributes defined by Akiyama et al. [Akiyama 2011]

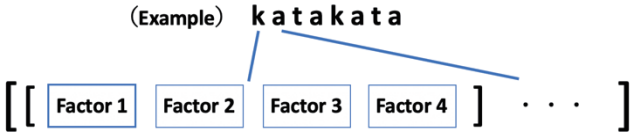

Figure 2. Feature vector (first step)

II. K of "katakata" belongs to C1 of the CVCV type. When CVCV type C1 focuses on Hamano's model (Table 1), it expresses "the surface is hard".

III. Since the meaning of the sound symbol of Hamano's sound symbol is "hard", the meaning is similar to that of Akiyama's factor analysis (Table 2) "soft - hard", so we combine these two impressions. The similarity relationship between the two impressions shall be investigated beforehand by a prior questionnaire.

IV. Since "soft - hard" contributes to the factor load amount of Factor 2 (0.4 or more), it weighs Factor 2 element. Figure3 show this weighting.

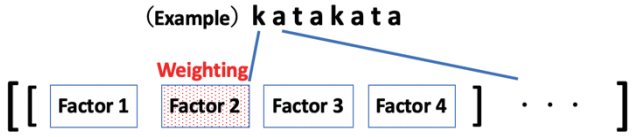

Figure 3. Weighting of feature values

V. If the onomatopoeia is repeating the same phoneme, the length of the feature vector is halved. This is due to dimensional compression.

VI. After halving the length, put the flag on whether the phoneme repeats or not on the last element. Figure 4 shows putting this flag.

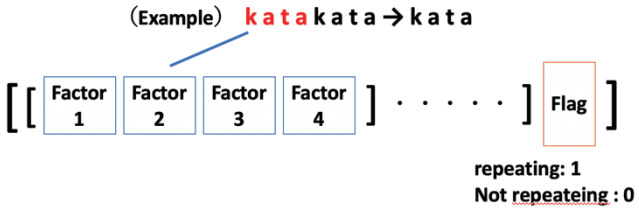

Figure4. Putting

This is the algorithm for finding the feature quantity from onomatopoeia. This feature quantity is input to the learner.

4. Results

4.1 Experiment 1 (simulation)

Classification experiments of mimetic words as shown in Fig. 3 were carried out. The mimetic words dealt with in this

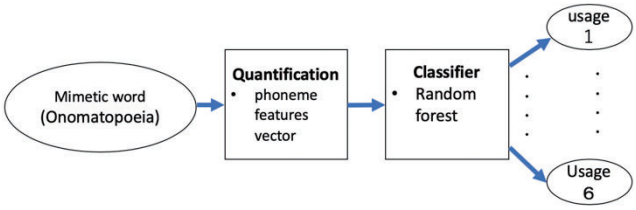

Table 1. Abstract of Experiment

experiment are 116 words chosen from onomatopoeia 6 usage a categories (“drop”, “flow”, “rain”, “soil”, “wave”, “window”) on nature that are published in the Japanese onomatopoeia dictionary. However, it excludes mimetic words such that there are multiple usage rules. The reason for these data is to show the effectiveness

of the proposed method by comparing the performance in the same situation as the experiment of the existing study Goriki et al. [Goriki 2018] Random Forest was used as the classifier. Evaluation of classification accuracy was made 20 times for 10-fold-cross-validation. That is, the mismatching word of the previous 116 words is divided into learning data and evaluation data, and classification accuracy is obtained. The evaluation index is the relevance ratio, accuracy and F value. Table 3 shows the experimental results. Both precision, recall and F-value higher than previous studies.

Table 3. experimental 1

	Precision	recall	F-value
Previous research	0.65	0.65	0.64
Proposed method	0.70	0.71	0.68

4.2 Experiment 2 (compare machine with human)

We conducted this experiment in order to compare experiments in order to compare comparing the accuracy between people and machines. In the experiment data, unknown onomatopoeia was used so as not to put in the person's prior knowledge. In this study, unknown onomatopoeia was defined as onomatopoeia not listed in the dictionary, and it was generated by preliminary survey with reference to the study. In this experiment, we first classify the generated 7 unknown onomatopoeia into people and use them as evaluation data. Then, the classification accuracy of the evaluation data is derived by letting the classifier learn 116 mimetic words that are used in Experiment 1 as training data. The evaluation index is the relevance ratio, accuracy and F value. Table 4 shows the experimental results.

Table4. experimental 2 results.

	Precision	recall	F-value
Proposed method	0.67	0.33	0.44

5. Discussion

In experiment 1, the classification accuracy exceeded the existing research as shown in this experiment, but the accuracy varied depending on the usage. In considering the characteristics of onomatopoeia with poor classification accuracy, we looked at the relationship between F value and the proportion of "words having only meaning of mimetic words" for each usage category. In specific, Pearson's product moment correlation coefficient, the has derived the relationship between "proportion of words having meaning only mimetic words" and "F value" for each usage category was -0.97. This demonstrates there is a very strong negative correlation. In other words, it can be said that the accuracy improves as the number of "words having meaning only in mimetic words" decreases. This is because onomatopoeia is a language that has originated directly from the sound, so it is thought that it is easy to capture the onomatopoeic sound symbolism as a feature.

On the other hand, experiment 2, the classification accuracy is better than the chance level (0.18), but not very high accuracy. However, there were two cases where mispredicted usage was injected to the usage with the second highest support number in the survey to generate unknown onomatopoeia. This is considered to be due to the existence of ambiguity in the onomatopoeia used in this experiment. Therefore, it is considered that there is a need to solve the prediction of the classifier as a multi-label problem instead of outputting only one usage.

6. Conclusion

In this paper, we proposed feature extraction of onomatopoeia according to phoneme sequence theory for automatic semantic usage classification of onomatopoeia with higher accuracy. In the existing onomatopoeia, the proposed method showed its effectiveness by comparing the accuracy on the simulation by the conventional approaches and 10-cross-validations. However, there is a problem in the accuracy of unknown onomatopoeia. In the future, we aim to make it possible to respond to ambiguous onomatopoeia by allowing classifiers to predict more than one usage.

References

[Agency for Cultural Affairs 1999] Agency for Cultural Affairs. 今後の日本語教育施策の推進について -日本語教育の新たな展開を目指して-調査研究報告書 本文, Retrieved January 4, 2019 from http://www.bunka.go.jp/tokei_hakusho_Shuppan/tokeichosa/nihongokyoiku_suishin/nihongokyoiku_tenkai/hokokusho/, 1999.

[Fijino 2006] Fujino, Y., Kikkawa, M., Yamada, T., Inoue, K., Nishina, E., Sport Onomatopoeia Data Base for Motor Learning, Japan Journal of Educational Technology,Japan Society for Educational Technology, vol.29,(Suppl), 5-8, 2006.

[Hinton 1995] L. Hinton, J. Nichols, and J. Ohara. Sound symbolism. Cambridge University Press, 1995.

[Akimoto 2007] M. Akimoto, 日本語教育におけるオノマトペの位置づけ『日本語学』, volume 26, pages 24–34. 2007.

[Ichioka 2009] Ichioka, K., Fukumoto, F. The Automatic Classification of Onomatopoeia Based on Co-occurrence from the Web and Sound Symbolism, The IEICE Transactions on Information and Systems (Japanese Edition), vol. J92-D No.3 pp.428-238, 2009.

[Urata 2017] Urata, D., Nakamura, T., Kanoh, M. Yamada, K., A Consideration on Usage Classification of Onomatopoeia using Acoustic Features, The 31st Annual Conference of the Japanese Society for Artificial Intelligence, 2G4-3, 2017.

[Goriki 2018] Goriki, M., Takeuchi, N., Urata, D., Nakamura, T., Kanoh, M., Yamada, K., An investigation of phoneme and acoustic features to auto-classify onomatopoeias into semantic usage category -A case report on mimetic words regarding “nature”-, 34st Fuzzy System Symposium, TF3-2, 2018.

[Hamano 2014] Hamano, S., 日本語のオノマトペ, Kurosio Publishers, 2014.

[Akiyama 2011] Akiyama, H., Komatsu, T., and Kiyokawa, S., Proposing an Objective Digitizing Method for Expressing One’s Impressions Derived from Onomatopoeias, HCI, vol.2011-HCI-142 No.23, pp.1-7, 2011.

The 33rd Annual Conference of the Japanese Society for Artificial Intelligence, 2019

Vibrational Artificial Subtle Expressions to Convey System's Confidence Level to Users

Takanori Komatsu [*1] Kazuki Kobayashi[*2] Seiji Yamada[*3]

Kotaro Funakoshi [*4] and Miki Nakano [*4]

[*1] Meiji University [*2] Shinshu University [*3] National Institute of Informatics/Tokyo Institute of Technology/SOKENDAI [*4] Honda Research Institute Japan, Co. Ltd.,

Artificial subtle expressions (ASEs) are machine-like expressions used to convey a system's confidence level to users intuitively. So far, auditory ASEs using beep sounds, visual ASEs using LEDs, and motion ASEs using robot movements have been implemented and shown to be effective. In this paper, we propose a novel type of ASE that uses vibration (vibrational ASEs). We implemented the vibrational ASEs on a smartphone and conducted experiments to confirm whether they can convey a system's confidence level to users in the same way as the other types of ASEs. The results clearly showed that vibrational ASEs were able to accurately and intuitively convey the designed confidence level to participants, demonstrating that ASEs can be applied in a variety of applications in real environments.

1. Introduction

Many studies in human-computer interaction have tried to use vibrational information as a communication channel with users based on the perceptual features of haptic sense [Ryu 2008]. Specifically, vibrational information was utilized to notify the user of the progress of the system's functions [Cauchard 2016], urgent information for pedestrians [Saket 2013] or tactile icons for blind people [Qian 2011]. This vibrational information was also utilized to represent the system's emotional states to users [Mathew 2005]. However, so far, there have been no studies that use vibrational information for conveying the system's confidence level to users in a complementary manner.

In terms of conveying system's confidence level, Komatsu et al. [2010] already proposed using artificial subtle expressions (ASEs) as machine-like expressions used to convey a system's confidence level to users intuitively in a complementary manner. Specifically, they proposed two simple beeping sounds used as "auditory ASEs": a flat sound (flat auditory ASE) and a sound with a decreasing pitch (decreasing auditory ASE). These auditory ASEs were added after the system's verbal suggestions. They then showed that suggestions followed by decreasing auditory ASEs intuitively conveyed a low system confidence level to users (Figure 1).

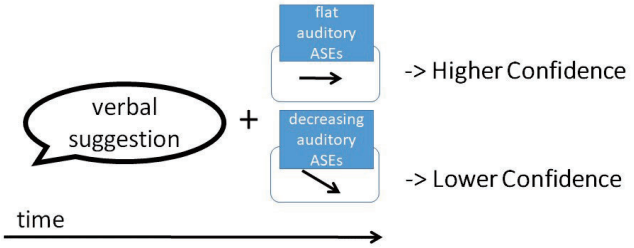

Figure 1. Auditory artificial subtle expressions (ASEs)

The purpose of this study is to propose "vibrational ASEs" based on our knowledge of "auditory ASEs." In this paper, we first describe the design of vibrational ASEs and then describe experiments done to confirm whether vibrational ASEs can convey a system's confidence level to users in the same way as auditory ASEs. Finally, we discuss the pros and cons of vibrational ASEs on the basis of the results of our experiments.

Contact: Takanori Komatsu, Meiji University, 4-21-1 Nakano, Tokyo 1648525, tkomat@meiji.ac.jp. This paper is a revised version of [Komatsu 2018].

2. Design of Vibrational ASEs

We think that vibrational ASEs should be added after a system's verbal suggestions to convey a higher or lower confidence level to users like auditory ASEs. In the case of auditory ASEs, a flat sound (a flat auditory ASE) conveys a higher confidence level, and a sound with a decreasing pitch (decreasing auditory ASE) conveys a lower confidence level to users. We thus prepared two vibration patterns used as vibrational ASEs: one to convey a system's higher confidence level, and the other, a lower confidence level. We assumed that vibrations with a fixed frequency (flat vibrational ASE) would convey a higher confidence level and that vibrations with a continuously or gradually decreasing frequency (decreasing vibrational ASE) would convey a lower confidence level; that is, the time variation pattern of the frequency of vibrations was almost the same as that of auditory ASEs (Figure 2).

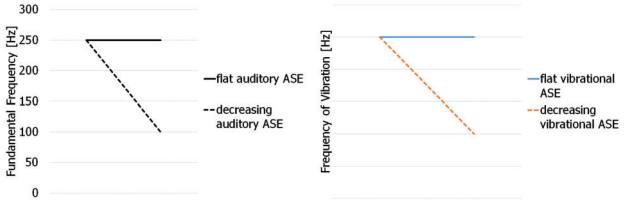

Figure 2. (left) Auditory ASEs and (right) vibrational ASEs at beginning

However, we cannot control the degree of frequency of the vibration motors on a smartphone because the vibration API of smartphones does not provide a method for controlling the frequency of the motors. It only provides a method for controlling the on/off statuses on the basis of vibration patterns.

Therefore, we prepared the following two patterns for flat and decreasing vibrational ASEs (Figure 3).

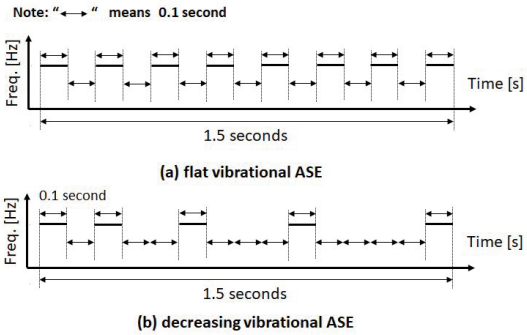

Figure 3. Vibrational ASEs. (a) Flat vibrational ASE and (b) decreasing vibrational ASE.

- Flat vibrational ASE: eight 0.1-second long vibrations with 0.1-second long intervals [Figure 3(a)].
- Decreasing vibrational ASE: five 0.1-second long vibrations. Lengths of intervals are 0.1, 0.2, 0.3, and 0.4 seconds [Figure 3(b)].

We preliminarily confirmed that gradually lengthening the intervals between vibrations made users feel the sensation of deceleration or decreasing velocity, while a fixed length of vibration intervals made users feel the sensation of a constant velocity. The total durations of flat and decreasing vibrational ASEs were both 1.5 seconds.

3. Experiment

3.1 Overview

We conducted an experiment to investigate whether the proposed vibrational ASEs were able to convey a system's confidence level to users accurately and intuitively; that is, whether the flat vibrational ASE conveys a higher confidence level and the decreasing vibrational ASE a lower confidence level.

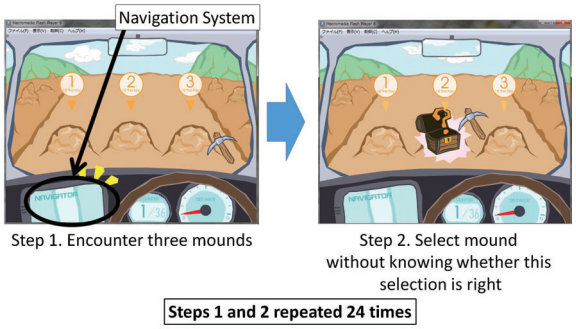

Figure 4. Driving treasure hunting video game

As an experimental setting, we used a "driving treasure hunting" video game (Figure 4). In this game, the game image scrolls forward on a straight road as if the participant is driving a car with a navigation system and with small three mounds of dirt appearing along the way. A coin is inside one of the three mounds, while the other two mounds contain nothing. The game ends after the participant encounters 24 sets of mounds (24 trials).

The purpose for each participant is to get as many coins as possible. Which of the three mounds has the coin is randomly assigned. In each trial, the navigation system to the left of the driver seat (circled in the left image of Figure 4) told them in which mound it expected the coin to be by using a verbal suggestion followed by a vibrational ASE. The participant could freely accept or reject the navigation system's suggestions. In each trial, even after the participant selected one mound among the three, he/she was not told whether the selected mound had the coin or not (only a question mark appeared from the opened treasure box, as shown in the right image of Figure 4). The participants were then informed of their total numbers of coins only after they finished all 24 trials. It took about three minutes to complete this game. This game setting was commonly used in most former studies on ASEs, and the design in this study is fairly standard in human factor literature; it is a variation of a lane change task, which is a ISO-standardized driving task (ISO 17387:2008).

3.2 Stimuli

In this experiment, the navigation system used Japanese speech to suggest to the participants the expected location of the coin, that is, "ichi-ban (no. 1)," "ni-ban (no. 2)," or "san-ban (no. 3)." These speech sounds were created by adding robotic-voice effects to the recorded speech of one of the authors. The duration of these three sounds was 0.5 seconds.

One of two vibrational ASEs was played immediately after the verbal suggestion (Figure 5). These two ASEs were the flat vibrational ASE or decreasing vibrational ASE. The suggestions followed by decreasing vibrational ASEs were designed to inform users of the system's lower level of confidence in its suggestions, while those with flat vibrational ASEs were to inform them of a higher level of confidence.

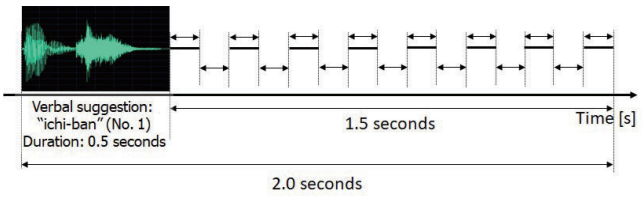

Figure 5. Speech waveform of suggestion "ichi-ban" with flat vibrational ASE

Here, the total length of a suggestion and a vibrational ASE was exactly 2.0 seconds (suggestion: 0.5 seconds, vibrational ASE: 1.5 seconds, and no interval between them). There were 6 variations of stimulus (3 suggestions × 2 ASEs). Among 24 trials of mound selection, each of these 6 variations was presented to the participants 4 times in a random order.

While the participants' played the game, we measured the response time, which was defined as the duration between the onset of the verbal suggestions and the participants' mound selection, and this was automatically measured by the experimental system implemented in the game environment. After playing the game, the participants were asked to answer the following two questions.

Q1: "Did you feel the vibrations during this game?"

Q2: "How many patterns of vibration did you notice?"

3.3 Participants

20 Japanese undergrads and graduate students participated (15 males and 5 females; 19 – 24 years old). These participants voluntarily responded to a call for participants from the authors. The participants were asked to be seated at a table, and an experimenter passed out a consent form with instructions on the experiment. These instructions and the experimenter never mentioned or explained the vibrational ASEs given after suggestions made to the participants. Afterward, a smartphone (Arrows M03, Fujitsu Limited, OS: Android 6.0.1) was passed to the participants, and they were asked to start the video game while holding the smartphone in their hands (Figure 6). The game was implemented in a web browser (Google Chrome: 60.0.3112.116) with JavaScript and the PixiJS library.

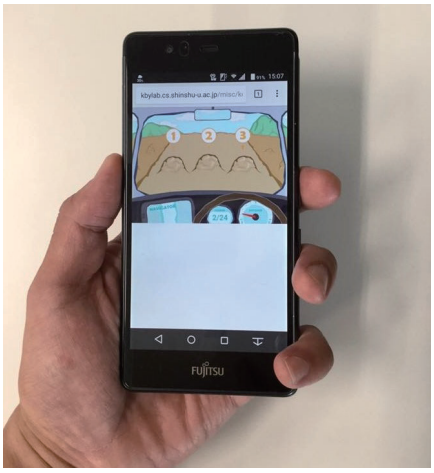

Figure 6. Smartphone and driving treasure hunting video game

3.4 Results

To investigate whether the vibrational ASEs could convey the designed confidence level to the participants or not, we calculated the rejection count, which indicates how many system suggestions were rejected by the participants (maximum rejection count: 12 times for each confidence level). For all 20 participants, the average rejection count of the 12 flat vibrational ASEs was 1.55 (SD = 1.99), while that of the 12 decreasing vibrational ASEs was 4.60 (SD = 4.13, Table 1).

Table 1. Average rejection counts for flat and decreasing vibrational ASEs

Type of vibrational ASE	Average rejection count
Flat	1.55 (SD = 1.99)
Decreasing	4.60 (SD = 4.13)

The rejection counts were analyzed with a dependent t-test (independent variable: flat/decreasing vibrational ASEs, dependent variable: rejection counts). The results showed significant differences between these two ASEs [$t(19) = 2.62$, $p = .017$, Glass' delta = 1.53], so we observed that suggestions with decreasing vibrational ASEs showed higher rejection counts compared with those with flat vibrational ASEs. Consequently, we confirmed that vibrational ASEs can convey the designed confidence level to the participants in the same way as auditory ASEs.

From the participants' answers to the two questions, Q1 and Q2, presented after the experiment, we found that all 20 participants felt vibrations during the game, but only 8 participants answered that there were two vibration patterns. We then compared the average rejection counts of the participants who were unaware that there were two vibrations with those of the other participants who were aware of this fact (Table 2). A 2 × 2 mixed ANOVA [within independent variable: vibration patterns (flat/dec.), between independent variable: awareness of two vibrations (Yes/No), dependent variable: rejection counts] showed that there were no significant differences in the interaction effects [$F(1,39) = 0.23$, n.s., effect size $f = 0.11$] and in the main effect of the between independent variable [$F(1,39) = 2.12$, n.s., effect size $f = 0.34$], but there was a significant difference in the main effect of the within independent variable [$F(1,39) = 6.82$, $p < .05$, effect size $f = 0.62$]. These results showed that all participants responded to the given stimuli in a similar way regardless of their awareness of the vibration patterns. This result clearly indicates that the participants responded to these vibrations intuitively without deeply considering what these patterns meant.

Table 2. Average rejection counts for two vibrational ASEs in terms of the participants' awareness of vibration patterns

Participants who noticed two types of vibrations	Average Rejection count for Flat ASE	Average Rejection count for Dec. ASE
Yes: 8 participants	2.00 (SD = 2.50)	5.75 (SD = 3.93)
No: 12 participants	1.25 (SD = 1.48)	3.83 (SD = 4.07)

3.5 Additional Experiment

We thus conducted a consecutive experiment to investigate whether simultaneously presenting verbal suggestions and the proposed vibrational ASEs could convey a system's confidence level to users accurately and intuitively. The experimental setting and procedure was completely the same as that of experiment 1 except for the timing at which the verbal suggestions and vibrational ASEs were presented.

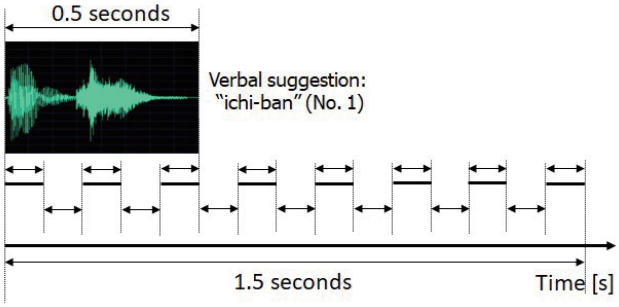

Figure 7. Speech waveform of suggestion "ichi-ban" and flat vibrational ASE in experiment 2

In this experiment, the vibrational ASEs were presented simultaneously with the verbal suggestions (Figure 7). The length of the suggestions with vibrational ASEs was exactly 1.5 seconds (suggestions: 0.5 seconds, vibrational ASEs: 1.5 seconds).

20 Japanese undergrads and graduate students participated (14 males and 6 females; 20 – 23 years old). These participants

voluntarily responded to a call for participants, and they did not participate in the former experiment.

To investigate whether vibrational ASEs presented simultaneously with verbal suggestions can convey the designed confidence level to the participants or not, we calculated the rejection counts. For all 20 participants, the average rejection count of the 12 flat vibrational ASEs was 1.65 (SD = 2.01), while that of the 12 decreasing vibrational ASEs was 5.30 (SD = 3.58, Table 3).

Table 3. Average rejection counts for flat and decreasing vibrational ASEs in experiment 2

Type of vibrational ASE	Average rejection count
flat	1.65 (SD = 2.01)
decreasing	5.30 (SD = 3.58)

The rejection counts were analyzed with a dependent t-test (independent variable: flat/decreasing vibrational ASEs, dependent variable: rejection counts). The results showed significant differences between the two ASEs [$t(19) = 3.92$, $p = .001$, Glass' delta = 1.82], so we confirmed that suggestions with decreasing vibrational ASEs showed a higher rejection count compared with those with flat vibrational ASEs, the same as in experiment 1. Therefore, we confirmed that vibrational ASEs presented simultaneously with verbal suggestions also could convey the designed confidence level to the participants.

Table 4. Average rejection counts for two vibrational ASEs in terms of the participants' awareness of vibration patterns

Participants who noticed two types of vibrations	Average Rejection count for Flat ASE	Average Rejection count for Dec. ASE
Yes: 11 participants	1.45 (SD = 2.06)	5.18 (SD = 3.90)
No: 9 participants	1.89 (SD = 1.91)	5.44 (SD = 3.13)

From the participants' answers for the two questions, Q1 and Q2, presented after the experiment, we found that all 20 participants had noticed that they felt vibrations during the game, and 11 participants answered that there were two vibration patterns. We then compared the average rejection counts of the participants who were unaware or aware of the two vibrations (Table 4). A 2 × 2 mixed ANOVA [within independent variable: vibration patterns (flat/dec.), between independent variable: awareness of two vibrations (Yes/No), dependent variable: rejection counts] showed that there were no significant differences in the interaction effects [$F(1,39) = 0.01$, n.s., effect size $f = 0.02$] and in the main effect of the between independent variable [$F(1,39) = 0.13$, n.s., effect size $f = 0.08$], but there was a significant difference in the main effect of the within independent variable [$F(1,39) = 14.39$, $p < .01$, effect size $f = 0.89$]. These results also clearly indicate that the participants still responded to these vibrations intuitively, the same as in the former experiment.

4. Discussions and Conclusions

We tested the template in the following versions. In this paper, we proposed a novel type of ASE that uses vibration, called vibrational ASEs. We implemented the vibrational ASEs on a smartphone and conducted experiments to confirm whether they can convey a system's confidence level to users in the same way as the other types of ASEs. The results clearly showed that vibrational ASEs were able to accurately and intuitively convey the designed confidence level to the participants.

One of the noteworthy achievements of this study was that it was found that vibration information can be utilized as ASEs in the same way as auditory, visual (LED-based), and motion ASEs. As already mentioned, most smart devices are equipped with vibration motors, so the results of this study will drastically increase the applicability of the ASEs into various kinds of devices. The other noteworthy achievement was that simultaneous usage of vibrational ASEs and verbal suggestions was shown to be possible. If the modalities of the main protocol and complementary protocol were the same, simultaneous usage would be difficult; for example, if verbal suggestions and auditory ASEs were presented simultaneously, the verbal suggestions would mask or overlap the auditory ASEs, and vice versa, so eventually, the main protocol and complementary protocol would interfere with each other. However, the results of this study clearly showed that it is possible to present the main protocol and complementary protocol simultaneously in the case that the modalities of these protocols are different. This finding would contribute to expanding the variety of stimuli for users and also to shortening the length of the stimuli.

References

[Cauchard 2016] Jessica R. Cauchard, Janette L. Cheng, Thomas Pietrzak, and James A. Landay. 2016. ActiVibe: Design and Evaluation of Vibrations for Progress Monitoring, In Proceedings of the CHI2016, 3261-3271.

[Komatsu 2010] Takanori Komatsu, Kazuki Kobayashi, Seiji Yamada, Kotaro Funakoshi, and Mikio Nakano. 2010. Artificial Subtle Expressions: Intuitive Notification Methodology for Artifacts, In Proceedings of the CHI2010, 1941-1944.

[Komatsu 2018] Takanori Komatsu, Kazuki Kobayashi, Seiji Yamada, Kotaro Funakoshi, and Mikio Nakano. 2018. Vibrational Artificial Subtle Expressions: Conveying System's Confidence Level to Users by Means of Smartphone Vibration, In Proceedings of the CHI2018, Paper No 487. Doi: 10.1145/3173574.3174052

[Mathew 2005] Deepa Mathew. 2005. vSmileys: Imaging Emotions through Vibration Patterns, In Proceedings of Alternative Access: Feelings & Games 2005, 75-80.

[Qian 2011] Huimin Qian, Ravi Kuber, and Andrew Sears. 2010. Towards developing perceivable tactile feedback for mobile devices, International Journal of Human-Computer Studies 69, 11 (2011), 705-719.

[Ryu 2008] Jonghyun Ryu, Jaehoon Jung, and Seungmoon Choi. 2008. Perceived Magnitudes of Vibrations Transmitted Through Mobile Device, In Proceedings of Symposium on Haptic Interfaces for Virtual Environments and Teleoperator Systems 2008, 139-140.

[Saket 2013] Bahador Saket, Chrisnawan Prasojo, Yongfeng Huang, Shengdong Zhao. 2013. Designing an Effective Vibration-Based Notification Interface for Mobile Phones, In Proceedings of the 2013 conference on Computer supported cooperative work companion (CSCW2013), ACM Press (2013), 1499-1504.

The 33rd Annual Conference of the Japanese Society for Artificial Intelligence, 2019

A think-programming method based on free texts “almost” in English

Keisuke NAKAMURA[*1]

[*1] Knowrel System, Inc.

This document describes a method for programming for simulating human-thinking based on free English texts and describes three PROLOG-like examples each consisting of a) such type “program” that is “almost” in English and that has natural language templates with variables, b) related query, and c) corresponding simulated “human-thought” result. In order to speed up executing English “programs” and queries that are separated with words and white spaces, we improved original algorithm used from 2012 for Japanese “programs” that are not so separated. We conclude that our think-programming method is useful for automatically simulating some types of real human thoughts that are able to be programmed “almost” in English.

1. Introduction

To use computer to automatically process knowledge and/or information written in natural language in the same manner as Prolog and to achieve comprehensive deduction and solution searching at the predicate logic level, in [Nakamura 2016] etc. we proposed that the knowledge be expressed in a format wherein variables are embedded in natural language.

This document describes 2) feature of the method, 3) examples of program, related query, and corresponding result, 4) our recent improvement for English white spaces, 5) conclusion.

2. Feature of our method

We respect Prolog. But our method differs in some points below. Detailed algorithms are shown in [Nakamura 2016].

・a person uses character types, delimiters, or escape characters to distinguish the constant portions and the variable portions of content that is equivalent to "literal" in Prolog and inputs the content into a computer.

・computer performs automatic unification and/or automatic derivation on text included in the input while treating variables as material that could span the boundaries of the subject, predicate, object etc. of the text.

3. Examples of program, query, and result

3.1 Example 1

```
[Progam]  C:\Users\Keisuke\Documents\humanote\1.jpl
   1: ice cream is cold food
   2: cold food is cooling
   3: $A is $B :- $A is $C ; $C is $B ;
[Query]
   ?ice cream is $X
[Result]
   :$X  = cold food
   :$X  = cooling
   time = 875msec
```

Line 3 teaches computer “transitivity rule” of human-thinking.

Contact: Keisuke NAKAMURA, KnowrelSystem,Inc., phone: +81-76-213-5211, fax: 5239, keisukebecome@icloud.com

Semicolon(;) is used for delimiter of literals because comma(,) in Prolog is too casually used in natural English.

Using lower case of alphabet, distinct case also is available.

It was implemented on 3.6-4.2GHz CPU, 8G Memory, Windows 10 and Visual C++2013. Demonstrations are enabled by downloading open beta version of our software HUMANOTE (see https://github.com/keisukebecome/humanote for public/)

3.2 Example 2

```
[Progam]  C:\Users\Keisuke\Documents\humanote\2.jpl
   1: ///@1.jpl
   2: my favorite food is ice cream
   3: what i eat is $X :- my favorite food is $X ;
[Query]
   ?what i eat is $X
[Result]
   …
   3: ///◆INC_START 2019/02/13_21:52:29  1.jpl
   4: ///LOAD … C:\Users\Keisuke\Documents\humanote\1.jpl
   5: ice cream is cold food
   6: cold food is cooling
   7: $A is $B :- $A is $C ; $C is $B ;
   8: ///◆INC_END  1.jpl
   9: my favorite food is ice cream
   10: what i eat is $X :- my favorite food is $X ;

   :$X  = cooling
   :$X  = cold food
   :$X  = ice cream
   time=3252msec
```

Line 1 at original Program (2.jpl) was expanded to Line 3-8 at resulted memory and computer do unification and derivation on the expanded Program in the memory.

Our system also enables recursive expansion and enables citation/reuse of programs placed in the internet, group LAN, and PC (the above example is PC case).

We call this method “LinkedOpenRule” (named after “LinkeOpenData”) which cites and uses not only new data (fact) in the internet etc. but also new rules both being updated daily, weekly and monthly by other users, groups and companies.

3.3 Example 3 (before improvement as to time)

```
[Progam]  C:\Users\Keisuke\Documents\humanote\3.jpl
   1: we can get to Noto from Kanazawa by car
   2: we can get to Kanazawa from Osaka by JR
   3: we can get to Sendai from Osaka by Shinkansen
   4: we can get to gyuutan shops from Sendai by foot
   5: we can get to Osaka from Toyonaka by Hankyu-line
   6: we can get to Hegura-island from Noto by boat
   7: we can get to $Z from $X by $A and $B :-
                              we can get to $Y from $X by $A ;
                              we can get to $Z from $Y by $B ;
[Query]
   ?we can get to $M from Toyonaka by $N
[Result]
   :$M  = Osaka
   :$N  = Hankyu-line

   :$M  = Kanazawa
   :$N  = Hankyu-line and JR

   :$M  = Sendai
   :$N  = Hankyu-line and Shinkansen

   :$M  = Noto
   :$N  = Hankyu-line and JR and car

   :$M  = Hegura-island
   :$N  = Hankyu-line and JR and car and boat

   :$M  = gyuutan shops
   :$N  = Hankyu-line and Shinkansen and foot

   time=124757msec
```

By this experiment, we found that 124757msec. for English program is over 15 times larger than 7818msec. for Japanese program with same logical structure.

In order to improve time, we reviewed original source codes and speeded up the basic algorithm of unification for “almost” English programs and related queries.

4. Speed up for English “program”

For speeding up, we focused on white spaces in English natural language texts that don’t exist so much in Japanese texts.

Two (one before and one after) characters neighboring each variable in the template was searched in targeted constant texts in original algorithm [Nakamura 2016].

New algorithm also checks another more before character if the original-variable-neighboring-before-character is white space like ‘ ‘.

The improvement result is that original 124757msec. was shorten to 9034msec. with other resulting content being same as the above-mentioned content.

It is only 7.24% of original time cost.

We think that this new algorithm is useful not only for other word-separated (i.e. inflected) natural language like French, German, Spanish and so on, but also agglutinative languages and analytic/isolated languages.

5. Conclusion

We conclude that our think-programming method is useful for automatically simulating some types of real human thoughts that are able to programmed “almost” in English.

6. Next

We will do as below,

- speed up more as to Japanese and English
- experiment as to analytic language such as Chinese language
- create a shared “LinkedOpenRule” web sites in each language with worldwide partners.

References

[Nakamura 2016] Keisuke Nakamura, “Method for Processing Knowledge or Information, Device, and Computer Program”, International Publication WO/2016/071942, the World Intellectual Property Organization (WIPO), 2016.

The 33rd Annual Conference of the Japanese Society for Artificial Intelligence, 2019

Affective Tutoring for Programming Education

Thomas James Tiam-Lee Kaoru Sumi

Future University Hakodate

This article discusses the use of artificial intelligence to detect student emotions while doing coding exercises for learning programming. Using data from programming students, we were able to build models for detecting confusion with as high as 70.46% accuracy. We applied this in a system for programming practice that provides affective-based feedback by offering guides and adjusting the difficulty of exercises based on the presence of confusion, and found that students given affective feedback were able to solve more exercises and gave up less times. Finally, we also discuss the future direction of this research by collecting a larger amount of data that can cover other affective states and handle finer-grained detection of affect.

1. Introduction

Recently, research on intelligent tutoring systems (ITS) have focused on modelling not only the cognitive, but also the affective states of the students [Harley 2017]. This is supported by studies that empirically correlate affect with student achievement [Rodrigo 2009] and self-regulated learning [Mega 2014]. While there have been several works on affect modelling on traditional ITS, recognizing emotions in complex learning tasks such as programming remains to be challenging [Bosch 2014].

Intelligent programming tutors (IPT) are a subclass of ITS that teach programming. In these systems, students interact with the system mostly by writing, testing, and debugging code to achieve certain tasks. Because of this, there is less direct interaction between the student and the tutor unlike that of traditional ITS. Despite this, it has been shown that students experience a rich set of emotions while doing coding tasks [Bosch 2013]. Thus, it is important for IPTs to be able to model these emotions so that appropriate responses could be made.

In this article, we discuss the use of facial features and logs (typing, compilation) to train machine learning models capable of recognizing academic emotions in a programming settings. We apply our models in a system for programming practice that offers guides and adjusts the difficulty of exercises based on the presence of confusion. Then, we discuss future work on collecting more data to handle finer-grained detection and more affective states.

2. Data Collection and Model Training

We trained models for recognizing confusion using data collected from 12 Filipino and 11 Japanese freshmen students. Each student had around 2 months of programming experience, and was taking a course on introductory programming during the time of the data collection. Each test subject was asked to solve a series of introductory programming coding exercises, in which they had to write the body of a function to perform a specified task. The exercises covered introductory programming concepts like variables, expressions, conditional statements, and loops.

The session lasted for 45 minutes or until all problems have been solved. Students were not allowed to skip an exercise. We logged all typing and compilation activity and recorded a video of the student's face throughout the session. After the session, each student was asked to provide affective state annotations to the session data. The affective state labels that we used are: engaged, confused, frustrated, and bored. This is based on a previous data that analyzed the common emotions that are experienced by novice programmers while coding [Bosch 2013]. Each annotation consisted of the start timestamp , the end timestamp, and the affective state label, to indicate that that emotion was felt during that interval. The student could make as many annotations as he wanted, and there were no restrictions to the length of the annotation intervals. The data collection process resulted to around 8 hours of session data and 44 emotion annotations in total.

Majority of the labels collected were *engaged* and *confused*, so we were only able to focus on these two states. We treated each interval as a Markov chain by dividing it into a sequence of discrete states, which may be a typing state, a non-typing state, a compilation error state, or a compilation with no error state. We included facial expression information from different action units (AU) information extracted using Affectiva SDK (https://www.affectiva.com). AUs are a taxonomy of fundamental facial actions, such as raising the cheek or opening the mouth. In this data collection, five AUs were consistently found across all test subjects, namely dimpler (AU16), lip press (AU24), lip suck (AU28), eye widen (AU5), and mouth open (AU27). Figure 1 shows some examples of these AUs. We used each of these AUs in each set of Markov chains. Figure 2 shows an example of a Markov sequence.

We trained hidden Markov models (HMM) for each affective state label, and classified unknown sequences by computing for the probability that the unknown sequence was generated by each model. Table 1 shows the accuracy of the models using leave one out cross fold validation. True positive (TP) refers to confused intervals correctly classified. False positive (FP) refers to confused intervals incorrectly classified. True negative (TN) refers to engaged intervals

Contact: Future University Hakodate, PhD Candidate, 116-2 Kamedanakanocho, Hakodate, Hokkaido 041-8655, 0138-34-6444, g3117002@fun.ac.jp

Figure 1: Examples of AUs

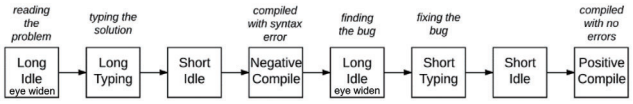

Figure 2: An example state sequence

correctly classified. False negative (FN) refers to the number of engaged intervals incorrectly classified.

Table 1: Results of leave-one-out cross fold validation

AU	TP	FP	TN	FN	Acc.	Kappa
no AU	14	10	14	6	63.64%	0.28
AU16	13	7	17	7	68.18%	0.35
AU24	12	6	18	8	68.18%	0.35
AU28	13	9	15	7	63.64%	0.27
AU5	9	10	11	14	45.46%	-0.08
AU27	15	8	16	5	70.46%	0.41

3. Programming Practice System with Affective Feedback

Using the models, we developed a system for coding practice. Our system is intended to be used with a web camera, which captures a video of the student's face. This, along with the logs is used to determine whether the student is more engaged or more confused. Figure 3 shows a screenshot of the system for programming practice. The student solves coding exercises by writing the body of a function according to some generated specifications. The specifications are automatically generated by combining different computational operations like arithmetic operations, conditional operations, and loops. The system provides an interface for the student to write code, test it by providing inputs to the function, and submit the code for checking. The system can automatically check the code by comparing its output against a set of automatically-generated test cases. The student can move on to the next exercise once a correct solution has been submitted. If a student is unable to solve an exercise for 7 minutes, he is allowed to give up and get a different exercise.

While the student is using the system, it attempts to detect the presence of confusion. When confusion is detected, it offers a guide to the student. If the student accepts the guide, a step by step visualization of the task is displayed, including some hints for each step. An example of the guide is shown in Figure 4. Additionally, the system also adjusts the level of the next exercise, measured by the number of

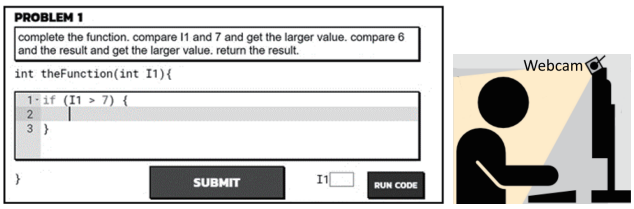

Figure 3: System for programming practice

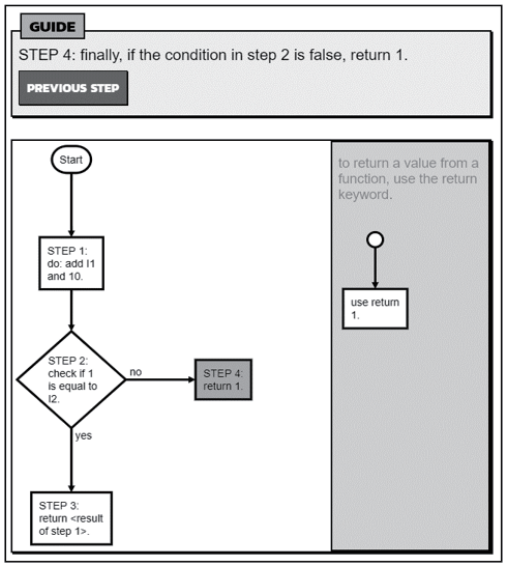

Figure 4: Guide when confusion is detected

operations, based on the presence of confusion. If confusion is detected, the level of the next exercise remains the same. If there is no confusion detected, the level of the next exercise increases. If the student gives up, the level of the next exercise is decreased.

4. Evaluation

We evaluated the system on 35 Japanese university students from Future University Hakodate, Japan. The students were from different year levels, from freshmen students to graduate school students. The students were divided into two groups, labeled Mode A (17 students) and Mode B (18 students). Students were divided such that each group had a balanced representation in terms of year level, age, sex, and months of programming experience. Each student was asked to use the system for 40 minutes.

Students in Mode A used a version of the system that does not offer any guide and does not adjust the level of the problems even when confusion is detected. In this group the problems were given in random difficulty. Students in Mode B featured affective feedback, offering a guide when confusion is detected and adjusting the level of the exercises according to the presence of confusion. The system was translated to Japanese for the evaluation.

We found that students who received affective feedback were able to solve more exercises and gave up of exercises fewer times. Figure 5 shows the number of problems solved

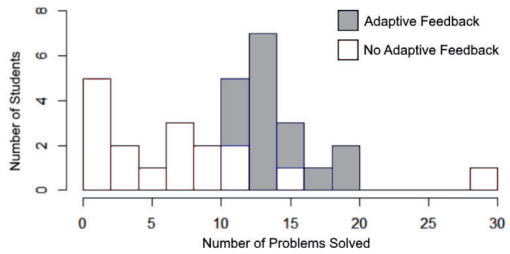

Figure 5: Number of solved exercises for each group

by the students in the two groups. At first glance, one might argue that the difference is due to the fact that the group that received affective feedback also received easier problems because of the automated difficulty adjusting. To investigate this, we further analyzed the data and found that the students who received affective feedback were able to solve more problems across problems of similar difficulty, showing that the offering of guides has a significant effect on the student performance. This is shown in Table 2.

Table 2: Percentage of problems solved across different difficulty levels. This shows that the group that received guides consistently outperformed the group that did not receive guides. There were too few data for difficulty greater than 7 to perform an appropriate comparison.

Difficulty	No feedback	Feedback	p-value
All	53.05%	90.23%	0.00016
1	55.11%	98.61%	0.00007
2 3	70.53%	97.42%	0.01
4 6	51.62%	94.42%	0.041

To evaluate the detection of confusion, we logged the instances in the session where the system detected confusion. If confusion was detected multiple times in a single exercise, we only considered the first instance. We showed these a replay of each of those instances starting from 30 seconds before the confusion was detected up to the point that it was detected. We then ask the student what he felt at that time, to which they could respond "very confused", "somewhat confused", or "not confused at all". To avoid biased responses, the student was not informed that these points in the session were points where the system detected confusion. Overall, 77.78% of all the instances where the system detected confusion match the actual emotion of the student ("very confused" or "somewhat confused").

We also asked the students to rate the exercises on a Likert scale from 1 to 5, with 1 being "very much", and 5 being "not at all" based on how fun the exercises were, and how helpful the exercises were in practicing programming. Across both groups, 62.68% of the students thought that the exercises were "very fun" or "fun" and 68.57% of the students thought that the exercises were "very helpful" or "helpful". However, we did not find any significant difference between the two groups. Although many students felt the exercises were a bit repetitive because of their auto-generated nature, this was a promising result.

5. Ongoing and Future Work

Although we achieved fairly good results in our experiments, we also identified limitations in our models. For instance, the data we have collected is not fine-grained. Since we did not restrict the length of the intervals of the annotations, most students reported emotions on a long intervals, resulting in coarse-grained data. We believe that there is also value in detecting emotion on a fine-grained level for automated tutors to respond more promptly to students. Furthermore, since we gave the students the freedom to provide as many annotations as they want, we only collected very few annotated intervals with respect to the session length. We did not collect enough data to cover other academic emotions such as frustration and boredom as well. Because of these, we were unable to use certain features that did not have enough observations in the data.

Due to these limitations, we performed another data collection process. The participants are 73 students taking up freshmen programming classes in the Philippines and in Japan. We used the same data collection methodology, except for the annotation part. This time, the system partitions the session data into intervals based on key moments such as the start and end of a series of key presses, compilation of the code, submission of the code, and the start of a new problem. A maximum of 150 intervals were selected and the student was asked to provide an annotation for each for these intervals. We added a fifth label called "neutral", which meant that there was no apparent emotion. The average length of the intervals is 17.24 seconds, resulting in fairly fine-grained and fixed point affect judgment data. We were able to collect 9,702 annotated intervals across around 49 hours of session data.

We have started to perform some initial analysis on this data, some of which are discussed in this article. We used OpenFace [Baltruaitis 2018] this time, which is a toolkit capable of not only extracting the presence of AUs, but also estimate the head pose (location and rotation) and the eye gaze. We trained different models using Weka to classify the presence of each emotion, selecting the best model for each task. Table 3 shows the results. In these models, we did not treat the data as time-series for the meantime. It can be seen that by combining face and log features, there is potential to classify some emotions above chance levels ($\kappa > 0.2$) in the fine-grained level.

We also looked at some correlations between certain features and affective state occurrence. To do this, we performed Wilcoxon signed-rank tests on the features and the affective states. Some of our findings are the following: the mean intensity of AU04 (brow lowerer) was significantly higher in reported intervals of frustrations than in all the other states combined ($p = 0.005$). Figure 6 shows examples of AU04. This is consistent with previous studies that correlate this AU with negative academic emotions. Document changes (insertions and deletions) occurred significantly more when students are engaged ($\mu = 0.77$) then when they are confused ($\mu = 0.44, p = 0.000000047$), frustrated ($\mu = 0.55, p = 0.0055$) or bored ($\mu = 0.38, p = 0.0015$),

Table 3: Accuracy and Cohen's Kappa (in parenthesis) for Classifying the Presence and Absence of Affective States

	Japanese Group				**Filipino Group**			
Features	Engaged	Confused	Frustrated	Bored	Engaged	Confused	Frustrated	Bored
pose+face	0.69 (0.39)	0.69 (0.11)	0.73 (0.13)	0.9 (0.13)	0.65 (0.28)	0.67 (0.08)	0.71 (0.16)	0.93 (0.17)
log	0.63 (0.26)	0.77 (0.01)	0.85 (0.07)	0.93 (0.00)	0.58 (0.07)	0.75 (0.00)	0.75 (0.00)	0.95 (0.00)
all	0.71 (0.42)	0.71 (0.18)	0.82 (0.27)	0.91 (0.16)	0.65 (0.30)	0.67 (0.10)	0.72 (0.22)	0.93 (0.1)

Figure 6: Prominent displays of AU04 (Brow Lowerer)

suggesting that typing is indicative of engagement. Compilations occurred significantly less when students were engaged ($\mu = 0.0037$) than when they were confused ($\mu = 0.0086, p = 0.0005$) or frustrated ($\mu = 0.0089, p = 0.0044$). In addition, compilations occurred significantly more when students were frustrated than when they were bored ($\mu = 0.015, p = 0.0043$).

6. Discussion

In this article, we trained models that classify student's academic emotions in the context of programming. Even though programming is generally viewed as a serious, solitary activity, it is interesting that students experience many emotions while doing it, and that these emotions could potentially be inferred through observable features on the face and on typing logs.

So far, our research shows that adaptive feedback based on emotion has a potential in helping students learn or practice coding. Majority of the students reported having fun in solving the exercises and reported that the exercises can be helpful in programming practice, and the guides offered show positive effects on the experience of each student. However, there is still much work to be done in this field, such as investigating how and when to respond to different affective states, the best type of feedback, and further improvement the model of the student's affect.

Affect detection is generally considered to be a challenging task caused by a variety of factors such as noise, individual differences, and the general complexities of human behavior. However, in our research, we show that predicting student emotions while engaged in a complex learning task is possible by using a combination of observable physical features as well as log information. We believe that this is a step in the right direction for the development of affect-aware intelligent tutoring systems for programming.

We believe that systems that can respond to the affective state of humans can be more effective in their interaction with them. For example, a system that can empathize with the student when he is frustrated can be more effective in steering him back towards the path of motivation. Although we have not yet explored many of these affective responses yet, it is something that we intend to investigate as a future direction of this work.

7. Conclusion

In this article we have summarized the research we have done on affective tutoring systems for programming. We discussed the models for classifying student emotion using face and log features and an application for coding practice. We also discussed the future possibilities and direction of this research.

References

[Baltruaitis 2018] Baltruaitis, T., Zadeh, A., Lim, Y.C., et al.: OpenFace 2.0: Facial Behavior Analysis Toolkit. IEEE International Conference on Automatic Face and Gesture Recognition, 2018.

[Bosch 2013] Bosch, N., DMello, S. and Mills, C.: Intelligent tutoring systems for programming education: a systematic review. in Proceedings of the International Conference on Artificial Intelligence in Education, pp. 11-20, 2013.

[Bosch 2014] Bosch, N. and Chen, Y. and DMello, S.: Its written on your face: detecting affective states from facial expressions while learning computer programming. in Proceedings of the International Conference on Intelligent Tutoring Systems, pp. 39-44, 2014.

[Harley 2017] Harley, J., Lajoie, S., Frasson, C., et al.: Developing emotion-aware, advanced learning technologies: A taxonomy of approaches and features. International Journal of Artificial Intelligence in Education 27(2), Springer, 2017.

[Mega 2014] Mega, C., Ronconi, L. and De Beni, R.: What makes a good student? How emotions, self-regulated learning, and motivation contribute to academic achievement. Journal of Educational Psychology 106(1), American Psychological Association, 2014.

[Rodrigo 2009] Rodrigo, M. M., Baker, R., Jadud, M., et al.: Affective and behavioral predictors of novice programmer achievement. ACM SIGCSE Bulletin 41(3), ACM, 2009.

International Session | International Session | [ES] E-1 Knowledge engineering

[2K3-E-1] Knowledge engineering

Chair: Tadahiko Murata (Kansai University), Reviewer: Yasufumi Takama (Tokyo Metropolitan University)
Wed. Jun 5, 2019 1:20 PM - 2:40 PM Room K (201A Medium meeting room)

[2K3-E-1-01] Mobile Website Creation based on Web Data eXtraction and Reuse

○Chia-Hui Chang[1], Yan-Kai Lai[1], Yu-An Chou[1], Oviliani Yenty Yuliana[1] （1. National Central University）

1:20 PM - 1:40 PM

[2K3-E-1-02] Reduction of Erasable Itemset Mining to Frequent Itemset Mining

○Tzung-Pei Hong[1,2], Chun-Ho Wang[2], Chia-Che Li[2], Wen-Yang Lin[1] （1. National University of Kaohsiung, 2. National Sun Yat-sen University）

1:40 PM - 2:00 PM

[2K3-E-1-03] Consideration of the relationship between explicit knowledge and tacit knowledge in an intellectual task

○Itsuki Takiguchi[1] （1. Graduate School of Humanities and Studies on Public Affairs Chiba University）

2:00 PM - 2:20 PM

[2K3-E-1-04] k-th Order Intelligences: Learning To Learn To Do

○Francisco J Arjonilla[1], Yuichi Kobayashi[1] （1. Graduate School of Science and Technology, Shizuoka University）

2:20 PM - 2:40 PM

The 33rd Annual Conference of the Japanese Society for Artificial Intelligence, 2019

Mobile Website Creation based on Web Data eXtraction and Reuse

Chia-Hui Chang, Yan-Kai Lai, Yu-An Chou, Oviliani Yenty Yuliana

Department of Computer Science and Information Engineering
National Central University

Abstract—Due to the rapid growth of mobile devices, using mobile devices to access the Internet is more and more popular. However, many websites are designed for desktop browsing and do not have Responsive Web Design (RWD) for mobile devices. Lacking mobile version for websites make it difficult for users to operate on mobile devices and may decrease the exposure rate or lose some commercial possibilities. However, abandon existing websites to create an RWD website (such as Wix) is not always a good idea since many services (e.g. backend management functions) need to be operated in a desktop GUI. In this paper we introduce a project called DeXaR (Data eXtraction and Reuse) to enable users to quickly and easily create an RWD website from existing website without programming. By incorporating automatic Web data extraction techniques to support Web Data ETL (Extract-Transform-Load) services, we are able to link contents of an existing website to the new website. In other words, we can keep mobile website synchronized with the existing website via data APIs such that users only need to maintain one copy of the data but it can be reused in mobile webpages. The user study on 35 students shows the design philosophy for mobile website creation from existing website is encouraging. However, further survey on the linkage of web data extraction needs to be explored.

1. Introduction

Due to the booming of smart handheld devices, there is an urgent need to browse the Web in mobile devices since people need to obtain information no matter where they are or what they want. While people spend more time on handheld devices to browse the web, most websites are designed for the desktop computers only and do not support small device browsing. Therefore, users must constantly zoom in and shift the display of the textual content and functional buttons on the device. These repetitive operations will cause users great distress and poor browsing experience.

In order to solve the problem in browsing web pages on handheld devices, the concept of Responsive Web Design (RWD) was proposed to enable the websites to dynamically adapt its layout to fit the size and orientation of the device on which it is viewed. Through CSS media query, web developers can check the capabilities of the device and apply corresponding stylesheets or style rules to control the display on different devices. By assigning different style sheets for different media, handheld devices can display the same website normally to avoid repeated zooming, panning and scrolling operations.

While RWD has been introduced to alleviate the website browsing problem on mobile devices, many organizations such as middle schools and hospitals still do not have mobile-device friendly websites because of extra cost and lack of proper IT staff. Meanwhile, creating an RWD website requires more web technologies such as HTML5.0, CSS or JavaScript, Node.js, etc.

In this paper, we introduced the DeXaR project to quickly create an RWD website from existing websites. Similar to existing mobile web design systems such as Wix and Weebly, it requires no programming to create a RWD website. Users can quickly create an RWD website by selecting a predefined template or customizing a page with various web components with page preview. However, different from existing mobile website design systems, this project features the idea of synchronizing the created mobile website and original website based on web data extract-transform-load APIs such that the same backend management system could be used to maintain the website.

To achieve this goal, the DeXaR project also includes a web data ETL system for data API creation by integrating web scraping techniques and web data extraction technologies, where the former helps download web pages and the later outputs the data in a tabular spreadsheet. The web data ETL system allows users to specify the web URLs (universal resource locator) and can extract data from a single web page that contains a list or multiple web pages that are generated from the same template to generate a data API endpoint. Thus, users can use the extracted data in existing web pages as input for mobile web page creation via the mobile web creator. This is especially helpful when there are list items since users do not need to input items one by one.

2. Related Work

Transforming desktop websites for better browsing experience on handheld devices has been a research topic in Web programming research. For example, Mohan et al. (1999) introduced InfoPyramid which provides a multimedia content description framework in a multi-abstraction, multi-modal content representation for adaptive delivery based on profile of client device. Xiao et al. (2009) also proposed a Web page transformation method by slicing the original page into page blocks iteratively to build a tree hierarchy of the transformed pages.

In addition, Nichols et al. (2008) introduced the Highlight system for creating and deploying mobile Web applications via a proxy server to clip and transform content from existing web pages for the mobile device. Koehl and Wang, enhanced the idea

Contact: Chia-Hui Chang, National Central University, Taoyuan City 32001, Taiwan (R.O.C), chia@csie.ncu.edu.tw

by introducing m.Site (2012) to allow site administrators to visually select web objects and assign attributes for adapting existing websites to mobile paradigm. However, Highlight and m.Site require administrators with front-end and back-end Web programming knowledge to modify or add features.

On the other hand, there are also tools for users with no programming background to create RWD websites. For example, WordPress, Wix and Weebly, etc. could generate HTML code for mobile webpages based on user specifications. Therefore, there would not be connection to existing websites. If users rely on the original desktop website for list item management, they may need to either manage two websites, or abandon the original website by creating responsible webpage for backend management. However, if we can reuse data from the existing websites and build linkages to the generated RWD website, the management efforts could be greatly reduced via automatic synchronization. As a result, we propose the DeXaR project to build a mobile website that allows users to focus on creating mobile websites instead of modifying the original website.

3. System Design

In order to quickly and easily create an RWD website from an existing website, we have developed two subsystems for responsible website creation and data ETL API creation. In addition to these two subsystems, we also develop deep web data extraction solutions. Due to space limitation, we focus on mobile website creation in this paper and give only overview of web data ETL system.

3.1 Mobile Website Creation

The mobile website creation provides two functions for page creation/editing and request response. As shown in Fig. 1, the website editor offers GUI (graphical user interface) for page creation and editing and keeps the configuration for each website in NoSQL (Not only SQL) database MangoDB. Upon the request of a page, the request renderer module coordinates with the request combiner to generate HTML and Javascript codes for browsing in mobile devices. Similarly, the page editor renderer coordinates with editor combiner to modify the GUI for page preview.

(1) Website Editor

Similar to commercial mobile website creator, the system also provide predefined templates, which are composed of web components. Users can select from predefined templates to create an RWD webpage. As shown in Fig. 1, the website editor manages mobile websites created by all users. Each website is maintained by a website manager class, which manages all web pages in a website. The settings for each website or webpage are stored in the Website Config Database. When adding or editing a web page, the page editor renderer calls editor combiner to produce the corresponding web code for page preview.

(2) Page Production

There are two cases that we need to generate HTML and Javascript codes for the created pages: one for page preview and one for official page request. Therefore, we have editor combiner and official combiner for respective webpage production. When a user browses a mobile webpage on smart handheld devices, the corresponding configuration is retrieved from the Website Config Database by the page request renderer which calls request combiner to generate the corresponding Web codes.

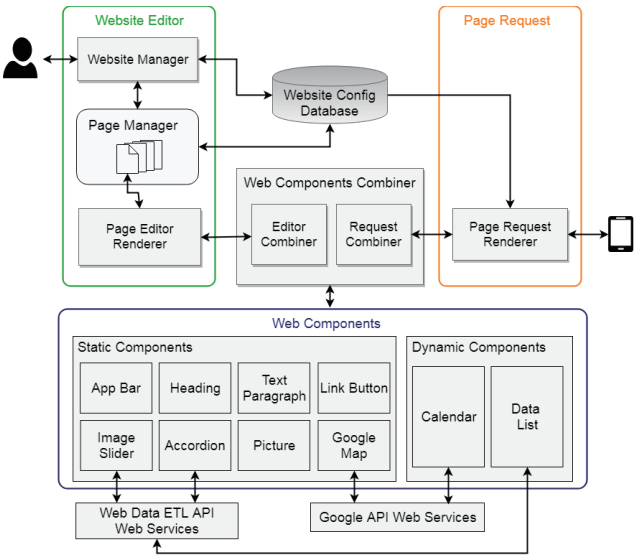

Fig. 1 Mobile Website Creator Architecture

(3) Static and Dynamic Web Components

To enrich the generated webpages, we have implemented a variety of web components including banner bar, heading, text paragraph, picture, link button, image slider, accordion, data list, calendar, maps, etc. Each web component includes an editor and a generator. The former is used in website editor for data setting, while the latter is used in web component combiner for code generation. Some web components use direct data from website Config database to generate static HTML code, while some use indirect access to extract data from data API dynamically.

(4) Design Methodology

To design a web-based development tool, we must consider the fluency of the user interface and the reusability of the self-made web component and the maintainability of the entire program. Therefore, we have adopted front-end engineering solutions React[1] to support single page application. React makes good use of JavaScript to manage the rendering and DOM object operation by encapsulating the elements of a webpage into components. Thus, whenever there is a change in the data on the page, the corresponding component will automatically reflect the change of the screen, which is very helpful for dealing with complex webpage interaction.

However, this kind of client-side rendering starts slowly since the main HTML content needs to be generated in the first request. To solve the above problem, we also use Node.js[2] since it can run JavaScript on the server side. By running Client-Side Rendering application on the server side, we can produce a complete page earlier. This not only improves the browsing experience on page loading, but also helps the search engine optimization (SEO) ranking of the mobile webpages.

[1] React, https://reactjs.org/
2 Node.js, https://nodejs.org/

3.2 Web Data ETL System

As mentioned before, Web data ETL system makes use of web scraping and data extraction techniques for data API generation. Web scraping involves fetching or crawling a page based on HTTP requests and scrape data for extraction based on HTML parsers such as Tidy, CyberNeko, BeautifulSoup, etc.

In the DeXaR project, we adopt unsupervised web data extraction systems including single-page record set extraction system MDR [Liu2003] and multiple-pages detail data extraction algorithm AFIS [Yuliana2018]. Through intuitive and easy-to-use graphical interface, users can specify how to crawl, extract, and output data results (e.g., data API endpoint or static export) automatically without writing a program. Note that there is no need to label data for training (as for supervised approaches). Instead, users only need to select data columns in the spreadsheet as shown in Fig. 6. The generated Web data API can be used in many applications such as synchronizing an existing website with its RWD version through dynamic data API services.

4. Demonstration[1]

In this section, we illustrate how to create a mobile website from an existing website. We will also show how data APIs generated by Web Data ETL System is used in creating mobile webpages for Hopkins West Junior High (HWJHS) school. This is a typical case with no mobile website and IT support. The homepage contains several data regions including banner, navigation bar, image slider, news list, event calendar, etc. By clicking on news article, we obtain more news list as shown in Fig. 2.

To create responsible webpages, users can choose a predefined template such as dashboard, news list, maps, calendar, etc. as shown in Fig. 3. Through website editor, users are free to add or delete web components as show in Fig. 4 where the left navigation bar shows the web components added in the current page. For static web components, the data can be copied-pasted from existing webpage or manually input. For dynamic web combiners, users can specify the extractor name and the corresponding data columns to be displayed (see Fig. 5), where the extractor is generated via web data ETL system. As shown in Fig. 6, we create a data API with multiple-page input from HWJH news pages (Fig. 2) to obtain the tabular output. Fig. 7 shows the generated RWD webpages.

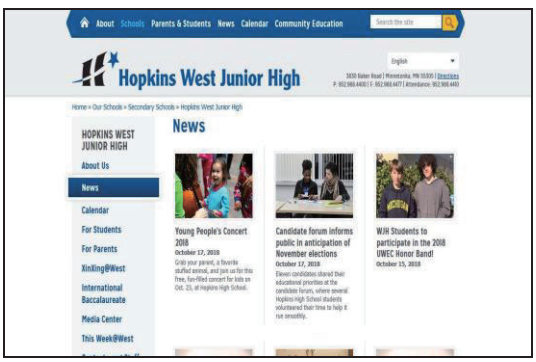

Fig. 2 The News Page of Hopkins West Junior High (HWJH)

Fig. 3 Predefined Template

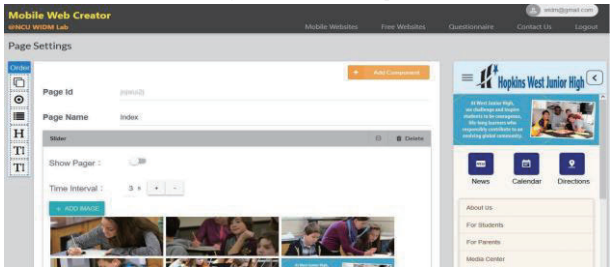

Fig. 4 Mobile webpage editing illustration (Page Editor)

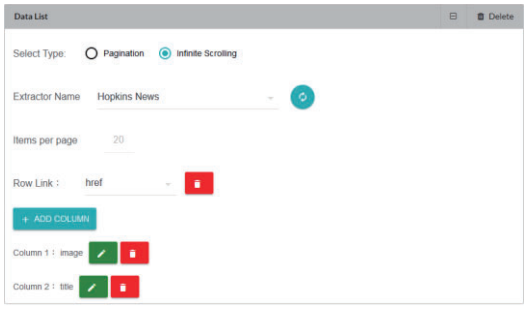

Fig. 5 Data List setting screen preview screen

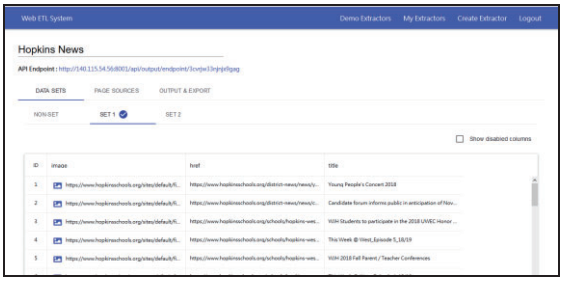

Fig. 6 Data extraction result from Web Data ETL System

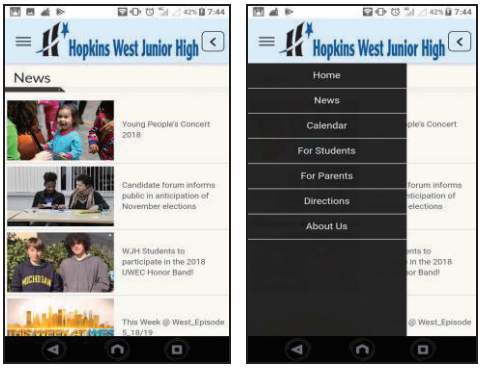

Fig. 7 A mobile webpage created based on the news page from HWJH

1 https://sites.google.com/site/nculab/project/dexar

5. Evaluation and Discussion

To evaluate the effectiveness of the proposed approaches, we run open demonstration several times and invite students to use the system to build a mobile website for any existing website. Then, a questionnaire of 7 questions (Table 1) is given to the test users. A total of 35 subjects replied the questionnaire. The scores for each question are given by 1~5 points, where one denotes very bad, very disagreeable or very difficult, and 5 denotes very good, very agree or very easy.

Table 1 Question list for the proposed questionnaire

	Questions
Q1	The interface is simple and easy to understand
Q2	The interface is easy to operate with high fluency
Q3	I don't need expertise to use the system
Q4	How easy is the tool to create a mobile website?
Q5	The completeness of the system in terms of functions and web components
Q6	I am interested in mobile website creation systems after using this tool
Q7	The quality and practicality of the established websites by this tool

We divide the users into two groups: with or without programming experience. Fig. 8 shows the experimental results. Students without web programming background gives higher score to the mobile website creation system than students with web programming background. Overall, most users can easily create a simple mobile website even without having any programming expertise. The interface is simple and easy to operate with fluent operational flow design.

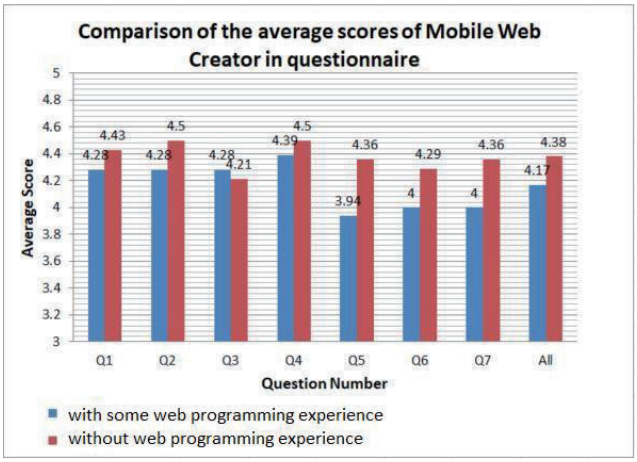

Fig. 8 Questionnaire scores for the mobile website creator system

While the experimental results seem to be great, most students only use static web components to create the mobile websites. Thus, it still lacks the evidence how web data ETL system can enhance the creation of mobile websites. Therefore, we plan to have the second run experiment to see whether web data ETL system could speed the mobile webpage creation in the future.

References

[Goto2016] K. Goto, & M. Toyama. Mobile web application generation features for SuperSQL. In Proceedings of the 20th International Database Engineering & Applications Symposium, 308-315.

[Koehl2012] A. Koehl, & H. Wang. m.Site: efficient content adaptation for mobile devices. In Proceedings of the 13th International Middleware Conference, 41-60. Springer-Verlag New York, Inc.

[Mohan1999] R. Mohan, J. R. Smith, C.S. Li, Adapting multimedia internet content for universal access. IEEE Transactions on Multimedia, 1(1), 104-114.

[Nichols2008] J. Nichols, Z. Hua, & J. Barton. Highlight: a system for creating and deploying mobile web applications. In Proceedings of the 21st annual ACM symposium on User interface software and technology, 249-258.

[Yuliana2018] O. Y. Yuliana and C.-H. Chang, A novel alignment algorithm for effective web data extraction from singleton-item pages, Applied Intelligence, 1–16.

[Toyama1998] M. Toyama. SuperSQL: an extended SQL for database publishing and presentation. In ACM SIGMOD Record, 27(2), 584-586.

[Xiao2009] I. Xiao, X. Luo, Q. Hong, D. Fu, H. Xie, & W.Y. Ma, W. Y. Browsing on small displays by transforming Web pages into hierarchically structured subpages. ACM Transactions on the Web (TWEB), 3(1), 4.

The 33rd Annual Conference of the Japanese Society for Artificial Intelligence, 2019

Reduction of Erasable Itemset Mining to Frequent Itemset Mining

Tzung-Pei Hong[*1,2], Chun-Ho Wang[*2], Chia-Che Li[*2], Wen-Yang Lin[*1]

[*1] National University of Kaohsiung, Kaohsiung, Taiwan

[*2] National Sun Yat-sen University, Kaohsiung, Taiwan

Frequent-itemset mining and erasable-itemset mining are two commonly seen and useful techniques in data mining. Although the two mining problems look contrary, they are actually close to each other. In this paper, we will show the erasable itemset mining problem can be reduced into the frequent-itemset mining problem and can be solved by the existing algorithms of finding frequent itemsets. By this way, the variants of erasable-itemset mining can be easily designed out based on the frequent itemset mining.

1. Introduction

The frequent-itemset mining is a very important step in the search for association rules [1][2][10]. It is mainly determined based on the occurrence frequency of the itemsets in the transactions. The erasable itemset mining problem, proposed by Deng et al in 2009 [5], aimed for the purpose of analyzing the factory production plan [5]. The problem assumes that a factory has some products to produce, and each product requires some kinds of raw materials and can gains some profits. The erasable itemset mining can be used to find out which combination of raw materials will not reduce the profit of the factory too much if they are removed. Although the frequent itemset mining and the erasable itemset mining seem to be relatively different, we will show in this paper that both of them are similar in nature and thus we can reduce the erasable itemset mining problem to the frequent itemset mining problem. The solutions for the frequent itemset mining problem can then be transformed back to form the results for the erasable itemset mining problem. We hope that based on this reduction, the transformation process can provide a novel and interesting design strategy for data analysis methods. The rest of this paper is organized as follows. Some related work is briefly reviewed in Section 2. The reduction process is proposed in Section 3. The correctness of the reduction is shown in Section 4. Conclusion is given in Section 5.

2. Related Work

2.1 Frequent Itemset Mining

Finding frequent itemsets and association rules from a transaction database is a very important research topic in data exploration nowadays. Among the existing algorithms, most of which were based on the Apriori algorithm [1][2] and the FP-tree algorithm [8]. The former approach generates and tests candidate itemsets level-by–level. It is composed of two parts. The first part is to find out the itemsets with large counts, called frequent itemsets or large itemsets; the second part utilizes the conditional probability to find the association rules from the large itemset. If the conditional probability of a possible rule is greater than or equal to the given minimum confidence, it is desired. An incremental mining approach is also proposed [3]

On the other hand, the FP-tree approach uses a tree structure called the frequent-pattern-tree (FP-tree) for efficiently mining association rules without generation of candidate itemsets [8]. The FP-tree can be thought of a compression structure for the database and stores only large items. It is also composed of two parts. The first part is to construct the FP-tree from the database by processing the transactions one by one; the second part utilizes a recursive mining procedure called FP-Growth to derive frequent patterns from the FP-tree.

2.2 Erasable Itemset Mining

Erasable itemset mining was proposed by Deng et al. in 2009 for analyzing production planning [5]. There are several algorithms for erasable itemset mining, such as META[12], MERIT [6], MERIT+ [4], MEI [11], and VME [7]. Some variants are also proposed [9].

Formally, let I is a set of m items. A product dataset, DB, contains a set of n manufactured products. Each product is represented by a subset of I and its profit. The gain of an itemset $X \subseteq I$ is the sum of the profits of the products which include at least one item in X. A set X is called an erasable itemset if its gain is equal to or less than a given threshold of the total profits of all products.

3. Reducing Erasable Itemset Mining to Frequent Itemset Mining

In this section, we reduce erasable itemset mining to frequent itemset mining. The transformation procedure we proposed is described with some examples interweaved in order to express the concept more easily.

3.1 The transformation procedure

In this subsection, we describe the transformation procedure for reducing the erasable itemset mining to frequent itemset mining. The procedure is described as follows.

STEP 1: Transform the product database into a corresponding transaction database.

STEP 2: Transform the threshold for erasable itemset mining into the one for frequent itemset mining.

STEP 3: Find the solutions of frequent itemsets.

Contact: Tzung-Pei Hong, National University of Kaohsiung, Taiwan, tphong@nuk.edu.tw

STEP 4: Transform the frequent itemsets into the erasable itemsets.

3.2 An example

Assume Table 1 is a product database with three fields.

Table 1: An example of a product database P

P		
PID	Items	Value
P_1	CE	150
P_2	BCD	150
P_3	CD	50
P_4	ADE	150

The items in the transaction database are just the complement of the items contained in the product. Taking P_1 as an example, since $P_1.Value$ is 150, there will be 150 identical transactions, T_1 to T_{150}, generated and put into the transaction database T. Since the items in P_1 are C and E, and the set of all the items in the product database are $\{A, B, C, D, E\}$, each derived transaction thus includes A, B and D. The final derived transaction database is shown in Table 2.

Table 2: The derived transaction database T

T							
TID	Items	TID	Items	TID	Items	TID	Items
T_1	ABD	T_{151}	AE	T_{301}	ABE	T_{351}	BC
T_2	ABD	T_{152}	AE	T_{302}	ABE	T_{352}	BC
⋮	⋮	⋮	⋮	⋮	⋮	⋮	⋮
T_{150}	ABD	T_{300}	AE	T_{350}	ABE	T_{500}	BC

Next in Step 2, the minimum threshold ratio r^T for frequent itemset mining is set. Assume in this example, the maximum threshold ratio, r^P, in erasable itemset mining is set at 0.6, then the minimum threshold ratio r^T is set as $1 - r^P$ (= 0.4).

In Step 3, any frequent itemset mining algorithm such as Apriori [2] or FP-Tree [8] can be used to mine all frequent itemsets from the derived transaction database. The mining results from the transaction database in Table 2 are shown in Table 3.

Table 3: Erasable itemsets mined from Table 2

Erasable itemsets	
Itemsets	gain
A	150
B	150
E	300
AB	300
AE	300

Finally in Step 4, the frequent itemsets are thought of as the erasable itemsets for the original product database.

4. The Correctness of the Reduction

In the section, we give a theorem to prove the correctness of the reduction process. That is, we will show the erasable itemsets from both the original erasable mining and from transformed frequent itemset mining are the same.

Theorem: The erasable itemsets from the original erasable mining are the same as the frequent itemsets obtained by the frequent itemset mining after the transformation procedure.

For proving the itemsets obtained by the two mining strategies (directly erasable itemset mining and transformed frequent itemset mining) are the same, the following two cases need to be considered.

(1) If an itemset is erasable, then it is a frequent itemset by the transformed frequent itemset mining.

(2) If an itemset is not erasable, then it is not a frequent itemset by the transformed frequent itemset mining.

Both of them can be proven from the definitions of the two mining problems based on the transformation process. The formal proof is skipped here. Below, we show the results of the product database in Table 1 directly mined by the META algorithm [5], which is commonly used in the erasable itemset mining. The results are shown in Table 4.

Table 4: The erasable itemsets directed mined by META

Erasable itemsets
A
B
E
AB
AE

Comparing the above results in Tables 3 and 4, we may find that the two results are identical, which indirectly show the correctness of the proposed procedure.

5. Conclusion

The erasable itemset mining looks for itemsets whose gain values are below a user-specified threshold, so that we can sacrifice the items in the erasable itemsets to plan the manufacture of products with limited money. While the frequent itemset mining is used to mine itemsets whose frequency is above a user-specified threshold, so that we can see that these items appear frequently. Although the frequent itemset mining and the erasable itemset mining seem to be relatively different, they have been shown that the two problems are similar in nature and can be designed in an interchangeable way. Note that we do not mean to actually solve the erasable itemset mining problem by the frequent itemset mining algorithms in real applications, but provide an effective design way to find out good algorithms to solve erasable itemset mining and its variants.

References

[1] R. Agrawal, T. Imieliński, and A. Swami, “Mining association rules between sets of items in large databases”, The ACM SIGMOD International Conference on Management of Data, pp. 207–216, 1993.

[2] R. Agrawal and R. Srikant, “Fast algorithm for mining association rules”, The 20th International Conference on Very Large Data Bases, pp. 487–499, 1994.

[3] D. W. Cheung, J. Han, V. T. Ng and C. Y. Wong, “Maintenance of discovered association rules in large databases: Agrawal approach”, The 12th IEEE International Conference on Data Engineering, pp. 106–114, 1996.

[4] T. Le, F. Coenen and B. Vo, “An efficient algorithm for mining erasable itemsets using the difference of NC-Sets”, The IEEE International Conference on Systems, Man, and Cybernetics Manchester, pp. 2270–2274, 2013.

[5] Z. H. Deng, G. D. Fang, Z. H. Wang and X. R. Xu, “Mining erasable itemsets”, The 8th International Conference on Machine Learning and Cybernetics, pp. 12–15, 2009.

[6] Z. H. Deng and X. R. Xu, “Fast mining erasable itemsets using NC_sets,” Expert Systems with Applications, Vol. 39, pp. 4453–4463, 2012.

[7] Z. H. Deng, “Mining top-rank-k erasable itemsets by PID_lists”, International Journal of Intelligent Systems, Vol. 28, Issue 4, pp. 366–379, 2013.

[8] J. Han, R. Mao, J. Pei and Y. Yin, “Mining frequent patterns without candidate generation: a frequent-pattern tree approach”, Data Mining and Knowledge Discovery, Vol. 8, Issue 1, pp. 53–87, 2014.

[9] B. Vo, T. P. Hong and B. Le, “A dynamic bit-vector approach for fast mining frequent closed itemsets,” Expert Systems with Applications, Vol. 39, Issue 8, pp. 7196–7206, 2012.

[10] W. Li, M. Ogihara, S. Parthasarathy and J. Zaki, “New algorithms for fast discovery of association rules”, The 3th International Conference on Knowledge Discovery and Data Mining, 1997.

[11] T. Le and B. Vo, “An efficient algorithm for mining erasable itemsets”, Engineering Applications of Artificial Intelligence, Vol. 27, pp. 155–166, 2014.

[12] T. Le, G. Nguyen and B. Vo, “A survey of erasable itemset mining algorithms”, Wires Data Mining Knowledge Discovery, pp. 356–379, 2014.

The 33rd Annual Conference of the Japanese Society for Artificial Intelligence, 2019

Consideration of the relationship between explicit knowledge and tacit knowledge in an intellectual task

Itsuki Takiguchi[*1]

[*1] Graduate School of Humanities and Studies on Public Affairs, Chiba University

In the execution of certain intellectual tasks, both explicit knowledge and tacit knowledge on the task are considered to be affecting. How does explicit knowledge and tacit knowledge affect the execution of task respectively? In this experiment, we investigated using four Origami tasks. As a result of the experiment, the following results were obtained. ① All the participants were able to complete the task. ② Variation in task time was large in tasks including new actions. From the above, it is concluded as follows. ① It is important that explicit knowledge is given in order to complete the intellectual task. ② If new information was included in the given explicit knowledge, tacit knowledge had a big difference in understanding and execution.

1. Introduction

When we look at the various actions from our morning getting up to sleep at night, it can be said that they are various kinds of task and accumulation of actions. In such task, even if it is an intellectual task that is somewhat complicated, such as cooking, sports, creative activities, if they are always doing them, we can do their intellectual task without any problems. This is because we have tacit knowledge about their intellectual task.

Tacit knowledge is knowledge of actions accumulated in the body by experience, and it is said that it is difficult to language and explain its contents. There is explicit knowledge as a knowledge division paired with this implicit knowledge. Explicit knowledge is a knowledge that can be symbolized, such as documentation or charting, and it can be said that it is relatively easy to acquire knowledge by looking at the symbolized one.

In the previous study, in a new intellectual task A and similar intellectual task B, if a person without knowledge of the intellectual task B experienced task B even once, they possible to perform intellectual task A as easily as those who have knowledge of task B.

As a problem of this experiment, it is not clear whether knowledge which is thought to be obtained by experiment is tacit knowledge or explicit knowledge, and the relationship between tacit knowledge and explicit knowledge for the intellectual task was unclear It is a point.

Therefore, in this research, we set the explicit knowledge for a certain intellectual task on the foundation and see the relationship between tacit knowledge and explicit knowledge for the intellectual task by seeing how tacit knowledge is involved in the task process investigated.

In this thesis, tacit knowledge and explicit knowledge were defined based on Nonaka (1996).

Contact：Itsuki Takiguchi, Graduate School of Humanities and Studies on Public Affairs, Chiba University
mail：moonbow.shooting@gmail.com

2. Experiment

2.1 Purpose

We examine the relationship between explicit knowledge and tacit knowledge in the execution of intellectual tasks using intelligent task called Origami. Given the procedure of symbolized task as a folding chart, compare the differences between the experiment participants in the execution, so that tacit knowledge

It is clear whether it is involved.

In this research, we conducted experiments using four types of origami tasks, "Organ", "Yakko-san" "Ship" "Motorboat" (Figure 1, Figure 2, Figure 3, Figure 4). The four tasks used in this study were selected according to the classification of folding methods and the number of task procedures.

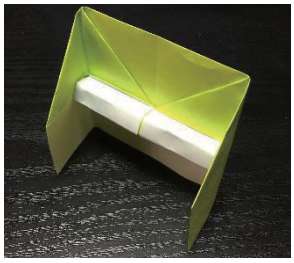

Figure 1 Organ

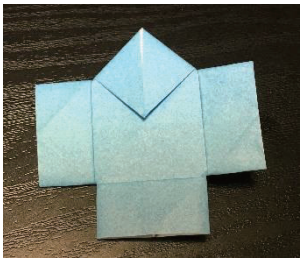

Figure 2 Yakko-san

Figure 3 Ship

Figure 4 Motorboat

First, similar to the classification of the basic folding method of origami in Maruyama (2013), we classify what is a plane deformed shape after deformation as a planar deformation and classify it as a three-dimensional deformed shape after deformation as a three-dimensional deformation.

Looking at the four types of tasks used in this experiment based on the above classification, "Organ" and "Yakko-san" contain both deformations of planar deformation and stereoscopic deformation, but mainly consists of three-dimensional deformation is there. On the other hand, "Ship" and "Motorboat" both contain only one deformation "turn over", but mainly consists of planar deformation.

Also, in "Organ" which is the problem of three-dimensional deformation, "Organ" has fewer task procedures and "Yakko-san" has more task procedures. Similarly, in "Ship" and "Motorboat" which is the problem of planar deformation, "Ship" has fewer task procedures and "Motorboat" has more task procedures.

If it is important to have formal knowledge about the task of folding origami, in the state given from the beginning in the formal knowledge of a fold, it is possible to fold each task to the end irrespective of participants It is considered possible. In addition, the variation in the tasking time among experimental cooperators in each task is reduced, and it can be considered that all the participants can finish the task in a certain time. It is thought that the task time of each task is that the task time becomes longer in the order of ship, organ, motorboat, Yakko-san, from the difference in the number of task procedures and the difference in task procedure related to deformation.

2.2 Method

(1) Participant

Nine university students (4 men, 5 females, 19 to 21 years old) participated. Both were undergraduates enrolled at the Faculty of Literature, Chiba University.

(2) Procedure

Based on Takiguchi (2017), we set experimental recording method and experiment time. I asked the participants to fold the origami of Organ, Ship, Yakko-san, and Motorboat. I take a photograph of the situation, and then asked questions about the problem. The experiment time was 40 minutes.

Firstly, we presented subjects with a fold of the task and an origami. After telling participants to refer to folding charts and referring to the tasks, we asked the participants to start to break down the task and took a picture of the situation. The shooting was done from the front so that the hand of the subject could be confirmed. A measurement was started from the point of time when the subject touched the origami, and the measurement was terminated when the task was completed. After completing the assignment, I asked the subjects the following question about the subject.

① Have you ever faced a problem before?
② Did you know how to break the task?
③ Has there been a part that the instructions were difficult to understand about the fold of the task?
④ Were there any places where it was difficult to break up the task, and what was difficult if there were any?

After finishing the question on the subject, we moved to the next task.

After completing all four tasks, we asked questions about the folding charts of subjects by referring mainly to the illustration part and the sentence part of the folding drawing and asked the questioner about experiments finished.

The order of assignment was randomly determined for each subject and experiments were carried out.

2.3 Result

Tasking time of each task was measured based on captured images. The measured results are summarized in a table (Table 1). Mark of "experience" in Table 1, they have never been experienced yet and none that knows how to fold as ×, they have a memory like folded before but they do not remember how to fold at the moment as △, and they had folded and remembered how to fold as ○. Also, the skewness, kurtosis, average value, standard deviation, and coefficient of variation were determined for each task in Table 2 and summarized in a table (Table 2).

And a box-breaking graph was created. (Figure 5)

Table 1 Task time(sec) and experience of participants

	Organ		Yakko-san		Ship		Motorboat	
ID	time	experience	time	experience	time	experience	time	experience
A	133	×	264	×	134	×	413	×
B	158	×	156	△	206	×	469	×
C	90	×	104	△	115	×	241	×
D	111	○	178	×	336	×	199	×
E	95	×	158	△	128	×	279	×
F	155	×	122	○	191	×	291	×
G	170	×	156	○	187	×	426	×
H	163	△	221	△	273	×	667	×
I	153	×	209	×	164	×	608	×

Table 2 Analysis values for each tasks

	Organ	Yakko-san	Ship	Motorboat
skewness	-0.625	0.465	1.068	0.508
kurtosis	-1.420	-0.171	0.658	-0.905
average	136.444	174.222	192.667	399.222
standard deviation	28.768	47.208	68.059	153.608
coefficient of variation	0.211	0.271	0.353	0.385

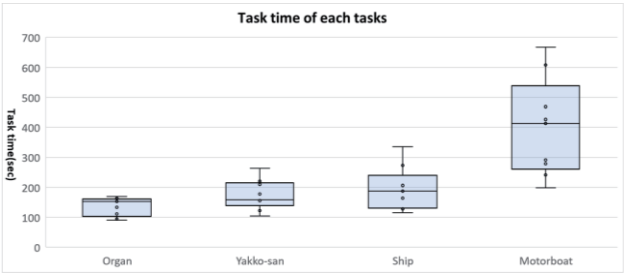

Figure 5 Box plot of task time

Looking at the experience of Table 1, we can see that in this experiment there were none of the experimental collaborators who had previously experienced the creation of a Ship and a Motorboat. Also, at Yakko-san, many participants are not remembering how to fold at the moment but remember that they have experienced before, or they have remembered folding methods before.

From Table 3, it can be seen that the skewness and kurtosis of each task are within the range of ± 1.5. Also, when comparing the values of average, standard deviation, and coefficient of variation for each task, you can see that the Organ, Yakko-san, Ship, Motorboat are increasing in that order in all the items.

As you can see from Figure 5, the Organ does not have much variation in task time, and he can be said that the variation in task time is small. For Ship, it seems there are variations in the tasking time compared to Organ and Yakko-san. It can be seen that the variation in the operation time of the Motorboat is larger than that of the other three. Also, it can be seen that there are no outliers for each task.

Regarding the question after the completion of each task, there were responses to Organ, Ship, and Motorboat for the part where the instruction of the folding chart was difficult to understand. For Organ, there are responses from five experimental collaborators, all of which are difficult to judge because there is no instruction as to whether to fold down by half or half against the folding method of the part corresponding to the keyboard part of the organ It was an answer that it was. For Ship, there were responses from six experimental collaborators, all of which were answers that the instruction of the folding drawing was difficult to see, of which four were to fold only the top one of the overlapping parts It was an answer that instructions were difficult to see. For Motorboat, eight replies from the participants replied that it was difficult to understand the instructions on the instructions that three of them will be turned upside down. The other 5 people answered that they had to worry about the order of folding up the left and right, and because they needed confirmation left and right unlike other tasks, they were caught in that place. There was no response from the participants to the Yakko-san.

Responses were obtained to Ship and Motorboat for places where it was difficult to break up the task. For Ship, there were responses from three people, and it was an answer that it was difficult to move all of them upside down. For Motorboat, there were responses from four people, and two of them answered that it was difficult to move upside down. The other two persons answered that the part folded so as to overlap on the left and right was hard to be folded due to a large number of papers overlapped and thick, which made it difficult to fold.

For the question after the task was completed, all the participants tasked while referring to illustrations mainly in the folding chart, and answered that the sentences were using it as an aid.

2.4 Discussions

Looking at the skewness and kurtosis values of each task in Table 2, we see that each task is within the range of ± 1.5. Also, looking at Figure 5, it does not appear that there are large outliers for each task. From the above, it can be said that it is appropriate to use the average value as the representative value and the standard deviation or the variation coefficient as the comparison of the variation size, according to the normal distribution of the numerical distribution of the task time in each task.

Looking at the variation in the task time within each task seen in Figure 5, it seems that the variation is increased in the order of Organ, Yakko-san, Ship, and Motorboat. This is also evident from the comparison of the values of the coefficient of variation in Table 2. From this it can be said that if it is assumed that only formal intelligence is important in origami, the variation in tasking time among experimental cooperators in each task is reduced, and it is possible that all participants can finish task in a certain time It can be said that the result was contrary to the assumed hypothesis. In addition, since the average value of each task increases in the order of Organ, Yakko-san, Ship, and Motorboat, it can be said that the total operation time in each task increases in the order of Organ, Yakko-san, Ship, and Motorboat. If the result is also important, when the task of each task is important, the result that Ship, Organ, Motorboat, and Yakko-san become larger from the difference of the number of task procedures and the task procedure related to the deformation It is contrary to the assumption that it is obtained.

In addition, with regard to Yakko-san, it cannot be seen that some variations between each participant can clearly show that those who have experience clearly were able to complete task earlier. However, it can be considered that the task time of participants who have never folded a fellow before it is higher than the average value of all the parties supports the assumption to some extent.

It is thought that the reason why Ship and Motorboat task time was more than Organ and Yakko-san was that there was no person who experienced Ship or Motorboat, and there was no experience of "turn over". On the other hand, since it is totally uneven despite being a new movement to all participants, we thought that there was something different about understanding and execution of the new behavior .

3. Discussions

Summarizing the results obtained in this experiment, the following two points can be said.

① If you get the folding chart, that is explicit knowledge, of origami, you can complete the task even if it is a task that has never folded before.

② From the results of task time variation, Yakko-san, Ship, and Motorboat, not only explicit knowledge but also tacit knowledge influences execution and understanding of the task.

In this experiment, all the participants were able to complete all tasks to the last. At Takiguchi (2017) and Takiguchi (2018), we could not finish the task to the very end by presenting samples of the task, presenting information that is not complete with respect

to the procedure of folding and how to fold. From these facts, it can be said that presenting the procedure of folding and the written explicit knowledge of how to fold has had a big influence on executing inexperienced tasks.

It can be concluded that tacit knowledge has an influence on the execution and understanding of explicit knowledge, based on the comparison of the average value in Yakko-san and the task time with inexperienced persons, the magnitude of variations in Ship and Motorboat.

In this experiment, it was important that explicit knowledge was given to the completion of origami, but the result that tacit knowledge had an influence on understanding and execution of given explicit knowledge was obtained.

Whether intellectual task is carried out or not is important for completing the task whether explicit knowledge is given, but individual tacit knowledge brings about a big difference to the understanding and execution of given explicit knowledge can be concluded.

4. Conclusions

Ship and Motorboat 's "turn over" is not intended in this experiment, so care must be taken when performing similar experiments.

The introduction of new action tasked effectively as a reinforcement of the possibility that tacit knowledge has an important influence on the execution and understanding of formal knowledge about the relationship between formal knowledge and tacit knowledge for tasks. However, it was not possible to deny the possibility of having a negative influence in the experiment which was supposed originally, and attention is necessary for a similar experiment to be carried out in the future.

Also, I would like to pay attention to the point that the folding chart of Ship became difficult to see part by printing.

Participants were tasking on the task with reference to both the illustration part and the sentence part of the folded drawing. It can also be said that the fact that the sentence is difficult to see is that part of the function as a folding chart has been lost.

I think that we can see the implications of tacit knowledge in terms of what we have been devised to accomplish the task from the missing information..

References

[Nonaka 1996] Ikujiro Nonaka, Hirotaka Takeuchi (Author) Katsuhiro Umemoto (Translation). Knowledge Creation Company 1996-03-21. Toyo Keizai Inc.

[Maruyama 2013] Manami Maruyama. Formation of stereoscopic image: psychological study using origami paper Brush up seminar proceedings for young image researchers 76-79, 2013-03-14. For the brush up seminar steering committee.

[Fukami 2000] Ezashi Fukami. Ogami Daizenshu. Narimido Publishing and Editorial Department (ed) Narumido Publishing

[Ueda 1955] Jiro Ueda. New Origami Origami. 1955-06-01. Fukuinkan bookstore

[Polanyi 1980] Michel Polanyi. Keizo Sato (Translation). Dimension of tacit knowledge: From language to non-language 1980-8-15. Kinokuniya Bookstore

[Osaki 2009] Masauru Osaki. Understanding tacit knowledge Tokyo Keizai University Humanities and Natural Sciences (127). 21-39, 2009-03-04. Tokyo Keizai University

[Igarashi 2012] Yuko Igarashi. A History of Origami and a Study on Origami as Child Care Education. Urawa Discourse (46). 45-68, 2012-02. Urawa University Junior College

[Takiguchi 2017] Itsuki Takiguchi. Akinori Abe. A study on the influence of experiential knowledge on intellectual task. The conference proceedings of the National Convention of the Society of Artificial Intelligence JSAI 2017 (0), 4 L 23 - 4 L 23, 2017. General Society of Artificial Intelligence

[Takiguchi 2018] Itsuki Takiguchi. Akinori Abe. A study on intellectual tasks influenced by the embodied knowledge. in New Frontiers in Artificial Intelligence. JSAI-isAI 2017 (Arai S., Kojima K., Mineshima K., Bekki D., Satoh K., Ohta Y. (eds)). Lecture Notes in Computer Science. vol 10838. pp. 51-62. Springer(2018)

The 33rd Annual Conference of the Japanese Society for Artificial Intelligence, 2019

k-th Order Intelligences: Learning To Learn To Do

Francisco J. Arjonilla[*1] Yuichi Kobayashi[*1]

[*1] Graduate School of Science and Technology, Shizuoka University

We propose a novel classification of intelligence based on distinguishing model exploitation from model exploration in order to improve our general understanding of intelligence and its limitations. For this purpose, we define computational problems by traditional function execution, which implicitly hold the model of the problem to solve, and learning problems by the meta-methods that produce computational methods. Learning problems are then assimilated to computational methods which hold implicit meta-models. The process is repeated iteratively, with each iteration named a *k*-th order intelligence. However, we show that the infinite sequence of classes of intelligence that emerges poses difficulties for meta-model exploration. We suggest using self-referential meta-models to break the escalation of orders, and we introduce some of the problems associated to this approach.

1. Introduction

The definition of intelligence is a highly debated topic that finds no consensus amongst researchers [Legg 2007]. In general, papers that tackle intelligence begin by offering a definition that is convenient for the topics dealt with and often matches the subjective view of the author on intelligence. Many of these definitions are too abstract or measure single capabilities. Intelligence includes concepts such as learning, exploration vs. exploitation, algorithms, knowledge representation, pattern recognition and many others. With such a broad scope, it is difficult to reconcile all aspects of intelligence in a single line of research for the purpose of unifying efforts into developing a plausible general theory of intelligence, hopefully facilitating collaborations and merging researches.

We propose a novel classification of Artificial Intelligence based on computational problems vs. learning problems that builds up from traditional algorithmic methods to general meta-models. In the next section we characterize computational problems and continue with learning problems on the following section. We then consider a different boundary for the learning agent such that we can equalize learning problems to computational problems, thus resulting in a hierarchical specification of meta-learning methods that emerge by induction. Lastly, we show how this hierarchy leads to fundamental problems to achieve General Intelligence.

2. Computational Problems

We start the discussion by defining computational problems as those problems solved by traditional function execution, where typically input data is processed and transformed to produce output data. The function realizes a fixed algorithm that holds an implicit model of the problem and the instructions to solve it. Hereupon, we will refer to these functions and problems as *first order intelligence* and *first order problems*, respectively. Typical examples are those informally referred as narrow intelligence, which include symbolic processing, calculation tasks, control algorithms and basically any function that yields output data. They are characterized by immutable algorithms that are specialized in concrete tasks. With respect to agent-environment systems, first order intelligence encompasses all the methods that imply exploitation of a model and enable an agent to interact and make changes to the environment, such as trained neural networks, expert systems, reactive systems and natural language processing, to name a few. Intuitively, first order intelligence is understood as *doing*.

3. Learning Problems

In contrast, learning problems are differentiated by the scope of the transformation. Rather than making changes to the environment, a learning process modifies the methods used in computational problems. Therefore, the target of a learning process is not the environment, but the agent itself. Learning problems arise when first order intelligence is unable to cope with computational problems due to a lack of an appropriate model [Unruh 1989]. In that case, learning processes generate candidate new models, *i.e.* functions, and test them against computational problems. We call these processes *second order intelligence*. Whereas first order intelligence exploits models, second order intelligence explores the model space. Representative examples include Bayesian networks, evolutionary programming and reinforcement learning. The common characteristic amongst these methods is that the output is a function, code listing or model, such that their input and output correspond to the ones that characterize first order intelligence, *i.e.* raw data. The functions produced are often defined by algorithmically choosing the appropriate weights. That is the case with neural network training algorithms such as gradient descent [Werbos 1990]. During training, the neural

Contact: Francisco J. Arjonilla (Paco), Graduate School of Science and Technology, Shizuoka University, 3-5-1 Johoku, Naka-ku, Hamamatsu City, +81 (0) 53-478-1604, pacoarjonilla@yahoo.es

network weights are adjusted until the measured error on the training data falls below a certain threshold, which represents the acceptance level of the neural network. This corresponds to second order intelligence because training does not affect the environment, but the resultant neural network does. After training, the neural network holds an implicit model of the training data in its weights, as characterized by first order processes. As opposed to doing, second order intelligence is understood intuitively as *learning to do*.

3.1 Learning Problems as Computational Problems

Let us now change the perspective on learning problems by redefining the boundaries of the agent by relocating the realization of first order intelligence to the environment. In other words, we consider the computing device, or at least the memory space reserved for first order processes, as external to our agent. Direct control of the environment is hence reduced to controlling what is executed in the first order computing device, which in turn controls the rest of the environment. The new boundaries redefine computational problems and learning problems as stated in the previous sections, yet this agent's computational processes hold meta-models, or models of models. Thus, learning problems for first order intelligence are the same as computational problems for second order intelligence. That is to say, learning problems are computational meta-problems in the domain of computational problems; exploration of a model is exploitation of a meta-model.

4. Higher Orders of Intelligence

In the previous sections we have treated first and second order intelligences, and how a second order intelligence is interpreted as a first order meta-intelligence. We now repeat the same process to arrive at third order intelligence from second order intelligence. In the same way that second order intelligence takes over first order intelligence when there are no models to cope with a problem, third order intelligence triggers when there are no meta-models available [Schmidhuber 2005]. However, third order processes are rarely found in Artificial Intelligence. One example is [Naik 1992] where a meta-neural network establishes the training parameters of a basic neural network, improving learning rates for solving problems that are similar to previously solved ones. Intuitively, third order intelligence is regarded as *learning to learn* (to do).

The next natural step is to consider higher order intelligences. These orders emerge when models, meta-models, meta-meta-models, … get exhausted. Hence, an infinite sequence of orders develops where exploration of a meta-model in the k-th order is exploitation of the meta-model in the $(k+1)$-th order [Turing 1939]. Unfortunately, higher orders are more complex, abstract and difficult to visualize intuitively: *learning to learn to learn to* … In A.I., there are no known methods that take the role of higher order intelligences. On the contrary, this role is taken by human researchers, who generally propose new methods corresponding to first order intelligence (*e.g.* GOFAI) or second/third order intelligence (*e.g.* machine learning). When the methods in A.I. fail for a given problem at some order, researchers ultimately perform exploration of the meta-models.

4.1 Breaking the Escalation of Orders

In order to overcome the lack of higher order processes, we propose a general meta-model that consists of a self-referential method that can modify itself. This way, the meta-model of this method is the model itself, effectively discontinuing the trend towards infinite orders by equalizing k-th order and $(k+1)$-th order for some k. Such a method is canonically realized by a function whose input and output data are the binary encoding of the function itself. Nevertheless, a self-referential function that can explore its own model conflicts with well-known problems of axiomatic systems related to incompleteness [Gödel 1931], inconsistency and the P *vs.* NP problem [Cook 1971].

References

[Cook 1971] Cook, S. A., *The Complexity of Theorem-Proving Procedures*, Proceedings of the third annual ACM symposium on Theory of Computing, ACM Press, 1971.

[Gödel 1931] Gödel, K., *Über formal Unentscheidbare Sätze der Principia Mathematica und verwandter Systeme I*, Monatshefte Für Mathematik Und Physik, 1939.

[Hutter 2001] Hutter, M., *Towards a Universal Theory of Artificial Intelligence based on Algorithmic Probability and Sequential Decisions*, Proceedings of the 12th European Conference on Machine Learning, 2001.

[Legg 2007] Legg, S., & Hutter, M., *Universal Intelligence: A Definition of Machine Intelligence*, Minds and Machines, 2007.

[Naik 1992] Naik, D. K., & Mammone, R. J., *Meta-neural networks that learn by learning,* International Joint Conference on Neural Networks, IEEE, 1992.

[Pfeifer 2001] Pfeifer, R., & Scheier, C., *Understanding intelligence,* The MIT Press, 2001.

[Schmidhuber 2005] Schmidhuber, J., *Gödel Machines: Self-Referential Universal Problem Solvers Making Provably Optimal Self-Improvements*, Artificial General Intelligence, Springer, 2005

[Sternberg 1977] Sternberg, R. J, *Intelligence, Information Processing, and Analogical Reasoning*, John Wiley & Sons, 1997.

[Turing 1939] Turing, A. M., *Systems of Logic Based on Ordinals*, Proceedings of the London Mathematical Society, 1939.

[Unruh 1989] Unruh, A., & Rosenbloom, P. S., *Abstraction in Problem Solving and Learning*, Proceedings of the 11th International Joint Conference on Artificial Intelligence, 1989.

[Werbos 1990] Werbos, P. J., *Backpropagation Through Time: What It Does and How to Do It*, Proceedings of the IEEE, 1990.

International Session | International Session | [ES] E-3 Agents

[2O5-E-3] Agents: reasoning and integration

Chair: Naoki Fukuda (Sizuoka University), Reviewer: Takayuki Ito (Nagoya Institute of Technology)
Wed. Jun 5, 2019 5:20 PM - 7:00 PM Room O (Front-left room of 1F Exhibition hall)

[2O5-E-3-01] Improving the Accuracy of the Collective Prediction by Maintaining the Diversity of Opinions: Preliminary Report

○Rui Chen[1], Shigeo Matsubara[1] （1. Kyoto University）

5:20 PM - 5:40 PM

[2O5-E-3-02] An Approach to Knowledge Graph Completion based on Discussion Agents using IBIS Structure

○Xiangyu Zhang[1], Shun Shiramatsu[2] （1. Department of Computer Science, Faculty of Engineering, Nagoya Institute of Technology, 2. Department of Computer Science, Graduate School of Engineering, Nagoya Institute of Technology）

5:40 PM - 6:00 PM

[2O5-E-3-03] Using Q-learning and Estimation of Role in Werewolf Game

○Makoto Hagiwara[1], Ahmed Moustafa[1], Takayuki Ito[1] （1. Nagoya Institute of Technology）

6:00 PM - 6:20 PM

[2O5-E-3-04] Inferring Agent's Goals from Observing Successful Traces

○Guillaume LORTHIOIR[1,2], Katsumi INOUE[1,2], Gauvain Bourgne[3] （1. SOKENDAI (The Graduate University for Advanced Studies), 2. National Institute of Informatics, 3. Sorbonne Université, UPMC CNRS, UMR 7606,LIP6, F-75005, Paris, France）

6:20 PM - 6:40 PM

[2O5-E-3-05] A New Character Decision-Making System by combining Behavior Tree and State Machine

○Youichiro Miyake[1] （1. SQUARE ENIX）

6:40 PM - 7:00 PM

Improving the Accuracy of the Collective Prediction by Maintaining the Diversity of Opinions: Preliminary Report

Rui Chen*1 Shigeo Matsubara*1

*1 Kyoto University

This study aims to improve prediction accuracy by fostering diversity of opinions. We take an approach to give incentive to agents and induce diverse opinions and focus the minority reward system. The previous study assumes that the number of agents is sufficiently large, but the number of agents may be small in real-world situations. We show that the minority reward system is not necessarily efficient if the number of agents is small such as 100. To overcome this drawback, we propose a method to improve the performance by tuning the threshold for determining the minority and show the preliminary result of the evaluation.

1. Introduction

This study aims to improve prediction accuracy by fostering diversity of opinions. The idea of collective prediction, i.e., the idea of group formation of agents can be supported by the diversity prediction theorem that given a group ("crowd") of predictive models, then the average squared error (collective error) is equal to the average individual error minus the variance between the individual signals (prediction diversity) [Page 07]. Forming a group whose diversity is large can make the collective error small. An approach for obtaining diverse opinions is to transform a prediction problem into a group formation problem [Lamberson 12].

Another approach is to give incentive to agents and induce diverse opinions [Mann 17]. Mann and Helbing propose an incentive scheme that rewards accurate minority predictions and show that this produces optimal diversity and collective predictive accuracy. They assume that the number of agents is sufficiently large, but the number of agents may be small. We show that the minority reward system is not necessarily efficient if the number of agents is small such as 100. To overcome this drawback, we propose a method to improve the performance by tuning the threshold for determining the minority and show the preliminary result of the evaluation.

2. Model

We consider a binary outcome, Y, which is the result of many independent factors, $x_1, x_2, \cdots, x_m$. The outcome is determined by the sign of the weighted average of $x_1, x_2, \cdots, x_m$.

$$Y = sign\Big(\sum_{i=1}^{m} \beta_i x_i\Big)$$

, where each contributing factor takes binary values such that $x_i \in \{-1, 1\}$. For example, Y is whether a stock price goes up or down. $x_1, \cdots, x_5$ are an economic trend, interest rate, exchange rate, political situation, and corporate performance, respectively.

There are n agents. Each agent chooses one factor at a given time. An agent choosing factor x_i observes the value of x_i and then votes according to that observation. The collective prediction, $\hat{Y}$, is given by the sign of the collective vote V, which is calculated as follows.

$$\hat{Y} = sign\Big(\sum_{i=1}^{m} \rho_i x_i\Big)$$

Collective accuracy, C, is defiend as the probability that the collective vote agrees with the ground truth given the distribution, ρ_i, of agents choosing each factor.

The reward function, $f(z)$, which determines the amount of the reward when an agent makes an accurate prediction as a function of the proportion, z. We consider the following three reward systems. In the minority reward system, agents are rewarded for an accurate prediction when the agents belong to the minority.

- Binary: $f(z) = 1$
- Market: $f(z) = 1/z$
- Minority: $f(z) = 1 - \alpha H(z - \theta)$, where H is the Heaviside step function. α and θ are control parameters.

Here, θ determines whether the population is a minority or not. If the population selecting factor x_i is less than θ, it is regarded as the minority. If α is set to 1, only the minority get rewarded. If α is less than 1, agents belonging to the majority also get paid. In the original minority reward system [Mann 17], $\alpha = 1$, and θ=1/2.

3. A criterion for determining the minority

In the study of Mann and Helbing [Mann 17], they assume that the number of agents is sufficiently large. If the number of agents is small, the followings may deteriorate the performance of the minority reward system.

Contact: Rui Chen, Kyoto University, Yoshida-honmachi, Sakyo-ku, Kyoto, 606-8501, chin@ai.soc.i.kyoto-u.ac.jp

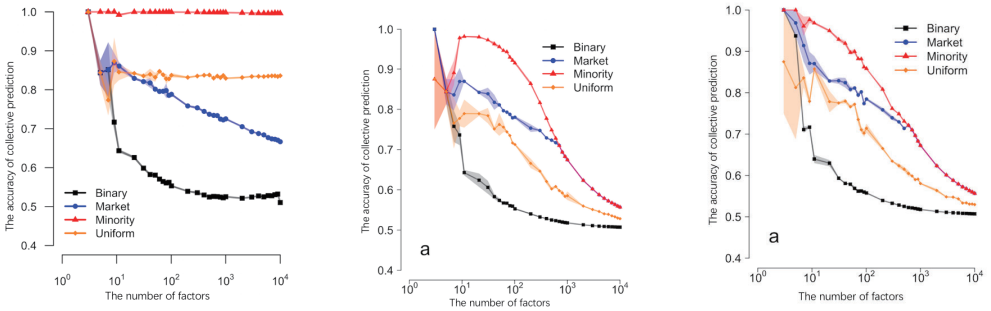

(a) large population $\theta = 0.5$ (b) small population $\theta = 0.5$ (c) small population $\theta = 0.6$

Figure 1: The accuracy of collective prediction

First, assume that the coefficients of only two contributing factors, x_1, x_2, are larger than zero. Here, the strategy of agents is represented by the probability of choosing x_1. An equilibrium is determined by the probability of choosing x_1 and the performances of x_1 and x_2. The performances of x_1 and x_2 are fixed. Thus, agents can change only the probability of choosing x_1. If the number of agents is large, fine-tuning can be achieved. However, if the number of agents is small, the tuning becomes coarse.

Second, when there are many factors whose coefficients are larger than zero, if the number of agents is small, the agents cannot cover all the factors. That is, only the factors having the high coefficients are chosen, and the factors having the low coefficients cannot be included in the prediction model, which deteriorates the performance of the collective prediction.

4. Experiments

To examine the observation in Section 3., we conducted the experiments. We compare the following three cases.

- Case1: Huge population, threshold $\theta = 0.5$.
- Case2: Small population (the number of agents $n = 100$), threshold $\theta = 0.5$.
- Case3: Small population (the number of agents $n = 100$), threshold $\theta = 0.6$. Also, pay 10% of the reward for agents belonging to the majority, i.e., $\alpha = 0.9$.

In Figure 1, (a), (b), and (c) correspond to Case1, Case2, and Case3, respectively. In each graph, the horizontal axis represents the number of factors, and the vertical axis represents the accuracy of collective prediction. The results of the three reward systems mentioned above and *Uniform* are plotted. *Uniform* means a uniform allocation of agents to factors.

Figure 1 (a) is a reproduction of the results by Mann and Helbing [Mann 17] and shows that the minority reward systems alwasy outperforms the other reward systems. Figure 1 (b), however, shows that the performance of the minority reward system drops and the market reward system is the best when the number of factors is less than ten. Also, we can observe that the performances decrease when the number of factors increases, although the minority reward system outperforms the other reward systems.

In Figure 1 (c), the performance drop of the minority reward system when the number of factors is arount 10 can be mitigated. The peak value of the accuracy in the minority reward system is around 0.97, and when the number of factors is equal to 1,000, the accuracy is 0.7.

This experiments confirmed our observation is correct and there is a possibility to improve the accuracy by tuning the threshold of determining the minority. Investigating how to find the optimal threshold is included in our future work.

5. Concluding remarks

We showed that the minority reward system is not necessarily efficient if the number of agents is small such as 100. To overcome this drawback, we proposed a method to improve the performance by tuning the criteria for determining the minority and showed the preliminary result of the evaluation.

Acknowledgments

This research was partially supported by a Grant-in-Aid for Scientific Research (A) (17H00759, 2017-2020) from Japan Society for the Promotion of Science (JSPS).

References

[Lamberson 12] Lamberson, P. J. and Page, S. E.: Optimal Forecasting Groups, *Management Science*, Vol. 58, No. 4, pp. 805–810 (2012)

[Mann 17] Mann, R. P. and Helbing, D.: Optimal incentives for collective intelligence, *Proceedings of the National Academy of Sciences*, Vol. 114, No. 20, pp. 5077–5082 (2017)

[Page 07] Page, S. E.: *The Defference: How The Power of Diversity Creates Better Groups, Firms, Schools, and Societies*, Princeton University Press (2007)

2O5-E-3-02

An Approach to Knowledge Graph Completion based on Discussion Agents using IBIS Structure

Xiangyu Zhang[*1] Shun Shiramatsu[*2]

[*1] Department of Computer Science, Faculty of Engineering, Nagoya Institute of Technology

[*2] Department of Computer Science, Graduate School of Engineering, Nagoya Institute of Technology

Knowledge Graph Completion Challenge 2018, a competition of interpretable AI systems to solve crime story, was held and we participated in it. Our approach is based on discussion agents using IBIS (issue-based information system), a kind of discussion structures. This paper is a part achievement of the design architecture. We design two types of agents: a discussion agent and a facilitation agent. The discussion agents generate hypotheses about the criminate. The facilitator agent ask questions to clarify the detail of the hypotheses. To manage the discussion on the hypotheses, IBIS structure is suitable because it has better interpretability. This approach based on the hypothesis generation has a possibility to be also utilized in the real-world discussion support.

1. Introduction

In recent years, along with the spread of deep learning, which process is difficult to understand, it is expected that the reason of deep learning result can be explainable. The need of artificial intelligence (AI) with interpretability is increasing.

Under such a background, Knowledge Graph Completion Challenge (KGC), a contest to recruit ideas and solutions, was held in November 2018. In this contest, Sherlock Holmes' mystery novel "Speckled Band" was taken as a theme, and a knowledge graph [kgc 18] describing its contents in RDF triple (KGC Data) was provided. The purpose of this completion is not only to find the correct answer through reasoning, but also more importantly, to give a compelling reason when interpreting the results. This means that it looks forward to establishing explainable and interpretable artificial intelligence.

A paper in last November [Shiramatsu 18] provided a design architecture, which is expected to give an idea to achieve the goal of KGC. The focus of this paper is to implement it this time. Here are some technical issues to solve:

- How to develop the generation logic of a hypothesis?
- What questions do the agents ask about a hypothesis?
- How can the facilitator agent evaluate the consistency of the hypothesis?

2. Related Work

2.1 Architecture for Knowledge Graph Complement

The design architecture gives a guide step by step to make sure to complete a system to reason murderer and motivation out from a mystery novel, the system is based on discussion agents.

Common knowledge is needed in this architecture since KGC Data only includes information of novel. And agents that can give multiple hypotheses are necessary.

When discussing, agents' actions include giving hypotheses, asking questions about a hypothesis, investigating clues, giving evidence.

It is also excepted that an agent can challenge other agents' hypotheses and give defenses.

After all discussion over, there will be a facilitator agent who evaluates the various hypotheses proposed by the previous agents, and then gives the score. The hypothesis with the highest score is regarded as the truth, and the suspect in the hypothesis is regarded as the prisoner.

2.2 IBIS Structure

Issue-based Information System (IBIS) structure [Kunz 70] offers a visual way to check agents' movement and system processing. Every time an agent has an action, there will be a node to represent it in IBIS structure. We use Web API of IBIS CREATOR, which is a Web-based IBIS editor implemented by Kamiya [Kamiya 19], for structuring discussion among the agents..

3. Material and Approach

3.1 Tools and Environment

Virtuoso is a server that combines relational, graph, and document data management with web application server and web services platform functionality. In this project, agents have to keep common knowledge besides KGC Data.

According to the instructions of the competition, the execution of reasoning should be carried out under three conditions to test the effect of reasoning in different situations:

a. using full knowledge graphs

b. using data with id numbers below 368 (10% incomplete)

c. using data with id numbers below 268 (25% incomplete)

It's hard to separate three execution conditions in one RDF triple data file. So the data file is downloaded, copied and deleted according to the execution conditions. The virtuoso server becomes necessary to give them different Graph IRI values to as a distinction.

In this system, Virtuoso is also used when agents use common knowledge for reasoning. The settings of Graph IRI this time is as Table 1.

Contact: Xiangyu Zhang, Nagoya Institute of Technology, Gokiso-cho, Showa-ku, Nagoya-shi 466-8555, E-mail: zhang.xiangyu@srmtlab.org

Table 1: Graph IRI

Data	Graph IRI
full knowledge graph	http://kgcdata/all
data with id below 368	http://kgcdata/368
data with id below 268	http://kgcdata/268
common knowledge	http://commonknowledge

For connecting KGC Data, this time program uses SPARQLWrapper library. SPARQLWrapper is a simple Python wrapper around a SPARQL service to remotely execute queries. It can help in creating the query invocation and, possibly, convert the result into a more manageable format.

3.2 Common Knowledge

It is necessary to add common knowledge. Since knowledge graph only include necessary information of novel, adding common knowledge can help agents understand things more like the real world.

There is a sample of common knowledge:

In the definitions of subjects "sister", "Julia" and "Helen", there are only two attributes for each other: "rdf:type" and "rdfs:labels". But if checking KGC Data, it is easy to know subject "sister" includes "Julia" and "Helen". So the relationship information among them is added. Table 2 shows this repair.

3.3 Program Design

Three technical issues were raised in the introduction section, here the first two are answered.

The first is, how to develop the generation logic of a hypothesis?

The agents will give a variety of hypotheses. There must be a logical chain to explain why a hypothesis is generated. The chain usually includes many rings. Here, agents use a chain called "why-chain". The chain represents the generation logic of a hypothesis. A classic scene is, before generating a hypothesis, the agents will look for the cause of death of a victim, there will be multi-steps to conclude the cause.

There is an explanation of “why-chain”.

For example, to speculate a victim's death, first of all, it must clarify what will be the cause of death. It includes a fatal injury, being poisoned, frozen or scared to death. The second step, the symptoms of each cause are different. If it is a fatal injury, the body of the victim must have a wound. If it is being poisoned, the victim will behave symptoms such as dizziness or vomiting before dying. If it is frozen to death, the skin of the victim may

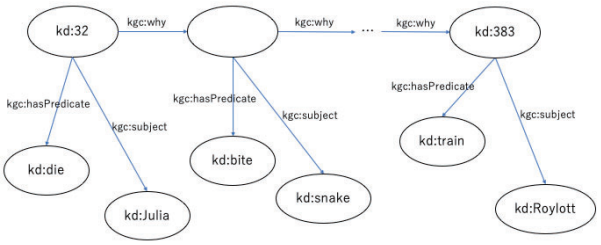

appear red. Next step, if the symptoms by the victim are likely to be poisoned, it may be one of these situations: poison, poisonous plants or bitten by poisonous animals [Matsushita 18]. Connect each ring in the chain with “kgc:why” and form a “why-chain”. Figure 1 is the "why-chain" of the hypothesis “How did Julia die”.

Make a summary of what may happen in the real world and put it in common knowledge. Before the agents give a hypothesis, they scan the KGC Data and common knowledge to make a matching. Then agents will give a hypothesis. The same technique can also be used to speculate a motivation of a suspect.

The second issue was raised in the introduction section is, what questions do the agents ask about a hypothesis?

Widely known, 5W1H are questions whose answers are considered basic in problem solving. They are often mentioned in police infestations. Their advantage is that none of them can be answered with a simple "yes" or "no". When agents do a reasoning, they use one or more to ask further questions.

The system includes several types of agents: the basic agent is named with BasicAgent, it has some common properties of all kinds of agents, such as "agent_id" "agent_name", "agent_type" and so on.

Then there are two main agents named DiscussionAgent and FacilitatorAgent. DiscussionAgent generates a hypothesis about who is the criminal. FacilitatorAgent asks questions according to 5W1H on the hypotheses, and DiscussionAgent gives sub-hypotheses as answers. There not only one instance of DiscussionAgents. They will be distinguished by id or name property.

There is a flag that is used to mark whether a hypothesis and its sub-hypotheses have all been discussed and answered. If it isn’t finished yet, the value of mark is "1", and the discussion

Table 2: repair of KGC Data

Resource	KGC Data	Repair
kd:sister	rdf:type kgc:person; rdfs:label “sister”@en;	rdf:type kgc:person; rdfs:label “sister”@en; kgc:ofPart <http://kgc.knowledge-graph.jp/data/SpeckledBand/Julia>; kgc:ofPart <http://kgc.knowledge-graph.jp/data/SpeckledBand/Helen>;
kd:Julia	rdf:type kgc:person; rdfs:label “Julia”@en;	rdf:type kgc:person; rdfs:label “Julia”@en; kgc:ofWhole <http://kgc.knowledge-graph.jp/data/SpeckledBand/sister>;
kd:Helen	rdf:type kgc:person; rdfs:label “Helen”@en;	rdf:type kgc:person; rdfs:label “Helen”@en; kgc:ofWhole <http://kgc.knowledge-graph.jp/data/SpeckledBand/sister>;

kd is a prefix for representing <http://kgc.knowledge-graph.jp/data/SpeckledBand/>

Table 3: remove subjects to narrow down suspect

Subject	Reason to remove
man	In KGC Data, the meaning of “man” is someone, it’s not the name of a specific person. Similarly, the “suspect” here is also a generic suspect. It just was used when the detective talks with his assistant or other characters in novel, not referring to someone who exists.
suspect	
Holmes	The premise of this reasoning process is that the detective and his assistant will not become murderers, so they are removed here. Of course, this situation is not absolutely true in reality, this issue will be discussed again in part of future work.
Watson	
mother-of-sister	The reason of removing them is that there are synonyms for these three subjects in KGC Data. That is, “mother-of-sister” is equal to “mother-of-Helen”, “father-in-law” is equal to “Roylott”, “friend-of-Roylott” is equal to “Roma”. In the process of reasoning, the words “mother-of-Helen”, “Roylott” and “Roma” appear far more frequently than the previous three synonyms. Using these three words will also make reasoning easier.
father-in-law	
friend-of-Roylott	

should be continued. If all doubtful points of the hypothesis are already discussed, then the value of mark turns to "0", meanwhile the discussion is completed, it should be summarized to report to the father hypothesis or gives a conclusion.

Finally, FacilitatorAgent evaluates the hypothesis.

3.4 Process

It is easy to extract all victims and characters from KGC Data using the SPARQL statement. The agent's action is to select one of victims to ask questions. The initial question is definitely "Who killed this dead person". To answer this question, according to the design structure, another agent should be expected to do a direct product using victims and all characters in the novel. But there is one point: in KGC Data, several of subjects which value of "kgc:type" is "person" are not needed.

Totally they are seven: "man", "suspect", "Holmes", "Watson", "mother-of-sister", "father-in-law", "friend-of-Roylott". Here Table 3 tells why these seven subjects are removed.

The elimination for these seven subjects will be done by agents using common knowledge actually. now the left subjects are called suspects. Agent will make a direct product between the victim who has been raised as a topic with the suspects. The form is isKiiledBy(victim, suspect) and it is passed on to other agents.

In processing, DiscussionAgent moves first, it gives a hypothesis once. With original hypothesis, FacilitatorAgent begins to ask questions according to 5W1H, they are "what" of 5W1H, "What could the suspect gain after killing the victim?", and "how", "How did the suspect kill the victims?". Then DiscussionAgent give sub-hypotheses for questions.

The why-chain is prepared for generating hypothesis for “how”, and there is also an idea to generate a hypothesis for “what”. Figure 2 is a view to explain the logic of how to generate a hypothesis of “What could Roylott gain after killing Julia”.

Firstly, agents catch all situations where “kgc:subject” is equal to “Julia” or “Roylott” and assign it to set A. Meanwhile agents catch situations that include “Julia” and “Roylott” at the same time and assign it to set B. Secondly, agents match special situations from set A or B using a special word list. If agents match succeed, they will give a hypothesis, if failed, agents will say “Roylott’s motivation is not clear”.

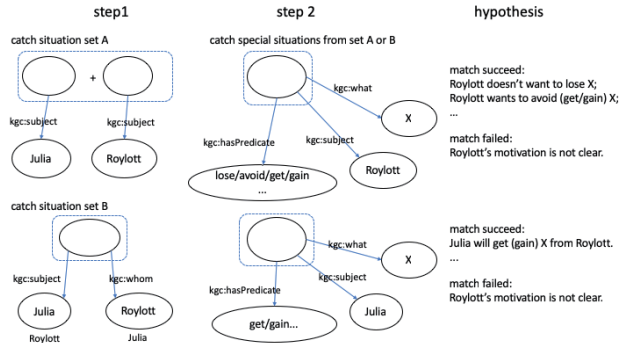

Figure 2: generate a hypothesis for question “what”

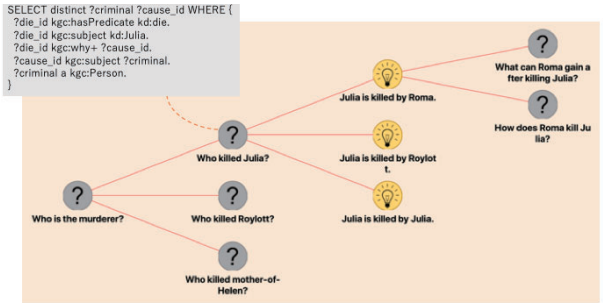

Figure 3: IBIS Structure

4. Conclusion and Future Work

In the Introduction section, three issues are excepted to be solved, then the key ideas of the previous two issues are provided in the Program Design section. To deal with how to develop the generation logic of a hypothesis, the key idea is to use a chain called "why-chain", a chain represents the generation logic of a hypothesis. To deal with what questions do the agents ask about a hypothesis, the key idea is that FacilitatorAgent will ask questions according to 5W1H.

In the current version of the implementation, every time an agent gives a hypothesis randomly. Other agents will ask sub-questions about it. Figure 3 is a view of agents’ actions with IBIS Structure.

Up to now, this paper's work is a half-finished product of the designed architecture. We will continue the development to enable agents to generate consistent hypotheses and answers for all questions.

And it is expected agents which have different hypotheses can challenge each other. It means they can give opposing views to others, this will make it a real discussion.

It is known that discussion among agents is not proposed to convince each other but to speaking to the third side. Here the third side is the facilitator agent. So how can the facilitator agent evaluate the consistency of the hypothesis? This is an important task for this system. This technical issue was generated in the introduction section but not answered yet, actually it is still under consideration.

If the methodology to generate sub-hypotheses to answer questions is established in the future, it has a possibility to be applied to supporting real-world discussion because such method can be used for giving logic behind discussion participants' ideas. Since our research team is currently developing a facilitator agent for supporting public debate [Kitagawa 19, Ikeda 17], we will also consider such direction towards the discussion support technology.

Acknowledgements

This work was partially supported by JSPS KAKENHI (17K00461).

References

[kgc 18] Knowledge Graph of "SpeckledBand", https://github.com/KnowledgeGraphJapan/Challenge/tree/master/rdf/SpeckledBand, 2018 (in Japanese).

[Shiramatsu 18] S. Shiramatsu , X. Zhang , A. Kamiya , M. Watanabe: Designing an Architecture for Knowledge Graph Completion based on Discussion Agents using IBIS Structure, in *Proc. of SIG-SWO*, 46(2), SIG-SWO-046-02, 2018. (in Japanese)

[Kunz 70] W. Kunz and HWJ. Rittel: Issues as Elements of Information Systems. in *Berkeley, California: Institute of Urban and Regional Development, University of California*, CiteSeerX 10.1.1.134.1741, 1970.

[Kamiya 19] A. Kamiya, K. Kitagawa, S. Shiramatsu, D. Shibata, K. Yoshino, S. Suzuki, T. Ito: Prototypes for Visualizing IBIS Structure and Discussion Progress towards Supporting Consensus Building in Web-based Discussion, in *Proc. of IPSJ 2019*, 1ZB-08 (in Japanese)

[Matsushita 18] Kamikotanaka 411 (K. Matsushita, T. Kaneko, K. Yoshikawa, K. Kobayashi, Y. Koyanagi, T. Ukai, F. Nishino, M. Oda): Knowledge Graph Completion Challenge, http://challenge.knowledge-graph.jp/results/results2018.html#2nd, 2018 (in Japanese)

[Kitagawa 19] Ko Kitagawa, Shun Shiramatsu, Akira Kamiya: Developing a Method for Quantifying Degree of Discussion Progress towards Automatic Facilitation of Web-based Discussion, in *Multi-Agent Systems and Agreement Technologies 16th European Conference, EUMAS 2018, and 6th International Conference, AT 2018, Revised Selected Papers*, Springer LNCS, 2019 (to appear)

[Ikeda 17] Yuto Ikeda, Shun Shiramatsu: Generating Questions Asked by Facilitator Agents Using Preceding Context in Web-based Discussion, in *Proceedings of the 2nd IEEE International conference on Agents*, pp. 127-132, 2017.

The 33rd Annual Conference of the Japanese Society for Artificial Intelligence, 2019

Using Q-learning and Estimation of Role in Werewolf Game

Makoto Hagiwara*1 Ahmed Moustafa*1 Takayuki Ito*1

*1Nagoya Institute of Technology

This paper introduces a novel construction strategy in Werewolf Game using reinforcement learning(RL). Werewolf Game is a type of incomplete information games in which the final results of the game is linked to the success or failure in communication. In this paper, we propose a model that uses RL and estimating other agent's role in order to learn playing strategy in Werewolf Game. In the proposed model, RL is used for deciding the actions of the learning agent and Naive Bayes classifier is used in order to estimate other agent's role. Up till now, there is no previous research that has effectively applied RL in Werewolf Game among existing AIwolfs in large scale environments. Therefore, by combining RL and estimation of other agent's role, we demonstrate through experimentation that the proposed approach achieved high level of performance in 11 people Werewolf Game.

1. Introduction

In this paper, we investigate the playing strategy of Werewolf Game, a cornerstone of communication games. Werewolf Game has two competing teams-villagers and wolves. In Werewolf Game, execution by vote or attack by werewolf eliminates the player from the game. The villagers win if all the werewolf players are eliminated. The werewolves win if enough number of villagers are eliminated so the number of villagers is even to the number of werewolves. In this regard, conversation becomes important to distinguish wolves from existing players.

In Werewolf Game, natural language is used for conversation. However, the processing of natural language by artificial intelligence (AI) remains a technical challenge. Towards this end, Osawa *et al* [Oosawa 14] have developed a special protocol for enabling AIwolf to conduct conversation. In this context, Toriumi *et al* [Toriumi 14] released a construction kit for developing intelligent agents that play the Werewolf Game using its developed protocol. In specific, Toriumi *et al* [Toriumi 14] attempted to solve the challenges for realizing sophisticated communication by developing an environment in which the intelligent agents play the Werewolf Game and gain collective intelligence via a contest. In this regard, a contest that involves the Werewolf Game was recently held for the first time as part of the Computer Entertainment Developers Conference (CEDEC2015) in Japan, with over 50 teams participating. Therefore, this paper adopts the conversation protocol proposed in [Toriumi 14] and the construction kit proposed in [Oosawa 14].

In the AIwolf contest held in CEDEC2018, the win rate of werewolf in the contest was about 30%. In this regard, Inaba *et al* [Inaba 12] researched the win rate in Werewolf BBS and estimated the percentage of this win rate. BBS is a web application for playing Werewolf Game on the Internet. The Construction kit that is proposed in [Oosawa 14] is built based on BBS. In specific, Inaba *et al* [Inaba 12] suggested that win rate of werewolf is about 50% in the same distribution of roles as that of the contest. Toriumi *et al* [Toriumi 16] suggested that AIwolf has shown performance to learn the win strategy in particular to Werewolf Game, and suggested that AIwolf has strong potential to play Werewolf Game. On the other hand, the win rate of werewolves in the contest held in CEDEC2018 demonstrated that the performance of werewolves in AIwolf is worse than that of villagers in AIwolf. In additon to this, only when the agents are assigned to the role of werewolves, these agents could learn game strategy not as single agents but as a group of agents. This is because information about the member or number of werewolves is known to the players of werewolves in the begining of the game. This factor is very important in Werewolf Game. Therefore, this paper focuses on improving the performance of werewolves in AIwolf.

It is difficult to use common game AI methods, such as tree search algorithms, because Werewolf Game is played through conversation with werewolf agents, i.e., AIwolf. Therfore, in Werewolf Game, it becomes necessary for AIwolf to adopt a voting strategy, because recent research [Doguro 18] has shown that voting information is linked to the estimation of werewolves. In this regard, Doguro and Matsubara [Doguro 18] suggested evaluating the effectiveness of voting information in estimating werewolves. As a result, it becomes important to define such actions as voting depends on game condition. Most of the existing AIwolf agents decide their actions by rule-based programs. Since WereWolf Game has variable conditions which depend on votes or the number of existing players, large state space is necessary to describe them. As a result, it becomes difficult to describe all proper actions in the game by rule-based programs. Therefore, it is important for AIwolf to learn the strategy in Werewolf Game by themselves.

In order to overcome this problem, we employ RL [Sutton 98], because RL is suitable for choosing a sequence of actions that lead to a strategy. In this regard, RL enables AIwolf to build a game playing strategy based on the sequence of these actions that exist in each state of Werewolf Game, and we propose that RL promotes the performance of AIwolf to succeed in the construction of game playing strategy.

In Werewolf Game, it is important to estimate the roles of other players, because information about the roles of other

Contact: Makoto Hagiwara, Nagoya Institute of Technology, hagiwara.makoto@itolab.nitech.ac.jp

players is important in the voting process. For example, estimation of role gives villagers information that tells them who are werewolves. This information enables the villagers to vote in order to decide the werewolf. In this regard, Toriumi *et al* [Toriumi 16] suggested correlation between voting and win rate in Werewolf Game played by AIwolf. Therefore, we expected that adopting estimation of other agent's role develop AIwolf. In estimation of other agent's role, Kaziwara *et al* [Kaziwara 16] suggested the effectiveness of SVM and Ookawa *et al* [Ookawa 17] suggested the effectiveness of deep learning. In the AIwolf contests held in CEDEC2017 and CEDEC2018, the AIwolf with Naive Bayes classifier won and adopted Naive Bayes classifier to estimate other agent's role.

In this paper, we employ these two methods, RL and estimation of other agent's role, to construct werewolf's strategy of action. Since there is no previous research to suggest the effectiveness of RL in Werewolf Game in large scale with existing AIwolf. Therefore, we examined the effectiveness of RL in Werewolf Game in 11 player with existing AIwolf.

2. Preliminaries

2.1 Werewolf Game

Werewolf Game is a conversation-based party game that is played using the communication abilities we possess as humans. When the game starts, all the players are randomly divided into either the villager side or the werewolf side, and then allocated to different roles. We summarize these roles in Table 1. The players in the villager side and possessed players do not know which side other players belong to; however, the werewolf players know the players of wolves.

In Werewolf Game, there are two phases, i.e., day phase and night phase. In the day phase, all players discuss who the werewolf are, and then select a player who becomes target for execution based on voting. In the night phase, the werewolf players attack a human player that is selected based on discussion with other players of the werewolf. Other players with specific abilities of their role can use their abilities at night. The executed player and the attacked player are eliminated form the game, and are not allowed to participate in further discussions or votes. Those player roles are not revealed until the game is over. A crucial aspect for villager players is to detect the lies presented by werewolf players in discussions. A crucial aspect for werewolf players is to manipulate discussion to their advantage by impersonating a role.

The villagers win if all werewolf players are eliminated. The werewolves win if enough number of villager players are eliminated so the number of villager players are even to the number of werewolf players.

2.2 Q-Learning

Q-learning [Watkins 92] is a model-free RL algorithm. In this context, Q-learning provides the learning agents with the capability of learning to act optimally in markovian environments by experiencing the consequences of their actions, without requiring these agents to build explicit models of their environments. In Q-learning, Q values estimate the values of actions and decide the learning agent actions. Through experiencing the consequences of their actions, Q-learning agents change Q values. In so doing, the Q values are updated using Equation (1):

role	ability
Seer	Every night, selecting one active player, you can know whether the player is werewolf or not.(divination)
Medium	Every night, you can know whether the player executed is werewolf or not.(medium result)
Knight	Every night, selecting one active player, you can guard the player.(guard) If target for guard is same as target for attack, player attacked is not eliminated from the game.
Werewolf	Every night, selecting one active player, you can attack the player.(attack)
Villager	the player of villager side. They don't have ability.
Possessed	the player of werewolf side. They don't have ability.

Table 1: Role ability

$$Q(s_t, a_t) = r_t + \gamma \max Q(s_{t+1}, a) \quad (1)$$

In this equation, s_t is the current state. a_t is the current action. γ is the learning rate. s_{t+1} is the next state. In Q values of next state, the highest value is used for updating Q values of the current state.

3. Proposed Model

First, we define state, reward and action in the proposed model as follows.

Definition One: Action

In the proposed model, three types of actions are available which are vote, attack and pronunciation. Vote is for choosing one player to eliminate from the game. Attack is for choosing one player to attempt to kill. Pronunciation is for choosing one pronunciation from the pronunciations set that is defined by the game protocol. This set of pronunciations also contains SKIP. SKIP means that I have nothing to talk. In the proposed model, the target of action consits of the player whose probability of being in some role is the highest among all players, the player who gets the most declarations of vote, the player who is not divined, the player whose results of divination include a result of being werewolf, the player whose results of divination include only result of being villager, the player whose time of votes of being werewolf is the highest among all existing players, and finally, any random player.

Definition Two: Pronunciation

In the proposed model, the pronunciation set that is defined in the game is limited by the game protocol. As shown in Table 2, the number and type of available pronunciations is limited. There are other types of pronunciations, however most of the existing AIwolf agents don't consider those types of pronunciations. Therefore, those pronunciations are not considered in the proposed model.

Definition Three: State

In the proposed model, there are six types of states which

type	example
Estimation	I think that PlayerA is werewolf.
vote declaration	I'll vote to PlayerA (this may be fake declaration.)
Result of ability	I divined PlayerA and found that PlayerA is werewolf.
Coming out	My role is Seer.

Table 2: Explaination about pronunciation

are day, turn, the number of players who declared that their role is seer (or medium) in discussion, the number of existing players of villager and werewolf, whether each werewolf is divined (boolean) and present number of declarations of vote to each werewolf.

Definition Four: Reward

The proposed model receives reward in the following three cases which are: when game is over, when attack is failed, when the player with ability or the player of werewolf side is eliminated.

The proposed model adopts Naive Bayes classifier to estimate other agents's roles based on the frequency of actions of every turn in the past games. As shown in Figure 1, we implemented the Naive Bayes classifier algorithm that is used by Cndl [Agent], which is an existing AIwolf agent, as a reference model. In addition, we present an algorithm that demonstrates the learning model in Algorithm 1.

Algorithm 1 Learning Model

```
function GETACTION(state)
    if Math.random() < ϵ then
        return action randomly
    else
        return action selected from top-3 Q value actions
function UPDATEQLIST
    for (s_t, s_{t+1}, a_t, r_t) in latest episode do
        Q(s_t, a_t) = r_t + γ max Q(s_{t+1}, a)
```

As shown in Algorithm 1, the proposed model calls *GETACTION* function, when the proposed model selects its action. In *GETACTION* function, there is an ϵ percent chance that the next action is selected randomly. Other than that, the proposed model selects the next action from the three available actions with the highest $Q(s_t, a_t)$ values in a_t using Boltzmann selection. When the game is over, the proposed model calls *UPDATEQLIST* function to update the Q values based on the sequences of (s_t, s_{t+1}, a_t, r_t) in the latest episode.

4. Experiment

4.1 Setup

We performed a set of experiments involving the rule-based model and the proposed RL model to show the efficiency of the proposed model. In these experiments, we used the AIwolf Server (ver0.4.11) [Oosawa 14]. In addition, the opponent agents (contest agents) that are used in the AIwolf competitions are built using Java Technology. In these experiments, we compared the win rate of the proposed RL model with that of the rule-based models, i.e., Cndl and Udon [Agent], when each player whose role was

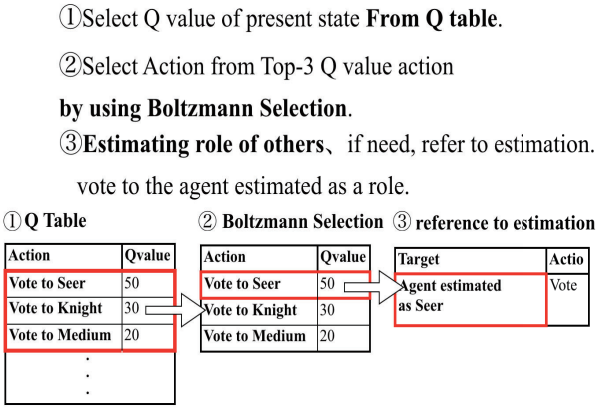

Figure 1: Overview of action decision in proposed model

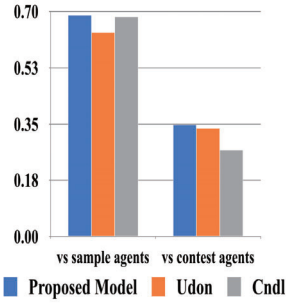

Figure 2: Result

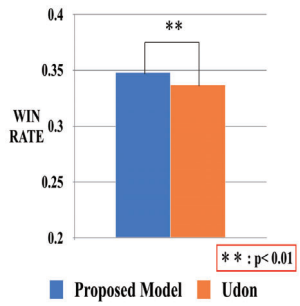

Figure 3: T-Test

werewolf played the game. It is important to note that Cndl won the 2017 AIwolf contest. In addition, Udon showed the highest win rate of werewolf in 2017 AIwolf contest. We executed 100,000 games among 10 sample agents (In this context, sample agents act almost randomly.) and an evaluation agent and executed 100,000 games among 10 contest agents and an evaluation agent. In this regard, Evaluation agent is the proposed RL agent or cndl or Udon. As for pre-training, we executed 2,000,000 games with sample agents and 50,000 games with contest agents.

4.2 Results

We demonstrate the results of these experiments in Fig 2. As shown in Figure 2, Udon's win rate against sample agents is lower than the win rate of both cndl and the proposed RL agent. In addition, we have conducted t-test and present the result of t-test in Fig 3. As shown in Fig 3, significant difference is shown between the proposed RL model win rate and Udon's win rate. In addition, we employed DQN instead of Q-learning in the same learning way as Q-learning. However, the win rate in the games among sample agents is higher but the win rate in the games among contest agents is lower than that of agent using Q-learning.

4.3 Discussion

In the game with sample agents, Udon has lower win rate than that of cndl [Agent]. However, in the game with contest agents, Udon has higher win rate than that of cndl. This is because Udon [Agent] adopts strategy to take in action of villager. Because sample agents decide target for vote and attack randomly, this Udon's strategy diminish their win rate versus sample agents. However, Udon's win

rate versus contest agents are better than cndl's win rate. These win rate suggest the effectiveness of Udon's strategy in Game with contest agents. Contest agents are different from sample agent in that their strategy is sophisticated enough that they adopt such strategies as power play (To decide target for execution by organized vote of werewolf side) or roler (To execute all agents who declared CO of specular role). The proposed RL agent showed better win rate than Agent cndl and Agent Udon. It is assumed that the pre-train in the games with sample agents promote the performance of the proposed model in the game with existing agents. In pre-train, the proposed model learned how to select the target for vote or attack in the game with sample agents. This helps the proposed model to select the target for vote or attack in the game with contest agents. As shown in Fig 3, there is a significant difference($p<0.01$) between the proposed model and Udon. Therefore, the proposed model showed that the performance of RL is no less than that of rule-based program in the Werewolf Game with existing model. In addition, we need adjustment to use DQN instead of Q-learning.

5. Related Work

Kaziwara *et al* [Kaziwara 14], [Kaziwara 15]; and Wang and Kaneko [Wang 17] researched Q-learning in AIwolf. In specific, Kaziwara *et al* [Kaziwara 14] adopted another protocol that is different from the proposed protocol by the authors in [Toriumi 14] and suggested the effectiveness of RL in Werewolf Game. In Kaziwara *et al* [Kaziwara 14], their agent used RL to learn the object to attack, vote and use ability of role. Their agent also used RL to learn choosing the role for impersonating their role when their roles are werewolf or possessed.

In Kaziwara *et al* [Kaziwara 15], the effectiveness of RL was demonstrated in the environment that adopts the proposed protocol in [Toriumi 14], and that selects opponent as sample agents. In this context, sample agents act almost randomly. In their work, they have defined state as "the probable collection of role based on talk in game" and defined action as "the target for attack, vote and use of ability", "condition of telling CO" and "impersonating a role in werewolf or possessed". In Kaziwara *et al* [Kaziwara 15], action is decided by multiplication of value of Q by the frequency of state. In their work, Kaziwara *et al* [Kaziwara 15] consider some types of roles but they did not consider all types of roles in Werewolf Game. Therefore, considerating all kinds of role in Werewolf Game, the proposed approach adopts a novel strategy that defines state using estimation of other agent's role and action using Q-learning.

On the other hand, Wang and Kaneko [Wang 17] defined action as "the target to which attack, vote and use ability of role", and defined state as CO, impression to other player(deceive, reliance and nothing) and role cleared in game. Both Kaziwara *et al* [Kaziwara 14], [Kaziwara 15] and Wang and Kaneko [Wang 17] employed heuristic method in state and action. Conversely, Wang and Kaneko [Wang 18] did not employ heuristic in action. In specific, Wang and Kaneko [Wang 18] employed DQN. No other research employed DQN in AIwolf. In this regard, Wang and Kaneko [Wang 18] suggested the effectiveness of DQN without heuristic action in Werewolf Game among 5 players with existing AIwolf. However, the proposed approach considers Werewolf Game among 11 players is more complex than that among 5 players.

6. Conclusion

This paper proposes a novel model that adopts RL for constructing a winning strategy and Naive Bayes classifier for estimating other agent's role in Werewolf Game. In the proposed model, the learning agent decides its actions based on RL. In addition, the learning agent decides the target for these actions based on estimation using Naive Bayes classifier. Thorough a set of evaluation experiments, the proposed model showed higher win rate than other existing models especially in 11 player Werewolf Game. The future work is set to investigated the necessary approaches that are needed in order to decrease the learning time.

References

[Agent] http://aiwolf.org/resource

[Doguro 18] Doguro,H., Matsubara,H.: Effectiveness Evaluation of Vote Information in Estimation Werewolf Using Neural Network, GAT2018, p1-4, 2018.

[Inaba 12] Inaba,M., Toriumi,F., Takahashi,K., et al.: The Statistical Analysis of Werewolf Game Data, GPW2012, p144-147, 2012.

[Kaziwara 14] Kaziwara,K., Toriumi,F., Oohashi,H., et al.: 強化学習を用いた人狼における最適戦略の抽出 (no English title), IPSJ vol2014, No.1, p597-598,2014.

[Kaziwara 15] Kaziwara,K., Toriumi,F., Inaba,M.: Design of Agent in "Are you a Werewolf?" using Reinforcement Learning, The 29th JSAI2015, p1F2-2, 2015.

[Kaziwara 16] Kaziwara,K., Toriumi,F., Inaba,M., et al: Development of AI Wolf Agent using SVM to Detect Werewolves, The 30th JSAI2016, p2F41,2016.

[Ookawa 17] Ookawa,T.,Yoshinaka,R.,Shinohara,A.: Development of AI Wolf Agent Deducing Player's Role Using Deep Learning,GPW2017,p50-55,2017.

[Oosawa 14] Osawa,H.,Toriumi,F.,Katagami,D.,et al.:Designing Protocol of Werewolf Game:Protocol for Inference and Persuasion, FAN2014, p78-81, 2014.

[Sutton 98] Sutton,R.S., Barto,A.G.: Introduction to reinforcement learning(Vol.135), MIT press,1998.

[Toriumi 14] Toriumi.F.,Kaziwara,K.,Osawa, H.,et al.: Development of AI Wolf Server,GPW2014,p127-132,2014.

[Toriumi 16] Toriumi,F., Shinoda,K., Inaba,M., et al.: Analysis of Agent Behaviors in First AI Wolf Contest, IPSJ vol2016-EC-41 No.3, p1-8,2016.

[Wang 17] Wang,T., Kaneko,T.:Comparation of Methods for Choosing Actions in Werewolf Game Agents, GPW2017, p177-182, 2017.

[Wang 18] Wang,T.,Kaneko,T.:Application of Deep Q Network in Werewolf Game Agents,GPW2018,p16-22,2018.

[Watkins 92] WATKINS, C., DAYAN, P.: Q-learning, Machine learning, 1992, 8.3-4: 279-292.

The 33rd Annual Conference of the Japanese Society for Artificial Intelligence, 2019

Inferring Agent's Goals from Observing Successful Traces

Guillaume Lorthioir[*1*2] Katsumi Inoue[*1*2] Gauvain Bourgne[*3]

[*1]National Institute of Informatics
[*2]Department of Informatics, SOKENDAI (The Graduate University for Advanced Studies)
[*3]CNRS & Sorbonne Universités, UMR 7606, LIP6

Intention recognition is the task of inferring the intentions and goals of an agent. Intention recognition has many applications. Especially, it can be very useful in the context of intelligent personal assistants like robots or mobile applications, smart environments, and monitoring user needs. We present a method to infer the possible goals of an agent by observing him in a series of successful attempts to reach them. We model this problem as a case of concept learning and propose an algorithm to produce concise hypotheses. However, this first proposal does not take into account the sequential nature of our observations and we discuss how we can infer better hypotheses when we can make some assumption about the behavior of the agents and use background knowledge about the dynamics of the environment. Then we talk about future work to improve our method.

1. Introduction

We are entering an era where new technologies are increasingly present, and soon artificial intelligence will be everywhere. Home automation, robotics, intelligent personal assistants, they will soon be interacting with humans on a daily basis. But for this, we need an artificial intelligence able to understand and interpret human's intention, which is not trivial. Even currently, there are many cases where the knowledge of an agent's intentions is useful, for cooperation or competition in a multi-agent system or even for a smart-phone application which tries to help the user to do something. The ISS-CAD problem [E-Martin et al., 2015] is a good illustration of this problem, where a free-flying robot is observing an astronaut performing a task in the International Space Station (ISS) and he has to help him.

This problem is called "Plan recognition" or "Intention recognition" and has been investigated in AI research and has many applications. [Schmidt et al., 1978] were the first ones to introduce the problem and treat it from a psychological point of view. [Charniak and Goldman, 1993] use Bayesian models and [Geib and Goldman, 2009] use also a probabilistic algorithm for the plan recognition. [Singla and Mooney, 2011, Ha et al., 2011] mix probabilistic and logic approaches, they found a very interesting field of application for plan recognition, which is digital games. [Carberry, 2001] describes the plan recognition problem and surveyed the current ways to tackle this problem. In this paper, we focus on a sub-field of intention recognition which is called "Goal-recognition" and which concern understanding of the goals of an agent several related recent work [Cardona-Rivera and Michael Young, 2017, E-Martin and Smith, 2017, Mirsky et al., 2017, Goldman et al., 2018, Vered et al., 2018] show that goal recognition is growing of interest.

However, there are only few approaches using propositional logic for goal recognition. It is this lack of literature that has led us to focus our work on this aspect of the goal recognition problem. [Hong, 2001] use propositional logic but he combines this to a graph representation, we use a different approach which consist of combining propositional logic and concept learning. We are among the first to do it. We try to guess the goal of the agent, the state of things that the agent is trying to achieve. Indeed, many previous work try to solve the plan recognition problem by using a set of possible goals for the agent and try to guess which one is more likely, as it is the case for example in the work of [Lang, 2004]. But often they assume that this set of possible goals is given, which is usually not the case.

In this paper, we will talk about the method to infer the possible goals of an agent by using concept learning that we introduced in our previous work [Lorthioir et al., 2018]. We review our method and describe the future extensions of this one. First, Section 2. will explain how to formalize the problem of inferring goals from the observation of successful scenarios as a concept learning task, we will explain how to use some assumptions on the agent decision process and the environment to improve the results of our algorithm in Section 3. We will detail a way to take into account the agents' preferences regarding their goals, and those provide additional information about the agents' goals in Section 4. Finally we will conclude this paper with Section 5.

2. Problem Formalisation

What is our problem exactly? Our objective is to infer the possible goals of an agent by observing him in a series of successful attempts to reach them. We thus assume some training process in which we observe the agent in a series of scenarios in which he performs actions in some environment until he satisfies one of the goals we are trying to guess. These observed scenarios will be modelled as a set of observed traces describing the successive states of the environment and actions of the agent. We consider environments with discrete time and no exogenous events: each action performed by the agent thus corresponds to a

Contact: Guillaume Lorthioir, National Institute of Informatics, 2 Chome-1-2 Hitotsubashi, Chiyoda, Tokyo, Japan, 101-8430, lorthioir@nii.ac.jp

change of state. Here we model the state of the environment as a series of discrete-valued attributes : N variables var_i with $i \in \{1, \ldots, N\}$ taking their values in variable domains $D_j = \{val_1^i, \ldots, val_{N_i}^i\}$. We build an atomic representation by converting all the couples $var_i = val_j^i$ into atoms $var_i^{val_j^i}$, denoting by $\mathcal{L}$ the set of all these atoms. A *state* S is then defined as a set of atoms $var_i^{val_j^i}$ from $\mathcal{L}$ where each var_i appears once and a *trace* is defined as a sequence of couples (S_i, a_i) where $S_i \subset \mathcal{L}$ is a state and a_i an action (taken from a finite set of actions $\mathcal{A}$). We do not go into the detail of the environment's dynamics, but they can be abstracted away by some function *next* from $2^{\mathcal{L}} \times \mathcal{A}$ to $2^{2^{\mathcal{L}}}$ which, given a state S and an action a gives the set of possible states that can be reached from S by performing a. When the environment is deterministic, $next(S, a)$ corresponds to a single state. Since they come from observations, traces are assumed to respect this dynamic, meaning that if i is not the last index of the trace, $S_{i+1} \in next(S_i, a_i)$.

To define successful traces we consider a special action `success` without effects ($\forall S, next(S, \texttt{success}) = \{S\}$), which the agent performs whenever he reaches his goal. A successful trace is thus a trace $T = (S_0, a_0), \ldots, (S_k, a_k)$ where $a_k =$`success` and for $i < k$, $a_i \neq$`success`. This means that a successful trace is a trace which ends in the first state where the goal of the agent is satisfied. Given a trace $T = (S_0, a_0), \ldots, (S_k, a_k)$, we denote by $endS(T)$ the last state S_k of a trace and by $intS(T)$ the set of intermediate states $\{S_0, \ldots, S_{k-1}\}$. The input of our problem is a set of successful traces $\Sigma = \{T_0, \ldots, T_l\}$ and our objective is to infer from that some hypothesis about the agent's goal, which will be expressed as a propositional formula over $\mathcal{L}$ which should be satisfied by some state (by interpreting states as the conjunction of their atoms) if and only if the goal is reached. We assume here that the goal depends only on the state and not on the way to reach it. The agent just needs to reach a state where the atoms composing the state satisfy his goal, no matter how he reaches it. We want the hypothesis written in the disjunctive normal form since an agent can have several goals. More precisely we want hypotheses of the form $H = C_0 \vee C_1 \vee ... \vee C_m$ where each $C_i = x_0 \wedge ... \wedge x_n$ is a conjunction of atoms of $\mathcal{L}$. Then, given $H = C_0 \vee C_1 \vee ... \vee C_m$, a state $S = \{y_0, \ldots, y_n\}$ satisfies H if and only if $\bigwedge_{y_i \in S} y_i \models H$, that is, if and only if there exists $i \in \{0, \ldots, m\}$ such that $C_i \subseteq S$.

Even without knowing anything about the behavior of the agents or the dynamics of the system, these observations give a series of states in which we know whether the goal is reached or not. Namely, we can build the set $S_{positive}$ of successful states by including in it all end-states of successful traces from Σ, that is, $S_{positive} = \{endS(T) | T \in \Sigma\}$. Likewise, we can build the set $S_{negative}$ of unsuccessful states by taking the union of all intermediate states, that is, $S_{negative} = \bigcup_{T \in \Sigma} intS(T)$. Given the definition of a successful trace, it means that the agent's goal is satisfied only by the elements of $S_{positive}$ and under no circumstances by an element of $S_{negative}$. The problem of inferring the goals of the agent is then equivalent to a concept learning problem where the states that we put in the set $S_{positive}$ are the positive examples and the states that we put in $S_{negative}$ are the negative ones. A hypothesis H will be said to be consistent with our data if it is satisfied by all the elements of $S_{positive}$ and by none of the elements of $S_{negative}$. We want to obtain such a hypothesis as an output of our problem. We created an algorithm to treat this problem and produce such a hypothesis, the algorithm can be found in [Lorthioir et al., 2018].

3. Inferring the Agent's Model and Environment Rules from Data

In previous sections, our input Σ, a set of successful traces, is reduced to two sets of states $S_{positive}$ and $S_{negative}$. By doing so, we do not use the information contained in Σ about the order of the explored states and the actions performed by the agents at each step. The advantage of ignoring these aspects is that we can infer possible goals without assuming more about the agent than what is induced by the definition of successful traces, that is, the agent stops (with a `success` action) as soon as his goal is reached and this goal is dependent only on the current state. However, if we know the dynamics of the environment, it seems sensible to derive some information based on what the agent chose to do given what it could have done. We explain in [Lorthioir et al., 2018] how to use such knowledge to improve the results of our algorithm.

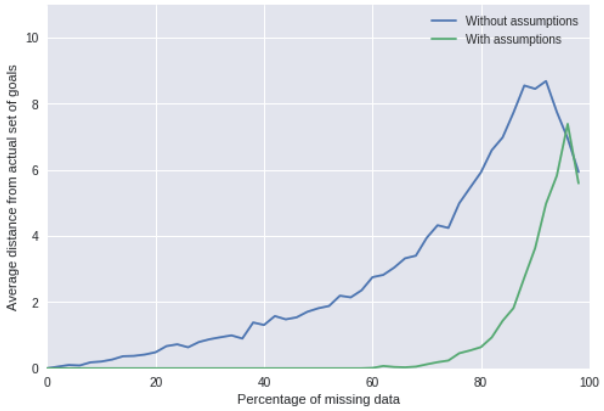

Figure 1: Comparison of the average syntactic distance from the actual goals in function of the percentage of missing data with and without assumptions on the agent.

Figure 1 allows us to see the point to have this last assumptions about the agent. On this figure the curves represent a distance similar to the Hamming one, between the hypothesis about the agent's goals generated by our algorithm and the actual agent's goals according to the percentage of data about the agent traces. More details about this distance can be found in [Lorthioir et al., 2018]. For this experiment we use the same amount of data for the two curve at the beginning. Then we make two assumptions on the agent which are that we know the action model of the agent and that we know that if he can reach his goal

with one move at the step $t-1$ then at the step t he will reach it. These are not very strong assumptions. These assumptions allow us to generate more data from the existing one. In total, we obtain almost three times more data with the assumptions about the agent than without the assumptions. As we can see in figure 1 it allows us to generate a hypothesis closer to the actual goals than when we use no assumptions.

Actually, we have two interesting methods that we wish to exploit for the deduction of the rules of action of agents and the environment. The first one is to use LFIT [Inoue et al., 2014] which is a framework for learning normal logic programs from transitions of interpretations, which means that, since we use a logical representation of the world, we will be able to infer the possible action model of the agent and the rules of the environment. Effectively, to use LFIT we just need a trace of the evolution of the states of the world in a chronological order. Which are in fact the same data that we use to infer the agent's goals. Which means that we do not need an important modification of the data collecting process to incorporate LFIT to our method, which is a good point. After processing these data with LFIT we will obtain a set of rules that correspond to the possible transition from a state of the world to another. We will then have for each state of the world (observed previously in the collected data), the different actions that the agent did when he was in this state and the states of the world that he reached after these actions. So we can infer a potential action model of the agent and the dynamic of the environment based on the observed transitions. But unfortunately LFIT is not really robust against the lack of data and the noise, especially the data need to cover as many transitions as possible between all the different possible states of the world. Which is not very convenient because usually the agent that we observe is not acting randomly and so, many possible transitions will never been observe. This is where our second method comes in. SMILE [Bourgne et al., 2007], another method that we can use to learn the action model of the agent. This method uses the same kind of data than LFIT so here also the modification of the data collecting process to use SMILE and our method are not too cumbersome. Even if SMILE is usually used for a multi-agent system because it is, in fact, the different agents who will learn information about the other agents of the system, we can just create an agent "Observer" who will learn the action model of the observed agent. SMILE is more robust to the lack of data than LFIT but not as effective in some cases. So we will choose which method to use based on the quantity of data obtained during the observation phase. We already tried SMILE and LFIT with our data to extract the action model of the agent and the rules of the environment. We obtained promising results and so, we want to continue in this way. But we do not have combined our method and these two algorithms yet.

4. Incorporating Agents' Preferences

To improve our method and provide some more interesting hypothesis about the agents' goals, we thought about incorporate a preferences function about the goals of these ones. Which means that our hypothesis will provide us with a set of possible goals for an agent and ordered these goals in function of the preferences of the agent. We want to start first with a simple model of preference, by simple we mean that if the agent prefers to reach the goal A rather than the goal B his preferences will not take into account the difficulty to reach these two goals. In other words, if for example the goal A is preferred to the goal B but to reach the goal A the agent needs twenty actions more than to reach the goal B, in this case, we might think that in function of the cost of the actions, the agent could finally prefer to reach B. But since we do not take into account the cost of the actions in our model we are not going to deal with this case right now. However, it's not really difficult to integrate this to our model because we can represent the cost of the agents' actions by some atoms that we will add to our representation of the world, but the computation time of our algorithm is likely to increase drastically. The process of inferring agents' preferences will take place after the goals inference in our method. Because, of course, we need to know the agents' goals to be able to order them. So once we have the agent's goals, we also need to know the agent's action model, then, for each intermediate state of the trace of the agent (see Section 2.) we can see if there is other reachable goals that the one reached in the final state of the trace and if so, compare the number of time that a goal has been preferred to another one. If between two goals one has always been preferred and if it happened several times, we can assume a strict preference between them $A > B$. Otherwise the preference will be more moderate $A \succeq B$.

Given an order of priority $>_p$ about the goals of an agent, we can translate the fact $A >_p B$ in a logic formula by assuming that if the agent finally reaches the goal B it is because the goal A was not reachable. Then we can translate this in the logic formula $A \vee \neg A \wedge B$ (where A and B are atoms conjunctions) by using our language $\mathcal{L}$ described in section 2. Likewise, if we have the preference $A >_p B >_p C$ on the agent's goals we can write this $A \vee \neg A \wedge B \vee \neg A \wedge \neg B \wedge C$. With such a translation we could write all the possible strict orders of preference on the agent's goals, and since the writing is still in disjunctive normal form (DNF) we can modify a bit our algorithm and return a disjunction of such DNF as a result and thus obtain the possible goals of the agent and his preferences for these goals. If the results are promising, we will then try to take into account the fact stated earlier, which is that under some special conditions the agents can change their preferences (especially considering the actions' cost).

5. Conclusion

We saw that the Intention Recognition and Goal Recognition have a wide variety of applications, especially in the coming years with the development of artificial intelligence,

robotics, and smart assistance. Unfortunately, several serious problems still slow down the use of plan recognition in large-scale real-world situations. [Carberry, 2001] describes these problems at the end of her paper. But we can also add another problem more related to our work, which is that in reality we do not really know when an agent reaches his goal, but we will come back on this problem later. We reminded our method and showed that it is quite different than the previous works on intention or goal recognition. Because few work are focused on using propositional logic for goal recognition and our formalisation of the problem allows us to use concept learning. This is very useful because the concept learning is well known and pretty easy to use, several algorithms already exist to treat concept learning. However, we made our own algorithm to control some generalisation bias and we have shown is efficiency in [Lorthioir et al., 2018]. We also showed that making some assumptions about the agent and his environment can drastically improve the goals deduction. This is why we plan to use LFIT or SMILE to infer the agents' models and the environment's rules to exploit such assumptions. This and the integration of the agents' goals preferences in our model will allow us to infer more refined hypotheses about the agent's goals. We were talking about the fact that in reality, we could not know when an agent reaches his goal. This is actually the main weakness of our method and we need to overcome this weakness. For this, a dynamic learning throughout the agent's actions might be efficient and more realistic. It could also be effective in a case where the agent changes goal along the way or in a case where the agent repeats the same cycle of actions, cases that we still can not solve with our method.

References

[Bourgne et al., 2007] Bourgne, G., El Fallah Segrouchni, A., and Soldano, H. (2007). Smile: Sound multi-agent incremental learning. In *Proceedings of the 6th international joint conference on Autonomous agents and multiagent systems*, pages 164–171. ACM.

[Carberry, 2001] Carberry, S. (2001). Techniques for plan recognition. *User Modeling and User-Adapted Interaction*, 11(5):31–48.

[Cardona-Rivera and Michael Young, 2017] Cardona-Rivera, R. E. and Michael Young, R. (2017). Toward combining domain theory and recipes in plan recognition. In *The AAAI 2017 Workshop on Plan, Activity, and Intent Recognition*, Palo Alto, California, USA.

[Charniak and Goldman, 1993] Charniak, E. and Goldman, R. P. (1993). A bayesian model of plan recognition. *Artificial Intelligence*, 64(5):53–79.

[E-Martin et al., 2015] E-Martin, Y., R-Moreno, M. D., and Smith, D. E. (2015). Practical goal recognition for iss crew activities. In *IJCAI the International Workshop on Planning and Scheduling for Space 2015 (IWPSS)*, Buenos Aires, Argentina.

[E-Martin and Smith, 2017] E-Martin, Y. and Smith, D. E. (2017). Goal recognition with noisy observations. In *The AAAI 2017 Workshop on Plan, Activity, and Intent Recognition*, Palo Alto, California, USA.

[Geib and Goldman, 2009] Geib, C. W. and Goldman, R. P. (2009). A probabilistic plan recognition algorithm based on plan tree grammars. *Artificial Intelligence*, 173(11):1101–1132.

[Goldman et al., 2018] Goldman, R. P., Friedman, S. E., and Rye, J. M. (2018). Plan recognition for network analysis: Preliminary report. In *The AAAI 2018 Workshop on Plan, Activity, and Intent Recognition*, New Orleans, Louisiana, USA.

[Ha et al., 2011] Ha, E., Rowe, J. P., Mott, B. W., and Lester, J. C. (2011). Goal recognition with markov logic networks for player-adaptive games. In *Proceedings of the Seventh AAAI Conference on Artificial Intelligence and Interactive Digital Entertainment 2011*.

[Hong, 2001] Hong, J. (2001). Goal recognition through goal graph analysis. *J. Artif. Int. Res.*, 15(1):1–30.

[Inoue et al., 2014] Inoue, K., Ribeiro, T., and Sakama, C. (2014). Learning from interpretation transition. *Machine Learning*, 94(1):51–79.

[Lang, 2004] Lang, J. (2004). A preference-based interpretation of other agents actions. In *International Conference on Automated Planning and Scheduling 2004*, volume 4, pages 33–42, Whistler. AAAI.

[Lorthioir et al., 2018] Lorthioir, G., Bourgne, G., and Inoue, K. (2018). Identifying goals of agents by learning from observations. In *MIWAI*.

[Mirsky et al., 2017] Mirsky, R., Stern, R., Gal, Y., and Kalech, M. (2017). Plan recognition design. In *The AAAI 2017 Workshop on Plan, Activity, and Intent Recognition*, Palo Alto, California, USA.

[Schmidt et al., 1978] Schmidt, C. F., Sridharan, N. S., and Goodson, J. L. (1978). The plan recognition problem: An intersection of psychology and artificial intelligence. *Artificial Intelligence*, 11(5):45–83.

[Singla and Mooney, 2011] Singla, P. and Mooney, R. J. (2011). Abductive markov logic for plan recognition. In *AAAI Proceedings of the twenty-fifth national conference on Artificial intelligence 2011*, pages 1069–1075.

[Vered et al., 2018] Vered, M., Pereira, R. F., Magnaguagno, M. C., Meneguzzi, F., and Kaminka, G. A. (2018). Online goal recognition as reasoning over landmarks. In *The AAAI 2018 Workshop on Plan, Activity, and Intent Recognition*, New Orleans, Louisiana, USA.

The 33rd Annual Conference of the Japanese Society for Artificial Intelligence, 2019

A New Character Decision-Making System by combining Behavior Tree and State Machine

Youichiro Miyake[*1]

[*1] SQUARE ENIX CO., LTD.

Abstract: We have developed a new decision-making system that combines behavior trees and state machines into a single system. The system has both flexibility of behavior tree and strict control of state machines to give a scalability to development of a character AI. The new decision-making system, we call the AI Graph, extends the node formalism to enable sharing nodes between FSMs and Behavior Trees, provides advanced techniques for code reuse using trays which organize code reuse and behavior blackboards, and also provides many features for integrating with detailed low-level character behavior

1. Overview

Originally, behavior Tree and state machine are independent technologies. They each have different good and bad points. The intent behind Behavior Trees[Isla 01,02.5a,5b] is to make a series of character behaviors whereas the intent behind Finite State Machines is to make a stable cycle of character actions. A new system, AI Graph, can have multilayers of both state machine and behavior tree. Any node of any layer can have a state machine or behavior tree as a lower layer (Figure 1).

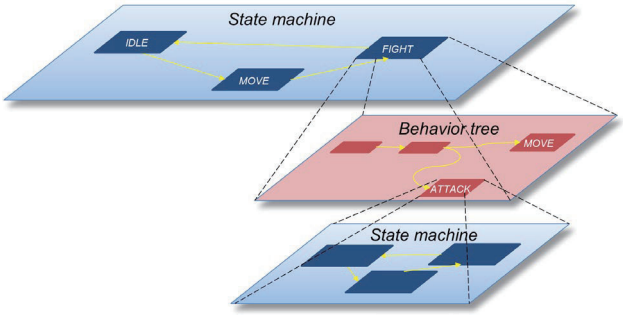

Figure 1. A concept of AI Graph

2. AI Graph Structure and Operation Principle

2.1 Operation principle

An AI Graph is a node based graph system to make a hierarchical structure with a GUI-based node graph tool during game development (Figure 2). AI program execute data made by the AI Graph tool. This is a data-driven system.

Level designers can make a multi-layered decision-making for each character by using a visual node graph tool called the AI Graph. For example, for the first step, a level designer makes a top layer state machine with several states by setting and connecting state machine nodes. Then the level designer can make a new state machine as a sub-state of one or more of the top-level states, or the designer can also make a new behavior tree inside any of the top-level states. Furthermore, the level designer can then make new state machines or behavior trees inside each subsequent sub-state. In this way, the level designer can make a hierarchical structure of state machines and behavior trees by simply editing nodes on the tool.

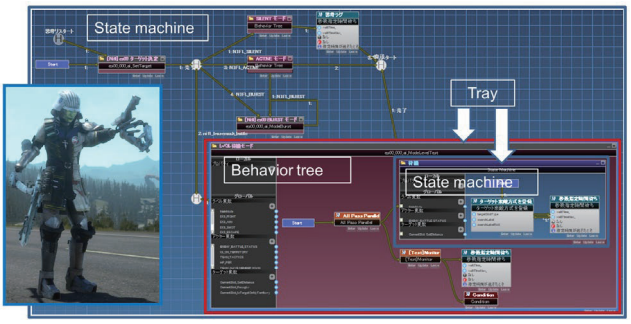

Figure 2. AI Graph tool image

Each layer of the AI Graph also has a blackboard system by which the designer can register variables used in the game. By connecting the blackboards of separate nodes, the different layers can share and use these variables.

2.2 Runtime execution process

An AI Graph user can generate data to be executed by the AI program. AI program execution process is :

(1) A decision making process executes a top layer. Go to (2).
(2) A decision making process executes a start node in the next layer.
a) When a node is primitive, after the node's process finishes, the next node is executed. Go to (2-a)
b) When a node is composite, the process executes a state machine or behavior tree in the node. Go to (2).

So the process continues executing nodes until it cannot go to a deeper layer. It then returns to a higher layer after finishing a lower layer.

When a state machine' transition happens in an upper layer, the state currently executing lower layers must be finished. In this case, after all processing of lower layers has finished, the transition occurs.

3. AI Graph Tool

By using the AI Graph tool, a user can make a state machine or behavior tree for each layer (Figure 3). To make the next layer, a user can select one node and make a state machine or behavior tree in it. In this way AI Graph makes a hierarchical nested structure. As requirements for a character increase in game development, and a developer wants to make character's decision making graph more precisely, the hierarchical nested structure allows developers to make as many layers as they want.

The AI Graph system has a real-time debug system that connects to and communicates with the game's run-time. Active nodes are high-lighted on the decision graph tool as they are executed. During development, this makes finding any problems in the decision graph much easier. AI Graph maintains scalability, variation, and diversity in character AI design through the course of development because of its data-driven approach. In this article, we will explain the AI Graph structure, operation principle, and examples from FINAL FANTASY XV.

AI Graph tool is used to make a character's decision making based on behavior trees and state machines. It has three regions (Figure 4). The center of the screen is a field to build a state machine and behavior tree graph by connecting nodes. The left vertically long window shows variables and nodes which are already made and can be re-used. The right vertically long window shows properties for customizing a node, and is called the property window. A node can be connected with another node by an arc. In a state machine, a node denotes a state and, an arc indicates transition of the state. In a behavior tree, a node denotes a behavior or operator of behavior tree and an arc is used to express behavior tree structure. A tray is used to enclose a state machine or a behavior tree. This enables a user to move one entire state machine or behavior tree by moving the tray, and it is also easy to see the layered architecture through the tray hierarchy.

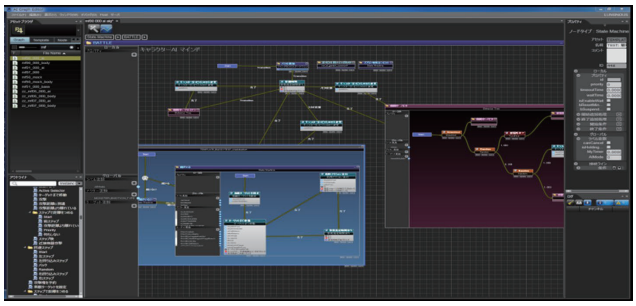

Figure 3. AI Graph Tool screen shot

3.1 Implementation Techniques of AI Graph Node.

In AI Graph, all nodes are re-used. For example, a node that can be used in a state machine can also be used in a behavior tree. But ordinarily the execution method of state machines and behavior trees are different. To make it possible for an AI node to be executed in both state machine and behavior tree, each AI Graph node has four components (Figure 4):

1. Start process (when a node is called)
2. Update process (while a node is executed)
3. Finalizing process (when a node is terminated)
4. A condition at terminate

For both behavior tree and state machine, the start process, the finalizing process and the update process are necessary to begin to execute, finalize and execute a node. The difference between them is what causes stopping a node. For a behavior tree, a node

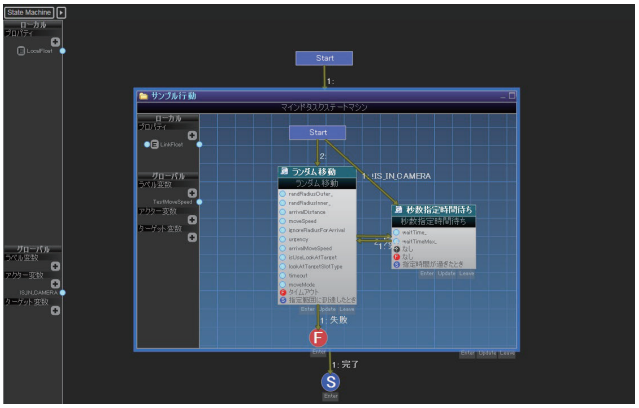

Figure 4. AI Graph Tool screen shot

terminates itself by judging an internal terminate condition while a state machine node is terminated by an external transition condition. Thus if a node has these four components, it can be executed in both behavior trees and state machines.

3.2 Data and Override

An AI Graph can be saved as an asset file. If an AI Graph is very fundamental for a character, it is repeatedly called and used. But the AI Graph is required to partially change the pattern, because it should be adjusted to each character. For example, when a state machine is saved as an asset file, a user will change a state of the state machine to make a more precise behavior tree or state machine in the state. A function to change a node is called an "override", much like C++.

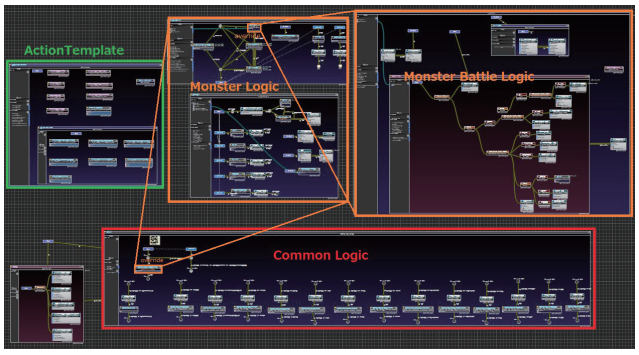

Figure 5. Overriding a monster's AI Graph

Furthermore, a monster's AI Graph can be created by overriding the graph repeatedly from common logic to monster battle logic (Figure 8). In this way, overriding methods makes AI Graph development easier and more effective.

3.3 Blackboard in AI Graph

Variables can be shared via blackboard with two types of blackboard (Figure 5). One is a local blackboard which belongs to a tray[Nii 86a,86b]. Variables of a local blackboard can be shared only in that local blackboard. The other is the global blackboard. Variables of the global blackboard can be shared with game and all characters' individual AIs. In the AI Graph tool, both blackboards are shown on the left side. And some variables are listed in them. To use variables of one local blackboard in a lower tray, the upper blackboard must be connected to the local blackboard of the lower layer included in the tray. Two connected blackboards can share variables.

These variables are used to describe the properties of a node and the transition conditions of a state machine, and so on. For example, the global variable "IS_IN_CAMERA" means whether an actor is in camera or not, and this variable can be used to describe a transition condition inside a state machine contained in a tray.

3.4 Parallel Thinking by AI Graph

For some situations, a character must think about two things at a time. AI Graph allows a character to have two concurrent thinking processes, and it is better to make two simple graphs rather than one big complex graph (Figure 6).

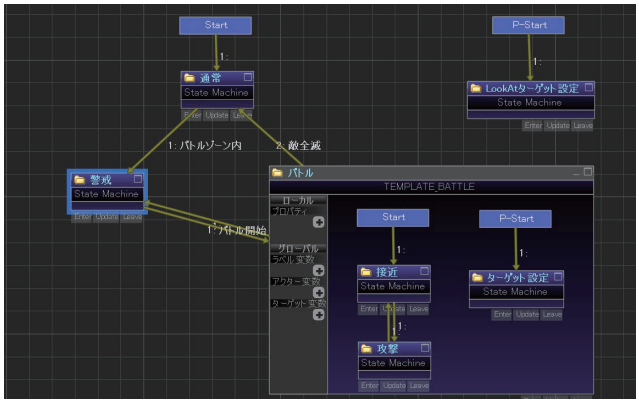

Figure 6. Parallel thinking

For example, one thinking process is a simple state machine to set a character behavior, and the other is a simple state to cause the character to look at a target that suddenly appears. The one state machine begins from a "START" node, and the other state machine begins from "PSTART" node.

The two state machines are executed concurrently. So the character can look around and search for a new target while it keeps attacking. Further, a behavior tree can execute two processes by a parallel node. For example, one behavior is to decide a target and the other is to approach and attack.

3.5 Interrupting the thinking process

It often happens that a character stops its thinking and must execute another specific action. An interrupt node interrupts a process of AI Graph when an interrupting condition is satisfied, and it executes the node linked to the interrupt node. For example, when a new game mission starts, monsters must rush to a player. After rushing into a player's position, they begin their original thinking process. In this case, two AI Graphs are prepared. One AI Graph includes an interrupt node (Figure 7). It causes the current tray to stop and the other Tray process to start when the transition condition connected to the interrupt node is satisfied. And after the tray process finishes, the process returns to the original process.

4. Use case of AI Graph in FINAL FANTASY XV

FINAL FANTASY XV is an RPG game in which a player travels in a large open world with three buddies while they fight with monsters and enemies in real-time (Figure 7). All characters have intelligence to make their decisions by themselves. Also for the player character, AI supports the player character's behaviors.

Figure 7. A player (left), a, monster, and a buddy character(right)

4.1 Body and Intelligence

AI Graph describes a character's intelligence and decision-making, but it does not describe physical body motion. It only gives an order of body motion via each node. And an AI Graph uses information required only for decision-making.

A character system consists of three layers: an AI layer, a body layer, and an animation layer. These three modules send messages to each other and share variables via blackboards.

AI Graph does not directly initiate animation data. AI Graph send a message to the animation layer via a body layer which consists of a state machine. Especially for shooting and damage behavior, AI Graph calls the special control nodes prepared in a body layer.

This three-layered architecture separates the roles to control a character between intelligence and physical body. And it also avoids increasing the size of an AI Graph (Figure 8).

A body layer represents a character's body as a node of a state machine. For example, a character's body state is expressed as running, jumping or climbing a ladder.

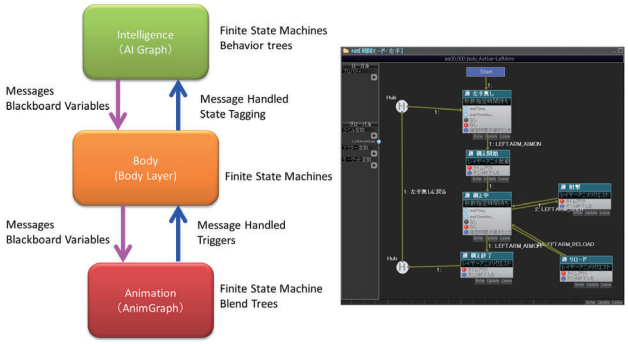

Figure 8. 3 layered system of character

4.2 AI development in game

For AI development, fast iteration is one of the most important features to keep AI improving until the end of development. As such a user should be able to reload an AI Graph without compiling when they want to make a change. In AI Graph Editor, an AI Graph can be compiled in the Editor independently from other systems' code. This an example of a data-driven system.

There are two debug windows (Figure 9). While a game program runs, an AI Graph keeps a connection with the program. This is called the visual node debugger. In this debugger, the active node currently being executed is highlighted in green. This enables a user to trace the active node in real-time.

The other debug window is in a game window. The window displays detailed logs which are generated from a character's AI Graph and AI Graph variables.

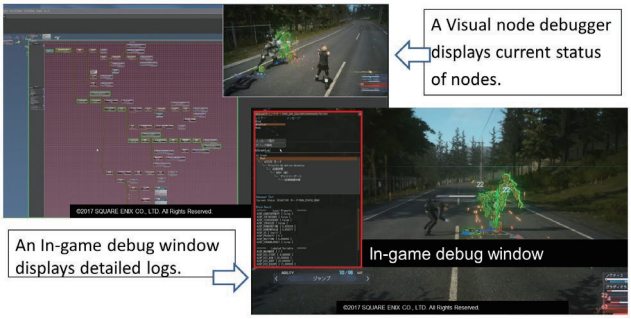

Figure 9 Visual node debugger (left) and In-game debug window (right)

5. Conclusion

As a game environment and game rules becomes more complex, a character is required to behave more smoothly and intelligently. When our project of next-gen AI development began, we realized and felt that improvement of our AI logic tool was required. After many discussions, an idea to combine both state machine and behavior tree was accepted and agreed to by the team. It allows a user to use both techniques in a nested hierarchical node structure to make a stable and flexible AI logic. We called this tool the AI Graph Editor. In this article, the basic principles and applied examples of AI Graph, and how these technologies are used in FINAL FANTASY XV which was released in 2016, are explained.

References

[Isla 01] D. Isla, R. Burke, M. Downie, B. Blumberg.: A Layered Brain Architecture for Synthetic Creatures. In Proceedings of IJCAI (2001).

[Isla 02] Damian Isla, Bruce Blumberg: Blackboard Architectures, AI Game Programming Wisdom, Vol.1, 7.1, pp.333-344 (2002).

[Isla 05a] Damian Isla: Managing Complexity in the Halo2 AI,Game Developer's Conference Proceedings. (2005).
http://www.gamasutra.com/view/feature/130663/gdc_2005_proceeding_handling_.php

[Isla 05b] Damian Isla.: Dude, where's my Warthog? From Pathfinding to General Spatial Competence", AIIDE(2005).
http://naimadgames.com/publications.html

[Nii 86a] H. Penny Nii: The Blackboard Model of Problem Solving and the Evolution of Blackboard Architectures, AI Magazine, Vol.7 Num.2, pp38-53(1986).
http://www.aaai.org/ojs/index.php/aimagazine/article/view/537

[Nii 86b] H. Penny Nii: Blackboard Application Systems, Blackboard Systems and a Knowledge Engineering Perspective, AI Magazine, Vol.7 Num.3, pp82-107(1986). .

International Session | International Session | [ES] E-2 Machine learning

[3B3-E-2] Machine learning: image recognition and generation

Chair: Masakazu Ishihata (NTT)

Thu. Jun 6, 2019 1:50 PM - 3:30 PM Room B (2F Main hall B)

[3B3-E-2-01] Design a Loss Function which Generates a Spatial configuration of Image In-betweening

○Paulino Cristovao[1], Hidemoto Nakada[1,2], Yusuke Tanimura[1,2], Hideki Asoh[2] （1. University of Tsukuba, 2. National Advanced Institute of Science and Technology of Japan (AIST)）

1:50 PM - 2:10 PM

[3B3-E-2-02] One-shot Learning using Triplet Network with kNN classifier

○Mu Zhou[1,2], Yusuke Tanimura[2,1], Hidemoto Nakada[2,1] （1. University of Tsukuba, 2. Artifical Intelligence Research Center, National Institute of Advanced Institute of Technology）

2:10 PM - 2:30 PM

[3B3-E-2-03] Cycle Sketch GAN: Unpaired Sketch to Sketch Translation Based on Cycle GAN Algorithm

○Takeshi Kojima[1] （1. Peach Aviation Limited）

2:30 PM - 2:50 PM

[3B3-E-2-04] Conditional DCGAN's Challenge: Generating Handwritten Character Digit, Alphabet and Katakana

○Rina Komatsu[1], Tad Gonsalves[1] （1. Sophia University）

2:50 PM - 3:10 PM

[3B3-E-2-05] Sparse Damage Per-pixel Prognosis Indices via Semantic Segmentation

○Takato Yasuno[1] （1. Research Institute for Infrastructure Paradigm Shift (RIIPS)）

3:10 PM - 3:30 PM

The 33rd Annual Conference of the Japanese Society for Artificial Intelligence, 2019

Design a Loss Function which Generates a Spatial configuration of Image In-betweening

Paulino Crsitovao[*1] Hidemoto Nakada[*2*1] Yusuke Tanimura[*2*1] Hideki Asoh[*2]

[*1] University of Tsukuba
[*2] National Institute of Advanced Industrial Science and Technology of Japan

Instead of generating image inbetween directly from adjacent frames, we propose a method based on inbetweening in latent space. We design a simple loss function which generates a latent space that represent the spatial configuration of image inbetween. Contrary to the frame based methods, this model can make plausible assumption about the moving objects in the image and can capture what is not seen in the images. Our model has three networks, all based on variational autoencoder, sharing same weights. We validate this model on different synthetic datasets. We show the details of our network architecture and the evaluation results.

1. Introduction

For machines to become more intelligent and autonomous is essential that they understand the world around them, by being able to learn and understand the semantics present in the data. One way to approach this issue is by using generative models. These models can learn the patterns present in the data and generate new similar sample. This work seeks to discover latent representations present in data also design an objective function which generates the spatial configuration of image inbetween. Image inbetween attempts to generate image interpolation from nearby frames. The generated image has to preserve the spatial configuration of the moving objects. Up to now, optical flow [Yi 15],[Mémin 98] and convolutional neural networks [Amersfoort 17] have been proposed to generate image interpolation. Both methods generate image inbetween directly from adjacent frames 1. The result is blur images and loss of contextual information, also they cannot capture what is not present in the the frames. When generating image inbetween preserving the spatial location, shape, color is relevant for some application, for this reason we design a simple model that is able to preserve the contextual representations of objects between nearby frames. This model find scope in several areas such as movie and animation industries where they have to draw each individual frame and in image inpaiting.
In section 2 we describe our proposed model to generate image interpolation, in section 3, we show the results and we present conclusion in the last section.

2. Proposed Method to Generate Image Inbetween

2.1 Model Overview

Our model is based on generative models, which have shown tremendous success in different field such as pattern recognition, image classification, natural language process and reinforcement learning. The proposed approach uses variational autoencoder to generate image inbetween.

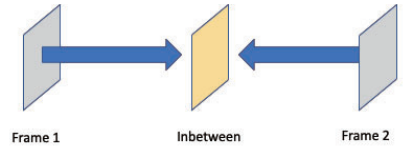

(a) Existing Approach: Directly interpolate image from other frames

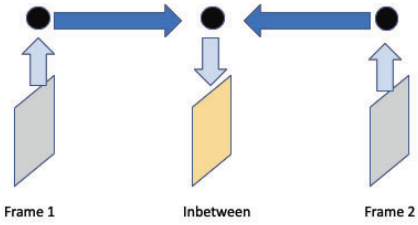

(b) Latent Model Interpolation

Figure 1: Comparison between existing approach and our

2.2 Proposed Loss Function to Generate Image Inbetween

Evaluating generative models means adjusting the internal weights of the network in order. to minimize an error measure. The error is usually given by a loss function. We optimize our network to minimize the distance between the image inbetween and ground truth in latent space. We follow a standard loss function for variational autoencoder. The model has three VAE each with its error function, we sum all errors function plus a an error function caused by the difference between the average latent space of the nearby frames and ground truth. We introduce a scalar hyper-parameter that we call coefficient α (below equation). The coefficient α is an adjustable parameter which express how much is relevant the difference between the Z1 and Z'. Next section we highlight the relevance of α.

Contact: paulinocristovao86@gmail.com

$$l_{(X_0,X_1,X_2)} = l_{VAE}(X_0) + l_{VAE}(X_1) + l_{VAE}(X_2) + \alpha(D_{KL}(q_{(X_1)}||\frac{q_{(X_0)} + q_{(X_2)}}{2}))$$

2.3 Effects of Coefficient α

The adjustable hyper-parameter α modifies the traditional variational autoencoder objective function. It places a restriction on the latent space. This coefficient constraint the latent representations to generate a latent space which represent the spatial configuration of inbetween objects in the image. For $\alpha = 0$ represents the traditional VAE, no restriction is placed in the latent model, increasing the value of α means increasing restrictions on the latent representations.

When evaluating images, the motion of large objects seems easy to evaluate however, evaluating small motion is more complex. We aim to be able to detect small and large changes between frames.

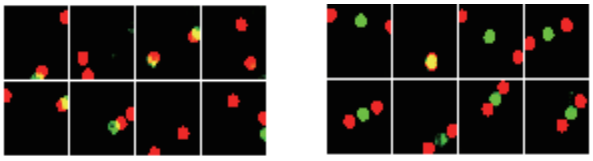

(a) $\alpha = 0$,epochs=5000 (b) $\alpha = 100$,epochs=5000

Figure 2: Inbetween Image: Red dots: Nearby Images; Green dot: Inbetween Image

3. Experiments

3.1 Data Preprocessing

We used synthetic datasets. Two scenarios were tested: first where the object has one variable influencing its rotation which we name "one degree of freedom" and second having two variables "two degrees of freedom". The images were reshape into size of 32x32. For training and testing we randomly sample a triplet images by giving a certain interval among the frames.

3.2 Network Implementation

The base of our model follows a variational autoencoders (VAE), the network model has three VAEs 3, all sharing same weights to reduce the number of hyper-paremeters. The encoder has four convolutional layers, first layer (128 nodes), second(256 nodes), third (512 nodes), fourth (1024 nodes), kernel size = 4 and stride 2. The decoder has four deconvolutional layers, first layer (512 nodes), second (512 nodes), third (256 nodes), fourth (64 nodes) with same kernel size and stride. We input a triplet image. For this work we ignore the output of the nearby frames 3.

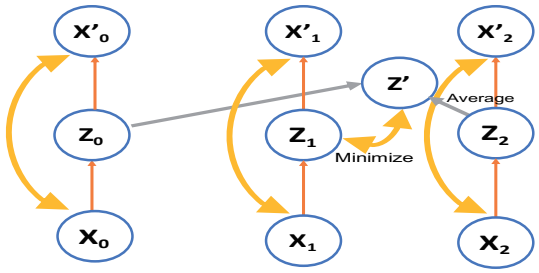

Figure 3: Network implementation

3.3 Reconstruction

The goal is to test the location accuracy

In this section, firstly we qualitatively demonstrate that our proposed model can reconstruct the input image. We tested the reconstruction object location, shape and color. Two scenarios is tested, on α equal to zero and α greater than zero.

3.3.1 One degree of freedom

Below results are for testing. We note that after strong coefficient $\alpha = 100$, the reconstruction test misses some features of the input data.

(a) $\alpha = 0$, epochs=10000 (b) $\alpha = 100$,epochs=10000

Figure 4: Teapot:1st row: Original Image, 2nd row:Reconstructed Image. Red box shows imperfect object reconstruction

3.3.2 Two degrees of freedom

We increase the complexity of the data, the rotation of the object is influenced by two variables.

(a) $\alpha = 0$, epochs=10000 (b) $\alpha = 100$,epochs=10000

Figure 5: Teapot: 1st row:Original Image, 2nd row:Reconstructed Image

3.3.3 Multiple Objects

The task of reconstructing 3 objects seems complex for the model, since it has to capture the pattern of each object and make correspondent matching while interpolating.

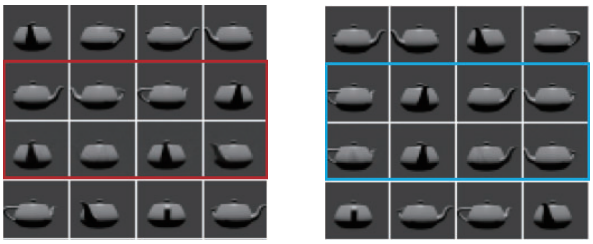

(a) $\alpha = 0$,epochs=10000 (b) $\alpha = 100$,epochs=10000

Figure 7: Teapot-Testing: 1st row:first image, 2nd row: ground truth, 3rd row: Inbetween Image, 4th row: second image. The red square box shows that with $\alpha = 0$ we have imperfect inbetween, Blue box show the correct inbetween

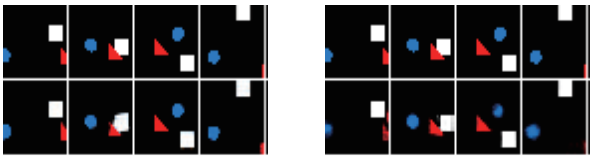

(a) $\alpha = 0$, epochs=15000 (b) $\alpha = 100$,epochs=10000

Figure 6: Mulitple Objects: 1st row:Original Image, 2nd row:Reconstructed Image

3.4 Image Inbetween

As the model was able to reconstruct its input image, even with strong restriction placed in the latent space, next we qualitatively demonstrate the image inbetween generated by our model 7. Using two nearby images with large displacement from one image to other, with zero coefficient the image inbetween does not preserve the accurate spatial location of the object, increasing the coefficient the model is able to generate the perfect image inbetween as we will show in the next section.

3.4.1 One degree of freedom

We trained the framework with images or rotating on x-axis with one degree of freedom. The testing size is 360, the test images used in training and testing are distinct. The images generated by our approach $\alpha = 100$ presents a fair inbetween 7.

3.4.2 Two and Six degrees of freedom

Previous examples we rotated the object in 360 degrees on x-axis, i.e. with one degree of freedom. It is easy to find the pattern of the data points as there are just 360 options or angles. We increased the complexity of the images by moving the object with two and six degrees of freedom. The results for two degrees are credible 8, while for six degrees (3 objects), the model does not perform well on testing phase 9.

3.5 Quantitative Evaluation

The goal here is to evaluate the complexity of the dataset in terms of its degree of freedom. We evaluate the same object in one degree and two degrees of freedom. The results indicates that the two degrees of freedom is more complex. Its MSE gives higher values 10.

3.6 Linear Latent Space Interpolation

We sample pair of images x1 and x2 and project them into latent space z1 and z2 by sampling from the encoder,

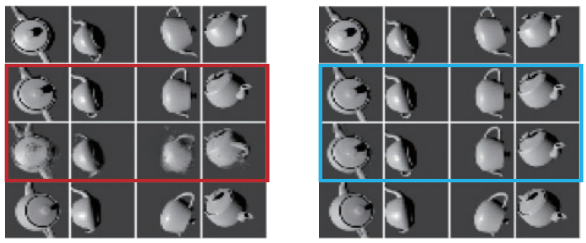

(a) $\alpha = 0$,epochs=15000 (b) $\alpha = 100$,epochs=15000

Figure 8: 2D Teapot-Testing: 1st row:first image, 2nd row: ground truth, 3rd row: Inbetween Image, 4th row: second image. The red square box shows that with $\alpha = 0$ we have imperfect inbetween, Blue box show the correct inbetween

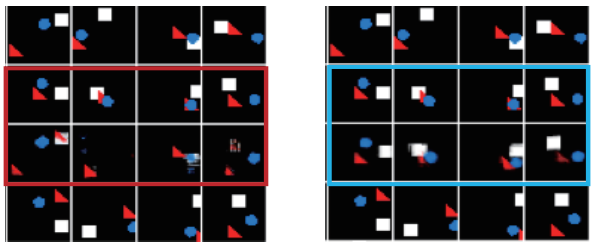

(a) $\alpha = 0$,epochs=15000 (b) $\alpha = 5$,epochs=15000

Figure 9: Multiple Objects - Testing: 1st row:first image, 2nd row: ground truth, 3rd row: Inbetween Image, 4th row: second image

then linearly interpolate between Z1 and Z2 and pass the intermediary points through the decoder to plot the input-space interpolations. The objective is to estimate the continuity in the latent space. Below figures show the generated smooth interpolation of two nearby points. The latent codes used to generate the nine intermediate images are equivalent to (P=0.9, to 0.1): We observe smooth transitions between pairs of examples, and intermediary images remain credible 11. This is an indicator that this model is not just restricting its probability mass exclusively around training examples, but rather has learned latent features that generalize well.

Linear latent space interpolation, indicate that there is a continuity in the latent space which allows a smooth interpolation. We show an example of 3 objects moving in random direction 12, we linearly interpolate the latent space and generate the possible trajectory between first frame and last frame. This model can predict a long-term frames and has the ability to capture their trajectory.

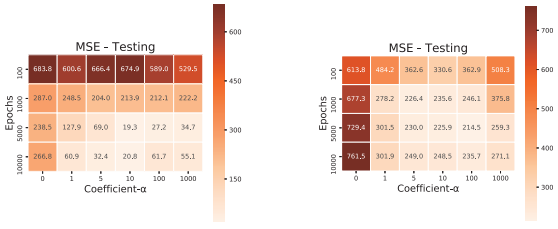

(a) one degree (b) two degrees

Figure 10: MSE loss

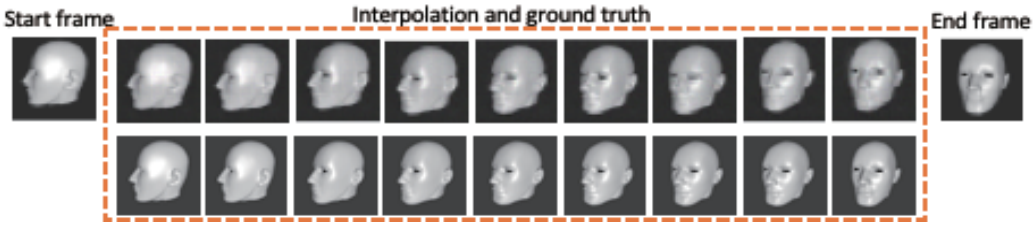

Figure 11: Linear Long-term Interpolation: Face turning to left side

Figure 12: Linear Long-term interpolation of 3 objects, we see the smooth interpolation from first frame and the last frame.

4. Related Work

The intention of unsupervised methods is to uncover the underlying latent representation of the data. Recent works on VAE [Higgins 17][Chen 18] [Berthelot 18] focus in disentangled the latent representations. This approach finds great application in scenario where there is a need to distinguish different characteristics present in the data, for instance, skin color, head pose, facial expression. A disentangled representation can be useful for natural tasks that require knowledge of the salient attributes of the data, which include tasks such as face and object recognition.
Our prosed model does not disentangle latent representations, it simply learn the pattern present in the data.

4.1 Improving Interpolation

While generating interpolation two fundamental characteristics have to be preserved: intermediate points along the interpolation are indistinguishable from real one and provide semantic and smooth morphing [Berthelot 18] The late characteristic is hard to achieve, for that reason [Berthelot 18] purpose a model based in variational autoencoder which introduce a regularizer which encourages interpolated data points to appear more indistinguishable from reconstructions of real data points. It is important to make a clear distinguish between image interpolation generated by latent model and our model. These latent model approaches cannot be used for our target application for the following reason, the dataset used by these models present some variation of the data, for instance in case of celebrity dataset mentioned earlier, it has many factors such as rotation of the head, skin color, age, gender, with or without glasses. The dataset we used does not present such characteristics in addition, we do not disentangle any specific factor of variations, we simply put a restriction on the latent model to generate an accurate image inbetween.

5. Conclusion

We present an alternative approach for generating an image inbetween by giving nearby frames which are non-consecutive images using a latent model. Our approach changes the Naive VAE objective function by introducing a hyper-parameter which constraint the latent representations. This model excels at predicting the image inbetwee in addition the model generalizes well for different datasets. For future, we will test this model on more complex data such as: Complex physical models, such as linked arms. Non-image data, for instance: text and audio data video i.e. video with fast motions and more moving objects. Finding better hyper-parameters between reconstruction and image inbetween.

Acknowledgement

This paper is based on results obtained from a project commissioned by the New Energy and Industrial Technology Development Organization (NEDO). This work was supported by JSPS KAKENHI Grant Number JP16K00116.

References

[Amersfoort 17] Amersfoort, V., et al.: Frame Interpolation with Multi-Scale Deep Loss Functions and Generative Adversarial Networks, *arXiv preprint arXiv:1711.06045* (2017)

[Berthelot 18] Berthelot, D., et al.: Understanding and Improving Interpolation in Autoencoders via an Adversarial Regularizer, *arXiv preprint arXiv:1807.07543* (2018)

[Chen 18] Chen, T. Q., et al.: Isolating Sources of Disentanglement in Variational Autoencoders, *arXiv preprint arXiv:1802.04942* (2018)

[Higgins 17] Higgins, I., et al.: beta-vae: Learning basic visual concepts with a constrained variational framework, in *International Conference on Learning Representations* (2017)

[Mémin 98] Mémin, E. and Pérez, P.: Dense estimation and object-based segmentation of the optical flow with robust techniques, *IEEE Transactions on Image Processing*, Vol. 7, No. 5, pp. 703–719 (1998)

[Yi 15] Yi, C., Liyun, C., and Chunguang, L.: Moving Target Tracking Algorithm Based on Improved Optical Flow Technology, *Open Automation and Control Systems Journal*, Vol. 7, pp. 1387–1392 (2015)

The 33rd Annual Conference of the Japanese Society for Artificial Intelligence, 2019

One-shot Learning using Triplet Network with kNN classifier

Mu ZHOU[*1*2] Yusuke TANIMURA[*2*1] Hidemoto NAKADA[*2*1]

[*1]筑波大学
University of Tsukuba

[*2]産業技術総合研究所 人工知能研究センター
Artifical Intelligence Research Center, National Institute of Advanced Institute of Technology

We propose a triplet network with a kNN classifier for the problem of one-shot learning, in which we predict the query images by given single example of each class. Our triplet network learns a mapping from sample images to the Euclidean space. Then we apply kNN classifier on the embeddings generated by the triplet network to classify the query sample. Our method can improve the performance of one-shot classification with data augmentation by processing the images. Our experiments on different datasets which are based on MNIST dataset demonstrate that our approach provides a effective way for one-shot learning problems.

1. Introduction

Deep learning has shown great achievement in various tasks related to artificial intelligence such as object recognition [Girshick 15], image classification [Kaiming 15], and speech recognition [Yu 14]. However, huge amounts of labelled data is necessary for these deep neural network models to train on. In contrast, humans are capable of one-shot learning, which is to learn a concept from one or only a few training example, contrary to the normal practice of using a large amount of data. This is evident in the case of learning a new thing rapidly - humans have no problem recognizing the new category with one or a few direct observation. However, it is a challenging task for machine to solve the classification and recognition problem with very few labelled training data.

2. Related work

Several studies have investigated few-shot learning and one-shot learning, one special type neural network is Siamese Neworks [Koch 15]. The idea of the Siamese Network is based on distance metric learning which is to learn the distance metric from the input space of training data by a contrastive loss, then keep the samples belonging the same class close to each other and separate the dissimilar samples. The similar one is Triplet Network [Hoffer 15] which is composed of 3 parameter-shared convolutional neural networks.

Inspired by Siamese Networks and Triplet Networks, we improve the Triplet Network and use a triplet loss [Schroff 15] in our work. The loss function is to minimize the distance between the data with same label and maximize the distance between the data with different label. Before we get the embeddings trained on networks, we do data augmentation on the training set with only one sample. Then we make the prediction to the embedded query points by finding the nearest embedded support point by using k-Nearest Neighbor classifier. The procedure of the whole work is shown in Figure 1.

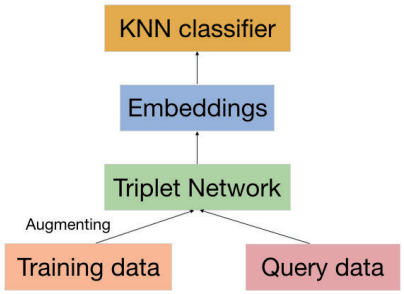

Figure 1: Prediction procedure.

3. Method

3.1 Triplet Network

In this research, we use the triplet network to learn the distance metric from inputs of triplet images. The triplet network is a horizontal concatenation triplet with 3 identical Convolutional Neural Networks (with shared parameters), these ConvNets are trained using triplets of inputs. The input triplet $(\vec{x_a}, \vec{x_p}, \vec{x_n})$ is composed of an anchor instance $\vec{x_a}$, a positive instance $\vec{x_p}$ (same class as the anchor), and a negative instance $\vec{x_n}$ (different class from the anchor). The network is then trained to learn an embedding function *f(x)* called triplet loss. The model architecture is shown in Figure 2.

3.1.1 Convolutional Networks

A series of breakthroughs in image classification came with the introduction of Convolutional Neural Networks (CNNs or ConvNets), where the image is input into a nested series of functions and convolved with filters, then output as feature vector. In our method, the ConvNet has 4 convolutional layers and is used as an embedding function. The ouput is passed through a fully connected layer resulting in a 128-dimensional embedding. In addition, we use ReLU as an activation function which is a common choice, especially for convolutional networks. The architecture of this ConvNet is as following:

- 1x{5x5-conv.layer (32 filters), 5x5-conv.layer (32 filters), batch normalization, max pool(2, 2), leaky relu,

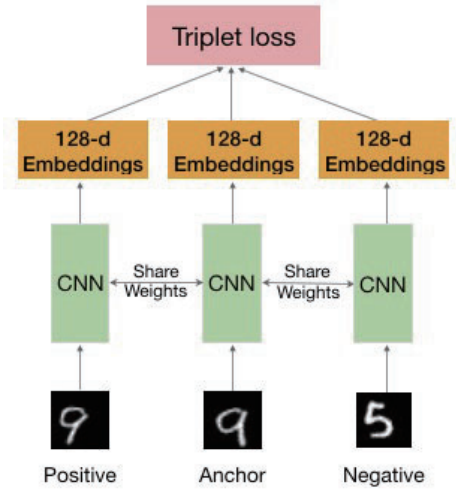

Figure 2: Triplet Network Model.

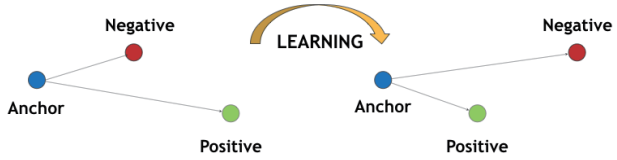

Figure 3: Triplet Loss Function.

dropout(0.25)},

- 1x{3x3-conv.layer (64 filters), 3x3-conv.layer (32 filters), batch normalization, max pool(2, 2), leaky relu, dropout(0.25)},
- 1x{fc-layer, batch normalization}.

3.1.2 Triplet Loss

Although we did not compare it to other loss function, we believe that the triplet loss is more suitable for this network, and triplet loss layer could improve the accuracy of ConvNets. A triplet loss is used to learn an embedding space for the images, such that embeddings of same class are close to each other, while those of different class are far away from each other. For the distance on the embedding space d, the loss of a triplet $(\vec{x_a}, \vec{x_p}, \vec{x_n})$ is:

$$L = max(d(x_a, x_p) - d(x_a, x_n) + \alpha, 0)$$

where α is a margin that is enforced between positive and negative pairs[Schroff 15]. In our research, the triplet loss minimizes the distance between the anchor and the positive, both of which have the same identity, and maximizes the distance between the anchor and a negative of a different identity, as shown in Figure 3.

3.2 kNN Classifier

The k-Nearest Neighbors algorithm is one of the simplest way to perform classification. Most kNN classifiers use Euclidean distances (also known as L2-norm distance) to measure the similarities between the instances which are represented as vector inputs. The L2-norm distance is as following:

$$d(\vec{x}, \vec{y}) = \sqrt{\sum_{i=1}^{n}(x_i - y_i)^2}$$

In our research, after we trained the dataset (both train and test dataset) on the Triplet Network, we obtained the embeddings of the data, each of which is a 128-dimensional feature vector. Then we used PCA (Principal component analysis) to reduce the dimension of the feature vectors. Since these vector embeddings are represented in shared vector space, we can calculate the similarity between the vectors by using the vector distance. Finally we used kNN classifier to calculate the distance between the test point and all the training points by giving the feature vector of labelled training and unlabelled test data. We gained the best choice of k and choose the corresponding classification that appears most frequently as the predictive class.

3.3 Data Augmentation

Data augmentation is the most common solution for one-shot learning, since it can help to increase the amount of relevant data in the dataset and boost the performance of neural networks. In our research, we augmented the images in the training dataset. As a result, a large amount of training images was created, through different ways of processing or combination of multiple processing, such as random rotation, shifts and shear, etc.

4. Experiment

4.1 Dataset

MNIST database (Modified National Institute of Standards and Technology database) is a large database of handwritten digits that is commonly used for training various image processing systems. The MNIST database contains 60,000 images for training and 10,000 images for testing. Figure 4 presents some of the digits from MNIST dataset.

4.1.1 Initial Dataset

To setup the training dataset, we chose whole digit images with label 0 to 4, while we randomly selected simple digit image with the label 5 to 9 from the MNIST dataset. This initial dataset was used for our comparison experiment. The count of each label on initial training dataset is shown in Figure 5.

4.1.2 Augmented Dataset

In addition to the initial dataset, we generated another training dataset by the technique of data augmentation. In our experiment, we augmented the single image. Due to the limitation of some digit images, (i.e. digit 9 may be recognized as digit 6 after the 180-degree rotation,) we did the random rotation operation with only 30 degrees combined with random zoom and random shifts. To ensure similar appearance of the amount of each label, we enlarged the images several times with similar amount. The count of

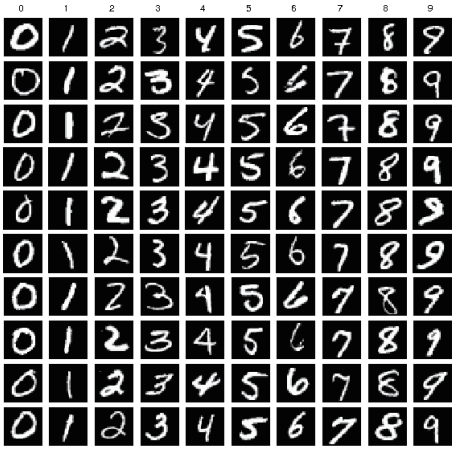

Figure 4: Samples from MNIST dataset.

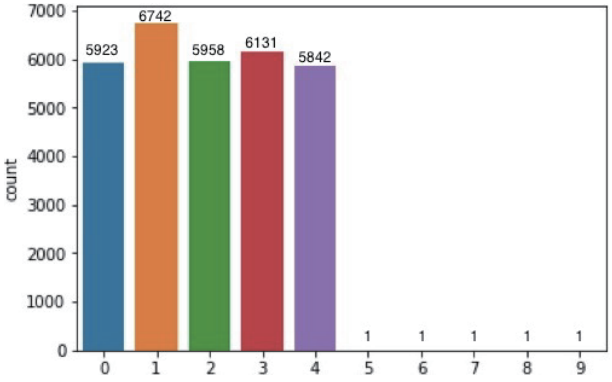

Figure 5: The initial dataset.

each label on augmented training dataset is shown in Figure 6.

4.2 Triplet Selection

Input triplets for Triplet Network were generated in two ways. One kind of triplets was produced by the augmented dataset, while another one was created by the initial dataset which was not augmented. For the first type, we randomly selected 1 sample (used as the anchor instance) from the dataset, then chose another one (used as the positive instance) from the same label. Then we randomly obtained the other sample (used as the negative instance) from any other label. Finally, we concatenated them as a triplet pair. However, for the other type created by initial dataset, we used the same image as the positive instance to overcome the limitation of lack of samples.

4.3 Results

We evaluated the performance of our model on above two datasets - initial dataset and augmented dataset, in order to judge the effectivity of data augmentation. To estimate the performance on Triplet Network in comparison to other model, we applied the CNN model on one-shot classification with the augmented dataset, as is mentioned above.

We obtained the embeddings of training points and test

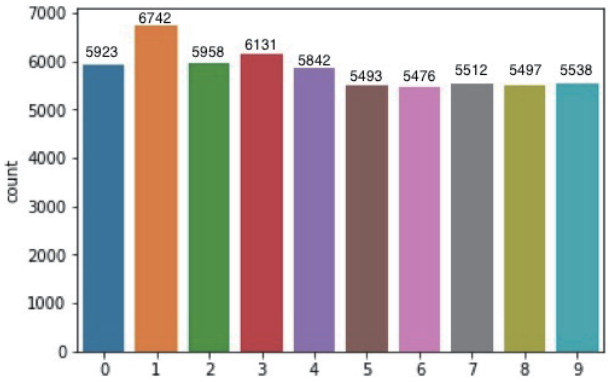

Figure 6: The augmented dataset.

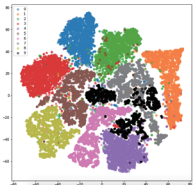

Figure 7: Embedding visualization of training points.

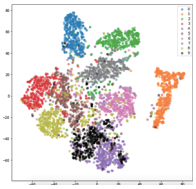

Figure 8: Embedding visualization of test points.

points from the Triplet Network, and we did visualization using t-SNE technique, as shown in Figure 7 and Figure 8. With these training points and test points, we evaluated the accuracy with different k ranging from 1 to 30, and selected the best choice of k. Figure 9 presents the accuracy of kNN classifier for different choice of k with augmented dataset in our Triplet Network model, and we get the best k (k=11) in this experiment. We predicted the label of test points with best k, and compared with the true label. The results are shown in Table 1, which present the accuracy of the test dataset with 1-shot classes (label 5 to label 9).

In our experiment on Triplet Network, the accuracy of the test dataset is 46.8% for 1-shot classes, while the accuracy

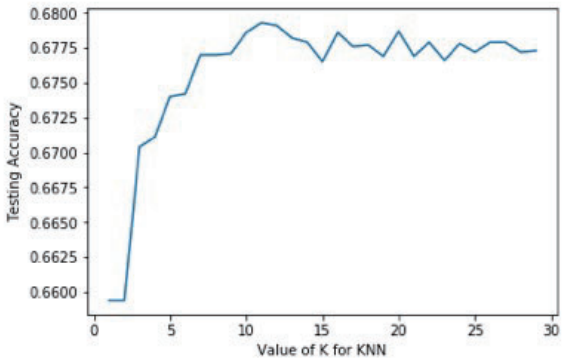

Figure 9: Accuracy of kNN classifer for different choices of k.

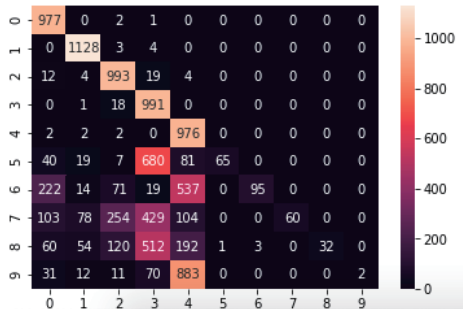

Figure 10: The result on TripletNN with initial dataset.

Figure 11: The result on TripletNN with augmented dataset.

is only 9.8% in the comparison experiment. This result suggests that data augmentation make sense and can obtain better prediction result than without data augmentation. In addition, the Triplet Network gives a better performance than the CNN model in this experiment.

Figure 10 and 11 show the results between actual labels and predicted labels in both datasets using Triplet Network. With regard to the accuracy of digit 9, it gets a low score since most of digit 9 are recognized as digit 4. This result implies that most written digit 9 are significantly similar to written digit 4, and the machine may not recognize them precisely with simple sample.

Method (dataset)	Accuracy					
	5	6	7	8	9	Average
TripletNN (not Agumented)	14%	18%	11%	6%	0%	9.8%
CNN (Augmented)	25%	26%	16%	24%	13%	20.8%
TripletNN (Augmented)	**42%**	**56%**	**66%**	**56%**	**14%**	**46.8%**

Table 1: Results of 1-shot classes.

5. Conclusion

In this work, we described how a Triplet Network model, inspired by the Siamese Network based on distance metric, can be used for one-shot learning. We used the embeddings of training points trained on kNN classifier and predict the label with the embedding of testing points by the classifier. We obtain significant improvement by the effectiveness of data augmentation. Of the 3 approaches tested, we achieved best results by augmenting the initial dataset with Triplet Network model. While in the contrast experiment on CNN model, data augmentation resulted accuracy of 20.8%. However, the experiment on Triplet model with initial dataset resulted accuracy of 9.8%, where almost all the data trained with 1 sample can not be recognized. This study therefore indicates that the benefits gained from data augmentation may work well on one-shot learning problem.

Although our experiment demonstrate a great improvement, the results are subject to certain limitations. For instance, since the differences between digit 9 and digit 4 are unable to be separated, most of digit 9 are recognized as digit 4 in the experiments. In addition, due to the computational constraint, our experiments were unable to explore how our approaches work on other much larger and complex datasets. Therefore, future work should focus on how to distinguish the difference between written digit 9 and digit 4 and how to enlarge the metric distance between digit 9 and 4. Furthermore, future studies need to be carried out in order to validate whether our approach does indeed help to solve the one-shot learning on other large and complex datasets, such as Fashion MNIST, Omniglot, Mini-Imagenet and e.t.

Acknowledgement

This paper is based on results obtained from a project commissioned by the New Energy and Industrial Technology Development Organization (NEDO). This work was supported by JSPS KAKENHI Grant Number JP16K00116.

References

[Girshick 15] Girshick, R.: Fast R-CNN, *IEEE International Conference on Computer Vision (ICCV) 2015* (2015)

[Hoffer 15] Hoffer, E. and Ailon, N.: Deep metric learning using triplet network, *International Workshop on Similarity-Based Pattern Recognition* (2015)

[Kaiming 15] Kaiming, H., Xiangyu, Z., Shaoqing, R., and Jian., S.: Delving deep into rectifiers: Surpassing human- level performance on imagenet classification, *arXiv preprint arXiv:1502.01852* (2015)

[Koch 15] Koch, G., Zemel, R., and Salakhutdinov, R.: Siamese neural networks for one-shot image recognition, *ICML Deep Learning Workshop* (2015)

[Schroff 15] Schroff, F., Kalenichenko, D., and Philbin., J.: Facenet: A unified embedding for face recognition and clustering, *Proceedings of the IEEE conference on computer vision and pattern recognition* (2015)

[Yu 14] Yu, D. and Deng, L.: *Automatic Speech Recognition: A Deep Learning Approach*, Springer Publishing Company (2014)

The 33rd Annual Conference of the Japanese Society for Artificial Intelligence, 2019

Cycle Sketch GAN: Unpaired Sketch to Sketch Translation Based on Cycle GAN Algorithm

Takeshi Kojima

Peach Aviation Limited

Unlike pixel image generation, sketch drawing generative model outputs a sequence of pen stroke information. This paper proposes Cycle Sketch GAN: the first model that learns to translate a sketch drawing from source domain to target domain in the absence of paired dataset. Based on Cycle GAN algorithm, this model uses Transformer Encoder architecture in generators. Transformer Encoder feeds the input stroke information in source domain and generates the parameters for output distribution, from which the stroke information in target domain is sampled by reparameterization trick. The negative log likelihood of the distribution is used as cycle consistency loss. This model is trained and evaluated by some QuickDraw datasets. Qualitative evaluation shows that this model can practically translate sketch drawings from source domain to target domain. Quantitative evaluation by user study showed that 42 % of the translated sketches is recognizable compared to 71 % of the human sketches.

1. Introduction

Unlike pixel image generation, sketch drawing generative model outputs a sequence of pen stroke information (See section 2.1 for details). Some recent researches focused on creating sketch drawing generative model [Ha 18][Song 18] by neural network. However, the research of sketch to sketch translation, which aims to transform a sketch from source domain to target domain especially without supervised dataset, was not yet conducted.

This paper proposes Cycle Sketch GAN: the first model that learns to translate a sketch drawing from source domain to target domain in the absence of paired dataset. Specifically, this unsupervised learning model can change a sketch drawing's partial shapes characteristic to source domain into ones characteristic to target domain while keeping the common features unchanged (See an example in Fig.1). To train this model, we need to prepare 2 domain datasets, but each data in one domain does not need to have paired data in the other domain. This model is based on Cycle GAN algorithm[Zhu 17]. However, several changes are implemented to solve the following 2 problems specific to sketch drawing process.

The first problem of unsupervised sketch to sketch translation is that the sketch drawing is a process of generating a sequence of stroke vector representations. Therefore, Convolutional Neural Network(CNN), which is used in basic Cycle GAN, should not be used for this solution. Cycle Sketch GAN solves this problem by using Transformer[Vaswani 17] Encoder architecture in a generator. Transformer has self-attention mechanisms and recently succeeded in improvements of several sequential data processing tasks mainly in NLP. Note that Transformder Decoder is not used in this paper because we have no supervised data. Instead, Transformer Encoder feeds input and directly generates sequential outputs.

The second problem is that drawing sketch requires the accurate generation of strokes. Therefore, cycle consistency loss function has to be like the form of reconstruction loss as in [Ha 18], instead of L1 or L2 Norm. Cycle Sketch GAN solves this problem as follows: Transformer Encoder feeds the input stroke in source domain and generates the parameters for output distributions. Stroke information in target domain is sampled from the distribution by reparameterization trick to enable backpropagation for the training. The negative log likelihood of the distribution is used as cycle consistency loss to improve accuracy.

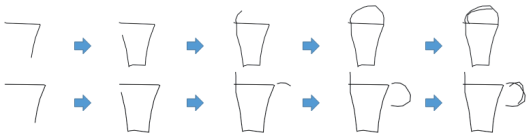

Figure 1: A visualized example of sequential stroke output process by Cycle Sketch GAN. This model can learn to translate a sketch drawing from source domain (Top: bucket) to target domain (Bottom: cup) in the absence of paired datasets. The common feature between 2 drawings (the body of bucket and cup) is unchanged.

2. Methods

2.1 Data Format

Based on [Ha 18], the data format of a sketch drawing for this model is a sequence of pen stroke actions $s = (s1, ...s_i, ..., s_{N_{max_s}})$, where $s_i = (\Delta_{x_i}, \Delta_{y_i}, p1_i, p2_i, p3_i)$. $\Delta_{x_i}, \Delta_{y_i}$ are the offset distance of ith pen movement in the direction of x axis and y axis. $p1_i, p2_i, p3_i$ are binary one-hot vector of 3 possible states at ith movement[*1]. $p1_i$ is an indicator that the pen is touching the paper for the ith pen movement. $p2_i$ is an indicator that the pen is lifted from the paper for the ith pen movement. $p3_i$ is an indicator that the drawing has ended. In case of $p3_i = 1$, Δ_{x_i} and Δ_{y_i} are defined to be 0.

2.2 Generator Architecture

This model uses Transformer[Vaswani 17] Encoder architecture as a generator to translate a sketch drawing stroke representation of domain S_A to domain S_B, and vice versa. Specifically, $s_A \in S_A$ is fed into one generator and translated to $\tilde{s_B} \in S_B$. In the same way, $s_B \in S_B$ is fed into the other generator and translated to $\tilde{s_A} \in S_A$. The architectures of these 2 generators are the same. This section omits the subscript A and B for simplicity.

Contact: t.kojima@flypeach.com

*1 [Ha 18] defines $p1_i, p2_i, p3_i$ as binary one-hot vector of 3 possible states at $i + 1$th movement.

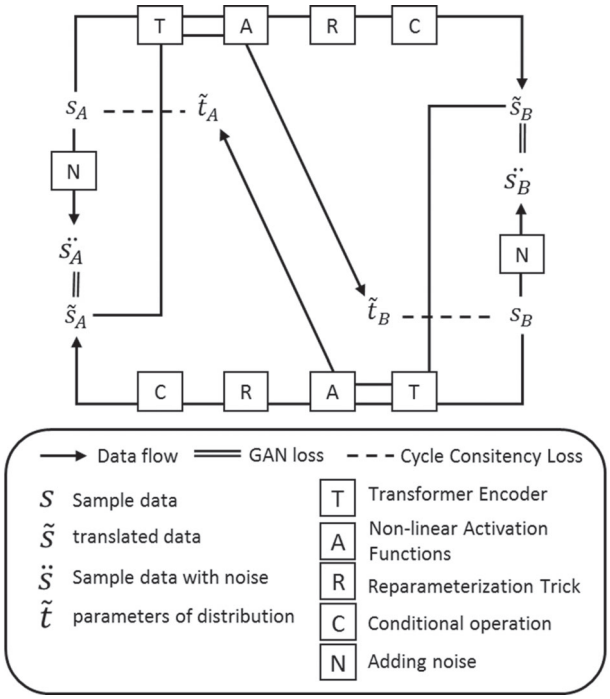

Figure 2: Overall image of Cycle Sketch GAN

The input s is concatenated with Positional Encoding [Vaswani 17] whose dimension size for ith position is ${N_{PE}}^{*2}$. The concatenated representation is fed into Transformer Encoder as input. Transformer Encoder has N_{TL}multiple stacked layers, each of which consists of N_{TA} multi-head attentions and a feed-forward network with dimension size of $4N_{TA}$, followed by a position-wise linear projection for the output below.

$$\begin{aligned}&(\mu_x, \mu_y, \hat{\sigma_x}, \hat{\sigma_y}, \hat{\rho_{xy}}, q1, q2, q3)_1 \\ &\quad .... \ (\mu_x, \mu_y, \hat{\sigma_x}, \hat{\sigma_y}, \hat{\rho_{xy}}, q1, q2, q3)_{N_{max_s}} \\ &\quad = TransformerEncoder([s; PE]) \end{aligned} \quad (1)$$

As described in [Ha 18], $(\mu_x, \mu_y, \hat{\sigma_x}, \hat{\sigma_y}, \hat{\rho_{xy}})$ are defined as the parameters for a bivariate normal distribution to describe Δx and Δy. $(q1, q2, q3)$ are the categorical distribution parameters to model the ground truth data $(p1, p2, p3)$. The following nonlinear functions are required to ensure that standard deviations are non-negative, that the correlation values are limited between -1 and 1.

$$\sigma_x = exp(\hat{\sigma_x}), \ \sigma_y = exp(\hat{\sigma_y}), \ \rho_{xy} = tanh(\hat{\rho_{xy}}) \quad (2)$$

The reparameterization trick for bivariate normal distribution is applied using $(\mu_x, \mu_y, \sigma_x, \sigma_y, \rho_{xy})$ to sample single value for each ith pen movements.

$$\begin{aligned}\begin{bmatrix} \tilde{\Delta x_i} \\ \tilde{\Delta y_i} \end{bmatrix} &= \begin{bmatrix} \mu_{x_i} \\ \mu_{y_i} \end{bmatrix} + L_i \begin{bmatrix} \epsilon_{x_i} \\ \epsilon_{y_i} \end{bmatrix} \\ where \ \ L_i &= \begin{bmatrix} \sigma_{x_i} & 0 \\ \rho_{xy_i}\sigma_{y_i} & \sqrt{1-{\rho_{xy_i}}^2}\sigma_{y_i} \end{bmatrix} \\ \epsilon_{x_i}, \epsilon_{y_i} &\sim N(0,1), \ \epsilon_{x_i}, \epsilon_{y_i} \in \mathbb{R} \end{aligned} \quad (3)$$

L_i is a lower triangular matrix after cholesky decomposition of covariance matrix of bivariate normal distribution.

∗2 Considering the case $N_{PE} > 5$, we use concatenation instead of addition.

Categorical reparameterization for $(q1, q2, q3)_i = q_i$ is also applied by using Gumbel Softmax[Jang 17] with temperature τ.

$$\begin{aligned}\tilde{q_i} &= softmax((q_i + g_i)/\tau) \\ where \ \ g_i &= -\log(-\log(u_i)) \\ u_i &\sim Uniform(0,1), \ u_i \in \mathbb{R}^3 \end{aligned} \quad (4)$$

In order to deceive discriminators as much as possible, generators calculate the following position-wise conditional operation before the data is fed into Discriminator.

$$\tilde{s_i} = \begin{cases} (0, 0, \tilde{q1}, \tilde{q2}, \tilde{q3})_i & if \ max(\tilde{q1}_i, \tilde{q2}_i, \tilde{q3}_i) = \tilde{q3}_i \\ (\tilde{\Delta x}, \tilde{\Delta y}, \tilde{q1}, \tilde{q2}, \tilde{q3})_i & otherwise \end{cases} \quad (5)$$

Here, for simplification, the sequence of functions (1) and (2) can be defined as $t = (t1, ..., t_i, ..., t_{N_{max_s}}) = G(s)$, where $t_i = (\mu_x, \mu_y, \sigma_x, \sigma_y, \rho_{xy}, q1, q2, q3)_i$. The sequence of functions (3), (4) and (5) can also be defined as $\tilde{s} = (\tilde{s}_1, \tilde{s}_2, ..., \tilde{s}_i, ..., \tilde{s}_{N_{max_s}}) = H(t)$. By using these expressions, 2 generators can be defined as:

$$\tilde{s_B} = H_B(G_B(s_A)), \ \ \tilde{s_A} = H_A(G_A(s_B)) \quad (6)$$

Note that the function $H_A(\cdot)$, $H_B(\cdot)$ does not contain any neural networks to be optimized.

2.3 Discriminator Architecture

The discriminator D is a multilayer convolutional neural network with instance normalization. Specifically, the discriminator regards the input s or $\tilde{s}$ as an image with height=N_{max_s}, width=5 and depth=1. The jth layer of D convolves the input of the layer with kernel size $(N_{Dk-height_j}, \ N_{Dk-weight_j})$ and stride size = N_{Ds_j} without padding, and outputs the tensor with channel size N_{Dc_j}, followed by instance normalization and activation. As an exception, the first layer and final layer does not have instance normalization. The final layer also has no activation function due to the restriction of the architecture of the discriminator in improved Wasserstein GAN optimization process [Gulrajani 17]. 2 discriminators, D_A for data A and D_B for data B are implemented with the same architecture described above.

2.4 Objective function

The objective function of this model contains adversarial losses and cycle consistency losses for both domains[Zhu 17]. As for the adversarial loss, this model uses improved Wasserstein GAN [Gulrajani 17] instead of the normal GAN [Goodfellow 14] to avoid mode collapse and to stabilize the training. The adversarial loss for data A is:

$$\begin{aligned}&\mathcal{L}^A_{GAN}(G_A, D_A, S_B, S_A) \\ &\quad = \mathbb{E}_{s_B}[D_A(H_A(G_A(s_B)))] - \mathbb{E}_{\ddot{s}_A}[D_A(\ddot{s}_A)] \\ &\qquad + \textit{gradient penalty for WGAN-GP} \\ &where \ \ddot{s}_A = noise(s_A) \end{aligned} \quad (7)$$

$noise(\cdot)$ is a function that adds random noises $U(-0.01, 0.01)$ into $(p1, p2, p3)$, and also into $(\Delta_{x_i}, \Delta_{y_i})$ if $q3_i = 1$ to prevent D from concentrating too much on discrete variables. The same as true for the adversarial loss of data B, $\mathcal{L}^B_{GAN}(G_B, D_B, S_A, S_B)$.

As for cycle consistency loss of data A, firstly the following cycled parameters are introduced.

$$(\tilde{t}_{A,1}, ..., \tilde{t}_{A,i}, ...\tilde{t}_{A,N_{max_s}}) = G_A(H_B(G_B(s_A)))$$
$$where\ \tilde{t}_{A,i} = (\tilde{\mu}_x^A, \tilde{\mu}_y^A, \tilde{\sigma}_x^A, \tilde{\sigma}_y^A, \tilde{\rho}_{xy}^A, \tilde{q1}^A, \tilde{q2}^A, \tilde{q3}^A)_i \quad (8)$$

Then, cycle consistency loss for data A is expressed as follows:

$$\mathcal{L}_{cyc}^A(G_A, G_B, S_A)$$
$$= \mathbb{E}_{s_A}\Big[- \frac{1}{N_{\max_s}} \sum_{i=1}^{N_s} \log\Big(\mathcal{N}(\Delta x_i^A, \Delta y_i^A \mid \tilde{w}_i^A)\Big)$$
$$- \frac{1}{N_{\max_s}} \sum_{i=1}^{N_{\max_s}} \sum_{k=1}^{3} pk_i^A \log(qk_i^{'A})\Big]$$
$$where\ \tilde{w}_i^A = (\tilde{\mu}_x^A, \tilde{\mu}_y^A, \tilde{\sigma}_x^A, \tilde{\sigma}_y^A, \tilde{\rho}_{xy}^A)_i$$
$$q1_i^{'A}, q2_i^{'A}, q3_i^{'A} = softmax(\tilde{q1}_i^A, \tilde{q2}_i^A, \tilde{q3}_i^A) \quad (9)$$

$\mathcal{N}(\Delta x_i^A, \Delta y_i^A \mid \tilde{w}_i^A)$ is the probability distribution function for a bivariate normal distribution. N_s is the point of last stroke in the sketch. This cycle consistency loss function is the same as the reconstruction loss function of [Ha 18] except that the distribution of $(\Delta x, \Delta y)$ is not modeled as a Gaussian mixture model (GMM). It can be said that the function is a special case of GMM size = 1. The same as true for the cycle consistency loss for data B, $\mathcal{L}_{cyc}^B(G_B, G_A, S_B)$.

The final objective function is:

$$\begin{aligned}\mathcal{L}(G_A, G_B, D_A, D_B) &= \mathcal{L}_{GAN}^A(G_A, D_A, S_B, S_A) \\ &+ \mathcal{L}_{GAN}^B(G_B, D_B, S_A, S_B) \\ &+ \lambda\mathcal{L}_{cyc}^A(G_A, G_B, S_A) \\ &+ \lambda\mathcal{L}_{cyc}^B(G_B, G_A, S_B) \quad (10)\end{aligned}$$

We aim to solve:

$$G_A^*, G_B^* = \arg\min_{G_A, G_B} \max_{D_A, D_B} \mathcal{L}(G_A, G_B, D_A, D_B) \quad (11)$$

3. Experimtents

3.1 Dataset

To evaluate Cycle Sketch GAN, full size of "Sketch-RNN QuickDraw Dataset" is used. QuickDraw Dataset contains hundreds of classes of sketch drawings. Each class is a dataset of more than 70K training samples and 2.5K test samples. In this paper, the following 6 classes are picked up from QuickDraw and made pairs: (bucket, cup), (suitcase, envelope), (sock, rollerskates). Note that each data in one class does not have paired data in the other class. The data format is changed according to section 2.1.

This experiment only uses the data whose size of the stroke actions does not exceed $N_{max_s} = 50$. Moreover, in order to equalize the training dataset size between paired classes, training data were randomly sampled from the class whose dataset size is larger than the other.

3.2 Implementation details

As for generators, the dimension size of Positional Encoding is set to be $N_{PE} = 251$. Transformer layer size is $N_{TL} = 12$, and the multihead attention size is $N_{TA} = 4$. As for the Discriminator, the hyper parameter values are set as followed:
$(N_{Dk-height_1}, N_{Dk-weight_1}, N_{Ds_1}, N_{Dc_1}) = (5, 5, 1, 128)$
$(N_{Dk-height_2}, N_{Dk-weight_2}, N_{Ds_2}, N_{Dc_2}) = (10, 1, 2, 256)$
$(N_{Dk-height_3}, N_{Dk-weight_3}, N_{Ds_3}, N_{Dc_3}) = (10, 1, 2, 512)$
$(N_{Dk-height_4}, N_{Dk-weight_4}, N_{Ds_4}, N_{Dc_4}) = (5, 1, 1, 1)$.

Figure 3: The original sketches by human (Row A, B) and the translated sketches by Cycle Sketch GAN (Row B', A').

All the activation functions in generators and discriminators are Leaky-ReLU activation. The temperature τ of Gumbel Softmax is set to be 1. λ in the final objective function is also set to be 1.

While training, minibatch SGD is used and the Adam optimizer is applied for the optimization process with $\beta_1 = 0$ and $\beta_2 = 0.9$ [Gulrajani 17]. The learning rate is fixed with 0.00005 during the training. The minibatch size is 128 and the iteration size is 30000 for generators. Discriminators and generators are mutually trained with the number of iterations of Discriminators per iteration of generators be set 5[Gulrajani 17].

Before generators feed data, the offsets $(\Delta x, \Delta y)$ in each classes is normalized using a single scaling factor [Ha 18] to adjust the offsets in the training set to have a standard deviation of 1. The test dataset is also normalized by that single scaling factor which is calculated by the training set of the same class.

2 types of data augmentation are applied into the training data for every iteration[Ha 18]. The first one is to stretch Δx and Δy respectively by multiplying random value drawn from $U(0.85, 1.15)$. The second one is to drop out strokes by dropping each point within line segments with a probability of 0.1.

Residual Dropout[Vaswani 17] is applied into Transformer Encoder with dropout rate = 0.1 during the training. At inference time, the dropout rate = 0, and also $\epsilon_x, \epsilon_y, g = 0$ in the reparameterization trick to produce the optimal translated drawings $\tilde{s_B}^* = H_B(G_B^*(s_A))$ and $\tilde{s_A}^* = H_A(G_A^*(s_B))$.

3.3 Results

3.3.1 Qualitative Evaluation

3 Cycle Sketch GAN models are trained by using 3 dataset pairs in QuickDraw (See section 3.1). Fig. 3 shows some examples of the translated sketch drawings from test data by the trained models. A and B rows are the randomly chosen sample drawings from each class test datasets. The drawings in B' rows are respectively the translated sketch drawings from the above A drawings. The

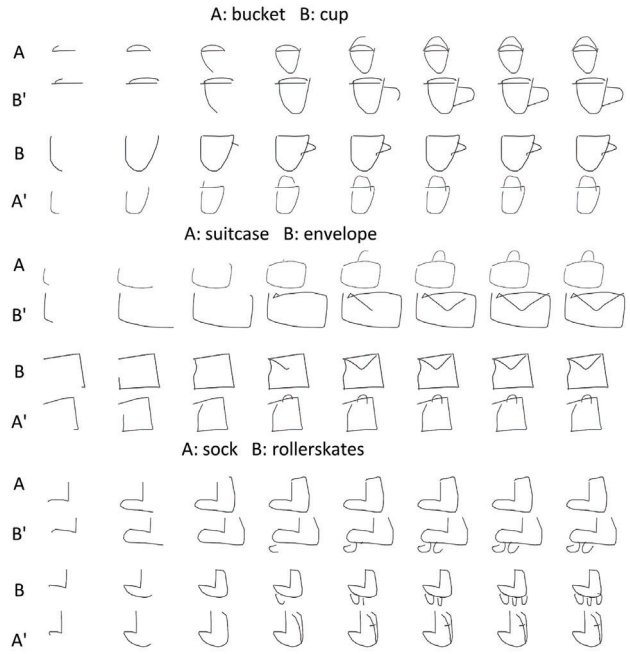

Figure 4: The stroke order of an original sketch by human (A, B) and the translated sketch by Cycle Sketch GAN (B', A').

same is true for A' and B. It shows that the common features are unchanged between the test sample drawing and the translated drawing, but the partial shapes characteristic to source domain are successfully transformed into ones characteristic to target domain, although some samples are failed to be translated.

Fig. 4 compares the order of the strokes between some test sample data and the translated data. Each row describes the snapshots of the strokes at the point of $i = 6, 12, 18, 24, 30, 36, 42, 48$ from the left to right. It clearly shows that the stroke order between original sketch and translated sketch are very similar from the start until some point. After that point, the stroke becomes different to express the characteristic feature for each domains.

3.3.2 Quantitative Evaluation

Class	Cycle Sketch GAN	Human
bucket	32.8($\pm$30.5)	57.6($\pm$25.9)
cup	43.0($\pm$28.5)	75.2($\pm$31.3)
suitcase	49.0($\pm$30.3)	54.4($\pm$27.0)
envelope	63.1($\pm$23.1)	85.8($\pm$18.7)
sock	38.4($\pm$26.1)	71.8($\pm$23.9)
rollerskates	30.8($\pm$14.8)	82.0($\pm$14.7)
Average	42.9	71.1

Table 1: User survey result

User study was also conducted on Amazon Mechanical Turk (AMT) to test the quality of translated sketch drawings. For each class, the survey results were collected from 20 participants. Specifically, participants see drawings one by one, and were asked "Do you think the drawing is (class name) ? ". Participants clicked on "yes" or "no" for the answer. For each dataset class, 55 drawings are surveyed, which consists of 25 of real sample sketches by humans, 25 of translated sketches by Cycle Sketch GAN, and 5 of trials (apparently irrelevant class sketches to check whether the participant's response was reliable or not). The order of showing these drawings are randomized.

Table. 1 shows the survey result, which lists the average percentage (and the standard deviation) of answering "yes" for each class surveys. Overall, 42 % of the translated sketches is recognizable compared to 71 % of the human sketch. There is apparent that some easy sketches such as envelope got higher recognition rate, while some complex sketches such as rollerskates got lower rate.

4. Conclusion and Future Work

This paper proposed Cycle Sketch GAN, the first model that learns to translate a sketch drawing from source domain to target domain in the absence of paired dataset. Qualitative and quantitative evaluation by some QuickDraw datasets demonstrates the effectiveness of this model. As a future work, the model needs to be improved to be able to translate complicated sketch drawings with higher quality. Using GMM as output distributions, or using Encoder-Decoder architecture as generators such as Seq2Seq might be effective. Furthermore, there might be a possibility that this unsupervised learning approach can be applied into other tasks that requires sequential data generation, such as unsupervised language translation[Lample 18], even though we need quite a lot of model changes and improvements.

References

[Goodfellow 14] Goodfellow, I., Pouget-Abadie, J., Mirza, M., Xu, B., Warde-Farley, D., Ozair, S., Courville, A., and Bengio, Y.: Generative Adversarial Nets, in *Advances in Neural Information Processing Systems 27*, pp. 2672–2680 (2014)

[Gulrajani 17] Gulrajani, I., Ahmed, F., Arjovsky, M., Dumoulin, V., and Courville, A. C.: Improved Training of Wasserstein GANs, in *Advances in Neural Information Processing Systems 30*, pp. 5767–5777 (2017)

[Ha 18] Ha, D. and Eck, D.: A Neural Representation of Sketch Drawings, in *International Conference on Learning Representations* (2018)

[Jang 17] Jang, E., Gu, S., and Poole, B.: Categorical Reparameterization with Gumbel-Softmax (2017)

[Lample 18] Lample, G., Ott, M., Conneau, A., Denoyer, L., and Ranzato, M.: Phrase-Based & Neural Unsupervised Machine Translation, in *Proceedings of the 2018 Conference on Empirical Methods in Natural Language Processing*, pp. 5039–5049 (2018)

[Song 18] Song, J., Pang, K., Song, Y., Xiang, T., and Hospedales, T. M.: Learning to Sketch With Shortcut Cycle Consistency, in *2018 IEEE Conference on Computer Vision and Pattern Recognition, CVPR 2018*, pp. 801–810 (2018)

[Vaswani 17] Vaswani, A., Shazeer, N., Parmar, N., Uszkoreit, J., Jones, L., Gomez, A. N., Kaiser, L. u., and Polosukhin, I.: Attention is All you Need, in *Advances in Neural Information Processing Systems 30*, pp. 5998–6008 (2017)

[Zhu 17] Zhu, J.-Y., Park, T., Isola, P., and Efros, A. A.: Unpaired Image-to-Image Translation using Cycle-Consistent Adversarial Networks, in *Computer Vision (ICCV), 2017 IEEE International Conference on* (2017)

The 33rd Annual Conference of the Japanese Society for Artificial Intelligence, 2019

Conditional DCGAN's Challenge: Generating Handwritten Character Digit, Alphabet and Katakana

Rina Komatsu[*1] Tad Gonsalves[*1]

[*1] Sophia University

Developing deep learning models has a great potential in assisting human tasks involving design and creativity. This study deals with generating handwritten characters using deep learning techniques. The task is not simply generating images randomly, but generating them conditionally, making a distinction according to the UI designates. To solve this task, we constructed the Conditional DCGAN model which includes the techniques from DCGAN and Conditional GAN. We tried training the models to be able to generate conditional images by adding label information as input to the Generator. Deep learning experiments were performed using 141319 training data consisting of 96 kinds of characters including digits, Roman alphabets and Katakana. The Generator trained by inputting random noise concatenated with the 96 kinds of characters, could generate each kind of character by just adding the appropriate label information.

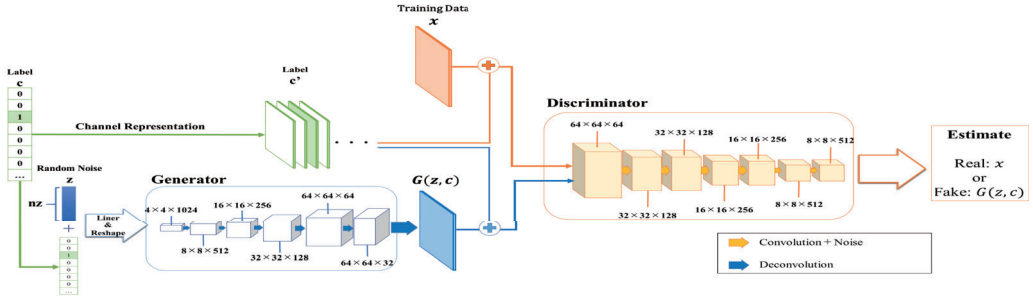

Figure 1. Proposed Conditional DCGAN which generates conditional handwritten characters

1. Introduction

Of late, more and more Deep Learning techniques which deal with generating images are been developed and as a result realistic images are being generated. In addition to being able to generate images that are realistic, the potential of deep learning is immense, such as supplementing blank areas and learning to imitate styles of famous painters to create artistic images.

To further test the potential of deep learning, we tried generating handwritten characters by developing a model called *Conditional DCGAN* which combines DCGAN with cGAN (Conditional GAN). A conditional label is added as additional input along with the image input to the model. The target kinds of character we dealt with in this study are not only digits, but also alphabets and katakana (Japanese script) and some special characters. The goal of this study is generating handwritten characters by making a distinction among more than 90 different kinds of them.

In our experiment, we obtained results by changing the dimensions of the random noise which is part of the input for the models. It can be inferred from our results that when the number of dimensions of noise falls below the number of labels, the model cannot generate images that are likely to be characters; and on the other hand, if the number of types exceeds 90, the model can generate the specified characters.

Contact: Rina Komatsu, Faculty of Science & Technology, Sophia University, Tokyo, Japan, r_komatsu@outlook.com

2. Related Work

We construct the model (the architecture shows in Figure 1) based on the techniques from DCGAN and cGAN. This section introduces generating method: GAN and DCGAN, also introduce cGAN to generate conditional images.

2.1 GAN & DCGAN

GAN: Generative Adversarial Net [Ian J. Goodfellow, 2014] is a generative network model that generates images by training a Generator and a Discriminator that are tied together in an adversarial relationship. The Generator plays the role of generating images from a given probability density distribution with random noise input, while the Discriminator plays the role of distinguishing the real input data from the fake data generated by the Generator. However, GAN has the weak points that the probability density distribution Generator learns is unable to indicate clearly and training Generator and Discriminator tend to unstable [Naoki Shimada et al, 2017].

DCGAN: Deep Convolutional Generative Adversarial Network [Alec Radford et al, 2015] is a generative model designed to solve this weak point by employing stable learning techniques such constructing fractional-strided convolution in Generator and strided convolution in Discriminator, in addition, instead of pooling layers, adapting batch normalization [Sergey

Ioffe et al, 2015] to each layer and so on. The Generator in DCGAN extends the information through upsampling from random noise input, while the Discriminator extracts feature maps through convolutions. As a result, DCGAN succeeds in generating more realistic images than GAN.

About how to calculate Loss GAN and DCGAN utilize Discriminator's output in loss function shown in formulae (1) and (2) to update each the parameters of each model. Formula (1) is loss function for Discriminator and (2) is the one for Generator. If the Discriminator learns good work in distinguishing, then log(D(x)) increases and 1-log(G(z)) decreases on the contrary. On the other hand, if the Generator reaches a matured level that deceives the Discriminator, then log(D(z)) increases.

$$L_D(G,D) = E\big[\log\big(D(x)\big)\big] + E[1 - \log(D(G(z)))] \quad (1)$$

$$L_G(G,D) = E[-\log(D(G(z)))] \quad (2)$$

where,
x is the training sample data, and
G(z) is the Generator's output from random noise z.

2.2 cGAN: Conditional GAN

cGAN: Conditional GAN [Mehdi Mirza et al, 2014] is the generative model which can output designated images by adding auxiliary information (represented as one-hot vector) such as a label corresponding with the kinds or modality to Generator after finishing training in the Generator and Discriminator.

Figure 2 shows a simplified structure of Conditional Adversarial Nets dealing with the auxiliary information. Random noise z and an auxiliary information y are input to the Generator combined forward to hidden layer. These jointed data help the Generator to suggest the probability density distribution to which the training sample data belongs. Also, training sample data *x* or generated ones G(*z*|*y*) and *y* are input to Discriminator combined in same.

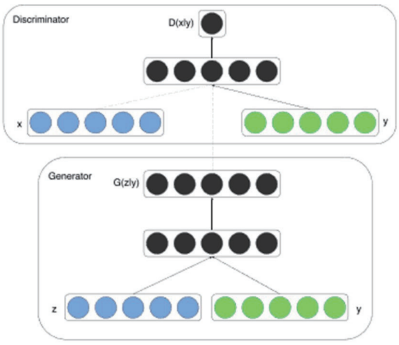

Figure 2. Simple Structure of Conditional Adversarial Net (adapted from Figure 1 in [Mehdi Mirza et al, 2014])

2.3 Conditional DCGAN (Constructed model in this study)

Figure 1 is the structure of proposed model in this study through trial and error finding stable training between Generator and Discriminator relatively quickly. In section 4 "Result" introduces the result using the Generator in this architecture.

Explaining details in this proposed model, Generator and Discriminator have the common factor that there is additional input named the auxiliary information represented one -hot (In this study, the auxiliary information is replaced to the label information related with the kind of characters). In Generator, the random noise z which consists of the number of dimensions nz and label information *c* are merged and input to Liner layers, then proceeded to up-sampling as output G(*z*,*c*) by deconvolution. In Discriminator, c is transposed to channel representation c' since Discriminator's input is represented with channel like training sample data x or G(*z*,*c*), then merged them and extract feature maps by convolution. When proceeded to convolution, input in each layer is added some noise for stable learning [Martin Arionsky et al, 2017].

Generator, Discriminator Loss is obtained by using the output from Discriminator like GAN and DCGAN. Formula (3) is loss function for Discriminator and (4) is the one for Generator.

$$L_D(G,D) = E\big[\log\big(D(x,c)\big)\big] + E[1 - \log(D(G(z,c),c))] \quad (3)$$

$$L_G(G,D) = E[-\log(D(G(z,c),c))] \quad (4)$$

3. Experiment

3.1 Handwritten character dataset

As the target for handwritten character dataset, we used ETL-1 Character Database [Electrotechnical Laboratory, 1973-1984] from Electrotechnical Laboratory (succeeding organization: National Institute of Advanced Industrial Science and Technology).

In the ETL-1 Character Database, the handwritten character images are grayscale and have a unified size of 64×63. The dataset contains 96 different characters: 10 Arabic numerals, 26 large alphabets, 12 special characters and 48 katakana letters. These handwritten characters were collected from 1445 writers, by making each writer write one character at a time on an OCR sheet. The total number of samples collected were 141,319.

In the training process of the Generator and the Discriminator, we treated this dataset as training sample data x.

3.2 Experiment Environment

The training of the Generator and Discriminator to distinguish 96 different kinds of characters is implemented in the Python programming language and Chainer deep learning library [Seiya Tokui et al, 2015]. We also used NVIDIA GeForce GTX 1080 Ti graphic boards to speed up the training as much as possible.

3.3 Experiment Setup

As an initial setting, the whole training sample images are resized to 64×64 and set the weight decay parameter λ= 0.00001.

The following steps count as 1 epoch. We repeated training the Generator and Discriminator for 100 epochs, every time employing a minibatch size 50.

Step 1:
This step consists in preparing the Generator's input, random noise and the label information. Random noise *z* is generated from uniform random distribution in the range [-1, 1], setting the number of dimensions as *nz*. Label information c is represented

with one-hot vector corresponding to the ID related to each type of character. The data shape of c becomes (batch size, label num, 1).

Step 2:

The z and c inputs are merged into the Generator to generate the output data G(z, c).

Step 3:

To the Discriminator, G(z,c) as fake data is input merged with c' which is represented in channel from c (The data shape of c' becomes (batch size, label num, h, w)). Next, the training sample data x is input merged with c'.

Step 4:

From the Discriminator's output, Generator and Discriminator Loss is calculated and the relevant parameters are updated in each model. As an optimization function, we employed the Adam function [Diederik P. Kingma et al, 2014]. The Adam function parameters in the Generator and Discriminator network models which assisted stable training in our study are shown in Table 1.

Table 1: Adam function parameters

Parameters	α	β_1
Generator	0.001	0.5
Discriminator	0.0002	0.5

4. Result

Using the Generator in our Conditional DCGAN, this section introduces the generated result changing *nz* =32,64,96(corresponding to the number of character kinds), 256,1024 and 4096(same to whole image size we set).

4.1 Generating conditional handwritten characters

To make sure the Generator output handwritten characters designating c, we prepared 5 kinds of characters. Figure 3 shows each kind of handwritten character image picked up from training sample data.

Figure 3. The targets for generating (picked up from ETL-1 Character Database)

Figure 4 is the result generated by using Generators of varying nz values. In the images depicted in Figure 4, vertical axis means the output changing label information and horizontal axis means the output using different random noise z.

From the results in *nz*=32,64 and 96, we can see that there are outputs which are likely handwritten characters, but they do not reflect the label information. Most output were the handwritten character not belong to the kind in training sample data. Also, same images are generated although changing z.

On the other hand, in Generator with nz set to 256, 1024, 4096, it is possible to generate by reflecting the designation of target character type. Thus, there is no confusion between similar characters such as "8" and "S", "シ" and "ツ" which are similar in shape. Moreover, in the result of changing the random noise, it was possible to generate an image in which its peculiarity appeared rather than a similar image, such as when the character is large or small, or the thickness of the line is different. Moreover, it was able to generate distinct characters despite the size being smaller (*nz* = 256; image size: 64 × 64).

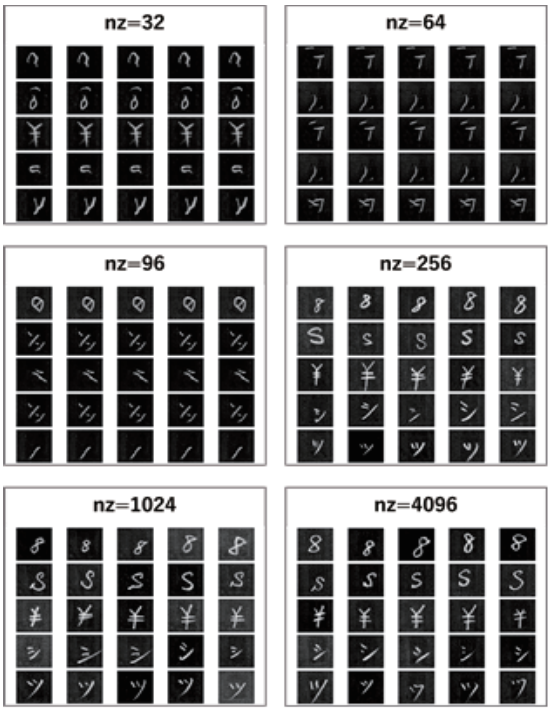

Figure 4. Conditional output from Generator changing nz

4.2 Loss changes in Generator and Discriminator

The Loss specific to the Generator and Discriminator for each epoch is shown in Figure 5.

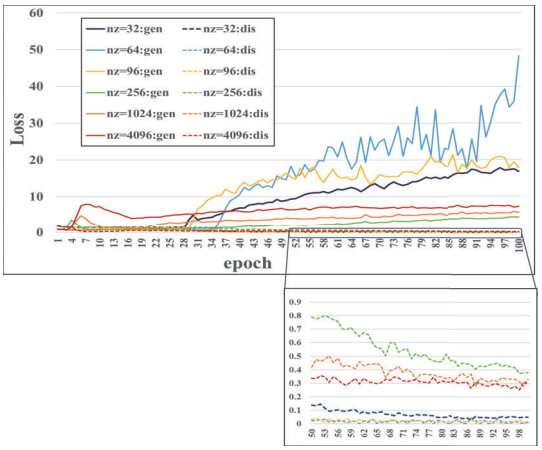

Figure 5. Loss changes from epoch 1-100.

As can be seen in Figure 5, in the model *nz* = 32,64,96, as the epochs progressed, the Generator Loss steadily increased, while the Discriminator loss gradually decreased near to 0. The difference in loss between Generator and Discriminator at epoch wider than the ones in conditional image generation. This result implies that gradient vanishing occurred in the Generator since Discriminator learned to distinguish between the real data and the fake data much before the Generator optimized to deceive the matured Discriminator [Ian Goodfellow, 2016].

Figure 6 shows the result of generating the whole of 96 kinds of characters as the target we set, from a larger *nz*=4096 to a smaller *nz*=256. Each Generator could output almost all kinds of handwritten images, making distinction just by changing the label information.

It can be inferred from our results that when the number of dimensions of noise falls below the number of labels, the model cannot generate images that are likely to be characters; on the other hand, if the number of types exceeds 90, the model can generate the specified characters.

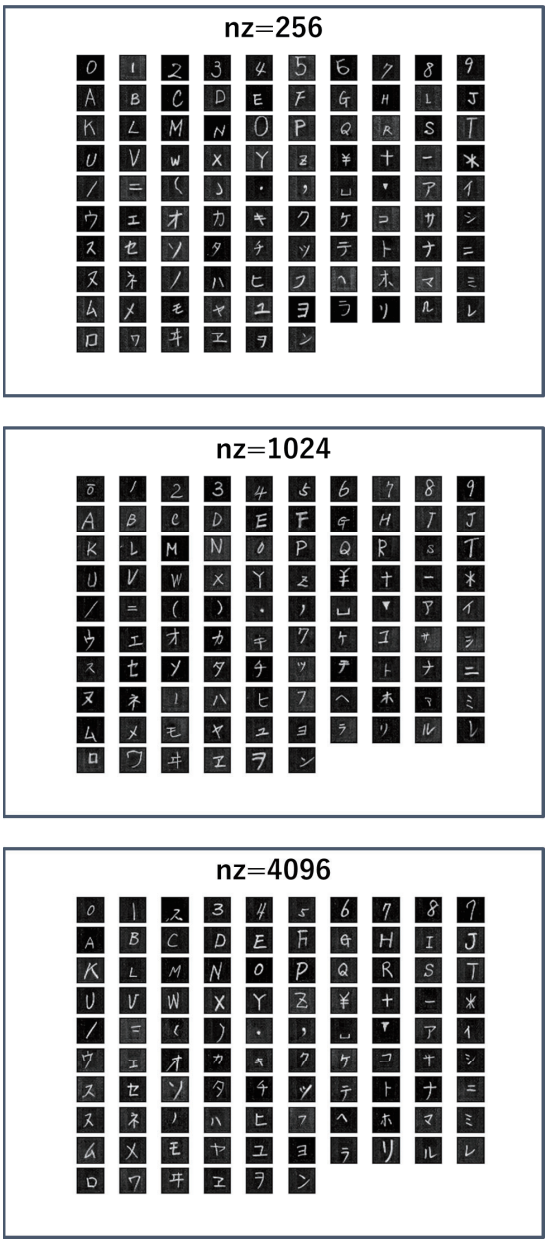

Figure 6. Handwritten characters produced by Generator

5. Conclusion and Future work

In this study, to be able to generate handwritten characters distinguishing among 96 different kinds of characters by adding UI designation, we constructed Conditional DCGAN. This model adapted DCGAN techniques using deconvolution for up-sampling at the Generator and convolution for extracting feature maps, and cGAN technique that adds label information to Generator and Discriminator. Through training our Generator and Discriminator with the dimension of random noise over the kinds, Generator could output the entire set of characters as a result.

In our future work, since the data shape of label information at the Discriminator in Figure 1 is (batch size, label num, h, w), large load will be applied to the model if dealing with over thousand kinds of characters like kanji. To solve this problem, constructing more compact Discriminator so that Discriminator's label information could keep the shape same as the one generated by the Generator and compressed through linear function. We want to try generating conditional images making distinction among over thousand kinds of images with compact Conditional DCGAN as the next challenge.

References

[Ian J. Goodfellow et al, 2014] Ian J. Goodfellow, Jean Pouget-Abadie, Mehdi Mirza, Bing Xu, David Warde-Farley, Sherjil Ozair, Aaron Courville & Yoshua Bengio: Generative Adversarial Nets, Advances in neural information processing systems, pp. 2672-2680, 2014.

[Naoki Shimada et al, 2017] Naoki Shimada & Takeshi Ooura: INTRODUCTION TO DEEP LEARNING WITH Chainer, Gijutsu-Hyohron Co (Japan), 2017.

[Alec Radford et al, 2015] Alec Radford, Luke Metz & Soumith Chintala: Unsupervised Representation Learning with Deep Convolutional Generative Adversarial Networks, arXiv preprint arXiv:1511.06434, 2015.

[Sergey Ioffe et al, 2015] Sergey Ioffe & Christian Szegedy: Batch Normalization: Accelerating Deep Network Training by Reducing Internal Covariate Shift, arXiv preprint arXiv:1502.03167, 2015.

[Mehdi Mirza et al, 2014] Mehdi Mirza & Simon Osindero: Conditional Generative Adversarial Nets, arXiv preprint arXiv:1411.1784, 2014.

[Martin Arjovsky et al, 2017] Martin Arjovsky & Léon Bottou: Towards Principled Methods for Training Generative Adversarial Networks, arXiv preprint arXiv:1701.04862, 2017.

[Electrotechnical Laboratory, 1973-1984] Electrotechnical Laboratory: Japanese Technical Committee for Optical Character Recognition, ETL Character Database, 1973-1984.

[Seiya Tokui et al, 2015] Seiya Tokui, Kenta Oono, Shohei Hido & Justin Clayton: Chainer: a Next-Generation Open Source Framework for Deep Learning, Proceedings of workshop on machine learning systems (LearningSys) in the twenty-ninth annual conference on neural information processing systems (NIPS). Vol. 5, pp. 1-6,2015.

[Diederik P. Kingma, 2014] Diederik P. Kingma & Jimmy Lei Ba: Adam: A Method for Stochastic Optimization, arXiv preprint arXiv:1412.6980, 2014.

[Ian Goodfellow, 2016] Ian Goodfellow: NIPS 2016 Tutorial: Generative Adversarial Networks, arXiv preprint arXiv:1701.00160, 2016.

The 33rd Annual Conference of the Japanese Society for Artificial Intelligence, 2019

Sparse Damage Per-pixel Prognosis Indices via Semantic Segmentation

Takato Yasuno[*1]

[*1] Research Institute for Infrastructure Paradigm Shift (RIIPS)

Efficient inspection and accurate prognosis are required for civil infrastructures with more than 30 years since completion. If we can detect damaged photos automatically per-pixels from the record of the inspection record and countermeasure classification of drone inspection vision, then it is possible that countermeasure information can be provided more flexibly, whether we need to repair and how large the expose of damage interest. A piece of damage photo is often sparse as long as it is not zoomed around damage, exactly the range where the detection target is photographed, is at most only one percent. In this paper, we propose three damage detection methods of transfer learning which enables semantic segmentation in an image with low pixels using damaged photos of drone inspection. Furthermore, we propose prognosis indices to make a decision repair-priority such as the counts index of pop-outs region and the per-pixel area counts index of each pop-out based on morphology image processing. In fact, we show the results applied this method using the 40 drone inspection images whose size is 6,000 x 4,000 on an infrastructure, where each image is partitioned into 400 crops, so the total number of input images is 16,000 for training deep neural network. Finally, future tasks of damage detection modeling are mentioned (211words).

1. Introduction

Deterioration of civil engineering structures is progressing in recent years, including a large number of concrete structures. Improving efficiency of scheduled inspections is a pressing issue, since the cost of inspections comprises a large proportion of maintenance costs for local governments, which are also experiencing manpower shortage for technical personnel. There are often opportunities to apply deep learning as a method for improving efficiency of inspections on social infrastructure and studies have been conducted on this issue. Dam general inspection is required for dam once every 30 years and as a result, images of damage have been accumulating (Ministry of Land, Infrastructure, 2013). If it were possible to utilize images of damage that are attached to inspection reports, data from scheduled inspections from past years can be input for the purpose of deterioration learning. If it could be possible to automatically calculate numerical scores for the extent of damage based on images of damage, this would be useful in deciding whether any repairs work should be performed and for setting the order of priority among candidates for repairs. There are past studies on detecting cracks in concrete on bridges, structures, plants, etc.

Especially, for dam structural health monitoring, it is important to prognosis pop-outs owing to be greater impact on the health of dam embankment. In area of low quality aggregates, as a result of the water absorption of the concrete, the soft stone having a high water absorption rate becomes saturated. When the freezing temperature is reached, pressure due to volume expansion occurs. However, the detection model for pop-out is only at its incipient stages, so it would be difficult to claim that this is an established means for concrete damage deterioration learning and prediction. This paper proposes a practical method applies semantic segmentation (segmentation) of concrete damage using images of damage from drone-base inspections. Results are shown from actually applying this method on sparse images of damage, focusing on images of pop-outs among images of damage to dam embankment. Finally, references will be made to issues of damage detection modeling as well.

Contact: Takato Yasuno, RIIPS on 5-20-8, Asakusabashi, Taito-ku, Tokyo, 111-8648, tk-yasuno@yachiyo-eng.co.jp

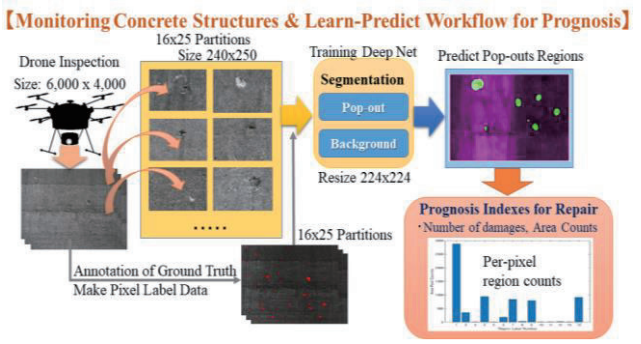

Figure 1: Monitoring concrete structures from drone-base inspection to train segmentation networks and damage prediction for prognosis indices.

2. Related Studies and Damage Images

2.1 Damage detection studies for civil infrastructures

Since 2002, there has been an accumulation of studies (Wu, 2002) (Chun, 2015) on resolving damage detection using neural networks (ANN) for the purpose of continuous surveillance of bridges. Many instances of damage detection modeling for machine learning have been conducted over the past 15 years, including the ANN, as well as the PCA, SVM, GA and other such solution methods (Gordan, 2017). Since the potential of convolutional neural networks (CNN) to exhibit high degrees of accuracy in classifying one million images into 1,000 classes was reported in 2012 (AlexNet, 2012), there has been active reporting of studies on solution methods of the CNN, which provides solutions with greater accuracy than conventional methods for label categorization of overall images, object detection and semantic segmentation at the pixel level. There have been a number of studies conducted on damage classification of at the whole-image level for cracks and corrosion of road pavement, structures and bridges, for detection of damage to civil engineering structures (Gopalakrishnan, 2018) (Ricard, 2018), as

well as damage segmentation at the pixel level (Hoskere, 2017). A report was made on a study that applied deep CNN to conduct four classes of damage segmentation, namely no damage, only separation, exposure of rebar (with and without rust), using 734 images of damage (Guillamon, 2018). The breakdown of the damage classes, however, indicated a distribution biased to the third class, for which there were 510 images, and as such, distortion in the training images cannot be denied. Dimensions of the images of damage were widely varied, being 640 x 480, 1,024 x 768, and 1,600 x 1,200. The potential for learning with the index that represents the degree of matching between prediction and reality, mIoU (class mean IoU) to the level of 0.6 to 0.8 was indicated by using some types of CNN models for fully convolutional networks (FCN) in entering images of such diverse dimensions. The use of the damage detection modeling that utilizes solution method of CNN, however, has just been started and as such, it would be difficult to claim that this is an established general-purpose method for damage detection in management of infrastructure. This paper proposes a practical method for damage segmentation with considerations for sparse characteristics of damage images from drone-base inspections. Furthermore, using the output of prediction RGB-images by the trained semantic segmentation, we propose two morphological indices such as the number of identified damages and the per-pixel counts of each damage region for prognosis to make a decision repair-priority.

Table 1: Comparison of the per-pixel counts between the target pop-outs region and the background region.

Example consisting of 40 damage drone inspection images	Total number of pixels per damage image	The number of pixels per image	Percentage per image
Background	954,339,801	23,858,495	99.4%
Damage to region of interest (ROI)	5,660,199	141,505	**0.6%**
Total per image	960,000,000	24,000,000	100.0%

2.2 Characteristics of Damage Images

This paper provides a practical observation on characteristics of images of damage, using 40 images of damage in which pop-out has been captured through drone-base inspection of dam embankment, whose size is 6,000 x 4,000. While generality cannot be guaranteed with these characteristics, they are considered to lead the way for utilizing images of damage. Characteristics of general conditions and damage for pop-out is as follows (CERI, 2016). Pop-out is a crater-like indentation generated by destruction due to the expansion of aggregate particles on the concrete surface. These are often observed in aggregates with high water absorption and in poor quality. Pop out is the meaning of “jumps out suddenly”. In the case of low-quality aggregate, as a result of the water absorption of the concrete, the soft stone having a high water absorption rate becomes saturated. At this time, when the freezing temperature is reached, pressure due to volume expansion occurs, the surface portion peels off, and then a crater-like hole is formed.

Table 1 shows the summary value for the damage area (region of interest: ROI) subject to detection, as well as other regions in the background, counted at pixel level. No advance manipulation was conducted on images to unify photographing distance and picture quality. The number of pixels per image was 24 million pixels. The proportion of these that include targeted damage was only 0.6%. The first characteristic of damage image is the sparsity of the area comprised of ROI.

3. Per-pixel Learning and Prognosis Indices

3.1 Damage segmentation for prediction

The FCN-Alex (Long, 2015), as well as the SegNet-VGG16 (Badrinarayanan, 2016) are compared where appropriate, as a method for learning transfers of semantic segmentation. The solution method used in this paper by itself does not present any innovation but the extremely sparse proportion of detection target ROI on any given image is a characteristic and the intention was to derive a practical method that can be applied to images of damage with sparse pixel labels. The FCN-Alex is a transfer learning of AlexNet and the CNN is implemented to the deepest layer, making it a deep neural net (DNN) of 23 layers in depth. Learning is possible with relatively short calculation time and prediction output for exhaustive detection of targeted damage can be achieved. SegNet-VGG16 is a method of transfer learning used to identify objects for automatic driving and a DNN with depth of 91 layers.

This paper applies the four deep neural networks described above to images of damage to compare calculation execution time, accuracy and prediction output image. There is a problem of no improvements being evident with loss functions when the SGDM is used in the optimization method for hyper parameters, as gradients of the detection target are eliminated due to the sparse characteristic of the damage image. In order to overcome this issue, the gradient of the detection target is captured with good sensitivity and the previously updated quantities are deleted where appropriate, and the RMSProp, which has a characteristic formula for error function that eliminates the amount of change in gradients of detection targets by taking square root of the amount of change in gradient, is adopted (Hinton, 2012) (Mukkamala, 2017). The weighting factor for the updating amount was set to 0.99. The learning coefficient for the overall model was set to 1E-5 and the minibatch was set to 32.

3.2 Morphological indices for prognosis

The word morphology commonly denotes a branch of biology that deals with the form and structure of animals and plants. We use the same word here in the context of mathematical morphology as a toll for extracting image components that are useful in the representation of region shape. We are interested also in morphological techniques for pre- or post-processing, such as morphological filtering, thinning, and pruning. In image-processing applications, dilation and erosion are used most often in various combinations (Serra 1992; Gonzalez 2008). This paper proposes some prognosis indices to make a decision repair-priority such as the counts index of pop-outs region and the per-pixel area counts index of each pop-out based on morphological image processing, such as dilation and erosion operation.

On the prediction of pop-out damage segmentation, there are some extremely small size of pop-outs, so that we may overlook

them. Also, the shape of pop-outs are not always like circle, but these are complex shape or partially connected with various size of pop-outs. This paper proposes two practical morphological operation, dilation and erosion, in terms of the union (or intersection) of an image with a translated shape called structuring element. At first, we translate the prediction RGB-image of pop-out segmentation into a binary mask image with pop-out foreground (1-valued pixel, white color) and with background (0-valued pixel, black color). Dilation is an operation that "grows" or "thickens" objects in the extremely small images of pop-outs. This growing is controlled by a shape referred to as a structuring element, such as linear, disk, octagon etc. This paper proposes the disk-shaped structuring element with radius r=3. Further, erosion "shrinks" or "thins" objects in a binary image like complex shape and partially connected with various size of pop-outs. This paper proposes these morphological operations applied to the masked prediction of pop-outs images. By these operation, it is possible to avoid overlooking the small pop-outs, and we can extract the complex shape or partially connected pop-outs, in order to count the number of pop-out and the each region pixel size more accurately and efficiently.

4. Applied Results

4.1 Training results

The input data was 40 images whose size is 6,000 x 4,000 from drone-base inspections of dam embankment. In order to bring them closer with the input size of deep pre-trained network, we partitioned each original image into 25 x 16 equal 400 crops whose size was 250 x 240. The usage rate of the training and test data was set to Train: Test = 99:1. The transition of loss function in the learning process applied to the pop-out segmentation is shown in Figure 2. The calculation conditions are 490 cycles per epoch for a total of 24,500 repeated calculations in 50 epochs. The loss value of the FCN-AlexNet is transitioning at a lower level than SegNet-VGG16. This FCN models, however, have large dispersion of loss values and their disadvantage is that they make for unstable learning processes. The loss function of the SegNet-VGG16 does not offer minimum values, but up and down fluctuations remain small early on, which can be interpreted to offer superior stability for the learning process.

Table 2: Comparison of indices for pop-out segmentation models.

DNN model	Time calculation	Mean mIoU	Weighted wIoU
FCN-AlexNet	466min.	0.5811	0.9861
SegNet-VGG16	832min.	**0.5967**	0.9856

Table 2 shows the calculation time, accuracy, mean-IoU and weighted-IoU index of respective segmentation model. The FCN-AlexNet offers a relatively short calculation time of 466 minutes. This net achieved the index such as mIoU = 0.5811, and wIoU = 0.9861. Meanwhile, the SegNet-VGG16 offers about two times calculation time compared with FCN-AlexNet, and indicates the score of mIoU of 0.5967 and wIoU of 0.9856. While each weighted wIoUs have almost no difference, but regarding the score of the mean mIoU the SegNet-VGG16 is superior with the FCN-AlexNet to select better pop-out predictor.

4.2 Prediction results

Figure 2 shows an output RGB-image of predictions for a test image whose size is 600 x 400, using the trained SegNet-base predictor of pop-out segmentation. Here, the region of prediction are shown in green color. In contrast, the region of background are shown in magenta color. Figure 3 shows the translated binary mask with pop-out foreground (1-valued) and with background (0-valued). We operated the morphological operations applied to the masked prediction of pop-outs images. Further, we compute the centroid of each pop-out region and set the pop-out number in order to represent the counts index accurately, here the total count of pop-outs is 14. Figure 4 shows the per-pixel counts of each region based on the morphological image pre-processing. Figure 5 shows the bar chart that we can visualize the volume indices of pop-outs and it is possible to compare the largest size, middle size, and extremely small size of pop-outs in order to make a decision of repair-priority for infrastructure manager.

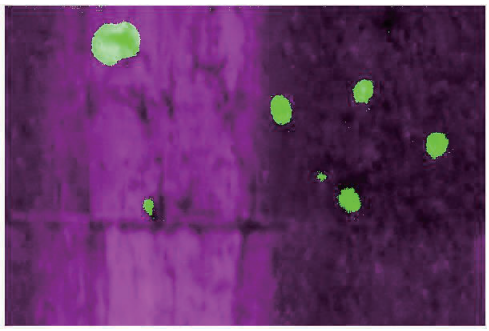

Figure 2: Trained SegNet-base prediction of pop-outs (RGB image) Here, green indicates prediction, magenta denotes background.

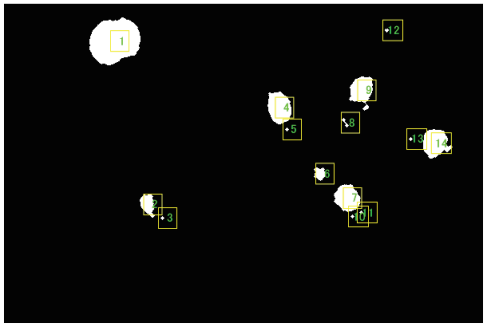

Figure 3: Counts index of identified pop-out centroid based on morphological operations with dilation and erosion.

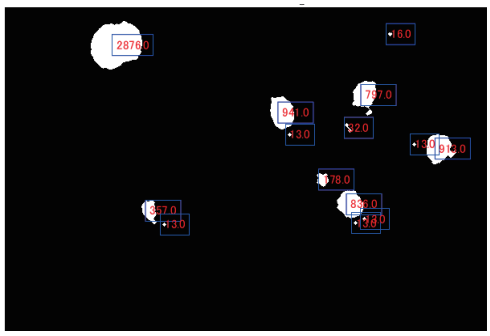

Figure 4: Per-pixel counts of each pop-out prediction region based on morphological image processing.

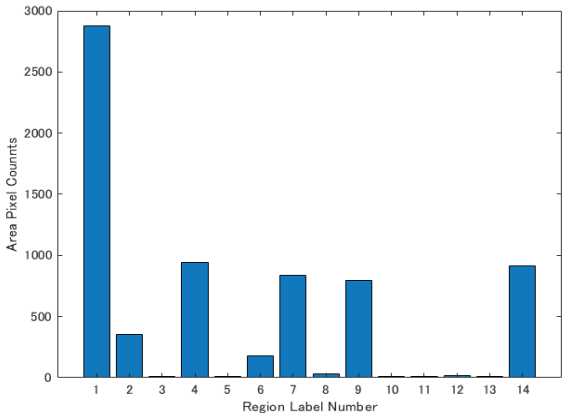

Figure 5: Area pixel count index of each pop-out for prognosis measure indices to make a decision regarding repair-priority.

5. Conclusion

5.1 Concluding remarks

This paper proposed a method for detecting pop-out by semantic segmentation, using images of damage obtained from drone-base inspections. In fact, we show the results applied this method using the 40 drone inspection images at a dam embankment, where each image is partitioned into 400 crops, so the total number of input images is 16,000 for training deep neural network. Based on transfer learning, per-pixel higher accurate prediction is possible, even to sparse damage images whose pop-out ratio per-pixel is only one percent compared with the background. The SegNet-VGG16 exhibited the better accuracy and achieved class mean mIoU index of 59.67% and weighted index wIoU of 98.56%. Furthermore, we demonstrated to compute some morphological indices, such as the counts index of identified pop-outs centroid and the per-pixel area counts index of each pop-out region for prognosis to make a decision repair-priority more accurately and efficiently.

5.2 Future works

The scope of this paper was the segmentation of pop-out for prognosis, using images from drone-base inspection of dam embankment. Monitoring various damages for standard dam inspection prescribes concrete crack, scaling, pop-outs, water leak, efflorescence etc (Ministry of Land, Infrastructure, 2013). In contrast, creation of dataset for training and prediction of various segmentation models for being predictive diagnosis before occurred pop-outs, such as “crack” and “scaling” are the issue for health monitoring. Infrastructure manager administrates a lot of aging structures other than dam well. Learning of damage segmentation models using a diverse range of images for a wide variety of other infrastructures will be the issue for the future. Predictor of damage segmentation intelligence created from scratch, i.e. U-Net by data mining accumulated images is also a challenging issue. Furthermore, 3-dimension segmentation is more useful for volume counting to measure the depth of damage.

[Acknowledgments] We would like to express our gratitude to obtain practical information about Deep Learning and Image Processing Toolbox for training and prediction from Mr. Shinichi Kuramoto and Mr. Takuji Fukumoto.

References

[Ministry of Land, Infrastructure 2013] Water Management Land Conservation Bureau River Environment Division : Dam General Inspection Procedure Commentary, 2013.

[CERI 2016] Public Works Research Institute CERI : Survey and Countermeasure Guidance on the Structure Suspected of Frost Damage (draft), 2016.

[Wu 2002] Wu, Z., Xu, B. Yokoyama, K. : Decentralized Parametric Damage Detection Based on Neural Networks, Comput. Civ. Infrastruct. Eng., 17, pp.175-184, 2002.

[Chun 2015] Chun, P., Yamashita, et al. : Bridge Damage Severity Quantification using Multipoint Acceleration Measurement and Artificial Neural Networks, 2015.

[Gordan 2017] Gordan, M., Razak, H.A. et al. : Recent Development in Damage Identification of Structures using Data Mining, Latin American Journal of Solids and Structures, pp.2373-2401.

[AlexNet 2012] Krizhevsky, A. et al. : ImageNet Classification with Deep Convolutional Neural Networks, NIPS, 2012.

[Gopalakrishnan 2018] Gopalakrishnan, K., Gholami, H. et al. : Crack Damage Detection in Unmanned Aerial Vehicle Images of Civil Infrastructure using Pre-trained Deep Learning Model, International Journal for Traffic and Transport Engineering, 8(1), pp.1-14, 2018.

[Ricard 2018] Ricard, W., Silva, L. et al. : Conclete Cracks Detection based on Deep Learning Image Classification, MDPI Proceedings, 2, 489, pp.1-6, 2018.

[Hoskere 2017] Hoskere, V., Narazaki, Y. et al : Vision-based Structural Inspection using Multiscale Deep Convolutional Neural Networks, 3rd Huixan International Forum on Earthquke Engineering for Young Researchers, 2017.

[Guillanmon 2018] Guillamon, J.R. : Bridge Structural Damage Segmentation using Fully Convolutional Networks, Universitat Politecnica de Catalunya, 2018.

[Long 2015] J. Long, E. Shelhamer, T. Darrell : Fully Convolutional Networks for Semantic Segmentation, CVPR, pp3431-3440, 2015.

[Badrinarayanan 2016] V. Badrinarayanan, A. Kendall, et al., SegNet: Deep Convolutional Encoder-Decoder Architecture for Image Segmentation, ArXiv:1511.00561v3, 2016.

[Hinton 2012] G. Hinton, N. Srivastava, K. Swersky : Lecture 6d – A Separate, Additive Learning Rate for Each Connection, Slides Lecture Neural Networks for Machine Learning, 2012.

[Mukkamala 2017] M.C. Mukkalmala et al.: Variants of RMSProp Adagrad with Logarithmic Regret Bounds, 2017.

[Serra 1992] Serra,J., Vincent,L.: An Overview of Morphological Filtering, Circuits, Systems and Signal Processing, 11(1), pp47-108, 1992.

[Gonzalez 2008] Gonzalez, R.C., Woods, R.E. : Digital Image Processing, 3rd ed., Prentice Hall, 2008.

[Yasuno 2018] T. Yasuno: Infra Machine Learning for Predictive Maintenance via Classification Models, 32th Journal of Society for Artificial Intelligence, 3Z1-04, 2018.

[Yasuno 2019] T. Yasuno, M. Amakata, J. Fujii, Y. Shimamoto : Color-base Damage Feature Enhanced Support Vector Classifier for Monitoring Quake Image, IAPR: CCIW, 2019.

(2019.Feb.15)

International Session | International Session | [ES] E-2 Machine learning

[3B4-E-2] Machine learning: social links

Chair: Lieu-Hen Chen (National Chi Nan University), Reviewer: Yasufumi Takama (Tokyo Metropolitan University)

Thu. Jun 6, 2019 3:50 PM - 5:30 PM Room B (2F Main hall B)

[3B4-E-2-01] Social Influence Prediction by a Community-based Convolutional Neural Network

Shao-Hsuan Tai[1], Hao-Shang Ma[1], ○Jen-Wei Huang[1] （1. National Cheng Kung University）

3:50 PM - 4:10 PM

[3B4-E-2-02] A Community Sensing Approach for User Identity Linkage

○Zexuan Wang[1], Teruaki Hayashi[1], Yukio Ohsawa[1] （1. Department of Systems Innovation, School of Engineering, The University of Tokyo）

4:10 PM - 4:30 PM

[3B4-E-2-03] Learning Sequential Behavior for Next-Item Prediction

○Na Lu[1], Yukio Ohsawa[1], Teruaki Hayashi[1] （1. The University of Tokyo）

4:30 PM - 4:50 PM

[3B4-E-2-04] Application of Unsupervised NMT Technique to Japanese--Chinese Machine Translation

○Yuting Zhao[1], Longtu Zhang[1], Mamoru Komachi[1] （1. Tokyo Metropolitan University）

4:50 PM - 5:10 PM

[3B4-E-2-05] Synthetic and Distribution Method of Japanese Synthesized Population for Real-Scale Social Simulations

○Tadahiko Murata[1], Takuya Harada[1] （1. Kansai University）

5:10 PM - 5:30 PM

The 33rd Annual Conference of the Japanese Society for Artificial Intelligence, 2019

Social Influence Prediction by a Community-based Convolutional Neural Network

Shao Hsuan Tai[*1] Hao-Shang Ma[*2] Jen-Wei Huang[*3]

[*1*2*3]Institute of Computer and Communication Engineer,
Department of Electrical Engineering,
National Cheng Kung University, Tainan, Taiwan

Learning social influence between users on social networks has been extensively studied in a decade. Many models were proposed to model the microscopic diffusion process or to directly predict the final diffusion results. However, most of them need expensive Monte Carlo simulations to estimate diffusion results and some of them just predict the size of the spread via regression techniques, where people who will adopt the information becomes unknown. In this work, we regard the prediction of final influence diffusion results in a social network as a classification problem to avoid expensive simulations with knowing the final adopters. We first address the problem on a deep neural network and utilize the diffusion traces to train the network. Furthermore, we propose a community-based convolutional neural network to capture the information of local structure with the aforementioned network. The proposed model is referred to as the Social Influence Learning on Community-based Convolutional Neural Network, SIL-CCNN. In the experiment, SIL-CCNN shows the promising results in both synthetic and real-world datasets.

1. Introduction

Nowadays people tend to share their life, emotions, and opinions to others on social network websites. Two representative diffusion models, Independent Cascade, IC, model and Linear Threshold, LT, model, were reformulated by Kempe [3]. However, there are several limitations of predicting the information diffusion using diffusion models. The influence probabilities between users and the active threshold of a user should be measured or learned from many personal features such as users' preferences and different relationships. In real social networks, the features are not easy to extract since the data sometimes is not complete. In addition, to get the results of IC/LT model, we need to conduct a huge number of simulations.

Actually, the prediction of the information diffusion process and the final diffusion results models can be regarded as a classification problem. Given the information sources and the network structure, the individuals are classified into active or inactive classes in the final diffusion result. The active class is corresponding to the individuals being influenced successfully in the information diffusion process. Some related works aim to predict the size of information spreads as a classification or regression problem [1, 7]. Different with diffusion models, these methods usually do not learn the individuals who are actually influenced by the information. We would like to know exactly who are influenced and who are not.

To overcome above limitations and solve the classification problem, we propose an influence prediction model based on community-based convolutional neural network. First, we consider the influence propagation process in the past to learn the influence between individuals. Then, most of the diffusion models consider the network structure, i.e., the relations between individuals, as their features. However, the information of the whole network structure may not be useful for the classification problem whereas the local network information of a single individual should be helpful. We try to embed the local structure of an individual into our model to learn the local relations. The community structure in social networks represents a cluster of individuals sharing connections that are stronger than those with individuals outside the community. The information diffusion in a community should be faster than outside the community. Therefor, we use the convolutional neural networks to mine the local relations within the community structure. The idea is that convolutional neural networks are good to extract the effects of a small group of individuals around an individual by extracting valuable relations from the structure. Finally, the influence traces and the community structure information are combined into our model as training features of the deep neural network. The proposed scheme is referred to as the Social Influence Learning on Community-based Convolutional Neural Network, SIL-CCNN.

The remainder of the paper is organized as follows. Works related to this work are outlined in Section 2. Section 3 details the proposed methodology. Experiment results and conclusions are presented in Section 4 and Section 5.

Contact: Jen-Wei Huang, Institute of Computer and Communication Engineer,
Department of Electrical Engineering,
National Cheng Kung University, Tainan, Taiwan.
Email: jwhuang@mail.ncku.edu.tw
Tel:(+886)-6-2757575#62347

2. Previous Work

In this section, we will briefly introduce other related works on diffusion models and the prediction of information spread size.

2.1 Diffusion Models

Diffusion models can be used to identify social influence by tracking information propagating through a social network. Nowadays, some diffusion models adopt the learning strategy to predict the activation since the technique of learning methodology has matured in these few years. Saito [6] first proposed a learning method for IC model. Wang [8] proposed a feature-enhanced approach, which considers not only temporal data in cascades but also additional features. Chou [2] proposed Multiple Factor-Aware Diffusion model, MFAD, that can consider many kinds of factors together. MFAD model adopts positive and unlabeled learning to train the classifiers for each individual.

2.2 Prediction of Information Spread Size

Different from diffusion models, the cascade prediction only focuses on predicting whether the information will become popular and widely spread. The problem is usually formulated as a classification or a regression problem to understand the size of potential influence of information.

Among the classification solutions of predicting information cascade, Cheng [1] proposed to use temporal and structural features for predicting the relative growth of a cascade size. As for the regression solutions, Tsur [7] proposed a content-based prediction model to include locations, orthography, number of words, lexicality, ease of cognitive process and emotional effect on various cognitive dimensions.

Our work aims to learn the hidden influence propagation from the data instances and the network structure directly without the huge number of diffusion simulations.

3. Methodology

In this section, we first propose an ordinary deep neural network model, SIL-DNN, for identifying traces of social influence. Second, we adopt a convolutional neural network to extract the local structure information of a network from the communities. Then, we propose Social Influence Learning on Community-based Convolutional Neural Network, abbreviated as SIL-CCNN, which combines the SIL-DNN and a community-based convolutional neural network to predict the final influential results.

Given a social network $\mathbb{G} = (\mathbb{V}, \mathbb{E})$, the node set $\mathbb{V}$ corresponds to the individuals, and $\mathbb{E}$ is the edge set indicating the relationships between individuals. Each influence trace (u, v, x) indicates that the nodes v adopt the information x and is influenced by source nodes u, where u and v are sets of nodes in $\mathbb{V}$. The architecture of SIL-DNN is presented in Fig. 1. In SIL-DNN, the number of neurons in the input layer is the same as the number of individuals in the social network $|V|$. The same setting is used in the output layer. For every trace, we put the vector of information sources as the input data of SIL-DNN and the output are the vector of influenced nodes. The input vector and output vector could be set as follows,

$$\begin{cases} y_i = 1, \text{if } i \in u \text{ for } (u, v, x) \\ y_i = 0, \qquad \text{otherwise,} \end{cases} \tag{1}$$

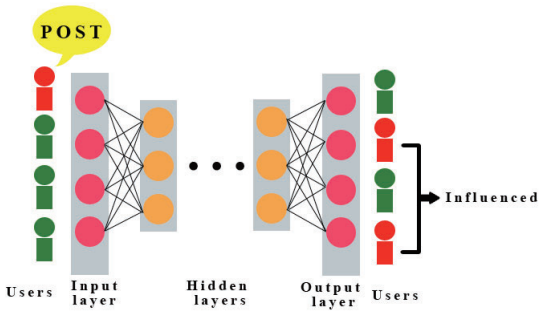

Figure 1: Social Influence Learning on Deep Neural Network Architecture

where y_i represents an individual i at the input layer. $i \in u$ for (u, v, x) indicates all traces that transmit the information x from user i. For example, an individual i provides an information x during the observation. The neuron of input layer $y_i^0 = 1$ for the information x. On the other hand, in the output layer, the $y_j = 1$ represents that node j is influenced by i and is classified as the active class. Otherwise, node j is classified into the inactive class.

3.1 Social Influence Learning on Community-based Convolutional Neural Network

In order to join the community structure to help us to predict the information diffusion results, we propose Social Influence Learning on Community-based Convolutional Neural Network, SIL-CCNN. The architecture of SIL-CCNN is presented in Fig. 2. First, we need to extract the community information in the network and form the relation matrix of each community. A list of relation matrix RM for communities in $COMM$ can be formulated. Then, we design a community-based convolutional neural network to deal with community-related information by extracting features through a convolutional layer and a pooling layer. For the input of the convolution layer, we extract the relation matrices of communities to represent the local network information of the individual. The relation matrix RM of a community is defined as follows,

$$RM = [rm_{ij}]_{d \times d}, rm_{ij} = \begin{cases} w_{ij}, (v_i, v_j) \epsilon E \\ 0, otherwise, \end{cases} \tag{2}$$

where d is the number of nodes in the community. The element rm_{ij} in the relation matrix represents the weight on the edge between node v_i and node v_j in a community. In addition, in order to account for differences in the size of communities, the community information matrices are normalized to the size of the largest community and have zero-padding.

However, if we randomly assign the order of nodes in relation matrices and put the matrices into the convolutional neural network, the small extracted region in the convolution layer would be meaningless. Therefore, we design an arrangement strategy to determine the relations of nearby

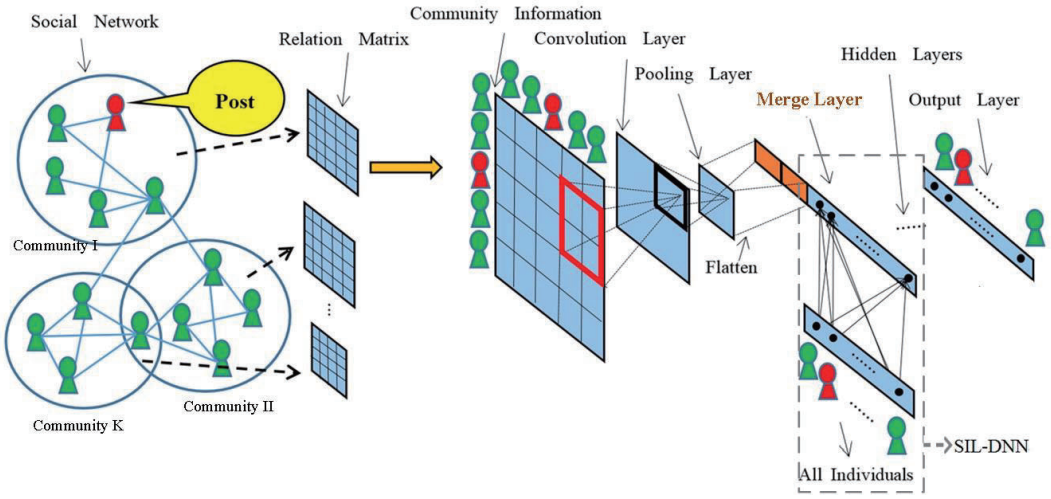

Figure 2: Social Influence Learning on Community-based Convolutional Neural Network architecture

elements. The order of individuals in each relation matrix is determined by the ranking of the number of degrees. The individual having the largest degree will be arranged to the leftmost of x-axis and the topmost of y-axis. Therefore, each block in different relation matrices shares the same weight matrix in the convolutional neural network.

In the pooling layer, we use max-pooling as our pooling function. Max-pooling is particularly well suited to the separation of features that are sparse. After the pooling layer, SIL-CCNN constructs a merge layer to combine the output of the pooling layer and the input vector of SIL-DNN. Then, several hidden layers are trained in SIL-CCNN before the output layer. Finally, a few hidden layers and one full-connected output layer are connected after the merge layer.

As for the detailed setting of neural network, the kernel size of the convolutional layer is defined to 3×3. In addition, we define a sigmoid function in the output layer and a cross-entropy objective function. In the training step, our goal is to minimize the following equation:

$$Q\left(W^t, W^r\right) = -\sum_{i}^{I} t_i \log y_i, \tag{3}$$

where I is the number of inputs, W^t is the weight matrices of traces, and W^r represents the weight matrices of the structure relation in SIL-CCNN. The weight matrix contains the relations between the individuals and the local structure information. The equation above is shown for one individual i at output layer k ranging over all target labels. Our objective function aims to minimize the cross entropy between the target t and the prediction y. As for the optimization, we use the well-known backpropagation algorithm and Adam [4] to compute the parameters in SIL-CCNN.

4. Experiments

In this section, we introduce experiments aiming at evaluating predicting performance in social networks using a synthetic dataset and a real-world dataset.

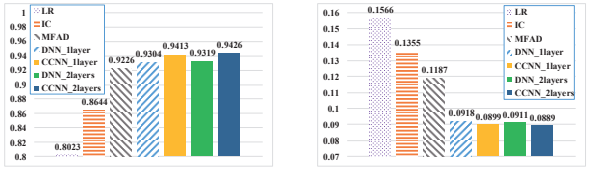

(a) Accuracy (b) MAE

Figure 3: Accuracy and MAE on the synthetic dataset of 5000 nodes

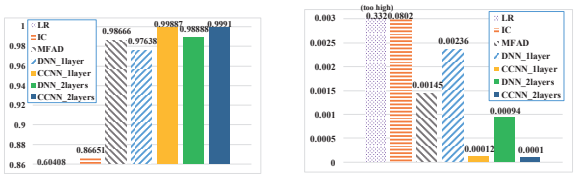

(a) Accuracy (b) MAE

Figure 4: Accuracy and MAE on twitter dataset

4.1 Dataset descriptions

Synthetic Data. Using the Lancichinetti-Fortunato-Radicchi (LFR) benchmark [5], we generate the synthetic dataset with 5000 nodes (2,666,674 traces). For the generation of diffusion data, we set the transmission probability uniformly between 0.1 and 1. We then choose a node at random to function as a source node and set it to be active.

Real Data. We crawl data from Twitter*1 for the period between September 2011 and May 2015. We use the experts in Healthcare Pundits*2 and Security*3 as the ini-

*1 https://twitter.com
*2 http://nursepractitionerdegree.org/top-50-health-care-pundits-worth-following-on-twitter.html
*3 http://www.marblesecurity.com/2013/11/20/100-security-

tial nodes, and crawl the followers of these experts to form a social network. The twitter data contains 20,453 users and 3,782,305 tweets. In this study, tweets were used as items, and the actions of sharing, replying, and liking are indications of the influence of a tweet.

4.2 Compared Methods

We include the following methods to predict the information diffusion results.

- **Logistic Regression** (LR). The in-degree and out-degree are included in a classifier for individual v.
- **Independent Cascade model** (IC). IC is a conventional diffusion model in which the probability of transmission from individual u to v is the ratio of items individual v adopted items from individual u.
- **Multiple Factor-Aware Diffusion model** (MFAD). MFAD is a diffusion model that can learn the social influence by multiple features [2].
- **SIL-DNN and SIL-CCNN**. We evaluated the performance of SIL-DNN and SIL-CCNN using one hidden layer (DNN_1layer, $CCNN\_1layer$) and two hidden layers ($DNN\_2layers$, $CCNN\_2layers$) in the following experiments.

4.3 Evaluated Metrics

We evaluate the performance of algorithms using the following two metrics.

- **Accuracy**. Accuracy is defined as the ratio of correct predicted answers over all answers in order to estimate the correctness of predictions.
- **Mean Absolute Error** (MAE). We computed the mean absolute error as follows: $MAE = \frac{\sum_{i=1}^{n}|y_i - x_i|}{n}$, where y_i is the truly adopted result of individual i, x_i is the estimated adoption probability of individual i, and n is the number of individuals in the network.

4.4 Results and Discussions

The comparison results on synthetic dataset is shown in Fig. 3. SIL-DNN and SIL-CCNN outperform the other three methods in the synthetic dataset. In addition, SIL-CCNN have higher accuracy and lower MAE than SIL-DNN using the same number of hidden layers. The results show that the information of the community structure actually helps the model to predict the influence results better. The proposed community-based CNN indeed extracts the local relations of individuals. Moreover, the performance of SIL-CCNN 2 layers is better than the SIL-CCNN 1 layer. Using more hidden layers also conducts a better result.

In the real twitter dataset, the results are shown in Fig. 4. SIL-DNN and SIL-CCNN still outperform the other three methods except for the DNN_1layer. We have examined the propagation results in these two datasets. We found that the influenced scale of the synthetic dataset is much larger than the Twitter dataset. This indicates that the diffusion results in synthetic dataset should be more difficult to predict. The superiority of SIL-CCNN over SIL-DNN shows that the performance can be improved by including the community information by the proposed community-based convolutional neural network.

experts-follow-twitter/

5. Conclusions and Future Works

In this work, we proposed two neural network architectures, SIL-DNN and SIL-CCNN, to identify social influences based on the propagation of information in a social network. The proposed framework makes it possible to obtain the diffusion results within the community. SIL-DNN and SIL-CCNN can predict the users who are actually influenced from the information without the Monte Carlo simulation. Experimental results demonstrate that SIL-DNN and SIL-CCNN both outperform existing methods.

For further improvement, we will design a strategy to extend the depth of SIL-CCNN in the future to overcome the problem with the insufficient number of traces. We also want to revise the structure of neural network to consider more features such as the content of items.

References

[1] J. Cheng, L. Adamic, P. A. Dow, J. M. Kleinberg, and J. Leskovec. Can cascades be predicted? In *In Proceedings of WWW*, pages 925–936, 2014.

[2] C.-K. Chou and M.-S. Chen. Multiple factors-aware diffusion in social networks. In *In Proceedings of PAKDD*, pages 70–81, 2015.

[3] D. Kempe, J. M. Kleinberg, and E. Tardos. Maximizing the spread of influence through a social network. In *In Proceedings of h ACM SIGKDD*, pages 137–146, 2003.

[4] D. Kingma and J. B. Adam. A method for stochastic optimization. In *In Proceedings of ICLR*, 2015.

[5] A. Lancichinetti and S. Fortunato. Benchmarks for testing community detection algorithms on directed and weighted graphs with overlapping communities. *Physical Review E*, 80, 2009.

[6] K. Saito, R. Nakano, and M. Kimura. Prediction of information diffusion probabilities for independent cascade model. In *In Proceedings of KES*, pages 67–75, 2008.

[7] O. Tsur and A. Rappoport. What's in a hashtag?: content based prediction of the spread of ideas in microblogging communities. In *In Proceedings of WSDM*, pages 643–652, 2012.

[8] L. Wang, S. Ermon, and J. E. Hopcroft. Feature-enhanced probabilistic models for diffusion network inference. In *In Proceedings of ECML-PKDD*, pages 499–514, 2012.

The 33rd Annual Conference of the Japanese Society for Artificial Intelligence, 2019

A Community Sensing Approach for User Identity Linkage

Zexuan Wang Teruaki Hayashi Yukio Ohsawa

Department of Systems Innovation, School of Engineering, The University of Tokyo

User Identity Linkage aims to detect the same individual or entity across different Online Social Networks, which is a crucial step for information diffusion among isolated networks. While many pair-wise user linking methods have been proposed on this important topic, the community information naturally exists in the network is often discarded. In this paper, we proposed a novel embedding-based approach that considers both individual similarity and community similarity by jointly optimize them in a single loss function. Experiments on real dataset obtained from Foursquare and Twitter illustrate that proposed method outperforms other commonly used baselines that only consider the individual similarity.

1. Introduction

In recent years, Online Social Networks (OSNs) such as Twitter, Facebook and Foursquare tend to become the central platform of people's social life. Tons of contextual (e.g. tweets, photos) and network structure related (e.g. users' profiles, relations) data is created every day on these OSNs, which is an important resource for many valuable applications such as user behavior prediction, and cross-domain recommendation. All such applications require a crucial step called User Identity Linkage (UIL) [Shu 17], which aims to identify and link the same person/entity across different OSNs. These linkages are also called anchor links as they help align different networks under the common scene that users usually don't explicitly claim the ownership of their different accounts, and due to privacy protection rules, personal information is always restricted inside each isolated OSNs.

Abundant literature has been focusing on the UIL problem, and the majority of them fall into two categories: (1) Structure-based approaches: these approaches focus directly on the structural features of a social network, such as user names, following relationship and common neighbors between different users [Malhotra 12, Kong 13], while the problem of those approaches lies on the difficulty to find an optimal distance function between nodes to evaluate their similarity as networks are not presented in the Euclidean space [Zhang 18]. (2) Embedding-based approaches: network embedding is a new way of network representation that is able to encode the network in a continuous low-dimensional vector space while effectively preserving the network structure, for example, [Zhou 18] proposed a dual-learning embedding paradigm to improve the linking result.

However, existing methods haven't paid enough attention to the social communities naturally formed by people in the real world. Users who have limited profile information could be evaluated easier when they are located in interest groups together with their close neighbors. To better resolve the UIL problem, we proposed a novel method called Community Sensing User Identity Linkage (CSUIL), which takes advantage of both structural and embedded features of a network by designing a jointly learning model. It aids user mapping by driving some of users to the same communities they belong to, which enhances the method's accuracy and generalization ability. Experiment results on real-world dataset show feasibility of our method.

Contact: Zexuan Wang, The University of Tokyo, 7-3-1 Hongo, Bunkyo-ku, Tokyo, Japan, wangzexuan@g.ecc.u-tokyo.ac.jp

2. Problem Definition

Definition 1 ***Social Network Graph*** *An unweighted and undirected network is denoted as $G = \{V, E\}$, where V is the set of nodes and each node represents a user, E is the set of edges reflecting connections between nodes.*

Definition 2 ***Node Embedding*** *In a given network $G = \{V, E\}$, node embedding (a sub-task of network embedding) learns a projection function $\psi : V \mapsto \mathbb{R}^{|V| \times d}$, where $d \ll |V|$. For each node $v_i \in V$, $\boldsymbol{\psi}(v_i) \in \mathbb{R}^d$ denotes its latent representation in the vector space.*

Definition 3 ***n-th order neighbors*** *The collection of all nodes which can be reached from the given root node $v_r \in G$ within exactly n hops, denoted as $C_r = \{v_i | hop(v_i, v_r) = n\}$.*

Definition 4 ***User Identity Linkage*** *Given two different networks, $G^S = \{V^S, E^S\}$ and $G^T = \{V^T, E^T\}$. The goal of User Identity Linkage (UIL) is to predict a pair-wise linkage between a user node v_s selected from the source network G^S and an unlabeled user node v_s in the target network G^T, which indicates the same user/entity (i.e., $v^s = v^t$).*

3. Community Sensing User Identity Linkage

This proposed method consists of three main components: network embedding, community clustering and latent space mapping. A brief overview is shown in Figure 1, where blocks are the core elements in each phase, green lines indicate structural information flow directions and blue lines show how algorithms connect different phases.

3.1 Network Embedding

The quality of the latent representation of each node in both source and target network is important to the results

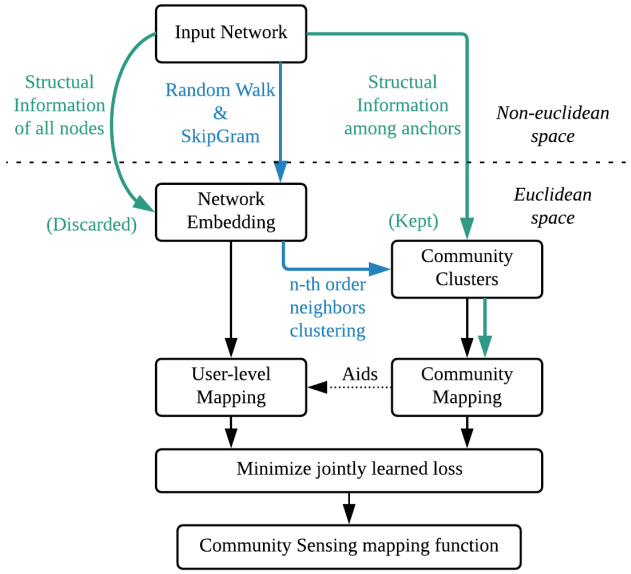

Figure 1: A brief overview of CSUIL

of the following clustering and mapping stages. Ideally, user nodes that have stronger connection, like sharing more common neighbors, or having shorter path between them should be closer to each other after they are projected into the latent space. To obtain the network embedding in good quality, an efficient model called DeepWalk [Perozzi 14] was adopted. DeepWalk mainly utilizes the truncated random walk and the SkipGram [Mikolov 13] model.

In particular, A random walk generator is first applied to the network, which will sample uniformly a random node $v_i \in G$ as the root of a random walk sequence W_{v_i}, then the generator samples uniformly from the neighbors of the last node visited until the maximum sequence length(l) is reached. The generated sequences could be thought of as short sentences, while the nodes within sequences are treated as words of a special kind of language. We could then obtain the embedding of nodes as a byproduct when updating the weight matrix in the derived SkipGram model, which aims to maximize the co-occurrence probability of nodes that appear within a window size w near the center v_j in the sequence W_{v_i}, that is to maximize the following log probability:

$$\max \quad \frac{1}{l}\sum_{i=1}^{l}\sum_{j=-w,j\neq 0}^{w} \log \Pr(v_{i+j}|v_i) \tag{1}$$

where $\Pr(v_{i+j}|v_i)$ is calculated with a hierarchical softmax function:

$$\Pr(v_{i+j}|v_i) = \frac{\exp(\boldsymbol{\psi}(v_{i+j})^{\mathrm{T}}\boldsymbol{\psi}(v_i))}{\sum_{m=1}^{l}\exp(\boldsymbol{\psi}(v_m)^{\mathrm{T}}\boldsymbol{\psi}(v_i))} \tag{2}$$

where $\boldsymbol{\psi}(v_i)$ is the embedding of node v_i we want to update at each training step and finally output to the next phase.

3.2 Community Clustering

In some supervised User Identity Linkage models such as PALE [Man 16], it only focuses on learning the user level, pair-wise matching patterns between source and target network. However, these methods failed to consider the social communities naturally formed by people in the real world. Some drawbacks may exist under such settings that users with very limited profile information could be hard to distinguish from others and the model may fall into over-fitting of local pair-wise features when trained with small amount of labeled data. More importantly, the knowledge contained in the structural relationship among anchor and non-anchor users in the original non-euclidean space is discarded after SkipGram is applied (shown by green lines in Figure 1) and later phases are not able to reuse such information.

Therefore, we made an assumption that compared to only considering the generated embedding or user-level similarity matching, the fact that which neighbors a user has in the original network, and which community a user belongs to could reveal more diffusible structural knowledge. Thus, we consider clustering the $n-th$ order neighbors of an anchor user to form their social community, the users in the same community have a closer relationship and higher similarity, which could be evaluated in some metrics including: the amount of common neighbors, or the minimum walk length between each other.

To utilize all the user information in a community, we reuse the structural information in the original network and derive a new embedding to represent this community by adopting the mean value of all community member embedding generated in Section 3.1 that are non-anchor nodes. The center that represents a certain community cluster C_i is denoted as μ_i:

$$\psi(\mu_i) = \frac{\psi(v_r) + \sum_{v' \in C_i}\psi(v')}{N+1} \tag{3}$$

where v_r is the root user, and N is the community size.

3.3 Latent Space Mapping

Let $\boldsymbol{z^s} = \psi(v^s)$ and $\boldsymbol{z^t} = \psi(v^t)$ be the node embedding generated in Section 3.1 and the final stage of CSUIL is Latent Space Mapping. In this phase, we try to find a mapping function from the source network to the target network Φ: $\mathbb{R}^{|V^s|\times d} \mapsto \mathbb{R}^{|V^t|\times d}$, that will minimize the distance between the predicted embedding $\Phi(\boldsymbol{z^s})$ and the true corresponding embedding $\boldsymbol{z^t}$ of $\boldsymbol{z^s}$ in the target network:

$$\min \quad \left\|\Phi\left(\boldsymbol{z^s}\right) - \boldsymbol{z^t}\right\|_F \tag{4}$$

We then train a novel two-inputs and two-outputs neural network model, which breaks down the whole task above into two simultaneously conducted parts: (1) minimize the distance between predicted and real user node (2) minimize the distance between predicted and real community center. The second sub-task will drive the mapping function to the direction that also exploits the relationship between community centers in both source and target networks to increase the generalization ability of the model on new unseen data.

Next, the design of the loss function could be one of the most critical parts of a machine learning model, a good loss function should reflect the error during training as well as the generalization error that guides parameters to optimize the model. Therefore, for the goal of above two sub-tasks, a new community sensing loss function is proposed as:

$$loss = (1-\gamma) \sum_{(v^s,v^t)\in\{S,T\}} \left\|\Phi(\boldsymbol{z^s};\theta) - \boldsymbol{z^t}\right\|_F + \gamma \sum_{\mu\in C} \left\|\Phi(\boldsymbol{\mu^s};\theta) - \boldsymbol{\mu}^t\right\|_F \quad (5)$$

where $\{S,T\}$ is the set of groundtruth anchor pairs, C is the set of community centers, F is the Frobenius norm, θ is the collection of all parameters in the model, and γ is the hyper-parameter of the weight coefficient of the community loss that could be co-optimized during the learning of the mapping function.

We finally employed a Multi-Layer Perceptron (MLP) model that does not require extensive feature selection or difficult parameter tuning to learn the optimized mapping function, while this model also has the flexibility of dealing with the non-linear relationships that may exist between the source and target network.

The whole algorithm design is shown in Algorithm 1.

Algorithm 1: CSUIL

Input: network $G(V,E)$, anchor nodes $\{S,T\}$, test nodes $\{S',T'\}$, community clustering parameter n, community loss parameter γ
Output: mapping function Φ, matching result list R
foreach *node* $v_i \in G$ **do**
  Generate the embedding of v_i as $\boldsymbol{z_i}$
end
foreach *anchor node pair* $\{s_i,t_i\}$ *in* $\{S,T\}$ **do**
  Reuse the original network structure information, cluster the n-order neighbors of s_i and t_i
  Derive the community center $\boldsymbol{\mu_i^s}$ and $\boldsymbol{\mu_i^t}$
end
Train the MLP model by jointly minimize the node mapping loss $\left\|\Phi(\boldsymbol{z^s};\theta) - \Phi(\boldsymbol{z^t})\right\|_F$ and community loss $\left\|\Phi(\boldsymbol{\mu^s};\theta) - \Phi(\boldsymbol{\mu^t})\right\|_F$
foreach *test node* $s'_i \in S'$ **do**
  Add the predicted t'_i to result list R
end
Evaluate(R,T')

4. Experiment

4.1 Data Preparation

A real-world social network dataset collected from Twitter and Foursquare [Zhang 15] is used in this experiment, which was released in [Liu 16]. All the sensitive personal information is removed under privacy concerns to form the final training and testing data. The ground truth of anchors is obtained by crawling users' Twitter accounts from their Foursquare homepage. Table 1 lists the statistics of this dataset.

Network	#Users	#Relations	#Anchors
Twitter	5,220	164,919	1,609
Foursquare	5,315	76,972	

Table 1: Statistics of Twitter-Foursquare Dataset

4.2 Evaluation Metrics

In this experiment, in a similar form to [Zhou 18], a metric called *Precision*@k was adopted, which is defined as:

$$Precision@k = \frac{\sum_{i}^{n} TOP_k(\Phi(\boldsymbol{z_i^s}))}{N} \quad (6)$$

where $TOP_k(\Phi(\boldsymbol{z_i^s}))$ is a binary output function (0 or 1), for each predicted embedding $\Phi(\boldsymbol{z_i^s})$, it tells whether the positive match $\boldsymbol{z_i^t}$ exists in the $top-k$ list or not, and N is the number of all testing nodes. In the context of UIL, as *Precision*@k is a metric of the true positive rate, it could be treated the same as *Recall*@k, and F_1@k.

4.3 Comparative Methods

We compare the proposed CSUIL with several existing embedding-based methods, and take them as the baseline of this task.

- **CSUIL**: the proposed method, it could explicitly exploit the individual as well as community features of a network, by jointly optimizing mapping functions that concentrate on user-level and community-level similarity respectively.
- **IONE**: Proposed in [Liu 16] and adopted as a baseline result, Input-Output Network Embedding (IONE) is a network embedding and partial network alignment method. It takes follower-ship and followee-ship as input and output contexts and generates all three representations together with the user node.
- **INE**: INE is a simplified version of IONE, which only consider node and input representation for matching.

4.4 Results

The performance results are illustrated in Table 2 and Figure 2. In the experiment, during the community clustering phase, the cluster size is set to first-order neighbors for the simplicity. Then we examine the ability of the final model (with training rate=90%) on the link prediction task. For CSUIL, we report the result in different settings of precision metrics k and community loss weight coefficient γ. For INE and INOE, we report the result in the original paper's default setting.

	Precision@k							
γ	P@1	P@5	P@9	P@13	P@17	P@21	P@25	P@30
INE	0.1108	0.2184	0.2975	0.3291	0.3703	0.4114	0.4304	0.4494
IONE	0.1899	0.3481	0.4494	0.4968	0.5253	0.5665	0.5854	0.6044
0.8	**0.2405**	**0.5190**	**0.6203**	**0.6835**	**0.7342**	**0.7722**	**0.7975**	**0.8165**

Table 2: Performance comparison between baselines

From the experiment results, we could conclude that:

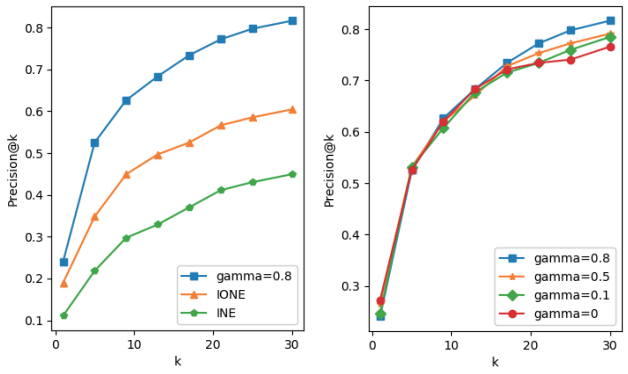

(a) Baselines (b) Precision on different γ

Figure 2: Link prediction precision results. X-axis is the different value of k, for the top-k list being evaluated; Y-axis is the precision result in percentage.

- Compared to the baseline model, INE and IONE, the best performance (when $\gamma = 0.8$, shown in Table 2 and Figure 2(a)) of our approach has an improvement from about 6% to 21 % at most in different settings of precision metrics, which shows the feasibility of this approach.
- Figure 2(b) also illustrates that by changing the setting of community loss weight coefficient γ, the ability of the model to sense more positive matching in a larger search space (higher k setting in precision), could be enhanced, which is an important improvement because many other papers only stress their performance at the $k = 30$ setting. However, adding too much weight to community loss may lead to a slight reduction of the ability to narrow the target to a finer scale (lower k in precision), compared with the $\gamma = 0$ setting.

5. Conclusion

In this paper, we aim to study the UIL problem by reusing the discarded knowledge in the original Online Social Network after network embedding. Not limited to anchor same users across networks, we would also like the community formed by close users to have a positive match across networks. This is because some users may have limited profile and it could be hard to distinguish them from others. However, in the context of a community, users share common features, and they will be driven to the correct direction where group of users with high similarity locates, even if community members are known little. This could also help to avoid overfitting the input data and increase the generalization ability of the method.

Therefore, we break down the main task into two simultaneously learned sub-tasks: User Mapping and Community Mapping, this is achieved by jointly optimizing the user loss and community loss in a single MLP model. Based on above theories, Community Sensing User Identity Linkage (CSUIL) is proposed. Results show that our approach outperforms current baseline models, and has the flexibility to adapt hyper-parameters for different needs or data input.

Acknowledgments

This work was funded by JSPS KAKENHI JP16H01836, JP16K12428, and industrial collaborators.

References

[Kong 13] Kong, X., Zhang, J., and Yu, P. S.: Inferring anchor links across multiple heterogeneous social networks, in *Proceedings of the 22nd ACM international conference on Information & Knowledge Management*, pp. 179–188ACM (2013)

[Liu 16] Liu, L., Cheung, W. K., Li, X., and Liao, L.: Aligning Users across Social Networks Using Network Embedding., in *IJCAI*, pp. 1774–1780 (2016)

[Malhotra 12] Malhotra, A., Totti, L., Meira Jr, W., Kumaraguru, P., and Almeida, V.: Studying user footprints in different online social networks, in *Proceedings of the 2012 International Conference on Advances in Social Networks Analysis and Mining (ASONAM 2012)*, pp. 1065–1070IEEE Computer Society (2012)

[Man 16] Man, T., Shen, H., Liu, S., Jin, X., and Cheng, X.: Predict Anchor Links across Social Networks via an Embedding Approach., in *IJCAI*, Vol. 16, pp. 1823–1829 (2016)

[Mikolov 13] Mikolov, T., Sutskever, I., Chen, K., Corrado, G. S., and Dean, J.: Distributed representations of words and phrases and their compositionality, in *Advances in neural information processing systems*, pp. 3111–3119 (2013)

[Perozzi 14] Perozzi, B., Al-Rfou, R., and Skiena, S.: Deepwalk: Online learning of social representations, in *Proceedings of the 20th ACM SIGKDD international conference on Knowledge discovery and data mining*, pp. 701–710ACM (2014)

[Shu 17] Shu, K., Wang, S., Tang, J., Zafarani, R., and Liu, H.: User identity linkage across online social networks: A review, *Acm Sigkdd Explorations Newsletter*, Vol. 18, No. 2, pp. 5–17 (2017)

[Zhang 15] Zhang, J. and Philip, S. Y.: Integrated Anchor and Social Link Predictions across Social Networks., in *IJCAI*, pp. 2125–2132 (2015)

[Zhang 18] Zhang, J.: Social Network Fusion and Mining: A Survey, *CoRR*, Vol. abs/1804.09874, (2018)

[Zhou 18] Zhou, F., Liu, L., Zhang, K., Trajcevski, G., Wu, J., and Zhong, T.: DeepLink: A Deep Learning Approach for User Identity Linkage, in *IEEE INFOCOM 2018-IEEE Conference on Computer Communications*, pp. 1313–1321IEEE (2018)

The 33rd Annual Conference of the Japanese Society for Artificial Intelligence, 2019

Learning Sequential Behavior for Next-Item Prediction

Na Lu Yukio Ohsawa Teruaki Hayashi

Department of System Innovation, School of Engineering, The University of Tokyo

A more precise recommendation plays an essential role in e-commerce. Representation learning has attracted many attentions in recommendation field for describing local item relationships. In this paper, we utilize the item embedding method to learn item representations and user representations. Our methods compute cosine similarity of user vector and recommended item vectors to achieve the goal of personalized ranking. Experiment on real-world dataset shows that our model outperforms baseline model especially when the number of the recommended item is relatively small.

1. INTRODUCTION

The sharp growth of e-commerce and the using mobile electronic device require a more precise prediction of next item that users would probably like to purchase. Data mining of users' behaviors aims at finding useful patterns from a large database. In this task, understanding users' history and features are one of the most critical parts.

To deal with this task, some models were developed based on last transaction information, which is mostly involving Markov chains[Chen 12]. This method mainly makes use of users' sequential transaction data to predict what will be the next item considering the last transaction event. The advantages of this method are that it could consider the time sequence and recommend a proper item for the next movement. Other general recommendation models would consider users' past purchase behavior as a whole to generate their overall taste (or features)[Rendle 10] . This method could generally grasp a user's interests. The most widely used method of general recommendation models is called collaborative filtering. The advantages of this method are that it could get users' interesting points. Thus, the recommendation could generate from users' whole behavior. However, this method discards subsequent information that may lack preciseness in next-item prediction.

Here a good recommendation model could consider not only the sequential information but also users' overall taste. A hierarchical representation model was proposed to combine both sequential information and user history transaction information [Wang 15]. The proposed hierarchical representation model used a two-layer model. One-layer aggregated all the sequential transactions, and in the second layer, this sequential information was aggregated with the user's overall taste. Then the combined information was used to predict item in the next transaction. This method was novel by setting different layers to combine two kinds of information. However, a better method has been proposed to learn item representations.

Contact: Na Lu, The University of Tokyo, 7-3-1 Hongo, Bunkyo-ku, Tokyo 113-8656 Japan, Department of Systems Innovation, School of Engineering,The University of Tokyo, Bldg.No.8. 507 , 080-1241-0956, luna@g.ecc.u-tokyo.ac.jp

For understanding sequence data, we utilize the Skip-Gram model for word representation learning in natural language process field [Mikolov 13] named as word2vec. Skip-Gram model learns word representations by predicting the context of this word. More precisely, word2vec get a word vector in a lower dimensional space compared with one-hot representation. This method was later generalized as item2vec for learning item representations [Barkan 16]. Item2vec treats users' subsequent behavior as a sentence in word2vec and creates item vectors.

By learning users' sequential data to generate item representations, we proposed a method for aggregating users' history behavior and general taste to build a recommendation system.

2. RELATED WORKS

A good recommendation system could improve users' decision-making process in this information overload era. The widely used recommendation methods include collaborative filtering, content-based filtering, and hybrid filtering. Despite the use of traditional methods, many approaches are proposed to improve the quality of recommendations. We first review some related work in this field.

2.1 Sequential Pattern Mining

Pattern mining is an essential branch of data mining, which consists of discovering frequent itemsets, associations, sub-graphs, sequential rules, etc. [Chen 96]. The target of sequential pattern mining is to detect sequential patterns by analyzing a set of sequential data, in which occurrence frequency is one of the target [Pei 04]. Item2vec embeds items into a low-dimensional representation by accounting the item co-occurrence in user records. That is, this model could generally capture the co-occurrence patterns of items in each transaction data.

2.2 Personalized Ranking

From the target of the recommendation system, it can be treated as a rating prediction problem or a personalized ranking problem [Rendle 09]. The task of personalized ranking is to provide a user with a ranked list of items, which matches a real-life scenario. An example is that an online retailer wants to give a personalized ranking item list that a user may probably buy in the recent future. For-

mer research for personalized ranking algorithms optimized through learning users' preferences on a set of items, which include BPR [Rendle 09], CliMF [Shi 12].

2.3 Item Representation Learning

The word embedding method [Mikolov 13] have attracted much attention from fields besides NLP. The recommendation is also to utilize this method for better performance, including clustering [Barkan 16] and regression. Representation learning in recommendation means getting relationships between items from a specific data set, which is called item embedding. Barkan and Koenigstein [Barkan 16] first proposed Item2Vec model which based on a neural item embedding model for collaborative filtering. In this method, item embedding is used to learn a better item representation but fail to give a personalized ranking recommendation. In this research, we propose an item embedding based method combined with users' history behaviors to provide a personalized next-item recommendation.

3. PROBLEM STATEMENT

In this section, we first introduce the problem formalization of recommendation based sequence behavior. We then describe the item embedding and recommendation for the next item in detail. After that, we talk about the learning and prediction procedure of this method.

3.1 Formalization

Let $U = \{u_1, u_2, ..., u_{|U|}\}$ be a set of users and $I = \{i_1, i_2, ..., i_{|I|}\}$ be a set of items, in which $|U|$ and $|I|$ denote to the total number of unique users and items, respectively. For each user u, the transaction history data T^u is given by $T^u = (T_1^u, T_2^u, T_3^u, ..., T_t^u)$, where $T_t^u \subseteq I$. The purchase history of all users is denoted as $T = \{T^1, T^2, T^3, ..., T^t\}$. Given the transaction data of all users, our task is to predict what the user will probably buy in the next time (eg. t-th), which is denoted as $R = \{R^1, R^2, R^3, ..., R^u\}$. Every R^i includes k items as recommendation: $R^i = \{R_1^i, R_2^i, ..., R_k^i, \}$.That is, we need to generate a personalized ranking R^i for user u_i in t-th transaction.

3.2 Item2Vec algorithm

Our purpose is to learn a recommendation model from a sequential transaction data which could also combine users' overall taste. In this section, we first explain Item2Vec algorithms in detail, which generate item embedding from sequential data. Then users' general taste will be concluded from one user's whole transaction data. At last, item representations and users' general taste will be combined to create a personalized ranking for a next-item recommendation.

To proposed our method for personalized ranking from a sequential user transaction data, we first need to have a look at Item2Vec specifically. Skip-gram with negative sampling (SGNS) was first introduced in word embedding by Mikolov et al. [Mikolov 13]. The neural embedding in natural language processing attempts to map words and phrases into a vector space of low-dimensional semantics and syntax. Skip-gram uses the current word to predict its context words. The item collection in Item2vec is equivalent to the sequence of words in word2vec, that is, the sentence. Commodity pairs that appear in the same collection are considered positive. For the set $w_1, w_2, ..., w_K$ objective function:

$$\frac{1}{K}\sum_{i=1}^{K}\sum_{j\neq i}^{K} log(w_j|w_i) \tag{1}$$

Same as word2vec, using negative sampling, define $p(w_j|w_j)$ as:

$$p(w_j|w_j) = \sigma(u_i^T v_j)\prod \sigma(-u_i^T v_k) \tag{2}$$

Finally, the SGD method is used to learn the max of the objective function and to obtain the embedding representation of each item. The cosine similarity between the two items is the similarity of items.

The cosine similarity between two vectors can be formalized as:

$$cos(v_1, v_2) = \frac{v_1 \cdot v_2}{|v_1||v_2|} \tag{3}$$

3.3 Proposed method

From Item2Vec method, all users' transaction data $T = \{T^1, T^2, T^3, ..., T^t\}$ is used to learn item representations. More specifically, Item2Vec algorithm inputs a large corpus of transactions and creates a vector space, in which every unique item is transformed as a vector in this space. Based on this, we produce item representations based on users' sequential transaction data.

The advantage of our methods is that we can introduce aggregation operations in forming user representations from their history transaction data. In this work, we propose two aggregation methods to get a user representation.

The first is average pooling. This method construct one vector by taking the average value from a set of vectors. Let $V = \{v_1, v_2, v_3, ..., v_l\}$ be a set of vectors. Average pooling of V can be formalized as:

$$f_{ave}(V) = \frac{1}{l}\sum_{i=1}^{l} v_i \tag{4}$$

Second is max pooling. This method construct one vector by taking the max value from a set of vectors. Thus, max pooling can be formalized as:

$$f_{max}(V) = \begin{bmatrix} max(v_1[1] & ... & v_l[1]) \\ max(v_1[2] & ... & v_l[2]) \\ ... & ... & ... \\ max(v_1[n] & ... & v_l[n]) \end{bmatrix} \tag{5}$$

From a user's transaction data T^i, we can get a user representation $\vec{u_i}$ from $f_{ave}(T^i)$ and $f_{max}(T^i)$ as $u_{i\vec{ave}}$ and $u_{i\vec{max}}$. Combine with top-K recommendation from item embedding, which is R^i, we re-rank R^i based on the weighted similarity with user u_i. The detail of re-ranking of recommendation R^i is in Algorithm 1.

In this way, we can combine u_i's general taste ($u_{i\vec{ave}}$ and $u_{i\vec{max}}$) and sequential prediction (R^i) to get a overall prediction.

Algorithm 1 Combination of user representation and top-K recommendation

Input: top-K recommendation R^i for u_i, user vector $u_{i\vec{ave}}$ and $u_{i\vec{max}}$, item set I
Output: R^i_{ave} and R^i_{max}

```
for j ≤ top − K ∗ 2 do
    if R^i_j ⊆ I then
        R^i_{ave−j} = cos(R^i_j, u_{iave}) and R^i_{max−j} = cos(R^i_j, u_{imax})
    else
        test_ size − 1
    end if
end for
sort R^i_ave and R^i_max from highest to lowest, choose top-K items from R^i_ave and R^i_max
return R^i_ave and R^i_max
```

Dataset name	# users	# items	# T
Online Retail	90,346	2553	397,923

Table 1: Basic Information about Online Retail dataset

4. EXPERIMENT AND DISCUSSION

In this section, we conduct empirical experiments to test the effectiveness of our method for a next-item recommendation. We first introduce the experimental data set, the baseline methods in our experiments. Then we compare our approach with the baseline model to study the effect of different aggregations. Finally, we make some analysis on the result of the experiments.

4.1 Dataset

We conduct our experiment on an open data set named 'Online Retail dataset' [UCI 15]. This data set includes transaction data from 2010.12.01 to 2011.12.09. Every row includes invoice number, product number, product name, sale quantity, sale time, unit price, customer ID, and customer's country. After deleting the row that has a default value, the data set basic information is in Table 1.

4.2 Evaluation and Discussion

We divided the dataset into train data and test data. Train data was used to train item2vec model to generate the item representations. Test data was used to evaluate the effectiveness of our method.

In the test data, we first remove the last transaction data from user u. So the remaining is $T^u_{n-1} = \{i_1, i_2, i_3, ..., i_{t-1}\}$. We use the learned model and remaining T^u to make a recommendation of top-K items located closer to each item in the learned vector space. Then these top-K items and user vector derived from T^u_{n-1} are combined to make the final top-K recommendation.

Here we use Recall as the prediction evaluation. The recall is formalized as below:

$$Recall(T^u_t, R^u_t) = \frac{T^u_t \bigcap R^u_t}{T^u_t}$$

top-K \ Method	Ave	Max
1	14.98%	20.25%
3	6.41%	8.43%
5	8.95%	7.54%
10	4.57%	6.13%
15	1.47%	7.75%
20	3.37%	3.85%

Table 2: Recall percentage improvement compared with baseline method

In our experiment, we set top-K=1,3,5,10,15,20 as the number of items that would be recommended to user u. In this experiment, the baseline method is the prediction derived from the item2vec method, which was not combined with a user vector. The comparison of these methods are as follows.

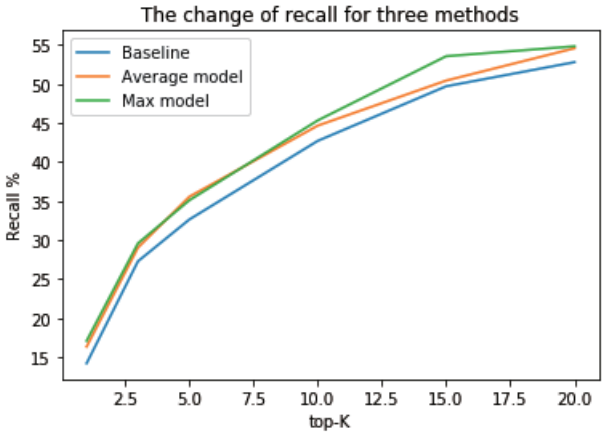

Figure 1: The change of recall for three methods

We can see that the average model and max model could improve over 10% of recall compared with the baseline model. That means if we recommend one item for a user, our model performed well by aggregating user's vector and item2vec prediction. However, this improvement declined with the increase in top-K, which means if we recommend a lot of items to a user at one time, our improvement is not as effective as recommending fewer items. Compared with the baseline model, the recall of the average model and max model are higher, and they get higher with the increase of top-K. If we provide more items for a user, the probability of correct prediction will be higher, just as Figure 1 shows above.

5. CONCLUSION

Representation learning has attracted many attentions in recommendation field for describing local item relationships. In this paper, we utilize the item embedding method to learn item representations from sequential transaction data. And we also constructed user representations to get a ranked list of items for a user. The experiment result

demonstrated that our proposed method for next-item recommendation outperformed baseline model in prediction recall. Specifically, our models get 14.98% and 20.25% improvement compared with baseline model in a top-1 recommendation, which means we get a distinct improvement when the number of the recommended item is relatively small.

6. ACKNOWLEDGEMENT

This work was funded by JSPS KAKENHI, JP16H01836, JP16K12428, and industrial collaborators.

References

[Chen 12] Chen, Shuo, et al. "Playlist prediction via metric embedding." Proceedings of the 18th ACM SIGKDD international conference on Knowledge discovery and data mining. ACM, 2012.

[Rendle 10] Rendle, Steffen, Christoph Freudenthaler, and Lars Schmidt-Thieme. "Factorizing personalized markov chains for next-basket recommendation." Proceedings of the 19th international conference on World wide web. ACM, 2010.

[Wang 15] Wang, Pengfei, et al. "Learning hierarchical representation model for nextbasket recommendation." Proceedings of the 38th International ACM SIGIR conference on Research and Development in Information Retrieval. ACM, 2015.

[Mikolov 13] Mikolov, Tomas, et al. "Distributed representations of words and phrases and their compositionality." Advances in neural information processing systems. 2013.

[Barkan 16] Barkan, Oren, and Noam Koenigstein. "Item2vec: neural item embedding for collaborative filtering." Machine Learning for Signal Processing (MLSP), 2016 IEEE 26th International Workshop on. IEEE, 2016.

[Chen 96] Chen, Ming-Syan, Jiawei Han, and Philip S. Yu. "Data mining: an overview from a database perspective." IEEE Transactions on Knowledge and data Engineering 8.6 (1996): 866-883.

[Pei 04] Pei J, Han J, Mortazavi-Asl B, et al. Mining sequential patterns by pattern-growth: The prefixspan approach[J]. IEEE Transactions on Knowledge & Data Engineering, 2004 (11): 1424-1440.

[Rendle 09] Rendle, Steffen, et al. "BPR: Bayesian personalized ranking from implicit feedback." Proceedings of the twenty-fifth conference on uncertainty in artificial intelligence. AUAI Press, 2009.

[Shi 12] Shi, Yue, et al. "CLiMF: learning to maximize reciprocal rank with collaborative less-is-more filtering." Proceedings of the sixth ACM conference on Recommender systems. ACM, 2012.

[UCI 15] https://archive.ics.uci.edu/ml/datasets/Online+Retail

The 33rd Annual Conference of the Japanese Society for Artificial Intelligence, 2019

Application of Unsupervised NMT Technique to Japanese–Chinese Machine Translation

Yuting Zhao*1 Longtu Zhang*2 Mamoru Komachi*3

Tokyo Metropolitan University

Neural machine translation (NMT) often suffers in low-resource scenarios where sufficiently large-scale parallel corpora cannot be obtained. Therefore, a recent line of unsupervised NMT models based on monolingual corpus is emerging. In this work, we perform three sets of experiments that analyze the application of unsupervised NMT model in Japanese–Chinese machine translation. We report 30.13 BLEU points for ZH–JA and 23.42 BLEU points for JA–ZH.

1. Introduction

Neural machine translation (NMT) has recently shown impressive results thanks to the availability of large-scale parallel corpora [Bahdanau 14]. NMT models typically fit hundreds of millions of parameters to learn distributed representations which may generalize better when data is redundant. Unfortunately, finding massive amounts of parallel data remains challenging for vast majority of language pairs, especially for low-resource languages, as it may be too costly to manually produce or nonexistent. Conversely, monolingual data is much easier to find, and many languages with limited parallel data still possess significant amounts of monolingual data.

Recently, remarkable results have been shown in training NMT systems relying solely on monolingual data in the source and target languages by using an unsupervised approach [Artetxe 18, Lample 18a]. They proposed unsupervised NMT models that are effective on English–French and English–German. Following their practice, we try to apply unsupervised NMT model to Japanese–Chinese translation.

In this work, we perform experiments from two data domains. They are divided into two types of monolingual corpus and quasi-monolingual corpus. Among them, the best BLEU score can reach 30.13 of ZH–JA and 23.42 of JA–ZH with using ASPEC-JC (Japanese Chinese language pairs) parallel corpus [Nakazawa 16] in the quasi-monolingual setting.

2. System Architecture

The unsupervised NMT model [Lample 18b] we used is composed of two encoder-decoder models for source and target languages and in series with back-translation models. The encoders will encode monolingual sentences into latent representations for respective decoders. One decoder is used as a translator to decode the latent representations, and the other decoder perform the denoising effect of a language model on the target side that refines the latent representation of the source sentence. Then, it jointly train two back-translation models together with the two encoder-decoder language models. In the forward translation, the model generates data which will be trained to the backward translation and in the backward translation, the model trained from the generated target to the source generates translations. The generated sentences from back-translation are added to the regular training set in order to regularize the model.

Contact: Yuting Zhao, zhao-yuting@ed.tmu.ac.jp

3. Experiment

3.1 Datasets

We prepare three data sets from ASPEC-JC (Japanese Chinese language pairs) parallel corpus [Nakazawa 16] and Wikipedia dump *1.

For quasi-monolingual data, the Japanese–Chinese portion of ASPEC-JC was used. Note that although this is a parallel corpus, we shuffled it and used it monolingually. In this paper, we call it ASPEC-Quasi. Official training/development/testing split contains totally 670,000 Chinese and Japanese sentences for training and 2,000+ sentences for evaluating and testing.

For monolingual data, the Japanese–Chinese portion of ASPEC-JC was also used. Note that we shuffled it monolingually and divided the monolingual Chinese and Japanese data into the first half and the second half. Then, they were staggered and combined to form two groups of monolingual data sets with a size of 335,000, and one group was randomly selected for experiment. In this paper, we call it ASPEC-Mono. In addition, we created a Japanese–Chinese monolingual corpus with a training size of 10 million from Wikipedia articles. As above, evaluation and test data are all official data from ASPEC-JC.

3.2 Preprocessing

Firstly, we tokenize Japanese and Chinese datasets separately. We use MeCab *2 with dictionary IPADic for Japanese and Jieba *3 with its default dictionary for Chinese. Secondly, we join the source and target monolingual corpora to learn fastBPE tokens with the vocabulary size of 30,000. Finally, we apply fastText [Bojanowski 17] on the

∗1 https://dumps.wikimedia.org/
∗2 http://taku910.github.io/mecab/
∗3 https://github.com/fxsjy/jieba

Corpora	Amount	JA-ZH	ZH-JA
ASPEC-Mono	335,000	8.9	10.37
Wikipedia	10,000,000	9.74	12.51
ASPEC-Quasi	670,000	**23.42** *(31.19)*	**30.13** *(39.18)*

Table 1: BLEU scores of 3 datasets. (The BLEU score of OpenNMT model is presented in parentheses)

BPE tokens. This way, we obtain cross-lingual BPE embeddings for Chinese and Japanese language pairs to initialize lookup tables. More specifically, we use the skip-gram model with ten negative samples, a context window of 5 words, and 512 dimensions.

3.3 Model

In this work, our models use transformer cells as basic units in the encoders and decoders with PyTorch toolkit version 0.5. We set the number of layers of both the encoders and decoders to 4, and the hidden layers is set to 512. Adam optimizer is used with a learning rate of 0.0001 and a batch size of 25. We set a maximum length of 175 tokens per sentence for each type of dataset and a dropout rate of 0.1. We also set random blank-out rate to 0.1 and word shuffle of 3.

BLEU score is used to evaluate translation in both directions with every iteration, and training will stop when the scores from the last 3 iteration did not improve any more.

4. Results and Discussions

The BLEU scores obtained by all the tested datasets are reported in Table 1.

Amount of data. Firstly, we see the results obtained from the complete monolingual datasets ASPEC-Mono and Wikipedia. As our baseline, the results of ASPEC-Mono obtained 8.9 BLEU points for JA–ZH and 10.37 BLEU points for ZH–JA. As the amount of sentences increases from 335,000 to 10,000,000, the results of Wikipedia obtained 9.74 BLEU points for JA–ZH and 12.51 BLEU points for ZH–JA. Comparing with ASPEC-Mono, scores have gone up in both directions despite of domain difference.

Quasi-monolinguality. Secondly, we see the results in the last row, which is from ASPEC-Quasi corpus. It gets 23.42 BLEU points for JA–ZH and 30.13 BLEU points for ZH–JA. This result exceeds all the previous two results. Moreover, the OpenNMT model using ASPEC-JC parallel corpus reports 31.19 BLEU points for JA–ZH and 39.18 BLEU points for ZH–JA. In contrast, the BLEU score of unsupervised NMT is lower than that of supervised NMT, but the gap is not big.

5. Related Work

From the work of Sennrich et al. [Sennrich 16], they proposed a straightforward approach to create synthetic parallel training data by pairing monolingual training data with an automatic back-translation.

Recently, Artetxe et al. [Artetxe 18] and Lample et al. [Lample 18a] have achieved substantial improvement for fully unsupervised machine translation. They leverage strong language models through training the sequence-to-sequence system as a denoising autoencoder.

6. Conclusion

Based on the above analysis, it can be inferred as follows:

- For monolingual data, the larger the data, the better the translation results.
- For quasi-monolingual data, the effectiveness of unsupervised NMT model on Japanese–Chinese is quite promising, even if it uses smaller training dataset.

From the experiment, we can see unsupervised NMT is effective in Japanese–Chinese machine translation. However, it is worth considering that why there is a huge gap between the results of using monolingual corpus and quasi-monolingual corpus on Japanese–Chinese unsupervised NMT. Even though the amount of monolingual Wikipedia corpus is 15 times more than that of ASPEC-Quasi corpus, the result is much worse. We hope to start from this significant gap and continue to study the factors affecting unsupervised NMT in Japanese–Chinese machine translation.

References

[Artetxe 18] Artetxe, M., Labaka, G., Agirre, E., and Cho, K.: Unsupervised Neural Machine Translation, in *Proceedings of ICLR* (2018)

[Bahdanau 14] Bahdanau, D., Cho, K., and Bengio, Y.: Neural Machine Translation by Jointly Learning to Align and Translate, in *Proceedings of ICLR* (2014)

[Bojanowski 17] Bojanowski, P., Grave, E., Joulin, A., and Mikolov, T.: Enriching word vectors with subword information, in *Proceedings of TACL*, pp. 135–146 (2017)

[Lample 18a] Lample, G., Conneau, A., Denoyer, L., and Ranzato, M.: Unsupervised Machine Translation Using Monolingual Corpora Only, in *Proceedings of ICLR* (2018)

[Lample 18b] Lample, G., Ott, M., Conneau, A., Denoyer, L., and Ranzato, M.: Phrase-Based & Neural Unsupervised Machine Translation, in *Proceedings of EMNLP*, pp. 5039–5049 (2018)

[Nakazawa 16] Nakazawa, T., Yaguchi, M., Uchimoto, K., Utiyama, M., Sumita, E., Kurohashi, S., and Isahara, H.: ASPEC: Asian Scientific Paper Excerpt Corpus, in *Proceedings of LREC*, pp. 2204–2208 (2016)

[Sennrich 16] Sennrich, R., Haddow, B., and Birch, A.: Improving Neural Machine Translation Models with Monolingual Data, in *Proceedings of ACL*, pp. 86–96 (2016)

The 33rd Annual Conference of the Japanese Society for Artificial Intelligence, 2019

Synthetic and Distribution Method of Japanese Synthesized Population for Real-Scale Social Simulations

Tadahiko Murata[*1]

[*1] Department of Informatics, Kansai University, Japan

Takuya Harada[*2]

[*2] Research Institute for Socionetwork Strategies, Kansai University, Japan

In this paper, we describe how synthesized populations are essential in real-scale social simulations (RSSS), and the current situation of the population synthesis for whole populations in Japan. RSSS is simulations using the real number of populations or households in social simulations. This paper describes how we have completed to synthesize multiple sets of populations based on the statistics of each local government in Japanese national census in 2000, 2005, 2010 and 2015. We have started to distribute those multiple sets of the synthesized populations for researchers of RSSSs in Japan. In distributing the synthesized populations, we should protect personal or private information in the synthesized populations. We show some scheme how to protect them using a cloud service or secure computations.

1. Introduction

In this paper, we try to develop a platform for Real-Scale Social Simulation (RSSS) by synthesizing whole households in Japan and providing the data of synthesized households for researchers who try to develop RSSS tools. RSSS is simulations using populations or households in the real scale.

Recently social simulations have attracted from many researchers to tackle with problems in our environments or communities. One of the most influential social simulations is the segregation model proposed by **Schelling (1971)**. In his model, he clearly shows how segregations happen due to the preference of residents to be a neighbor of the same race or group. His model shows that segregations can happen even if there is no hostility among races. His model is quite interesting and meaningful to give understanding of conflict and cooperation. He was awarded the 2005 Novel Memorial Prize in Economic Science.

Although Schelling's model is quite significant, interpretation is required to apply his model to real situations. If we are able to directly conduct simulations with real-scale environments and real-scale residents, it is easy to draw insight from simulation results. That is why RSSS has much attention from many researchers recently.

In order to conduct RSSS, real-scale populations are required. For example, when **Murata & Konishi (2013)** optimized the number of polling places with considering the voting rate and the number of polling places in a city using a scheme of RSSS, they should synthesize the population in the city and measure the distance of polling places from their homes. When **Murata & Du (2015a)** assessed effects of the pension program for each household in Japan, they should create and simulate demographic movement of all prefectures in Japan for 25 or over 100 years according to the statistics of Japanese census conducted in 2010.

2. Synthetic reconstruction methods

Tadahiko Murata; Address: Kansai University, 2-1-1, Ryozenji, Takatsuki, Osaka 569-1095, Japan; Phone: +81-72-690-2429, FAX; +81-72-690-2491; murata@kansai-u.ac.jp .

Since RSSS researchers should face to synthesize populations in the target area of their social simulation sooner or later, we have synthesized populations using the available statistics in each local government such as city, town and village in Japan according to the national census in 2000, 2005, 2010 and 2015. The number of cities, towns and villages in Japan is 1741 in the national census in 2015).

Methods synthesizing populations with individual attributes are known as Synthetic Reconstruction method (SR method) (**Wilson, 1976**). Originally an SR method employs real samples from the real statistics. That method increases the number of individuals from the samples in order to fit the real statistics. Here, we prefer using the term "synthesize" to the term "reconstruct" in this paper. Since a reconstruction method is expected to generate exactly the same attributes of each individual in the population, however, it is impossible to reconstruct the same attributes from a small number of statistics. Therefore, we can only synthesize a population that has the same statistical characteristics using SR methods. **Lenormand & Deffuan (2013)** compared SR methods that employ samples with a synthetic method without samples. They showed the synthetic method without samples is better than the former one.

We employ a synthetic method without samples in this paper. The basis of our method is a method proposed by **Ikeda et al. (2010)**. They proposed a method for synthesizing households of nine family types according to the nine real statistics using a simulated annealing method **(Davis, 1987)**. **Fig. 1** shows the nine

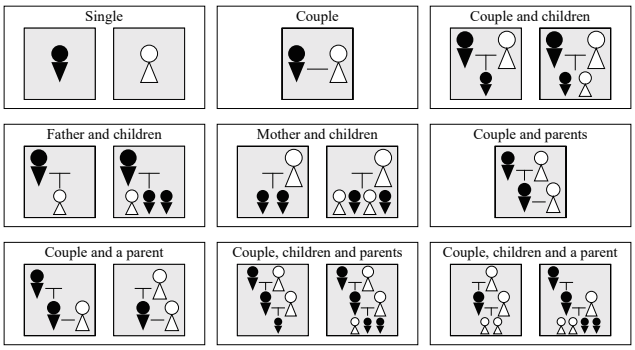

Fig. 1 Nine Family Types.

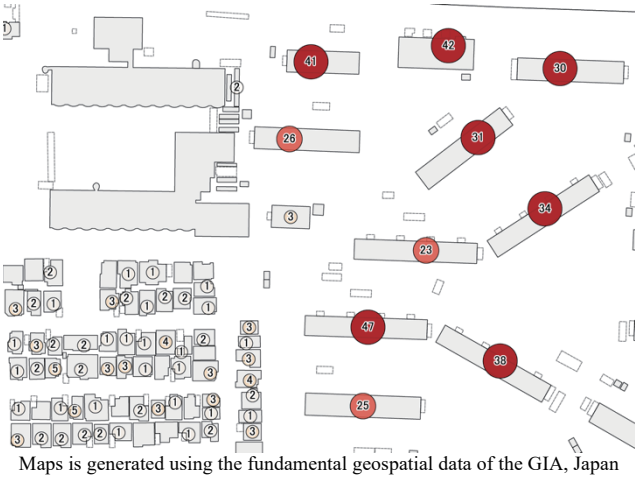

Maps is generated using the fundamental geospatial data of the GIA, Japan

Fig. 2 Households Projection on buildings.

family types they synthesized. 95% households in Japan come from these family types. Each family member has attributes of sex, age, kinship in its household. **Murata & Masui (2014, 2015b)** modified the objective function and a transition method in their simulated annealing method. Although their method (Ikeda, 2010; Murata, 2014, 2015b) can synthesize a population that has the same statistical characteristics with the real statistics, their method tried to synthesize a reduced population with only 500 or 1,000 households. The synthesized population is too small for social simulations in a real city, town or village.

In order to cope with the problems arisen in the reduced number of populations, we tried to synthesize exactly the same number of individuals in a target area such as states, counties, and prefectures using statistics of prefectures **(Murata, 2016, 2017a)**. We first increased the number of real statistics for each family type and modified a transition method (Age-Changing method) in their SA method by considering role in a family (2016). We then proposed another transition method (Age-Swap method) in their SA method that keeps the distribution of the initial population that is fit to the real statistics (2017a). Age-changing method has a better performance in reducing the error when the number of transitions in an SA method is relatively small. On the other hand, Age-swap method can reduce better than Age-changing method when the number of transitions in an SA method is relatively large.

When we increase other attributes such as geographical characteristics **(Harada, 2017)** or occupation and income **(Murata, 2017b)** to the synthesized population, populations by local governments such as city, town or village are required **(Murata, 2018)**. There are finer statistics that are statistics for each "basic unit block." The number of "basic unit blocks" in Japan is around 1.9 millions. A population synthesis method using statistics of "basic unit block" is proposed by Harada & Murata (2018). We have conducted population synthesis using the above algorithms with high performance computers in Osaka University. **Fig. 2** shows an example of a household projection on buildings in a map of Japan. Each figure in a circle shows the number of households residing in the corresponding building.

Table 1 Distributed Synthetic Populations.

Organization	Synthesized Area	Statistics
RTI International, USA	All states, USA Population: 300 million	2010 US Decennial Census 2007-2011 American Community Survey
CDRC: Consumer Data Research Center, UK	England & Wales, UK Population: (53 + 3) million	2011 UK Census
Kansai University, Japan	Japan Population: 120 million	2000 National Census 2005 National Census 2010 National Census 2015 National Census

3. Synthesized Population Distribution

Using the above synthetic methods, we have generated synthesized populations for whole Japan. We are trying to prepare the database of synthesized populations using database. There are only two organizations that distributes synthetic populations in the national level in the world. **Table 1** shows the distributed synthesized populations. Those organizations distribute nation-wide populations of their country.

Although they are distributing only one set of synthesized populations, we have synthesized 10 sets of populations now. Since any methods synthesizes populations based on the limited number of statistics, there is no guarantee that the synthesized population is exactly the same as the real population. Therefore, RSSS should be conducted on several sets of populations and find common outcome from the simulations, or a unique outcome among them. When we find a common result, it seems to be obtained from any populations with the same statistical characteristics of the real population. When we find some unique result, we should carefully see how the obtained result is caused. In order to conduct such multiple simulations, we distribute several sets of populations.

We are distributing synthetic populations with the following notations.

1) The synthetic populations do not contain any data of the real households and individuals.
2) The synthetic populations contain only the same statistical characteristics of the real households and individuals.
3) The synthetic populations do not contain any statistical characteristics that are not used in the synthetic process.
4) The synthetic population will be updated when latest statistics become available.
5) Simulations or analysis using the synthetic populations should be conducted on multiple sets of populations.
6) Outcomes of simulations and analysis should NOT be released any personal or private information that is relating to real households or individuals.

Although synthesized populations are not real populations, residents may consider that their privacy is offended by releasing

their personal information such as their occupations, income or educational back grounds. Therefore, we require researchers to conduct their simulations or analysis using multiple sets of synthesized populations in Item 5). We also require researchers not to release outcomes of their simulations or analysis in any forms that enables others to identify or estimate a private information in a certain household.

4. Further Challenges for Data Protection

In order to protect the personal or private information in the synthesized populations, we are planning to employ a cloud service that enables simulations using the synthesized populations. By employing a cloud-style service, we do not have to distribute the synthesized data themselves to researchers but allow them to access the synthesized data in their RSSSs. In order to realize such an interface for accessing the synthesized populations, we should develop online programming tools for utilizing the synthetic populations in simulations or analysis.

Another way to protect personal information is to employ secure computation (Chida, 2014). The secure computation enables users to utilize sensitive data without allowing them to see exact values of them.

5. Conclusion

In this paper, we show the current status of population synthesis of whole populations in Japan. We have developed multiple sets of synthesized populations with the same statistical characteristics of the real populations in Japan. In synthesizing the populations, we utilized the statistics conducted in 2000, 2005, 2010, and 2015. After synthesizing the populations with sex, age, kinship in their household, we are increasing attributes of each individual such as geospatial data, occupation, and income. We hope enriching such synthesized population will help researchers who try to develop real-scale social simulations or analyze micro data to see characteristics of our communities or environments.

Acknowledgement

Part of this research is funded by Foundation for the Fusion of Science and Technology in 2017, JSPS KAKENHI 17K03669 in 2017, and Tateishi Science and Technology Foundation in 2018. Synthesized populations are generated using the large-scale computing systems (VCC) of Cybermedia Center, Osaka University.

References

[Chida, 2014] K. Chida, G. Morohashi, H. Fuji, F. Magata, A. Fujimura, K. Hamada, D. Ikarashi, R. Yamamoto, Implementation and evaluation of an efficient secure computation system using 'R' for healthcare statistics, J. of the American Medical Informatics Association, Vol. 21, Is. e2, pp. 326-331, 2014.

[Davis, 1987] L. Davies: Genetic algorithms and simulated annealing; Research Notes in Artificial Intelligence, Los Altos, CA: Morgan Kaufumann, 1987.

[Harada, 2017] T. Harada, T. Murata, Projecting household of synthetic population on buildings using fundamental geospatial data, SICE Journal of Control, Measurement, and System Integration, Vol. 10, No. 6, pp. 505-512, 2017.

[Harada, 2018] T. Harada, T. Murata, Geospatial data additional method using basic unit blocks, Proc. of SICE Symposium on Systems and Information 2018, 6 pages, 2018 (in Japanese).

[Ikeda, 2010] K. Ikeda, H. Kita, M. Susukita, Estimation method of individual data or regional demographic simulations, Proc. of SICE 43rd Technical Com. on System Engineer, pp. 11-14, 2010 (in Japanese).

[Lenormand, 2013] M. Lenormand, G. Deffuant, Generating a synthetic population of individuals in households: Sample free vs sample-based methods, Journal of Artificial Societies and Social Simulation, vol. 16, no. 4, pp. 1-9, 2013.

[Murata, 2013] T. Murata, K. Konishi, Making a Practical Policy Proposal for Polling Place Assignment Using Voting Simulation Tool, SICE Journal of Control, Measurement, and System Integration, Vol. 6, No. 2, pp. 124-130, 2013.

[Murata, 2014] T. Murata and D. Masui, "Estimating agents' attributes using simulated annealing from statistics to realize social awareness", Proc. of 2014 IEEE Int'l Conf. on System, Man & Cybernetics, pp. 717-722, 2014.

[Murata, 2015a] T. Murata, N. Du, Comparing income replacement rate by prefecture in Japanese pension system, Advances in Social Simulation, pp. 95-108, 2015.

[Murata, 2015b] T. Murata and D. Masui, "A two-fold simulated annealing to reconstruct household composition from statistics", Proc. of 2015 IEEE Int'l Conf. on System, Man & Cybernetics, pp. 1133-1138, 2015.

[Murata, 2016] T. Murata, T. Harada, D. Masui, Modified SA-based household reconstruction from statistics for agent-based social simulations", Proc. of 2016 IEEE Int'l Conf. on Systems, Man, & Cybernetics, pp. 3600-3605, 2016.

[Murata, 2017a] T. Murata, T. Harada, D. Masui, Comparing transition procedures in modified simulated-annealing-based synthetic reconstruction method without samples, SICE Journal of Control, Measurement, and System Integration, vol. 10, no. 6, pp. 513-519, 2017.

[Murata, 2017b] T. Murata, S. Sugiura, T. Harada, Income allocation to each worker in synthetic populations using basic survey on wage structure, Proc. of 2017 IEEE Symposium Series on Computational Intelligence, pp. 471-476, 2017.

[Murata, 2018] T. Murata, T. Harada, Synthetic method for population of a prefecture using statistics of local governments, Proc. of 2018 IEEE Int'l Conf. on Systems, Man, & Cybernetics, pp. 1171-1176, 2018.

[Schelling, 1971] T. Schelling, "Dynamic models of segregation, Journal of Mathematical Sociology, Vol. 1, pp. 143-186, 1971.

[Wilson, 1976] A. G. Wilson, C. E. Pownall, A new representation of the urban system for modeling and for the study of micro-level interdependence, Area, vol.8, no. 4, pp. 246-254, 1976.

International Session | International Session | [ES] E-3 Agents

[3H3-E-3] Agents: safe and cooperative society

Chair: Ahmed Moustafa (Nagoya Institute of Technology), Reviewer: Takayuki Ito (Nagoya Institute of Technology)

Thu. Jun 6, 2019 1:50 PM - 3:30 PM Room H (303+304 Small meeting rooms)

[3H3-E-3-01] An Autonomous Cooperative Randomization Approach to Prevent Attacks Based on Traffic Trends in the Communication Destination Anonymization Problem

○Keita Sugiyama[1], Naoki Fukuta[1] （1. Shizuoka University）

1:50 PM - 2:10 PM

[3H3-E-3-02] Cooperation Model for Improving Scalability of the Multi-Blockchains System

○Keyang Liu[1], Yukio Ohsawa[1], Teruaki Hayashi [1] （1. University of Tokyo, Graduate school of engineer）

2:10 PM - 2:30 PM

[3H3-E-3-03] Effect of Visible Meta-Rewards on Consumer Generated Media

○Fujio Toriumi[1], Hitoshi Yamamoto[2], Isamu Okada[3] （1. The University of Tokyo, 2. Rissho University, 3. Soka University）

2:30 PM - 2:50 PM

[3H3-E-3-04] Toward machine learning-based facilitation for online discussion in crowd-scale deliberation

○Chunsheng Yang[1], Takayuki Ito[2], Wen GU[2] （1. National Research Council Canada, 2. Nagoya Institute of Technology）

2:50 PM - 3:10 PM

[3H3-E-3-05] An automated privacy information detection approach for protecting individual online social network users

○Weihua Li[1], Jiaqi Wu[1], Quan Bai[2] （1. Auckland University of Technology, 2. University of Tasmania）

3:10 PM - 3:30 PM

The 33rd Annual Conference of the Japanese Society for Artificial Intelligence, 2019

An Autonomous Cooperative Randomization Approach to Prevent Attacks Based on Traffic Trends in the Communication Destination Anonymization Problem

Keita Sugiyama*1 Naoki Fukuta*2

*1 Faculty of Informatics, Shizuoka University
*2 College of Informatics, Academic Institute, Shizuoka University

The communication destination anonymization problem is one of the problems to be resolved under some trade-offs in the cyber security field. Several approaches have been proposed for the communication destination anonymization problem such as Wang's U-TRI. However, due to the trade-offs that the user cannot take too expensive costs to make the network performance improved while keeping its security level, there remains the issues to make anonymization even over a short period of time while giving a good throughput. In this paper, we present an overview of the approach to solve this issue by introducing autonomously coordinating multiple end-hosts and a simulation environment to analyze it.

1. Introduction

When defending facilities with the camera network or patrolling ponds for avoiding illegal disposals by drones, the networks constituting them also need to be protected at the same time in order to operate them properly. It is mentioned that the anonymity of communication destination in such network is often implemented for this purpose [Wang 17]. U-TRI [Wang 17] has been proposed by Wang et al as one of the approaches for that purpose. However, it is mentioned that U-TRI still suffers from an issue when attackers are allowed to utilize their observed traffic trends [Wang 17]. In this paper, we present an overview of the approach to solve this issue by introducing autonomously coordinating multiple end-hosts and a simulation environment to analyze it.

2. Background and Related Work

2.1 Communication Destination Anonymization

It is one of the security problems on enterprise local networks that attackers are able to gather intelligence such as which end-hosts are online and which end-hosts are important by sniffing traffic in the networks. In order to prevent this problem, identifiers appear in network traffic need to be anonymized. PHEAR [Skowyra 16] and U-TRI [Wang 17] are methods to anonymize addresses in the local network. U-TRI implement anonymity by updating identifiers representing the communication destination and source in VIRO, which is a method of efficiently routing packets using the Software Defined Network, at random intervals based on idea of Moving Target Defense [Jajodia 11].

Contact: Keita Sugiyama, Faculty of Informatics, Shizuoka University, 3-5-1 Johoku, Naka-ku, Hamamatsu-shi, Shizuoka 432-8011 Japan, cs15050@s.inf.shizuoka.ac.jp

2.2 Attacks Based on Traffic Trends

As mentioned in the original Wang's U-TRI paper [Wang 17], U-TRI leaves the problem to allow attackers to attack based on traffic trends. Although the detail is not clearly mentioned there, the following cases can happen. For example, on the system where multiple clients are managed by a server, it is expected that packets whose destination address or source address is the address of the server appear frequently since multiple clients communicate with the server. In such a case, even if the address of each end-host is updated in a certain period, it is not difficult for the attacker to identify the address of the server by investigating the appearance situation of the address in a shorter period than the address-update interval. The primary factor of that is that, U-TRI implements anonymity in the medium to long term, but anonymity is not implemented in the short term. It is possible to make that hard by making the address-update interval very short for the purpose of implementing anonymity. However, shortening the address-update interval disorderly is not a practical solution since it is expected that the network performance will be greatly impaired by increasing the packet loss rate.

In this way, U-TRI leaves the possibility of traffic analysis utilizing the fact that it is difficult to implement short-term communication destination anonymity and that the tendency of traffic tends to be biased due to the nature of the system. In this paper, we will proceed with the necessary discussion to propose a method to effectively implement short-term anonymity.

3. Overview of Proposed Approach

The aim of our proposed approach is to implement a short-term anonymity in consideration of the trade-offs with the network performance while implementing the communication destination anonymity in the medium to long term like the U-TRI does. In addition, it is also required to

	Address	The First Observed Time	The Last Observed Time
1	~~f0:00:38:4e:8f:29~~	00:00:12	00:08:12
2	~~5e:11:59:50:df:30~~	00:00:12	00:04:12
3	~~ef:fe:27:b7:3d:10~~	00:04:12	00:08:12
4	~~a0:50:88:8a:5f:33~~	00:08:12	00:12:12
5	~~bf:2c:f8:9d:db:48~~	00:08:12	00:13:30
6	**be:9a:70:5b:9f:54**	00:12:12	00:13:30

Figure 1: The recently updated addresses estimated by the attacker.

change the strategy automatically and autonomously in consideration of the current traffic trends since network traffic changes over time.

Regarding the former requirement, the approach that each end-host determines the address-update frequency according to its own importance level is considered as one of the ways of satisfying the requirements.

Regarding the latter requirement, the approach that each end-host determines the address-update frequency according to its own packet transmission/reception status and packet loss is considered as one of the methods satisfying the requirements.

Therefore, it is possible for each end-host to determine its own address-update frequency in consideration of its own importance level, packet transmission/reception status, and its potential or current level of packet losses. Here, an issue is found using this approach. The issue of this approach is that the attackers are able to predict the most recently updated address, that is, the address likely to be the address pointing to the end-host whose address is being updated frequently, by excluding addresses that have not been observed for a long time and addresses that have been observed for a long time among the observed addresses. Figure 2 shows how an attacker predicts the most recently updated address from the observed addresses. Entries 1 to 4 are the addresses that have not been observed for a long period of time. Entry 5 is an address that is being observed for a long period of time. The attacker predicts that entry 6 is the address that was most recently updated.

In this way, it becomes an issue when attackers are able to gain much profit by attacking the end-host with high frequency of address-updates if the address-update frequency can be predicted by attackers. In order to solve this issue, we also require the ability that allows each end-host to cooperate with other end-hosts for giving attackers uncertainty about their own importance level.

4. Calculation of Attack-Success Rate by Simulator

In this work, we are preparing a prototype simulator to evaluate effectiveness our approach. The prototype of simulator has a mechanism to analyze the differences among the original U-TRI and our approach regarding their abilities to prevent an attack which utilizes its poor implementation of anonymity of communication destination (Attacker A) and an attack which predicts an end-host whose update frequency of the addresses is high (Attacker B).

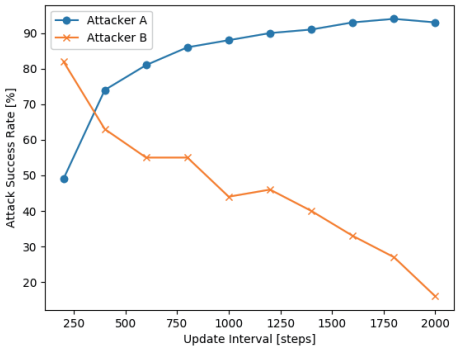

Figure 2: Attack-success rate of each attacker against the address-update interval of the server. The number of end-hosts except for the server = 6, the address-update interval of end-host except for the server = 2000 [steps].

On a situation with a network which has one server and six cameras where each camera communicates with the server, we analyze the attack-success rate of each attacker in the case where the attack-success condition is to attack the server. Figure 2 shows the results on that condition. It shows the attack-success rate when only the address-update interval of the server is changed while the address-update interval of end-hosts are fixed except for the server.

5. Conclusion

In this paper, we presented an overview of the approach to prevent attacks based on the traffic trends which is unavoidable in the original U-TRI, which provides the communication destination anonymization problem in the cyber security field by autonomously coordinating multiple end-hosts. In addition, we presented a prototype simulator to analyze differences among the original U-TRI and our approach.

References

[Jain 11] Jain, S., Chen, Y., and Zhang, Z.-L.: VIRO: A scalable, robust and namespace independent virtual Id routing for future networks, *2011 Proceedings IEEE INFOCOM*, pp. 2381–2389 (2011)

[Jajodia 11] Jajodia, S., Ghosh, A. K., Swarup, V., Wang, C., and Wang, X. S.: *Moving Target Defense: Creating Asymmetric Uncertainty for Cyber Threats*, Springer Publishing Company, Incorporated (2011)

[Skowyra 16] Skowyra, R., Bauer, K., Dedhia, V., and Okhravi, H.: Have No PHEAR: Networks Without Identifiers, in *Proceedings of the 2016 ACM Workshop on Moving Target Defense*, pp. 3–14 (2016)

[Wang 17] Wang, Y., Chen, Q., Yi, J., and Guo, J.: U-TRI: Unlinkability Through Random Identifier for SDN Network, in *Proceedings of the 2017 Workshop on Moving Target Defense*, pp. 3–15 (2017)

The 33rd Annual Conference of the Japanese Society for Artificial Intelligence, 2019

Cooperation Model for Improving Scalability of the Multi-Blockchains System

Liu Keyang Ohsawa Yukio Teruaki Hayashi

Department of System Innovation, Graduate School of Engineering, The University of Tokyo

Scalability is an open question of the blockchain. Ongoing solutions, like Sharding and Side-chain, try to solve it within an independent blockchain system. We propose a cooperation model by constructing a system of multiple blockchains. In this model, secure cross chain operations can help to handle more requests. The gossip channel can help to refresh the states of other blockchains. Through manage interactions among blockchain systems, this model can limit their misbehaviors and improve scalability.

1. INTRODUCTION

Blockchain, a solution to decentralized systems, can solve problems in fields like finance[Eyal 2017], supply chain[Abeyratne 2016], crowdsourcing [Li 2018]. Currently, blockchain can provide two functions. First, a blockchain can work as a securely distributed ledger[Ren 2018]. Second, a blockchain can provide a reliable distributed calculating platform. By using smart contracts[Underwood 2016], all participants can execute functions correctly and give the same output.

Generally, a decentralized system is more robust and trusted than a centralized system. However, the scalability is its weakness. Scalability problem is the long latencies or superfluous messages caused by growing participants. Usually, it is a result of the consensus algorithm[Karame 2016]. Many solutions try to solve this problem within a blockchain system. Sidechain shifts some assets into a sidechain to realize faster responses[Back 2014]. Sharding technology tries to split participants into several shardings for parallel processing[Luu 2016]. All these works sacrifice security or consistency for the efficient responses.

This work tries to solve the scalability problem through cooperative problem-solving. In this model, each blockchain system is an independent agent. The contributions of this work are 1. A protocol for delivery versus payment(DVP) problem. 2. The framework of Blockchain's cooperation model.

2. RELATED WORKS

Sharding is an exciting idea that split blockchain into several shardings so they can handle requests simultaneously. This idea shares some similarity with multiple blockchains system. Elastico[Luu 2016] and Rapid chain[Zamani 2018] are some great implementations of this solution. In these systems, the randomness of each sharding limits the possibility of collusion and planned attacks. However, they give up security or consistency to some degree. To solve this problem, we propose a framework to weaken secure assumptions of each blockchain. By considering possible attack happens, this work focus on limiting the effect of attacks. Hence, our model allows more sacrificing of security on individual blockchain while providing better services.

Chen et al[Chen 2017] and Kan et al[Kan 2018] had finished some works about the communication between different blockchains. They simulate Internet stack and TCP protocol to create the Inter blockchain communication protocol. Although these methods are functional, they are also fragile to malicious attacks. Besides, they ignored the achievements of the consensus algorithm which is very useful in DVP problem. This work will consider the case that some blockchains are controlled or created by attackers. We can prove that these attacks cannot affect other blockchains.

3. PROBLEM MODEL

This part will clarify assumptions and notations of this model. First, $N = 1, 2, ...n$ represents the set of agents. Each agent i is a distributed network that maintains one blockchain $B_i[]$ with all terminated blocks list linearly. The participants of each agent run the consensus algorithm to maintain the blockchain and provide their services to users. Terminated block means at least $f_i > 0.5$ participants have confirmed and stored the block. f_i is the parameter of each agent's consensus algorithm.

Second, all block contents two parts: header and body. A header contains at least the hash of the previous Block, metadata of the body, and signatures of the creator. For convenience, all blockchains' contents, like transactions or Key-Value pair, is unified under an abstracted class – log. Each agent should support two operations: $verify$ and $check_i$. $verify(log, h)$ will return the validity of one log before the h^{th} block $B_i[h]$ according to the rule of the blockchain. Taking a Bitcoin's transaction as an example, input should be a subset of unspent transaction output (UTXO), and the sum of inputs should be larger than the sum of outputs. $check_i(log)$ returns the position of one log in B_i. It will return -1 when it does not exist. Hence, the

Contact: Liu Keyang, University of Tokyo, 7-3-1 Hongo, Bunkyo-ku, Tokyo 113-8656 Japan, Department of Systems Innovation, School of Engineering,The University of Tokyo, Bldg.No.8. 507 , 070-4336-1780, stephenkobylky@gmail.com

following property held:

- a.(Validity) $\forall h > 0$ and $log \in B_i[h]$, $verify_i(log, T) = True$ for $T < h$ and $verify_i(log, T) = False$ for $T > h$.
- b.(Agreement) If $check_i(log) == True$, log can be accessed from at least f_i part of participants in agent i.

Third, we assume adding one legal log into a blockchain consume resources for all agents. Under this condition, cross chain operation becomes a DVP problem. Off-line cost's DVP problem is the job of exchanges. This work focus on the online DVP problem between two agents. Cooperation model will guarantee the payment's validity stick to the delivery of goods.

Last, we allow an agent itself can work improperly or attack some other agents. Since an agent can work independently, agents need some mechanism to control the effect of attacks. One naive way is creating a higher layer blockchain among different agents so it can be byzantine fault tolerate. This work uses another lightweight method. We create an externality of each cross-chain operation without affecting other agents. However, these externalities can prove the existence of misbehavior and punish the agent by detaching it from the network.

4. COOPERATION MODEL

This section includes the detail of the cooperation model. To begin with, we defined two extended functions for each participant of agents in our model.

4.1 Extended operation

Define a condition log $clog1 = log1||log2||j||h1||h2$ represents $log1$ is a cross chain operation related to $log2$ in agent j. The expiration height for a condition log is $h1$ and $h2$ in agent i and j. All participants of agents maintain a waiting list(WL) for cross chain log and condition log. WL supports a function $condcheck()$. When $clog1$ and $log1$ are stored together in WL, $condcheck(log1) = clog$ and $condcheck(clog1) = log1$. In other cases, it returns the existence of input log in WL.

Next, we need to define the extended function $checkEX_i(log1)$. Let $checkEX_i(log1)$=-1 if $condcheck(log1) = True$. If $condcheck(log1) = clog1$, $checkEX_i(log1) = check_i(clog1)$. In other cases,$checkEX_i(log1) = check_i(log1)$. $checkEX_i(clog1) = check_i(clog1)$

Then, we define function $verifyEx(log, h)$ in algorithm 1.

4.2 Workflow

By using previous notations, the operations to WL are following:

- When the new terminated block contains a condition log $clog1$, all participants add $clog1$ and $log1$ into their WL.

Algorithm 1 verifyEx

Input: log1 or clog1, h
Output: True or False

```
if Input is normal log then
  if condcheck(log1)! = clog1 then
    return verify(log1, h)
  else
    return checkEX_i(clog1) ≥ 0 & checkEX_i(log_1) < 0 & checkEX_j(clog2) ≥ 0 & verify(log1, h)
  end if
else if condcheck(clog)! = False then
  return False
else
  return h < h_1 & verify(log1, h)
end if
```

- Expire: When $B_i[h1]$ is terminated $clog1$ is removed from WL. When$checkEX_j(log2) \geq 0$ and $checkEX_i(log1) \geq 0$ $log1$ and $clog1$ is removed.

the workflow of cross chain operations are following:

- 1. Register: A user submits $clog1$ to one participant. Participants check $verifyEX_i(clog1, h_t)$ where h_t is the current height of blockchain B_i. If it returns True, commit $clog1$ to next block.
- 2. Condition-commit: If the newest terminated Blocks contain $clog1$, all participants add $clog1$ and $log1$ to their WL.
- 3. Pre-commit: User submits $log1$ to one participant.The participant checks $verifyEX_i(log1, h)$. If it is true, commit $log1$ to next block.
- 4. Commit: When the height of blockchain reaches $h1$, participant check $checkEX_i(log1)$ and $checkEX_j(log2)$ to determine whether to expire $clog1$.

The workflow of a success cross chain operation looks like Figure 1.

Till now, we have clarified main steps of a cross chain operation. The final step is to broadcast the latest view, like the hash of last terminated block header, of both agents. One agent can use a gossip channel to notify other agents of updating. This gossip is not necessary to be received or confirmed. However, an agent can reveal a fork by identifying an unmatched view of one agent.

4.3 Communication rule

In the cooperation model, each blockchain is an agent to act. Hence, verifying the status of one agent demands sufficient supports from its participants. Due to the property of agreement, secure connection with one agent i anchors to the parameter f_i. For a given possibility p , the required confirmations m_i should satisfied $(1 - f_i)^{m_i} < p$. Hence, $m_i \geq \frac{p}{\ln(1-f_i)}$.

A secure communication requires enough participants of agent i asks for m_j confirmations from agent j independently. The communication cost is $O(m_i * m_j)$ per time.

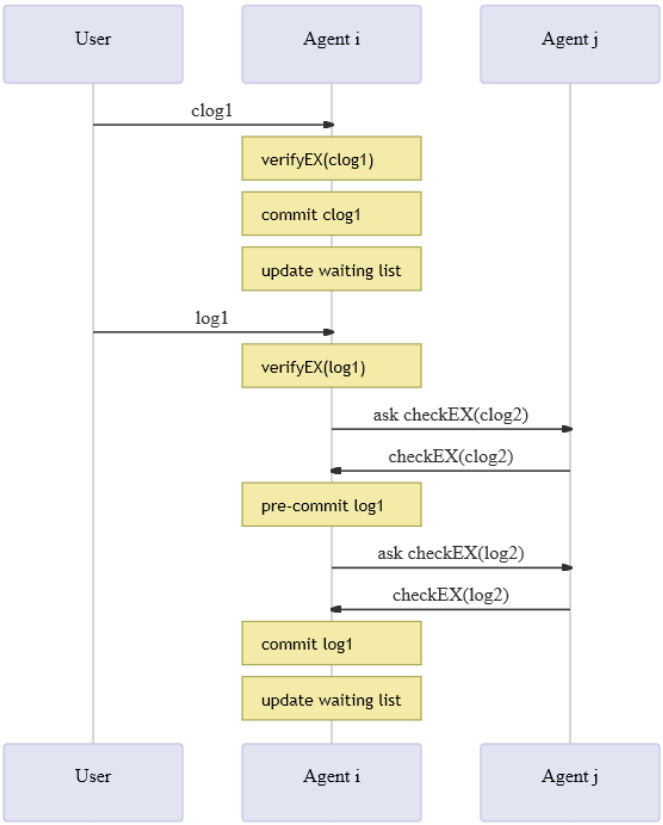

Figure 1: The work flow of one cross chain operation.

An efficient way is to select some proxies to do this communicate. Once selected proxies confirmed $checkEX_j()$, they can spread the gossip information among agent i. Under this method, the cost is $O(m_i)$. For preventing collusion, participants should randomly select proxies.

5. ANALYSIS AND EXPERIMENT

5.1 Function analysis

To view other possible situations of this protocol, we can consider the states of WL. WL can allow three statues:1. Null,2. $clog1$ and $log1$, 3. $log1$. Table 1 shows the result of VerifyEX and CheckEX, where the condition is the 3rd line in Algorithm 1. When a user submits $clog1$, only case 1 and case 3 can continue. Case 3 means new condition log is a supplement to an expired one which jumps to the final stage. When a user submits $log1$ at case 3, participants can detect that it is a rejected log. As a result, on one can admit a existed cross chain operation $log1$ without satisfying a condition $clog1$. This is the cost of agreement in a blockchain.

Assumes log' is conflicted with $log1$, which indicates the terminated blockchain can only contain one of them. The condition for committing log', $checkEX_i(log1)$ should be less than 0. Since termination requires admissions of at least half of all participants, they can exclude the possibility of conflicts within the blockchain. Once a terminated block contains log', it is impossible to activate $log1$ in case 3 any more. The reason is $clog1$ is also conflicted with log'.

Func \ WL	Null	Clog&log	log
VerifyEX(clog)	Verify(Log)	False	Verify(Log)
CheckEX(clog)	check(clog)	check(clog)	check(clog)
VerifyEX(log)	Verify(Log)	condition	Verify(Log)
CheckEX(log)	check(log)	check(clog)	-1

Table 1: Result of VerifyEX(ignore h) and CheckEX

Hence, by using the property of Blockchain, this protocol can solve the DVP problem of cross chain operations.

5.2 Security analysis

This part provides some brief proofs of security. Generally, there are two types of attacks: agent's misbehaviors and communication attacks. During the protocol, the only information needed about other agent is function $checkEX$ which affect by WL and terminated blocks. Hence, Adjusting can detect the counterfeit WL and B_i. Once attacker Eve controls the agent j, j can reply to other agents arbitrary and support any cross-chain operations. After completing a cross chain operation, Eve can create a fork to repeal the existed log. In this case, agents that received the previous view of j will anchor to the elder branch and reject new branch inherit the identity of j. The network will wait for j recovering the former branch and continue its services. Here, the gossip channel creates an externality of an agent so that it cannot change its termination within the network. The higher rate to verify gossip, the higher termination the model can propose.

Besides, there are some network attacks like Sybil attacks and DDOS attack among agents. Sybil attack means the attacker create several agents in the model to arrange attacks. However, these bot agents need to spend enough resources to convince users of other agents for one round attack. Hence, this attack is not profitable if users can manage their risk. Another way is isolating one agent like Man in the Middle(MITM) attack to block gossips. This attack is very costly when the target is a distributed network. A fixed and reliable channels can also resolve this attack. In a word, the resilience against manufactured identities depends on the value of each agent. Lastly, DDOS attacks also worth considering. Attackers can attack waiting list by creating many useless conditional logs. The solution can be charging an additional fee for registering cross chain operation. Indeed, cross chain operations require extra payment for stronger termination and complex procedures. The most significant problem relates to the gossip channel where redundancy informs can block useful gossip. Hence, the gossip channel needs some rule for filtering. Agents can require a signature for each message, limit frequency of source agents, create some periodical routes.

5.3 Experiment

This work intended to improve the scalability of one agent through cross chain operation. The experiment evaluated the average latency and gossip burden for different rates of cross chain operations in the worst case. Latency is evaluated by the number of blocks for solving same amount

of requests. Gossip represents the number of message sent in gossip channel when discard rate is 0.5. The result(Figure 2) shows a linear growth of latency with inter log rate and stable average gossip message related to the number of agents. The increasing of latency relates to the size of condition logs. In the experiment, we assume condition log spending double space compare to other logs.

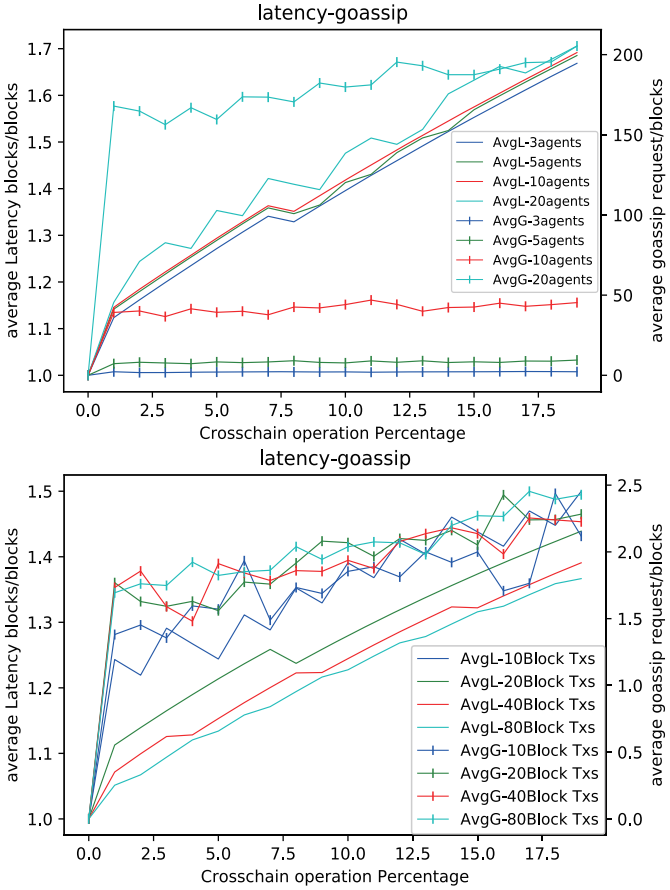

Figure 2: Average latency and gossip according to cross operation rate when transactions terminate immediately. The first picture shows the number of gossips is square to the system's scale. The second picture shows the system do not accumulate gossips or latency as time goes by.

6. CONCLUSION

This work proposes a cooperation model for improving scalability. Under the cooperation model, cross chain operation can create externality of each agent and spread it through gossip channel. The termination of one agent can partly rely on other agents and agent can pay more attention to achieve agreements. On the other hand, cross chain operation extends the ability of one agent and allow a more flexible exchange between different digital assets. We can still optimize this work in many ways. Condition log and gossip message can be compressed to reduce latency and burden of gossip channel. A gossip checking protocol can detect forks faster. The future works will focus on the consensus design under the cooperation model and optimization of gossip channel and related protocols.

7. ACKNOWLEDGMENT

This work was funded by JSPS KAKENHI, JP16H01836, JP16K12428, and industrial collaborators.

References

[Eyal 2017] Eyal I. Blockchain technology: Transforming libertarian cryptocurrency dreams to finance and banking realities[J]. Computer, 2017, 50(9): 38-49.

[Abeyratne 2016] Abeyratne S A, Monfared R P. Blockchain ready manufacturing supply chain using distributed ledger[J]. 2016.

[Li 2018] Li M, Weng J, Yang A, et al. Crowdbc: A blockchain-based decentralized framework for crowdsourcing[J]. IEEE Transactions on Parallel and Distributed Systems, 2018.

[Karame 2016] Karame G. On the security and scalability of bitcoin's blockchain[C]//Proceedings of the 2016 ACM SIGSAC Conference on Computer and Communications Security. ACM, 2016: 1861-1862.

[Back 2014] Back A, Corallo M, Dashjr L, et al. Enabling blockchain innovations with pegged sidechains[J]. URL: http://www. opensciencereview. com/papers/123/enablingblockchain-innovations-with-pegged-sidechains, 2014.

[Luu 2016] Luu L, Narayanan V, Zheng C, et al. A secure sharding protocol for open blockchains[C]//Proceedings of the 2016 ACM SIGSAC Conference on Computer and Communications Security. ACM, 2016: 17-30

[Ren 2018] Ren Z, Cong K, Aerts T, et al. A scale-out blockchain for value transfer with spontaneous sharding[C]//2018 Crypto Valley Conference on Blockchain Technology (CVCBT). IEEE, 2018: 1-10.

[Chen 2017] CHEN Z, Zhuo Y U, DUAN Z, et al. Inter-Blockchain Communication[J]. DEStech Transactions on Computer Science and Engineering, 2017 (cst).

[Kan 2018] Kan L, Wei Y, Muhammad A H, et al. A Multiple Blockchains Architecture on Inter-Blockchain Communication[C]//2018 IEEE International Conference on Software Quality, Reliability and Security Companion (QRS-C). IEEE, 2018: 139-145.

[Zamani 2018] Zamani M, Movahedi M, Raykova M. RapidChain: scaling blockchain via full sharding[C]//Proceedings of the 2018 ACM SIGSAC Conference on Computer and Communications Security. ACM, 2018: 931-948.

[Underwood 2016] Underwood S. Blockchain beyond bitcoin[J]. Communications of the ACM, 2016, 59(11): 15-17.

The 33rd Annual Conference of the Japanese Society for Artificial Intelligence, 2019

Effect of Visible Meta-Rewards on Consumer Generated Media

Fujio Toriumi*1Hitoshi Yamamoto*2Isamu Okada*3

*1The University of Tokyo *2Rissho University*3Soka University

Consumer Generated Media(CGM) are useful for sharing information, but information does not come without cost. Incentives to discourage free riding (receiving information, but not providing it) are therefore offered to CGM users. The public goods game framework is a strong tool for analyzing and understanding CGM and users' information behaviors. Although it is well known that rewards are needed for maintaining cooperation in CGM, the existing models hypothesize the linkage hypothesis which is unnatural. In this study, we update the meta-reward model to identify a realistic situation through which to achieve a cooperation on CGM. Our model reveals that restricted public goods games cannot provide cooperative regimes when players are myopic and never have any strategies on their actions. Cooperative regimes emerge if players that provide first-order rewards know whether cooperative players will give second-order rewards to the first-order rewarders. In the context of CGM, active posting of articles occurs if potential commenters/responders can ascertain that the user posting the article will respond to their comments.

1. Introduction

Consumer generated media (CGM) are the most active information sharing platforms in which users generate contents by voluntary participation. They include information sharing sites such as Wikipedia and TripAdviser, and question/answer forums such as Yahoo Answers. CGM reflect positive traits of the Internet because, in CGM, aggregating users' voluntary participation bears values, and thus they have network externality in which the more active users are, the more the values of the CGM are.

CGM rely on user-provided information and thus fail if information is not provided. Getting users to provide information generally requires effort costs including time costs and click costs[Nakamura 14]. Therefore, CGM users are given incentives to discourage free riding, a situation in which users receive information, but do not provide it. While huge CGM never worry about freeriding, many managers of small-sized CGM pay attention to it. CGM can be regarded as a kind of public goods game–a social dilemma game in which users may refrain from paying costs (that is, free riding), although they could benefit substantially if they contributed.

To avoid the free-rider problem, many CGM adopt incentive systems for users to receive comments as appreciation for posting articles. These comments are considered rewards for contributing to the public goods game. Moreover, many real CGM systems provide Like buttons to react to comments, which can be regarded as meta-rewards. This is because comments also give psychological benefits to original article providers as well as Like buttons give psychological benefits to their receivers.

Toriumi et al. [Toriumi 16] used a public goods game model to show that meta rewards are required to maintain cooperation. A meta reward is a reward for those who gave a reward to cooperative users. Many CGMs implement a function that allows other users to express their gratitude to those who provided information, and the users who expressed their gratitude can also be given something as a reward.

However, the model has an unrealistic hypothesis which called Linkage hypothesis: Whoever performs the first-order sanction (rewards) also performs the second-order one. This hypothesis is needed for the theoretical rationale of meta sanctions because, if the second-order sanctions are independent of the first-order sanctions, third-order free riders who shirk the second-order sanctions only are possible, and thus cooperation through meta sanctions collapses. Experimental studies have no consensus on this linkage hypothesis. Some experiments support the linkage between the first-order sanctions and cooperative behaviors [Horne 01, Horne 07] while others deny it [Yamagishi 12, Egloff 13]. The linkage hypothesis between the first-order and second-order sanctions is partially supported by an experiment of a one-shot public goods game [Kiyonari 08].

In this paper, we will model our CGM public goods game without assuming the linkage hypothesis between the first- and second-order rewards. While a previous model [Toriumi 16] uses the same parameter, r_i, as the probabilities of giving rewards and giving meta rewards, our model separates the former probability from the latter.

2. Models and Methods

In this section, we develop a model that reflects real CGM by extending the CGM model proposed by Toriumi et al. [Toriumi 12]. We then define an adaptive process of players in the model to explore feasible solutions of strategies for promoting and maintaining cooperation. Third, we introduce several scenarios to provide insight for managing real CGM by comparing their performances. Finally, we set parameter values to perform our simulation.

2.1 A restricted meta reward game model

We consider N agents playing a restricted meta reward game. The game is run for a discrete time and each period is referred to as a round. In each round, all agents play three

連絡先: Fujio Toriumi, tori@sys.t.u-tokyo.ac.jp

sequential steps in serial order. Using the case of Agent i as an example, Agent i has its own strategy denoted by (b_i, r_i, rr_i), which we will explain later.

In the first step, the agent provides its own token into a public pool with probability b_i and otherwise does not. In CGM, a contribution and a non-contribution are, respectively, regarded as an information-providing behavior and a non-providing behavior. If a token is provided by Agent i, i must pay a cost κ_0, also the other $N-1$ players receive a benefit, ρ_0.

In the second step, rewards for providing a public good may occur. In CGM, posting a comment to an information provider is regarded as a reward. If and only if Agent i provides a token, the other $N-1$ agents consider whether or not they will give a reward to Agent i. Agent $j(\neq i)$ gives a reward to Agent i with probability $p_{r_{i\to j}}$ and otherwise does not. This probability is calculated as $p_{r_{i\to j}} = \varepsilon \cdot r_j$, where r_j is j's own reward parameter and ε is an expected rate of meta rewards newly introduced in this model to consider the third challenge of the above-mentioned prior studies. If a reward is given, Agent i gains a constant benefit, ρ_1, while Agent j must pay a constant cost, κ_1.

In the third step, meta rewards for giving rewards may occur. In our model, meta rewards from contributors are possible in the first step only to consider the second challenge of the previous studies, thus making this model a restricted game. In CGM, a reply to comments is regarded as a meta reward. If and only if Agent i received a reward from Agent j, Agent i can decide whether to give a meta reward to Agent j with probability rr_i, and otherwise not. While Toriumi et.al.[Toriumi 12] assumes that $r_i = rr_i$, our model assumes that these are independent of each other to consider the linkage hypothesis. If a meta reward is given, Agent j gains a constant benefit, ρ_2, while Agent i must pay a constant cost, κ_2.

Each agent plays the above three steps four times in each round. When all agents complete these steps, each agent's final payoff at each round is regarded as its fitness value.

2.2 Simulation scenarios

In the restricted meta reward game, there is no incentive to give meta rewards, and thus players never provide meta incentives. To consider this point, we introduce players' expectations of meta rewards. We then explore how these expectations are reflected in the probability of providing rewards using the following three scenarios that are different values of expected rates of meta rewards, ε.

1. No reference ($\varepsilon = 1.0$): players do not use any reference
2. Social reference ($\varepsilon = \frac{1}{N}\sum_k rr_k$): players use the average rate of meta rewards in the group
3. Individual reference ($\varepsilon = rr_i$): players use cooperator i's probability of meta rewards

Scenario 1 is a baseline. Scenario 2 describes a situation that players can get information on a providing rate of meta rewards in CGM. For instance, we suppose a system in which seeing all meta rewards for rewards by others is possible. Scenario 3 describes a situation that visualizes a providing rate of meta rewards for information provided in CGM. In this scenario, we assume that players can decide whether or not to provide meta rewards to a cooperator after they check the providing rate of meta rewards of the focal cooperator.

Table 1: Simulation Parameters

Param	Value
N	100
Simulation steps	1000
μ (benefit-cost ratio)	2.0
δ (discount ratio)	0.8
ρ_0 (benefit of cooperation)	2.0
κ_0 (cost of cooperation)	1.0

2.3 Parameter setting

For simplicity, we set the values of the parameters above by installing two new intervening parameters: δ and μ.

$$\kappa_0 = 1.0 \tag{1}$$

$$\rho_n = \mu \cdot \kappa_n \tag{2}$$

$$\kappa_n = \delta \cdot \kappa_{n-1}, \tag{3}$$

where $n = 1, 2$.

At first, we simulate the case of $\mu = 2$ and $\delta = 0.8$ to clarify the performances of each scenario. Then, we investigate the influences of the cost-reward ratios in Section 3.2. Table 1 shows the values of the other parameters in the simulation.

3. Simulation Results

3.1 Comparison of three scenarios

We simulate 100 runs with different random seeds in each scenario, and show the averages and the variances of values using error-bars in Figs.1, 2, and 3. In these figures, the vertical axes show the step numbers while the horizontal axes show the average parameter values: Cooperation indicates cooperation rates, b_i, Reward indicates reward rates, r_i, and MetaReward indicates meta reward rates, rr_i.

As shown in Fig.1, the cooperation rate in Scenario 1 decreases at about 100 steps while increasing at the beginning. This is due to the decrease in reward rates. The rate gradually decreases immediately after the beginning and reaches 0.1 at 20 steps. No reward never bears cooperation.

Scenario 2 faces the same mechanism and thus neither scenario can maintain a cooperative regime.

In Scenario 3, on the other hand, the cooperation rate increases from the beginning, then the meta reward rate also increases and, finally, the reward rate increases, therefore maintaining a stable cooperative regime as shown in Fig.3.

Why does Scenario 3 promote cooperative regimes while Scenario 1 does not? This is quite surprising because parameter value ε is 1 in Scenario 3 while it is less than 1 in

Scenario 1. We then analyzed the time series of cooperation rates, reward rates, and meta reward rates in Scenario 3 in comparison with Scenario 1. At the beginning of the simulation, cooperative rates increased in both scenarios. However, the next phenomena are different. In Scenario 3, the meta reward rates increased before the reward rates increased. This is because players with high meta reward rates tend to receive more rewards than those with low meta reward rates. If the number of players who give rewards is sufficiently large, the high meta reward rates bear the benefit of the rewards and are larger than the costs of meta rewards. Therefore, players with high meta reward rates benefit more than those with low meta reward rates.

The more players with high meta reward rates there are, the greater the probability of receiving meta rewards when giving rewards. Therefore, players who tend to give rewards gain more benefit than those who do not, and thus the reward rates increase. High reward rates enhance the benefit of cooperation and, therefore, cooperative players have an advantage over defective players. Cooperative regimes stay robust.

3.2 Influence of cost-reward ratios

In our model, the rate of the reward benefit on the reward cost is important for promoting cooperative regimes[Toriumi 16]. Therefore, we simulated many cases with different values of μ and δ. Figure 4 shows the average rate of cooperation in 1000th step with in 50 runs per each case. In this figure, the x axis indicates μ, the y axis indicates δ, and the color bar indicates the average cooperation rates.

The scopes of μ and δ are, respectively, $0.0 \leq \mu \leq 5.0$ and $0 \leq \delta \leq 1.0$. This figure shows that

1. Cooperative regimes emerge only in Scenario 3
2. Cooperative regimes never emerge if $\mu < 1.4$ and
3. Cooperative regimes emerge if approximately $\mu \cdot \delta > 1.0$

Among these, Result 2 is consistent with a previous study [Toriumi 12] that demonstrated that cooperative regimes require a substantially large benefit of rewards compared with their costs. Our result adds the insight that it also requires a sufficiently larger value of μ in our model than the previous study's model. This is because the expected values of meta rewards are small if μ is small, and thus the incentive to give rewards vanishes.

Next, we consider Result 3. As a result of our simulation, condition $\mu \cdot \delta > 1.0$ is necessary for promoting cooperation. In terms of the relationship between rewards and meta rewards, if the benefit of meta rewards is greater than the cost of rewards, players may receive a benefit through giving rewards, and thus there are incentives to give rewards. This indicates that

$$\rho_2 > \kappa_1 \tag{4}$$

is required. If $\kappa_1 > 0$ is satisfied, equations $\rho_2 = \mu \cdot \kappa_2 = \mu \cdot \delta\kappa_1$ are satisfied, and thus the necessary condition of reward behaviors is

$$\mu \cdot \delta = \frac{\rho_2}{\kappa_1} \quad > \quad 1.0. \tag{5}$$

Strictly on this point, players do not always receive meta rewards and thus we should consider the average rate of meta rewards, $\overline{rr_i}$. Therefore,

$$\overline{rr_i} \cdot \mu \cdot \delta > 1.0 \tag{6}$$

is the necessary condition.

If this condition is satisfied, players who give rewards to other players at sufficiently large rates of meta rewards have an advantage. This also means that cooperative agents are given incentives from which they should receive a large amount of meta reward rates. This mechanism works and therefore players with large amounts of both reward rates and meta reward rates have survival advantages and, finally, cooperative regimes emerge.

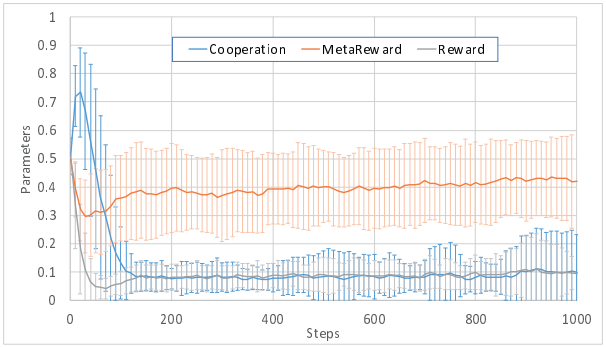

Figure 1: Result of Scenario 1

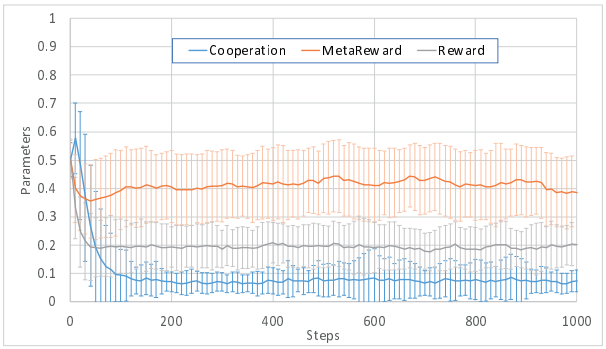

Figure 2: Result of Scenario 2

4. Discussion

While our main results support the importance of meta-rewards for activating CGM, we must state the

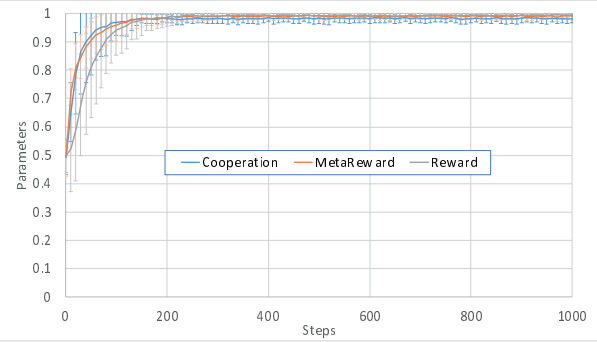

Figure 3: Result of Scenario 3

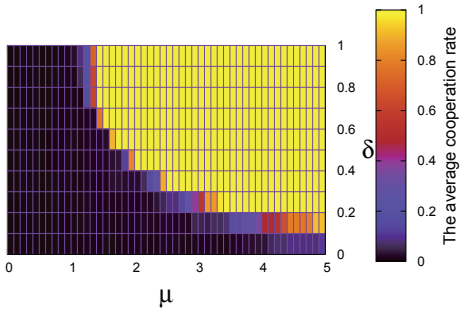

Figure 4: Change μ, δ in Scenario 3

other important drivers of real posting including brand image[Kim 16], attention seeking, communication, archiving, and entertainment[Sung 16]. Moreover, we have no option but to accept the future study on the empirical data that support that the original article providers respond to other commenters replies to sustain posting on CGM.

We developed a restricted public goods games model to overcome the mismatches found between previous models and actual CGM. Our model reveals that restricted public goods games cannot provide cooperative regimes when players are myopic and never have any strategies on their actions. Cooperative regimes emerge if players that give first-order rewards are given information that reveals whether cooperative players will give second-order rewards to the first-order rewarders. In the context of CGM, if users who post articles reply to commenters/responders, active posting of articles occurs if potential commenters/responders can ascertain that the user posting the article will respond to their comments.

This study should be extended. First, the present version of our model describes two types of players actions: cooperation as posting information and defect as non-posting. However, defect behaviors in CGM can be divided into two types: do nothing and post inadequate information. This issue should be introduced in a future version. Second, while our model assumes that all players can observe all information, this is not realistic. We are interested in the influence when the frequency of information accessibility depends on the quality of the information.

References

[Egloff 13] Egloff, B., Richter, D., and Schmukle, S. C.: Need for conclusive evidence that positive and negative reciprocity are unrelated, *Proceedings of the National Academy of Sciences*, Vol. 110, No. 9, pp. E786–E786 (2013)

[Horne 01] Horne, C.: The enforcement of norms: Group cohesion and meta-norms, *Social psychology quarterly*, pp. 253–266 (2001)

[Horne 07] Horne, C.: Explaining norm enforcement, *Rationality and Society*, Vol. 19, No. 2, pp. 139–170 (2007)

[Kim 16] Kim, A. J. and Johnson, K. K.: Power of consumers using social media: Examining the influences of brand-related user-generated content on Facebook, *Computers in Human Behavior*, Vol. 58, pp. 98–108 (2016)

[Kiyonari 08] Kiyonari, T. and Barclay, P.: Cooperation in social dilemmas: Free riding may be thwarted by second-order reward rather than by punishment., *Journal of personality and social psychology*, Vol. 95, No. 4, pp. 826–42 (2008)

[Nakamura 14] Nakamura, H., Gao, Y., Gao, H., Zhang, H., Kiyohiro, A., and Mine, T.: Tsunenori Mine. Toward Personalized Public Transportation Recommendation System with Adaptive User Interface, *3rd International Conference on Advanced Applied Informatics* (2014)

[Sung 16] Sung, Y., Lee, J.-A., Kim, E., and Choi, S. M.: Why we post selfies: Understanding motivations for posting pictures of oneself, *Personality and Individual Differences*, Vol. 97, pp. 260–265 (2016)

[Toriumi 12] Toriumi, F., Yamamoto, H., and Okada, I.: Why do people use Social Media? Agent-based simulation and population dynamics analysis of the evolution of cooperation in social media, in *Proceedings of the The 2012 IEEE/WIC/ACM International Joint Conferences on Web Intelligence and Intelligent Agent Technology-Volume 02*, pp. 43–50 (2012)

[Toriumi 16] Toriumi, F., Yamamoto, H., and Okada, I.: Exploring an Effective Incentive System on a Groupware, *Journal of Artificial Societies and Social Simulation*, Vol. 19, No. 4 (2016)

[Yamagishi 12] Yamagishi, T., Horita, Y., Mifune, N., Hashimoto, H., Li, Y., Shinada, M., Miura, A., Inukai, K., Takagishi, H., and Simunovic, D.: Rejection of unfair offers in the ultimatum game is no evidence of strong reciprocity, *Proceedings of the National Academy of Sciences*, Vol. 109, No. 50, pp. 20364–20368 (2012)

The 33rd Annual Conference of the Japanese Society for Artificial Intelligence, 2019

Toward machine learning-based facilitation for online discussion in crowd-scale deliberation

Chunsheng Yang[*1], Takayuki Ito[*2], and Wen Gu [*2]

[*1] National Research Council Canada [*2] Nagoya Institute of Technology

The objective of this paper is to develop machine learning-based facilitation agent for facilitating online discussion in collective intelligence, particularly for online discussion in deliberation. The main idea is to model facilitator's human behaviour by using machine learning technique, case-based reasoning paradigm,. After introducing the details of the proposed machine learning-based approach for facilitation of online discussion, the paper presents some preliminary results along with some outline of the on-going research tasks and future work. The results demonstrate that it is feasible and effective to develop machine learning-based agent for smoothing the discussion and achieving a consensus.

1. Introduction

Deliberation is defined as the activity of small group of people who make the best solution for themselves [Ito 2017]. Over centuries, such decision-making process never changed. This deliberation process is controlled by a small group of powerful people who make the policies without incorporation of public opinion from crowd, and excludes the most people's involvement during the decision-making. Such an approach is becoming inadequate because many important ideas are not properly incorporated. Today, democratically, most people or crowds have to be involved in deliberation.

With the rapid development of Internet, the Internet-based online discussion in crowd-scale deliberation [Klein 2011] or in collective intelligence has attracted many efforts from researchers in social science and computer science. Online crowd decision-making support has received an amount of research interests, and some such support systems have been developed. For instance, Climate CoLab at MIT [Introne 2011] was a pioneer project which aims at harnessing the collective intelligence of thousands of people around the world to make arguments on global climate issues. The project developed a web-based crowdsourcing platform to facilitate the online argumentation [Klein 2011, Gurkan 2010, Klein 2007] democratically. Another example is COLLAGREE developed at Nagoya Institute of Technology (NiTech); it is a web-based online discussion platform [Ito, 2014], which provides a facilitator the support for managing online discussion to effectively achieve the consent through various mechanisms, including facilitation, incentives [Ito 2015], discussion-tree [Sengoku 2016], and understanding. The project team has applied the COLLAGREE to political applications such as city planning forum to collect the crowd opinion from public. For example, NiTech and Nagoya City used COLLAGREE for generating the consent for Next Generation Total City Planning. With the help of COLLAGREE, the Nagoya City gathered many opinions from public citizens. On the other hand, the people from city can understand the importance of next generation city plan. Eventually a consent decision can be achieved democratically. Such online argumentation platforms or forums require the facilitators having systematic methodologies to efficiently guild the discussion toward to consensuses by integrating ideas and opinions and avoiding flaming.

Existing online discussion systems or collective intelligence support systems require the human facilitators to conduct facilitation in order to guide/ensure the online discussion towards consensus. However, human facilitators-based online discussion systems remain several challenging issues such as human bias, time/location restriction, and human resources constrains. To address these challenges, relieve some burden of facilitators, and reuse the prior experience and skills of the facilitators, it is desirable that more advanced techniques are available for supporting the automated facilitation to achieve the consensuses efficiently.

Fortunately, the advancement of machine learning and multi-agent systems techniques provides a venue for developing facilitator agent to automate facilitations for large-scale online discussion. One of machine learning techniques available is case-based reasoning (CBR), which provides an effective reasoning paradigm for modeling the human cognition behaviors in solving real-world problems. CBR-based approach has been widely applied to many applications such as fault diagnostics [Yang 2003], recommendation systems, and judge supporting systems [Lopes 2010]. We believe in that machine learning-based facilitation, specifically, CBR-based method should be a good solution to crowd-scale deliberation or online discussion facilitation. Therefore, we propose a CBR approach to facilitating the crowd-scale online discussion in order to achieve a consensus efficiently. The main idea is to develop CBR-based facilitation actions/mechanisms, including better idea generation, smooth discussion, avoiding negative behavior and flaming, and maintaining online discussion, consensus-oriented guidance and navigation, and so on. The paper mainly discuss the basic ideas on developing machine learning-based facilitation agent and some on-going research tasks and future work.

Following this Section, the paper presents the proposed CBR-based approach for facilitating the online discussion in details;

Chunsheng Yang, National Research Council Canada, 1200 Montreal Road, Room370a@M50, Ottawa, ON, Canada, Chunsheng.Yang@nrc.gc.ca, Tel 1-613-993-0262

Section III discusses the on-going research tasks and future work; and the final Section concludes the paper.

2. Machine learning-based facilitation agent

Machine learning techniques have been widely applied to various real-world problems and have been achieved great success in developing machine learning-based modeling technologies. Today, the machine learning-based modeling technology has become a powerful tool for building models to explain, predict, and describe system or human behaviors. The main task is to develop the data-driven models from the historic data or past experience by using machine learning algorithms. The developed models have the given ability to explain, predict, and describe the system or human behaviour. For example, in the prediction applications, the machine learning-based models can forecast the system operating status, including failures or faults. With such predictions the proactive actions can be taken to maintain the system availability. In this work, we contemplate to use a case-based reasoning approach or paradigm to model facilitators' behavior or facilitation by using their experience accumulated in past.

2.1 CBR-based modeling for cognition

CBR is rooted in the works of Roger Schank on dynamic memory and the central role that a reminding of earlier episodes (cases) and scripts (situation patterns) has in problem solving and learning [Schank 1983]. Today, Case-based reasoning is a paradigm for combining problem-solving and machine learning to solve real-world problems. It has become one of the most successful applied intelligences for modeling human cognition. The central tasks in CBR-based methods and systems [Amodt 1994] are: "to identify the current problem situation, find a past case similar to the new one, use that case to suggest a solution to the current problem, evaluate the proposed solution, and update the system by learning from this experience. How this is done, what part of the process that is focused, what type of problems that drives the methods, etc. varies considerably, however". A general CBR-based system or agent can be described by a reasoning cycle composed of the following four steps:

- RETRIEVE the most similar case from existing case bases;
- REUSE the solution in the case to solve the problem such as flaming, wrong post to the issue, distraction post;
- REVISE the proposed solution if necessary;
- RETAIN the parts of this case into a case base for future problem solving.

2.2 Case composition and definition

In general a case documents relationships between problems and its solutions. CBR solves a new problem by adapting similar solutions used for a similar problem in the past. For online discussion facilitation, a case can be defined as three components (as shown as Figure 1): online discussion case description, facilitation action, and case management. Following is the brief description for each components.

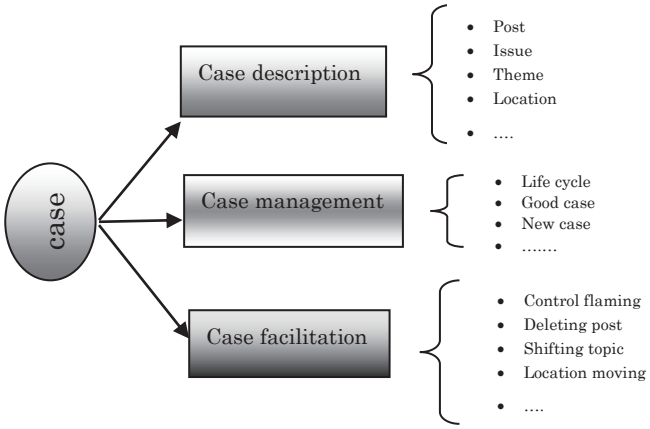

Fig.1 The case composition for online discussion

Case Description: This component contains discussion post, issue related to discussion, topics, theme, and so on. Post could be a free text, or a group of sub posts.

Case Management: This component consists of necessary case management information such as case status, case life cycle, case type, case consistence, and so on.

Case Facilitation: This component records the facilitation actions conducted by human facilitator over the past online discussion. The main facilitation could be flaming control, topic shift, post combination, post deletion, idea promotion, and so on.

From online discussion practice such as Nagoya City Planning, we have collected the data to create cases based on the case definition. It is especially useful to create facilitation cases which documents how a facilitator guided the online discussion; what kind of facilitation was used; how a facilitation action was taken, and so on.

2.3 Similarity computation

Based on the case definition above, a CBR method must provide a similarity algorithm for computing the similarity between two cases. Using computed similarity, the similar cases can be retrieved from a case base. In this work, we provide a global similarity algorithm, which computes the global similarity (sim) using Equation 1.

$$sim = \frac{\sum_{i=1}^{N} \omega_i sim_i(f_i, f_i')}{\sum_{i=1}^{N} \omega_i} \quad \cdots\cdots\cdots\cdots (1)$$

where, *sim* is the global similarity of two problems; N is the number of features or attributes that contribute to similarity; ω_i is the weigh coefficient of each feature; sim_i is a local similarity; f_i, f_i' are the i^{th} features in a case and given problem description. It is computed with Nearest Neighbor *(NN)* distance algorithm (*NN* method) for regular types of the features. For a free "text" feature, we use natural language processing techniques to compute local similarity. Particularly, we used IE (Information Extraction) method to compute the text similarity by using the library provided in OpenNPL package [Weber 2001]. We used the Maximum Entropy algorithms implemented in the OpenNLP package to compute the local similarity for two text messages as expressed as Equation 2.

$$sim_i\ (f_i, f_i') = \frac{|f_i \cap f_i'|}{(|f_i| \cup |f_i'|)} \ldots\ldots\ldots\ldots\ldots (2)$$

2.4 CBR-base facilitation agent framework

Once the case base is created, the CBR-based facilitation agent is ready constructed in online discussion system or platform. In general, such a facilitation agent can be implemented following the designed framework showed as in Table 1.

Table 1, the pseudocode for facilitation agent framework
(*Note: CB: case bases, C: case from Post, C': retrieved case from CB, FA: facilitation action from C')*

Input: *caseBase (plain text file, CB);*
Steps:
CB =Loadthecasebaseinmomorry (CB text file);
C= GetOnlineDiscussionCase (post ,issue, theme);
C'= StartReasonningCycle(C) ;
⇨ *RrtriveCase(C,SIM());*
⇨ *SolutionAdaptation(C')*
⇨ *ReviseCase(C');*
⇨ *RetainCase(C');*
FA =AdaptatFacilitation(C');
ExecuteFAcilication (FA);
Stop

As described in Table 1, the first step is to load the cases (stored in external files or database) into memory given a case composition and configuration mapping information. Once the case base is loaded into memory, a facilitation agent can execute the CBR reasoning cycles to retrieve the similar case in a case base for obtaining facilitation action give a post, issue and theme. Second step is to adapt the facilitation from the similar case for given case; the third step is to modify the case if necessary; the last step is to retain the revised case and save it back to the case base as a new case. The final step is to execute the facilitation action based on adapted facilitation action to the current post if it requires a facilitation action.

3. Discussion and Future Work

This paper mainly reports our ongoing research project. The objective is to present the ideas for developing machine learning-based agent for online discussion facilitation. Therefore many tasks are ongoing. Since focusing on CBR-based approach for facilitation, we only discuss the CBR related ongoing tasks. The other machine learning-based methods for automated facilitation will be reported in other papers.

3.1 Case structure extension and similarity algorithm

The case defined above is a basic structure. To reflect the various online discussion and complexity of facilitator's behaviour, the case structure may become complicated and complex. The similarity computation algorisms have also to be further investigated and extended from existing simple algorithm. For example, we are exploring a graph-based case structure in order to build case from a group post instead of one individual post [Gu 2018]. On the other hand, we have to investigate new algorithms for computing similarity of graph-based online discussion cases

Cases can be created either from historic data or simulation data. In this work, we conducted an online discussion forum to collect the real data. The forum was set up as a "CBR approach to support facilitation in COLLAGREE". We created the theme for an online discussion in the laboratory. The online discussion was managed and guided by a facilitator who maintains the online discussion in three phases: divergence, convergence, and evaluation. The facilitator used the support vehicle provided to navigate the forum from divergence to convergence to evaluation. Using collected data, we created some cases which reflect the facilitator's facilitation during online discussion. However, to enrich the facilitation more data are required for case creation. One way is to conduct the simulation to generate more facilitation data for creating more cases.

3.2 Machine learning-based case adaptation

In CBR research area, one remaining challenge is case adaptation. It is normal that we can't retrieve a similarity case from a case base to obtain a similar facilitation action for controlling and managing online discussion in practice. Therefore, the CBR-based agent has to adapt a facilitation action. To this end, we have to build the ability for agent to learn a new facilitation action. This motivates us to investigate the machine learning-based case adaptation methods for facilitation agent.

3.3 Case base management

This is a vital research topic for any CBR-based applications. The existing cases are manually created from the forum data collected in COLLAGREE. This is a time-consuming task and requires rich domain knowledge to understand the contents in the post or opinion. With the increasing of the collected data, manual case creation will be a challenge. An automated case creation mechanism is expected and necessary. Therefore two necessary research topics are described as follows:

(1) Automated case generation: As we discussed above, automated case creation is desirable to relieve the burden of manual case creation. From the viewpoint of machine learning, automated case creation is a supervised learning problem. It requests the annotated information to decide the case property or types. To do this sentiment analysis of the post contents is inevitable and vital for determining the case types: positive, natural, and negative. Another challenge is machine translation of language. During the online discussion it may encounter the multiple language. When generating cases from different language the automated machine translation is required.

(2) Case base management: In this work, the case base management still remains a challenge. To manage the case base efficiently, case redundancy and consistence have to be investigated in order to ensure the quality and integrity

of the case bases. Another challenge is case adaptation from the existing case and case updating to existing cases.

3.4 Validation and evaluation

Validation and evaluation for a CBR-based systems is always a challenge issue in developing CBR-based applications. It requires many efforts to design the procedures and methods. In this work, the following tasks will be conducted:

(1) Continue to collect the data from online discussion forum using COLLAGREE and create more cases for evaluation;
(2) Evaluate the performance of CBR-based systems for facilitation support by comparing the results with one from human facilities; and
(3) Validate the scalability of cases crossing different themes, even domains.

4. Conclusions

This paper reported an ongoing research project. The objective is to develop a machine learning-based facilitation agent for online discussion system to perform the automated facilitation in crowd-scale deliberation. After describing the proposed approach, we discussed some on-going research tasks and future work.

ACKNOWLEDGMENT

This work was supported by the JST CREST fund (Grant Number: JPMJCR15E1), Japan. We would like to thank all project members and related people for their contribution in the studies and the experiments. We are also grateful for all participants at Ito-Lab, Nagoya Institute of Technology in online discussion on CBR application to COLLAGREE.

References

[Amodt, 1994] A. Aamodt and E. Plaza, “Case-based reasoning: Foundational issues, methodological variations, and system approaches”, AI Communications, Vol. 7 No. i, 1994.

[Gu, 2018] W. Gu, A. Moustafa, T. Ito, M. Zhang. and C. Yang, “A Case-based Reasoning Approach for Automated Facilitation in Online Discussion Systems”, The Proceedings of The 2018 International Conference on Knowledge, Information and Creativity Support Systems (KICSS 2018), Thailand, Nov. 2018

[Gurkan , 2010] A. Gurkan, L. Iandoli, M. Klein, and G. Zollo, “Mediating debate through on-line latrge-scale atgumentation: Evidence from the field”, Information Science Vol. 180, No. 19, 2010, pp. 3686-3702

[Ito, 2015] T. Ito, Y. Imi, M. Sato, T. K. Ito, and E. Hideshima,”Incentive Mechanism for Managing Large-Scale Internet-Based Discussions on COLLAGREE”, Collective Intelligence 2015, May 31 – June 2, 2015, the Marriott Santa Clara in Santa Clara, CA (poster).

[Ito, 2014] T. Ito, Y. Imi, T. K. Ito, and E. Hideshima, “COLLAGREE: A Faciliator-mediated Large-scale Consensus Support System”, Collective Intelligence 2014, June 10-12, 2014. MIT Cambridge, USA. (poster)

[Ito, 2017] T. Ito, T. Ostuka, S. Kawasa, A. Sengoku, S. Shiramatsu, T.K. Ito, E. Hideshima, T. Matsuo, T. Oishi, and R. Fujita, “Experimental results on large-scale cyber-physical hybird discussion support”, International Jouran of Crowd Science, Vol. 1 No. 1, 2017

[Introne , 2011] J. Introne, R. Laubachar, G. Olson, and T. Malone, “The Climate Colab: Large scale model-based collaborative planning”, Proceedings of International Conference on Collaboration Technologies and Sytems (CTS 2011), 2011

[Klein, 2011] M. Klein, “Toward crowd-scale deliberation”, DOI: 10.13140/RG.2.2.12264.06401 , Massachusetts Institute of Technology, available at https://www.researchgate.net/publication/317613473Towards_Crowd-Scale_Deliberation

[Klein, 2012] M. Klein, “Enabling large-scal deliberation using attention-mediation metrics”, Computer Supported Cooperative Work(CSCW), Vol. 21, No. 4/5, pp.449-473, 2012

[Klein, 2007] M. Klein, “Achieving collective intelligence via large-scale on-line argumentation”, CCI working paper, 2007-001, April, 2007

[Lopes, 2010] E. C. Lopes and U. Schiel, “Integrating Context into a Criminal Case-based Reasoning Model”, the proceedings of 2nd International Conference on Information, Process, and Knowledge management, 2010

[Schank, 1983] R. C. Schank. “Dynamic Memory”, Cambridge Univ. Press, 1983.

[Sengoku, 2016] A. Sengoku, T. Ito, K. Takahashi, S. Shiramatsu, T.K. Ito, E. Hideshima and K. Fujita, “Discussion Tree for Managing Large-Scale Internet-based Discussion” , Collective Intelligence 2016, Stern School of Business New York University , June 1-3, 2016

[Weber, 2001] R. Weber, D. W. Aha, N. Sandhu, H. Mounoz-Avila, “A textual case-based reasoning framework for knowledge management applications”, Proceedings of Knowledge Management by Case-Based Reasioning; Experience and Management as Resue of Knowledge (CWCBR 2001), 2001

[Yang, 2003] C. Yang, R. Orchard, B. Farley, and M. Zaluski, Authoring Cases from Free-Text Maintenance Data, in Proceeding of IAPR International Conference on Machine Learning and Data Mining (MLDM 2003), Leipzig, Germany, July 5-7, 2003, pp.131-140

The 33rd Annual Conference of the Japanese Society for Artificial Intelligence, 2019

An automated privacy information detection approach for protecting individual online social network users

Weihua Li[*1], Jiaqi Wu[*1]

Quan Bai[*2]

[*1] Auckland University of Technology, New Zealand

[*2] University of Tasmania, Australia

Abstract: Massive private messages are posted by online social network users unconsciously every day, some users may face undesirable consequences. Thus, many studies have been dedicated to privacy leakage analysis. Whereas, there are very few studies detect privacy revealing for individual users. With this motivation, this paper aims to propose an automated privacy information detection approach to effectively detect and prevent privacy leakage for individual users. Based on the experimental results and case studies, the proposed model carries out a considerable performance.

1. Introduction

Online social networks (OSNs) have become ubiquitous in people's activities. The popularization of OSNs turns out to be a double-edged sword. On one hand, it provides convenience for people to communicate, collaborate, and share information. On the other hand, OSNs also come with serious privacy issues. Without given much attention by the users, a massive amount of private information can be accessed publicly through OSNs. Users may expose themselves to a wide range of "observers", which include not only relatives and close friends, but also strangers and even stalkers. This raises a serious cybersecurity issue, i.e., online privacy leak.

Online privacy leak means that an individual user shares his/her private information to people who he/she does not know well or even strangers on the Internet. This can be very dangerous for general Internet users, especially with the booming of OSNs. It is necessary to have a tool to assist general users to make better use of OSNs and protect them from leaking privacy information [Wang 11] [Hasan 13]. Hence, it is essential to detect privacy leakage in OSNs and remind individual online social network users before posting any privacy-related message. Under this motivation, in this paper, we propose a novel privacy detection framework for individual users of OSNs by using a Deep Learning approach. Twitter has been used as the source of data for training and validating our proposed framework since it is the biggest microblogging social media in the world [Mao 11]. Based on the generic definition of privacy and the characteristics of OSNs, the definition of "individual privacy" in OSNs have been formally defined. Furthermore, a deep learning-based approach has been developed and utilized to extract privacy-related entities from the messages posted by the users.

The rest of the paper is organized as follows. Section 2 reviews the existing research work regarding data leaks on OSNs. Section 3 introduces the automated privacy information detection framework. In Section 4, two experiments have been conducted to evaluate the proposed framework by using a real-world dataset collected from Twitter. Section 5 concludes this study, as well as the limitations and future work.

Contact: Dr Weihua Li, Auckland University of Technology, 55 Wellesley St E, Auckland, 1010, NZ, +64 09921 9999

2. Related Work

Privacy leakage detection in OSNs has attracted great attention to many researchers. A few studies have been conducted to analyze user privacy revealing on Twitter. People are very cautious about their personal information, e.g., home address, phone number, etc., but they consciously or unconsciously disclose their plans and activities through posting information in OSNs [Humphreys 10]. Publishing such messages online can possibly raise serious security issues. For example, a message saying "going out for holiday" implies that no one stays at home, which may cause robbery. Therefore, users should be reminded before delivering such event-related information. Mao, Shuai and Kapadia (2011) present a detection approach to analyzing three types of sensitive tweets, i.e., drunk, vacation and disease tweets. The research on privacy issues is not restricted to Twitter. Acquisti and Gross (2006) investigate the privacy concerns of users on Facebook. Dwyer, Hiltz, and Passerini (2007) compare the trust and privacy issues between Myspace and Facebook. Bhagat, Cormode, Srivastava, and Krishnamurthy (2010) show that privacy can be revealed by predicted social graph.

Whereas, very few studies investigate how to detect individual privacy information and protect individual OSNs users from online privacy leak. Therefore, in this study, instead of assisting the organizations, we target the individual online users and keep them away from privacy leakage. As almost all the posts by users are unstructured data, the information extraction plays a pivotal role in the proposed framework.

Named Entity Recognition (NER) is an important method for extracting domain-specific information [Nadeau 07]. Given the context of privacy detection domain, NER can assists users in identifying privacy-related entities after given sufficient training. Traditionally, Conditional Random Field (CRF) classifier has been employed for NER due to its robustness and reliability. Gomez-Hidalgoy et al. (2010) proposed a mechanism which is capable of detecting named entities, e.g., a company, brand, or person, using NER. Nowadays, Bi-directional Long Short-Term Memory with Conditional Random Field (Bi-LSTM CRF) model becomes more popular as it achieves more promising results [Lample 16]. Therefore, we utilize Bi-LSTM CRF for privacy-related entities extraction. Privacy Information Detection.

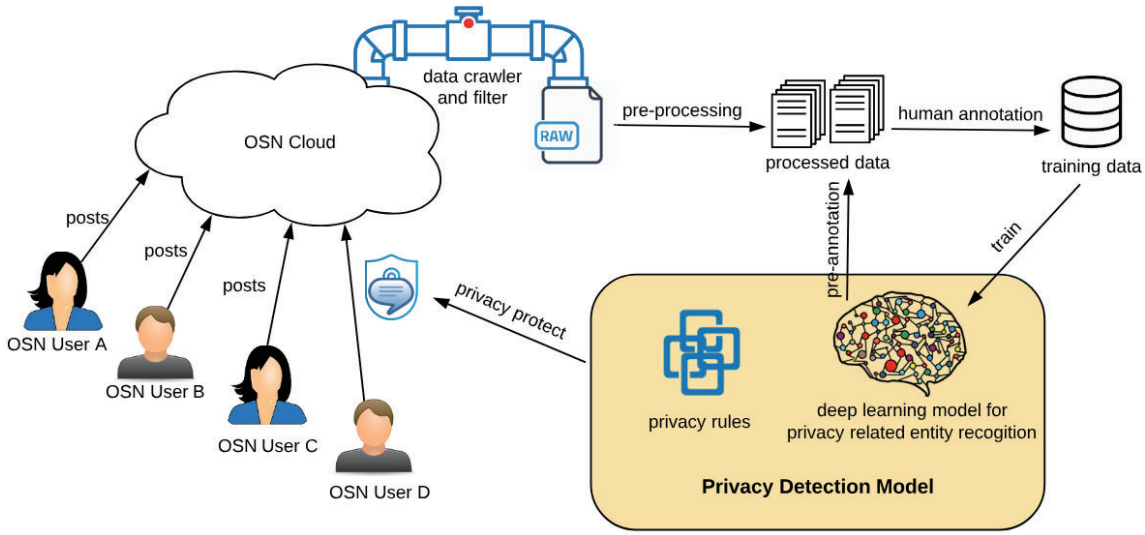

Fig 1 The Proposed Privacy Detection Framework

3. Privacy Information Detection Framework

3.1 Definition of Privacy

"Privacy" has a very broad meaning, which generally refers to the people's right to keep their personal matters and relationships secret [Gehrke 11]. In this sense, the privacy information is associated with something personal, as well as the matters of past, present, and future. Given the generic definition, in this paper, the privacy information that users tend to publish on the OSNs is defined as a sequence of words, stating or implying any individual's personal information, preferences, events that he or she involved.

Based on the definition given above, the privacy information incorporates four categories of entities, i.e., PERSON, TRAIT, PREF, and EVENT. More specifically, PERSON refers to any expression that identifies a real person; TRAIT represents the personally identifiable information, such as birth date and phone number; PREF refers to an individual's preference or hobbies; EVENT indicates the matters or activities that one involves anytime anywhere. Therefore, given a word sequence, the judgment of privacy information can be summarized as a rule as follows:

$$\exists \mathrm{PERSON} \wedge (\exists \mathrm{TRAIT} \vee \exists \mathrm{PREF} \vee \exists \mathrm{EVENT}) \longrightarrow \mathrm{P(message)}$$

3.2 The Automated Privacy Detection Framework

Our automated privacy information detection framework is demonstrated in Figure 1. The framework illustrates how the privacy detection model gets trained and utilized.

Users keep posting messages to the OSNs hosting in the cloud. Such raw unstructured and public data can be obtained through crawlers or APIs provided by the OSNs. For example, Twitter allows developers to search public tweets if the proposed project is approved. Given the context of privacy detection, the potential privacy-related data should be filtered and downloaded. Pre-processing is conducted based on specific rules, such as removing meaningless words and characters and parsing word sequences to tokens. The processed data are supposed to be further enriched by running through the pre-annotation if a privacy-detection NER model is available. Next, human involvements, i.e., manual annotation, are required. Specifically, according to the aforementioned definition of privacy information, it is essential to recognize the privacy-related entities, i.e., PERSON, TRAIT, PREF, and EVENT. The annotation also aims to figure out these four types of entities from the processed data. The annotated dataset is then fed into the deep learning model for training.

The privacy detection model consists of two components, i.e., a deep learning model for privacy-related entities recognition and privacy definition rules. For any posting messages by the OSN users, the proposed model is capable of judging whether the message is privacy-related or not. Moreover, as the privacy rules are properly defined, the privacy detection model can also explain the reason why the message is potentially privacy-related. Using a single deep learning model for private messages classification definitely loses the capability of justification.

3.3 Privacy-Related Entities Recognition

The privacy-related entities recognition plays an important role in the entire framework. There are two major aspects affecting the performance of an NER model, i.e., the annotation approach and the algorithm.

In this study, the Bi-LSTM CRF model has been employed for privacy-related entities recognition in our model, as it is capable of achieving more promising results compared with that of other classic algorithms when being applied to NER [Lample 16]. Bi-LSTM can learn long-term dependency due to the structure of the 'cell' in the hidden layer. Moreover, it can adjust the impact of previous states on the current states through the forget gate, input gate and output gate in the 'cell' [Graves 05]. However, it lacks the feature analysis on the sentence level, which can be solved by CRF. It can consider contextual conditions to make global optimal predictions. Combining the LSTM and CRF together can label sequence effectively when ensures to extract contextual features [Huang 15].

In regards to the annotation approach, BIO encoding scheme is utilized to tag entities in NER task [Kim 04]. BIO encoding scheme is a standard method which can solve the joint segmentation problem in labelling sequence by transforming them into raw labelling problem. Specifically, 'B-' is used as a prefix of an entity, implying the beginning of an entity; prefix 'I-' tags other characters indicating the tag is inside of an entity and 'O' is used for characters which do not belong to any pre-defined entities. For example, privacy-related entities fall into BIO scheme are normally annotated as follows:

I	*watch*	*a*	*movie*	*with*	*Christine.*
B-PERSON	**B-EVENT**	**I-EVENT**	**I-EVENT**	**O**	**B-PERSON**

4. Experiments

Two experiments have been conducted to evaluate the proposed privacy detection framework. The first experiment aims to train a privacy-related entities recognition model using Bi-LSTM CRF model. The second experiment gives some case studies to further demonstrate the effectiveness of the proposed privacy detection model.

4.1 Data description

Twitter is one of the largest OSNs, which enables users to conduct online social activities, including the distribution of any ideas or information. In Twitter, the messages that are posted and interacted by users are known as "tweets". Twitter provides APIs, allowing developers to search and store tweets. Therefore, we utilize Twitter API to collect 18k tweets by searching for some terms which potentially result in privacy leakage, such as pronouns, sensitive words, plans, etc.

4.2 Experiment 1

In Experiment 1, a privacy detection model based on Bi-LSTM CRF is trained to recognize the privacy-related entities. Through which, the users can be prompted before potential privacy leakage occurs. According to the definition of privacy and BIO encoding scheme mentioned previously, nine tags have been defined, i.e., 'B-PERSON', 'I-PERSON', 'B-TRAIT', 'I-TRAIT', 'B-PERF', 'I-PERF', 'B-EVENT', 'I-EVENT' and 'O'. Around 200 tweets have been annotated manually by applying these nine tags.

In this experiment, we leverage three traditional evaluation metrics as follows:

- **Precision**: the percentage that privacy-related entities can be labelled correctly among all the entities which are labelled privately in the test dataset.
- **Recall**: the percentage that privacy-related entities can be labelled correctly among all the actual privacy entities in the test dataset.
- **F1-score**: the weighted average of precision and recall, which takes both the two measures into account.

After 50 epochs' training, the performance of the deep learning model is demonstrated in Table 1.

Table 1 Performance of Privacy-Related Entities Recognition

Entity	Precision	Recall	F1-score
PREF	0.99	0.67	0.8
TRAIT	0.68	0.88	0.77
PERSON	0.98	0.93	0.95
EVENT	0.77	0.67	0.71
Avg/Total	**0.86**	**0.83**	**0.84**

4.3 Experiment 2 Case Study

In this experiment, we further demonstrate the effectiveness of the proposed privacy detection model by selecting three tweets posted recently and analyzing the results produced by the model.

Case 1: Adam and I are having lunch tomorrow.

Results: Adam (B-PERSON) and I (B-PERSON) are having (B-EVENT) lunch (I-EVENT) tomorrow.

Explanations: Based on the privacy rules, this tweet is privacy-related since it mentions both PERSON and EVENT.

Case 2: Watching a movie is a good way to relax!

Results: Watching (B-EVENT) a (I-EVENT) movie (I-EVENT) is a good way to relax!

Explanations: This tweet is just a simple statement regarding "Watching a movie", which is not a private one.

Case 3: My son is crazy about coke.

Results: My (B-PERSON) son (I-PERSON) is crazy about coke (B-PREF).

Explanations: This tweet talks about PERSON and PREF, it is privacy-related.

5. Conclusion and Future Work

In this paper, we presented a privacy information detection framework for individual OSN users. The objective is to protect end users from potential privacy leakage before posting any messages. The proposed framework explains the process of data collection, processing, model training and how it works. Both privacy rules and Bi-LSTM CRF model are leveraged in the privacy detection model. Thus, the proposed model is equipped with the capability of both detection and results explanation.

This study is still very preliminary and there is huge space for further investigation and extension. In the future, we intend to utilize a larger training dataset for performance evaluation and improve the performance of the privacy-related entities recognition by fine-tuning the parameters of Bi-LSTM CRF. Moreover, different tweets are associated with different degrees of privacy leakage. How to evaluate and score the privacy-leakage degree is also under our consideration.

References

[Wang 11] Wang, Y., Norcie, G., Komanduri, S., Acquisti, A., Leon, P. G., & Cranor, L. F. "I regretted the minute I pressed share: A qualitative study of regrets on Facebook.". *Proceedings of the seventh symposium on usable privacy and security*,pp.10 (2011).

[Humphreys 10] Humphreys, L., Gill, P., & Krishnamurthy, B. "How much is too much? Privacy issues on Twitter." *Conference of International Communication Association* (2010).

[Mao 11] Mao, H., Shuai, X., & Kapadia, A. "Loose tweets: an analysis of privacy leaks on Twitter." *Proceedings of the 10th annual ACM workshop on Privacy in the electronic society*. (2011).

[Hasan 13] Hasan, O., Habegger, B., Brunie, L., Bennani, N., & Damiani, E. "A discussion of privacy challenges in user profiling with big data techniques: The excess use case." *Big Data (BigData Congress), 2013 IEEE International Congress on*. (2013).

[Wang 17] Wang, Q., Bhandal, J., Huang, S., & Luo, B. "Classification of private tweets using tweet content." *Semantic Computing (ICSC), 2017 IEEE 11th International Conference on.*(2017).

[Aborisade 18] Aborisade, O., & Anwar, M. "Classification for Authorship of Tweets by Comparing Logistic Regression and Naive Bayes Classifiers." *2018 IEEE International Conference on Information Reuse and Integration (IRI)*. (2018).

[Lample 16] Lample, G., Ballesteros, M., Subramanian, S., Kawakami, K., & Dyer, C. "Neural architectures for named entity recognition." *arXiv preprint arXiv:1603.01360* (2016).

[Bengio 94] Bengio, Y., Simard, P., & Frasconi, P.. "Learning long-term dependencies with gradient descent is difficult." *IEEE transactions on neural networks* Vol.5, No.2, pp.157-166 (1994).

[Graves 05] Graves, A., & Schmidhuber, J. "Framewise phoneme classification with bidirectional LSTM and other neural network architectures." *Neural Networks* Vol.18, No.5-6, pp. 602-610 (2005).

[Huang 15] Huang, Z., Xu, W., & Yu, K. "Bidirectional LSTM-CRF models for sequence tagging." *arXiv preprint arXiv:1508.01991* (2015).

[Bhagat 10] Bhagat, S., Cormode, G., Srivastava, D., & Krishnamurthy, B. "Prediction Promotes Privacy in Dynamic Social Networks." *WOSN*. (2010)

[Acquisti 06] Acquisti, A., & Gross, R. "Imagined communities: Awareness, information sharing, and privacy on the Facebook." *International workshop on privacy enhancing technologies.* (2006)

[Dwyer 07] Dwyer, C., Hiltz, S., & Passerini, K. "Trust and privacy concern within social networking sites: A comparison of Facebook and MySpace." *AMCIS 2007 proceedings,* pp. 339 (2007).

[Kim 04] Kim, J. D., Ohta, T., Tsuruoka, Y., Tateisi, Y., & Collier, N."Introduction to the bio-entity recognition task at JNLPBA." *Proceedings of the international joint workshop on natural language processing in biomedicine and its applications.* pp.70-75 (2004).

[Wu 15] Wu, Y., Xu, J., Jiang, M., Zhang, Y., & Xu, H. "A study of neural word embeddings for named entity recognition in clinical text." *AMIA Annual Symposium Proceedings*, Vol. 2015, p. 1326 (2015).

[Nadeau 07] Nadeau, D., & Sekine, S. "A survey of named entity recognition and classification." *Lingvisticae Investigationes*, Vol.30, No.1, pp.3-26. (2007).

[Gehrke 11] Gehrke, J., Lui, E., & Pass, R. "Towards privacy for social networks: A zero-knowledge based definition of privacy." *Theory of Cryptography Conference*, pp. 432-449 (2011).

[Gomez-Hidalgo 10] Gomez-Hidalgo, J. M., Martin-Abreu, J. M., Nieves, J., Santos, I., Brezo, F., & Bringas, P. G. (2010, August). Data leak prevention through named entity recognition. In Social Computing (SocialCom), 2010 IEEE Second International Conference on (pp. 1129-1134). IEEE.

[3J3-E-4] Robots and real worlds: Human Interactions

Chair: Yihsin Ho (Takushoku University), Eri Sato-Shimokawara (Tokyo Metropolitan University)
Thu. Jun 6, 2019 1:50 PM - 3:10 PM Room J (201B Medium meeting room)

[3J3-E-4-01] Automatic Advertisement Copy Generation System from Images

○Koichi Yamagata[1], Masato Konno[1], Maki Sakamoto[1] （1. The University of Electro-Communications）

1:50 PM - 2:10 PM

[3J3-E-4-02] Eye-gaze in Social Robot Interactions

Koki Ijuin[2], ○Kristiina Jokinen Jokinen[1], Tsuneo Kato[2], Seiichi Yamamoto[2] （1. AIRC, AIST Tokyo Waterfront, 2. Doshisha University）

2:10 PM - 2:30 PM

[3J3-E-4-03] A Team Negotiation Strategy that Considers Team Interdependencies

○Daiki Setoguchi[1], Ahmed Moustafa[1], Takayuki Ito[1] （1. Nagoya Institute of Technology）

2:30 PM - 2:50 PM

[3J3-E-4-04] Identity Verification Using Face Recognition Improved by Managing Check-in Behavior of Event Attendees

○Akitoshi Okumura[1], Susumu Handa[1], Takamichi Hoshino[1], Naoki Tokunaga[1], Masami Kanda[1] （1. NEC Solution Innovators, Ltd.）

2:50 PM - 3:10 PM

The 33rd Annual Conference of the Japanese Society for Artificial Intelligence, 2019

Automatic Advertisement Copy Generation System from Images

Koichi Yamagata[*1], Masato Konno[*1], Maki Sakamoto[*1]

[*1] Graduate School of Informatics and Engineering, The University of Electro-Communications

When we want to sell something, the presence of a good advertisement copy often affects sales. In this research, we develop an automatic advertisement copy generation system. Most existing systems only enter keywords, and the potential image of the product is not necessarily reflected by keywords only. We propose a method to generate advertisement copies using images as input to convey potential messages and the world view. This method uses Word2vec and color information of ad images, and both were confirmed to be effective by evaluation experiments. In the evaluation experiments, the mean score of the proposed method was significantly larger than 4 out of 7, and most of the subjects answered positively to ad copies of our method.

1. Introduction

Advertisement copies describe the features of products with a short number of characters and impact sentences, which are factors that greatly contribute to building brands such as companies and promoting purchase willingness of products. In recent years, there have been many researches on the generation of Japanese sentences and advertisement copy generation. In existing researches, however, they did not focus on describing potential messages and the view of the world that the producer wanted to convey.

In this research, we propose a method to generate appropriate copies reflecting color and sensitivity of given images by using a database that maintains the relationship between color and words.

There are also several prior studies on the relationship between color and sensitivity. Iiba et al. [Iiba 13] focused on the relationship between color and word sensibility, and constructed a system that recommends appropriate colors and fonts for textual sensibility images considering the effect reminiscent of the color of words. Further, Nakamura et al. [Nakamura 12] focused on the relationship between color and lyrics and constructed a music retrieval system with color as input. In this research, we focus on the relationship between colors and words and aim to automatically generate advertisement copies with color input.

Recently, in the field of natural language processing, various methods handling words as distributed expressions are increasing. Mikolov et al. [Mikolov 13] developed Word2vec which is a new model that improves the precision of vector operation of words considering the similarity between words in sentences. In this research, we utilize Word2vec to extract synonyms from a large corpus.

Existing researches on advertising copying were mainly methods of inputting words and keywords, and they were not taken into consideration to convey the latent message or the world view that the creator wished to convey. On the other hand, in this research, we construct an automatic advertisement copy generation system using images as inputs. Color information is extracted from the input image, and a large number of advertisement copies are generated by using a database that maintains the relationship between words and colors, from which adequate copies are determined as outputs.

Contact: Koichi Yamagata, UEC, 1-5-1, Chofugaoka, Chofu, Tokyo182-8585, Japan, koichi.yamagata@uec.ac.jp, 042-443-5535

2. Methods

The flow of the proposed method is as follows:

1. Color information contained in given image is extracted, and some keywords are extracted from the database storing the relationship between words and colors.
2. From the lyrics database, some phrases including the keywords extracted in step 1 are searched and extracted as sentence templates.
3. By using a deep neural network (dnn) based classification model that classifies words used for ad copies or not trained by ad copies corpus, word candidates are selected from the word extracted in step 1.
4. The noun in the template sentences extracted in step 2 are replaced by the words selected in step 3, and they are taken as copy candidate sentences.
5. The ad copy candidate sentences are evaluated by the similarities given by Word2vec, and the most evaluated ad copy candidate sentence is outputted.

In step 1, we utilize the word-color database constructed by [Konno 18]. This database was constructed based on the idea of the relation between sensitivities and music/colors studied by [Nakamura 11]. In this database, among the songs released between 1968 and 2017, we defined words that were often used for lyrics as primitive words (PWs), and each PW has a 45-dimensional color information vector obtained by a psychological experiment. Figure 1 shows 45 colors to define the 45-diensional color vector space. For words other than PWs that were not psychologically tested, latent semantic analysis was performed on them, and color information vectors were given based on the similarities with PWs.

In step 3, pytorch is used as a dnn library. The input data is a bag-of-words vector of a sentence to be classified, and the output data is “copy” or “not-copy”.

In step 4, we use Word2vec model which learned 100,000 songs of Japanese lyrics corpus, and which contains similarities with a poetic point of view. Using this model, we calculate the similarities between words (nouns, verbs, adjectives etc.) contained in sentences and evaluate candidate sentaQSZQences of ad copies.

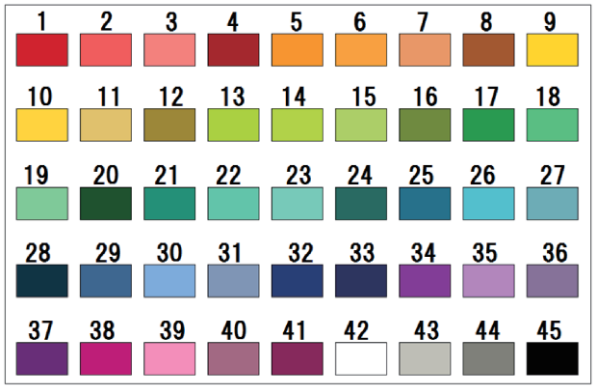

Fig. 1: 45 colors to define the 45-dimmensional color vector space.

3. System Evaluation

In order to evaluate our system, we conducted an evaluation experiment with 30 subjects (7 females and 23 men, mean age = 22.63). We adopted 20 advertisement images actually used from four categories (beverage and food, travel, beauty, fashion), and we prepared five ad copies for each advertisement image by five methods:

A) original ad copy
B) proposed method
C) proposed method without Word2vec
D) proposed method without using the image
E) RNN

For example, when input image was a picture of three can coffees against the background of the night sky, an ad copy of method B (translated into English) was “You will surely drink it tonight”, method C outputted “You laugh, even the deadly midnight dropping the mountain, forever”, method D outputted “Eat coffee and coffee”, method E outputted “Feel coffee and go”.

Subjects were asked to evaluate a total of 100 advertisement copies for the images including the original ad copies and the ad copies outputted by the proposed method. The subjects evaluated the following questionnaires on a scale from 1 to 7:

i. Is it appropriate as an ad copy in this category?
ii. Is it appropriate as an ad copy regardless of category?
iii. Is the grammar of the ad copy appropriate?
iv. Does the ad copy follow the impression of the image?

Table 1 shows the results of the questionnaires (averages and standard errors of scores). We can see that the mean score of the proposed method B is much larger than 3, and most of the subjects answered positively to our method. Comparing the methods A and B, we can see that the proposed method is slightly less than the scores of original advertisements. However, it is not so bad and the difference is small. In the food category, it is confirmed that the proposed method has smaller score differences with respect to the original advertisement. Comparing the methods B and C, we can see that the use of Word2vec is effective. Comparing the methods B and D, we can see that the use of images is effective. Comparing the methods B and E, we can see that the proposed method is much better than the RNN method.

Table 1: Results of questionnaires to evaluate each method (averages and standard errors of scores)

	i	ii	iii	iv
A	5.29±0.07	5.75±0.06	6.03±0.06	5.37±0.07
B	4.90±0.07	5.17±0.06	5.55±0.06	4.22±0.08
C	2.82±0.07	3.15±0.08	3.31±0.08	2.51±0.06
D	4.23±0.08	3.92±0.08	3.81±0.09	3.20±0.07
E	3.18±0.07	2.74±0.07	2.05±0.06	2.75±0.07

4. Conclusion

This study proposed a method to generate advertisement copies using images as input to convey potential messages and the world view. This method uses not only Word2vec but also color information of images, and both were confirmed to be effective by evaluation experiments. In the evaluation experiments, the mean score of the proposed method was significantly larger than 4 out of 7, and most of the subjects answered positively to our method. The proposed method was slightly less than the scores of original advertisements. However, it was not so bad and the difference was small.

References

[Iiba 13] Iiba, S., Doizaki, R., and Sakamoto, M.: Color and Font Recommendations based on Mental Images of Text, Transactions of the Virtual Reality Society of Japan, 18(3), pp.217-226 (2013)

[Nakamura 12] Nakamura, T., Utsumi, A., and Sakamoto, M.: Music Retrieval Based on the Relation between Color Association and Lyrics, Transactions of the Japanese Society for Artificial Intelligence, Volume 27, Issue 3, pp. 163-175, 2012.

[Mikolov 13] Mikolov, T., Yih, W., Zweig, G.: Linguistic Regularities in Continuous Space Word Representations, Conference of the North American Chapter of the Association for Computational Linguistics: Human Language, Technologies (NAACL-HLT-2013) (2013)

[Konno 18] Konno, M., Suzuki, K, and Sakamoto, M.: Sentence Generation System Using Affective Image, 2018 Joint 10th International Conference SCIS and 19th ISIS, 678-682.

[Nakamura 11] Nakamura, T., Kawanishi, K., and Sakamoto, M.: A Possibility of Music Recommendation Based on Lyrics and Color, Transactions of the Japanese Society for Artificial Intelligence, Transactions on Fundamentals of Electronics, Communications and Computer Sciences, Volume J94-A, pp.85-94, No.2 (2011)

The 33rd Annual Conference of the Japanese Society for Artificial Intelligence, 2019

Eye-gaze in Social Robot Interactions – Grounding of Information and Eye-gaze Patterns

Koki Ijuin[*1] Kristiina Jokinen[*2] Tsuneo Kato[*1] Seiichi Yamamoto[*1]

[*1] Doshisha University [*2] AIRC, AIST Tokyo Waterfront

This paper examines human-robot interactions and focuses on the use of eye-gaze patterns in evaluating the partner's understanding process. The goal of the research is to understand better how humans focus their attention when interacting with a robot and to build a model for natural gaze patters to improve the robot's engagement and interaction capabilities. The work is based on the AIST Multimodal Corpus which contains human-human and human-robot interactions on two different activities: instruction dialogues and story-telling dialogues. The preliminary experiments show that there are differences in the eye-gaze patterns given expected and non-expected responses, which affects their understanding and grounding of the presented information. The paper corroborates with the hypothesis that eye-gaze patterns can be used to predict grounding process and provide information to the speaker about how to proceed with the presentation, so as to support the partner's understanding and building of the mutual knowledge. Some consideration is given to future improvements in methodology.

1. Introduction

The goal of the research is to understand better how humans focus their attention when interacting with a robot and to build a model for natural gaze patters to improve the robot's engagement and interaction capabilities. The work follows from the pilot study (Jokinen 2018) in which human gaze patterns were studied when they interacted with a humanoid Nao robot using the WikiTalk application (Jokinen and Wilcock 2014) which allowed the user to navigate among Wikipedia topics, and is also related to eye-gaze in second-language learning with robots (Fujio et al. 2018).

In this paper, we focus on eye-tracking technology and its use in instruction giving and story-telling activities. The hypothesis examined in the paper is that there is a difference between the interlocutor's eye-gaze patterns depending on how their understanding proceeds, i.e. if the partner's utterance is understood, misunderstood or non-understood. By measuring eye-gaze activity in the communicative context we build a model that enables estimation of the partner's level of understanding, and consequently, modification of the presentation if the partner eye-gaze signals problems in the grounding of information. Such a model can help the humanoid robot to better tailor its presentations to the human user, i.e. to enable the use of the partner's eye-gaze signals to establish an appropriate way to continue. In particular, it will enable us to study how eye-gaze is used in grounding information and creating mutual understanding of the discussion topic.

Smooth interaction requires that the partners can easily understand each other and are able to build their conversation on mutual knowledge of what has been discussed. The process of creating such mutual knowledge is called grounding, i.e. the partners ground the semantics of their utterances in the context of their interaction and the context of their world knowledge, Clark & Wilkes-Gibbs (1986).

Earlier work shows that in social situations, humans are sensitive to another person's gaze: it constructs new shared knowledge, communicates experiences, and creates social linkages (Argyle & Cook, 1976; Kendon, 1967). Visual attention is important in cognitive studies (Skarrat et al. 2012), and e.g. turn-taking is commonly coordinated by gaze (Jokinen et al., 2013). Broz et al. (2015) provides an overview of the work on eye gaze and human robot interaction.

Contact: Kristiina Jokinen, AIRC AIST Tokyo Waterfront, Koto, Aomi, Tokyo, *kristiina.jokinen@aist.go.jp*

2. Data collection setup

Experiments were set-up using the lab's SMI eye-tracker and the Nao robot, to collect eye-tracking data. Fig 1. Shows the setup. Each participant had two conversations, one with a human partner (HHI) and one with a humanoid robot (HRI). The conversations were about 10 minutes long. One of the experimenters played the role of the human partner but was different from the one who gave instructions to the participant.

The experiment was conducted in Japanese or English depending on the participant's preferred language. The instructions were the same for both HRI and HHI conditions. Before the experiments, the participants signed a consent form and filled in a pre-experiment questionnaire of their background and expectations. After each interaction (HRI and HHI), they filled in another questionnaire focussing on their experience in the interaction.

Data consists of 30 participants (20 Japanese, 10 English), each having both HHI and HRI conversation. The participants (10 female) were students and researchers, age 20-60, with experience on IT, but no experience on robots. Of the participants, 14 had instruction and 16 chat dialogues.

Data analysis has started using the standard gaze frequency and duration measurements, annotations and statistical analysis,

to analyse the user's gaze patterns during interaction with the robot and with a human partner. Special attention is paid to gesturing and head nodding, and conversational instances such as turn-taking, feedback, and problem cases.

3. Annotation and Analysis

3.1 Annotation Method

Annotation for duration of utterances were done with automatic silence segmentation of ELAN. The audio files which were recorded with eye tracker were used to annotate utterances. Automatic silence segmentation was conducted two times with different thresholds of loudness for determining the silence. The one with low threshold annotates both participant's and partner's utterances, and the other one with high threshold annotates only participant's utterances. The values of those thresholds were manually set by each conversation. The segmentation of partner's utterances was calculated by subtracting those automatic segmentations.

After the segmentation, the participant's utterances in human-robot conversations were manually classified into four types from the perspective of robot's feedback to that utterances: Correct-Understood, Miss-Understood, None-Understood, and Other. Correct-Understood (CU) were tagged to the utterance which robot recognized and gave the correct feedback, Miss-Understood (MU) were tagged to the utterance which robot recognized but gave the unexpected or wrong feedback, and None-Understood (NU) was tagged to the utterance which robot did not recognized and did not give any feedback.

To annotate the eye gaze activities of participants automatically, we created the robot detection system with OpenCV3. We used cascade classifier to detect the position of robot's face in video recorded with eye sight camera of eye tracker. The robot's face was detected as rectangle, and the rectangle of robot's body was estimated with the position of robot's face. After detecting the robot's face and body, the eye gaze activities were automatically annotated into two groups; Gaze Face and Gaze Body, by judging whether the coordinates of gaze point captured by the eye tracker were in those detected rectangles or not. Fig 2 shows the result of robot detection system and gaze point of the participant.

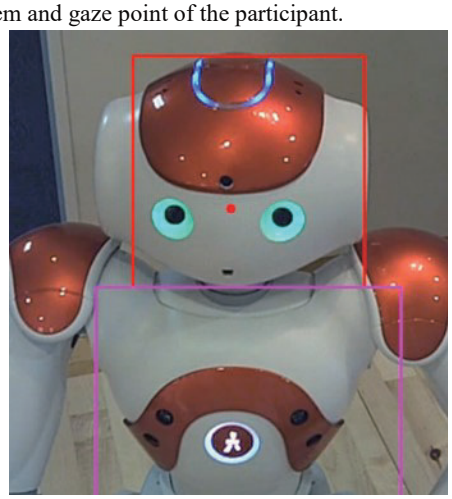

Figure 2 Snapshot of the result of robot detection system. Red rectangle represents the robot's face, purple rectangle represent, the estimated robot's body, and red dot represents the point of participant's gaze

3.2 Methodology of analyses of eye gaze activities

In order to verify how the participant uses his/her eye gaze activities, we conducted quantitative analyses of eye gaze activities during utterances, pauses just before the beginning of utterances, and pauses just after the end of utterances.

We used Gazing Ratios in order to understand how the participant uses eye gaze activities during the human-robot conversations.

Gazing Ratio is defined as:

$$\frac{1}{N}\sum^{N}\left(\frac{DG_{(i)}}{\text{duration of } i\text{-th } w}\right.$$

where $DG_{(i)}$ represents that the duration of participant's gaze toward the robot during *i*-th window. Three types of windows were used: before utterance window, during utterance window, and after utterance window. *N* represents the total number of windows. Gazing Ratio was calculated for each utterance type (CU, MU, and NU).

4. Preliminary Results

The Gazing Ratios were calculated with the data of 19 participants. Figure (ppt p. 26) shows that the temporal change of Gazing ratio for each utterance type in human-robot conversations. The results of eye gaze activities show that the participants tend to gaze away from the robot after they finishes speaking regardless of correctness of robot's feedback. After the robot gives feedback, the participants shift their gaze to the robot again. However, when the robot does not give any feedback to the participants, the participants keep gaze away to the robot for a while, and then they gaze at the robot again.

These results suggest that after the participants answer the

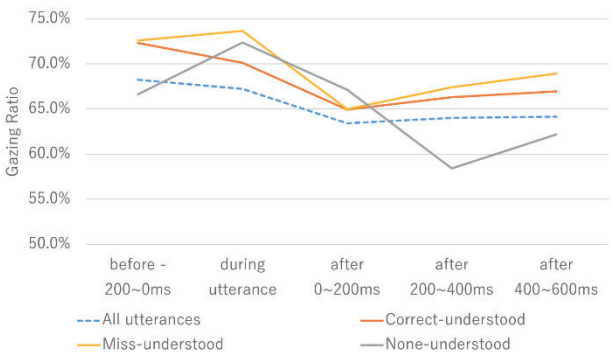

Figure 3 Gazing Ratios of participant during utterances, before the beginning of utterances, and after the end of utterances

question from the robot, they gaze away from the robot during the interval that the robot starts speaking, and if the robot does not start speaking, the participants soon realize that there is something wrong with the conversation so that they gaze at the robot in order to monitor what is going on to the robot.

This quantitative difference of eye gaze activities according to the robot's reaction might be useful to predict the participant's state whether he/she is waiting for the robot's feedback or not.

5. Conclusions

This paper has presented preliminary studies concerning eye-gaze in human-robot interaction and focused especially on the understanding of the presented information. Such grounding is important for the human-robot interaction to progress smoothly and for the robot to exhibit context-aware capability, i.e. be able to take the user's multimodal signals in the given conversation al context into account. The work is based on the AIST Multimodal Corpus which includes eye-tracking data on natural interactions between two humans and between a human and a robot.

The work continues on further analysis and annotation of the corpus and building computational models of the use of eye-gaze in signaling the interlocutors' understanding. As the corpus contains both human-human and human-robot interactions in similar conversational situations, further research is focused on studying the differences in the human gaze behaviour in the two types of conversational settings. This will deepen our knowledge of the function of gazing in interaction in general and the role of being able to detect and analyse gaze-patterns also in human-robot interactions.

Acknowledgement

This paper is based on results obtained from *Future AI and Robot Technology Research and Development Project* commissioned by the New Energy and Industrial Technology Development Organization (NEDO).

References

Argyle, M. and Cook, M. (1976). Gaze and Mutual Gaze. Cambridge University Press, Cambridge.

Broz, F., Lehmann, H., Mutlu, B., and Nakano, Y. (Eds.) (2015). Gaze in Human-Robot Communication. John Benjamins Publishing Company.

Clark, H. & Wilkes-Gibbs D. Referring as a collaborative process. *Cognition 22:*1-39, 1986

Fujio, S., Ijuin, K., Kato, T., Yamamoto, S. (2018). Measurement of Gaze Activities of Learners with Joining-in-type RALL System, Proceedings of the 2018 IEICE General Conference, March 2018 (In Japanese)

Jokinen, K., Furukawa, H., Nishida, M., Yamamoto, S. (2013). Gaze and Turn-taking behaviour in Casual Conversational Interactions. ACM Transactions on Interactive Intelligent Systems (TiiS) Journal, Special Section on Eye-gaze and Conversational Engagement, Vol 3, Issue 2.

Jokinen, K. and Majaranta, P. (2013). Eye-Gaze and Facial Expressions as Feedback Signals in Educational Interactions. In D. Griol Barres, Z. Callejas Carrión, R. López-Cózar Delgado (Eds.) Technologies for Inclusive Education: Beyond Traditional Integration Approaches. Chapter 3, pp.38-58. Hershey, PA: Information Science Reference, IGI Global.

Jokinen, K. and Wilcock, G. "Multimodal Open-domain Conversations with the Nao Robot." In Natural Interaction with Robots, Knowbots and Smartphones - Putting Spoken Dialog Systems into Practice. Springer Science+Business Media, 2014. pp. 213-224

Kendon, A. (1967). Some functions of gaze–direction in social interaction. *Acta Psychologica*, 26 (1): 22–63.

Skarratt, P.A. et al. 2012. Visual cognition during real social interaction. *Frontiers in human neuroscience*. 6, (Jan. 2012), 196

A Team Negotiation Strategy that Considers Team Interdependencies

Daiki Setoguchi[*1] Ahmed Moustafa[*1] Takayuki Ito[*1]

[*1] Nagoya Institute of Technology

ABSTRACT

In automated negotiation, team negotiation is poised as one of the most important negotiation techniques. A team is a group where multiple interdependent agents participate in negotiations as a negotiating party during the course of negotiations. Existing team negotiation strategies did not consider the change in decisions due to the interdependencies within the team. In this paper, we propose a team negotiation strategy that considers the interdependencies within the same team. Towards this end, in the proposed negotiation strategy, we first set the parameters that represent the interdependencies that exist within the team in both directions. Thereafter, a voting process is performed in each direction. By weighting the degree of dependency of each team member, a change in agent decision due to its dependency relationships is measured. A comparative experiment with the existing team negotiation strategies showed the efficiency of the proposed strategy.

1. Introduction

Numerous researches on automated negotiation agents have been done in multiagent research fields [1, 2]. Negotiation has emerged as an important social activity wherein different people with different targets seek to reach an agreement in order to satisfy each other's interests and is indispensable in the real world where various goals exist. Therefore, automated negotiation is attracting attention as it can bring the benefits of negotiation in order to solve real life problems. In this regard, it is thought that it can be applied to route change interference and scheduling system in e-commerce system and transportation system [1, 2, 3]. One of the most important automated negotiation techniques is team negotiation [4, 5]. A team is a group where multiple interdependent agents participate in negotiations as a negotiating party during negotiations. There are numerous negotiation scenarios between multiple groups in the real world such as negotiations between a couple and a real estate agent, a negotiation between a friend and a travel agency.

In these scenarios, the team in the negotiation participates in the negotiation as a single party, but cannot be regarded as one agent. This is because they may have internal conflicting preferences when making team decisions. Even if one of the team members is unlikely to accept the proposal from the negotiating partner, this proposal may be compromised and accepted when another member accepts it. In this way, since all the team members have individual preference information and are affected by the decision of other agents, linear preference information cannot be expressed as one agent. Therefore, it is important to negotiate with the dependency amongst the team members.

However, the existing team negotiation approaches did not consider interdependencies within the team during negotiation [4, 5]. As teams are interdependent by nature in team negotiations, interdependencies must be considered during these negotiations. For example, when an agent in a team accepts the opponent's proposal, the agent that depends on that agent becomes more likely to accept the same opponent's proposal by the degree of dependency. In this context, it becomes necessary to evaluate these changes in decisions due to dependencies within the team.

In this paper, we propose a team negotiation strategy that considers the dependency relationships within this team. The proposed negotiation strategy, bidirectionally sets the parameters that express these dependency relationships that exist within the team. By setting bidirectional dependencies within the team, it becomes possible to express unilateral dependencies. In each mechanism, when the voting process is performed, by weighting the dependency degree of each team member, change of agent decision according to the dependency relation is expressed.

2. Proposed Team Negotiation Strategy

First, we define interdependencies within the team as follows. Let parameter $w(a, b)$ define Agent A 's dependency on Agent B, and each team member sets parameters to all other team members according to its dependency relationships. This is defined as the degree of dependency from agent A to agent B. When there are N team members, the dependency $W(a)$ that Agent A receives can be defined by Equation (1).

$$W(a) = \Sigma\, w(i, a) \quad (1)$$

Where $w(i, a)$ is the degree of dependency that Agent A receives from Agent i. For example, when there are three team members, their interdependencies can be represented as shown in Figure 1.

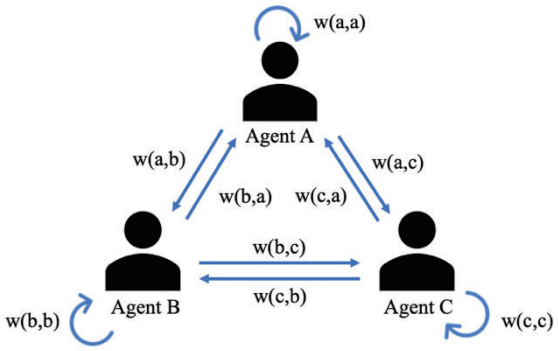

Figure 1: Dependency relationships amongst three team members

As shown in Figure 1, we can see that the dependencies between Agent A and Agent B, Agent B and Agent C, Agent A

Contact: Daiki Setoguchi, Nagoya Institute of Technology, setoguchi.daiki@itolab.nitech.ac.jp

and Agent C can be defined from both directions. By this, it can also be defined in a state that depends unilaterally.

Members with a high degree of dependency who receive it can be regarded as members with high decision and speaking rights within the team because other members are strongly influenced by their opinion. Therefore, members with high dependence are members of high importance within the team, and if the utility value of members with high importance is high, other members can easily compromise. Conversely, members with low importance depend heavily on other members, so they depend on the utility values of other members. Since the importance value in the team at this time has a difference in importance depending on the members, the weighted sum by importance rather than the sum of the utility values of simple team members is the utility value of the team. For example, utility values of members with high importance are simply added with a simple summation, but other members are influenced by the dependency within the team, and the utility value increases. Therefore, it is necessary to calculate the increment of the utility value due to the dependency relationship. Therefore, when the utility value of Agent A is assumed to be $u(a)$, the utility value of the team can be defined by Equation (2).

$$U = \Sigma\, u(i)\, W(i) \tag{2}$$

Where $u(i)$ is the utility value obtained by Agent i. $W(i)$ is the importance level of Agent i and can be regarded as the decision power that Agent i has in the team. In this research, we propose a novel team negotiation strategy that maximizes the utility value U of the whole team.

2.1 Accept/Reject Opponents' Offer

The Accept mechanism for a team determines whether to accept the proposed bid from the negotiating partner. Towards this end, all team members need to vote regarding the proposed bid by the opponent. Let $s(a)$ be the acceptance function employed by Agent A in order to assess the proposed bid. $s(a)$ is a function that returns 1 when Agent A chooses acceptance, and 0 if not. Here, the acceptance function is defined by Equation (3).

$$f = \Sigma\, s(i)\, W(i) \tag{3}$$

Where $s(i)$ represents s is a variable that returns 0 or 1 as to whether or not the Agent i accepted. $W(i)$ is the importance level of Agent i. In other words, it is synonymous with $W(i)$ in the team judged to be accepted when Agent i accepted. Therefore, when voting is done, it is necessary to obtain the importance degree of the accepted member as the voting right and the acceptance function as the sum of the importance degree. As a result of voting in this way, accept as a team if the acceptance function exceeds half the size of the team. Since the acceptance function is the sum of the importance of the received members in the team, when it exceeds half the size of the team, members who exceed the majority in the team accepted the other party's bid. Therefore, accept the proposal of the negotiating partner as a team's decision. Otherwise, the team starts the offer proposal mechanism.

2.2 Offer Proposal

The Offer mechanism decides and transmits the bid to be proposed to the negotiating partner as a team. The proposed approach employs a voting mechanism that selects widely accepted candidates such as Borda count [6]. Submit the bid that each team member wishes to propose within the team. After that, each team member evaluates all the submitted bids by using its own utility function. Let the utility value obtained when Agent A accept Agent B's proposed Bid is $u'_{A(b)}$. Agent A has a dependence on agent B for $w(a, b)$, and it is necessary to weight it when evaluating it depending on the degree of dependency. The utility value $u_{A(b)}$ for Agent B's proposed Bid for Agent A is as follows. Next, we evaluate and rank all the bids submitted within the team by Equation (4).

$$u_{A(b)} = u'_{A(b)}\,\{1.0 + w(a, b)\} \tag{4}$$

Where $u'_{A(b)}$ is the utility value when accepting B's proposed. Also, $w(i, a)$ is the degree of dependency that Agent A receives from Agent i. Assign the score from the set [0, |A| - 1] to the submitted bid along with its ranking. | A | is the total number of bids submitted. All team members make this ranking, and the highest score bid is sent to the negotiating partner as the team's proposed bid.

3. Experiment And Discussion

In this experiment, we use GENIUS which is a general-purpose negotiation platform as evaluation environment [7]. GENIUS is an open source software, aimed at negotiation simulation and the development of automated negotiation agents. Since GENIUS supports Java API that is necessary for agent development, development becomes easy with basic knowledge of Java programming. We set the experiment setting as follows. The Automated Negotiating Agents Competition (ANAC), an international competition of automated negotiation agents, employs this simulator, where several researches on automated negotiation agents are actively conducted. In addition, the negotiation problems used in the past ANAC competition have been prepared as a standard, and they support the development of an effective negotiation strategies in various negotiation problems. We set the experiment setting as follows.

- We set up 3 team members and use 3 agents of Atlas 3, Caduceus, PonPokoAgent.
- We also used Farma as a negotiating partner. All the agents used for the experiments received high ranking results at ANAC competitions.
- We used two parts, partydomain and Domain 8, implemented in GENIUS as a negotiation domain.
- Negotiating with setting the maximum time of negotiations to 180 turns, the agents negotiated 10 times for each team member's permutation. That is, 3! × 10 = 60 automated negotiations were made in one negotiation domain.
- We set the following two interdependencies in the team.

	Agent A	**Agent B**	**Agent C**
Agent A	0.5	0.2	0.3
Agent B	0.3	0.6	0.1
Agent C	0.2	0.1	0.7

Table 1: Dependency within the team

	Agent A	Agent B	Agent C
Agent A	0.6	0.2	0.2
Agent B	0.3	0.5	0.2
Agent C	0.3	0.3	0.4

Table 2: Dependency within the team

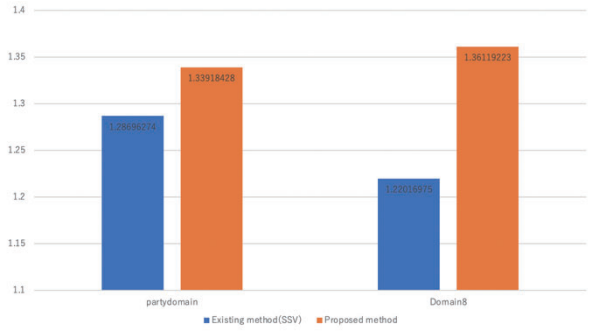

Figure 2: Average negotiation result (Table1)

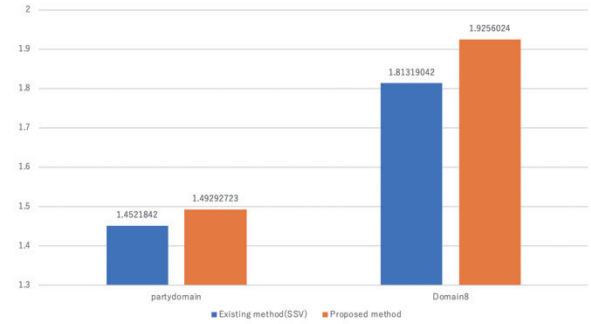

Figure 3: Average negotiation result (Table2)

The results of the experiment are shown in Figure 2 and Figure 3. As demonstrated in Figure 2, the results show that the score increases by about 0.05 for partydomain and about 0.14 for Domain 8. Since the number of team members is three, the increase in score per person is increased by about 1.8% for party domain and about 4.7% for Domain 8. As demonstrated in Figure 3, the results show that the score increases by about 0.04 for partydomain and about 0.11 for Domain 8. Since the number of team members is three, the increase in score per person is increased by about 1.3% for party domain and about 3.7% for Domain 8. Table 3 shows the results of examining the number of agreement proposal candidates in order to investigate the difference in increment by the negotiation domain.

Domain Name	Issues	Total Bid
partydomain	6	3072
Domain8	8	6561

Table 3: Comparison of size of negotiation space

From Table 3, when comparing partydomain and Domain 8, the total number of bids is larger in Domain 8. As the total number of Bids increases, the options of the proposed Bid spread, so the probability of agreeing on the same agreement decreases and the difference in the agreement proposal based on the strategy is largely reflected. From Figure 2, Figure 3 and Table 3, it can be seen that the utility value of the team is increasing as the total number of agreement proposals is larger. Therefore, as the total number of agreement proposals increases, the difference between the utility values of existing teams and the proposed method teams increases, so it can be concluded that the proposed method adapts to the utility value of the team that changes according to the dependency relationship.

4. Conclusions And Future Work

In this paper, we proposed a novel negotiation strategy that considers the interdependencies within the team in team negotiation scenarios. Towards this end, the proposed strategy implements appropriate considerations by setting the parameters that represent the interdependencies within the team, and then, using these parameters to weigh the relationship in each direction. A comparative experiment with the existing team negotiation strategies demonstrated the efficiency of the proposed strategy. As for future research, planned to investigate how to quantify the parameters that represent the interdependencies in actual negotiation problems. In addition, it become very difficult to simulate the actual negotiation scenarios unless there is a method to formulate appropriately from these scenarios. As another research direction, we also plan to study the change in the dependency score due to the change in the negotiating partner. As the negotiation partner changes, the result changes accordingly, so we plan to investigate how the agreement proposals change with the proposed approach.

References

[1] Kanamori, R., Takahashi, J. and Ito, T. “Evaluation of Traffic Management Strategies with Anticipatory Stigmergy”, Journal of Information Processing, Vol.22, No.2(2014).

[2] Sen, S. and Durfee, E. H. “On the design of an adaptive meeting scheduler.”, Artificial Intelligence for Applications, 1994., Proceedings of the Tenth Conference on. IEEE (1994).

[3] Kraus, S. “Strategic Negotiation in Multiagent Environments”, MIT press (2001).

[4] Sánchez-Anguix, Víctor, V., Botti, V., Julián, V., & García-Fornes, A. “Analyzing intra-team strategies for agent-based negotiation teams.” The 10th International Conference on Autonomous Agents and Multiagent Systems-Volume 3. International Foundation for Autonomous Agents and Multiagent Systems, 2011.

[5] Sanchez-Anguix, V., Julian, V., Botti, V., & Garcia-Fornes, A. “Reaching unanimous agreements within agent-based negotiation teams with linear and monotonic utility functions.” IEEE Transactions on Systems, Man, and Cybernetics, Part B (Cybernetics) 42.3: 778-792, 2012.

[6] Nurmi, Hannu. “Voting systems for social choice.” Handbook of Group Decision and Negotiation. Springer, Dordrecht, 2010. 167-182.

[7] Lin, R., Kraus, S., Baarslag, T., Tykhonov, D., Hindriks, K., & Jonker, C. M. “Genius: An integrated environment for supporting the design of generic automated negotiators.” Computational Intelligence 30.1 (2014): 48-70.

The 33rd Annual Conference of the Japanese Society for Artificial Intelligence, 2019

Identity Verification Using Face Recognition Improved by Managing Check-in Behavior of Event Attendees

Akitoshi Okumura[*1] Susumu Handa[*1] Takamichi Hoshino[*1] Naoki Tokunaga[*1] Masami Kanda[*1]

[*1] NEC Solution Innovators, Ltd.

This paper proposes an identity-verification system using continuous face recognition improved by managing check-in behavior of event attendees such as facial directions and eye contact (eyes are open or closed). Identity-verification systems have been required to prevent illegal resale such as ticket scalping. The problem in verifying ticket holders is how to simultaneously verify identities efficiently and prevent individuals from impersonating others at a large-scale event at which tens of thousands of people participate. We previously developed Ticket ID system for identifying the purchaser and holder of a ticket. This system carries out face recognition after attendants check-in using their membership cards. The average face-recognition accuracy was 90%, and the average time for identity verification from check-in to admission was 7 seconds per person. The system was proven effective for preventing illegal resale by verifying attendees of large concerts; it has been used at more than 100 concerts. The problem with this system is regarding face-recognition accuracy. This can be mitigated by securing clear facial photos because face recognition fails when unclear facial photos are obtained, i.e., when event attendees have their eyes closed, are not looking directly forward, or have their faces covered with hair or items such as facemasks and mufflers. In this paper, we propose a system for securing facial photos of attendees directly facing a camera by leading them to scan their check-in codes on a code-reader placed close to the camera just before executing face recognition. The system also takes two photos of attendees with this one camera after an interval of about 0.5 seconds to obtain facial photos with their eyes open. The system achieved 93% face-recognition accuracy with an average time of 2.7 seconds per person for identity verification when it was used for verifying 1,547 attendees of a concert of a popular music singer. The system made it possible to complete identity verification with higher accuracy with shorter average time than Ticket ID system.

1. Introduction

Identity verification is required in an increasing number of situations. Let us take an example of a case in which many people are admitted to an event. It used to be that in such cases, having a document, such as a ticket or an attendance certificate, checked was sufficient to gain entry; the need for personal authentication was not seriously considered due to the limited amount of time for admitting all participants. Many events with high ticket prices had designated seating, so it was not necessary to assume that some tickets may have been counterfeit. However, the advent of Internet auctions in recent years has made it easier to buy and sell tickets at the individual level. This has resulted in an increase in illegal ticket scalping, i.e., tickets being purchased for resale purposes. Equity in ticket purchasing is required not only by ticket purchasers but also by event organizers and performers [Chapple 16]. Consequently, event organizers have had to deal with complaints about malicious acts by undesignated individuals who take advantage of fans by buying and selling tickets on the Internet. In many cases, therefore, any ticket buying and selling outside the normal sales channels is prohibited. Ticket-sales terms now often stipulate that tickets are invalid when people apply for them using a pseudonym or false name and/or false address or when they have been resold on an Internet auction or through a scalper. Illegally resold tickets have in fact been invalidated at amusement parks and concert halls [JE 15]. Verification has therefore become a more important social issue than ever before. The problem in verifying ticket holders is how to simultaneously verify identities efficiently and prevent individuals from impersonating others at a large-scale event at which tens of thousands of people participate. To solve this problem, we previously developed Ticket ID system that identifies the purchaser and holder of a ticket by using face-recognition software [Okumura 17]. Since the system was proven effective for preventing illegal resale by verifying attendees at large concerts of popular music singers and groups, they have been used at more than 100 concerts. However, it is necessary to improve face-recognition accuracy because face recognition fails when unclear facial photos are obtained, i.e., when event attendees have their eyes closed, not looking directly forward, or have their faces covered with hair or items such as facemasks and mufflers. We propose an identity-verification system for attendees of large-scale events using continuous face recognition improved by check-in behavior of event attendees such as facial directions and eye contact (eyes are open or closed).

Akitoshi Okumura, NEC Solution Innovators, Ltd.
2-6-1 Kitamikata, Takatsu-ku, Kawasaki, Kanagawa 213-8511

2. Ticket ID System Using Face Recognition

2.1 Outline of Ticket ID System

Thorough verification for preventing individuals from impersonating others is in a trade-off relationship with efficient verification. The problem in verifying ticket holders is how to simultaneously verify identities efficiently and prevent individuals from impersonating others at a large-scale event in which tens of thousands of people participate. The solution should be suitable within practical operation costs for various

sized events held in various environments including open air. As a practical solution combining efficiency, scalability, and portability for a large-scale event, we developed Ticket ID system, which consists of two sub-systems, a one-stop face recognition system (one-stop system) and a check-in system [Okumura 17]. The one-stop system uses the high-speed and high-precision commercial face recognition product NeoFace [NEC 17]. The one-stop system is implemented in a commercially available tablet terminal, and the recognition result is displayed with regard to the facial-photo information of 100,000 people within about 0.5 seconds. The check-in system supports identity verification of attendees. A venue attendant checks in by placing his/her membership card on the card reader and initiates face recognition by the taking of his/her photos. The following steps make up the ticket-verification procedure from ticket application to admission [Okumura 17]:

Step 1: Tickets to popular events are often sold on a lottery basis at fan clubs or other organizations where membership is registered. Individuals applying for tickets register their membership information as well as their facial photos. In the same way for an ordinary ID photo, the registered facial photo is a clearly visible frontal photo taken against a plain background. The face must not be obstructed by a hat, sunglasses, facemask, muffler, or long hair.

Step 2: Event organizers notify ticket winners, i.e., successful applicants that have been selected.

Step 3: On the day of the event, venue attendants receive membership cards from attendees, and use a card reader to verify that attendants entering the venue are successful applicants at the event venue, as shown in Fig. 3.

Step 4: The attendants use the one-stop system to confirm that the photo taken at the time of application and the collation photo show the same person. The attendants explain the verification through face recognition to the attendees and instruct them where to stand in front of the terminal. Then, they execute the face-recognition process using the terminal to confirm the attendees are those who applied for the tickets.

Step 5: The admission procedure is carried out in accordance with the face-authentication results.

2.2 Problems with One-stop System

The average time for identity verification from check-in to entry admission was 7 seconds per person, and the average accuracy of face recognition was 90%. It is necessary to improve face-recognition accuracy by securing clear facial photos because face recognition fails when unclear facial photos are obtained, i.e., when event attendees have their eyes closed, are not looking directly forward, or have their faces covered with hair or items such as facemasks and mufflers. When face recognition fails, venue attendants have to verify attendees carefully by direct visual inspection. This increases the mental and physical burden on attendants, which makes attendees have an unreliable impression of the system. When face-recognition accuracy is 90%, two attendees are successively verified without face recognition failure with a probability of 81%. This means that 19% of attendees may experience face-recognition failure or observe it in front of them. Improving face-recognition accuracy is critical for decreasing attendants' stress and attendees' waiting time.

3. Continuous-Face-Recognition System

3.1 Managing Check-in Behavior of Attendees

We propose an identity-verification system for attendees of large-scale events using continuous face recognition improved by managing check-in behavior of the attendees. The proposed system enables attendees to check in themselves (check-in doers are not attendants, but attendees). While the previous system is equipped with a card reader, the proposed system verifies attendees with a QR code reader set up at the same position for recognizing faces of attendees standing still in front of a venue attendant, as shown in Fig. 4. Managing facial directions and eye contact are two major issues regarding facial recognition. The proposed system addresses these issues with the following methods:

1) Managing facial direction

The proposed system secures facial photos of attendees directly facing a camera by leading them to scan their QR codes just before executing face recognition. We found most people spontaneously look at the code-reader, i.e., turn their faces to the reader during check-in. The face-recognition camera of the proposed system is placed at the same position as the code-reader, as shown in Fig. 4, which makes it possible to take an attendee's photo when directly facing the camera when the photo is taken just after check-in.

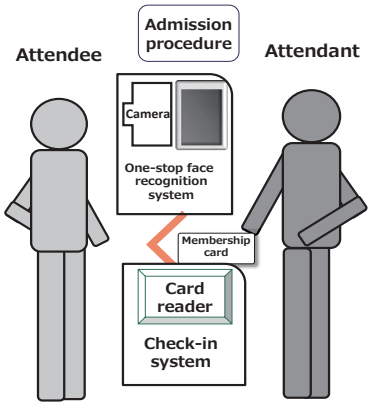

Fig. 3 One-stop face-recognition system

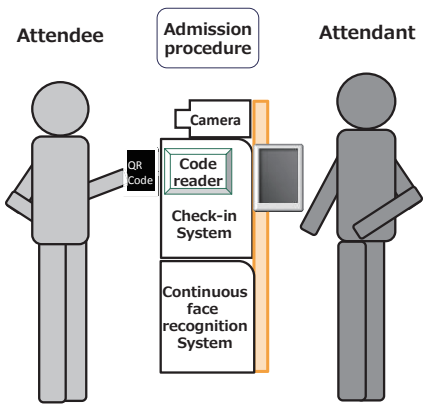

Fig. 4 Continuous face-recognition system

2) Managing eye contact

The proposed system uses a continuous-face-recognition system for accepting two photos of attendees successively taken with a single camera after an interval of 0.5 seconds to obtain facial photos with their eyes open. Few people spontaneously keep their eyes closed longer than 0.5 seconds because human blink duration is on average between 0.1 and 0.4 seconds [Bentivoglio 97]. Few people spontaneously blink twice in 0.5 seconds because human blink rate is between 7 and 17 per minute [Nosch 16]. It is possible to manage eye contact of attendees when we take the first photo at the same time of them scanning a QR code and then take the second photo after an interval of 0.5 seconds with a single camera.

3.2 Configuration of Proposed System

Figure 5 shows a configuration of the proposed system including event-attendee control platform and continuous-face-recognition system. The configuration is almost the same as that of the previous system [Okumura 17] except for a check-in doer and a QR code reader. While check-in doers of the previous system are attendants, those of the proposed system are attendees. While the previous system uses a card reader to scan membership cards, the proposed system uses a QR-code reader to scan tickets with QR codes. When attendees check in at a location that has the proposed system installed, they scan their QR-coded tickets. The attendee-management system provides the attendees the tickets in advance of the event day. Attendees can obtain tickets with QR codes with their smartphones. The ticket has the concert name, date and time, venue, QR code containing attendee's membership information, his/her name, seat number, registered photos, and so on.

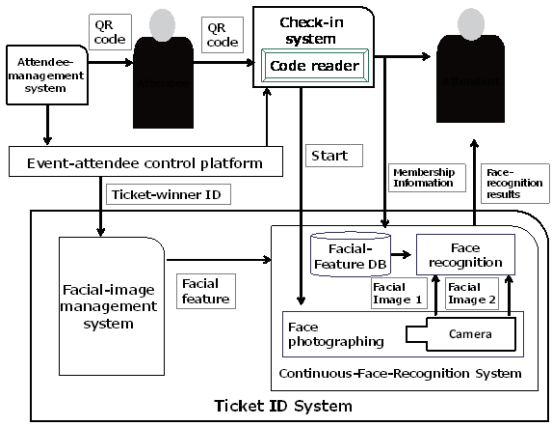

Fig. 5 Configuration of proposed system

3.3 Identity-Verification Procedure

An attendee's identity is verified with the procedure shown in Fig. 6. When attendees scan their QR codes, a check-in system performs ticket-winner check as well as showing the attendants the member information of the attendees, which is retrieved from the ticket-winner database with search keys of membership numbers obtained through a QR code reader. Scanning a QR code automatically activates continuous face recognition by taking two photos of the attendee after an interval of 0.5 seconds. When either photo is verified with the registered photo of the attendee, face recognition is successful. When attendees are ticket winners and face recognition is successful, the verification is successful. Otherwise, verification fails.

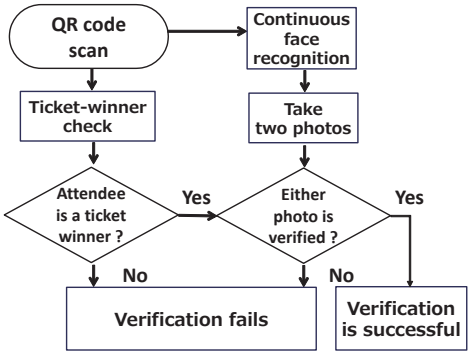

Fig. 6 Flowchart of verification

3.4 Operational Steps

The proposed system has the following operational steps from ticket application before the event day to admission on the event day:

Step 1: Ticket application is the same as that of the one-stop face-recognition system described in Section 2.1.

Step 2: Event organizers notify ticket winners, i.e., successful applicants that have been selected. They can obtain attendee's tickets including their QR codes and registered facial photos.

Step 3: At the check-in site on the event day, attendees scan their QR codes with the code reader according to attendant's instruction.

Step 4: Attendants can confirm that attendees are successful applicants who applied for the tickets.

Step 5: If identity is verified, the attendee is admitted entry. Otherwise, identity is verified by an attendant with direct visual inspection of the facial photo on the ticket.

4. Demonstration of Proposed System

4.1 Results

Six sets of the proposed system were used for a popular concert on November 17, 2018 in Tottori prefecture, Japan. Face recognition was carried out for 1,547 attendees. Face-recognition accuracy was 93%, and identity-verification time was 2.7 seconds on average in cases in which face recognition was not successful. No cases of attendees impersonating others were reported for the concert. The false reject rate (FRR) was 7% and the false accept rate (FAR) was 0%. There were two reasons for recognition failure: The first was that faces of incorrect attendees were detected when photos contained other attendees behind the correct attendee. The second was that the attendees had their faces covered with hair or items such as facemasks and mufflers. Failure was not observed due to the fact that attendees had their eyes closed or were not directly facing a camera.

4.2 Discussion

Table 1 compares the results of our previous and proposed systems. The average identity-verification time was 4.3 seconds shorter than that of the previous system because of changing check-in doers and improving face-recognition accuracy. The proposed system does not require handing over a membership

card between attendants and attendees. The face-recognition accuracy of the proposed system was 3% higher than that of the previous system. This resulted in decreasing the number of direct visual inspections, which increases identity-verification time.

There was a problem with face detection in that faces of incorrect attendees were detected when photos contained other people behind an attendee. This can be solved by choosing the face with the largest face area among all the detected faces. Face recognition failed when attendees had their faces covered with hair or items. There were no cases in which attendees had their eyes closed or were not directly facing a camera in the two successive photos, i.e., in the first photo and second photo taken after 0.5 seconds. Managing facial direction and eye contact of attendees worked as expected. It is difficult to solve the problem of when the faces of attendees are covered with hair or items because there would be no differences between the first and second photos on the attendee's covered faces. The attendee's cooperation is necessary for solving this problem.

Table 1 Results of our previous and proposed systems

	Previous system	Proposed system
Identity-verification time	7 seconds	2.7 seconds
Face-recognition accuracy	90%	93%
Check-in doer	Attendant	Attendee
Reasons for recognition failure	Attendees had their eyes closed.	
	Attendees were not directly facing camera.	
		Incorrect attendee's faces were detected.
	Attendees had their faces covered with their hair or items.	

5. Future Issues

Faces of incorrect attendees were detected when they stood behind a correct attendee. This can be solved by choosing the face with the largest face area among all the detected faces. If this improvement does now work, we are preparing a partitioning screen to be placed behind the correct attendee to prevent incorrect attendees from being photographed.

The largest obstacle remaining to improving face-recognition accuracy is that of covered faces. This problem could be solved with attendee's cooperation. We have been developing an identity-verification system using face recognition from selfies taken by attendees with their smartphone cameras [Okumura 18]. Self-photographing is regarded as helpful for securing clear facial photos because attendees can control intrinsic parameters such as their expressions, facial hair, and facial directions. We are planning to use of this system with the proposed system for solving the problem of covered faces.

The proposed system has been widely reported in the mass media. The system is highly regarded from reviews on the Internet [Hachima 18]. It was used to carry out face recognition for more than 100,000 attendees in 2018. Though no cases of attendees impersonating others were reported for any of these events, i.e., the FAR was 0%, the FAR should be more carefully examined from the view-point of preventing impersonation. It is necessary to evaluate the robustness against impersonation with pseudo attack tests. These tests should include disguise and lookalike tests. A disguise test makes people's facial appearances as similar to each other as possible by using facial paraphernalia such as facial hair, glasses, and makeup. A lookalike test is conducted for those, such as twins or similar looking siblings, with similar facial features. A disguise test will reveal considerable disguise methods and help in creating operational manuals for venue attendants to detect these methods. A lookalike test will disclose the technical limitations of current face-recognition methods and help in establishing next-generation technology.

6. Conclusion

We proposed an identity-verification system for attendees of large-scale events using continuous face recognition improved by managing check-in behavior of the attendees. The proposed system could secure facial photos of attendees directly facing a camera by leading them to scan their QR codes on a QR-code reader placed close to the camera just before executing face recognition. The system took two photos of attendees with this one single camera after an interval of 0.5 seconds to obtain facial photos with their eyes open. The system achieved 93% face-recognition accuracy with an average identity-verification time of 2.7 seconds per person when it was used for verifying 1,547 attendees at a concert of a popular music singer. The system made it possible to complete identity verification with higher accuracy with shorter average time than the previous system. We plan to improve our system to further streamline the verification procedure.

References

[Chapple 16] Chapple,J.: Ticket resale? NO, says Japanese music business (Aug. 23, 2016), available from < https://www.iq-mag.net/2016/08/ticket-resale-no-says-japanese-live-business-resaleno/#.W_01Jk8Un3g>.

[JE 15] JE fandom: Johnny's Tracks Illegally Sold Tickets for Arashi's Japonism Tour (Oct. 25, 2015), available from <https://jnewseng.wordpress.com/2015/10/25/johnnys-tracks-illegally-sold-tickets-for-arashis-japonism-tour/>.

[Okumura 17] Okumura, A., etc.: Identity Verification of Ticket Holders at Large-scale Events Using Face Recognition, *Journal of Information Processing*, Vol. 25, pp. 448-458 (Jun. 2017)

[NEC 17] NEC: Face Recognition, available from < https://www.nec.com/en/global/solutions/safety/face_recognition/index.html>.

[Bentivoglio 97] Bentivoglio AR, etc.: Analysis of blink rate patterns in normal subjects, Mov Disord. 12(6) pp1028-1034, (Nov. 1997)

[Nosch 16] Nosch DS, etc,: Relationship between Corneal Sensation, Blinking, and Tear Film Quality, Optom Vis Sci. ,93(5) pp471-481, (May. 2016)

[Okumura 18] Okumura, A., etc: Identity Verification for Attendees of Large-scale Events Using Face Recognition of Selfies Taken with Smartphone Cameras, *Journal of Information Processing*, Vol. 26, pp. 779-788 (Nov. 2018)

[Hachima 18] Hachima: Concerts of Hikaru Utada were successfully operated, available from < http://blog.esuteru.com/archives/9218587.html>. (Nov.2018) (in Japanese)

International Session | International Session | [ES] E-2 Machine learning

[4D3-E-2] Machine learning: living environment

Chair: Junichiro Mori (The University of Tokyo)

Fri. Jun 7, 2019 2:00 PM - 3:40 PM Room D (301B Medium meeting room)

[4D3-E-2-01] Privacy-Preserving Resident Monitoring System with Ultra Low-Resolution Imaging and the Examination of Its Ease of Installation

○Takumi Kimura[1], Shogo Murakami[1], Ikuko Egushi Yairi[1] （1. Sophia University）

2:00 PM - 2:20 PM

[4D3-E-2-02] Trees Detection on Google Street View Images Using Deep Learning and City Open Data

○Lieu-Hen Chen[1], Hao-Ming Hung[1], Cheng-Yu Sun[1], Eric Hsiao-Kuang Wu[2], Toru Yamaguchi[3], Eri Sato-Shimokawara[3], Hao Chen[1] （1. Nantional Chi Nan University, 2. National Central University, 3. Tokyo Metropolitan University）

2:20 PM - 2:40 PM

[4D3-E-2-03] Scoring and Classifying Regions via Multimodal Transportation Networks

○Aaron Bramson[1,2,3,4], Megumi Hori[1], Zha Bingran[1], Hirohisa Inamoto[1] （1. GA Technologies, 2. RIKEN Center for Biosystems Dynamics Research, 3. Ghent Univeristy, 4. UNC - Charlotte）

2:40 PM - 3:00 PM

[4D3-E-2-04] Evaluating Road Surface Condition by using Wheelchair Driving Data and Positional Information based Weakly Supervision

○Takumi Watanabe[1], Hiroki Takahashi[1], Yusuke Iwasawa[2], Yutaka Matsuo[2], Ikuko Eguchi Yairi[1] （1. Sophia Univ., 2. Univ. of Tokyo）

3:00 PM - 3:20 PM

[4D3-E-2-05] Prediction of the Onset of Lifestyle-related Diseases Using Regular Health Checkup Data

○Mitsuru Tsunekawa[1], Natsuki Oka[1], Masahiro Araki[1], Motoshi Shintani[2], Masataka Yoshikawa[3], Takashi Tanigawa[4] （1. Kyoto Institute of Technology, 2. SG Holdings Group Health Insurance Association, 3. Japan System Techniques Co.,Ltd., 4. Juntendo University）

3:20 PM - 3:40 PM

The 33rd Annual Conference of the Japanese Society for Artificial Intelligence, 2019

Privacy-Preserving Resident Monitoring System with Ultra Low-Resolution Imaging and the Examination of Its Ease of Installation

Takumi Kimura [*1] Shogo Murakami [*1] Ikuko Egushi Yairi [*1]

[*1] Graduate School of Science and Technology, Sophia University

Monitoring systems using infrared array sensors allow monitoring of residents while protecting their privacy. However, since such a sensor is vulnerable to subtle movements, accuracy of posture classification is low, and limits the locations and methods available for installation. This study proposes a posture classification method with higher accuracy. Over 93% accuracy was achieved in posture classification by RGB conversion of infrared array sensor images and successfully decreased loss due to displacement by DCNN. Additionally, this research considers methods to create artificially simulated data for postural-behavioral study. To check the validity of this method, postures of 3 subjects were examined using a classifier with studied simulation data. Finally, simulation environments with different sensor altitudes and angles were created to examine the ease of installation for the proposed method. As a result, the experiments showed that accuracy was highest at approximately 90% when the sensor was located 50cm below the height of the target and when the tilt angle was within ±2°.

1. Introduction

Resident monitoring systems are useful in detecting abnormal conditions of residents. However, as every move is under inspection, privacy issues arise. As a solution, usage of infrared array sensors has been proposed to preserve privacy as well as to avoid physical burden on the target. [Okada 13][高木 16][楠亀 17]. Such sensors can be placed in various places as they solely rely on temperature data obtained from the infrared sensor to detect the target. Spatial information and light measurements received from the sensors are used to identify the posture and location of the target and to observe their changes.

It is known that sensor installation angle is a factor for decreased classification accuracy, but the analysis on its effects are yet insufficient. Acquisition of learning data for machine learning is key in improving classification accuracy. To solve the aforementioned tasks, this paper assesses the classification accuracy by the single 8x8 infrared array sensor, proposes the methods of artificially creating simulated data to study postures for machine learning, and analyzes the effects caused by the angle of the installed infrared array sensor.

2. A resident monitoring system using ultra low-resolution infrared array sensor imaging

2.1 Posture classification system

To examine posture classification accuracy, a data collection device including an infrared array sensor was developed. A diagram of the device is shown in Figure 2. This device composes of a Raspberry Pi3 Model B mounted with a Grid-EYE (AMG8833) sensor. The Grid-EYE will output an 8x8 pixel image data of the surface temperature for objects detected in the observation space. Temperatures between 0°C -80°C can be detected with a step increment of 0.25°C.

Deep Convolution Neural Network (DCNN), is an effective method for high accuracy image recognition. It is used in this study to examine the obtained infrared image data for use in the production of a posture classifier. Figure 3 shows the structure of the DCNN used.

2.2 Posture classification experiment of a subject using DCNN

A posture classification experiment was conducted on 3 subjects to check the operation of the posture classification system and to evaluate the performance of the DCNN. The first two experiments were conducted in a 9.5m^2 Japanese-style room at roughly 13°C room temperature. Here, the data of a male subject of age 24 and height of 170cm, and a female subject of age 20 and a height of 160cm was obtained. The experiment for the third subject was done in a 20m^2 room with a room temperature of roughly 11°C. The subject was male, of age 22, and was 170cm in height. For all three scenarios, the sensor was placed 140cm from ground level such that the entire body of each subject could be observed.

The subjects were stationed 1-3m away from the sensor and were told to stand, sit, or lie down within the view of the sensor. A total of 14983 frames worth of data were obtained. 10% of the above data were randomly selected and studied by the classifier, then were used to classify the remaining 90%. The result of posture classification, evaluation of accuracy, and recall ratio are shown in Table 1.

Considering practical use, a resident monitoring system needs to be able to detect instantaneous dangerous incidents such as slips and therefore it is desirable for the F-measure to be above 90%. Experimental results showed an F-measure of roughly 87%. It is probable that directly inputting 8x8 temperature data to the DCNN is insufficient for image feature extraction.

However, since DCNN is known to have high accuracy object detection for colored images, focus was placed on converting data

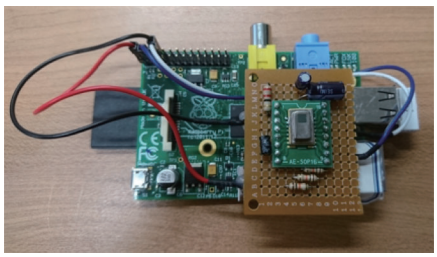

Fig. 1 A posture recognition device equipped with an 8×8 infrared array sensor.

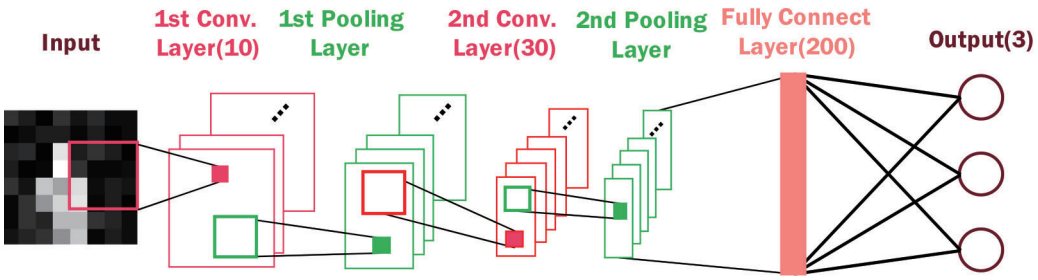

Fig. 2 Illustration of DCNN structure used in 2.2 experiment.

from the infrared array sensor into RGB and inputting them to the DCNN to improve the accuracy of the classifier. [Simonyan 15] This was done by mapping temperature data into a color space and using that as a reference to convert images to RGB. Data were then divided into R, G, and B, and were separately inputted to the DCNN. The classification results after RGB conversion, evaluation of accuracy, and recall ratio are shown in Table 2. In comparison to Table 1, the number of misclassifications decreased, and F-measure was above 90% for all postures. From such results, it could be concluded that RGB conversion of data led to less number of misclassifications. RGB converted data were used for DCNN input hereafter.

3. Learning data generator construction and evaluation of classification accuracy

3.1 Learning data generation procedures

Using the DCNN posture classifying method previously evaluated in 2.2, methods to generate simulation learning data without subject-based experiments were made. The infrared images handled in this research are for a room temperature distribution represented by 8x8 image pixels. Therefore, it can be theorized that placing a human model in the view of the sensor would require less effort while outputting results like those of the subject based experiments. For such a reason, a Unity program including physics engines and functions was used to simulate this environment and was used to produce learning data. This learning data generator was made to arbitrarily set the height and physique of the human model, the tilt and altitude of the sensor, and the size of the room. As for physique, the human model was composed of several body parts including the head, arms, and torso, with each part having its own temperature distribution that could also be arbitrarily changed. For this research, the radiant heat distribution obtained from a real environment experiment was used to set parameters for each body part. As for posture, the human model had 3 types of postures namely, “stand”, “sit” or "lie down”.

After running the learning data generator, ray tracing was performed from the sensor. Whenever the ray hit the human model, the radiant heat information of the human model on the incident spot was recorded. When the ray did not hit the model, the preset radiant heat or temperature of the background was recorded. Simulation by the learning data generator is depicted in Figure 3.

3.2 Learning method evaluation using simulated learning data

DCNN with studied simulation data were used to classify real environment data. The real data used were the same data as those used in 2.2. Simulation data collection was done by placing a human model randomly 1m-3m away from the sensor with three postures— either “stand”, “sit” or "lie down”. Room temperatures

Table 1 Posture classification results of 8x8 infrared array sensor images by DCNN.

Posture classification results

Recognition	Answer		
	Stand	Sit	Lie down
Stand	3582	266	15
Sit	496	5243	435
Lie down	185	590	4171

Posture classification evaluations

	Stand	Sit	Lie down
Accuracy	0.92726	0.84921	0.84331
Recall ratio	0.84025	0.85965	0.90262
F-measure	0.88161	0.85440	0.87196

Table 2 Action classification result of 8x8 RGB converted images of infrared array sensor.

Posture classification results

Recognition	Answer		
	Stand	Sit	Lie down
Stand	3929	137	20
Sit	217	5620	113
Lie down	121	336	4490

Posture classification evaluations

	Stand	Sit	Lie down
Accuracy	0.96158	0.94454	0.90762
Recall ratio	0.92079	0.92237	0.97123
F-measure	0.94074	0.93332	0.93835

and sizes were set according to real data. The human model also corresponded with subjects from the experiment, and the learning data generator was run for 30 minutes outputting 50000 sample data for each simulated subject. Finally, the posture classifier was used to analyze the obtained data. Table 3 shows the posture classification and evaluation results. Results show that average F-measure was relatively low— generally under 80%. From observing misclassified examples, it was hypothesized that such classification accuracy loss occurred due to the existence of high-temperature pixels in the background. Therefore, background elimination was conducted by analyzing the temperature difference in each data, estimating and eliminating background parts, and leaving only the human model in the data. The background elimination process is shown in Figure 4. This elimination method was applied to both simulated learning data and real data used for classification and evaluation. Then, classification was repeated for the second time. Table 4 shows the classification and evaluation results. Results showed that all classification average F-measures increased from under 80% to over 90% accuracy. From such results, it was safe to say that background elimination method was effective when using simulated learning data to classify real data.

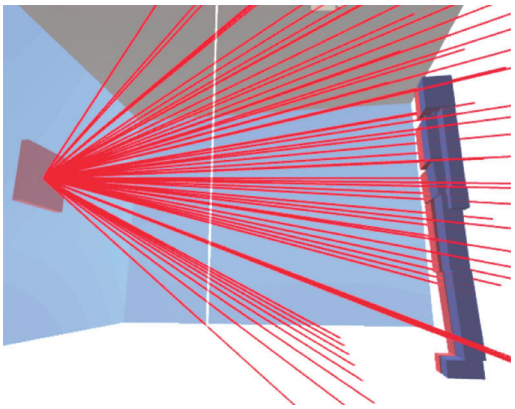

Fig. 3 The learning data generator simulating 8x8 infrared array sensing of a human in a room.

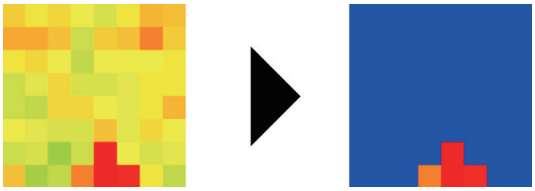

Fig. 4 Process of background elimination algorithm.

4. Evaluation on classification accuracy effects due to the system installation condition

So far, this research had fixed the sensor at a height of 140cm to successfully classify the postures with over 90% accuracy. However, it was never tested to confirm the range of heights this high accuracy rate can be sustained. In implementation, it is highly likely that the sensor will be slightly displaced or tilted from external factors. Therefore, the effect and degree of these factors against classification accuracy were tested, and system installation conditions were considered.

4.1 Evaluation on installation height

Using the learning data generator, the sensor height was changed from 50-170cm with a step increment of 10cm, and the human model height was set at either 170cm, 160cm, or 150cm. Then, for each condition, an evaluation of classification accuracy was performed. The results are shown in Figure 6. For all models, the accuracy peaked when the sensor height was 50cm below the model height.

4.2 Evaluation on sensor tilt

Next, the degree of effect on accuracy by the sensor angle were inspected. The human model height was set at 170cm, and sensor installation height was set at 120cm. Tilt range was set from -5° to 5° with increments of 1°. As for learning data, the preceding data without any tilt was used. Results are summarized in Figure 7. Results show that when the sensor is tilted upwards to 2°, the F-measure is over 90%, but when the tilt reaches 5°, the F-measure is decreased to roughly 86%. When the sensor is tilted down, F-measure is sustained at a high value until -1°. However, a tilt of over -2° drastically decreases the F-measure until under 80% at -

Table 3 Action classification results of the real data by learning with the simulated data.

Posture classification results

Recognition	Answer		
	Stand	Sit	Lie down
Stand	3306	537	216
Sit	959	5129	1274
Lie down	5	427	3130

Posture classification evaluations

	Stand	Sit	Lie down
Accuracy	0.81449	0.69669	0.87872
Recall ratio	0.77424	0.84179	0.67749
F-measure	0.79385	0.76239	0.76509

Table 4 Effects of background image removal on action classification of the real data by learning with the simulated data.

Posture classification results

Recognition	Answer		
	Stand	Sit	Lie down
Stand	4130	0	0
Sit	201	5665	585
Lie down	0	217	4185

Posture classification evaluations

	Stand	Sit	Lie down
Accuracy	1.00000	0.87816	0.95070
Recall ratio	0.95359	0.96311	0.87736
F-measure	0.97624	0.91867	0.91256

5°. Since this research takes privacy preservation as a serious consideration, the number of image pixels used are very low. Therefore, the posture classification relied heavily on high-temperature distributions per row, and a one-row difference gave an extensive impact on classification results.

The high-temperature distribution change caused by the sensor tilt was assumed to be the major cause of the decrease in classification accuracy.

5. Evaluation on classification accuracy effects due to the system installation conditions

In chapter 4, the influence on classification by installation height and sensor tilt were investigated to consider potential external effects upon real implementation. As a result, it was found that installation height yielded highest accuracy at height 50cm below the height of the target, and that sensor tilt largely impacted the classification accuracy.

With these results in mind, real implementation is further considered. Assuming the wall were to be perpendicular, the sensing device could be installed 50cm below the target height after the height of the target is measured. On the other hand, if a wall installation is difficult, then there may be a need to call a specialist to install the device.

A solution to this installation problem could be to create a personalized classifier for the target by inputting the target's room information data into the learning model. Although this method requires meticulous interview on the house conditions, by utilizing the learning data generator one can simulate and obtain data corresponding to the target room and apply the resident monitoring system

6. Conclusions

This paper justified that an infrared array sensor resident monitoring system using an infrared array sensor image with 8x8 pixels would output over 90% accuracy for posture action classification of the target. Noise analysis was performed on a tilt and it was concluded that approximately 90% accuracy was sustained for tilt angle within ±2° by extending the classifier. In addition, posture pattern learning data simulation was taken into consideration, and through comparison against real data, a high accuracy classifier construction was achieved. As for further research, an improvement in simulated learning data, learning data generator, and learning algorithm will be continued for application in a real environment.

Acknowledgements

We would like to show our gratitude to Yuki Kato, Motoharu Sakurai, and all the supporters for their participated and assistance. This research was conducted under the support of 23rd and 24th year of Heisei period research grant from the Support Center for Advanced Telecommunications Technology Research, Grant-in-Aid for Scientific Research B(17H01946), and Grant-in-Aid for challenging Exploratory Research (16K12537).

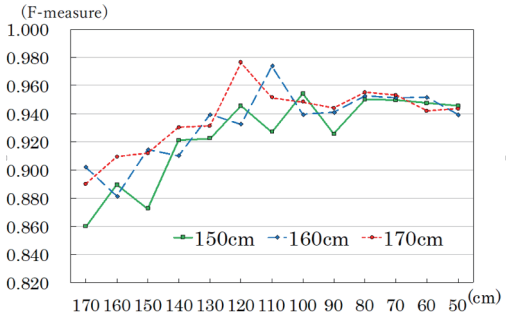

Fig. 5 Accuracy for various sensor altitudes.

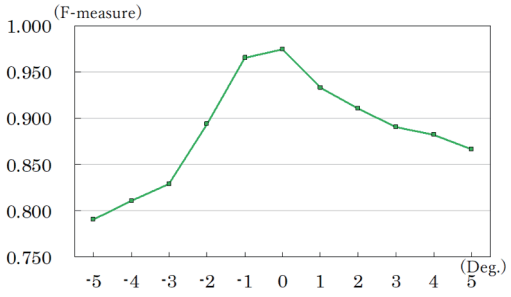

Fig. 6 Accuracy for vertical sensor tilt.

References

[Okada 13] R. Okada and I. Yairi, "An indoor human behavior gathering system toward future support for visually impaired people," Proc. of the 15th International ACM SIGACCESS Conference on Computers and Accessibility, no. 36, Washington, Oct. 2013.

[高木 16] 高木, 高橋, 大塚, "温度センサを用いた高齢者の見守り," 第8回データ工学と情報マネジメントに関するフォーラム (DEIM 2016), P6-1, 福岡, 2016.

[楠亀 17] 楠亀, 米田, 式井, シラワン, 野坂, 久保, "サーモカメラによる非接触温冷感センシング, "Panasonic Technical Journal, pp.118-122, vol.63, no.2, Nov. 2017.

[Simonyan 15] K. Simonyan and A. Zisserman, "Very Deep Convolutional Networks for Large-Scale Image Recognition," International Conference on Learning Representations (ICLR), May 2015.

The 33rd Annual Conference of the Japanese Society for Artificial Intelligence, 2019

Trees Detection on Google Street View Images Using Deep Learning and City Open Data

Lieu-Hen Chen[*1] Hao-Ming Hung[*1] Cheng-Yu Sun[*1] Eric Hsiao-Kuang Wu[*2] Toru Yamaguchi[*3] Eri Sato-Shimokawara[*3] Hao Chen[*1]

*1 National Chi Nan University, Taiwan *2 National Central University, Taiwan *3 Tokyo Metropolitan University, Japan

For almost every cities and towns, street trees play an important role in representing seasonal change of the street view. Nowadays, lots of countries start promoting open data. Among these data, very useful information related to street trees are well documented with free access by many city governments. At the same time, Google Street View provides the view of a certain surrounding by composing stitched images which are shot by specialized vehicles moving along streets and alleys. However, few research reports have been published on utilizing city open data for trees detection on Google Street View. Therefore, in this study, we aim to perform trees detection on Google Street View Images by utilizing Deep Learning technologies and city open data.

1. Motivation and Research Background

Street Trees are an indispensable component of great neighborhoods. Street trees play an important role for:

1. representing the style of a city, trees provide beauty and aesthetic appeal for the urban landscape.
2. improving environmental quality, especially for reducing air pollution.
3. strengthening urban amenity because trees provide spaces for rest and relaxation.

Therefore, street trees management is always an important issue for city and county governments. It is especially true for cities such as Tokyo and Washington DC where have beautiful cherry blossom seasons.

Nowadays, many countries start promoting open data. The concept of open data is that certain data should be freely available to everyone to use and republish as they wish, without restrictions from copyright, patents or other mechanisms of control. Among the open data provided by some city governments, very useful information related to street trees are well documented with free access. For example, many well documented information of street trees can be accessed form the open database of Taipei and New York city, as shown in figure 1 and figure 2. These useful information includes: tree species, tree height, diameter at breast height, growth status, and position.

Figure 1. Tree's data in Taipei

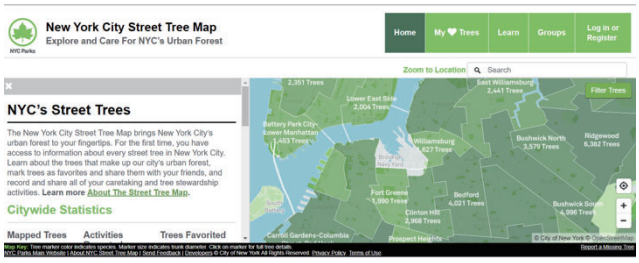

Figure 2. Tree's data in New York

At the same time, Google Map has become the most common tool used for exploring street maps. There are many services available on Google Map. And Google Street View is one of the feature derived from Google Map for improving users' perception of real world. It shows the view of a certain surrounding composed by stitched photographs shot by specialized vehicles moving along streets and alleys. However, these street images are static, no matter which season is now. Moreover, as shown in figure 3, it is still difficult to accurately locate trees on street images by using Google API because of the

Contact:
Lieu-Hen Chen, National Chi Nan University, No. 303, Daxue Rd., Puli Township, Nantou County 545, Taiwan, +886-49-2910-960#4861, +886-49-2915-226, lhchen@csie.ncnu.edu.tw
Hao-Ming Hung, National Chi Nan University, No. 303, Daxue Rd., Puli Township, Nantou County 545, Taiwan, +886-49-2910-960#4861, +886-49-2915-226, d3764291@gmail.com
Cheng-Yu Sun, National Chi Nan University, No. 303, Daxue Rd., Puli Township, Nantou County 545, Taiwan, +886-49-2910-960#4861, +886-49-2915-226, s106321526@mail1.ncnu.edu.tw
Eric Hsiao-Kuang Wu, National Central University, No. 300, Zhongda Rd., Zhongli Dist., Taoyuan City 320, Taiwan, +886-3-4227151, +886-3-4226062, hsiao@csie.ncu.edu.tw
Toru Yamaguchi, Tokyo Metropolitan University, 6-6 Asahigaoka, Hino-shi, Tokyo, Japan 191-0065, +81 42 585 8606, yamachan@tmu.ac.jp
Eri Sato-Shimokawara, Tokyo Metropolitan University, 6-6 Asahigaoka, Hino-shi, Tokyo, Japan 191-0065, +81 42 585 8606, eri@tmu.ac.jp
Hao Chen, National Chi Nan University, No. 303, Daxue Rd., Puli Township, Nantou County 545, Taiwan, +886-49-2910-960#4861, +886-49-2915-226, s107321517@mail1.ncnu.edu.tw

GPS position bias of moving vehicles and the image stitching algorithm.

Figure 3. The shifting problem of tree positions on street picture due to GPS errors

Therefore, in this study, we aim to develop a new approach which detects trees position on Google Street View Images by utilizing Deep Learning technologies and city open data. The remainder of this paper is organized as follows: in section 2, the related works are introduced; in section 3, our prototype system are explained; in section 4, the current experiment results are shown; and finally in section 5, the conclusion are discussed.

2. Related Works

2.1 Trees Detection

In comparison with the number of research works developed for detecting car and people, there are fewer papers published on solving street trees detection problem. In 2006, Wajid Ali proposed a tree detecting method by using the color and texture of trees as the basis for detection in a forest environment [1]. Later, Y. Lu and C. Rasmussen proposed a tree trunk detection algorithm by using contrast templates in 2011 [2]. These studies have good results with limitations of vertical trees on grass fields. In addition, Harri Karrtinen et al. evaluated the quality, accuracy, and feasibility of automatic tree extraction methods, mainly based on laser scanner, which requires high precision and expensive instruments to collect and detect data from trees [3]. It is still very difficult to detect trees images because trees have very complex and various textures and shapes.

2.2 Machine Learning Technologies

Machine learning technologies have been widely applied in solving many problems such as object recognition and route planning, and have achieved many good results in recent years [4]. For example, in1995, C. Cortes and V. Vapnik proposed the Support Vector Machine algorithm which separates the attribute space with a hyperplane to maximize the margin between different classes [5]. Later, in 1997, M. Dorigo, L. Gambardella used the Ant Colony Optimization approach to solve the Traveling Salesman Problem successfully [6].

3. System Implementation

Our system can be divided into the following three stages:

3.1 Adopting Deep Learning approaches for trees image segmentation.

In our prototype system, we trained U-Net and Seg-Net for Deep Learning as shown in figure x. Both U-Net and SegNet are kinds of Convolution Neural Networks. The U-Net was developed for biomedical image segmentation in 2015 [7]. SegNet was developed for autonomous driving applications to enable vehicles understand road scenes in 2016 [8]. For the research convenience, we try to reduce the network size and complexity by pre-categorizing trees images into several groups based on the tree species and seasons. Then each CNN is trained separately for different groups.

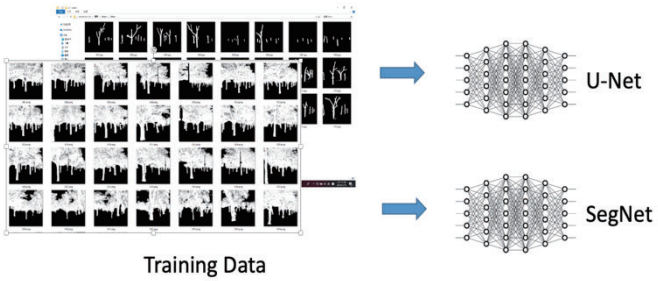

Figure 4. System Flow 1

3.2 Selecting appropriate Deep Learning models for tree segmentation.

By cross referencing the city open data, and the location/compass/time information of Google Street View images, appropriate Deep Learning models are then used for image segmentation of tress. For example, as shown in figure y, our system first determines that there should be a tree contained in the image, according to its GPS and compass information. Then we select the U-Net and Seg-Net which are trained by using deciduous trees images in Spring for image segmentation.

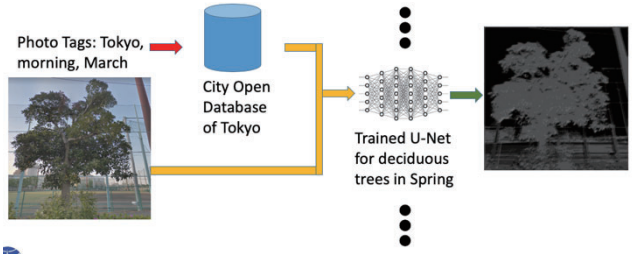

Figure 5. System Flow 2

3.3 With the segmentation results as the guidance, adopting conventional image processing approaches to detect and extract useful information of trees on street pictures.

Currently, we adopted the flood fill algorithm with the segmentation results as the guidance for edge extraction. One of the results is shown in figure 6.

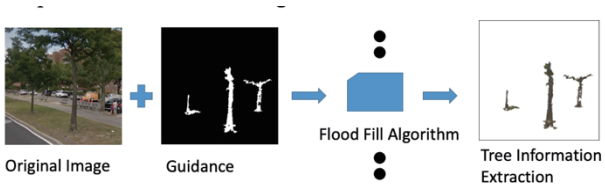

Figure 6. System Flow 3

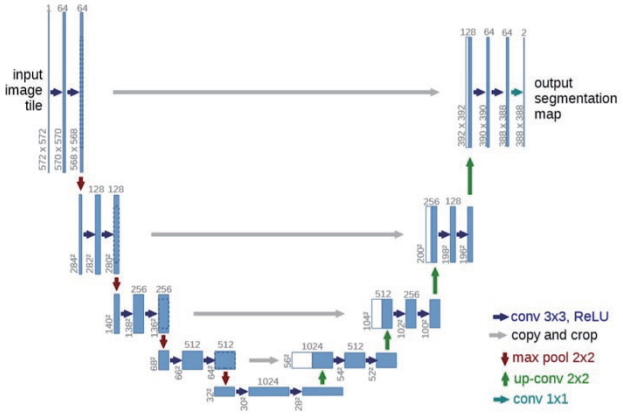

Figure 7. U-Net

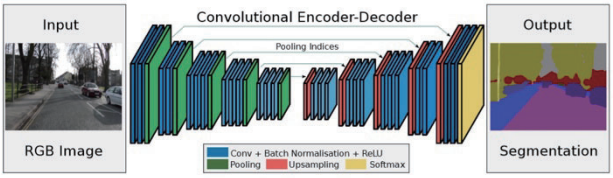

Figure 8. Seg-Net

4. Current Experiment Results

Up to now, we use 100 street view pictures for experiment, Only 40 labeled positive training data are used currently, 30 pictures for testing data, And 30 pictures for negative training data are not adopted yet.

Figure 9. Street Picture in Puli

Figure 10. Segmentation Result use Seg-Net

Figure 10 illustrates an image segmentation result of Seg-Net for a Google Street View picture of Puli, Taiwan in figure 9. The blue regions are for sky, red regions for buildings, white regions for cars, black regions for road, and green regions for plants which are our target for further processing.

Figure 11 is another example of the original street images. And figure 12 illustrates it segmentation results of U-Net trained by deciduous trees images in summer respectively.

Figure 11. A street image which contains multiple trees.

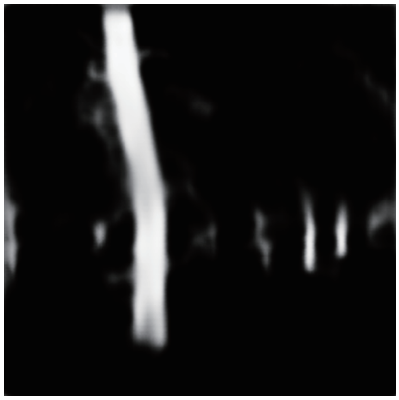

Figure 12. Segmentation Result using U-Net which is trained by trees images in summer.

5. Conclusion

In this research, by utilizing Deep Learning technologies and city open data, we developed a street trees detection method. And we are currently collecting and labeling more images of the 10 most common street trees in 4 seasons for training the Deep Learning models and fine tuning them. There are many parts remained at the conceptual-level, especially at the stage 3, in our prototype system. In addition, more research efforts are required for extracting and separating the shapes of overlapping tree crowns. However, the experiment result still shows that our system has the potentials to:

1. Provide an effective approach for automatically monitoring and managing street trees in smart cities.
2. Severe as a useful tool for users to explore and share the great values of trees in cities and towns.

Acknowledgment

This project is partially supported by No. NSC- 107-2218-E-002 - 048 -.

References

[1] Wajid Ali. “Tree Detection using Color, and Texture Cues for Autonomous Navigation in Forest Environment”. Umea University, 2006.

[2] Y. Lu and C. Rasmussen, "Tree trunk detection using contrast templates," 2011 18th IEEE International Conference on Image Processing, Brussels, 2011, pp. 1253-1256.

[3] Batty M. “Smart cities, big data”. Environment and Planning B: Planning and Design, 39: 191-193, 2012.

[4]ThomasLiebig, NicoPiatkowski, ChristianBockermann, KatharinaMorik, "Dynamic route planning with real-time traffic predic- tions", 2015

[5] CORINNACORTES,VLADIMIRVAPNIK,"Support-VectorNetworks ", 1995

[6] Marco Dorigo, Luca Maria Gambardella, "Ant Colony System: A Cooperative Learning Approach to the Traveling Salesman Problem", 1997

[7] Olaf Ronneberger, Philipp Fischer, Thomas Brox, "U-Net: Convolutional Networks for Biomedical Image Segmentation ", 2015

[8] Vijay Badrinarayanan, Alex Kendall, Roberto Cipolla, "SegNet: A Deep Convolutional Encoder-Decoder Architecture for Image Segmentation", 2016

The 33rd Annual Conference of the Japanese Society for Artificial Intelligence, 2019

Scoring and Classifying Regions via Multimodal Transportation Networks

Aaron Bramson[*1,2,3,4] Megumi Hori[*1] Zha Bingran[*1] Hirohisa Inamoto[*1]

[*1] GA Technologies Inc.
[*2] RIKEN Center for Biosystems Dynamics Research
[*3] Ghent University
[*4] University of North Carolina at Charlotte

In order to better understand the role of transportation convenience in location preferences, as well as to uncover transportation system patterns that span multiple modes of transportation, we score geographic regions according to properties of their multimodal transportation networks. The various scores are then used to classify regions by their dominant mode of transportation, and rank/cluster regions by their transportation features. Specifically, we analyze the train, bus, and road networks of major cities and neighborhoods of Japan to classify them as being train-centric, bus-centric, or car-centric. We also generate scores based on various transportation features to rank cities by their access to public transportation and to categorize/cluster neighborhoods of major cities by their transportation and accessibility properties. We find that business hubs (having low populations) are conveniently reachable via public transportation but vary greatly in their automobile accessibility. Suburban regions have lower connectivity overall but are typically strongly connected to at least one business area. As increasingly rural areas rely more strongly on the road and bus networks, but the network features do not correlate highly with population density.

1. Introduction

Transportation networks can be considered multi-graphs or multilayer networks insofar as there are links of different types connecting nodes representing locations. However, they are also fundamentally geographically embedded which constrains the network structure and requires the inclusion of continuous distance and time weights in discrete network measures. This fusion of network and geographic metrics offers the opportunity to augment network similarity measures as well as fill crucial data gaps about transportation efficiency, accessibility, connectivity, and policies.

2. Data

The geographic foundation of our analysis is a 54,127m^2 (125m inner radius) hexagonal grid covering all of Japan. This is used to define locations as the centers of each hex using GoogleMap's coordinates of Tokyo Station (139.7649361E, 35.6812405N) as a fixed reference point. In order to compare cities and regions within cities, we define a region as all hexes with centroids within 20 km of a selected point. We chose a variety of points across the Tokyo, Kyoto, and Osaka Metropolitan areas to capture a diversity of situations (city centers, suburban bed towns, rural areas, etc.).

2.1 Network Data

We utilize four interwoven networks representing distinct modes of transportation: train/subway, bus/streetcar, road, and walking. The train/subway network represents stations as nodes and train routes as links. In this way, express trains that skip stations are captured by links directly connecting the stations used by that route. The bus network is similarly constructed among bus stops. Our road network is constructed via OpenStreetMaps in which the nodes are intersections and links are road segments; both restricted to roads tagged as *tertiary* or above.

In addition to these networks we include a "walking network". This walking network connects each node of the train network to (1) the closest location of our hex grid as well as (2) any location within 500m of each station. It also connects each bus station to the (1) closest location (2) any location within 200m, and (3) any train station within 200m (when both train and bus networks are included). The third type of link represents a transfer from train to bus. The walking network also connects the nodes of the road network to each location of the hex grid. Finally, we create walking links to convert the location hex grid into a regular k=6 lattice network to allow (slow) transit on foot where no other mode of transportation is available. This walking network is included in all analyses because it is necessary to connect each of the transportation networks to the geographic foundation.

For each link we include a weight equaling the traversal time. For the train and bus data this is set from respective schedules using the average traversal time for that link for that type of train/bus (e.g., local, express). For the road network we calculate the traversal time based on the length of the road segment and the official speed limit (i.e., not considering traffic congestion or actual speeds). For the walking network we assume an average speed of 4kph (15 minutes per km). This slower-than-average speed is used to account for congestion as well indirect walking routes.

In addition to the travel times, we also incorporate a transfer time where appropriate to account for both moving from one platform to another as well as the waiting time for the next train/bus/taxi/etc. Specifically, we add 5 minutes when switching between trains of different lines or types at the same station, and 3 minutes for switching modes: (train ↔ bus, train ↔ road, or bus ↔ road (walking time is already included in the walking link connecting stations, bus stops and intersections).

Contact: Aaron Bramson, GA Technologies, Roppongi Grand Tower 40F, Roppongi 3-2-1, Minato-ku, Tokyo, 106-6290, JAPAN, 03-6230-9180, bramson@ga-tech.co.jp

Although only a rough approximation of the interstitial time gap, it sufficiently summarizes the variance across locations, times of day, walking speeds, congestion conditions, etc. without adding unnecessary complication to the network model.

2.2 Demographic Data

In order to assess practical (versus potential) accessibility we incorporate data regarding the population distribution into our analysis. We take 250m^2 square grid population data obtained from [eStat2018] using grid coordinates from [geoSpacial2018]. Then we resample it to our hex grid using overlap proportions to interpolate the hex populations.

3. Methods

To compare neighborhoods within a city we collect the locations within a 5km radius of multiple secondary and tertiary city centers (these regions overlap). We isolate the transportation networks to within the region of analysis and apply scoring methods to the individual and combined transportation networks. Our most basic evaluation utilizes standard network measures such as diameter, eccentricity profiles, and betweenness profiles along with their time/distance weighted versions. Additionally, we will include specifically geographic and transportation-focused measures such as the profile of times to travel to each regional location, a profile of the number of people reachable within 5, 10, 15, 20 minutes, and the population weighted load on the transportation network to reach the region center.

3.1 Network Measures

To start we calculate several standard network measures (mean degree, mean betweenness, mean eigenvector centrality, mean eccentricity, diameter, clustering coefficient, alpha and beta indices, etc.) on of the following transportation networks: train+walk, bus+walk, road+walk, train+bus+walk, and train+bus+road+walk. We do this for each of several focal areas within Tokyo, Kyoto, and Osaka. This battery of tests allows us to examine both differences in transportation networks for each area and differences among areas for each transportation network.

For each transportation network we calculate the travel times using Dijkstra's algorithm: breadth-first summation of traversed edges' time weights. The core algorithm is augmented to handle transfer times at appropriate junctures. Isochrones are sets of locations binned by travel time, although most of our measures can and do utilize the real-valued traversal times.

3.2 Geotemporal Measures

As a basic measure of accessibility, we compute time-weighted number of hexes reachable form each hex: $\sum_j 1 / t_{ij}$ in which t_{ij} is the shortest time from hex i to hex j. Collecting the population data allows us to determine the *sociability score* of each location; that is, the number of people who can reach each location weighted by the time it takes to reach it. We simplify and generalize the measure from [Biazzo2018] to handle continuous travel time values and averaged edge traversal times. For each hex grid space i we calculate $\sum_j P_j / t_{ij}$ in which P_j is the population of grid space j and t_{ij} is again the shortest time from hex i to hex j. We furthermore include geotemporal versions of certain network measures, such as the time-weighted eccentricity (longest, shortest-time path from the center to the periphery) and time-weighted betweenness.

Figure 1. Isochrone map of Tokyo centered on Tokyo Station using the train+walk network. Darker colors indicate shorter travel times.

3.3 Machine Learning Techniques

In addition to providing a profile of the multifaceted transportation system, the network and geotemporal measures above are also fuel for clustering and discriminant analysis. We apply an ensemble of available measures of whole-network similarity [Soundarajan2014] (*NetSimile* [Berlingerio2012], N*ormalized LBD* [Richards2010], *Graphlets* [Pržulj2004]) as a basis for distance calculations in addition to standard vector-based methods. Using those distance measures we then apply an ensemble of available unsupervised learning techniques (K-means, spectral clustering, affinity propagation, agglomerative clustering, Gaussian mixture) on the regional profiles to score, cluster, and classify them.

4. Results and Conclusions

This is still a work in progress, but preliminary results reveal cities clustered into those which have a dense rail system (e.g. Tokyo), dense regions that instead rely on buses for public transportation (e.g. Kyoto), and regions with weak public transportation that require automobiles (e.g. small cities and suburbs). Although we expected these features to correlate well with population density; we instead find that other factors heavily influence the type and convenience of a transportation network; factors such as average income, percent of commercial properties, and age demographics.

Within cities we see a familiar pattern of easily accessible central regions with low populations and regions of higher population density further out, with populations again tapering down even further out. These suburban regions often have convenient public transport to the city centers, but locally require buses and/or cars for daily transportation. An analysis of

demographics on the presence of children and elderly within the household should also correlate well with a high score on car-centric transportation. These and other results create a multi-faceted scoring of properties by their transportation and demographic features. Our current efforts aim to summary and visualize these results in an intuitive and interactive way that will lead to greater insights and deeper questions.

While most applications of machine learning to transportation networks aim at traffic prediction, flow efficiency, and rerouting, we are particularly interested in identifying cities with underdeveloped public transportation systems and regions within cities with poor accessibility. Related to the latter point, we will uncover differences in regional accessibility by mode of transportation (e.g., areas that are only convenient if one has access to a car). Identifying under- and over-serviced areas can help in policy decisions including infrastructure planning and housing development. Finally, the fusion of geographic and network measures to score areas by the convenience of, and their reliance on, varying modes of transportation can inform decisions for location services (such as apartment hunting, ride sharing, and new store positioning).

4.1 Future Work

We will extend this analysis by including additional demographic and geographic data in the analysis. Our primary purpose here is scoring and clustering areas by transportation accessibility. Future work will examine the relationship between accessibility and socio-economic factors such as unemployment, income, home-ownership, household structure, age profile, crime, etc. We are also interested in identifying network community structure differences [Bohlin2014] among the transportation modes; that is, which geographic regions are considered to be parts of which neighborhoods when considering different networks. Finally, we wish to pursue question of robustness and efficiency via knockout and detour analyses. This can address response to accidents/failures, and further to identify required structural and throughput changes required to adapt to short-term passenger changes (e.g. the Olympics) and long-term demographic changes (e.g., aging population).

Finally, we are strongly interested in the impact of bicycle ride-sharing programs on transportation flow. Although these programs have long been popular in Europe and China, and bicycles usage is high across Japan, there is very little data or analysis on bicycle usage and its interaction with other transportation modes. The recent growing popularity of bicycle-sharing programs will provide additional data to foster more advanced impact studies.

References

[Berlingerio2012] Michele Berlingerio, Danai Koutra, Tina Eliassi-Rad, Christos Faloutsos. “NetSimile: A scalable approach to size-independent network similarity” *CoRR, Abs*/1209.2684, 2012.

[Biazzo2018] Indaco Biazzo, Bernardo Monechi, and Vittorio Loreto, Universal scores for accessibility and inequalities in urban areas, *arXiv*:1810.03017v1, 2018.

[Bohlin2014] Ludvig Bohlin, Daniel Edler, Andrea Lancichinetti, and Martin Rosvall. "Community detection and visualization of networks with the map equation framework." In *Measuring Scholarly Impact*. Springer, 2014, pp. 3-34.

[eStat2018] Official Statistics of Japan. www.e-stat.go.jp “統計データ/ 国勢調査/ 2015 年/ 5 次メッシュ（250m メッシュ）/ その1人口等基本集計に関する事項” (accessed December 12, 2018).

[geoSpacial2018] Association for Promotion of Infrastructure Geospatial Information Distribution. www.geospatial.jp “都道府県別 250m メッシュ” (accessed December 12, 2018).

[Richards2010] Whitman Richards and Owen Macindoe. “Decomposing Social Networks.” *2010 IEEE Second International Conference on Social Computing* 2010, pp 114-119.

[Soundarajan2014] Sucheta Soundarajan, Tina Eliassi-Rad, and Brian Gallagher. "A guide to selecting a network similarity method." In *Proceedings of the 2014 SIAM International Conference on Data Mining*, pp. 1037-1045. Society for Industrial and Applied Mathematics, 2014.

[Pržulj2004] Nataša Pržulj, Derek G. Corneil, and Igor Jurisica. "Modeling interactome: scale-free or geometric?" *Bioinformatics* 20, no. 18 2004, 3508-3515.

The 33rd Annual Conference of the Japanese Society for Artificial Intelligence, 2019

Evaluating Road Surface Condition by using Wheelchair Driving Data and Positional Information based Weakly Supervision

Takumi Watanabe[*1] Hiroki Takahashi[*1] Yusuke Iwasawa[*2] Yutaka Matsuo[*2] Ikuko E. Yairi[*1]

[*1] Graduate School of Science and Engineering, Sophia University
[*2] Graduate School of Technology Management for Innovation, The University of Tokyo

Providing accessibility information on sidewalks for mobility impaired people is an important social issue. Until now, the authors have evaluated the accessibility of sidewalks by estimating the road surface condition by supervised learning on the accelerometer data mounted on wheelchairs. Video recording and data labeling to accelerometer data based on the video for teacher data require enormous costs and become problematic. This paper proposed and evaluated a novel weakly supervised road surface condition evaluation system of using positional information automatically acquired at driving as a label. The evaluation result showed that weakly supervised learning method using locational label captured detailed features of road surfaces, and classified moving on slopes, curb climbing, moving on tactile indicators, and others with a mean F-score of 0.57 and accuracy of 0.71 close to those of supervised learning method.

1. Introduction

Providing accessibility information on sidewalks for mobility impaired people, such as elderly people and wheelchair users, is one of the important social issues. The conventional methods for gathering accessibility information are as follows: a system that experts evaluate images of sidewalks for each case [Ponsard 06], a crowdsourcing method to recruit volunteers to take pictures of sidewalks and evaluate them [Hara 14, Cardonha 13]. All these methods are based on human power and thus gathering large-scale accessibility information is difficult. Because of the recent expansion of intelligent gadgets, such as smartphones and wristwatch-shaped vital sensors, there is a growing movement of sensing human activities [Swan 13, Nagamine 15]. The authors have been proposing a system which evaluates road surface condition by machine learning using accelerometer data. This system focuses on the fact that the observed values of the accelerometer mounted on a wheelchair is influenced by the condition of the road surfaces. In machine learning, however, video recording and video-based labeling to acceleration data for teacher data require a huge cost and become a serious problem. In various machine learning fields, weakly supervised learning [Zhou 18] methods that do not require conventional detailed teacher labels have been proposed [Oquab 15, Gidaris 18, You 18]. In this paper, the authors propose and evaluate the road surface condition evaluation system by weakly supervised learning which uses positional information labels which can be automatically acquired at the time of driving and thus does not require conventional detailed labels. Our contributions are as follows: we propose a novel method of weakly supervised learning of extracting feature representations of the road surface condition from accelerometer data without conventional detailed labels; we verify the effectiveness of our method using actual data.

Contact: Takumi Watanabe, Graduate School of Science and Engineering, Sophia University, Tokyo, 102-8554 Japan, 03-3238-3280, watanabe@yairilab.net

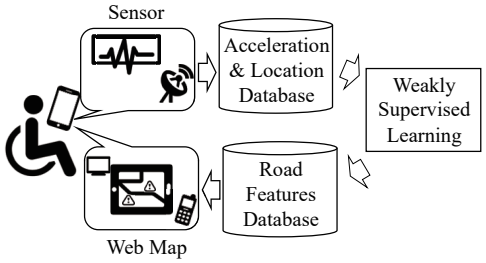

Figure 1 Outline drawing of road surface condition evaluation system by wheelchair sensing and weak supervision.

2. Road surface condition evaluation system

Figure 1 shows an outline of the proposed system. Vibration waveforms of wheelchair movement are collected by an accelerometer mounted on a wheelchair. Extracting road surface information from vibration waveforms using machine learning, the extracted data is accumulated and visualized on a web map. Extracting influence of the road surface condition from the raw accelerometer data is not easy [Lara 12, Liu 17]. Therefore, it is important to convert observed accelerometer data to indexes which represent the condition of the road surface. Some methods for expressing the road surface condition in several discrete classes by creating acceleration data classifiers using machine learning have been proposed [Iwasawa 12, Iwasawa15, Iwasawa 16], and a method for acquiring more detailed road surface features than applied several discrete labels by using feature values extracted from pre-trained DCNN is proposed [Takahashi 18]. However, these methods depend on detailed road surface condition labels and require enormous costs.

3. Road surface condition evaluation by weakly supervised learning

Dataset

The total of nine wheelchair users, including six manual wheelchair users(M1~M6) and three Powered wheelchair users(P1~P3), participated in the experiment. Their actions while

driving about 1.4 km of a specified route around Yotsuya station in Tokyo were measured by an accelerometer (iPod touch) mounted on the lower part of the wheelchair seat, and positioning data of Quasi-Zenith Satellite System (QZSS) was measured at the same time. In order to confirm the situation where the acceleration data sample was acquired, the video of the participant's driving state and the driving road surface condition were taken during the experiment. Acceleration values in the x, y, and z axes of the accelerometer were sampled at 50 Hz, and the total of 1,341,142 samples (about 8 hours) was obtained.

Weakly supervised label

For the training of DCNN, positional information was used as a weakly supervised label as a method of weakly supervised learning. For the positional information in this paper, we checked the location where the accelerometer data was measured by visual observation of the recorded video and used the GPS data (latitude, longitude) acquired on Google Map website as positional information. In assigning labels to the acceleration data, all the sidewalks traveled at the time of the experiment were divided into meshes of an uniform width, and a grid belonging at the time of the measurement of the acceleration data was assigned as a weakly supervised label (as shown in Figure 2). Labels were generated under the conditions of a grid width of 3 m, 4 m, and 5 m.

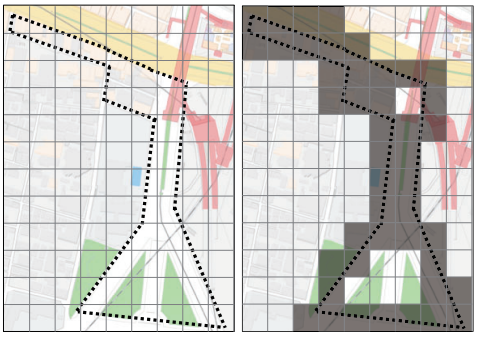

Figure 2 Outline of grids to be weakly supervised label. The left shows how all the sidewalks were divided into meshes, and the right shows how each grid was assigned as a label.

Weakly supervised DCNN

The three axes of acceleration data were segmented into 28502 and 6692 pieces by a sliding window method with a window size of 400 (about 8 seconds) and 100 (about 2 seconds) respectively and overlapping rate of 0.5. As shown in Figure 3, the DCNN used for weakly supervised learning is composed of 7 layers of an input layer, 4 convolutional layers, one fully connected layer, and an output layer. By using the hierarchical structured network and training functions in layers from input to output, feature extractor h and the classifier f those are effective for classification are trained simultaneously.

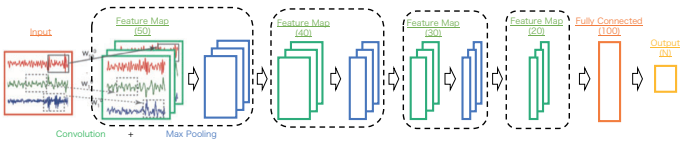

Figure 3 Illustration of the DCNN structure.

Acquisition and Clustering of feature representations

The procedure of acquiring road surface feature representations from weakly trained DCNN and clustering the similar condition road surfaces based on the extracted feature representations is described in order from Step 1 to Step 5.

Step 1: Acquisition of an output pattern of all data

For the DCNN model trained with eight participants data sets as a training data, the remaining one participant data set was input to the DCNN and 100 units output pattern in the fully connected layer was extracted as feature representations of each segmented data.

Step 2: Clustering of feature representations

After compressing the acquired 100-dimensional feature values to a dimension whose cumulative contribution rate exceeds 80% by principal component analysis, clustering was performed on the compressed feature values using the k-means method.

Step 3: Visualization on a map

Clusters generated in Step 2 were color-coded and each point of each cluster was visualized on a map.

Step 4: Analysis of clustering results

Visually comparing the plot result obtained in Step 3 and the recorded video during driving, the road surface condition belonging to each cluster was analyzed.

Step 5: Optimum grid width, window size, and number of clusters

Based on Step 3 and Step 4, the optimum grid width and window size were selected, then a number of clusters that captures the most detailed features of the road surface conditions were selected under best grid width and window size.

4. Qualitative evaluation by clustering

a) Selection of optimum grid width

Plot results with a grid width of 3 m, 4 m, and 5 m with a cluster number of 5 and a window size of 400 were compared.

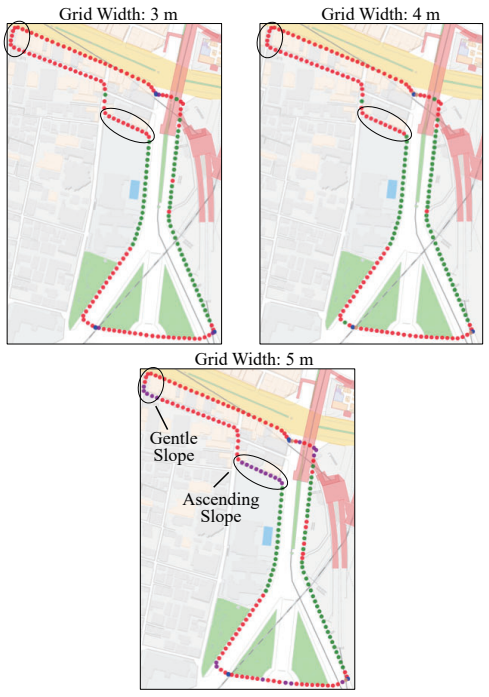

Figure 4 Comparison of clustering results under each condition of a grid width of 3 m, 4 m, and 5 m.

As shown in Figure 4, at the grid width of 5 m, the DCNN captured the features of the ascending slope the most. From this result it is considered that the larger the grid width is, the larger the range of the road surface learned as one label in the DCNN, and DCNN captured an ascending slope where features are easier to read in the larger range.

b) Selection of optimum window size

Plot results with a window size of 100 and 400 with a cluster number of 5 and a grid width of 5 m were compared. As Shown in Figure 5, at the window size of 400, DCNN captured the features of the ascending slope the most. From this result, it is considered that the larger window size is, the larger each segmented training sample in DCNN, and DCNN captured an ascending slope where features are easier to read in the larger range.

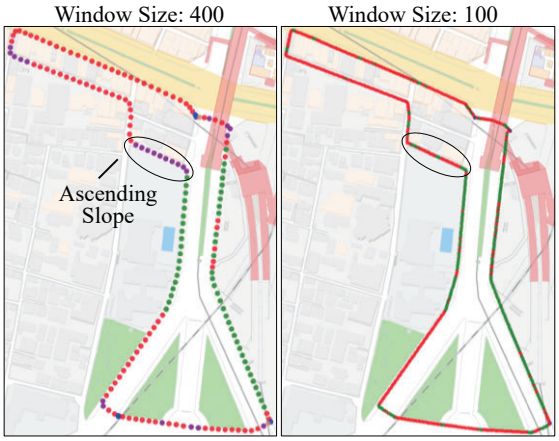

Figure 5 Comparison of clustering results under each condition of a window size of 400 and 100.

c) Selection of the optimum number of clusters

Plot results with the number of clusters 5 to 10 with a grid width of 5 m window size of 400 were compared. As shown in Figure 6, the ascending slope and descending slope were classified into one cluster respectively, and curbs were classified into a specific cluster. Table 1 shows the number of clusters that classified the most detailed road surface condition for each user.

d) Comparison with conventional labeling method

As a result of comparing Figure 5 and clustering result of feature values extracted from detailed labeled trained DCNN, it was shown that weakly supervised method captured more detailed road surface features than the conventional DCNN.

5. Quantitative evaluation of features acquired from weakly supervised DCNN

Evaluation method

Using feature values extracted from weakly trained DCNN as an input, a new classifier was trained as a classification task of four types of labeled road surfaces: slope, curb, braille block, and others. These four types represent typical features of road surfaces, so this method evaluates feature values extracted from weakly supervised DCNN whether they are useful as an indicator of the condition of the road surface.

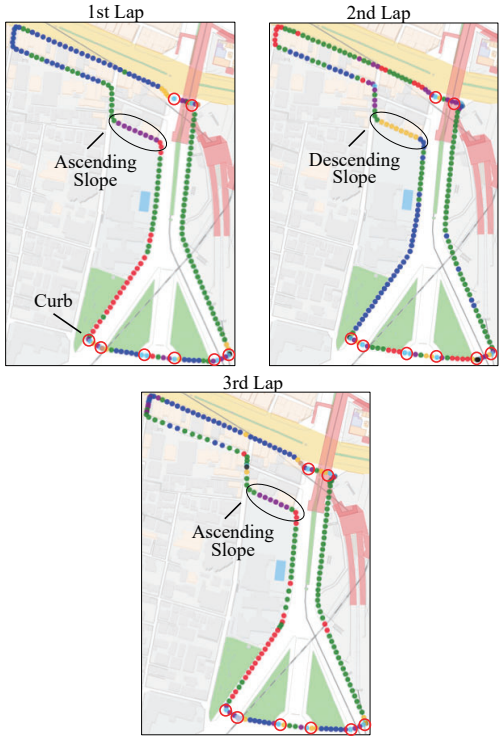

Figure 6 Clustering result with the number of clusters 9 in grid width 5 m and window size 400.
The 1st and 3rd lap are clockwise, so the slope is ascending.
The 2nd lap is counterclockwise, so the slope is descending.

Table 1 Optimum number of clusters for each participant.

Participant	M1	M2	M3	M4	M5	M6	P1	P2	P3
number of clusters	10	8	9	8	9	8	9	9	9

Table 2 Performance comparison between supervised DCNN and weakly supervised DCNN method.

Method	Supervised DCNN	SVM	LR
Mean F-Score	0.58	0.57	0.54
Accuracy	0.81	0.71	0.74

Comparison with Supervised DCNN

Table 2 is a comparison of the classification score. The mean F-score and the accuracy of each class were used as evaluation indexes. Supervised DCNN is the conventional method of training the dataset with DCNN labeled four types of road surfaces. SVM
uses feature values extracted from weakly supervised DCNN as an input and uses Support Vector Machine as a classifier. LR uses feature values extracted from weakly supervised DCNN as an input and uses Logistic Regression as a classifier. As a result, in LR, the mean F-Score was 0.04 points lower than the supervised DCNN, and the accuracy was 0.07 points lower than the supervised DCNN. From this result, it is considered that weakly supervised method misclassified others which occupy more than 70 % of the four labels into a slope, curb, or braille

block, and classified the three types of the road surface to the same degree as Supervised DCNN.

6. Conclusion

In this paper, we proposed a novel method to evaluate road surface condition by weakly supervised learning using positional information as a label and accelerometer data. As a result, it was shown that feature representations acquired by Weakly Supervised DCNN can capture more detailed features of road surfaces than feature values by conventional supervised DCNN, and quantitatively estimate road surface condition. As a future work, we will propose a method to acquire higher-precision feature representations based on new weak label generation method and conduct a detailed analysis of what kind of road surface conditions DCNN with the position information extracts.

Acknowledgments.

We are deeply grateful to all participants of the experiment. This study was supported by Tateishi Science and Technology Foundation in FY2011-2012, the research grant by Chiyoda-ku(CHIYODAGAKU) in FY 2014-2016, and JSPS KAKENHI Grant Number 17H01946.

References

[Ponsard 06] Ponsard, C. and Snoeck, V.: Objective accessibility assessment of public infrastructures, in *10th Int. Conf. on Computers Helping People with Special Needs,* pp. 314–321, Linz, Austria (2006)

[Hara 14] Hara, K.: Scalable methods to collect and visualize sidewalk accessibility data for people with mobility impairments, in *Proc. Adjunct Publication of the 27th Annual ACM Symposium on User Interface Software and Technology*, pp. 1–4, Honolulu, HI, USA (2014)

[Cardonha 13] Cardonha, C., Gallo, D., Avegliano, P., Herrmann, R., Koch, F., and Borger, S.: A crowdsourcing platform for the construction of accessibility maps, in *Proc. 10th Int. Cross-Disciplinary Conf. on Web Accessibility*, p. 26 Rio de Janeiro, Brazil (2013)

[Swan 13] Swan, M.: The Quantified Self: Fundamental Disruption in Big Data Science and Biological Discovery, *Big Data*, Vol. 1, No. 2, pp. 85–99 (2013)

[Nagamine 15] Nagamine, K., Iwasawa, Y., Matsuo, Y., and Yairi, I. E.: An Estimation of Wheelchair User's Muscle Fatigue by Accelerometers on Smart Devices, in *Adjunct Proc. 2015 ACM Int. Joint Conf. on Pervasive and Ubiquitous Computing and Proc. 2015 ACM Int. Symposium on Wearable Computers*, UbiComp/ISWC'15 Adjunct, pp. 57–60, New York, NY, USA (2015)

[Zhou 18] Zhou, Z. H.: A brief introduction to weakly supervised learning, in *National Science Review*, Vol. 5, No. 1, pp. 44-53, (2018)

[Oquab 15] Oquab, M., Bottou, L., Laptev, I., and Sivic, J.: Is object localization for free?-weakly-supervised learning with convolutional neural networks, in *Proc. IEEE Conf. on Computer Vision and Pattern Recognition*, pp. 685-694, Boston, MA, USA (2015)

[Gidaris 18] Gidaris, S., Singh, P., and Komodakis, N.: Unsupervised Representation Learning by Predicting Image Rotations, in *6th Int. Conf. on Learning Representations*, Vancouver, BC, Canada, (2018)

[You 18] You, Z., Raich, R., Fern, X. Z., and Kim, J.: Weakly Supervised Dictionary Learning, in *IEEE Trans. Signal Proc.*, Vol. 66, No. 10, pp. 2527-2541, (2018)

[Lara 12] Lara, O. D. and Labrador, M. A.: A survey on human activity recognition using wearable sensors, in *IEEE Commun. Surveys Tutorials*, Vol. 15, No. 3, pp. 1192–1209, (2012)

[Liu 17] Liu, H., Taniguchi, T., Tanaka, K., Takenaka, Y., and T. Bando: Visualization of driving behavior based on hidden feature extraction by using deep learning, in *IEEE Trans. Intelligent Transportation Systems*, Vol. 18, No. 9, pp. 2477–2489, (2017)

[Iwasawa 12] Iwasawa, Y. and Yairi, I. E.: Life-logging of wheelchair driving on web maps for visualizing potential accidents and incidents, in *PRICAI 2012: Trends in Artificial Intelligence*, pp. 157–169, Springer (2012)

[Iwasawa 15] Iwasawa, Y., Nagamine, K., Matsuo, Y., and Eguchi Yairi, I.: Road Sensing: Personal Sensing and Machine Learning for Development of Large Scale Accessibility Map, in *Proc. 17th Int. ACM SIGACCESS Conf. on Computers & Accessibility,* pp. 335–336ACM (2015)

[Iwasawa 16] Iwasawa, Y., Yairi, I. E., and Matsuo, Y.: Combining Human Action Sensing of Wheelchair Users and Machine Learning for Autonomous Accessibility Data Collection, in *IEICE Trans. on Information and Systems*, Vol. E99-D, No. 4, pp. 115–124 (2016)

[Takahashi 18] Takahashi, H., Nagamine, K., Iwasawa, Y., Matsuo, Y., and Yairi, I. E.: Quantification of Road Condition from Wheelchair Sensing Data Using Deep Convolutional Neural Network, in *IEICE Trans. Information and Systems*, Vol. J101-D, No. 6, pp. 1009-1021 (2018) (In Japanese)

The 33rd Annual Conference of the Japanese Society for Artificial Intelligence, 2019

Prediction of the Onset of Lifestyle-related Diseases Using Regular Health Checkup Data

Mitsuru Tsunekawa[*1] Natsuki Oka[*1] Masahiro Araki[*1] Motoshi Shintani[*2]
Masataka Yoshikawa[*3] Takeshi Tanigawa[*4]

[*1] Kyoto Institute of Techonology [*2] SG Holdings Group Health Insurance Association
[*3] Japan System Techniques Co.,Ltd. [*4] Juntendo University

This study proposes a method for predicting the onset of lifestyle-related diseases using periodical health checkup data. We carefully examined insurance claims data to identify the onsets of the diseases and used them as correct answers for supervised learning. We adopted the undersampling and bagging approach to address the class imbalance problem. We aimed to predict whether lifestyle-related diseases, other than cancer, will develop within one year. The precision and recall of the proposed method were 0.32 and 0.89, respectively. Compared with a baseline that sets thresholds for each examination item and considers their logical sum, it was found that much higher precision could be obtained while maintaining recall, which is meaningful as it allows for the suppression of the number of targets for health guidance, without increasing the negligence of those that are likely to become severely ill.

1. Introduction

Many people have recently begun using Internet mail-order sales, greatly increasing the number of deliveries. Consequently, the social interest in the work environment and health management of courier drivers is increasing. If appropriate health guidance can reduce the occurrence of drivers' lifestyle-related diseases and prevent severe idiopathic illnesses during driving, medical expenses and traffic accidents can be decreased. We, therefore, aimed to use drivers' regular health checkup data to predict the onset of lifestyle-related diseases as accurately as and ensure provision of appropriate health guidance.

Many studies have used machine learning and data mining techniques to predict disease onset from medical data. For example, [Weng 17] highlighted the superiority of machine learning techniques to predict cardiovascular risk from routine clinical data; [Yatsuya 16] predicted the occurrence probability of myocardial infarction or cerebral infarction using health examination results. Morevoer, [Uematsu 17] proposed a model that predicts pneumonia hospitalization using the Lasso logistic regression of regular health checkup data, which is similar to our research model in that it tries to predict using periodical health checkup data of healthy people. Our study objective was to predict whether lifestyle-related diseases, other than cancer, will develop within one year, using regular medical examination data of Courier drivers.

2. Target Data

2.1 Data overview

We used insurance claims and regular health checkup data of employees from the SG Holdings Group Health Insurance Association. Health insurance claims data is created when a person is injured or ill and visits a medical institution, whereas health checkup data is taken regularly (typically once a year). The two datasets were anonymized and linked with a hash code for uniquely identifying patients. In this study, disease onsets were extracted from the insurance claims data and used as correct answers for onset prediction; the health checkup data is used as input for onset prediction.

Health insurance claims data includes disease name codes and medical examination dates etc. Details of the health checkup data are provided later.

In this study, we analyzed the insurance claims data from 1996 to 2017 and the health checkup data from 2006 to 2018, of individuals aged 15-74 years; the total health checkup data was 961,906 sheets for 156,145 people, and the total insurance claims data was 1,617,078 sheets for 108,581 people.

2.2 Disease names as prediction targets

An individual's diagnosed diseases names were obtained by searching through the disease name codes included in the health insurance claims data and corresponded with those in the ICD-10. Table 1 presents the ICD-10 codes and the corresponding disease names to be predicted (hereinafter, referred to as "severe disease names").

2.3 Feature values used for prediction

The following examination items of health checkup data were used as feature values for prediction: Health examination data included not only the numerical data of inspection results, but also the results of a questionnaire on lifestyle habits, and the judgment results of six levels derived from the examination data by medical institutions. Items of abdominal girth and visual acuity judgment, heart rate, visual acuity judgment, fundus judgment, and metabolic judgment were removed, since the ratio of missing values was

Contact: Mitsuru Tsunekawa, Kyoto Institute of Technology, and E-mail: m-tsune@ii.is.kit.ac.jp

Table 1: ICD-10 codes of severe disease names.

ICD-10	disease name
E10	Insulin dependent diabetes mellitus
E11	Non-insulin dependent diabetes mellitus
E14	Diabetes mellitus other than the above
I20	Angina pectoris
I21, I22	Acute myocardial infarction
I42	Cardiomyopathy
I44 I49	Arrhythmia, Conduction defects
I60, I690	Subarachnoid hemorrhage
I61, I691	Intracerebral hemorrhage
I63, I693	Cerebral infarction

50% or more. The health examination data also included findings freely described by doctors; however, we excluded them because natural language understanding is necessary for use of free description.

Health examination data items used as input features are as follows:
Sex; Age; Height; Weight; Body fat percentage; Systolic blood pressure; Diastolic blood pressure; Number of red blood cells; Hemoglobin; Hematocrit; Platelet count; GOT; GPT; γ-GTP; Total cholesterol; HDL cholesterol; LDL cholesterol; Neutral fat; Uric acid; Creatinine; eGFR; HbA1c; Questions about medicine to lower blood pressure, insulin injection, or medicine to lower blood sugar, medicine to ameliorate dyslipidemia, stroke, chronic renal failure, anemia, smoking habits, weight change from the age of 20 years, exercise habits, walking habits, walking speed, weight change over the past year, eating speed, meal just before going to bed, after dinner snacks, skipping breakfast, drinking habits, drinking alcohol amount, sleeping time, willingness to improve lifestyle habits, and willingness to receive health guidance; Judgments on urinary protein and urine sugar; Representative judgment; Judgments on physical measurements, hearing ability, blood pressures, anemia, liver function, renal function, uric acid and gout, blood sugar, sugar metabolism, and urinalysis; Examination judgment.

2.4 Characteristics of data

The data typically have two characteristics. First, considerable imbalance: For example, in 2017, the proportion of people diagnosed with severe diseases was only 4.5%. The learning of such unbalanced data may be greatly affected by the properties of a large number of negative examples, persons who are not diagnosed with severe diseases. Therefore, a method that can successfully learn this imbalanced data must be adopted.

Second, classifying data as positive or negative is not easy. In this study, we aimed to predict whether a person who is healthy at the time of a regular health checkup will be diagnosed with one of the severe diseases within a year of the checkup. Consequently, data was positive if the person will fall sick within a year, and negative if not. Therefore, it was necessary to accurately judge the presence or absence of illness at the time of a health checkup.

The point at which the target disease name first appeared in an employee's insurance claims data was not necessarily the point when he/she first developed the disease. It is not uncommon for individuals with previously diagnosed diseases to join a health insurance association in an industry with large personnel flow. However, because the data used in this study belonged to a health insurance association, it was only available for the period of joining the association; the insurance claims data before entering the association could not be confirmed. The next section describes how we addressed this problem.

3. Data selection and machine learning method

3.1 Data selection

We addressed the classification problem of predicting whether individuals will suffer severe illness within one year, by using medical examination data. The data selection method for positive and negative data was as follows.

First, to address the previously mentioned data availability problem, we used the following method and determined whether the insurance claims data of an individual's first-time diagnosis of a severe disease was actually first. We first calculated the hospital visit interval for the same disease after receiving the diagnosis of a disease. If the hospital visit interval was shorter than the interval between the day of joining the health insurance association and the day of first-time diagnosis of a severe disease, the diagnosis was judged to be actually first; alternatively, if the visit interval was greater, it was judged not to be first. The visit interval was calculated using three interval data, which we regarded as sufficient. The specific procedure was as follows (see also Figure 1):
1) Extract the oldest data (*) with a severe disease name from an individual's insurance claims data. 2) Select three consecutive data with the same disease name that are newer than the extracted data and calculate the hospital visit intervals. 3) Retrieve the individual's oldest insurance claims data (**) and calculate the interval between data (**) and data(*). 4) If the maximum of the three values calculated in "2)" is smaller than that calculated in "3)," regard data (*) as the first-diagnosis data of the disease.

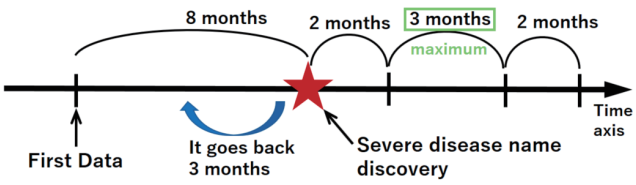

Figure 1: Method of judging the genuineness of the first diagnosis.

Next, the positive health checkup data was chosen from the data included within the range of one year or less before the first appearance of the severe disease. When there were multiple data in the range, we adopted the oldest one. We also considered the amount of changes in the health checkup

data, calculated the differences between the chosen data and the previous data and between the chosen data and the two previous data, and added them to the feature set (Figure 2). Since some items in the health checkup data would have changed with the development of the disease, we considered that the discrimination accuracy improved by explicitly adding the change amount to the feature set.

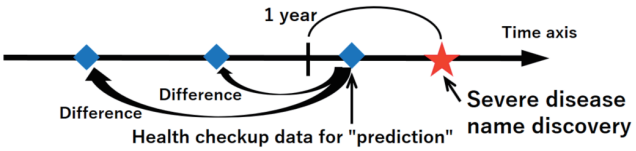

Figure 2: Selection of positive data.

For negative data, however, we excluded data of individuals who had been diagnosed with a severe disease even once and used only the remaining data. Furthermore, if there is no insurance claims data after more than one year from when the health checkup data was extracted, the possibility is that the individual may have been diagnosed with a severe disease within one year of data extraction. This is possible if the person leaves the job. Therefore, to eliminate this possibility, we excluded the data of individuals with no insurance claims data after one year or more from the extracted health examination data. As with the positive data, we calculated the differences using three consecutive health examination data and added them to the feature set (Figure 3).

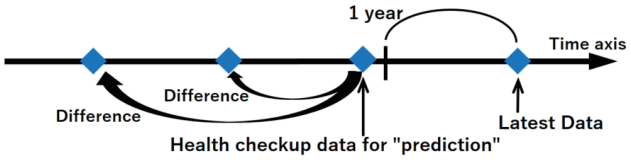

Figure 3: Selection of negative data.

There were cases in which an individual had multiple medical examination data that fit the selection criteria. This was common in both positive and negative data. However, we used only one data per individual to prevent data imbalance. If we did not select the oldest data for positive data, we used data after being diagnosed with one of the severe diseases; however,for negative example, we can select data at any point in time.

Thus, we obtained 1255 positive data and 37664 negative data, with 133 features. The missing values were filled with the median values.

3.2 Machine learning method

In this study, undersampling and bagging [Wallace 11] was adopted as an effective learning method for imbalanced data. Bagging is a method of improving classification accuracy by combining classifiers which are called weak learners. We used decision trees without pruning as classifiers because they were unstable and resulted in higher performance. Undersampling created balanced data.

4. Results and discussion

There were 500 weak learners. Even if the number of weak learners was changed to range between 100 and 500, there was little change in recall and precision; however, if the number was less than 100, the precision decreased. Since the decision tree used for the weak learners was an algorithm not affected by the scale, data scaling was not performed. We used 70% of the dataset for learning and 30% for evaluation. Table 2 presents the confusion matrix of the proposed method. The positive precision and recall were 0.32 and 0.89, respectively.

Table 2: Confusion matrix of the proposed method.

		Predicted class	
		Positive	Negative
Actual class	Positive	334	43
	Negative	700	10600

We used a judgment category table[*1] that was officially released by the Japan Society of Ningen Dock as the baseline method. A threshold value for each item was set and discrimination was carried out by logical OR operation on each item. We only used the items that were common to the input features of this study. The total number of items used was 13. The table classified health checkup data into four categories: No abnormality, Mild abnormality, Follow-up required, and Medical treatment required.

The precision-recall curves of the proposed method and the baseline method are shown in Figure 4. The thresholds of three categories, excluding "No abnormality," were used to plot the precision-recall curve of the baseline method. For the proposed method, we changed the ratio of the positive and negative examples in undersampling as follows: 1:0.25, 1:0.5, 1:1, 1:2, 1:4, 1:8, and 1:16. We added another precision-recall curve of the proposed method in which the number of features was reduced to 13 in order to compare with the baseline method using the same features.

Since the graph of the proposed method lies clearly above that of the baseline method, the proposed method can be considered superior to the baseline method. The results demonstrated that much higher precision could be obtained by the proposed method when the recall was about the same degree as the baseline method; increasing precision while maintaining recall is meaningful as it allows for the suppression of the number of targets for health guidance, without increasing the negligence of those who are likely to become severely ill.

We identified the features that were important for classification. The top 3 were HbA1c, metabolism judgement, and the question about taking insulin injection or a drug that lowers blood glucose. Metabolic judgement refers to the judgment of the danger of metabolic syndrome in six levels from the health checkup data. HbA1c is one of the indicators used to judge diabetes, prescribing insulin injection and medication to lower blood glucose is a treatment

*1 https://www.ningen-dock.jp/wp/wp-content/uploads/2013/09/Dock-Hantei2018-20181214.pdf

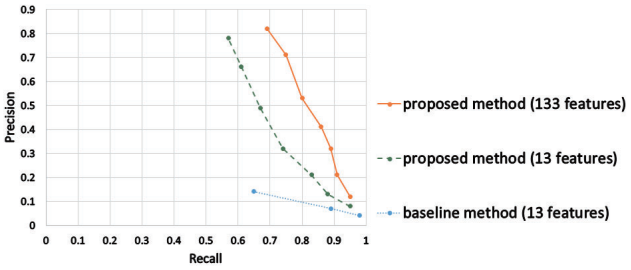

Figure 4: Precision-recall curves of the proposed method and the baseline method.

related to diabetes. Thus, diabetes can be easily distinguished using health checkup data. Among the positive data, the number of diabetes mellitus was as high as 74%; therefore, if identify diabetes, the result would have a high overall accuracy. To confirm this assumption, we focused solely on diabetes and its prediction. Positive cases were defined as persons diagnosed with diabetes mellitus; negative cases comprised patients with severe diseases other than diabetes and healthy people. The created dataset comprised 921 positive and 37998 negative cases. As a result of classification, the positive precision and recall were 0.34 and 0.92, respectively. The confusion matrix is shown in Table 3.

Table 3: Confusion matrix for diabetes prediction using the proposed method.

		Predicted class	
		Positive	Negative
Actual class	Positive	254	23
	Negative	494	10906

Next, to compare with diabetes, we tried to predict the second most frequent angina using the proposed method. As before, positive cases were defined as persons diagnosed with angina pectoris, and negative cases consisted of patients with severe diseases other than angina pectoris and healthy people.

The created dataset comprised 229 positive and 38690 negative cases. As a result of prediction, the positive precision and recall were 0.03 and 0.90, respectively. Table 4 shows the confusion matrix. As evident, the precision reduced and angina pectoris was difficult to discriminate.

Table 4: Confusion matrix for angina pectoris prediction uising the proposed method.

		Predicted class	
		Positive	Negative
Actual class	Positive	62	7
	Negative	1755	9852

5. Conclusion

5.1 Summary

In this study, we proposed a method to predict the onset of lifestyle-related diseases other than cancer, using periodical health checkup data, and a method to select learning data based on the insurance claims data. When all target disease names were identified as positive cases, we obtained positive precision and recall values, 0.32 and 0.89, respectively. Compared to the judgment category table, which the Japan Society of Ningen Dock used as a baseline, it was found that much higher precision could be obtained when the recall was about the same degree.

5.2 Future tasks

In this study, doctors' findings from the health examination data were excluded; however, applying natural language processing to this part will allow the data to be used. As another method of coping with imbalanced data, we plan to use an anomaly detection method that constructs a model using data of healthy people as normal data and detecting data that does not fit the model. We also plan to predict the onset of lifestyle-related diseases after more than one year of a regular medical examination.

A major limitation of this study was that although insulin injection and drugs that lower blood glucose should not be prescribed before receiving a diagnosis of diabetes, the item "Do you take insulin injection or a drug that lowers blood glucose" was used as one of the main items to predict the onset of diabetes. This means that the selection process of positive and negative data need to be reconsidered.

References

[Weng 17] Weng, F. S., Reps, J.,Kai, J., Garibaldi, M. J., and Qureshi, N.: Can Machine-learning Improve Cardiovascular Risk Prediction Using Routine Clinical Data?, PLoS One, 12(4), doi:10.1371/journal.pone.0174944 (2017).

[Yatsuya 16] Yatsuya, H., Iso, H., Li, Y., Yamagishi, K., Kokubo, Y., Saito, I., Sawada, N., Inoue, M., and Tsugane, S.: Development of a Risk Equation for the Incidence of Coronary Artery Disease and Ischemic Stroke for Middle-aged Japanese Japan Public Health Center-Based Prospective Study. Circulation Journal, 80(60), 1386-1395 (2016).

[Uematsu 17] Uematsu, H., Yamashita, K., Kunisawa, S., Otsubo, T., and Imanaka, Y.:Prediction of Pneumonia Hospitalization in Adults Using Health Checkup Data, PLoS One, 12(6), doi:10.1371/journal.pone.0180159 (2017).

[Wallace 11] Wallace, C. B.,Small, K., Brodley, E. C., and Trikalinos, A. T.: Class Imbalance, Redux, IEEE 11th International Conference on Data Mining, IEEE Xplore, doi:10.1109/ICDM.2011.33 (2011).

International Session | International Session | [ES] E-5 Human interface, education aid

[4H2-E-5] Human interface, education aid: human evaluation

Chair: Naohiro Matsumura (Osaka University)

Fri. Jun 7, 2019 12:00 PM - 1:40 PM Room H (303+304 Small meeting rooms)

[4H2-E-5-01] Recognition of Kuzushi-ji with Deep Learning Method

○Xiaoran Hu[1], Mariko Inamoto[2], Akihiko Konagaya[1] （1. Tokyo Institute of Technology, 2. Keisen University）

12:00 PM - 12:20 PM

[4H2-E-5-02] Computerized Adaptive Testing Method using Integer Programming to Minimize Item Exposure

○Yoshimitsu MIYAZAWA[1], Maomi UENO[2] （1. The National Center for University Entrance Examinations, 2. The University of Electro-Communications）

12:20 PM - 12:40 PM

[4H2-E-5-03] Maximizing accuracy of group peer assessment using item response theory and integer programming

○Masaki Uto[1], Duc-Thien Nguyen[1], Maomi Ueno[1] （1. University of Electro-Communications）

12:40 PM - 1:00 PM

[4H2-E-5-04] Waveform Processing of Electrocardiogram with Neural Network and Non-contact Measurement using Kinect for Driver Evaluation

○HAO ZHANG[1], Takashi IMAMURA[1] （1. Niigata University）

1:00 PM - 1:20 PM

[4H2-E-5-05] Probability based scaffolding system using Deep Learning

○Ryo Kinoshita[1], Maomi Ueno[1] （1. The University of Electro-Communications.）

1:20 PM - 1:40 PM

The 33rd Annual Conference of the Japanese Society for Artificial Intelligence, 2019

Recognition of Kuzushi-ji with Deep Learning Method: A Case Study of Kiritsubo Chapter in the Tale of Genji

Xiaoran Hu[*1] Mariko Inamoto[*2] Akihiko Konagaya[*1]

[*1] Tokyo Institute of Technology [*2] Keisen University

Reading ancient documents is one of fundamental works on the study of national literature. However, due to the use of kuzushi-ji (classical cursive handwriting characters) in the ancient documents, it requires a lot of knowledge and labor to read. This paper uses an End-to-End method with attention mechanism to recognize the continuous kuzushi-ji in phrases. Compared with the traditional recognition model with Connectionist Temporal Classification (CTC), our approach can get higher accuracy of recognition. The method can recognize phrases written by kana (47 different characters) with the accuracy 78.92% and recognize phrases containing both kanji (63 different characters) and kana with accuracy 59.80%.

1. Introduction

Kuzushi-ji (classical cursive handwriting characters) is general name for the outdated hiragana and kanji that are not used in school education of Japan since 1900. However, the works of Japanese classical literature, especially those before the Edo period, were almost written by kuzushi-ji. As a result, the classical literature can only be read by experts and most literary works are buried without being digitized. In order to deal with this problem, it is necessary to develop the method that aims to reprinting old ancient documents automatically. Recently, some methods were proposed to recognize kuzushi-ji, especially three-character string. The model that combines neural network with connectionist temporal classification won the challenge of recognizing kuzushi-ji (21th PRMU Algorithm Context) [1] in 2017. However, the performance of those models with various length continuous kuzushi-ji is not so good. This paper uses an End-to-End method that can recognize continuous kuzushi-ji with any length in phrases. The method uses the convolutional layers of VGG [2] and BLSTM [3] as encoder, using LSTM with attention mechanism [4] as decoder. To explain the result of two model, this paper use Grad-CAM [5] to visualize the network.

2. Method

2.1 Dataset

The training dataset of kuzushi-ji is from the Center for Open Data in the Humanities [6]. We select 47 kana and 63 kanji characters from 15 books as training dataset. The original training dataset is a set of images with single kana as shown in Fig1. In order to build arbitrary length character dataset, the original dataset does image banalization and combine single character images to form phrases. The model sets the input size of training images as width 32, height 300 pixels. To ensure kana on images are not deformed, the padding place of image is white.

The test dataset of various length continuous kuzushi-ji phrases is from a chapter of ancient roles, Kiritsubo, in the tale of Genji, which is written by unknown writer in Edo period. Separating images into many phrase images have been finished by hands. There are 137 images containing only kana and 159 images containing both kana and kanji.

The book of training dataset and test dataset are written by different persons. So the handwriting style is different between two datasets, which can decrease the accuracy of prediction. So we uses the phrases of the tale of Genji as labels of training dataset to reduce the differences between training and testing of our neural network models.

Fig1. Screenshot of original Training dataset「あ」
http://codh.rois.ac.jp/char-shape/unicode/U+3042/

2.2 Encoder: CNN + BLSTM

An original method for extracting the sequential features form images is to use convolutional neural network, however the native approach does not make use of the spatial dependencies between the features. So, we use the encoder that combines CNN and BLSTM to get the feature vectors from input images.

As shown in Fig2(a), the encoder first uses the convolutional layers to process the images to get robust and high-level features of images. In this process, two dimensional image converts to one dimensional feature map. A two-layer Bidirectional Long-short term memory (BLSTM) network [3] is applied after convolutional neural network to enlarge the range the feature sequences of input images.

2.3 Decoder: LSTM with Attention Mechanism

The decoder of model is LSTM with Attention mechanism. Connectionist temporal classification (CTC) uses a scoring function proposed in 2006[8], which deals with sequence problems where the timing is variable. However, CTC is limited in character recognition in phrases because it does not consider the dependencies between labels. Different from CTC method, attention based LSTM model can predict current label relying on

Contact: Akihiko Konagaya, The school of computing, Tokyo institute of Technology, kona@c.titech.ac.jp

the results of previous labels [7]. So, we adopted attention based model as decoder. In order to compare the performance of CTC and attention models, our decoder has the two models in its structure as shown in Fig2(b).

3. Experiments

3.1 Implementation

The structure of CNN in encoder is the convolutional layers of VGG16, which has 5 blocks. The memory units of each layer of BLSTM is 256. CTC based model and attention based model use the same encoder. To fit the input size of CTC model, there is a fully connected layer between BLSTM and CTC. The max step of attention model is set as 11 so that kuzushi-ji's recognition model can recognize up to 10 characters in a phrase. The parameters of CNN use pre-trained weights of VGG16, which are open on GitHub [8].

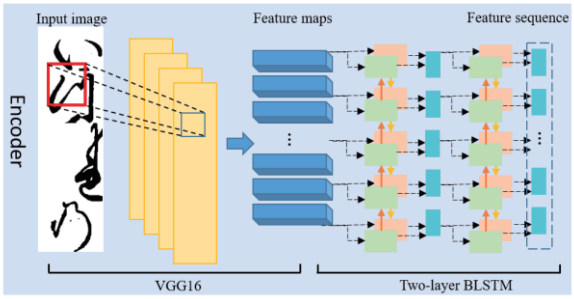

(a) Encoder structure

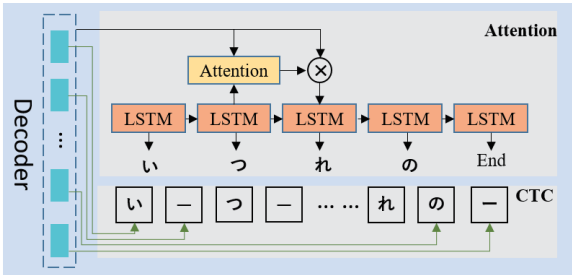

(b) Decoder structure of Attention and CTC

Fig2. Encoder and decoder structures of continuous kuzushi-ji recognition model

3.2 Prediction Accuracy on Test Dataset

We perform two sets of experiments: one on kana dataset and the other on kana-kanji dataset. Table 1 shows the prediction results of different models. It indicates that the performance of attention model is much better than the one of CTC model. In the both models, the performance on kanji-kana dataset is not so good as kana dataset mainly due to the lack of sufficient number of kanji images in the original dataset.

Table1. The accuracy of prediction

Model	Kana dataset	Kanji-kana dataset
CTC	60.14%	48.16%
Attention	78.92%	59.80%

3.3 Comparison of CTC and Attention Model Results

Fig3 shows the difference of focusing points between two models when recognizing the phrases image "思ひあかり." Both model can give correct prediction, however, compared with CTC based model, attention based model can figure out more precise character positions on the image.

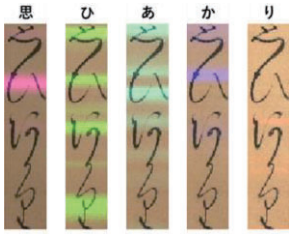

(a) Visualization result of CTC based model

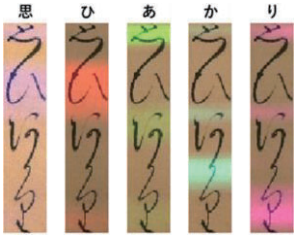

(b) Visualization result of Attention based model

Fig3. Visualization result between two models: the highlight colors mean the positions where neural network focuses on when predicting a target character.

4. Conclusion

This paper proposes a deep learning method to recognize continuous kuzushi-ji phrases using the images of the tale of Genji. Compared with previous model, the proposed model with attention mechanism gets high accuracy of prediction.

Our future task is to improve the performance of recognizing kanji-kana mixed images by enhancing the decoding capability.

Acknowledgements

I would like to express my gratitude to the members of the Konagaya laboratory and Genji Pictorial DB Study Group for valuable comments and discussions in promoting this research.

References

[1] https://sites.google.com/view/alcon2017prmu/コンテスト結果
[2] Simonyan, Karen, and Andrew Zisserman. Very Deep Convolutional Networks for Large-Scale Image Recognition. Computer Science, 2014.
[3] Graves, Alex, Abdel-rahman Mohamed, and Geoffrey Hinton. Speech recognition with deep recurrent neural networks. ICASSP, 2013.
[4] Xu, Kelvin, et al. Show, attend and tell: Neural image caption generation with visual attention. International conference on machine learning. 2015.
[5] Selvaraju, et al. Grad-cam: Visual explanations from deep networks via gradient-based localization. ICCV, 2017.
[6] http://codh.rois.ac.jp/index.html.en
[7] Graves, Alex, et al. Connectionist temporal classification: labelling unsegmented sequence data with recurrent neural networks. Proceedings of the 23rd international conference on Machine learning. ACM, 2006.
[8] Dabbish, Laura, et al. Social coding in GitHub: transparency and collaboration in an open software repository. ACM, 2012.

The 33rd Annual Conference of the Japanese Society for Artificial Intelligence, 2019

Computerized Adaptive Testing Method using Integer Programming to Minimize Item Exposure

Yoshimitsu MIYAZAWA*1 Maomi UENO*2

*1The National Center for University Entrance Examinations, Tokyo, Japan,
*2The University of Electro-Communications, Tokyo, Japan

Computerized adaptive testing (CAT) estimates an examinee's ability sequentially and selects test items that have the highest accuracy for estimating the ability. However, conventional CAT selects the same items for examinees who have equivalent ability. Therefore, tests cannot be used practically under circumstances in which the same examinee can take a test multiple times. As described herein, we propose CAT that minimizes item exposure and which adaptively selects different items for examinees of equal ability, while retaining accuracy. This paper presents the method's effectiveness through a simulation experiment and with item pools used by actual test providers. Results confirmed that 1) the proposed method yielded the shortest test length. 2) The proposed method controls exposure and selects different items for different examinees. The non-uniformity of estimation was low. 3) The average item exposure of the proposed method was the lowest.

1. Introduction

Computerized adaptive testing (CAT) estimates an examinee's ability after every answer and selects an item with the highest accuracy of estimating the ability[Linden 10][Ueno 10][Ueno 13].

This item selection presents an important benefit: the number of items to be selected and the testing time can be decreased for an examinee without reducing the accuracy. Furthermore, the abilities of all examinees are measured using the same degree of accuracy. Nevertheless, conventional CAT has the following two shortcomings.

1. Conventional CAT is inapplicable for conditions in which the same examinee takes a test multiple times because the same group of items tends to be selected when the same examinee takes a test multiple times.

2. Conventional CAT provides the same items to examinees of equivalent ability. Therefore, not all items in an item pool can be used effectively. Excessive item exposure engenders disclosure of the item contents to examinees, and might therefore degrade reliability[Way 98].

Items with estimated difficulty and discrimination parameters must be prepared in advance to conduct CAT. Huge amounts of time and other costs thereby arise for test item preparation, especially for high-stakes tests. Accordingly, it is desirable to use all items in an item pool for the implementation of a test. We propose a framework of new CAT that resolves these difficulties in this study.

Constrained CAT (CCAT) is proposed to resolve difficulties posed by excessive exposure [Linden 10, Linden 98]. The method reported by van der Linden et al.[Linden 98, Linden 10], a constrained CAT method, constitutes an item set in which the number of exposed items and necessary answer times, and selects an item with the most information from the item pool at every item selection. This method can control exposure and can select a different item for each examinee. However, deviation of accuracy in the selected items produces great differences among examinees in terms of the test length and accuracy.

We propose a CAT to resolve this difficulty. It can select a different item while maintaining equal accuracy, even for an examinee with the same ability. Specifically, we propose a CAT method that can select items 1) with uniform test length, and 2) with uniform accuracy among tests, but 3) the items are not identical.

This study proposes CAT item selection using integer programming. The approach of the proposed method is described as presented below. 1) A group that satisfies test constraints as Fisher information is assembled using integer programming for minimizing item exposure. 2) An item that has the highest information is selected from the group.

The proposed method uses integer programming for minimizing item exposure and satisfying upper and lower bounds of information. Accordingly, a different item set can be selected, even for an examinee with equal ability. Moreover, the improved diversity of item selection is expected to encourage thorough use of items in an item pool and to mitigate deviation in exposure.

This paper demonstrates the effectiveness of the proposed method through simulation experiments and experiments using actual data.

2. Item Response Theory

In CAT, ability is estimated based on Item Response Theory (IRT)[Lord 80, Lord 68] to select items with the highest estimation accuracy[Baker 04, Linden 16a, Linden 16b]. Item response theory is a recent test theory based on mathematical models for which practical use is in progress lately

Contact: Yoshimitsu MIYAZAWA, The National Center for University Entrance Examinations, 2-19-23, Komaba, Meguro-ku, Tokyo, Japan, 03-5478-1275, miyazawa@rd.dnc.ac.jp

in widely diverse areas related to computer testing.

The two-parameter logistic model (2PLM) has been used for many years as an item response model that is broadly applicable to such binary data. This study also adopts 2PLM, for which the probability of a correct answer given to item i by an examinee j with ability $\theta \in (-\infty, \infty)$ is assumed as

$$p(u_i = 1|\theta) = \frac{1}{1 + \exp[-1.7a_i(\theta - b_i)]}. \quad (1)$$

The standard error of ability estimation based on the item response theory is known to approach the reciprocal of Fisher information asymptotically [Lord 80]. Accordingly, item response theory usually employs Fisher information as an index representing the accuracy.

In 2PLM, the Fisher information is defined when item i provided to an examinee with ability θ using the following equations[Birnbaum 68].

$$I_i(\theta) = \frac{[p'(u_i = 1|\theta)]^2}{p(u_i = 1|\theta)[1 - p(u_i = 1|\theta)]} \quad (2)$$

where

$$p'(u_i = 1|\theta) = \frac{\partial}{\partial\theta} p(u_i = 1|\theta). \quad (3)$$

That result implies that the examinee ability can be ascertained near ability θ using an item with much Fisher information $I_i(\theta)$. Accordingly, it is expected that ability estimation can be implemented by selecting items with much Fisher information at a given ability for each examinee. Based on this concept, an item selection method of computerized based testing, CAT, presents items with much Fisher information. The total of Fisher information of an item set contained in a test presented to an examinee is called test information, which represents the test estimation accuracy.

3. Computerized Adaptive Testing

In CAT, items are selected from a given item set with known item parameters, using the following procedures.

1. The examinee ability is initialized.
2. An item that maximizes Fisher information for given ability is selected from the item pool and is presented to an examinee.
3. The estimated ability of the examinee is updated from the correct/wrong answer data to the item.
4. Procedures 2 and 3 are repeated until the update difference of the estimated ability of the examinee reaches a constant value ϵ or less.

Consequently, for a small number of items to be selected compared with a fixed test, repeating item selection based on maximizing information and estimation of an examinee ability engenders high ability estimation accuracy.

Unfortunately, in CAT, it is highly likely that the same set of items will be selected for examinees who have equal ability. Conventional CAT cannot be used practically under situations in which the same examinee can take a test multiple times. In addition, to follow the normal distribution for ability items with high information, the average value $\theta = 0$ is frequently selected. Therefore, some items in an item pool might not be used effectively. Excessive exposure of items leads to disclosure of the item contents to examinees, and might therefore degrade the test reliability[Way 98].

To resolve this difficulty, we propose a CAT method that minimizes item exposure. It can select a different item while maintaining the same accuracy, even for an examinee with equal ability.

4. Proposed Method

The concept of the proposed method is to assemble a group with test constraints as Fisher information, but with different items using integer programming, to select an item with higher information, and to minimize item exposure from the group. Details of the proposed method are described below.

1. The estimated ability of an examinee is initialized.
2. The group maximizing Fischer information is assembled using the integer programming presented below.

$$\text{Minimize } y = \sum_{i=1}^{I} e_i x_i \quad (4)$$

subject to

$$\sum_{i=1}^{I} I(\theta_k) x_i \geq r_k, k = 1, 2, \cdots, K \quad (5)$$

$$\sum_{i=1}^{I} I(\theta_k) x_i \leq s_k, k = 1, 2, \cdots, K \quad (6)$$

$$\sum_{i=1}^{I} x_i = n(\text{Test length}) \quad (7)$$

To expand the method proposed by Adema (1989) [Adema 92] in which test forms are assembled using integer programming, we propose an optimization problem in which we embed an objective function minimizing item exposure. The lower boundaries and the upper boundaries of test information function at a set of the examinee's ability, $\Theta = \{\theta_1, \ldots, \theta_K\}$, is r_k and s_k. Also, $I(\theta_k)$ denotes the test information function at the examinee's ability θ_k. The exposure count of item i is e_i. If item i is selected into the group, then $x_i = 1$; otherwise $x_i = 0$.

3. An item is selected from a group. Then response data are generated with the given true ability and item parameters.
4. Ability $\hat{\theta}$ is estimated by expected a posteriori (EAP) [Baker 04].

表 1: Results obtained using simulation data

Item pool size	methods	Avg. test length	non-uniformity of estimation	Max. No. exposure item	Avg. exposure item
500	CAT	19.99 (2.26)	0.03	1000	39.98 (120.93)
	CCAT	23.99 (6.2)	0.21	60	47.98 (23.15)
	Proposal	9.35 (2.15)	0.09	65	18.7 (17.1)
1000	CAT	21.33 (2.15)	0.03	1000	21.33 (82.22)
	CCAT	28.37 (8.98)	0.86	30	28.37 (6.75)
	Proposal	9.73 (2.46)	0.09	42	9.73 (8.74)
2000	CAT	22.48 (2.1)	0.02	1000	11.24 (57.47)
	CCAT	28.56 (11.35)	2.33	15	14.28 (3.19)
	Proposal	9.61 (2.66)	0.08	19	4.8 (4.02)

表 2: Results obtained using actual data

Item pool size	methods	Avg. test length	non-uniformity of estimation	Max. No. exposure item	Avg. exposure item
978	CAT	14.82 (3.41)	0.05	1000	15.15 (78.5)
	CCAT	26.56 (6.36)	0.19	30	27.15 (8.42)
	Proposal	11.99 (3.15)	0.07	75	12.26 (10.31)

5. Procedures 2–4 are repeated until the update difference of the estimated ability decreases to ϵ or less.

The proposed method selects an item from a different group for each examinee. Accordingly, a different item is expected to be selected, even to an examinee of equivalent ability. Furthermore, improved diversity of item selection is anticipated to encourage thorough use of items in an item pool and to mitigate deviation in exposure.

5. Simulation Experiment

The simulation experiment procedure is the following.

1. An item pool comprising 500, 1000, or 2000 items is generated. The true values of parameters of each item are set randomly from $a_i \sim U(0,1)$, $b_i \sim N(0,1)$.
2. The true ability of an examinee is sampled from $\theta \sim N(0,1)$.
3. The estimated ability of an examinee is initialized to $\hat{\theta} = 0$.
4. An item is selected from an item pool using each method. Then response data are generated with the given true ability and item parameters.
5. The ability $\hat{\theta}$ is estimated using EAP.
6. Procedures 4 and 5 are repeated until the update difference of the estimated ability decreases to ϵ or less. Also, ϵ is set to 0.05, which is used conventionally for actual CAT[Linden 10].
7. Procedures 2–6 are repeated 1000 times to obtain statistical values for the following indices using a delivery pattern and answer data obtained: a) the length of a test, b) the non-uniformity of ability estimation accuracy, and c) the exposure of each item.

Table 1 presents the results. Results confirmed that the proposed method yielded the shortest test length under all conditions. Selecting an item with less information for the initial value of θ rather than selecting an item with more information is known to achieve faster convergence of ability estimation when the initial value of θ is distant from the true ability of an examinee. The proposed method constrains the number of items with uniformity conditions. Therefore, it has a property of not selecting items with an extremely large amount of information only to a certain estimated value. This property shortens the test length, thereby reducing the exposure of items. The proposed method also indicates the smallest standard deviation of test length under all conditions. The proposed method selects items from an item set of uniform information. Therefore, it can render the number of items to take for convergence of the estimated ability uniform.

The non-uniformity of estimation using conventional CAT was lowest. It repeatedly selects some item sets with much information. However, the proposed method controls exposure and selects different items for each examinee. The non-uniformity of estimation was low because of the deviation of measurement accuracy in the selected items.

The maximum exposure was the least when CCAT was used. Results demonstrate that CCAT can constrain maximum exposure directly in the same manner as the fraction of different items. This result is interpreted as attributable to the exposure setting to use as many items in an item pool as possible in this experiment. The averages of exposure obtained using the proposed method were the lowest. Actually, CCAT constrained only the maximum of expo-

sure directly, so that the deviation of exposure could not be controlled.

6. Simulation Using Real Data

This chapter explains evaluation of the effectiveness of the proposed method using real data. An experiment was conducted using an item pool of real data. The item pool contained 978 items. Table 2 presents the experimentally obtained results. Table 2 suggests the following characteristics: 1) The test length produced using the proposed method is the shortest. The standard deviation of test length produced using the proposed method is the smallest, which suggests that the test length selected to examinees has little dispersion. 2) Non-uniformity of estimation by the proposed method is the second highest to CAT, so the same accuracy was maintained using the proposed method. 3) The maximum exposure was smallest by CCAT. The average tended to be small when obtained using the proposed methods.

7. Conclusions

This study has examined a proposed CAT implementation in which different items can be selected, even by an examinee with equivalent ability, while maintaining equal accuracy. Specifically, we proposed a method by which a group is assembled using integer programming: an item is selected from the group. Using simulation experiments and experiments using real data, some points have been verified as benefits of the proposed method.

参考文献

[Adema 92] Adema, J. J.: Implementations of the branch-and-bound method for test construction problems, *Methodika*, Vol. 6, No. 2, pp. 99–117 (1992)

[Baker 04] Baker, F. B. and Kim, S.-H. eds.: *Item Response Theory: Parameter Estimation Techniques*, CRC Press (2004)

[Birnbaum 68] Birnbaum, A.: Some latent trait models and their use in inferring an examinee's ability, in Lord, F. M. and Novick, M. R. eds., *Statistical theories of mental test scores*, pp. 397–479, Addison-Wesley (1968)

[Linden 98] Linden, van der W. J. and Reese, L. M.: A model for optimal constrained adaptive testing, *Applied Psychological Measurement*, Vol. 22, No. 3, pp. 259–270 (1998)

[Linden 10] Linden, van der W. J. and Glas, C. A. W. eds.: *Elements of Adaptive Testing*, Springer (2010)

[Linden 16a] Linden, van der W. J. ed.: *Handbook of Item Response Theory, Volume One: Models*, Chapman and Hall/CRC (2016)

[Linden 16b] Linden, van der W. J. ed.: *Handbook of Item Response Theory, Volume Two: Statistical Tools*, Chapman and Hall/CRC (2016)

[Lord 68] Lord, F. and Novick, M. R.: *Statistical Theories of Mental Test Scores*, Addison-Wesley (1968)

[Lord 80] Lord, F. M.: *Applications of Item Response Theory To Practical Testing Problems*, Lawrence Erlbaum Associates (1980)

[Ueno 10] Ueno, M. and Songmuang, P.: Computerized adaptive testing based on decision tree, in *Advanced Learning Technologies (ICALT), 2010 IEEE 10th International Conference on*, pp. 191–193 (2010)

[Ueno 13] Ueno, M.: Adaptive testing based on bayesian decision theory, in *International Conference on Artificial Intelligence in Education*, pp. 712–716 (2013)

[Way 98] Way, W. D.: Protecting the integrity of computerized testing item pools, *Educational Measurement: Issues and Practice*, Vol. 17, pp. 17–27 (1998)

The 33rd Annual Conference of the Japanese Society for Artificial Intelligence, 2019

Maximizing accuracy of group peer assessment using item response theory and integer programming

Masaki Uto*1 Duc-Thien Nguyen*1 Maomi Ueno*1

*1 University of Electro-Communications

With the wide spread of large-scale e-learning environments, peer assessment has been widely used to measure learner ability. When the number of learners increases, peer assessment is often conducted by dividing learners into multiple groups. However, in such cases, the peer assessment accuracy depends on the method of forming groups. To resolve that difficulty, this study proposes a group formation method to maximize peer assessment accuracy using item response theory and integer programming. Experimental results, however, have demonstrated that the method does not present sufficiently higher accuracy than a random group formation method does. Therefore, this study further proposes an external rater assignment method that assigns a few outside-group raters to each learner after groups are formed using the proposed group formation method. Through results of simulation and actual data experiments, this study demonstrates that the method can substantially improve peer assessment accuracy.

1. Introduction

As an assessment method based on a social constructivist approach, peer assessment, which is mutual assessment among learners, has become popular in recent years. One common use of peer assessment is for summative assessment. The importance of this usage has been increasing concomitantly with the wider use of large-scale e-learning environments [Suen 14, Shah 14]. Peer assessment, however, entails the difficulty that the assessment accuracy of learner ability depends on rater characteristics such as severity and consistency. To resolve that difficulty, item response theory (IRT) models incorporating rater parameters have been proposed [Eckes 11, Uto 18]. The IRT models are known to provide more accurate ability assessment than average or total scores do because they can estimate the ability considering rater characteristics [Uto 16, Uto 18].

In learning contexts, peer assessment has often been adopted for group learning situations such as collaborative learning and active learning [Staubitz 16, Suen 14, Nguyen 15]. Specifically, learners are divided into multiple groups in which they work together, and peer assessment is conducted within the groups. However, in such cases, the ability assessment accuracy depends also on a way to form groups. For example, if a group consists of learners who tend to assess others randomly, their abilities are difficult to be estimated accurately. Therefore, group optimization is important to maximize the accuracy of peer assessment. However, no studies have focused on this issue.

For the reason, this study proposes a new group formation method that maximizes peer assessment accuracy based on IRT. Specifically, the method is formulated as an integer programming (IP) problem that maximizes the lower bound of the Fisher information (FI) measure: a widely used index of ability assessment accuracy in IRT. The method is expected to improve the ability assessment accuracy because groups are formed so that the learners in the same group can assess one another accurately. However, experimental results demonstrated that the method did not present sufficiently higher accuracy than that of a random group formation method. The result suggests that it is generally difficult to assign raters with high FI to all learners when peer assessment is conducted only within groups.

To alleviate that shortcoming, this study further proposes an external rater assignment method that assigns a few optimal outside-group raters to each learner after forming groups using the method presented above. We formulate the method as an IP problem that maximizes the lower bound of the FI for each learner given by assigned outside-group raters. Simulations and actual data experiments demonstrate that assigning a few optimal external raters using the proposed method can improve the peer assessment accuracy considerably.

Contact: Masaki Uto, 1-5-1, Choufugaoka, Choufu-shi, Tokyo, Japan, 042-443-5627, uto@ai.lab.uec.ac.jp

2. Peer assessment data

This study assumes that peer assessment data $\boldsymbol{U}$ consists of rating categories $k \in \mathcal{K} = \{1, \cdots, K\}$ given by each peer-rater $r \in \mathcal{J} = \{1, \cdots, J\}$ to each learning outcome of learner $j \in \mathcal{J}$ for each task $t \in \mathcal{T} = \{1, \cdots, T\}$. Letting u_{tjr} be a response of rater r to learner j's outcome for task t, the data $\boldsymbol{U}$ are described as $\boldsymbol{U} = \{u_{tjr} \mid u_{tjr} \in \mathcal{K} \cup \{\text{-1}\}, t \in \mathcal{T}, j \in \mathcal{J}, r \in \mathcal{J}\}$, where $u_{tjr} = -1$ denotes missing data.

Furthermore, this study assumes that peer assessment is conducted by dividing learners into multiple groups for each task $t \in \mathcal{T}$. Here, let x_{tgjr} be a dummy variable that takes 1 if learner j and peer r are included in the same group $g \in \mathcal{G} = \{1, \cdots, G\}$ for task t, and which takes 0 otherwise. Then peer assessment groups for task t can be described as $\boldsymbol{X}_t = \{x_{tgjr} \mid x_{tgjr} \in \{0, 1\}, g \in \mathcal{G}, j \in \mathcal{J}, r \in \mathcal{J}\}$. Consequently, when peer assessment is conducted among group members, the rating data u_{tjr} become missing data if learners j and r are not in the same group ($\sum_{g=1}^{G} x_{tgjr} = 0$).

The purpose of this study is to estimate the learner ability accurately using IRT for peer assessment [Uto 16] from the data $\boldsymbol{U}$ by optimizing the groups $\boldsymbol{X} = \{\boldsymbol{X}_t \mid t \in \mathcal{T}\}$.

3. IRT for peer assessment

The IRT for peer assessment [Uto 16] has been formulated as a graded response model that incorporates rater parameters. The model defines the probability that rater r responds in category k to learner j's outcome for task t as

$$P_{tjrk} = P^*_{tjrk-1} - P^*_{tjrk}, \tag{1}$$
$$P^*_{tjrk} = [1 + \exp(-\alpha_t\gamma_r(\theta_j - \beta_{tk} - \varepsilon_r))]^{-1}$$

Here, θ_j denotes the ability of learner j; γ_r reflects the consistency of rater r; ε_r represents the severity of rater r; α_t is a discrimination parameter of task t; and β_{tk} denotes the difficulty in obtaining category k for task t ($\beta_{t1} < \cdots < \beta_{tK-1}$); $P^*_{tjr0} = 1$, and $P^*_{tjrK} = 0$.

In IRT, the standard error estimate of ability assessment is defined as the inverse square root of the FI. More information implies less error of the assessment. Therefore, FI can be regarded as an index of the ability assessment accuracy. For the above model, FI of rater r in task t for a learner with ability θ_j is calculable as

$$I_{tr}(\theta_j) = \alpha_t^2\gamma_r^2 \sum_{k=1}^{K} \frac{\left(P^*_{tjrk-1}Q^*_{tjrk-1} - P^*_{tjrk}Q^*_{tjrk}\right)^2}{P^*_{tjrk-1} - P^*_{tjrk}}, \tag{2}$$

where $Q^*_{tjrk} = 1 - P^*_{tjrk}$.

The FI of multiple raters for learner j in task t is definable by the sum of the information of each rater. Therefore, when peer assessment is conducted within group members, the FI for learner j in task t is calculable as shown below.

$$I_t(\theta_j) = \sum_{\substack{r=1 \\ r\neq j}}^{J} \sum_{g=1}^{G} I_{tr}(\theta_j) x_{tgjr} \tag{3}$$

A high value of FI $I_t(\theta_j)$ signifies that the group members can assess learner j accurately. Therefore, if we form groups to provide great amounts of FI for each learner, then the ability assessment accuracy can be maximized.

4. Group formation method

Based on this idea presented above, we formulate the group formation optimization method (designated as *PropG*) as an IP problem that maximizes the lower bound of FI for each learner. Specifically, *PropG* for task t is formulated as the following IP problem.

$$\text{maximize} \quad y_t \tag{4}$$
$$\text{subject to} \quad \sum_{\substack{r=1 \\ r\neq j}}^{J} \sum_{g=1}^{G} I_{tr}(\theta_j) x_{tgjr} \geq y_t, \quad \forall j, \tag{5}$$
$$\sum_{g=1}^{G} x_{tgjj} = 1, \quad \forall j, \tag{6}$$
$$n_l \leq \sum_{j=1}^{J} x_{tgjj} \leq n_u, \quad \forall g, \tag{7}$$
$$x_{tgjr} = x_{tgrj}, \quad \forall g, j, r \tag{8}$$

The first constraint requires that FI for each learner j be larger than a lower bound y_t. The second constraint restricts each learner as belonging to one group. The third constraint controls the number of learners in a group. Here, n_l and n_u represent the lower and upper bounds of the number of learners in group g. In this study, $n_l = \lfloor J/G \rfloor$ and $n_u = \lceil J/G \rceil$ are used so that the numbers of learners in respective groups become as equal as possible. This IP maximizes the lower bound of FI for learners. Therefore, by solving the problem, one can obtain groups that provide as much FI as possible to each learner.

4.1 Evaluation of group formation methods

To evaluate the effectiveness of *PropG*, we conducted the following simulation experiment. 1) For $J = 30$ and $T = 5$, the true IRT model parameters were generated randomly. 2) For the first task $t = 1$, learners were divided into $G \in \{3, 4, 5\}$ groups using *PropG* and a random group formation method (designated as *RndG*). For *PropG*, the FI values were calculated using the true parameter values. 3) Given the created groups and the true model parameters, peer assessment data were sampled randomly for the current task t based on the IRT model. 4) Given the true rater and task parameters, the learner ability was estimated from the data generated to date. 5) RMSE between the estimated ability and the true ability were calculated. 6) Procedures 2) – 5) were repeated for the remaining tasks. 7) After 10 repetitions of the procedures described above, the average values of RMSE were calculated.

Fig. 1 presents the results. Results demonstrate that RMSE decreases with the decreasing number of groups G or with increasing numbers of tasks or learners because the number of data for each learner increases. Generally, the increase of data per learner is known to engender improvement of the ability assessment accuracy [Uto 16]. Comparing the group formation methods, however, *PropG* does not decrease RMSE sufficiently. The results indicate that it is difficult to form groups to sufficiently increase the peer assessment accuracy. To overcome this shortcoming, we further propose the assignment of outside-group raters to each learner, given the groups created using *PropG*.

5. External rater assignment

The proposed external rater assignment method (designated as *PropE*) is formulated as an IP problem that maximizes the lower bound of information for learners given by the assigned outside-group raters. Specifically, given a group formation $\boldsymbol{X}_t$, *PropE* for task t is defined as folllows.

$$\text{maximize :} \quad y'_t \tag{9}$$
$$\text{subject to :} \quad \sum_{r\in \boldsymbol{C}_{tj}} I_{tr}(\theta_j) z_{tjr} \geq y'_t, \quad \forall j \tag{10}$$
$$\sum_{r\in \boldsymbol{C}_{tj}} z_{tjr} = n^e, \quad \forall j \tag{11}$$
$$\sum_{j=1}^{J} z_{tjr} \leq n^J, \quad \forall r \tag{12}$$
$$z_{tjj} = 0, \quad \forall j \tag{13}$$

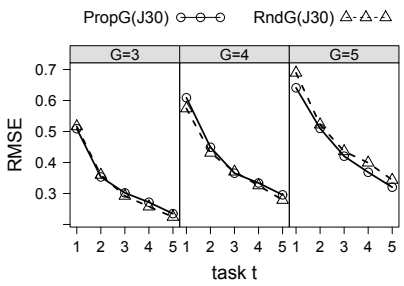

Figure 1: RMSE values of group formation methods in the simulation experiment.

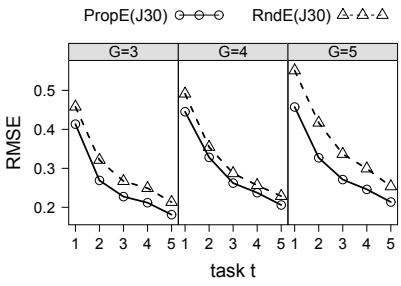

Figure 2: RMSE values of external rater assignment methods for each G and t in the simulation experiment.

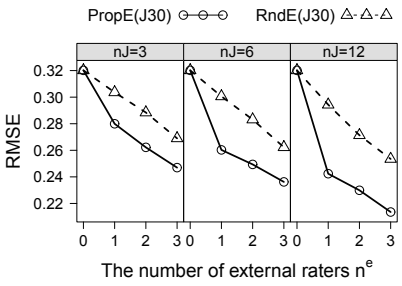

Figure 3: RMSE values of external rater assignment methods for each n^J and n^e in the simulation experiment.

Here, $\boldsymbol{C}_{tj} = \{r \mid \sum_{g=1}^{G} x_{tgjr} = 0\}$ is the set of outside-group raters for learner j in task t given a group formation $\boldsymbol{X}_t$. In addition, z_{tjr} is a variable that takes 1 if external rater r is assigned to learner j in task t; it takes 0 otherwise. Furthermore, n^e denotes the number of external raters assigned to each learner; n^J is the upper limit number of outside-group learners assignable to each rater. Here, n^e and n^J must satisfy $n^J \geq n^e$. The increase of n^J makes it easier to assign optimal raters to each learner, although differences in the workload among the learners increases.

The first constraint in the IP restricts that the FI for each learner given by the assigned outside-group raters must exceed a lower bound y'_t. The second constraint requires that n^e number of outside-group raters must be assigned to each learner. The third constraint restricts that each learner can assess at most n^J number of outside-group learners. The objective function is defined as the maximization of the lower bound of the FI for learners given by assigned external raters. Therefore, by solving the proposed method, an external rater assignment z_{tjr} is obtainable so that n^e outside-group raters with high FI are assigned to each learner.

5.1 Evaluation of external rater assignment

To evaluate the performance of the proposed method, we conducted the following simulation experiment, which is similar to that conducted in 4.1. 1) For $J = 30$ and $T = 5$, the true model parameters were generated randomly. 2) For the first task $t = 1$, learners were divided into $G \in \{3, 4, 5\}$ groups using *PropG*. Then, given the created groups, $n^e \in \{1, 2, 3\}$ outside-group raters were assigned to each learner using *PropE* and a random assignment method (designated as *RndE*). Here, we changed the value of n^J for $\{3, 6, 12\}$ to evaluate its effects. In *PropG* and *PropE*, FI was calculated using the true parameter values. 3) Peer assessment data were sampled randomly for current task t following the IRT model, given the true model parameters, the formed groups and the rater assignment. 4) The following procedures were identical to procedures 4) – 7) of the previous experiment.

Fig. 2 shows the RMSE for each t and G when $n^J = 12$ and $n^e = 3$, and Fig. 3 shows the RMSE for each n^e and n^J when $G = 5$ and $t = 5$. In Fig. 3, the results for $n^e = 0$ correspond to *PropG*. Results show that the accuracy of the external rater assignment methods tends to increase concomitantly with decreasing number of groups and increasing number of tasks and assigned external raters n^e because the number of rating data for each learner increases. Furthermore, Fig. 3 shows that both external rater assignment methods reveal the lower RMSE than *PropG* in all cases, which suggests that the addition of the external raters is effective to improve the ability assessment accuracy. Comparison of the external rater assignment methods reveals that *PropE* presented higher accuracy than *RndE* in all cases. Furthermore, the RMSE difference between *PropE* and *RndE* tends to increase with increasing n^J value because the increase of n^J makes it easier to assign optimal raters to each learner.

From those results, we infer that the proposed method can improve the peer assessment accuracy efficiently when a large value of n^J and a small value of n^e are given.

6. Usage in actual e-learning situations

PropG and *PropE* require IRT parameter estimates to calculate FI. Although the experiments described above used the true parameter values, they are practically unknown. Therefore, this section presents a description of how to use *PropG* and *PropE* when the IRT parameters are unknown in actual e-learning situations. We consider the following two assumptions for using *PropG* and *PropE* in an e-learning course. 1) More than one task is offered in the course. 2) All tasks were used in past e-learning courses at least once, and past learners' peer assessment data corresponding to the tasks were collected. Although the second assumption might not necessarily be satisfied in practice, it is necessary to estimate the task parameters.

Under the second assumption, we can estimate the task parameters. Given task parameter estimates, we can use *PropG* and *PropE* through the following procedures under the first assumption. 1) For the first task, peer assessment is conducted using randomly formed groups. 2) The rater parameters and learner ability are estimated from the obtained peer assessment data. 3) For the next task, group formation and external rater assignment are conducted using *PropG* and *PropE* given the parameter estimates. 4) Repeat procedures 2) and 3) for remaining tasks.

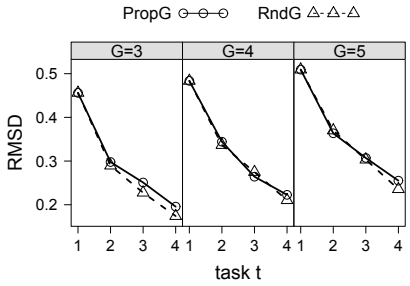

Figure 4: RMSDs of group formation methods in the actual data experiment.

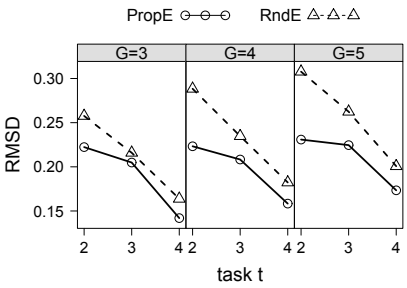

Figure 5: RMSDs of external rater assignment methods for each G and t in the actual data experiment.

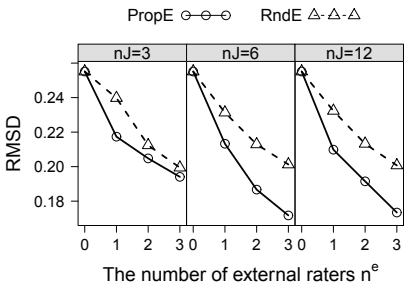

Figure 6: RMSDs of external rater assignment methods for each n^J and n^e in the actual data experiment.

7. Actual data experiment

This section evaluates the effectiveness of *PropG* and *PropE* using actual peer assessment data based on the above usage. We gathered actual data using the following procedures. 1) As subjects for this study, 34 university students were recruited. 2) They were asked to complete four essay writing tasks offered in NAEP. 3) After the participants completed all tasks, they were asked to evaluate the essays of all other participants for all four tasks using a rubric with five rating categories. Furthermore, we collected additional rating data (designated as *five raters' data*) for task parameter estimation. The data consist of ratings assigned by 5 graduate school students to the essays gathered in the experiment above.

Using the actual data, we conducted the following experiments. 1) The task parameters in the IRT model were estimated using the five raters' data. 2) Given the task parameter estimates, the rater parameters and learner ability were estimated using the full peer assessment data. 3) For the first task, $G \in \{3, 4, 5\}$ groups were created randomly. 4) The peer assessment data without peer-rater assignment were changed to missing data. 5) From the peer assessment data up to the current task, the rater parameters and learner ability were estimated given the task parameters estimated in Procedure 1). 6) RMSD between the ability estimates and that estimated from the complete data in Procedure 2) was calculated. 7) For the next task, $G \in \{3, 4, 5\}$ groups were formed by *PropG* and *RndG*. Then, given the groups formed by *PropG*, $n^e \in \{1, 2, 3\}$ external raters were assigned to learners by *PropE* and *RndE* under $n^J \in \{3, 6, 12\}$. Here, *PropG* and *PropE* used the task parameters obtained in Procedure 1) and the current estimates of ability and rater parameters to calculate FI. 8) For the remaining tasks, procedures 4) – 7) were repeated. 9) After repeating the procedures described above 10 times, the average values of the RMSD were calculated.

Fig. 4 presents results of each group formation method. Figs. 5 and 6 show those of the external rater assignment methods. Fig. 5 presents results for each $t \geq 2$ and $G \in \{3, 4, 5\}$ when $n^J = 12$ and $n^e = 3$. Fig. 6 shows those for each n^e and n^J when $G = 5$ and $t = 4$. Results show similar tendencies to those obtained from the simulation experiments. Specifically, comparing the group formation methods, *PropG* does not improve the accuracy much, while the assessment accuracy is improved drastically by introducing external raters. Furthermore, the proposed external rater assignment method realizes the higher accuracy than the random assignment method when n^J is large and n^e is small.

8. Conclusion

This study proposed the group formation method and external rater assignment method to improve peer assessment accuracy using IRT and IP. The experimentally obtained results showed that the external rater assignment method, which assigns a few optimal outside-group raters to each learner, improved the accuracy dynamically, although the proposed group formation method did not improve the accuracy sufficiently.

References

[Eckes 11] Eckes, T.: *Introduction to Many-Facet Rasch Measurement: Analyzing and Evaluating Rater-Mediated Assessments*, Peter Lang (2011)

[Nguyen 15] Nguyen, T., Uto, M., Abe, Y., and Ueno, M.: Reliable Peer Assessment for Team-project-based Learning using Item Response Theory, pp. 144–153 (2015)

[Shah 14] Shah, N. B., Bradley, J., Balakrishnan, S., Parekh, A., Ramchandran, K., and Wainwright, M. J.: Some Scaling Laws for MOOC Assessments, in *KDD Workshop on Data Mining for Educational Assessment and Feedback (ASSESS 2014)* (2014)

[Staubitz 16] Staubitz, T., Petrick, D., Bauer, M., Renz, J., and Meinel, C.: Improving the peer assessment experience on MOOC platforms, in *Proceedings of the Third (2016) ACM Conference on Learning@ Scale*, pp. 389–398ACM (2016)

[Suen 14] Suen, H. K.: Peer assessment for massive open online courses (MOOCs), *The International Review of Research in Open and Distributed Learning*, Vol. 15, No. 3, pp. 312–327 (2014)

[Uto 16] Uto, M. and Ueno, M.: Item Response Theory for Peer Assessment, Vol. 9, No. 2, pp. 157–170 (2016)

[Uto 18] Uto, M. and Ueno, M.: Empirical comparison of item response theory models with rater's parameters, *Heliyon, Elsevier*, Vol. 4, No. 5, pp. 1–32 (2018)

The 33rd Annual Conference of the Japanese Society for Artificial Intelligence, 2019

Waveform Processing of Electrocardiogram with Neural Network and Non-contact Measurement using Kinect for Driver Evaluation

Hao ZHANG [*1]

Takashi IMAMURA [*2]

[*1]Graduat School of Science and Technology, Niigata University

[*2] Faculty of Engineering, Niigata University

In recent years, the measurement method of biological information using non-contact sensor have become popular. And, in-vehicle measurement systems for a driver evaluation are also needed in order to decrease the serious traffic accidents. In this research, improvement method of heart rate measurement with high accuracy by using the non-contact sensor “Kinect” is examined. As the reliable biological information, the Holter monitor of electrocardiograph is combination used for measurement experiment. Moreover, to extract high level features from electrocardiogram, a neural network based autoencoder has also constructed. In this paper, about the constructed neural network, the effectiveness of abnormal R wave detection through learning for waveform characteristics of electrocardiogram and the possibility of application for reconstruction of the heart rate signal from Kinect are discussed.

1. Introduction

According to a highway survey of 1000 drivers, the driver who experienced sleepiness during the operation was 78% of the total. In addition, "Front Carelessness" occupies about half of all accidents and about 40% in the death accident. It is thought that the factor which exists in this "front carelessness" is different by the driver, and there is insufficient attention and concentration as one of the big factors. Therefore, it is necessary to improve the attention to the operation, to operation of the quick handle, and the quick brake, the existence of the obstacle on the road, the sudden change of the curvature of the road, so maintenance and control of tension are necessary.

Recently, the driver's load is reduced by the various driving assistance, there is a possibility that attention is insufficient by lowering the tension. On the other hand, if the tension is too high, there may be a possibility that the physical strength and the mental state are exhausted early, and sleepiness may occur. It is thought that the extreme state of the tension seems to lead to the lowering of the accident avoidance capacity. It is said that the tension of the driver can be evaluated using electroencephalogram, blood pressure, electrocardiogram (ECG) [Deguchi 2006]. The purpose of this study is to develop a system to evaluate the feeling of tension by measuring the R-R interval variation of drivers during driving.

In this research, two kinds of technique to measure R-R interval variation are used. First one is acquisition for ECG with an electrocardiograph by using multifunctional wireless Holter monitor and recorder "CarPod" (Medilink inc.). It is an typical method of contact measurement, and it is also used in medical test for sleep apnea by its high accuracy. It can be used in daily life environment without disturbance for several behaviors or works. However, it is not suitable for the actual situation of vehicle driver monitor. Because, it is required to put the 3 or 5 electrodes on human skin directory.

Second one is sensing method using non-contact sensing such as Infrared sensors or cameras. "Kinect" (Microsoft Corp.) is typical example of such kinds of sensor which has already been put into practical use as a product of home game interface. And several researchers were tried to acquire the heart rate waveform by the changes of the luminance value (RGB) from the human face [Nakamura 2015].

On the other hand, although it is easy to acquire the electrocardiogram itself, there are still many unresolved parts about the analysis method and application method of information obtained from the detected waveform. Fundamental analysis is based on frequency analysis. For example, Yokoyama et al. Proposes a method to evaluate heart rate variability using the power spectrum which is frequency information of electrocardiogram and the amplitude spectrum extracted from the amplitude information [Kiyoko 1999]. In addition, recent developments in deep learning have been studied and applied to electrocardiograms. Takahashi et al. Has proposed the feature extraction from the electrocardiogram using stained convolutional extraction autoencoder (SCDAE) [Takahashi 2017]. Their research showed that robust feature extraction is possible for waveform changes due to observation objects and heart rate variability by using autoencoder.

In this paper, we propose a neural network (NN) - based autoencoder, which extracts high - level features from normal waveforms, and detects a location with abnormal electrocardiograms compared to required examination data. And, it is also possible to compare the electrocardiogram feature extracted by the autoencoder with the heartbeat waveform obtained from Kinect and to analyze the heartbeat characteristics from the RGB information.

Contact: ZHANG Hao, Niigata University,8050 Ikarashi-2nocho Nishiku-Niigata-JAPAN,950-2181,025-262-7475, ima@eng.niigata-u.ac.jp

2. The Proposed Method

2.1 Summary of Techniques

The fixed length data divided by the sliding window method in the electrocardiogram waveform does not consider labels for heartbeat interval or arrhythmia, so it is easy to use the acquired data [Noriyasu 2018]. Autoencoder (Ae) is a dimension compression algorithm using neural network. the weight of the AE is trained through neural network layer used to reconstruct the input data, which is of high dimensionality. As a result of the training, we can obtain a higher-level representation of the input data [Takahashi 2017].

The proposed method consists of three steps: Generate Partial Time-series, Autoencoder Pre-learning, Abnormal Inspection and R Wave Detection.

- Generate partial time-series of fixed length data from normal and abnormal data
- Autoencoder pre-learning and extracting normal data features
- Inspecting data abnormally with the trained autoencoder
- Constructing the R wave detector using discrete wavelet transform (MODWT)

(1) Generate Partial Time-series

ECG data X divided into fixed length D by slide window method

$$\mathrm{X}=(X_1,\ldots,X_R)$$

Here, $X_r$is the r-th section, and R is the total number of spaces. The fixed length D and shift of the sizes of stride S are given as parameters.

(2) Autoencoder Pre-learning

Input $\mathrm{X}=(X_1,\ldots,X_R)$,We use NN based deep autoencoder in MATLAB 2017A. As shown in Fig. 2, it is possible to obtain a low dimensional feature which holds information representing data.

The encoder section of the autoencoder is represented by encoder (・), and the decoder section is represented by decoder(・). The feature of the r-th section is expressed by

$$Z_r=\mathrm{encoder}(X_r)$$

As a result of applying the decoder to the encoder result Z_r which is the low dimensional feature quantity,

$$Y_r=\mathrm{decoder}(Z_r)$$

is similar to the original signal X_r.

The loss function for calculating how much the neural network matches the original data is the mean square error (mase sparse) between the original signal X_r and the decoded result Y_r,

$$\mathrm{E}=\frac{1}{2R}\sum_{r=1}^{R}(X_r-Y_r)^2$$

Which is an indicator of poor performance of the neural network.

(3) Abnormal Inspection

An autoencoder has the function of bringing an abnormal waveform closer to a normal waveform. Using this function, it is possible to check waveform abnormality.

(4) R Wave Detector

The R-wave detector was constructed using the discrete wavelet transform (MODWT) to emphasize the R peak of the ECG waveform.

'Sym4' wavelet is similar to 'QRS' complex, so it is suitable for 'QRS' detection. For comparison, the results of extracted 'QRS' complex and the results with 'sym4' wavelet are shown in Fig.1.

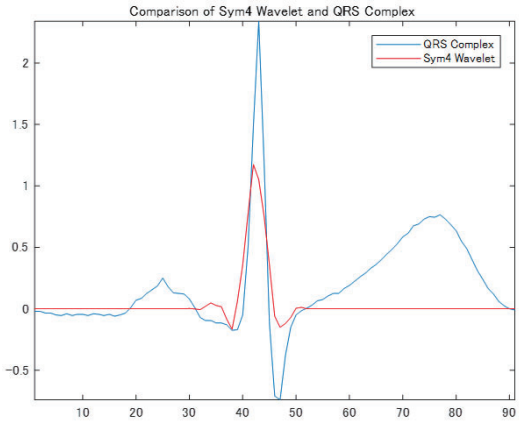

Fig.1 Comparison of 'QRS' and 'sym4' wavelets

3. Experiments

3.1 Measurement Experiment

Measurement experiments were made of electrocardiogram and Kinect. The resting state was maintained for more than 1 hour before starting the measurement. In the measurement at rest, the subject was chosen to be the most comfortable sitting position. The measurement time of the electrocardiograph and Kinect is half hour and one minute. The subjects were healthy 25 years old men without arrhythmia, heart disease, and autonomic neuropathy.

3.2 Numerical Experiment

In this experiment, we rely on MATLAB 2017A, fixed length D = 100 Samples,S =1 Samples in the sliding window system, hidden layer set 160, and an autoencoder was constructed as shown in Fig. 2.

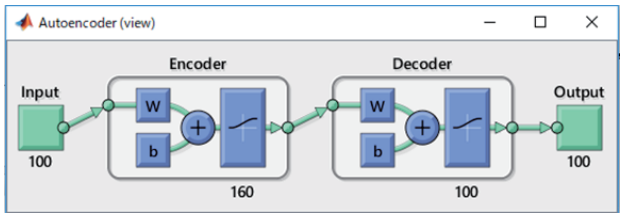

Fig. 2 Block diagram of Autoencoder

The normal part of the measured ECG waveform was chosen, and 10000 samples were trained as training data and 5000 samples were tested.

Fig. 3 shows the learning curve of Ae. The mean square error (mase sparse) between the decoded result Y_r and the original signal X_r is only 3.5195e-05 when the number of calculations is 3000, which shows that high accuracy learning has been performed.

This is because the amount of information can be greatly lost by reducing the dimension of the autoencoder. Fig.4 shows the following. We calculate the square error (MSE) of the restored signal Y_r and the original data X_r by selecting a random one waveform feature. Error division of individual data is shown. It seems to have succeeded in maintaining the waveform characteristic and restoring it.

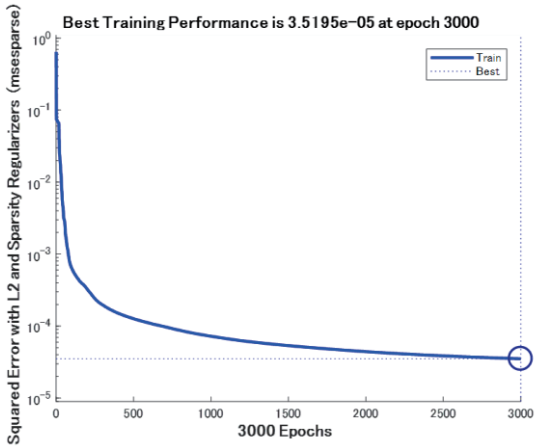

Fig. 3 Learning Curve of Ae

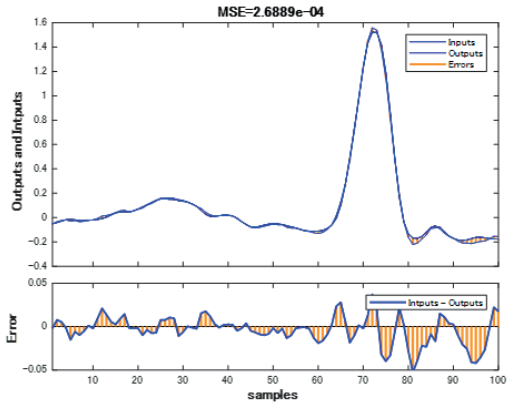

Fig. 4 Waveform Feature

And, the threshold of the error is set to 0.55 (the minimum value exceeding the maximum value of the training data error), and through the test data experiment, the error becomes 0 in the normal case of the electrocardiogram. In addition, two R-wave anomalies were found by the pre-learning Autoencoder from 5-minute data.

Finally, we measured the total heart rate 330 and average heart rate 66 for 5 minutes using MODWT.

4. Heart Rate Measurement Using Kinect in Driving Situation

In order to examine the characteristics of heart rate signal in driving situation, experimental setup using several measurement method as shown in previous section and driving simulator is constructed. In this section, several measurement problem not only signal processing issue but also installation of measurement devices are described through the experimental setups.

4.1 Driving Heart Rate Measurement Using Kinect

As the human heart contracts, the volume of the blood vessel changes. The amount of reflection of light also changes according to the changes. It is able to obtain the reflected light from the capillary of the face with Kinect. Then, it becomes possible to acquire a heartbeat waveform.

However, environmental light conditions will be always change in actual driving situation. And the driver also has driving behavior such as maneuvering the steering wheel on the curve or at the intersection. According to them, drastically changes of the light condition and driving behavior have possibility of making disturbance for visual sensing. Therefore, position of installation for Kinect is also important to consider in order to acquire the driver's face in stable.

4.2 Fixture Design with DS-6000

In order to measure the driver to a better angle with Kinect, the fixture points and its device is designed considering with several structures and dimensions of cockpit of the typical vehicle. In this research, driving simulator "DS-6000" (Mitsubishi Precision Inc.) is used for driving environment. It is simulated for the driving cockpit of typical type of car and their component such as driver's sheet, steering wheel, shift lever and pedals. Especially, driving instruments such as speed and gas meter are also set in the back of steering wheel.

For in-vehicle measurement, it is also important to keep enough fields of view for driver. On the other hand, to make better acquisition of driver's face, it is expected to put the non-contact sensors in front of the face. To satisfy these constraints, the upper side of the front windows is selected and the fixture of Kinect sensor was designed as shown in Fig. 5.

Fig. 5 Experimental setup of Kinect on Driving simulator

4.3 Measurement Result

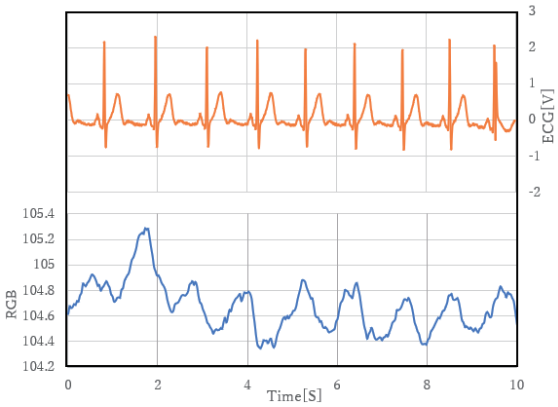

Fig. 6 Comparison of RGB heartrate waveforms and ECG waveforms

The experiment in driving situation with a subject driver has been conducted using constructed experimental setup as shown in previously. The measurement results in this experiment as shown in Fig.6. In this figure, red line shows heart rate waveform obtained by the electrocardiograph, and blue one shows the heart beat waveform measured by Kinect.

Through the simple comparison, heart beat have weakness of overall waveform for typical heart rate signal while heart rate signal has stability. However, it has possibility that the peak points of heart beat can be indicate the R wave characteristic based on the waveform reconstruction techniques.

5. Conclusion

In this paper, we propose a new method of analysis of electrocardiogram waveform data using an NN based autoencoder. At first, the waveform feature of a high level was extracted after the longtime waveform of the electrocardiogram was cut into the fixed length by the slide window system, and the high accuracy automatic encoder was prepared by adjusting various parameters. In addition, abnormal electrocardiogram was passed through a trained autoencoder, and abnormal R wave was accurately detected. Finally, more accurate heart rate information was obtained using MODWT.

As a future problem, the heart rate data of the RGB acquired from the face by Kinect has some correspondence with the electrocardiogram waveform, but it is not easy to detect heartrate. Therefore, it is expected that Kinect's heartbeat data will be processed with an autoencoder that extracts high level waveform features, and concrete connection with electrocardiogram will be examined. With that continuation, we will experiment a plurality of subjects and measure the R-R interval to achieve the final purpose of evaluating the driver's tension.

References

[Deguchi 2006] Mitsuo Deguchi, Junichi Wakasugi, Tatsuya Ikegami, Shinji Nanba, Masaki Yamaguchi, Evaluation of Driver Stress Using Motor-vehicle Driving Simulator, IEEJ Trans, SM,Vol.126,No.8, 2006.

[Nakamura 2015] Koru Nakamura, Tsukasa Sugiura, Takata Tomohiro, Tomoaki Ueda, KINECT for Windows SDK Programming, syuuwa System, 2015.

[Kiyoko 1999] Kiyoko Yokoyama, Junichirou Ushida, Takayoshi Yoshioka, Osamu Ozeki, Yosaku Watanabe, Kazuyuki Takata, Proposal of the Evaluation Method of the Heart Rate Variability using the Frequency Information of the Electrocardiogram, T.IEE Japan, Vol.199-C, 1999.

[Takahashi 2017] Thu Takahashi, Keiichi Ochiai, Yusuke Fukazawa, Feature extraction and arrhythmia classification from 2-lead ECG using stacked convolutional denoising autoencoders, 2017 Information Processing Society of Japan, IPSJ SIG Technical Report, 2017.

[Noriyasu 2018] Noriyasu Omata, Yoshihiro Nakanura, Susumu Shirayama, Extracting Long-term Patterns from Electrocardiogram Waveform using Deep Learning, The 32nd Annual Conference of the Japanese Society for Artificial Intelligence, 2018

The 33rd Annual Conference of the Japanese Society for Artificial Intelligence, 2019

Probability based scaffolding system using Deep Learning

Ryo Kinoshita Maomi Ueno

Graduate school of Informatics and Engineering, The University of Electro-Communications.

Recently, a great deal of interest in the learning science field has arisen in the use of software to scaffold students in complex tasks. However, most of those software tools have been unable to adapt to individuals To solve the problem, IRT-based approaches to predict student's performance have been proposed. These studies show predicting students' correct answer probability with high accuracy is of critical importance. However, IRT-based approach doesn't predict student's performance accurately when the test data are sparse or imbalanced. To achieve high accuracy in those situations, we proposed a novel scaffolding system based on deep learning. We show proposed method can predict student's performance more precisely than traditional IRT method.

1. Introduction

The leading metaphor of human learning has recently been transferred from instructionism to social constructivism. In the context, the Zone of Proximal Development(ZPD) was introduced by [Vygotsky 62, Vygotsky 78]. [Bruner 96] also emphasized the social nature of learning and reported importance of "scaffolding". He defined scaffolding as steps taken to reduce the degrees of freedom in carrying out some task so that children can concentrate on difficult task.

To carry out effective scaffolding, teachers need to estimate student's ability on ZPD and predict their performances after scaffolding. Therefore, [Collins 89] worked on a new assessment method called "dynamic assessment," which provided a cascadig sequence of hints (called graded hints) to understand how much supports students needed to complete tasks.

Recently, a great deal of interest in the learning science field has arisen in the use of software to scaffold students in complex tasks. However, most of those software tools have been unable to adapt to individuals

[Ueno 15, Ueno 18] proposed a novel Item Response Theory(IRT) to represent the individual student's development as the increase of the latent ability variable and then to provide optimal help by predicting the performance given several hints. They assumed that the optimal student's correct answer probability exists for a student's successful performance. Their results revealed that the adaptive hint function is the most effective for learning when they determined 0.5 to be the correct answer probability. Thus, to predict students' correct answer probability with high accuracy is of critical importance.

However, IRT-based approach has some disadvantages. 1) IRT is not robust when students' data are sparse or imbalanced. 2) General IRT models assumes that students' ability has only a single dimensionality

Meanwhile, there are many studies which utilize deep neural networks(deep learning) for educational data mining[Piech 15, Le 18]. They reported high accuracies in various tasks, because deep neural networks can be trained to achieve high accuracy for training data. Furthermore, deep neural networks can includes several abilities in the hidden layers and be relatively robust.

Therefore, we propose a novel scaffolding system for adaptive learning based on deep learning, Deep Response Model(DRM), to predict students' performances with high accuracy. It consists of two independent layers, Student Layer and Item Layer, combined their outputs to predict students' performances

The experiment shows that DRM can predict students' performances more precisely than traditional IRT model in time series data.

2. Dynamic Assessment

The scaffolding process requires dynamic assessment to predict learner performance when a teacher ' s help is presented to them, as explained previously. Brown and her team compared the performance of children's responses to IQ test items under two conditions. The first was "static assessment," which involved children trying to solve problems under conventional test conditions, for which they received no help or guidance. The same children were also tested on the same items under dynamic conditions of providing a series of graded hints. The results demonstrated that dynamic assessment provided a stronger basis for predicting learning outcomes than static measures did. The most important result was that the greatest learning gain tended to be achieved by children who only needed the minimum number of hints. The magnitude of the 'gap' between assisted and unassisted performance indicated by the amount of help needed was therefore prognostic of individual differences in learning outcomes. Assessing how much help a learner needed to succeed provided more decisive information about readiness for learning than determining how often they failed when doing the same, untutored tasks. Consequently, dynamic assessment integrated the assessment of learners' prior knowledge with the task of helping them to learn.

An important difficulty associated with previous studies is that the number of hints needed was not a reliable mea-

連絡先: Ryo Kinoshita,Graduate school of Informatics and Engineering,The University of Electro-Communications, 1-5-1 Chofugaoka, Chofu-shi, 182-8585, Japan,kinoshita@ai.is.uec.ac.jp

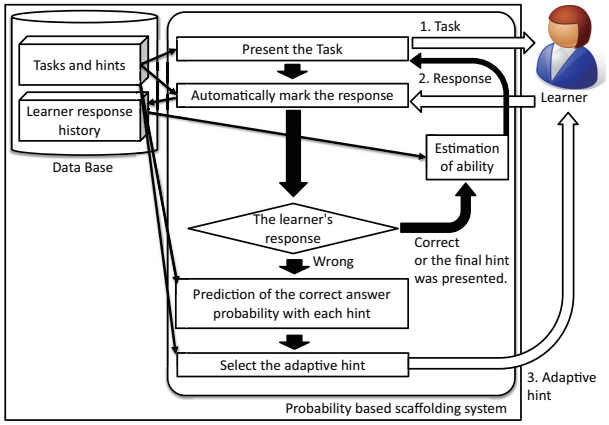

Fig. 1: Outline of the probability-based scaffolding system

sure of dynamic assessment because it depended strongly on the task difficulty. In addition, earlier studies were unable to predict how much support a learner needed for solving a task that had not been presented to the learner.

3. Item Response Theory

This section briefly introduces IRT, a recent test theory based on mathematical models, which is being used widely in various areas and adaptive learning. It has three main benefits:

1)It can assess ability while minimizing the effects of heterogeneous or aberrant items, which have low estimation accuracy.

2)The students' responses to different items can be assessed on the same scale.

3)It predicts the individual probability of correct response to a problem based on past response data.

This section introduces the two-parameter logistic model(2PLM), which is an extremely popular IRT model. For the 2PLM, u_j denotes the response of a student to item j. In this model, $u_j = 0$ shows the student answered item j incorrectly and $u_j = 1$ shows the student answered item j correctly.

In the 2PLM, the probability of correct answer given to item j by a learner with ability $\theta \in (-\infty, \infty)$ is assumed as

$$P_j(u_j = 1|\theta) = \frac{1}{1 + exp(-1.7a_j(\theta - b_j))} \tag{1}$$

where $a_j \in [0, \infty)$ is the j$^{\text{th}}$ item's discrimination parameter expressing the discriminatory power for students' abilities of item j, and $b_j \in (-\infty, \infty)$ is the j$^{\text{th}}$ item's difficulty parameter expressing the degree of difficulty of item j.

4. Proposed Deep Learning Model

We developed a scaffolding system to solve the programming trace problem. Fig. 1 depicts an outline of the system framework.

Especially, this paper introduce proposed model for estimating students' ability and predicting the correct answer probability. Fig. 2 shows a process of the proposed method. It consists of two neural networks, Student Layer and Item Layer, to separate students' ability from item traits. Then, it combines two outputs to predict students' response.

Proposed method predicts a response $u_{ij} \in \{0, 1\}$ given by student $i \in \{1, ..., I\}$ for item $j \in \{1, ..., J\}$ as follows.

The input of Student Layer, $\boldsymbol{s}_i \in \mathbb{R}^I$ is a one-hot vector, where only the i$^{\text{th}}$ element is 1 and the others are 0. Then, it calculates two-layered feed forward networks.

$$\boldsymbol{\theta}_1^{(i)} = tanh\left(\boldsymbol{W}^{(\theta_1)}\boldsymbol{s}_i + \boldsymbol{b}^{(\theta_1)}\right) \tag{2}$$

$$\boldsymbol{\theta}_2^{(i)} = tanh\left(\boldsymbol{W}^{(\theta_2)}\boldsymbol{\theta}_1^{(i)} + \boldsymbol{b}^{(\theta_2)}\right) \tag{3}$$

$$\theta_3^{(i)} = \boldsymbol{W}^{(\theta_3)}\boldsymbol{\theta}_2^{(i)} + b^{(\theta_3)} \tag{4}$$

We use hyperbolic tangent as an activate function:

$$\tanh(x) = \frac{\exp(x) - \exp(-x)}{\exp(x) + \exp(-x)} \tag{5}$$

$W^{(\theta_1)}$,$W^{(\theta_2)}$are weight matrices:

$$\boldsymbol{W}^{(\theta_1)} = \begin{pmatrix} w_{11}^{(\theta_1)} & w_{12}^{(\theta_1)} & \dots & w_{1I}^{(\theta_1)} \\ w_{21}^{(\theta_1)} & w_{22}^{(\theta_1)} & \dots & w_{2I}^{(\theta_1)} \\ \vdots & \vdots & \ddots & \vdots \\ w_{|\boldsymbol{\theta}_1|1}^{(\theta_1)} & w_{|\boldsymbol{\theta}_1|2}^{(\theta_1)} & \dots & w_{|\boldsymbol{\theta}_1|I}^{(\theta_1)} \end{pmatrix}$$

$$\boldsymbol{W}^{(\theta_2)} = \begin{pmatrix} w_{11}^{(\theta_2)} & w_{12}^{(\theta_2)} & \dots & w_{1|\boldsymbol{\theta}_1|}^{(\theta_2)} \\ w_{21}^{(\theta_2)} & w_{22}^{(\theta_2)} & \dots & w_{2|\boldsymbol{\theta}_1|}^{(\theta_2)} \\ \vdots & \vdots & \ddots & \vdots \\ w_{|\boldsymbol{\theta}_2|1}^{(\theta_2)} & w_{|\boldsymbol{\theta}_2|2}^{(\theta_2)} & \dots & w_{|\boldsymbol{\theta}_2||\boldsymbol{\theta}_1|}^{(\theta_2)} \end{pmatrix}$$

$W^{(\theta_3)}$ is a weight vector.

$$\boldsymbol{W}^{(\theta_3)} = \begin{pmatrix} w_1^{(\theta_3)} & w_2^{(\theta_3)} & \dots & w_{|\boldsymbol{\theta}_2|}^{(\theta_3)} \end{pmatrix}$$

$\boldsymbol{b}^{(\theta_1)} = \left(b_1^{(\theta_1)}, b_2^{(\theta_1)} ... b_{|\boldsymbol{\theta}_1|}^{(\theta_1)}\right)$, $\boldsymbol{b}^{(\theta_2)} = \left(b_1^{(\theta_2)}, b_2^{(\theta_2)} ... b_{|\boldsymbol{\theta}_2|}^{(\theta_2)}\right)$ are bias parameter vectors, and $b^{(\theta_3)}$ is a bias parameter.

This model considers the last value of Student Layer,$\theta_3^{(i)}$, as a student parameter of i

In the same way, the input of Item Layer, $\boldsymbol{q}_j \in \mathbb{R}^J$ is a one-hot vector, where only the j$^{\text{th}}$ element is 1 and the others are 0. Then, it calculates two-layered feed forward networks.

$$\boldsymbol{\phi}_1^{(j)} = tanh\left(\boldsymbol{W}^{(\phi_1)}\boldsymbol{q}_j + \boldsymbol{b}^{(\phi_1)}\right) \tag{6}$$

$$\boldsymbol{\phi}_2^{(j)} = tanh\left(\boldsymbol{W}^{(\phi_2)}\boldsymbol{\phi}_1^{(j)} + \boldsymbol{b}^{(\phi_2)}\right) \tag{7}$$

$$\phi_3^{(j)} = \boldsymbol{W}^{(\phi_3)}\boldsymbol{\phi}_2 + b^{(\phi_3)} \tag{8}$$

$\boldsymbol{W}^{\phi_1}$,$\boldsymbol{W}^{(\phi_2)}$ are weight matrices:

$$\boldsymbol{W}^{(\phi_1)} = \begin{pmatrix} w_{11}^{(\phi_1)} & w_{12}^{(\phi_1)} & \dots & w_{1J}^{(\phi_1)} \\ w_{21}^{(\phi_1)} & w_{22}^{(\phi_1)} & \dots & w_{2J}^{(\phi_1)} \\ \vdots & \vdots & \ddots & \vdots \\ w_{|\boldsymbol{\phi}_1|1}^{(\phi_1)} & w_{|\boldsymbol{\phi}_1|2}^{(\phi_1)} & \dots & w_{|\boldsymbol{\phi}_1|J}^{(\phi_1)} \end{pmatrix}$$

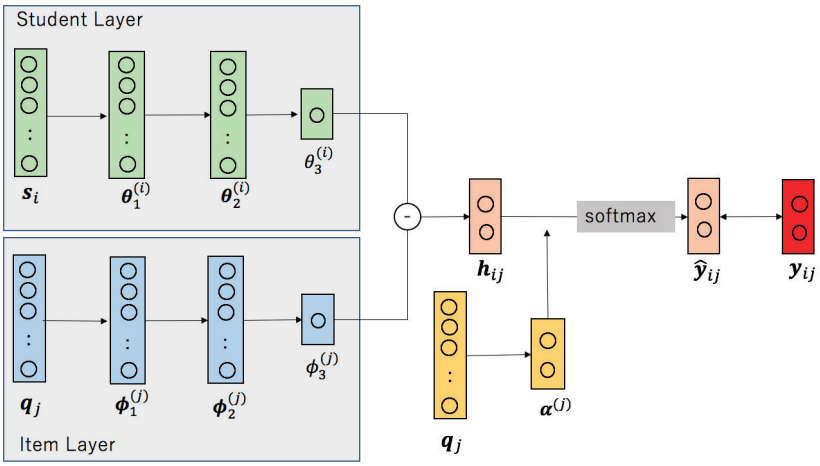

Fig. 2: Proposed Deep Learning model

$$\boldsymbol{W}^{(\phi_2)} = \begin{pmatrix} w_{11}^{(\phi_2)} & w_{12}^{(\phi_2)} & \dots & w_{1|\phi_1|}^{(\phi_2)} \\ w_{21}^{(\phi_2)} & w_{22}^{(\phi_2)} & \dots & w_{2|\phi_1|}^{(\phi_2)} \\ \vdots & \vdots & \ddots & \vdots \\ w_{|\phi_2|1}^{(\phi_2)} & w_{|\phi_2|2}^{(\phi_2)} & \dots & w_{|\phi_2||\phi_1|}^{(\phi_2)} \end{pmatrix}$$

$\boldsymbol{W}^{(\phi_3)}$ is a weight vector:

$$\boldsymbol{W}^{(\phi_3)} = \begin{pmatrix} w_1^{(\phi_3)} & w_2^{(\phi_3)} & \dots & w_{|\phi_2|}^{(\phi_3)} \end{pmatrix}$$

$\boldsymbol{b}^{(\phi_1)} = \left(b_1^{(\phi_1)}, b_2^{(\phi_1)} ... b_{|\phi_1|}^{(\phi_1)}\right)$, $\boldsymbol{b}^{(\phi_2)} = \left(b_1^{(\phi_2)}, b_2^{(\phi_2)} ... b_{|\phi_2|}^{(\phi_2)}\right)$ are bias parameter vectors, and,$b^{(\phi_3)}$is a bias parameter.

This model considers the last value of Item Layer,$\phi_3^{(j)}$, as an item parameter of j.

Then, a student parameter and an item parameter are combined to predict the student response.

Specifically, proposed model outputs response probabilities $\hat{\boldsymbol{y}}_{\boldsymbol{i,j}} = (\hat{y}_{i,j}^{(0)}, \hat{y}_{i,j}^{(1)})$ using hidden layer $\boldsymbol{h}^{(i,j)} = (h_0^{(i,j)}, h_1^{(i,j)})$ and softmax function.

$$\boldsymbol{h}^{(i,j)} = (W^{(y)})^T(\theta_3^{(i)} - \phi_3^{(j)}) + \boldsymbol{b}^{(y)} \tag{9}$$

$$\begin{aligned} \hat{y}_{i,j}^{(c)} &= softmax(\boldsymbol{\alpha}^{(j)} \circ \boldsymbol{h}^{(i,j)}) \\ &= \frac{exp(\alpha_c^{(j)} * h_c^{(i,j)})}{\sum_c exp(\alpha_c^{(j)} * h_c^{(i,j)})} \end{aligned} \tag{10}$$

$\boldsymbol{W}^{(y)} = (w_1^{(y)}, w_2^{(y)})$, $b^{(y)} = (b_1^{(y)}, b_2^{(y)})$ are weight vector and bias vector. $\circ$ in equation(10) indicates Hadamard product. In the process, we implement attention function $\boldsymbol{\alpha}$, which is calculated based on the question vector $\boldsymbol{q}_j$ as follows:

$$\boldsymbol{\alpha}^{(j)} = softmax(\boldsymbol{W}^{(\alpha)}\boldsymbol{q}_j + \boldsymbol{b}^{(\alpha)}) \tag{11}$$

$\boldsymbol{W}^{(\alpha)}$ is a weight matrix:

$$\boldsymbol{W}^{(\alpha)} = \begin{pmatrix} w_{11}^{(\alpha)} & w_{12}^{(\alpha)} & \dots & w_{1J}^{(\alpha)} \\ w_{21}^{(\alpha)} & w_{22}^{(\alpha)} & \dots & w_{2J}^{(\alpha)} \end{pmatrix}$$

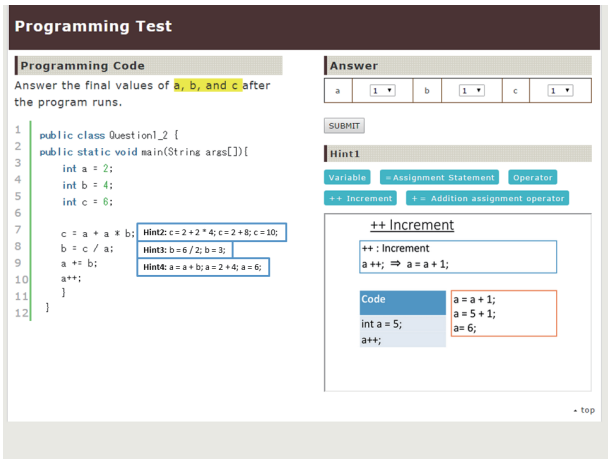

Fig. 3: Dynamic Assessment System

$b^{(\alpha)} = (b_1^{(\alpha)}, b_2^{(\alpha)})$ is a bias vector.

With attention, the model can consider other traits of items like a discrimination or label balance.

This model are trained to reduce the following loss function.

$$Loss = -\sum_i \sum_j \sum_{c \in (0,1)} \boldsymbol{y}_{i,j}^{(c)} \log \hat{\boldsymbol{y}}_{i,j}^{(c)} \tag{12}$$

Loss shows a classification error between response probability $\hat{\boldsymbol{y}}$ and true response $\boldsymbol{y}$, where $\boldsymbol{y}_{i,j}^{(c)} = 1$ when student i answered item j correctly, and otherwise, $\boldsymbol{y}_{i,j}^{(c)} = 0$.

5. Actual Data Experiment

This section presents a description of evaluation of the effectiveness of the proposed model using actual time-series data. Actual data were gathered through the following procedures using the dynamic assessment system we developed. The system is shown in Fig. 3.

(1)82 university students who are not familiar with programming were enrolled.

(2) They tried to solve the 19 items in order with hints about grammar of programming.

Table. 1: Prediction accuracy of learner's performance

Item	2	3	4	5	6	7	8	9	10	
DRM	**52.50%**	**72.15%**	**62.82%**	**58.44%**	75.00%	**61.04%**	**62.67%**	67.11%	**63.16%**	
DRM w/o attention	**52.50%**	**72.15%**	58.97%	57.14%	**76.32%**	**61.04%**	58.67%	65.79%	60.53%	
IRT	51.22%	69.51%	56.10%	53.66%	69.51%	57.32%	58.54%	**68.29%**	57.32%	
Item	11	12	13	14	15	16	17	18	19	Average
DRM	**70.42%**	**67.57%**	**80.26%**	**79.73%**	**87.84%**	65.76%	**97.37%**	**92.00%**	73.68%	**71.64%**
DRM w/o attention	69.01%	**67.57%**	71.05%	**79.73%**	83.78%	**67.57%**	96.05%	**92.00%**	**76.32%**	70.34%
IRT	59.76%	62.20%	76.83%	74.39%	81.71%	60.98%	86.59%	84.15%	73.17%	66.73%

In this experiment, u_{ij} are defined as follows:

$$u_{ij} = \begin{cases} 1 & (\text{student } i \text{ answered item } j \text{ correctly} \\ & \text{without any hints}) \\ 0 & (otherwise) \end{cases}$$

The data includes much missing, which account for over 7%.

We employ Chainer*1, one of frameworks on deep learning, for implementation and optimization of proposed model. The parameters are updated iteratively for 1500 times using batch learning. We use adaptive moment estimation(Adam)[Kingma 14] as an optimizer.

On the other hand, we adopt 2 PLM as a comparative method. The parameters were estimated using Markov chain Monte Carlo algorithm with following prior distributions.

$$\theta \sim N(0,1), \quad \log a \sim N(0,1), \quad b \sim N(1,0.4) \qquad (13)$$

$N(\mu, \sigma)$ denotes normal distribution with mean μ and standard deviation σ.

Using the actual data, we calculate the accuracy as following:
1) All models are trained using full data and hold only their item parameters, Item Layer weights and bias.
2) Student parameters are estimated using actual data between item 1 to item $j (j = 1, ..., J-1)$.
3) Student responses for item $j+1$ are predicted.
4) Each agreement rate between their predictions and true responses are calculated

Table 1 presents the results. As shown in table 1, the proposed model predict students' response the most precisely for the almost all of items. In addition, result shows the average of agreement rates of the proposed model over all items are much higher than traditional IRT model.

Furthermore, proposed method with attention achieve higher accuracy than without attention. Thus, the effectiveness of attention was shown.

Here, Bonferroni's multiple comparison test using p-values of Wilcoxon signed-rank test shows there are significant differences between three models at 0.05 significance level. It showed proposed model outperformed the conventional model in terms of response predictions.

6. Conclusion

This study proposed a novel scaffolding system using deep learning method. Experiments conducted with actual data demonstrated that the proposed model can predict students' responses more precisely than a traditional model.

Although this study specifically addressed only response prediction, it can be useful for response prediction with hints and has potential to apply for adaptive learning. These are left as subjects for future work.

Reference

[Bruner 96] Bruner, J.: The Culture of Education, Harvard University Press (1996)

[Collins 89] Collins, A., Seely Brown, J., and E Newmann, S.: Cognitive Apprenticeship: Teaching the Craft of Reading, Writing, and Mathematics, Vol. 18, pp. 453–494 (1989)

[Kingma 14] Kingma, D. P. and Ba, J.: Adam: A Method for Stochastic Optimization, arXiv:1412.6980 (2014)

[Le 18] Le, C. V., Pardos, Z. A., Meyer, S. D., and Thorp, R.: Communication at Scale in a MOOC Using Predictive Engagement Analytics, in Artificial Intelligence in Education - 19th International Conference, AIED 2018, London, UK, June 27-30, 2018, Proceedings, Part I, pp. 239–252 (2018)

[Piech 15] Piech, C., Bassen, J., Huang, J., Ganguli, S., Sahami, M., Guibas, L. J., and Sohl-Dickstein, J.: Deep Knowledge Tracing, in Cortes, C., Lawrence, N. D., Lee, D. D., Sugiyama, M., and Garnett, R. eds., Advances in Neural Information Processing Systems 28, pp. 505–513, Curran Associates, Inc. (2015)

[Ueno 15] Ueno, M. and Miyasawa, Y.: Probability Based Scaffolding System with Fading, in Conati, C., Heffernan, N., Mitrovic, A., and Verdejo, M. F. eds., Artificial Intelligence in Education, pp. 492–503, Cham (2015), Springer International Publishing

[Ueno 18] Ueno, M. and Miyazawa, Y.: IRT-Based Adaptive Hints to Scaffold Learning in Programming, IEEE Transactions on Learning Technologies, Vol. 11, No. 4, pp. 415–428 (2018)

[Vygotsky 62] Vygotsky, L.: Thought and Language, Harvard University Press (1962)

[Vygotsky 78] Vygotsky, L.: Mind in Society, Harvard University Press (1978)

∗1 https://chainer.org/